

GBF1 recruitment to membranes: domains and interacting proteins

by

Calvin John Chan

A thesis submitted in partial fulfillment of the requirements for the degree of

Doctor of Philosophy

Department of Cell Biology
University of Alberta

© Calvin John Chan, 2020

Abstract

The Golgi complex resides at the center of the cellular trafficking pathway, where it functions in the modification, sorting, and trafficking of over one third of human proteins to their correct cellular destination. Initiation of vesicle formation at the Golgi requires activation of small GTPases of the ADP-ribosylation factor (Arf) family. The Golgi-specific Brefeldin-A resistance factor 1 (GBF1), is the only large guanine nucleotide exchange factor (GEF) that regulates Arf activation at the *cis*-Golgi and is actively recruited to membranes through a feed forward mechanism upon a reduction in active Arf-GTP.

Previous studies have demonstrated that GBF1 recruitment requires (a) heat labile and protease sensitive component(s). However, the domains in GBF1 involved in its recruitment, as well as the Golgi-localised protein interactors responsible remain unknown. In this thesis, we first demonstrate using a series of GBF1 deletion mutants that domains HDS1 and HDS2 are essential in the localisation and recruitment of GBF1 to Golgi membranes. To identify GBF1 regulators at the membrane, we further established a method pairing the proximity biotinylation (BioID) based proteomic assay with organelle enrichment to identify Golgi specific GBF1 interacting partners. Unlike past studies on GBF1 interacting proteins, this method allows for the capture of transient, weak, and/or poorly soluble proximal proteins. High-confidence putative interactors were screened via shRNA knockdown and two novel GBF1 interactors were identified and confirmed using coimmunoprecipitation: C10orf76 and ZnT6. Fluorescence and electron microscopy revealed C10orf76 to be a peripheral membrane Golgi-localised protein involved in Golgi maintenance, secretion, and regulation of GBF1 recruitment. C10orf76 exchanges rapidly between free and bound forms, and treatment with the GBF1 inhibitory drug, brefeldin A,

increases the residence time of C10orf76 on the membrane. Our phylogenetic analysis suggests that C10orf76 was likely present in the last eukaryotic common ancestor, but subsequently lost from the plant and yeast model systems, *Arabidopsis thaliana* and *Saccharomyces cerevisiae*. However, C10orf76 orthologues were identified in other plant and yeast species including *Marchantia polymorpha* and *Schizosaccharomyces pombe*. These data suggest that other more evolutionarily conserved GBF1 regulators likely exist. Using fluorescence recovery after photobleaching (FRAP) we demonstrate that another novel regulator, ZnT6, while not essential in recruiting GBF1, plays a role in modulating GBF1 cycling on and off membranes. Knockdown of ZnT6 appears to prevent a fraction of GBF1 from cycling off the membrane. Overexpression reduces the overall fraction of membrane-bound GBF1 and increases the rate of exchange between free and bound forms. We hypothesize that ZnT6 may facilitate the release of GBF1 from the membrane. However, whether this may be due to a direct interaction between ZnT6 and GBF1, or the role of ZnT6 in zinc import into the Golgi lumen remains unclear. Our work has generated new insights into the regulation of GBF1 recruitment to Golgi membranes, and offers a more nuanced picture of the dynamic cellular processes that likely shape GBF1 function in mammalian cells.

Preface

A version of Chapter 3 has been published as, “The Arf-GDP-regulated recruitment of GBF1 to Golgi membranes requires domains HDS1 and HDS2 and a Golgi-localised protein receptor.” (Quilty et al., 2019). All copyright belongs to the respective authors.

Initial construction and preliminary testing of the EGFP-tagged GBF1 truncation library used in Chapter 3 was performed in collaboration with Douglas Quilty for my undergraduate degree. Construction of this plasmid truncation library and initial live-cell imaging of the constructs were described in Douglas Quilty’s 2016 doctoral thesis (Quilty, 2016). However, none of the data developed as part of that thesis are reproduced here. All data shown in Chapter 3 were obtained during my time as a graduate student in the Department of Cell Biology, University of Alberta. Dr. Paul Melançon helped in the planning of experiments, data analysis, and writing of the final manuscript.

A version of Chapter 4 and 5 has been published as, “BioID performed on Golgi-enriched fractions identify C10orf76 as a GBF1 binding protein essential for Golgi maintenance.” (Chan et al., 2019). All copyright belongs to the respective authors.

Initial construction and characterization of the BirA*-FLAG and BirA*-FLAG-GBF1 cell lines, preparation of samples for mass spectrometry, and the shRNA screen was done with the help of undergraduate student Roberta Le. Mass spectrometry and SAINT analysis was done by Dr. Etienne Coyaud and Estelle M.N. Laurent in Dr. Brian Raught’s lab in the Department of Medical Biophysics at the University of Toronto, Toronto, ON, Canada. Several reagents used in the BioID assay were provided by Drs. Nicolas Touret and Ing Swie Goping. The electron microscopy was performed with Dr. Nasser Tahbaz. The GBF1 mutants used for the co-immunoprecipitation assays were generated with the help of undergraduate student Khadra

Ahmed. The luciferase assay was performed with help from undergraduate student Kaylan Burns. Pulldowns were performed with advice from Dr. Richard Wozniak and with reagents provided by Dr. Thomas Simmen. The phylogeny of C10orf76 was examined using advice and guidelines suggested by Dr. Joel Dacks and Dr. Lael Barlow. Dr. Paul Melançon helped in the planning of experiments, data analysis, and writing of the manuscript.

The work contained in Chapter 6 has not been published. The construction of the ZnT6 knockdown cell line and the luciferase secretion assay was performed with help from undergraduate student Kaylan Burns.

All other components of this thesis are my original work completed under the supervision of Dr. Paul Melançon, who also provided advice and comments during the writing of this thesis.

Dedication

For my mom.

Acknowledgments

The deepest gratitude to my supervisor, Dr. Paul Melançon, for finding and believing in me before it all began. And for respecting me as a researcher, and standing behind my vision in every way. Your tireless faith and patience allowed me to grow as an independent thinker. Your perspicacity and wisdom lit the light we needed to navigate the many roadblocks on our journey. Your feedback and criticism continually sharpened this body of work. Despite some challenging times, your office was always my first site of refuge. Never forget that your career has set the foundation for many new researchers to follow. While we may not have arrived at the destination we hoped for, I don't think our journey any less worthwhile.

To my committee members and mentors Drs. Gary Eitzen and Nicolas Touret, for always keeping our path true. Your nurturing feedback and advice mapped the rough and uneven terrains of the project. You saw value in the work even when our destinations were unclear. Your numerous ideas and recommendations shaped the product we have today.

A thank you to Dr. Richard Wozniak for serving on both my candidacy exam and defense committees, as well as for teaching me the value of a strong control. Your insight helped us unravel some of the most complex knots in our work.

A deep thanks to our collaborators Dr. Etienne Couyaud, Dr. Brian Raught, and Estelle M.N. Laurent. Your delicate work on the mass spectrometry and statistical analysis for our project laid the soil by which my research could blossom.

To my fellow graduate student, Sol Herrera, for lending me your strength when I had none, and for your friendship, when by luck I sat down beside you that first day in CELL 545. I've long forgotten the words we exchanged that day, but I will never forget your kind presence. I have you to thank for troubleshooting the many protocols I've come to lean on time and time

again, and for your keen eye in reviewing my numerous assignments, proposals, and reports. You were an anchor in the most turbulent weather.

To Douglas Quilty, thank you for being a friend and teacher. In more ways than you know, you made this work possible.

A deep gratitude to all the high school and undergraduate research students who I've had the joy to teach. Roberta Le, your passion and dedication to the BioID project carried the work forward during an uncertain beginning. Khadra Ahmed and Kaylan Burns, your tireless hours in the lab allowed for the great strides in our research. And lastly, Amy McNeil and Patricia Feng, your excitement for science reminded me of why it all began.

And of course, a sincerest thank you to my external examiner, Dr. Nava Segev. Your advice and kind words at our past meetings taught me the importance of perseverance. Science isn't always easy, but that only makes it all the more worthwhile.

Table of Contents

1	Chapter 1: Introduction	1
1.1	The endomembrane system and the early secretory pathway	2
1.1.1	The ERGIC	4
1.1.2	The Golgi Compartment and intra-Golgi traffic	5
1.1.3	Golgi membrane lipid composition	8
1.1.4	The COPI trafficking machinery	10
1.2	Small GTPases at the Golgi	11
1.2.1	Rabs	12
1.2.2	ADP-ribosylation factors (Arfs)	13
1.3	Arf guanine nucleotide exchange factors (ArfGEFs)	14
1.4	Golgi-specific brefeldin-A resistance factor 1 (GBF1)	18
1.4.1	GBF1 domains	24
1.4.2	GBF1 interacting partners and a putative receptor	25
1.5	Arf GTPase activating proteins (ArfGAPs)	27
1.6	Hypothesis and thesis plan	29
2	Chapter 2: Materials and Methods	31
2.1	Reagents	32
2.2	Cell culture	35
2.2.1	Construction of Flp-In T-Rex HeLa cell lines containing tetracycline operator regulated BirA*-tagged transgenes	36
2.2.2	Construction of Flp-In T-Rex HeLa cell lines containing a tetracycline operator regulated EGFP-GBF1 and stably expressing a non-targeting or ZnT6-specific shRNA	37
2.3	Expression plasmids	38
2.3.1	pEGFP-GBF1 truncation library	38
2.3.2	mCherry-ERGIC53 plasmid	39
2.3.3	mCherry-C10orf76, FLAG-C10orf76, and the EGFP-C10orf76 truncations	39
2.3.4	mCherry- and EGFP-ZnT6	41
2.3.5	Additional plasmids	41
2.4	Antibodies and streptavidin conjugates	41
2.5	Site-directed mutagenesis	43
2.6	Cell plating, transient transfections, and immunofluorescence	44
2.7	Fluorescence microscopy	44
2.7.1	Epifluorescence microscopy	44
2.7.2	Electron microscopy	45
2.7.3	Fluorescence recovery after photobleaching (FRAP)	45
2.8	Image quantitation and analysis	46
2.8.1	Li's intensity correlation quotient	46
2.8.2	Fraction signal at Golgi structures	46
2.9	Lentiviral particle production and transduction	47
2.10	Proximity-dependent biotinylation and Golgi membrane enrichment	51
2.11	Mass spectrometry and analysis	52
2.12	Western blotting and quantitation	54
2.13	Co-immunoprecipitation	55
2.14	Secretion assays and plate reading	56

2.15	Membrane isolation and peripheral membrane protein extraction	57
2.16	Homology searching for protein orthologues.....	57
3	Chapter 3: GBF1 domains HDS1 and HDS2 are required for GBF1 localisation and recruitment.....	59
3.1	Background and current understanding of GBF1 domain function	60
3.2	Results.....	62
3.2.1	HDS1 and HDS2 are involved in targeting GBF1 to the Golgi	62
3.2.2	Interaction between HDS1, HDS2, and the membrane is sensitive to formaldehyde fixation.....	72
3.2.3	HDS1 and HDS2 domains alone fail to localise to Golgi structures	74
3.2.4	The catalytic Sec7d is not required for the active recruitment of GBF1 to the Golgi ..	76
3.3	Discussion.....	79
3.3.1	DCB, HUS, Sec7ds are not needed for GBF1 localisation or recruitment to Golgi membranes	79
3.3.2	HDS1 and HDS2 are likely essential in targeting GBF1 to Golgi membranes.....	80
3.3.3	Sec7d is not required for additional recruitment of GBF1 to Golgi structures	82
3.3.4	GBF1 localisation to other membrane sites	83
4	Chapter 4: Analysis of Golgi fractions obtained from proximity biointylation with GBF1 chimera identifies unique proximal partners	85
4.1	Background on BioID and rationale for using a Golgi enrichment procedure.....	86
4.1.1	Known GBF1 interactors and the putative GBF1 receptor	86
4.1.2	Proximity-based biotinylation approaches to studying the GBF1 interactome	87
4.2	Results of BioID Analysis	92
4.2.1	Characterization of the BirA*-FLAG and BirA*-FLAG-GBF1 HeLa cell lines	92
4.2.2	BioID analysis using Golgi-enriched fractions identify unique proximal partners	98
4.3	Results of the shRNA screen.....	103
4.4	Discussion.....	110
4.4.1	Enrichment of Golgi organelles improved identification of certain proximal partners using BioID.....	110
4.4.2	Comparison to previously published attempts at identifying GBF1 membrane interactors	111
4.4.3	Limitations of the BioID method and SAINT analysis	112
4.4.4	Limitations of the shRNA screen	114
5	Chapter 5: C10orf76 is a novel GBF1 interacting partner essential for Golgi maintenance.....	116
5.1	Background on C10orf76	117
5.2	Results.....	118
5.2.1	C10orf76 is essential for Golgi maintenance.....	118
5.2.2	C10orf76 is required for maintaining cellular secretion	120
5.2.3	C10orf76 interacts with the C-terminal half of GBF1	122
5.2.4	C10orf76 interaction is not sufficient to target GBF1 to the Golgi	124
5.2.5	C10orf76 depletion does not impair GBF1 activity	127
5.2.6	C10orf76 is a Golgi-localised protein but is not sensitive to BFA	129
5.2.7	C10orf76 is a peripheral protein that cycles on and off Golgi membranes.....	131
5.2.8	C10orf76 truncations fail to reveal a Golgi localising domain	136
5.2.9	C10orf76 is likely present in the last eukaryotic common ancestor, similar to GBF1	138

5.3	Discussion.....	142
5.3.1	Links between C10orf76, PI4K, and GBF1	142
5.3.2	Is C10orf76 a GBF1 co-receptor?	143
6	Chapter 6: ZnT6 is a novel GBF1 interacting partner and may regulate GBF1 dynamics at the Golgi.....	147
6.1	Background on ZnT6.....	148
6.1.1	Zinc transporters at the Golgi.....	148
6.1.2	ZnT5 and 6 are structurally unique compared to other ZnT proteins	149
6.2	Results.....	150
6.2.1	ZnT6 is a novel GBF1 interactor.....	150
6.2.2	ZnT6 depletion alters GBF1 dynamics on the membrane, but not distribution or recruitment.....	153
6.2.3	ZnT6 overexpression reduces Golgi-localised GBF1 and alters GBF1 cycling on and off membranes	158
6.2.4	ZnT6 depletion does not significantly impact GBF1 activity or secretory activity.....	163
6.3	Discussion.....	166
6.3.1	ZnT6 is a novel GBF1 interactor and regulates GBF1 cycling on and off membranes 166	
6.3.2	Does GBF1 regulation involve zinc?	168
7	Chapter 7: General Discussion	170
7.1	Synopsis.....	171
7.2	Pairing organelle isolation with BioID	172
7.3	GBF1 membrane binding and the HDS1 and HDS2 domains.....	173
7.4	ZnT6 and other zinc binding proteins in the BioID analysis	175
7.5	Potential roles of C10orf76 in GBF1 regulation.....	179
7.6	Future experiments, BioID analysis, and other GBF1 regulators	183
7.7	GBF1 recruitment at other membrane sites	186
7.8	Concluding remarks	189
8	References.....	190
9	Appendix.....	205
9.1	Total peptide counts and associated Bayesian false discovery rates for proteins identified from whole cell lysates.....	206
9.2	Total peptide counts and associated Bayesian false discovery rates for proteins identified from enriched Golgi fractions.....	292

List of Tables

Table 2.1 List of chemicals and reagents	32
Table 2.2 Commercial kits	33
Table 2.3 Commonly used buffers and solutions	34
Table 2.4 Primers used for generating Flp-In T-Rex HeLa cells expressing various BirA*-tagged transgenes	36
Table 2.5 Primers used for generating the pEGFP-C1-GBF1 truncation library	38
Table 2.6 Primary antibodies used in immunofluorescence	41
Table 2.7 Secondary antibodies used in immunofluorescence	42
Table 2.8 Primary antibodies used in western blots	42
Table 2.9 Secondary antibodies used in western blots	43
Table 2.10 Streptavidin conjugates	43
Table 2.11 List of Sigma-Aldrich MISSION shRNA encoding plasmids used	49
Table 4.1 Total spectral counts and SAINT scores for candidate GBF1 interactors identified in whole cell lysate (WCL) and Golgi-enriched fractions, as indicated	102
Table 5.1 Accession numbers and associated E-values for BLASTp searches using human C10orf76 as a query	141

List of Figures

Figure 1.1 Schematic depiction of the human secretory pathway.	3
Figure 1.2 Domain organization of the Sec7 family of ArfGEFs in human cells.	17
Figure 1.3 Mechanism of Arf activation by the sec7d and its inhibition by BFA.	22
Figure 1.4 Diagram depicting the activation and inactivation of Arf by GBF1 at cis-Golgi membranes.	23
Figure 3.1 Colocalization and average intensity correlation analysis of GBF1 truncations.	65
Figure 3.2 N205-1856, N390-1856, N885-1856, and C1-1275 localise to mCherry-ERGIC53-positive Golgi structures.	67
Figure 3.3 GBF1 truncations lacking HDS1 or HDS2 fail to co-localise with mCherry-ERGIC53.	70
Figure 3.4 Western blotting confirms protein size for EGFP-tagged GBF1 truncations.	71
Figure 3.5 Localisation of GBF1 truncations appears sensitive to formaldehyde fixation.	73
Figure 3.6 HDS1 and HDS2 domains alone fail to localise to Golgi structures.	75
Figure 3.7 BFA stimulates Golgi recruitment of GBF1 truncations.	78
Figure 4.1 Depiction of the proximity-based biotinylation technique BioID with GBF1.	90
Figure 4.2 Application of the proximity-based biotinylation technique BioID for identifying GBF1 interactions on Golgi membranes.	91
Figure 4.3 Both BirA*-FLAG and BirA*-FLAG-GBF1 are expressed at low levels upon induction with doxycycline.	95
Figure 4.4 BirA*-FLAG-GBF1 biotinylates Golgi proteins vastly different than BirA*-FLAG.	96
Figure 4.5 BirA*-FLAG-GBF1 can be recruited to and biotinylates proximal proteins at Golgi structures.	97
Figure 4.6 Venn diagram depicting the high-confidence candidates identified in the BioID experiment.	101
Figure 4.7 Knockdown of nearly all high-confidence GBF1 proximal proteins identified by BioID had little impact on GBF1 distribution at 72 hours.	107
Figure 4.8 Confirmation of knockdown for high-confidence GBF1 proximal proteins identified by BioID.	108
Figure 4.9 Knockdown of C10orf76 redistributed GBF1 and altered its recruitment.	109
Figure 5.1 C10orf76 appears essential for Golgi maintenance.	119
Figure 5.2 C10orf76 depletion impairs cellular secretion.	121
Figure 5.3 C10orf76 interacts with the C-terminal half of GBF1.	123
Figure 5.4 The L1246R mutation abrogates Golgi localisation in the N885-1856 truncation.	125
Figure 5.5 C10orf76 interaction appears not to be impaired by the L1246R mutation.	126
Figure 5.6 C10orf76 depletion does not prevent β-COP recruitment.	128
Figure 5.7 C10orf76 localises to GBF1 positive Golgi structures but appears insensitive to BFA.	130
Figure 5.8 C10orf76 is a peripheral membrane protein.	133
Figure 5.9 C10orf76 cycles on and off membranes rapidly.	134
Figure 5.10 C10orf76 overexpression prevents Golgi fragmentation in knockdown cells.	135
Figure 5.11 N- and C- terminal c10orf76 truncations fail to localise to ERGIC53-positive Golgi structures.	137

Figure 5.12 C10orf76 is likely an ancestral protein.	140
Figure 6.1 ZnT6 interacts with GBF1	152
Figure 6.2 ZnT6 knockdown does not significantly alter GBF1 distribution or recruitment.	155
Figure 6.3 ZnT6 depletion alters GBF1 cycling on and off Golgi membranes.	156
Figure 6.4 Golgi isolation reveals more membrane-bound GBF1 in ZnT6-depleted cells.	157
Figure 6.5 ZnT6 overexpression reduces quantity and recruitment of juxtannuclear GBF1.	160
Figure 6.6 Fraction of juxtannuclear GBF1 appears to be sensitive to the amount of transfected ZnT6.	161
Figure 6.7 ZnT6 overexpression alters GBF1 cycling on and off Golgi membranes.	162
Figure 6.8 ZnT6 knockdown does not impair COP recruitment.	164
Figure 6.9 ZnT6 knockdown does not significantly alter secretory activity.	165
Figure 7.1 Models for ZnT6 regulation of GBF1 cycling.	178
Figure 7.2 Potential model for C10orf76 mediated recruitment of GBF1.	182

List of Symbols and Abbreviations

ADP	adenosine diphosphate
Arf	ADP-ribosylation factor
Arl	ADP-ribosylation factor-like
ATP	adenosine triphosphate
BIG	brefeldin A-inhibited guanine nucleotide exchange factor
BFA	brefeldin A
C10orf76	chromosome 10 open reading frame 76
COP	coatamer protein
DCB	dimerization and cyclophilin binding
ddH ₂ O	double distilled water
DMSO	dimethyl sulfoxide
EGFP	enhanced green fluorescent protein
EM	electron microscopy
ER	endoplasmic reticulum
ERES	ER exit sites
ERGIC	ER-Golgi intermediate compartment
FBS	fetal bovine serum
g	gram
GAP	GTPase activating protein
GBF1	Golgi-specific BFA resistance factor 1
GDP	guanosine diphosphate
GEECs	GPI-Aps enriched early endosomal compartments
GEF	guanine nucleotide exchange factor
GGA	Golgi-localising, Gamma-adaptin ear domain homology, Arf binding protein
GTP	guanosine triphosphate
HDS	homology downstream of sec7d
HUS	homology upstream of sec7d
IF	immunofluorescence
IP	immunoprecipitation
kDa	kilodalton
ManII	mannosidase II
mCherry	monomeric Cherry (red fluorescent protein)
min	minute
PBS	phosphate buffer saline
PCR	polymerase chain reaction
PH	plekstrin homology
PI4K	phosphatidylinositol 4-kinase
PI4P	phosphatidylinositol 4-phosphate
SLC30A5	solute carrier family 30 member 5
SLC30A6	solute carrier family 30 member 6
SNARE	soluble N-ethylmaleimide sensitive factor attachment receptor
VSV	vesicular stomatitis virus

YFP
ZnT

yellow fluorescent protein
zinc transporter

Chapter 1: Introduction

1.1 The endomembrane system and the early secretory pathway

In eukaryotic cells, the endomembrane system is the collection of membrane-bound organelles that work in concert to sort, modify, package, and transport lipids and proteins (Bonifacino and Glick, 2004). The majority of proteins and lipids destined for secretion or roles in the endomembrane system are initially synthesized at the endoplasmic reticulum (ER). From there, correctly synthesized, folded, sorted, and modified proteins then enter the bidirectional secretory pathway, moving through each compartment in a sequential manner. Beginning from the ER, synthesized components are trafficked out of ER exit sites into the ER-Golgi intermediate compartment (ERGIC), then the individual cisternae of the Golgi complex (*cis*, *medial*, and *trans*), through the *trans*-Golgi network (TGN), and onwards to various endosomal compartments, and the plasma membrane (see figure 1.1 for a depiction of the endomembrane system). Analysis of the human genome suggests that approximately one-third of encoded proteins enter the secretory pathway (Braakman and Bulleid, 2011; Chen et al., 2005a). Proteomic studies also suggest that seven percent of human proteins are involved in the biogenesis and maintenance of the pathway, indicating the importance of the pathway's organelles in cell survival and function (Gilchrist et al., 2006).

The research described in this thesis focuses specifically on protein regulators involved in maintenance of the ERGIC and Golgi compartments and the membrane traffic that occurs at these sites. For this reason, we will not discuss in detail ER, TGN, endosomal, and plasma membrane traffic.

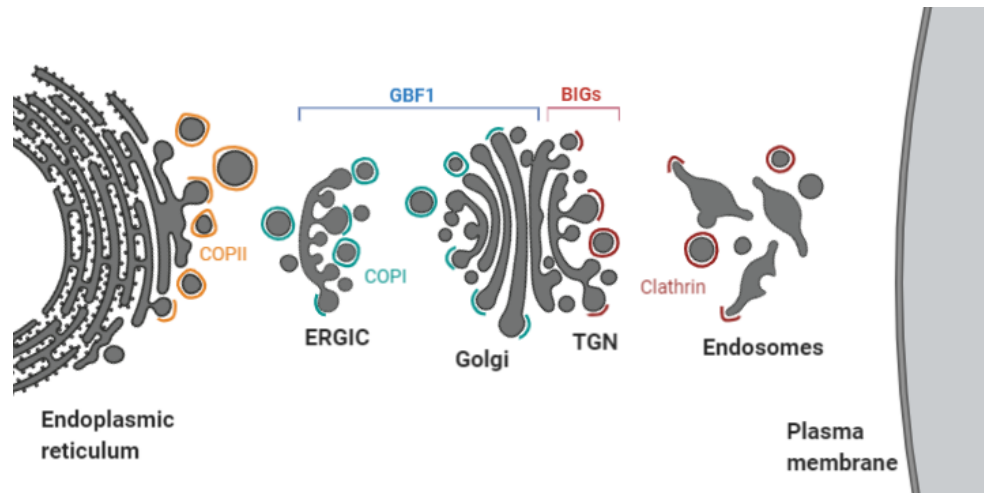


Figure 1.1 Schematic depiction of the human secretory pathway.

The secretory pathway is comprised of multiple membrane-bound compartments that exchange cargo through membrane carriers in a bi-directional manner. As described in the text, newly synthesized cargo at the ER can be trafficked anterograde through the ERGIC, Golgi, TGN, and endosomal compartments to the plasma membrane. These trafficking steps are mediated by various coat protein complexes: COPII (orange) functions at ER exit sites, COPI (blue) functions at ERGIC and Golgi, clathrin (red) functions at the TGN, endosomes and plasma membrane. COPI-mediated traffic involves the large ArfGEF, GBF1. Clathrin mediated traffic at the TGN is requires the large ArfGEFs, BIG1 and BIG2. Figure is adapted from (Szul and Sztul, 2011) and created using BioRender.

1.1.1 The ERGIC

In mammalian cells, newly synthesized cargo at the ER can be sorted into ER exit sites (ERES) where they are then packaged into COPII vesicles and trafficked to the ERGIC – also referred to as vesicular tubular clusters (VTCs) or pre-Golgi compartments. ERGIC structures are membranous organelles that function as an additional bidirectional sorting station (Appenzeller-Herzog and Hauri, 2006). Erroneously sorted ER proteins (including those with ER retention or retrieval sequences) are returned to the ER through COPI-mediated retrograde traffic. Proteins destined for secretion or other organelles in the endomembrane system will continue through anterograde traffic to the Golgi (Appenzeller-Herzog and Hauri, 2006).

ERGIC structures are most commonly marked using the cargo receptor, ERGIC-53, from which the structures were originally identified (Schweizer et al., 1988). The organelle was initially thought to be subdomains of the *cis*-Golgi or ER, but electron microscopy and three-dimensional reconstruction has demonstrated that the compartments are distinct and non-continuous with either ER or Golgi membranes (Fan et al., 2003).

Two competing models have been proposed for the biogenesis and maintenance of ERGIC structures. The first is the transport complex model which postulates that ERGIC clusters are transient structures that arise through fusion of ER-derived COPII vesicles; these clusters are then thought to fuse to give rise to the *cis*-Golgi (Stephens and Pepperkok, 2001). Using correlative video/light electron microscopy and tomography, researchers have observed the formation of ERGIC-like saccular carriers from ER membranes in a COPII dependent process (Mironov et al., 2003). The formation of ERGIC-like clusters has also been observed with COPII vesicles *in vitro* (Xu and Hay, 2004). This model however has been criticized for its reliance on studies observing the traffic of overexpressed vesicular stomatitis virus glycoprotein, VSV-G,

which may not reflect normal cell physiology (Appenzeller-Herzog and Hauri, 2006).

Furthermore, live-cell imaging experiments using fluorescently labelled ERGIC-53 and labeled cargo has demonstrated that the structures remain stationary while cargo can freely transit through, suggesting that ERGIC structures are likely stable compartments (Ben-Tekaya et al., 2005). Based on these observations, a stable compartment model was proposed.

In this second model, ERGIC receives ER-derived COPII vesicles, following which, cargo will dissociate from their receptors. Receptors are likely recycled to the ER while cargo may continue through anterograde traffic from the ERGIC to the *cis*-Golgi. ERGIC to Golgi traffic requires components including Rab1, p115, GM130, giantin, SNAREs and the COPI and COPII coats (Appenzeller-Herzog and Hauri, 2006).

Apart from its role in bidirectional traffic, the ERGIC has also been suggested to facilitate, at least to some degree, protein quality control and sorting. Proteomics analysis of isolated ERGIC structures and electron microscopy has shown an enrichment of chaperones at ERGIC sites (Breuza et al., 2004; Zuber et al., 2001). Furthermore, unfolded VSV-G has been observed at ERGIC and *cis*-Golgi sites in several studies, prior to being retrieved for ER-associated degradation (Hammond and Helenius, 1994; Spiro and Spiro, 2001). However, the molecular mechanism guiding retrieval is unclear.

1.1.2 The Golgi Compartment and intra-Golgi traffic

Following sorting at the ERGIC, cargo proteins may continue through anterograde traffic to the Golgi. The Golgi is a critical organelle within the secretory pathway and functions in both sorting and post-translational protein and lipid modification (Boncompain and Perez, 2013). In mammalian cells, the Golgi is usually considered as a series of stacked polarized cisternae, with the *cis* face receiving cargo from the ERGIC, while the *trans* face (along with the TGN) is

involved in cargo sorting for post Golgi export (to sites including the endosomes and plasma membrane). These cisternae are linked in a lateral ribbon-like structure and held in close proximity to the microtubule organizing center (Wei and Seemann, 2010). Within the Golgi ribbon, Golgi stacks (formed by approximately five to eight cisternae each) can be classified into *cis*, *medial*, and *trans* based on their proximity to the ER, their biochemical composition, and the protein and lipid modifications they perform (Pfeffer, 2003). This level of sub-compartmentalization allows for sequential modifications to take place as cargo enters from the *cis*-Golgi and departs through the *trans* face towards the TGN. Individual compartments are also best resolved by electron microscopy or high-resolution optical microscopy using Golgi markers such as p115, mannosidase II, and TGN46 (for the *cis*, *medial*, and *trans* cisternae, respectively) (Nelson et al., 1998; Velasco et al., 1993; Zhao et al., 2002).

Recent work has demonstrated that individual cisternae appear spatially organized such that Golgi enzymes localise preferentially to the cisternae interior, while the trafficking machinery reside largely at the periphery (Tie et al., 2018). Apart from its role in secretory traffic, it is also of note that the Golgi has emerged in recent years as a platform for a range of cellular processes: regulation of mitosis (Rabouille and Kondylis, 2007), sensor for cell stress (Sasaki and Yoshida, 2015), directed migration (Millarte and Farhan, 2012), cellular signaling (Mayinger, 2011), and even autophagy (Yamamoto et al., 2012).

Protein traffic through the Golgi compartments has been shown to involve numerous proteins, with COPI playing a central role in organelle maintenance and intra-Golgi traffic (Popoff et al., 2011). ADP-ribosylation factors (Arfs) are activated by guanine nucleotide exchange factors to recruit components needed for cargo sorting and vesicle formation. These vesicles are then moved along microtubules towards their target membranes at which point

docking and fusion occurs; this involves tethering factors (such as p115, GM130, giantin, golgin-84), regulatory proteins (such as Rab1), and SNAREs (Szul and Sztul, 2011). While the importance of COPI-mediated intra-Golgi traffic is well agreed upon, the exact mechanism by which cargo transits through the Golgi remains heavily discussed and debated. Multiple models have been proposed to explain how COPI vesicles support Golgi traffic, the most recognized include some element of cisternal maturation. In the cisternal maturation model, membrane components and anterograde cargo from the ERGIC fuse to form the *cis*-cisternae. The cargo then moves through the Golgi in bulk as the cisternae “matures” (i.e. transformed from *cis*, to *medial*, to *trans*), by losing early acting Golgi enzymes and acquiring late acting ones. As such, the majority of cargo remains within the cisternae while COPI-mediated vesicle traffic recycles and transports Golgi enzymes to remodel the compartments (Glick and Nakano, 2009). The cisternal maturation model is useful for explaining the traffic of large cargo that cannot fit in conventional COPI vesicles including scales in algae, and collagen in mammalian cells (Becker and Melkonian, 1996; Bonfanti et al., 1998). Cisternal maturation has since been visualized in yeast, with cells containing defective COPI proteins exhibiting slowed maturation – indicating a role for COPI in cisternae remodeling (Losev et al., 2006; Matsuura-Tokita et al., 2006).

Mathematical models of Golgi traffic have suggested that cisternal maturation is a natural consequence of vesicle trafficking homeostasis. These models evaluate the exchange of cargo between theoretical vesicular compartments based on assumptions such as low rate of random homotypic vesicle fusion, no heterotypic vesicle-vesicle or compartment-compartment fusions, and multiple classes of molecules that influence vesicle budding and fusion rates (Mani and Thattai, 2016). In their modeling approaches, the authors found that without fine tuning, the

majority of stochastic and unstable compartment composition will naturally, over time, settle into a homeostatic state with maturation events.

Despite cisternal maturation being the favoured model, several additional observations have emerged challenging this view. For instance, cisternal maturation fails to account for the observation of anterograde cargo in COPI vesicles or the different rates of transit for different cargos (Beznoussenko et al., 2014; Glick and Luini, 2011). Since then, multiple other trafficking mechanisms have been proposed. In one, anterograde transport is mediated by both vesicle and cisternal maturation. COPI is thought to mediate the production of two populations of cargo carriers: one for the recycling of Golgi enzymes needed for cisternal maturation, and another for the anterograde transport of cargo. Electron tomography has also revealed the presence of tubular intra-cisternal connections in the Golgi which allow for the movement of cargo from cisternae to cisternae without leaving the luminal space (Marsh et al., 2004; Trucco et al., 2004). Formation and maintenance of these tubules may or may not require the function of COPI. It has also been suggested that the Golgi may go through continuous fusion and fission events such that the original compartment will remain while smaller membrane-bound fragments may be free to fuse with another cisternae, carrying cargo with it (Pfeffer, 2010). Currently, no single mechanism has been able to completely explain intra-Golgi traffic, and the mechanisms involved remain a major unresolved question in the field. In reality, Golgi traffic probably relies on multiple mechanisms of cargo transport.

1.1.3 Golgi membrane lipid composition

Similar to its location in the secretory pathway, the Golgi has a membrane lipid composition intermediate between that of the ER and the plasma membrane (Jackson et al., 2016). How the exact membrane lipid composition of the Golgi is generated and maintained remains poorly

understood but likely involves both vesicular traffic and non-vesicular lipid transport (Lev, 2010). Eukaryotic membranes can be generally split into two camps corresponding to two dynamic membrane recycling systems – one centered around the ER, including ERGIC and the *cis*-Golgi and the other centered around the plasma membrane, including the TGN and endosomes. Golgi membranes, similar to that of the ER, contain largely neutral lipids including phosphatidylcholine and phosphatidylethanolamine (Jackson et al., 2016). Anionic lipids such as phosphatidylserine, phosphatidic acid, phosphatidylinositols, and the phosphatidylinositol phosphorylated derivatives: phosphoinositides, are present at the *cis*-Golgi, but are much more enriched at the TGN. The phosphatidylinositides, despite being less abundant at the *cis*-Golgi play essential roles in membrane trafficking (Balla, 2013; Burke, 2018). Specifically, the Golgi is a major site of phosphatidylinositol 4-phosphate (PI4P) production through the kinase, phosphatidylinositol 4-phosphate kinase beta, PI4KB.

PI4KB is part of the type III phosphatidylinositol 4 kinase family, which contains PI4KA and PI4KB. These phosphoinositide kinases generates phosphoinositides by phosphorylating different hydroxyl groups in the inositol headgroup (Burke, 2018). PI4KA localises to the plasma membrane and is involved in the production of PI4,5P₂ and PI3,4,5P₃ signaling lipids. PI4KB localises to the Golgi to produce PI4P required for lipid transport and membrane trafficking. Cells expressing a kinase inactive form of PI4KB exhibit impaired Golgi traffic and altered Golgi morphology (Godi et al., 2004; Godi et al., 1999). Aside from its enzymatic activity, PI4KB is also thought to facilitate protein-protein interactions including the recruitment of Rab11 (involved in TGN to plasma membrane traffic) to the TGN (De Graaf et al., 2004). Recruitment of PI4KB to Golgi membranes requires activation of the small ADP-ribosylation factor, Arf1 – which is also involved in vesicle formation and the recruitment of the COPI coat

(Godi et al., 1999). Constitutively active Arf1 leads to increased PI4KB and PI4P production at the Golgi. However, the interaction between Arf1 and PI4KB is likely indirect as no association between Arf1 and PI4KB has yet been observed (Haynes et al., 2004).

1.1.4 The COPI trafficking machinery

As mentioned, the COPI coat is required for multiple stages of ER to Golgi traffic, including the retrieval of cargo from the *cis*-Golgi to the ERGIC and ER, as well as intra-Golgi traffic (Szul and Sztul, 2011). Coat proteins are essential to the formation of vesicles through their membrane deformation capacity and function to drive cargo sorting through cargo and cargo receptor interactions. The approximately 700 kDa COPI coat is composed of seven coatomer subunits (α , β , β' , γ , δ , ϵ , ζ) which are further subdivided into two subcomplexes: the α , β' , ϵ trimeric subcomplex and the β , γ , δ , ζ tetrameric subcomplex (Eugster et al., 2000; Waters et al., 1991). Structural analysis has shown that the COPI coat resembles the double-layer like structure of the COPII coat (Lee and Goldberg, 2010). The α , β' , ϵ trimeric subcomplex likely composes the outer layer of the coat while the β , γ , δ , ζ tetrameric subcomplex forms the inner layer. The COPI coat also displays isoform specific subcellular localisation. Both the γ and ζ subunits have two distinct isoforms (γ_1 , γ_2 , ζ_1 , and ζ_2). Analysis performed in the mouse 3T3 cell line suggests that approximately 50% of COPI coat is $\gamma_1\zeta_1$ (primarily *cis*-Golgi), approximately 30% with $\gamma_2\zeta_1$ (primarily TGN), approximately 20% $\gamma_1\zeta_2$, and less than 5% with $\gamma_2\zeta_2$ (Beck et al., 2009; Moelleken et al., 2007).

Recruitment of the COPI coat requires the activation of Arf small GTPases. The transmembrane Golgi proteins, p23 and p24 (also known as TMED9 and 10) have also been previously suggested to facilitate this process (Zhao et al., 1999). Activated, membrane-bound Arf helps recruit the COPI coat *en bloc* – a process starkly different from that of the COPII and

clathrin coats which are recruited as two successive layers (Hara-Kuge et al., 1994). Site-directed photolabeling studies suggests that there are multiple protein-protein interaction sites between Arfs and the COPI coat including with the β , β' , γ , and δ subunits (Zhao et al., 1997; Zhao et al., 1999). Upon recruitment, the COPI coat can directly facilitate cargo sorting through interaction with sorting signals present on cargo proteins (Arakel and Schwappach, 2018). The di-lysine (KKxx and KxKxx) motifs have been well characterized and shown to interact with the α and β' subunits. COPI can also interact with cargo receptors including the KDEL receptor to mediate sorting into the COPI vesicle. Continued polymerization of COPI generates membrane curvature. Eventual scission of the COPI vesicle appears to require formation of Arf1 oligomers, although the exact mechanism by which scission *in vivo* is driven by Arf1 is unclear but likely involves additional auxiliary proteins (Beck et al., 2008).

Following scission, the COPI-derived vesicles are then thought to undergo uncoating. Release of COPI requires Arf inactivation or GTP hydrolysis (Presley et al., 2002). Current understanding suggests that uncoating is likely incomplete, and that residual COPI may facilitate vesicle recognition and tethering. Studies have shown that vesicle tethering components including p115, the trafficking protein particle II (TRAPPII), and even the conserved oligomeric Golgi (COG) protein complex interacts with COPI, and may be recruited by residual COPI after uncoating (Guo et al., 2008; Miller et al., 2013; Yamasaki et al., 2009).

1.2 Small GTPases at the Golgi

Two major families of small GTPases function to regulate vesicular transport and membrane trafficking at the early Golgi compartments: ADP-ribosylation factors (Arfs) and Ras related in brain (Rabs) (Pylypenko et al., 2017; Sztul et al., 2019). Both families belong to the Ras superfamily of regulatory GTPases. These proteins cycle between a GTP-bound and a GDP-

bound form. The GTP-bound conformation is generally considered ‘active’, as this form allows stable interaction with membranes and recruitment of downstream effectors. GTP binding and subsequent hydrolysis requires the activity of the specific guanine nucleotide exchange factors (GEFs) and GTPase activating proteins (GAPs).

1.2.1 Rabs

For Rabs, the GDP-bound form can interact with Rab escort proteins (REPs) and GDP dissociation inhibitors (GDIs). Newly synthesized Rabs are recognized by REPs which present the protein for C-terminal geranylgeranylation. Rabs can then be activated at membrane sites by corresponding GEFs and dissociate from the Rab-REP complex. Upon inactivation by GAPs, inactive Rabs become a substrate for GDIs, which can extract Rab-GDP from the membrane. These GDI-bound Rab are now ready to be reinserted into a membrane site for another round of activation.

The best known Rab at the ER and *cis*-Golgi compartments is Rab1 (Ypt1 in the yeast, *Saccharomyces cerevisiae*), which is comprised of two key isoforms (Goud et al., 2018; Segev et al., 1988). Both Rab1a and Rab1b have been thought to play largely redundant functions in mammalian cells due to their high sequence similarity. However, recent work has suggested that they likely do harbor independent non-redundant functions; Golgi fragmentation caused by Rab1a knockdown cannot be completely rescued by overexpression of Rab1b, and vice versa (Aizawa and Fukuda, 2015). Rab1 interacts with several components of the COPII coat and is thought to facilitate protein sorting and formation of COPII vesicles at ER exit sites (Slavin et al., 2011). Rab1 has also been implicated in facilitating the docking and fusion of COPII vesicles at target membranes by recruiting tethering factor p115 (Allan et al., 2000; Moyer et al., 2001). Furthermore, Rab1 is also thought to be involved in COPI traffic. Yeast Ypt1 has been shown to

genetically interact with the Golgi-localised GEFs, Gea1/2, which regulates COPI coat recruitment (Jones et al., 1999). Overexpression of GDP-arrested Rab1 has also been shown to impair COPI recruitment to the Golgi (Alvarez et al., 2003).

1.2.2 ADP-ribosylation factors (Arfs)

The other major small GTPase family involved in ER to Golgi traffic is the Arf family, which includes the Arfs, the Arf-like proteins (Arfs), and SARs (Melançon et al., 1987; Sztul et al., 2019). Within the Arf subfamily, there are six mammalian Arfs, all of which are highly conserved and share over 65% sequence identity. All six Arfs are also N-terminally myristoylated. These Arf proteins can be subdivided into three classes based on their sequence homology: Class I (Arf1-3), Class II (Arf 4-5), and Class III (Arf6); humans lack Arf2. Class I Arfs are the most evolutionarily conserved and share approximately 96% sequence identity and they are found in all eukaryotes examined to date (Donaldson and Jackson, 2011). Class II Arfs are believed to have arisen through divergent evolution from Class I Arfs and retain approximately 90% sequence identity (Schlacht et al., 2013). Class III Arfs share the least similarity, with approximately 60% sequence identity compared to the other Arf classes.

Class I and class II Arfs primarily localise throughout the secretory pathway including the ERGIC, Golgi, TGN, and endosomal compartments (Donaldson and Jackson, 2011). However, they have also been observed at other membrane locations including lipid droplets and the mitochondria (Ackema et al., 2014; Wilfling et al., 2014). Arf6 (the only human Class III Arf) localises to the endosomes and plasma membrane where it facilitates endocytosis. Surprisingly, none of the Golgi-localised Arfs are essential for Golgi maintenance and function. Depletion of any one of Arf1, 3, 4, or 5 yields no obvious phenotypes (Volpicelli-Daley et al., 2005). Double knockdown of distinct pairs can lead to varying phenotypes indicating that Arfs

may function in pairs for specific trafficking functions. Currently, the overlapping functions and distribution of Arf proteins are not well understood and require further study.

The primary way in which Arf proteins affect cellular processes is through their ability to recruit effector proteins – primarily in their GTP-bound forms (Sztul et al., 2019). Currently, over 20 Arf effectors have been identified. These include coat proteins (ex. COPI), adaptor proteins (ex. GGAs at the TGN), tethering proteins, (ex. golgi-160 at the TGN), lipid modifying enzymes, and lipid transporters.

All Arfs, like other small GTPases, contain the canonical G domain with two nucleotide sensitive regions: switch 1 and switch 2 (Nawrotek et al., 2016). But unlike others, Arfs also contain an interswitch region. In the GDP-bound form, the variable N-terminal helix and myristoyl group interacts with the core of the Arf GTPase which shields the myristate and the N-terminal membrane binding regions. This alters the conformation of the interswitch region which blocks GTP binding – creating an autoinhibitory effect. This autoinhibitory effect is relieved upon displacement of the N-terminal groups in the presence of membranes. Upon GTP binding, the interswitch region again switches confirmation, now obstructing the retraction of the N-terminal helix and myristate, ensuring that the protein stably interacts with the membrane. Because of the autohibitory effect, Arf GEFs cannot activate their corresponding Arfs without the presence of membrane. Unlike other GTPases such as Rabs, Arfs are not known to interact with escort proteins or GDIs.

1.3 Arf guanine nucleotide exchange factors (ArfGEFs)

Activation of Arfs through the nucleotide exchange reaction is facilitated by Arf guanine nucleotide exchange factors (ArfGEFs). The human genome encodes fifteen ArfGEFs which can be subdivided into six related families: GBF, BIG, cytohesins, EFA6/Psd, BRAG/IQSec, and

FBX (Figure 1.2) (Sztul et al., 2019). The GBF and BIG ArfGEFs are commonly referred to as the large ArfGEFs due to their size (>160 kDa) (Mouratou et al., 2005). The BRAG/IQSec range in size from 100-150 kDa, while the small ArfGEFs including the cytohesins, EFA6/Psd, and FBX fall below 80 kDa (Cox et al., 2004). All known ArfGEFs share a conserved approximately 200 residue *sec7* domain (*sec7d*) which encodes the catalytic activity required to facilitate nucleotide exchange (Casanova, 2007). The domain is named after the yeast *sec7* protein – the yeast BIG family member. Additional domains in each ArfGEF allows for the diverse localisation and regulation of the proteins. Because Arfs cannot be activated without the presence of membrane, cytosolic ArfGEFs are thought to be inactive, and are activated upon their recruitment to membrane sites. The recruitment strategies of each ArfGEF varies. For instance, the cytohesins, BRAG/IQSecs, and EFA6/PSDs interact with membranes via their plekstrin homology (PH) domains downstream of *sec7d*. The PH domains of cytohesin bind PIP2 and PIP3, while the ones in the BRAG/IQSecs, and EFA6/PSDs bind anionic lipids more promiscuously (DiNitto et al., 2003). The GBF and BIGs lack PH domains and their recruitment to membranes has been less thoroughly studied but is believed to involve a combination of lipid binding domains and protein-protein interactions (Bouvet et al., 2013; Monetta et al., 2007; Quilty, 2016). Lastly, FBX8, the sole representative of the FBX subfamily shares no common domains with the other ArfGEFs apart from *sec7d* (Yano et al., 2008). Its regulation and recruitment strategies remain unexplored.

As previously mentioned, Arf activation through *sec7d* requires the presence of membranes to lift the autoinhibitory effect of the N-terminal helix and myristate (Nawrotek et al., 2016). Upon being primed by the membrane, ArfGEFs can toggle the interswitch region of the Arf and briefly secure the Arf-GDP on the membrane prior to the release of the nucleotide

(see figure 1.3) (Renault et al., 2003). Following this, sec7d inserts a glutamate into the Arf active site which competes with and displaces the nucleotide, allowing the formation of a nucleotide free complex. Now vacant, the Arf active site is free to bind the abundant GTP, which stabilizes its membrane-bound conformation.

Arf activation at the Golgi is largely regulated by the large ArfGEFs: GBF1, BIG1, and BIG2. These large ArfGEFs have been shown to have orthologs in all eukaryotic organisms sequenced to date (Pipaliya et al., 2019). Specifically, GBF1 acts at the ERGIC and *cis*-Golgi interface, while BIG1 and BIG2 at the TGN and endosomes (Sztul et al., 2019). It is important to note that GBF1 has also been shown to regulate other cellular activities at other membrane sites, which will be discussed in more detail in subsequent sections (Ackema et al., 2014; Gupta et al., 2009; Wilfling et al., 2014). In the early secretory pathway, GBF1 is thought to activate Arf1 and Arf4 to drive COPI-mediated vesicular traffic; only the depletion of Arf1 and Arf4 together appears to inhibit COPI traffic (Manolea et al., 2008; Volpicelli-Daley et al., 2005). GBF1 has also been suggested to activate Arf5 to support maintenance of the TGN. Although whether this activation takes place at the TGN or at early Golgi compartments remain debated. In the late secretory pathway, BIG1 and BIG2 are thought to activate Arf1 and Arf3 to facilitate recruitment of the clathrin adaptors AP1 and AP2 (Shinotsuka et al., 2002). The additional non-trafficking function of the BIGs are not as well investigated, but their localisation to alternative sites including the nucleus suggest they do have additional cellular roles (Padilla et al., 2008). Lastly, Arf5 – like Arf6 – is also thought to be activated by BRAGs for post-TGN clathrin mediated traffic (Moravec et al., 2012).



Figure 1.2 Domain organization of the Sec7 family of ArfGEFs in human cells.

As described in the text, humans express 15 total ArfGEFs which can be categorized into six subfamilies: GBF, BIGs, BRAG/IQsec, cytohesin, EFA6/Psd, and FBX. Representatives for each subfamily is shown with their corresponding names (including alternate names), domain organization, and protein length in amino acids. Each protein is aligned based on the location of their sec7 domains. Domains are colour coded. DCB: dimerization and cyclophilin binding domain, HUS: homology upstream of sec7d, HDS1-4: homology downstream of sec7d, PH: plekstrin homology domain, CC: coiled-coil domain, IQ: IQ motif, and FBox: FBox motif. Figure is adapted from (Casanova, 2007).

1.4 Golgi-specific brefeldin-A resistance factor 1 (GBF1)

GBF1 is the only large ArfGEF that functions at the *cis*-Golgi and ERGIC and is essential for the maintenance of COPI traffic. In humans, GBF1 is the sole GBF species, but *Saccharomyces cerevisiae* has been shown to have two distinct genes: Gea1p and Gea2p. Interestingly, the proteins appear to be redundant, at least under normal growth conditions, as expression of either copy is alone sufficient to maintain cell growth and secretory traffic (Peyroche et al., 1996). However, the proteins share only approximately 50% sequence identity, suggesting that they are likely functionally distinct, and probably serve non-redundant functions that have yet to be identified. GBF exists as single copies in both *Arabidopsis thaliana* and *Drosophila melanogaster*; in these model systems they are referred to as GNOM and Garz respectively (Mouratou et al., 2005).

In human cells, GBF1 is thought to activate Arf1 and Arf4 to facilitate the formation COPI vesicles at both *cis*-Golgi and ERGIC membranes (Sztul et al., 2019). This is because only the simultaneous depletion of these two Arfs but no other pair inhibits COPI traffic (Volpicelli-Daley et al., 2005). GBF1 functions on both ERGIC and *cis*-Golgi membranes. COPI vesicle traffic from the *cis*-Golgi is required for the retrieval of cargo to ERGIC structures in a retrograde manner, and to sustain continued anterograde traffic through the Golgi stack. At the ERGIC, COPI vesicles are thought to facilitate both retrograde and anterograde traffic. Both retrieval of cargo to the ER and anterograde traffic to the *cis*-Golgi can be blocked by COPI mutants (Beck et al., 2009). However, whether COPI vesicles directly move cargo from ERGIC to *cis*-Golgi, or if the retrieval of trafficking components from the *cis*-Golgi to ERGIC mediated by COPI is in turn required to sustain anterograde traffic remains incompletely resolved.

GBF1 has been shown to cycle rapidly on and off membranes similar to COPI and Arf, with $t_{1/2}$ of approximately 20 seconds (Szul et al., 2005; Ting-Kuang et al., 2005; Zhao et al., 2006). The cycling of GBF1 also appears to be tied to its nucleotide exchange activity. GBF1 mutants unable to catalyze nucleotide exchange remain on membranes significantly longer ($t_{1/2}$ approximately 53 seconds). Mechanistic details on how GBF1 cycling and nucleotide exchange activity on the membrane is regulated remains incomplete.

GBF1 was initially identified in mammals as a BFA resistance factor (hence the name) after the isolation of mutant Chinese hamster ovary (CHO) cells that grew in the presence of the fungal metabolite, brefeldin A (BFA), which blocks protein secretion and causes Golgi disassembly (Yan et al., 1994). Additional studies have since revealed that GBF1 is in fact BFA sensitive, and provides BFA resistance only when overexpressed (Claude et al., 1999). BFA acts as an uncompetitive inhibitor of the catalytic *sec7d* (Mansour et al., 1999; Peyroche et al., 1999). *In vitro* studies have shown that BFA fits into a hydrophobic cavity that exists in the transitory Arf-GDP-*sec7d* complex, creating an abortive reaction intermediate (Figure 1.3). This Arf-GDP-*sec7d* complex exists in the early stages of the nucleotide exchange reaction prior to the release of GDP, and BFA insertion blocks the conformational change needed to move the catalytic glutamate residue into position to electrostatically expel the bound nucleotide (Mossessova et al., 2003; Renault et al., 2003). As a result, BFA inhibition is thought to stabilize GBF1 and Arf on the membrane, preventing further cycling of either proteins (Ting-Kuang et al., 2005; Zhao et al., 2006). This stabilization likely contributes to the observed increase in GBF1 at Golgi structures following BFA treatment. It is important to note, however, that the BFA induced GBF1-Arf-GDP abortive complex has been observed *in vitro*, but not yet confirmed *in vivo*. In fluorescence recovery after photobleaching (FRAP) studies, BFA treatment

blocks GBF1 cycling on and off membranes, confirming the ability of BFA to “trap” membrane-bound GBF1. However, imaging experiments revealed that while GBF1 is actively recruited to membranes upon BFA treatment, the majority of Arfs appear to be rapidly released from membranes, which contradicts the conclusion that BFA traps Arfs in a membrane-bound GBF1-Arf complex (Chun et al., 2008). Overexpression of GBF1 has been shown to increase the amount of residual membrane-bound Arf present at the Golgi, which researchers have argued may be due to the formation of the abortive complex (Ting-Kuang et al., 2005). Likewise, using bimolecular fluorescence complementation assays with GBF1 and Arfs tagged to split YFP, researchers have observed juxtannuclear YFP signal in BFA treated cells, suggesting that some Arfs remain in close proximity to the membrane “trapped” GBF1. However, it’s unclear if the reformed YFP can dissociate rapidly under these conditions. Reconstitution of most split fluorophore complexes of the GFP-family, including YFP, have been shown to be irreversible (Kökoer et al., 2018; Wong and O’Bryan, 2011). As such, the YFP fluorescence observed at juxtannuclear sites after BFA treatment may not represent what would naturally occur *in vivo*. Likewise, the potential influence of residual GBF1 activity due to overexpression also complicates interpretation. As such, the stability of the GBF1-Arf abortive complex, should it exist *in vivo*, remains debated.

Outside the use of exogenous drugs, recent work has shown that under WT conditions, the recruitment of GBF1 to membrane sites appear to be sensitive to changes in regulatory Arf-GDP levels (Quilty, 2016) (Figure 1.4). Conditions such as overexpression of ArfGAPs or constitutively inactive Arfs can increase GBF1 levels at the Golgi. Most *cis*-Golgi-localised Arfs appear to be able to regulate GBF1 recruitment, including Arf1, 3, and 5 (Quilty et al., 2014). However, non-myristoylated Arfs are not, suggesting that regulatory Arf-GDP is likely acting at

the membrane – potentially through modulating membrane-bound GBF1 interactors. This regulatory feed-forward mechanism likely helps modulate and maintain steady-state Arf activation in cells.

Also of note is that GBF1 is also a binding partner of the positive-strand RNA enterovirus protein 3A (Wessels et al., 2007). The exact role of GBF1 in facilitating the replication of positive-strand RNA viruses is unclear, however, the use of GBF1 inhibitory drugs such as BFA have been shown to reduce viral replication (Lanke et al., 2009).

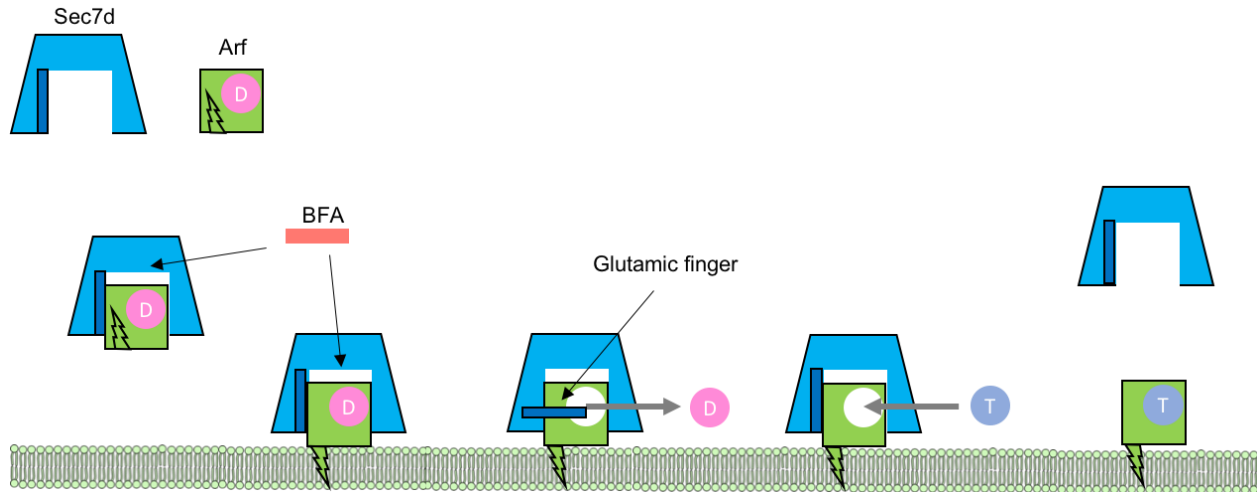


Figure 1.3 Mechanism of Arf activation by the sec7d and its inhibition by BFA.

From left to right, sec7d first interacts with Arf-GDP, which in principle can occur in either the cytoplasm or on the membrane. Following this interaction the Arf interswitch toggle occurs exposing the N-terminal extension and myristoyl group. This GTP-like conformational change secures Arf on the membrane prior to GDP expulsion. A second conformational change in sec7 moves the negatively charged glutamate residue into position for electrostatic attack and expulsion of GDP, forming the nucleotide free intermediate. The more abundant GTP replaces GDP, stabilizing the Arf in its membrane-bound conformation. The GEF is now free to dissociate from the activated Arf. Two different steps in this reaction can be inhibited by either BFA treatment or a glutamine to lysine mutation in the sec7d. The initial interaction between the GEF and Arf can be trapped by BFA (red block), which fits into the interface between Arf-GDP and the sec7d. This prevents the conformational changes required for nucleotide exchange, forming the abortive sec7d-BFA-Arf-GDP complex. A second step in the reaction can be trapped by the glutamine to lysine mutation (E794K in GBF1). Mutating the glutamine residue prevents the expulsion of GDP from the bound Arf, trapping both the GEF and Arf-GDP in an inactive membrane-bound conformation.

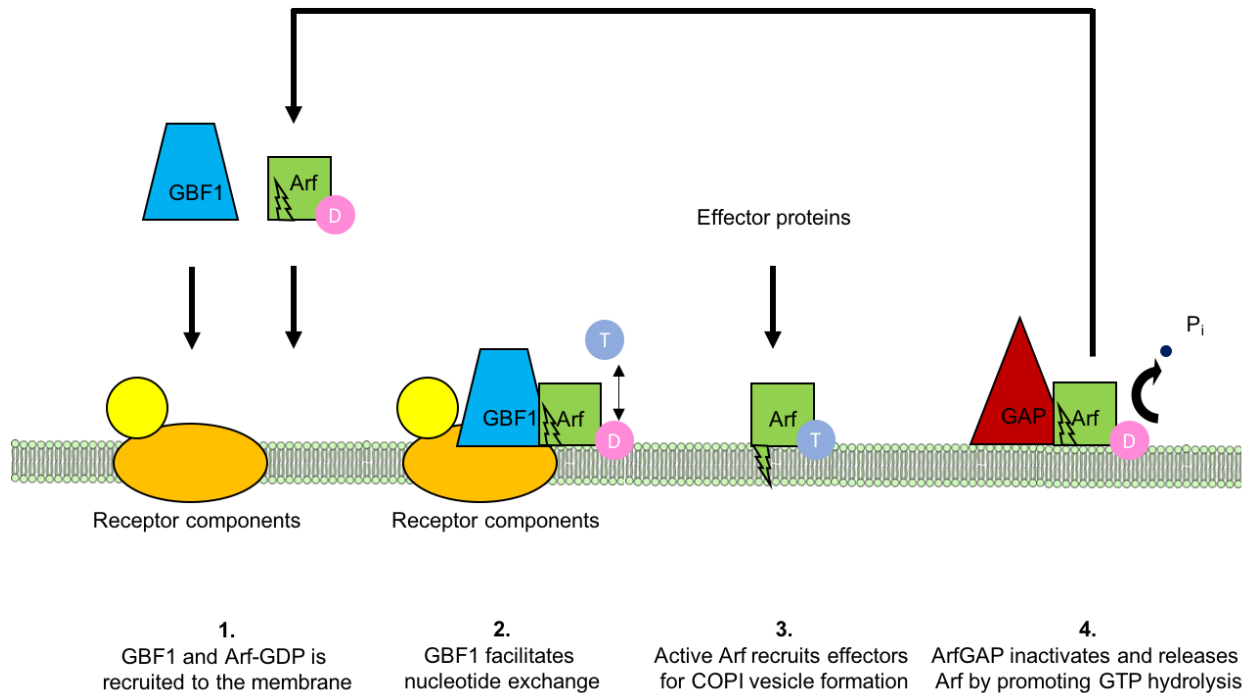


Figure 1.4 Diagram depicting the activation and inactivation of Arf by GBF1 at ArfGAP at *cis*-Golgi membranes.

GBF1 facilitates the activation of Arfs at the *cis*-Golgi and ERGIC membranes. 1) Arf nucleotide exchange occurs at the membrane, and therefore, requires the co-recruitment of both Arf and GBF1. Membrane recruitment of Arfs likely occur through the N-terminal myristate moiety as well as potential interactions with unknown membrane receptors. Likewise, GBF1 recruitment requires interactions with membrane lipids as well as unidentified membrane components. 2) GBF1 facilitate nucleotide exchange by displacing GDP nucleotide and allowing more abundant GTP to bind, thus activating the Arf. 3) GTP-bound Arf stably interacts with the membrane via the N-terminal myristate moiety and can now modulate the activity of effector proteins such as the COPI coat. 4) GTP-bound Arfs can be subsequently inactivated by GTP hydrolysis facilitated by the activity of ArfGAPs. Inactivated Arfs are now free to return to the cytosol where it may participate in another round of activation.

1.4.1 GBF1 domains

In animal cells, GBF1 is composed of six evolutionarily conserved domains: DCB, HUS, sec7d, HDS1, HDS2, and HDS3 (Figure 1.2). As described earlier, the sec7d remains the best characterized due to its essential catalytic function in all known ArfGEFs (Goldberg, 1998; Mouratou et al., 2005).

Upstream of the sec7d is the dimerization and cyclophilin binding (DCB) domain and the homology upstream of sec7d (HUS). The DCB and HUS domains located at the N-terminus of GBF1 have been previously shown in both mammalian (Ramaen et al., 2007) and plant systems (Grebe et al., 2000) to facilitate dimerization through DCB-DCB and DCB-HUS interactions. This was demonstrated through a series of yeast two-hybrid systems and further confirmed through co-immunoprecipitation experiments. Furthermore, previous work has suggested that these domains were involved in facilitating the targeting of GBF1 to ERGIC and Golgi membranes (Bouvet et al., 2013). Studies in *A. thaliana*, also suggested that the DCB domain was involved in cyclophilin 5 binding – a peptidylprolyl *cis/trans*-isomerase (PPIase). However, further studies were unable to confirm the interaction and cyclophilin 5 binding has never been observed in mammalian cells (Anders et al., 2008).

In the C-terminal half of GBF1 are the homology downstream of sec7d (HDS1, HDS2, and HDS3) domains. Protein structure predictions had previously shown HDS1 to contain an amphipathic helix thought to be involved in lipid binding (Bouvet et al., 2013). Tagged HDS1 fragments were shown to bind lipid droplets *in vivo*, artificial phosphatidylcholine droplets *in vitro*, and the lipid droplet protein, adipose triglyceride lipase *in vitro* (Bouvet et al., 2013; Ellong et al., 2011). Mutations in the helix abrogated lipid droplet localisation, further confirming HDS1's role in lipid droplet targeting and lipid binding. Little research has been done

on the further downstream HDS2 and HDS3 domains. Deletion experiments found HDS3 to be dispensable for both Golgi and lipid droplet localisation (Bouvet et al., 2013). Likewise, loss of HDS2 and HDS3 did not interfere with GBF1's role in polio virus replication or secretion (Belov et al., 2010). Currently, the exact domains involved in GBF1 membrane binding and recruitment remains unresolved and will require further study.

1.4.2 GBF1 interacting partners and a putative receptor

The first published interacting partner for GBF1 is the tethering factor p115 (Sztul and García-Mata, 2003). p115 is essential for Golgi maintenance and assembly, and is associated with multiple secretory compartments including COPII and COPI vesicles, ERGIC, and the *cis*-Golgi (Allan et al., 2000; Alvarez et al., 1999). Upon recruitment by activated Rab1, p115 is thought to facilitate vesicle tethering and fusion. However, the precise mechanism by which p115 participates in this process remains unclear, but likely involves additional interacting partners including GM130, giantin, and ER-Golgi SNAREs (Nakamura et al., 1997; Shorter et al., 2002; Sonnichsen et al., 1998). P115 interaction with GBF1 was first identified in a yeast two-hybrid screen and further confirmed by co-immunoprecipitation (Sztul and García-Mata, 2003). The interaction appears essential as introduction of a competing peptide in cells lead to Golgi disruption. However, the interaction appears dispensable for membrane targeting of both proteins. The exact function of the p115-GBF1 interaction remains unresolved.

Interestingly, the p115 interacting partner, Rab1, has also been shown to interact with GBF1 in a GTP-dependent manner (Monetta et al., 2007). More specifically, the Rab1b isoform appears to bind directly to the N-terminal half of GBF1 (sequences upstream of sec7). Constitutively active Rab1b appears to recruit additional GBF1 to peripheral ERGIC structures, and depletion of Rab1b slows Arf1 cycling on and off Golgi membranes. Whether the Rab1a

isoform plays a similar redundant function has not yet been investigated. These previous reports on both Rab1b and p115 suggest that the two proteins likely regulate GBF1-mediated vesicle trafficking through some unexplored mechanism, potentially as a part of a larger protein complex (Sztul and Lupashin, 2009).

Lastly, both GMH1 and GGAs (GGA1, 2, and 3) have also been shown to interact with GBF1 in previously published co-immunoprecipitation studies. GMH1, also known as UNC50, is a Golgi-localised protein with unknown function (Chantalat et al., 2003). However, despite the observed interaction, deletion of GMH1 in yeast had negligible impact on the localisation of the yeast GBF1 homologs. The reported interaction between GBF1 and GGAs was initially suggested as a potential mechanism by which GGAs may be recruited to the TGN (Lefrançois and McCormick, 2007). Overexpression of non-catalytic GBF1 also reduced recruitment of GGAs to the membrane. However, extensive imaging studies have demonstrated that GBF1 localises specifically to *cis*-Golgi membranes (Quilty, 2016; Zhao et al., 2006; Zhao et al., 2002), for this reason it is unlikely that GBF1 acts as a direct receptor for GGAs at the TGN *in vivo*. Rather, GBF1 activity may produce downstream effects that regulate GGA distribution.

In vitro experiments performed using isolated Golgi membranes has shown the existence of some unknown protein factor required for GBF1 membrane binding. Interfering with membrane protein integrity either through treatments with trypsin or elevated temperatures abrogated GBF1 binding *in vitro* (Quilty et al., 2019). These observations suggest that some protein factor is likely either interacting with GBF1 directly to facilitate recruitment, or rapidly modifying membrane conditions to allow for GBF1 binding. However, despite the number of GBF1 interactors identified, none of these proteins have been shown to be essential for the targeting and recruitment of GBF1 to the membrane, suggesting that our understanding of the

protein components involved remains incomplete. While Rab1 and p115 likely play critical roles in this process, additional work must be done to identify the remaining components.

Outside the *cis*-Golgi, GBF1 has also been suggested to play additional cellular functions. As mentioned, HDS1, has been shown to bind lipid droplets *in vivo*, artificial phosphatidylcholine droplets *in vitro*, and the lipid droplet protein, adipose triglyceride lipase *in vitro* (Bouvet et al., 2013; Ellong et al., 2011). Depletion of GBF1, Arf, and β COP all led to an increase in lipid droplet deposition, suggesting that GBF1 mediated COPI vesicular traffic may play a role in lipid droplet homeostasis. Although the exact mechanisms by which this occurs remain unclear. GBF1 has also been shown to localise to the plasma membrane where it facilitates several different cellular processes. The first is the activation of Arf1 at the leading edge of cells for migration and chemotaxis; impaired GBF1 activity or lack of Arf1 activation causes a loss of cell polarity and migratory potential (Busby et al., 2017; Mazaki et al., 2012). In select cell types, GBF1 is also recruited to the plasma membrane to initiate clathrin and dynamin independent endocytosis (CLIC/GEEC). Both processes appear to be Arf1 dependent, but the Arf1 effectors involved are unknown (Gupta et al., 2009; Sathe et al., 2018). More recently, GBF1 has also been shown to modulate mitochondrial positioning and mitophagy in an Arf1 dependent manner (Ackema et al., 2014; Walch et al., 2018). The mechanisms by which GBF1 is recruited to these various sites and functionally controlled remain unclear. However, the emergence of these observations solidifies the importance of GBF1 as a major regulator of cellular physiology.

1.5 Arf GTPase activating proteins (ArfGAPs)

As mentioned, the inactivation of Arfs requires the activity of Arf GTPase activating proteins (ArfGAPs). Unlike other small GTPases, Arfs display no detectable intrinsic GTPase activity

and rely largely on the activity of ArfGAPs to facilitate GTP hydrolysis (Campa and Randazzo, 2008). ArfGAPs are unified by the presence of the catalytic GAP domain consisting of four cysteine zinc-finger motifs and a catalytic arginine residue. At the Golgi there exists two key subfamilies: ArfGAP1, and ArfGAP2 and 3 (Kahn et al., 2008). ArfGAP1 localises primarily to the *cis*-Golgi. Apart from interacting with Arfs, ArfGAP1 has also been shown to interact with the COPI coat, COPI cargo proteins, and cargo receptors to facilitate COPI vesicle formation (Huber et al., 1998; Lee et al., 2005; Yang et al., 2002). ArfGAP2 and ArfGAP3 resulted from a gene duplication event and are approximately 58% identical to each other (Schlacht et al., 2013). However, neither share sequence similarity to ArfGAP1. Currently, the exact localisation of each ArfGAP within the Golgi remains debated (East and Kahn, 2011). Overexpression of ArfGAP1 results in the redistribution of Golgi enzymes to the ER, a phenotype expected of increased Arf1 inactivation; this mimics inhibition of Arf1 activation using BFA or overexpressing a dominant negative GTP binding defective Arf (Donaldson et al., 2005). Overexpression of ArfGAP2 or ArfGAP3 do not have this effect, suggesting that only ArfGAP1 regulates Arf1 at the ER-Golgi interface. ArfGAP3 has been suggested to primarily localise to TGN and endosomes where it facilitates post-Golgi traffic (Shiba et al., 2013). Impaired localisation of the TGN mannose 6-phosphate receptor and the plasma membrane epidermal growth factor receptor in ArfGAP3 depleted cells could only be rescued by catalytically active ArfGAP3 but not ArfGAP1 or ArfGAP2. This indicates potential unique functions for ArfGAP3. However, other reports have suggested a *cis*-Golgi localisation for ArfGAP3, and that both ArfGAP2 and ArfGAP3 can influence COPI coat recruitment to the Golgi (Kartberg et al., 2010). Current understanding is further complicated by the observations that single and double knockdowns of any of the three ArfGAPs are not lethal, indicating some level of functional redundancy (Frigerio et al., 2007).

Only knockdown of all three leads to Golgi collapse similar to a β COP knockdown; re-expression of any of the three ArfGAPs can recover Golgi morphology. Clearly, additional studies into the ArfGAPs are needed to thoroughly elucidate the exact functional roles of each one, and the level of redundancy between them.

1.6 Hypothesis and thesis plan

As described, the activity of the Golgi is essential for protein secretion and maintenance of the secretory pathway. Failure to efficiently maintain Golgi traffic results in the collapse of the organelle and eventual cell death. GBF1 is the only large ArfGEF that appears to function at the early secretory pathway and is essential for ERGIC to Golgi, and intra Golgi traffic. Loss or inhibition of GBF1 activity impairs Arf1 activation at the ERGIC and Golgi, and blocks COPI vesicle formation. Furthermore, GBF1 has also been shown to play essential roles in lipid droplet and mitochondrial homeostasis, cell migration and chemotaxis, and clathrin and dynamin independent endocytosis – all of which similarly require Arf1 activation by GBF1. Since the activation of Arfs *in vivo* appear membrane dependent, the recruitment of their corresponding ArfGEFs to the membrane is required for Arf activation. The majority of GBF1 localises to *cis*-Golgi structures at steady state, and previous studies have shown that the recruitment of GBF1 to the membrane appears to involve a combination of protein and membrane components; the HDS1 domain of GBF1 interacts with PI4Ps and disruption of Golgi membrane proteins via trypsin or high-temperature treatment abrogates GBF1 membrane recruitment. Based on these previous observations, we hypothesize that GBF1 interaction and recruitment to Golgi membranes require specific interactions between a number of protein components present on the *cis*-Golgi and critical domains found within GBF1. To test our hypothesis and identify these components we utilized a range of molecular techniques. The identification of essential GBF1

domains was performed using live-cell imaging coupled with the use of fluorescently-tagged mutant constructs and pharmacological inhibitors. The identification of GBF1 interacting partners at the membrane was done using a protein-interactome approach coupled with knockdown and overexpression studies. By probing the GBF1 domains and protein partners involved in Golgi targeting, our goal was to shed light on the mechanisms that regulate GBF1 and the maintenance of the secretory pathway. Furthermore, by improving our understanding of GBF1 regulation at the Golgi, we may then set the stage for future studies into understanding GBF1 recruitment and regulation at other essential membrane locations.

The following chapter will detail the reagents, materials, and techniques used for the experiments described in the subsequent research chapters – 3, 4, 5, and 6.

Chapter 2: Materials and Methods

2.1 Reagents

In this study, all chemicals, reagents, enzymes, and commercial products used were performed according to manufacturer's instructions – unless otherwise stated.

Table 2.1 List of chemicals and reagents

Chemical/Reagents	Supplier
2-mercaptoethanol	Sigma
6x Sample Buffer (loading dye)	Promega
10x DPBS pH 7.4 (Dubecco's phosphate buffered saline)	Gibco (Invitrogen)
30% acrylamide/bis (29:1)	Bio-rad
Acetone	Fisher Scientific
Agarose (ultrapure)	Invitrogen
Ammonium persulfate	Bio-rad
Ampicillin	Novopharm
Bactotryptone	BD Biosciences
Bacto-yeast	BD Biosciences
Biotin	Sigma
BP clonase enzyme	Invitrogen
Brefeldin A	Sigma
Bromophenol blue	Sigma
Calf intestinal alkaline phosphatase (CIAP)	Invitrogen
CHAPS detergent	Thermo Scientific
CO ₂ -independent medium	Gibco (Invitrogen)
Coelenterazine	Gold Biotechnology
Complete, EDTA-free protease inhibitor cocktail	Roche
Difco LB (Luria-Bertani) broth, Miller	BD Biosciences
Difco LB (Luria-Bertani) agar, Miller	BD Biosciences
DTT (dithiothreitol)	Sigma
DMEM (Dulbecco's Modified Eagle Medium)	Gibco (Invitrogen)
DMSO (dimethyl sulfoxide)	Sigma
dNTPs (deoxyribosenucleotide triphosphate)	Invitrogen
Doxycycline hydrochloride	Fisher
EDTA (ethylenediamine-tetraacetic acid)	Sigma
EGTA (ethyleneglycol-tetraacetic acid)	Sigma
Ethanol (95%)	Fisher Scientific
Fetal Bovine Serum (FBS)	Gibco (Invitrogen)
GeneRuler 1kb DNA Ladder	Fermentas
O'GeneRuler 1kb DNA Ladder	Fermentas
Glycylglycine	Fisher Scientific
Glycerol	Fisher Scientific
Halt protease inhibitor cocktail (100x)	Thermo Scientific
HEPES	Sigma

Hydrochloric acid	Fisher Scientific
Hygromycin B in PBS (50mg/mL)	Invitrogen
IGEPAL CA-360	Sigma
Isopropanol	Fisher Scientific
Kanamycin sulfate	Gibco (Invitrogen)
L-glutamine	Gibco (Invitrogen)
LipoD293 reagent	FroggaBio
Lipofectamine 2000	Invitrogen
LR clonase enzyme	Invitrogen
Magnesium chloride	BDH
Magnesium sulphate	Fisher Scientific
Methanol	Fisher Scientific
MISSION transduction particles	Sigma
Odyssey blocking buffer (PBS)	LI-COR Biosciences
Opti-MEM	Gibco (Invitrogen)
Paraformaldehyde	Sigma
Penicillin/streptomycin	Gibco (Invitrogen)
Platinum Pfx DNA Polymerase	Invitrogen
Potassium chloride	BDH
Precision Plus Dual Colour Protein Standard	Bio-rad
Prolong Gold with DAPI antifade reagent	Molecular Probes (Invitrogen)
Prolong Gold antifade reagent	Molecular Probes (Invitrogen)
Protein A sepharose	GE Healthcare
Protein G sepharose	GE Healthcare
Puromycin	Sigma
Restriction endonucleases	Invitrogen or NEB
Sequabrene	Sigma
Sodium chloride	Fisher Scientific
SDS (sodium dodecyl sulfate)	Bio-rad
Sodium hydroxide (5N and 10N)	Fisher Scientific
Subcloning efficiency DH5 α competent cells	Invitrogen
Sucrose	Sigma
SYBR Safe DNA gel stain	Molecular Probes (Invitrogen)
T4 DNA Ligase	Invitrogen
TEMED (tetramethylethylenediamine)	Sigma
Tris-base	Invitrogen
Tris-HCl	Invitrogen
Triton X-100	VWR
Trypsin (0.25%)-EDTA	Gibco (Invitrogen)
Tween-20	Fisher Scientific
UltraPure Distilled Water	Invitrogen
Urea	Sigma

Table 2.2 Commercial kits

Commercial Kit	Supplier
Plasmid Maxi Kit	Qiagen
Plasmid Midi Kit	Qiagen
QIAprep Spin Mini Prep Kit	Qiagen
QIAquick Gel Extraction Kit	Qiagen
QIAquick PCR Purification Kit	Qiagen

Table 2.3 Commonly used buffers and solutions

Solution	Composition
4x separating gel pH 8.8	0.4% (w/v) SDS, 1.5 M Tris-HCl, pH 8.8
4x stacking gel pH 6.8	0.4% (w/v) SDS, 0.5 M Tris-HCl, pH 6.8
5x Ling's solubilizing buffer	150 mM sucrose, 50 mM Tris-HCl pH 8.0, 20 mM dithiothreitol, 10% (w/v) SDS, 5 mM EDTA
50x TAE	2 M Tris base, 5.71% (v/v) glacial acetic acid, 50 mM EDTA, pH 8.0
Cell freezing medium	15% (v/v) DMSO in FBS
CHAPS lysis buffer	1% (w/v) CHAPS, 10 mM Tris-HCl pH 7.4, 150 mM NaCl, 1 mM EDTA, 2x protease inhibitor
Homogenization buffer	10 mM Tris-Cl pH7.6, 0.25 M Sucrose, 150 mM KCl, 1.0 mM MgCl ₂ , 2x protease inhibitor
IGEPAL C-630 lysis buffer	1% (v/v) IGEPAL C-630, 50 mM HEPES-HCl, pH 7.4, 100 mM NaCl, 1.5 mM MgCl ₂ , 2x protease inhibitor
Luciferase assay buffer	25mM glycyglycine pH 7.8, 15 mM K ₂ PO ₄ pH 7.8, 15mM MgSO ₄ , 4 mM EGTA, 1.4 μM coelenterazine
Luciferase lysis buffer	0.1% Triton X-100, 25 mM glycyglycine pH 7.8, 15mM MgSO ₄ , 4 mM EGTA, 1 mM dithiothreitol
Paraformaldehyde (4%)	4% (w/v) paraformaldehyde, 0.1 mM CaCl ₂ , 0.1 mM MgCl ₂
Permeabilization buffer	0.1% (v/v) Triton X-100, 0.05% (w/v) SDS in PBS
Running buffer	25 mM Tris-HCl, 190mM glycine, 0.1% (w/v) SDS
SOC medium	2% (w/v) bactotryptone, 0.5% (w/v) bacto-yeast extract, 10 mM NaCl, 2.5 mM KCl, 10 mM MgCl ₂ , 20 mM glucose
TBS-T	50 mM NaCl, 0.5% (v/v) Tween-20, 20 mM Tris-HCl, pH 7.5
Transfer buffer	25mM Tris-HCl, 190 mM glycine, 20% (v/v)

2.2 Cell culture

Multiple cell lines were used in this thesis. Commercially obtained lines include: HeLa cells (ECACC; Sigma-Aldrich, 93031013) and HEK293 cells (ATCC, CRL-1573). The five separate lines of Flp-In T-Rex HeLa cells containing various tetracycline operator regulated transgenes were either previously developed in the lab or generated specifically for experiments in this thesis. Transgenes include: an Enhanced GFP (EGFP)-tagged GBF1 (construction described in (Quilty et al., 2018)), BirA*-FLAG, BirA*-FLAG-GBF1, BirA*-FLAG-GBF1(885-1856), GBF1-BirA*-FLAG, and GBF1(885-1856)-BirA*-FLAG. HeLa cells expressing both EGFP-GBF1 and either a non-targeting shRNA or ZnT6-specific shRNA were also developed for this thesis.

Wild-type (WT) HeLa cells and HEK293 cells were maintained in DMEM medium supplemented with 10% FBS, 100 µg/mL penicillin and 100 µg/mL streptomycin in a 5% CO₂ incubator set at 37° Celsius. Flp-In T-Rex HeLa cells containing tetracycline operator regulated transgenes were cultured in DMEM medium supplemented with 10% FBS, 100 µg/mL penicillin, 100 µg/mL streptomycin, 100 µg/mL hygromycin in a 5% CO₂ incubator set at 37° Celsius. To stimulate transgene expression, 2 µg/mL doxycycline would be added 24 hours prior to the experiment. HeLa cells stably expressing EGFP-tagged GBF1 and shRNAs were maintained in DMEM medium supplemented with 10% FBS, 100 µg/mL penicillin, 100 µg/mL streptomycin, 100 µg/mL hygromycin, and 5 µg/mL puromycin in a 5% CO₂ incubator set at 37° Celsius. To stimulate transgene expression, 2 µg/mL doxycycline would be added 24 hours prior

to the experiment. For all live-cell imaging experiments, all cells were kept in CO₂-independent medium supplemented with 10% FBS.

2.2.1 Construction of Flp-In T-Rex HeLa cell lines containing tetracycline operator regulated BirA*-tagged transgenes

Relevant genes (full-length GBF1 or GBF1 aa 885-1856) were first introduced into the pcDNA5-pDEST-BirA*-FLAG-N-ter plasmid, or pcDNA5-pDEST-BirA*-FLAG-C-ter plasmid obtained from the Gingras lab (Couzens et al., 2013) using the Gateway cloning method according to guidelines by Invitrogen. In short, the relevant GBF1 regions were PCR amplified using forward (fwd) and reverse (rvs) primers (Table 2.4) ends containing either *attB1* or *attB2* sequences to allow for recombination with the *attP1* and *attP2* sites in the pDONR 221 plasmid.

Recombination was performed using the BP clonase by Invitrogen. N-FWD and N-RVS primers were designed for cloning genes downstream of the BirA*-FLAG sequence in the pDEST-BirA*-FLAG-N-ter plasmid. C-FWD and C-RVS primers were designed for cloning genes upstream of the BirA*-FLAG sequence in the pDEST-BirA*-FLAG-C-ter plasmid.

Table 2.4 Primers used for generating Flp-In T-Rex HeLa cells expressing various BirA*-tagged transgenes

Primer Name	Primer Sequence
AttB1 GBF1 N- FWD	GGGG <u>ACAAGTTTGTACAAAAAAGCAGGCT</u> TGGTGGATAAGAATATTTACA TC
AttB2 GBF1 N- RVS	GGGG <u>ACCACTTTGTACAAGAAAGCTGGGTT</u> TAGTTGACTTCAGAGG
AttB1 885-1856 N-FWD	GGGG <u>ACAAGTTTGTACAAAAAAGCAGGCT</u> TGGAGGAACAGACAGGCC
AttB1 GBF1 C- FWD	GGGG <u>ACAAGTTTGTACAAAAAAGCAGGCT</u> TGACCATGGTGGATAAGAATA TTTAC
AttB2	GGGG <u>ACCACTTTGTACAAGAAAGCTGGGTT</u> GTTGACTTCAGAGGTG

GBF1 C-
RVS

AttB1 GGGGACAAGTTTGTACAAAAAAGCAGGCTTGACCATGGAGGAACAGACAG
885-1856 GCC
C-FWD

attB1 and attB2 sites are underlined

Following recombination into the pDONR 221 plasmid, the genes were then moved into the corresponding pDEST-BirA*-FLAG-N-ter plasmid or pcDNA5-pDEST-BirA*-FLAG-C-ter plasmid with a second round of recombination facilitated by the LR clonase by Invitrogen. The completed pDEST-BirA*-FLAG-N-ter and pcDNA5-pDEST-BirA*-FLAG-C-ter plasmids containing the corresponding GBF1 sequences were then sequenced by Sanger sequencing to ensure successful and error-free cloning.

The pDEST-BirA*-FLAG-N-ter or pcDNA5-pDEST-BirA*-FLAG-C-ter plasmids containing corresponding GBF1 sequences were integrated into the HeLa Flp-In T-Rex cell line (Couzens et al., 2013) using the Flp-In system according to guidelines by Invitrogen. The plasmids were co-transfected into the cells with pOG44 in a 1:9 ratio. Stable population of cells containing the BirA*-FLAG or FLAG-BirA* tagged transgenes were selected for with 150 µg/mL hygromycin over a period of 14 days. In all cases, stimulation of the tetracycline operator was done using 2 µg/mL doxycycline for 24 hours.

2.2.2 Construction of Flp-In T-Rex HeLa cell lines containing a tetracycline operator regulated EGFP-GBF1 and stably expressing a non-targeting or ZnT6-specific shRNA

The Flp-In T-Rex HeLa cells containing a tetracycline operator regulated EGFP-GBF1 previously generated in the Melançon lab (Quilty et al., 2018) were cultured and transduced with lentiviral particles containing packaged MISSION shRNA encoding TRC2-pLKO-puro plasmids (Sigma; see sub-section 2.9 for lentiviral particle production and transduction details). Successful

integration of the MISSION shRNA encoding plasmids were selected for in 5 µg/mL puromycin over a period of 14 days. Successful depletion of target genes in these cell lines were confirmed by western blotting.

2.3 Expression plasmids

2.3.1 pEGFP-GBF1 truncation library

The pEGFP-GBF1 wild-type and its truncated derivatives used in Chapter 3 were generated as part of my undergraduate research project in collaboration with Douglas Quilty (Quilty et al., 2018). The domain boundaries used for the library are based on previously published research (Mouratou et al., 2005). Construction was achieved through PCR amplification of select GBF1 regions using forward and reverse primers with SacII and SbfI restriction sites, respectively. These sites allowed for the directional insertion of the GBF1 truncation into a pEGFP-C1 vector. Successful and error-free cloning was confirmed by Sanger sequencing.

Table 2.5 Primers used for generating the pEGFP-C1-GBF1 truncation library

Primer Name	Primer Sequence
GBF1 WT Forward	<u>CCGCGGGATGGTGGATAAGAATTACATCATTAAACGGAGAA</u>
GBF1 WT Reverse	<u>CCTGCAGGTTAGTTGACTTCAGAGGTGGGAATAGGG</u>
205-1856 Forward	<u>CCGCGGTGAGCTATGTGGGAACCAACATGAAGAAG</u>
390-1856 Forward	<u>CCGCGGTGGAAGGCACAGCTTTGGTTCCTTAT</u>
565-1856 Forward	<u>CCGCGGAGTCTGGTCAACTTTATACCACACACCTACTG</u>
696-1856 Forward	<u>CCGCGGTAAACAAAAAGAAGCTGCTGATCACTGGC</u>
885-1856 Forward	<u>CCGCGGAGCCCAGGAACAGACAGG</u>
1065-1856 Forward	<u>CCGCGGAGATGCCATCAAACCGAGGAGAG</u>
1276-1856 Forward	<u>CCGCGGTGAAGCCTCCAGATGCTCTACAG</u>
1533-1856 Forward	<u>CCGCGGATGACTCACGCACCCTCTGG</u>
1645-1856 Forward	<u>CCGCGGGGCTCACCATCCTGGACTTCATG</u>
1-204 Reverse	<u>CCTGCAGGTTACTTGGGTCTTCTTTAAACTGAGGTAACCT</u>
1-389 Reverse	<u>CCTGCAGGTTACTTCTGGGAGGACTGTGTGAAGC</u>
1-564 Reverse	<u>CCTGCAGGTTACACAGGAAAGGCATTCTTGACAGC</u>
1-695 Reverse	<u>CCTGCAGGTTACTTAATTTCAATTAGTTCCCGTGGATC</u>
1-884 Reverse	<u>CCTGCAGGTTACATCACGATTTCTCATTCTTGATGGCATG</u>
1-1064 Reverse	<u>CCTGCAGGTTACTCCTCCCGCTGTAGAGAGATCTTACC</u>
1-1275 Reverse	<u>CCTGCAGGTTACACGCCTGAGCCAATACACTCC</u>

1-1532 Reverse	<u>CCTGCAGGTTAAGCTTCAATCTTTCGGCCACCTGA</u>
1-1644 Reverse	<u>CCTGCAGGTTACCACAGGGCAGCAAAGGT</u>

The SacII (CCGCGG) and SbfI (CCTGCAGG) restriction sites are underlined

2.3.2 mCherry-ERGIC53 plasmid

The mCherry-ERGIC53 plasmid was generated by removing the EGFP open reading frame from the pEGFP-ERGIC53 plasmid (Ben-Tekaya et al., 2005), and replacing it with the mCherry open reading frame obtained from a mCherry-C1 vector. The EGFP open reading frame was removed by restriction enzyme digestion with AgeI and BglII. The mCherry open reading frame was PCR amplified using forward and reverse primers with AgeI and BglII restriction sites, respectively (Forward primer: TATTTAACCGGTAGTGAGCAAGGGCGAGGAG; reverse primer: TACCTAAAGATCTCTTGTACAGCTCGTCCATGCC; corresponding restriction sites are underlined). The PCR amplified fragments were first digested then ligated into the ERGIC53 containing plasmid fragment. Successful and error-free cloning was confirmed by Sanger sequencing.

2.3.3 mCherry-C10orf76, FLAG-C10orf76, and the EGFP-C10orf76 truncations

All C10orf76 constructs used in this thesis was derived from a previously published codon-optimized FLAG-C10orf76 (Blomen et al., 2015). This previously published construct contains 63 additional nucleotides at the 3' end of the C10orf76 open reading frame prior to reaching a stop codon. To avoid having these 21 additional amino acids potentially interfere with the FLAG-tagged construct we generated a new FLAG-C10orf76 lacking the additional peptide by PCR amplifying the FLAG-C10orf76 continuous open reading frame for sub cloning using AgeI and BamHI restriction sites. The forward and reverse primers contained an AgeI or BamHI restriction site, respectively, and the reverse primer was designed to integrate a stop codon at the end of the C10orf76 sequence (Forward primer:

GGAACAACCGGTACCATGGACTACAAGGAC; Reverse primer:

GGCGGATCCTTAGCTGATGGTGCTGAACTC; the AgeI and BamHI restriction sites are underlined and the stop codon is **bolded**). The amplified fragment was then ligated into a mCherry-C1 vector with the mCherry open reading frame removed by digestion with AgeI and BamHI. Successful and error-free cloning was confirmed by Sanger sequencing.

The mCherry-C10orf76 plasmid was constructed by PCR amplifying the C10orf76 open reading from the same published codon-optimized FLAG-C10orf76 (Blomen et al., 2015) in a similar manner. The forward and reverse primers contained SacII and BamHI restriction sites, respectively, for insertion into the mCherry-C1 vector (Forward primer:

ATACCGCGGATGCCCAGGTGGAAAAGAG; Reverse primer:

GGCGGATCCTTAGCTGATGGTGCTGAACTC; restriction sites are underlined and the stop codon is **bolded**). Successful and error-free cloning was confirmed by Sanger sequencing.

The two EGFP-tagged C10orf76 truncations-were generated in a similar manner to the pEGFP-C1-GBF1 truncations described in section 2.3.1 by PCR amplification and ligation into a pEGFP-C1 vector. The same published codon-optimized FLAG-C10orf76 (Blomen et al., 2015) was used as a template. The forward and reverse primers contained SacII and BamHI restriction sites, respectively (C1-483 Forward: ATACCGCGGATGCCCAGGTGGAAAAGAG; C1-483

Reverse: GGCGGATCCTTAGCAGGGCAGGTTCTTG; N439-688 Forward:

ATACCGCGGATAGGCCTCTCGTGTGCG; N439-688 Reverse:

GGCGGATCCTTAGCTGATGGTGCTGAACTC; restriction sites are underlined). Successful and error-free cloning was confirmed by Sanger sequencing.

2.3.4 mCherry- and EGFP-ZnT6

The mCherry- and EGFP-tagged ZnT6 plasmids were generated by modifying a previously published HA-tagged ZnT6 plasmid (Fukunaka et al., 2011). The ZnT6 open reading frame was PCR amplified using forward and reverse primers containing SacII and SbfI restriction sites, respectively (Forward: ACCGCGGGCATGGGGACAATTCATCTCTTTC; Reverse: GTCATACCTGCAGGTCATGGTCTTGGTTG; restriction sites are underlined). These amplified fragments were then ligated into either an EGFP-C1 or mCherry-C1 vector. Successful and error-free cloning was confirmed by Sanger sequencing.

2.3.5 Additional plasmids

The FLAG-Rab32 and EGFP-Drp1 plasmids were obtained from the Simmen lab (Eura et al., 2003; Ortiz-Sandoval et al., 2014).

2.4 Antibodies and streptavidin conjugates

Antibodies and streptavidin conjugates used in this thesis for labeling of proteins and biotin are listed in the tables below. The tables are separated based on categories: primary antibodies used in immunofluorescence, secondary antibodies used in immunofluorescence, primary antibodies used in western blots, and secondary antibodies used in western blots, and streptavidin conjugates. Streptavidin-Cy3 was used for immunofluorescence and Alexa Fluor 690 streptavidin was used for western blotting. All streptavidin conjugates were used without a secondary antibody

Table 2.6 Primary antibodies used in immunofluorescence

Antibody	Dilution	Source
Mouse anti- β -coatamer protein I (COPI) (clone m3a5) monoclonal	1:250	Sigma
Mouse anti-GBF1 (clone 25)	1:400	BD Biosciences

monoclonal		
Rabbit anti-GBF1 (9D2) IgG	1:400	(Zhao et al., 2006)
polyclonal		
Mouse anti-P115 (7D1)	1:1000	Dr. Gerry Water, Princeton University, Princeton, USA
monoclonal		
Sheep anti-TGN46 polyclonal	1:500	AbD Serotec
Rabbit anti-Giantin (polyclonal)	1:500	Dr. Edward K.L. Chan, University of Florida Health, Jacksonville, USA
Mouse anti-FLAG monoclonal	1:100	Rockland

Table 2.7 Secondary antibodies used in immunofluorescence

Antibody	Dilution	Source
Alexa Fluor 488 goat anti-mouse	1:500	Molecular Probes (Invitrogen)
Alexa Fluor 488 goat anti-rabbit	1:500	Molecular Probes (Invitrogen)
Alexa Fluor 546 donkey anti-sheep	1:500	Molecular Probes (Invitrogen)
Alexa Fluor 647 donkey anti-mouse	1:500	Molecular Probes (Invitrogen)
Alexa Fluor 647 donkey anti-rabbit	1:500	Molecular Probes (Invitrogen)

Table 2.8 Primary antibodies used in western blots

Antibody	Dilution	Source
Rabbit anti-EGFP polyclonal	1:2000	Eusera
Mouse anti-GBF1 (clone 25) monoclonal	1:2000	BD Biosciences
Rabbit anti-GBF1 (9D4) IgG polyclonal	1:2000	(Claude et al., 2003)
Rabbit anti-C10orf65 (HPA053580)	1:500	Sigma
Rabbit anti-Giantin (polyclonal)	1:1500	Dr. Edward K.L. Chan, University of Florida Health, Jacksonville, USA
Mouse anti-FLAG (monoclonal)	1:1000	Rockland
Mouse anti-tubulin (Clone DM 1 A)	1:1000	Sigma

Mouse anti-GM130 monoclonal	1:250	BD Bioscience
Mouse anti-VDAC1	1:5000	Abcam
Rabbit anti-GOSR1 (EP1768Y) monoclonal	1:500	Abcam
Rabbit anti-CANT1 (PA5-92914) polyclonal	1:500	Invitrogen
Rabbit anti-ZnT6 polyclonal	1:500	Proteintech

Table 2.9 Secondary antibodies used in western blots

Antibody	Dilution	Source
Alexa Fluor 680 goat anti-rabbit	1:10000	Molecular Probes (Invitrogen)
Alexa Fluor 750 goat anti-mouse	1:10000	Molecular Probes (Invitrogen)

Table 2.10 Streptavidin conjugates

Streptavidin conjugate	Dilution	Source
Streptavidin-Cy3	1:1000	Invitrogen
Alexa Fluor 690 streptavidin	1:10000	Molecular Probes (Invitrogen)

2.5 Site-directed mutagenesis

To generate the L1244R mutation in the pEGFP-C1-GBF1-N885-1856 plasmid, we utilized site-directed mutagenesis. Mutant strand synthesis was performed through thermocycling using primers containing the L1244R mutation (Forward:

GGTTGCCTACGGGCGCCATGAACTCCTCAAG; Reverse:

CTTGAGGAGTTCATGGCGCCCGTAGGCAACC; the altered bases are underlined).

Following thermocycling, amplification results were digested with DpnI and transformed into chemically competent DH5α *Escherichia coli*. Successful mutation was confirmed by Sanger sequencing.

2.6 Cell plating, transient transfections, and immunofluorescence

Imaging experiments were performed with tissue culture cells plated and grown on glass coverslips in 6-well plates. For live-cell imaging, 25CIR #1 circular glass coverslips from Fisher Scientific were used. For fixed-cell imaging, #1.5 glass coverslips by Corning were used. Coverslips were sterilized by washing in 70% ethanol and the alcohol removed by ignition in an open flame. Transfection of plasmids for transient expression of proteins were performed on cells grown to approximately 60-70% confluency using Lipofectamine 2000 (Invitrogen, Carlsbad, CA) according to manufacturer's instructions. These cells were then cultured for approximately 18 hours to allow for protein expression prior to imaging.

2.7 Fluorescence microscopy

For fixed-cell imaging, cells were washed in pre-warmed 37° Celsius PBS and fixed in 4% paraformaldehyde at room temperature for 20 minutes. Cells were then washed twice in room temperature PBS and permeabilized in permeabilization buffer. Cells were then double-labeled with various primary and secondary antibodies for one hour each, washed three times in PBS, and mounted on glass slides.

For live-cell imaging, slides were transferred to Attofluor cell chambers (Invitrogen, Carlsbad, CA) with pre-warmed 37° Celsius CO₂ independent media supplemented with 10% FBS (Gibco Laboratories, Grand Island, NY).

2.7.1 Epifluorescence microscopy

Both live- and fixed-cell epifluorescence experiments were performed on a DeltaVision Elite (GE Healthcare, Buckinghamshire, UK) microscope equipped with a front-illuminated sCMOS camera driven by softWoRx 6 (GE Healthcare, Buckinghamshire, UK). Fixed cell imaging was performed at room temperature, while live-cell imaging was performed with the microscopy

chamber warmed to 37° Celsius. Images were acquired using a 60x 1.4 NA oil objective (Olympus, Richmond Hill, CAN) with focus maintained using the UltimateFocus feature. Z-slices were acquired with an optical section spacing of 0.35 µm and 25 optical sections were acquired per image for a sample depth of 8.74 µm. Images were then deconvolved using softWoRx 6 before being processed and analyzed using FIJI (National Institutes of Health, Bethesda, MD).

2.7.2 Electron microscopy

Electron microscopy experiments were performed with the help of electron microscopist Dr. Nasser Tahbaz (University of Alberta, Edmonton, Canada). Cells were grown in 10 cm dishes to approximately 80% confluency and fixed in Karnovsky fixative (2% paraformaldehyde and 2% glutaraldehyde). Cells were then pelleted by centrifugation at gradually increasing speeds before secondary fixation in 1% osmium tetroxide for one hour. This was followed by staining with 1% uranyl acetate in water over night and dehydrated in increasing concentrations of ethanol. Pellets were then embedded in epoxy resin – Epon 812 (EMS #14120) – and sectioned using the UltracutE ultramicrotome (Reichert Jung). Imaging was performed with a Jeol JEM-2100 transmission electron microscope.

2.7.3 Fluorescence recovery after photobleaching (FRAP)

For FRAP experiments, images were acquired on a Quorum Technologies WaveFX microscope with a Yokagawa CSU 10 spinning disk confocal scan-head and a 60x 1.42NA oil objective. Imaging was driven by the Perkin Elmer's Volocity program and photobleaching was performed using the Andor iQ3 live-cell imaging software.

2.8 Image quantitation and analysis

2.8.1 Li's intensity correlation quotient

Li's intensity correlation quotient was used to confirm the co-localisation of the EGFP-tagged GBF1 truncations with the mCherry-ERGIC53 marker (Li et al., 2004). Li's ICQ is a pixel-intensity correlation measurement not based on any object-recognition approach. Pixels at identical positions between the two channels are compared to their respective image mean intensities. The method is based on the principle that the sum of the differences from the mean for all pixels in an image should equal zero. As such, for two sets of random, unrelated images, the sum of their product of their differences will also tend to zero. However, if the intensities are dependent, their products will tend to a positive value. Or if they are segregated, with opposite intensities for pixels at identical positions, the products will tend to a negative value. To achieve these calculations for images with multiple Z-slices (approximately 10 slices per cell / image), image files free of pixel saturation were imported into FIJI (National Institutes of Health, Bethesda, MD). The pre-installed plugin, coloc2, was used to calculate Li's ICQ value and generate corresponding intensity plots. A minimum of 10 cells from three independent replicates were used.

2.8.2 Fraction signal at Golgi structures

Quantification of fraction signal at Golgi structures was carried out using FIJI (National Institutes of Health, Bethesda, MD) with a minimum of 10 cells from three independent replicates. Areas of interest were highlighted using the freehand selection tool and average pixel intensity values and area size was measured and exported into Excel spreadsheets (Microsoft, Redmond, WA). The total Golgi intensity was corrected for cytosolic intensity and the total cell

intensity was further corrected for intensity of the image background. The equation used for the correction of signal at the Golgi is:

$$\textit{Fraction signal at Golgi} = \frac{\textit{Golgi area (Golgi intensity - cytosol intensity)}}{\textit{Cell area (cell intensity - background intensity)}}$$

For recruitment measurements, the fold recruitment was calculated as: fraction signal at the Golgi after BFA / fraction signal at the Golgi prior to BFA. Where applicable, statistical significance was measured using two-tailed upaired *t*-tests on Excel (Microsoft, Redmond, WA). A single asterisk indicates a *p*-value below 0.05, two asterisks for *p*-values below 0.01, and three asterisks for *p*-values below 0.001.

2.9 Lentiviral particle production and transduction

Plasmids encoding shRNAs targeting genes of interest were obtained from the Sigma-Aldrich MISSION human shRNA library. To generate the lentiviruses containing these shRNA encoding plasmids, HEK293 cells grown to 80% confluency in 6-well plates were cotransfected with the shRNA encoding plasmid and the Sigma Aldrich MISSION lentiviral packaging mix using LipoD293 DNA In Vitro transfection reagent (FroggaBio). The secreted lentiviral particles were collected over a period of 3 days and filtered with 0.45 µm low protein binding PVDF syringe filters (Millex). The lentiviral particles were then stored at -80° Celsius. Lentiviral titer was determined with 2 mL ten-fold serial dilution of the lentivirus preparation from 1 x 10⁻¹ to 1 x 10⁻⁵. 1 mL of lenvirus dilution added to HeLa cells on 6-well plates with 8 µg/mL Sequabrene (Sigma). Cells were then incubated with the lentivirus for 24 hours prior to replacing the media with DMEM with 10% FBS and 5 µg/mL puromycin to select for transduced cells. Puromycin resistant colonies were counted 48 hours post puromycin addition to calculate viral titer.

$$\frac{\textit{Transforming Units}}{\textit{mL}} = \textit{\# of puromycin resistant clones} \div \textit{dilution}$$

shRNA knockdowns were performed on tissue culture cells by transduction of the lentiviral particle pools containing the appropriate shRNA plasmids (two per genes of interest; multiplicity of infection at two) with 8 $\mu\text{g}/\text{mL}$ Sequabrene (Sigma). Cells were then incubated with the lentivirus for 24 hours prior to replacing the media with DMEM with 10% FBS and 5 $\mu\text{g}/\text{mL}$ puromycin to select for transduced cells. All shRNA knockdown time values refer to time post-transduction.

Table 2.11 List of Sigma-Aldrich MISSION shRNA encoding plasmids used

Gene Symbol	Gene ID	Refseq ID	TRC ID	Oligo Sequence
GBF1	8729	NM_004193.1	TRCN0000157212	CCGGGCGAGTATGCTTCCTACTGTTCTCGA GAACAGTAGGAAGCATACTCGCTTTTTTG
GBF1	8729	NM_004193.1	TRCN0000155498	CCGGCGAGCACTACTTGTACATGATCTCG AGATCATGTACAAGTAGTGCTCGTTTTTTG
C10orf76	79591	NM_024541.2	TRCN0000131024	CCGGCTGGACCTGATGGTAGAGTTTCTCG AGAAACTCTACCATCAGGTCCAGTTTTTTG
C10orf76	79591	NM_024541.2	TRCN0000130013	CCGGGCTCAGATTTAGGGTAAGATACTCG AGTATCTTACCCTAAATCTGAGCTTTTTTG
CANT1	124583	NM_138793.2	TRCN0000051902	CCGGGAACTGGGTGTCCAACAACAACCTCG AGTTGTAGTTGGACACCCAGTTCTTTTTG
CANT1	124583	NM_138793.2	TRCN0000051899	CCGGCGGCTGGGATTCGGTATCGAACTCG AGTTCGATACCGAATCCAGCCGTTTTTG
TMEM87A	25963	NM_015497.2-209slc1	TRCN0000143983	CCGGCCTCTTCAGAAATACCACTATCTCGA GATAGTGGTATTTCTGAAGAGGTTTTTTG
TMEM87A	25963	NM_015497.2-1662slc1	TRCN0000144956	CCGGGAACGAATGATCACACACTTTCTCG AGAAAGTGTGTGATCATTCTTTTTTTG
TMEM115	11070	NM_007024.4	TRCN0000147505	CCGGGAAGGTAAAGATATGCCAGAACTCG AGTTCTGGCATACTTTACCTTCTTTTTTG
TMEM115	11070	NM_007024.4	TRCN0000180504	CCGGGCCCTCATCTGAGGTAAGAATCTCG AGATTCTTACCTCAGATGAGGGCTTTTTTG
RHBDD2	57414	NM_001040456.1	TRCN0000060384	CCGGCGCTATCATCTTCCTGTCATTCTCGA GAATGACAGGAAGATGATAGCGTTTTTG
RHBDD2	57414	NM_001040456.1	TRCN0000048639	CCGGCCTTCGCAACTGGCAAGTTTACTCGA GTAAACTTGCCAGTTGCGAAGGTTTTTG
GOSR1	9527	NM_004871.2	TRCN0000060383	CCGGGCGACAGGTATAGTTCTGATACTCG AGTATCAGAATAACCTGTCGCTTTTTTG
GOSR1	9527	NM_004871.2	TRCN0000060384	CCGGGCAGGATTATACACATGAATTCTCG AGAATTCATGTGTATAATCCTGCTTTTTG

SLC30A6 (ZnT6)	55676	NM_017964.2	TRCN0000043670	CCGGGCAAGTTGTTACGGGAATTTACTCG AGTAAATTCCCCTAACAACCTTGCTTTTTG
SLC30A6 (ZnT6)	55676	NM_017964.2	TRCN0000043671	CCGGCGATGCTTTCTATTCGGAATACTCGA GTATTCCGAATAGAAAGCATCGTTTTTG
SLC30A5 (ZnT5)	64924	NM_024055.2	TRCN0000042824	CCGGCCAGATAATTGGATCACTAAACTCG AGTTTAGTGATCCAATTATCTGGTTTTTG
SLC30A5 (ZnT5)	64924	NM_024055.2	TRCN0000042826	CCGGCGAATCATATGATCTCCTAAACTCG AGTTTAGGAGATCATATGATTCGTTTTTG
ZDHHC17	23390	NM_015336.2	TRCN0000134447	CCGGGCTGCCATCAATAACAGAATACTCG AGTATTCTGTTATTGATGGCAGCTTTTTTG
ZDHHC17	23390	NM_015336.2	TRCN0000138466	CCGGCCCAGAATATCAAGGGCGAATCTCG AGATTCGCCCTTGATATTCTGGGTTTTTG

2.10 Proximity-dependent biotinylation and Golgi membrane enrichment

Proximity-dependent biotinylation was performed with the Flp-In T-Rex HeLa cell lines containing tetracycline operator regulated BirA*-FLAG or BirA*-FLAG-GBF1, as described (Roux et al., 2013). Briefly, cells were grown to approximately 80% confluency in five 15 cm culture dishes and treated with 0.1 µg/mL doxycycline for six hours to allow for expression of the BirA*-FLAG proteins. This was followed by further supplementation with 50 µg/mL exogenous biotin and cultured for an additional 24-hours. Cells were then collected by treatment with 0.25% trypsin-EDTA (Gibco, Carlsbad, CA) and followed by neutralization with DMEM containing 10% FBS. Cells were pelleted by centrifugation at 300 x g for 10 minutes in a Sorvall RT7 benchtop centrifuge with a RTH-750 swinging bucket rotor. The cells were washed in PBS to remove residual medium and re-pelleted.

For preparation of Golgi-enriched membrane fractions, the pelleted cells were resuspended in ice-cold homogenization buffer and homogenized by 20 passages through a cell homogenizer (Isobiotec, Heidelberg, Germany) with a 16 µm clearance. The homogenates were centrifuged at 800 x g for 10 minutes at 4° Celsius to pellet nuclei and unbroken cells. The supernatant was collected, adjusted to 1.2 M sucrose and layered in a sucrose gradient for organelle separation by density centrifugation (Sucrose layers from top to bottom: 0.25 M, 1.0 M, 1.2 M, 1.3 M, 2 M). Samples were centrifuged at 23,000 x g for three hours in an Optima ultracentrifuge with a SW 41 Ti swinging bucket rotor (Beckman Coulter, Mississauga, Canada) at 4° Celsius. Enriched-Golgi fractions were collected between the 0.25 M and 1.0 M sucrose interface, washed with PBS, and pelleted by centrifugation at 163877.9 x g for 20 minutes in an Optima TLX Benchtop Ultracentrifuge with a TLA-100.4 rotor (Beckman Coulter, Mississauga, Canada) at 4° Celsius.

2.11 Mass spectrometry and analysis

Both the mass spectrometry and SAINT analysis was performed by our collaborators Etienne Coyaud, Estelle M.N. Laurent, and Brian Raught in the Department of Medical Biophysics at the University of Toronto (Chan et al., 2019). The BirA*-FLAG and BirA*-FLAG-GBF1 cells pellet and Golgi fractions prepared were shipped on dry ice overnight from the University of Alberta to the University of Toronto. The following protocols were not performed by us at the University of Alberta but are included for clarity and completeness.

Briefly, cell pellets and Golgi fractions were resuspended in 10 mL and 5 mL of lysis buffer respectively (50 mM Tris-HCl pH 7.5, 150 mM NaCl, 1 mM EDTA, 1 mM EGTA, 1% Triton X-100, 0.1% SDS, 1:500 protease inhibitor mixture (Sigma), 1:1000 benzonase nuclease (Novagen) and incubated at 4° Celsius for one hour on an end-over-end rotator. Samples were then briefly sonicated to disrupt any visible aggregates and centrifuged at 45000 x g for 30 minutes at 4° Celsius. Supernatants containing solubilized proteins were then collected and 30 µL of packed, pre-equilibrated Streptavidin-Sepharose beads (GE) were added and the mixture incubated for three hours at 4° Celsius. Beads were pelleted by centrifugation at 2000 rpm for two min, collected, and transferred with 1 mL of lysis buffer to fresh tubes. The beads were then washed once with 1 mL lysis buffer and then twice with 1 mL of 50 mM ammonium bicarbonate pH 8.3. The beads were then collected, and transferred with fresh ammonium bicarbonate into another fresh tube before being washed twice more with 1 mL ammonium bicarbonate. Protein peptides were separated from the beads by tryptic-digestion using 1 µg MS-grade TPCK trypsin (Promega, Madison, WI) dissolved in 200 µL of 50 mM ammonium bicarbonate pH 8.3 and incubated overnight at 37° Celsius. Beads were then pelleted again by centrifugation at 2000 x g for two minutes and supernatants collected in clean tubes. The pellets were washed twice with

150 μ L 50 mM ammonium bicarbonate to collect any residual peptides and these washes were pooled with the first eluates. These samples were then lyophilized and resuspended in 0.1% formic acid. One fifth of the sample was analyzed per single MS run.

Peptides were separated using high performance liquid chromatography conducted using a 2 cm pre-column (Acclaim PepMap 50 mm x 100 μ m inner diameter (ID)), and 50 cm analytical column (Acclaim PepMap, 500 m x 75 μ m diameter; C18; 2 μ m; 100 Å, Thermo Fisher, Waltham, MA). The setup was run using a 120 min reversed-phase buffer gradient at 225 nL/min on a Proxeon EASY-nLC 1000 pump in-line with a Thermo Q-Exactive HF quadrupole-Orbitrap mass spectrometer. A parent ion scan was performed first using a resolving power of 60000, then up to the twenty most intense peaks were selected for MS/MS (minimum ion count of 1000 for activation) using higher energy collision induced dissociation (HCD) fragmentation. Dynamic exclusion was activated such that MS/MS of the same m/z (within a range of 10ppm; exclusion list size = 500) detected twice within 5 seconds were excluded from analysis for 15 seconds.

For protein identification, raw files containing the identified peptide sequences were converted to the .mxXML format using Proteowizard (v3.0.10800; (Kessner et al., 2008)), then searched using X!Tandem (v2013.06.15.1; (Craig and Beavis, 2004)) against the HumanRefSeq Version 45 (database containing 36113 entries). Search parameters specified a parent MS tolerance of 15 ppm and an MS/MS fragment ion tolerance of 0.4 Da with up to two missed cleavages allowed for trypsin. No fixed modifications were set but oxidation of methionine was allowed as a variable modification. Data were analyzed using the trans-proteomic pipeline (Pedrioli, 2010) via the ProHits 5.0.2 software suite (Liu et al., 2010). Proteins were identified with a iProphet cut-off of 0.9 (corresponding to a \leq 1% probabilistic false discovery rate;

(Nesvizhskii et al., 2003)). Targets with 2+ unique peptides were analyzed with SAINT Express v. 3.6.1 to identify high-confidence interactors (Choi et al., 2011; Teo et al., 2014). The four controls were collapsed to the highest two spectral counts for each hit. Proteins identified with 2+ unique peptides and scoring above a Bayesian False Discovery Rate of 1% were high-confidence proximity interactors. All data are now publicly available on the MassIVE archive (www.massive.ucsd.edu) with ID: MSV000083866.

2.12 Western blotting and quantitation

For western blotting, proteins were separated by SDS-PAGE and transferred to nitrocellulose membrane at 376 mA for two hours in transfer buffer. The membrane was then blocked in Licor Odyssey blocking reagent (Licor Biotechnology, Lincoln, NE) for at least one hour. Incubation in primary antibody took place in 50% Licor Odyssey blocking reagent either overnight at 4° Celsius or one hour at room temperature. Membranes were then washed in PBS thrice before further incubation in fluorescent secondary antibodies for one hour in 25% Licor Odyssey blocking reagent at room temperature. This was followed by two 10 minute washes in TBST, and three additional five minute washes in PBS. Membranes were then scanned on a Licor Odyssey scanner (Licor Biotechnolgy, Lincoln, NE)

Quantitation of immunoblots were performed with Licor's Image Studio Lite software version 5.0 (Licor Biotechnology, Lincoln, NE). Band intensities were quantified by manually drawing a rectangle around the region of interest. Total signal was corrected for background based by subtracting the intensity of a 3-pixel width region above and below the selected band. Quantitated intensities were exported to Excel worksheets (Microsoft, Redmond, WA) where mean, standard deviation, and normalization calculations were performed.

2.13 Co-immunoprecipitation

HeLa cells at approximately 60-70% confluency were transfected with the plasmids indicated using Lipofectamine 2000 (Invitrogen) according to manufacturer instructions and cultured for 18 hours to allow for protein expression. Cells were then washed twice with PBS and lysed in detergent buffers as indicated (either CHAPs lysis buffer or IGEPAL C-630 lysis buffer).

For co-immunoprecipitation experiments, a 10 cm dish of transfected cells at approximately 90% confluency were lysed in 500 μ L CHAPs (FLAG pulldown). Lysates were centrifuged at 800 x g for five minutes at 4° Celsius to pellet nuclei and any intact cells. Supernatants were precleared with protein A sepharose beads and a 25 μ L aliquot was collected for subsequent use as the input fraction of the co-immunoprecipitation. The rest was incubated overnight with 4 μ L rabbit anti-FLAG antibodies (Sigma) at 4° Celsius on a rocking platform. 25 μ L of protein A sepharose beads were added the next day and the samples further incubated at 4° Celsius on a rocking platform for one hour. Beads were pelleted by centrifugation at 800 x g for five minutes at 4° Celsius, washed thrice in 500 μ L CHAPs buffer. After the third wash, beads were pelleted again, and resuspended in 25 μ L of 2x sample buffer for western blotting. 10 μ L of the pelleted sample was run for the pulldown (represents approximately 28.5% of original lysates). 20 μ L of the precleared supernatant sample was loaded for the input (represents approximately 2% of original lysates).

Co-immunoprecipitation experiments performed using the IGEPAL C-630 lysis buffer (EGFP pulldown) were done as previously described for ZnT6 (Suzuki et al., 2005). For each condition, a 10 cm dish of transfected cells at approximately 90% confluency was lysed in 1 ml IGEPAL C-630 lysis buffer. Samples were rotated for two hours at 4° Celsius. Following incubation, lysates were centrifuged at 800 x g for five minutes at 4° Celsius to pellet nuclei and

any intact cells. Supernatant was collected and precleared using protein G sepharose beads. A 300 mL aliquot was collected and proteins precipitated with three volumes of acetone for two hours at -20° Celsius. Precipitates were collected by centrifugation at 20,400 x g for 15 minutes at 4° Celsius and resolubilized with 200 µL Ling's solubilizing buffer and sample buffer. This was then used as the input fraction for the co-immunoprecipitation. The rest of the lysates were immunoprecipitated with 4 µL rabbit anti-EGFP antibodies (Sigma) at 4° Celsius on a rocking platform overnight. 25 µL of protein G sepharose beads were added the next day and the samples further incubated for one hour at 4° Celsius on a rocking platform. Beads were pelleted by centrifugation at 800 x g for five minutes at 4° Celsius. The collected beads were then washed thrice in 500 µL IGEPAL C-630 lysis buffer, then resuspended in 60 µL Ling's solubilizing buffer with sample buffer for western blotting. 25 µL of the pelleted sample was run for the pulldown (represents approximately 30% of original lysates). 20 µL of the precleared supernatant sample was loaded for the input (represents approximately 3% of original lysates).

2.14 Secretion assays and plate reading

HeLa cells were transduced with appropriate shRNA plasmid containing lentiviruses and transfected with a pNL1.3CMV[SecNluc] plasmid (Promega) encoding a NanoLuciferase. Secretion measurements were performed as previously described (Kumar et al., 2016). On the day of the experiment, cells were washed with serum-free medium to remove any already secreted luciferase and placed in fresh medium with or without BFA. After a two hour incubation period, the medium was assessed for the presence of luciferase using the luciferase substrate coelenterazine (Gold Biotechnology). Total cell luciferase was measured similarly after lysis in luciferase lysis buffer. Signal was quantitated with a fluorescence microplate reader (BioTek). Fraction of secreted luciferase was calculated as:

Fraction luciferase secreted

$$= \frac{\text{Total signal from growth medium}}{\text{Total signal from growth medium} + \text{total signal from lysed cells}}$$

Both total signal from growth medium and total signal from lysed cells were background corrected by subtracting the signal measured from wells containing coelenterazine alone without enzyme. Where applicable, statistical significance was measured using two-tailed upaired *t*-tests on Excel (Microsoft, Redmond, WA). A single asterisk indicates a *p*-value below 0.05, two asterisks for *p*-values below 0.01, and three asterisks for *p*-values below 0.001.

2.15 Membrane isolation and peripheral membrane protein extraction

Cells were grown and homogenized as previously described section 2.11. The post-nuclear supernatant was collected and transferred to fresh tubes for and centrifuged again on a benchtop Optima TLX ultracentrifuge with a TLA 100.4 rotor at 55,000 rpm for one hour at 4° Celsius. The membrane pellet was collected was either resolubilized in 2x sample buffer for western blotting or used in peripheral membrane protein extraction experiments.

For peripheral membrane protein extraction, the membrane pellet was resuspended in either ice-cold PBS with 2x Halt protease inhibitor or 0.1 M Na₂CO₃ pH 11.3 and incubated on ice for 30 minutes. Following incubation, membranes were re-pelleted and solubilized in 2x sample buffer for western blotting.

2.16 Homology searching for protein orthologues

C10orf76 orthologues were identified using homology searches performed with BLASTp on a representative sampling of eukaryotic organisms. The human C10orf76 protein sequence was obtained from NCBI (NP_078817.2) and used as the initial query sequence in a bi-directional

search. Putative top hits retrieved using the human C10orf76 query were deemed as positive hits only if they also retrieved the human C10orf76 sequence in a reciprocal BLASTp search.

Additional BLASTp and tBLASTn searches were performed using the *S. pombe*, *M.*

polymorpha, and *T. spiralis* C10orf76 orthologues to identify potential divergent sequence in *S.*

cerevisiae, *A. thaliana*, and *C. elegans* respectively, though none of which revealed any positive

hits. An E-value cutoff of 10^{-12} was applied to all searches.

Chapter 3: GBF1 domains HDS1 and HDS2 are required for GBF1 localisation and recruitment

A version of this chapter has been previously published (Quilty, D., C.J. Chan, Y. Katherine, A. Bain, G. Babolmorad, and P. Melançon. 2019. The Arf-GDP-regulated recruitment of GBF1 to the Golgi membranes requires domains HDS1 and HDS2 and a Golgi-localized protein receptor. *Journal of Cell Science*. 132). All copyright belongs to the respective authors.

Initial construction and preliminary testing of the EGFP-tagged GBF1 truncation library was performed in collaboration with Douglas Quilty for my undergraduate degree. Dr. Paul Melançon helped in the planning of experiments, data analysis, and writing of the manuscript. Construction methodology and initial live-cell imaging of the constructs was also described in Douglas Quilty's 2016 doctoral thesis (Quilty, D. 2016. A molecular mechanism for GBF1 recruitment to cis-Golgi membranes. In Department of Cell Biology. Vol. Doctor of Philosophy. University of Alberta, Edmonton, Alberta, Canada. 174). However, none of the data presented as part of that thesis are reproduced here. All data in this chapter were obtained during my time as a graduate student in the Department of Cell Biology, University of Alberta.

3.1 Background and current understanding of GBF1 domain function

As discussed in Chapter 1, mammalian GBF1 is comprised of six evolutionarily conserved domains: DCB, HUS, sec7d, HDS1, HDS2, and HDS3 (Mouratou et al., 2005). Among them, sec7d remains the best characterized; it is the only known catalytic domain in GBF1, and is essential in carrying out the nucleotide exchange reaction that activates Arfs (Goldberg, 1998). Sec7d is also the site of non-competitive inhibition by the fungal toxin, BFA (Mansour et al., 1999; Peyroche et al., 1999). The inhibitory activity of BFA is unique in that the drug does not bind to GBF1 itself, rather *in vitro* studies suggest that the drug fits into a hydrophobic cavity created in the transitory Arf-GDP-sec7d complex, leading to an abortive reaction intermediate. This Arf-GDP-sec7d complex exists in the early stages of the nucleotide exchange reaction prior to the release of GDP, and BFA insertion blocks the conformational change needed to move the catalytic glutamate residue into position to electrostatically expel the bound nucleotide (Mossessova et al., 2003; Renault et al., 2003). As such, BFA treatment has been thought to stabilize GBF1 and Arfs on the membrane, preventing further cycling (Ting-Kuang et al., 2005; Zhao et al., 2006). This stabilization likely contributes to the observed increase in GBF1 at Golgi structures following BFA treatment. Additionally, recruitment is also driven by the accumulation of inactive regulatory Arf-GDP following the global loss of GBF1 activity (Quilty, 2016). However, as mentioned in the introduction, formation of Arf-GDP-sec7d complex *in vivo* remains unclear. Imaging studies have suggested that unlike GBF1, majority of Arfs do not remain trapped at the membrane following BFA treatment (Chun et al., 2008). Other reports using a split YFP assay suggest some Arfs remain in close proximity to membrane “trapped” GBF1 (Ting-Kuang et al., 2005). Likewise, overexpressing GBF1 can allow for increased Arf1 retention at the membrane following BFA treatment, suggesting that some GBF1 may form an

abortive reaction complex with Arf, thus trapping it on the membrane. However, criticisms including whether the reformed YFP may keep GBF1 and Arf in close proximity, and whether the increased retention of Arfs on the membrane reflects an artifact of residual GBF1 activity due to overexpression, have all challenged the interpretation. These observations have raised multiple questions about the mechanistic effects of BFA in living cells. As such, the formation of the GBF1-Arf abortive complex, as well as its stability *in vivo* remains incompletely resolved.

The DCB and HUS domains located at the N-terminus of GBF1 have been previously shown in both mammalian (Ramaen et al., 2007) and plant systems (Grebe et al., 2000) to facilitate dimerization through DCB-DCB and DCB-HUS interactions. Furthermore, previous work has suggested that these domains were involved in facilitating the targeting of GBF1 to ERGIC and Golgi membranes (Bouvet et al., 2013). However, whether the requirement of the DCB and HUS domains were due to their role in dimerization or some other unknown function remains unclear.

The C-terminal half of GBF1 contains the HDS1, HDS2, and HDS3 domains. Protein structure predictions had previously shown HDS1 to contain an amphipathic helix thought to be involved in lipid binding (Bouvet et al., 2013). Tagged HDS1 fragments were shown to bind lipid droplets *in vivo*, artificial phosphatidylcholine droplets *in vitro*, and the lipid droplet protein, adipose triglyceride lipase *in vitro* (Bouvet et al., 2013; Ellong et al., 2011). Mutations on the helix abrogated lipid droplet localisation, further confirming HDS1's role in lipid droplet targeting and lipid binding. Prior to our own study, little research had been done on the further downstream HDS2 and HDS3 domains. Deletion experiments found HDS3 to be dispensable for both Golgi and lipid droplet localisation (Bouvet et al., 2013). Likewise, loss of HDS2 and

HDS3 did not interfere with GBF1's role in polio virus replication or secretion (Belov et al., 2010).

The following subsections will describe the characterization of an EGFP-tagged GBF1 truncation library. By comparing the localization of various GBF1 truncation mutants with and without exposure to the inhibitory drug brefeldin A, we identify domains likely involved in the targeting and recruitment of GBF1 to Golgi membranes.

3.2 Results

3.2.1 HDS1 and HDS2 are involved in targeting GBF1 to the Golgi

To begin characterizing the protein-protein interactions that may facilitate the recruitment and targeting of GBF1 to Golgi membranes, we first began by attempting to determine the minimal domain regions required for Golgi membrane binding. To this end, we developed a GBF1 truncation library using the domain boundaries from a previously published sequence homology study (Mouratou et al., 2005). In this library, each of the six conserved domains and inter-domain regions were progressively deleted, beginning at either the N- or C-terminal ends (Figure 3.1). These constructs are named based on which end of the protein is truncated – N or C – followed by the amino acid residues retained; for example, N885-1856 indicates the deletion of the N-terminal half and that only residues 885-1856 are present. Initial live-cell imaging performed with Douglas Quilty showed that of the 18 truncations examined, only four exhibited a juxtannuclear localisation: N205-1856, N390-1856, N885-1856, and C1-1275. All constructs that lacked either HDS1, HDS2, or both, remained evenly distributed across the cytosol and failed to localise to any clear cellular structures. These observations led to two conclusions: HDS1 and HDS2 may be essential for membrane binding, and the catalytic Sec7d may be dispensable. However, without a Golgi marker, we were unable to confirm that the juxtannuclear

localisation of these constructs corresponded to the Golgi. Likewise, we were unable to confirm whether the Golgi was disrupted by any of the constructs that appeared strictly cytosolic.

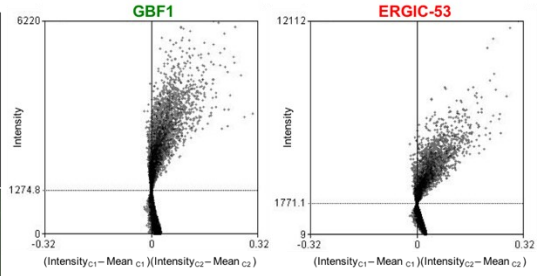
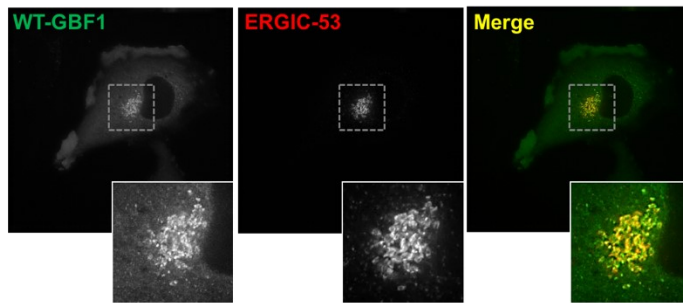
To extend this initial work, we generated an mCherry-ERGIC53 marker for use in new live-cell co-localisation studies with the EGFP-tagged GBF1 truncations. This marker was co-transfected with each of the EGFP-tagged GBF1 truncations, full length EGFP-GBF1, or EGFP alone. Similar to the initial live-cell imaging, we found that N205-1856, N390-1856, N885-1856, and C1-1275 all exhibited clear co-localisation with the mCherry-ERGIC53 marker (Figure 3.2). This confirmed the original live-cell findings that HDS1 and HDS2 appear essential for targeting of GBF1 to early Golgi structures. To further confirm co-localisation, we utilized Li's intensity correlation quotients (ICQ), which ranges from -0.5 for asynchronous patterns and 0.5 for complete overlap. This technique was chosen over other common methods as ICQ measures changes in intensity rather than overlap in signal. Consequently, the method is largely insensitive to any potential erroneous overlap between ERGIC53 and any non-membrane-bound EGFP-tagged protein in the cytosol. The average ICQ values observed for N205-1856, N390-1856, N885-1856, and C1-1275 are 0.266, 0.320, 0.300, and 0.300 respectively (Figure 3.1). These values are comparable to the average ICQ observed with the EGFP-tagged WT GBF1 plasmid (0.333) and vastly different from the average ICQ for EGFP alone (0.026). ICQ values for truncations that failed to localize to the Golgi were not measured. A summary figure of the co-localisation analysis can be found in figure 3.1 and the images for N205-1856, N390-1856, N885-1856, and C1-1275 along with the corresponding intensity plots in figure 3.2. Using the mCherry-ERGIC53 marker, we were also able to confirm that the Golgi remained intact in cells transfected with truncations that failed to be targeted to any clear membrane structures (Figure 3.3). Together, these observations suggest that these truncations did not interfere with Golgi

function or maintenance. Lastly, we performed western blots with an antibody recognizing the EGFP-tag (Figure 3.4). We were able to verify the truncation sizes, suggesting that the lack of localization to the Golgi is not due to poor protein stability and the cleavage of the EGFP-moiety from the GBF1 truncation. Smaller truncations appear to be expressed at higher levels as observed by western blotting. However, cells of similar expression levels were selected for imaging experiments shown in figure 3.2 and 3.3.

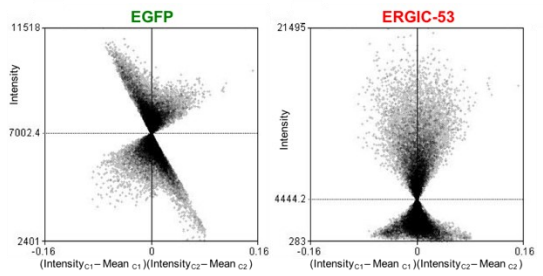
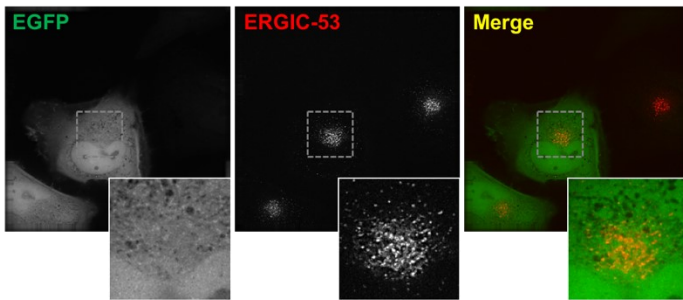
	Sequence Depiction	Co-localization w/ ERGIC53	Average ICQ
WT-GBF1		✓	0.333
	EGFP tag alone	X	0.026
N205-1856		✓	0.266
N390-1856		✓	0.320
N565-1856		X	
N656-1856		X	
N885-1856		✓	0.300
N1065-1856		X	
N1276-1856		X	
N1533-1856		X	
N1645-1856		X	
		X	
		X	
		✓	0.300
		X	
		X	
		X	
		X	
		X	
		X	

Figure 3.1 Colocalization and average intensity correlation analysis of GBF1 truncations. (Left) Cartoon depiction of the pEGFP-GBF1 truncation library highlighting the domains and inter-domain regions each construct contains. (Middle and Right) HeLa cells were co-transfected with the corresponding EGFP-GBF1 truncation and mCherry-ERGIC53. Images were acquired by live-cell wide-field fluorescence microscopy, and constructs that exhibited clear co-localisation with the ERGIC53 marker across three independent replicates are indicated with a checkmark (Middle). For constructs exhibiting clear co-localisation, further analysis was performed using Li's intensity correlation quotients (Right). A minimum of 35 cells were examined. The average ICQ is obtained from several images like those in Figure 3.2. (n=3).

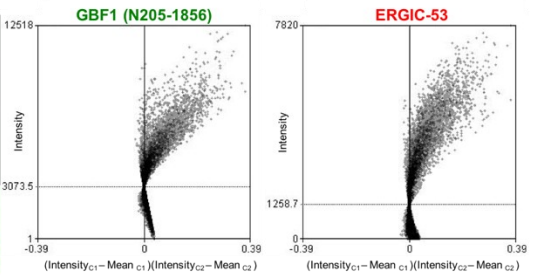
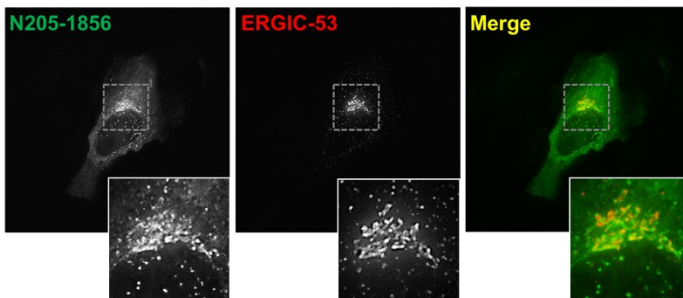
WT-GBF1



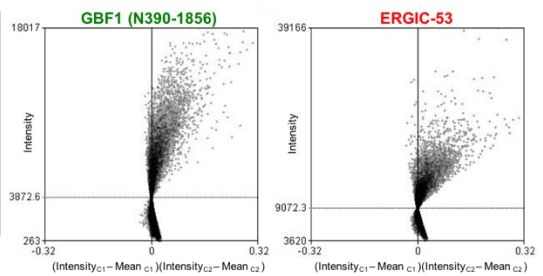
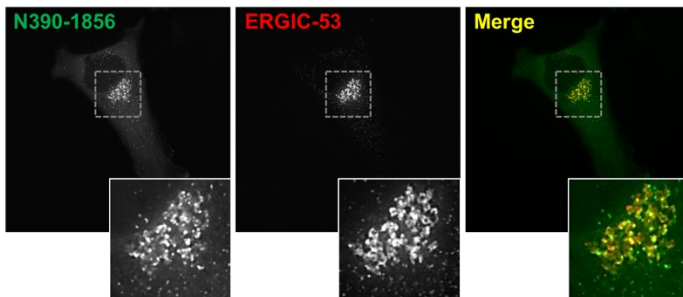
EGFP



N205-1856



N390-1856



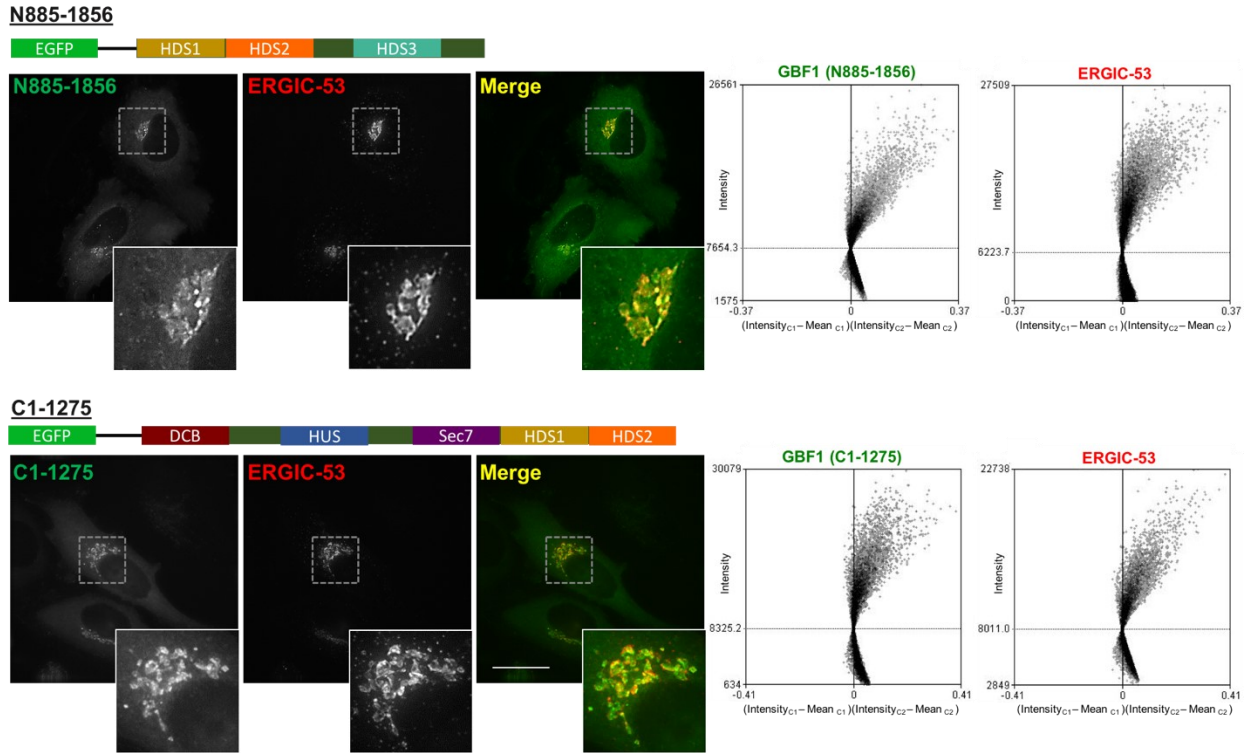
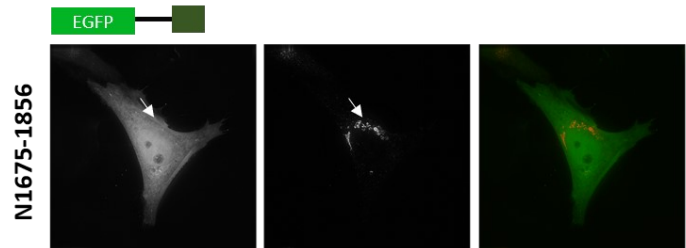
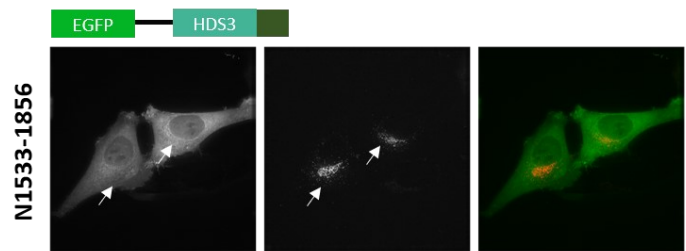
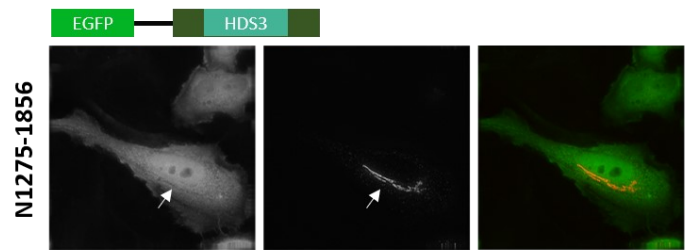
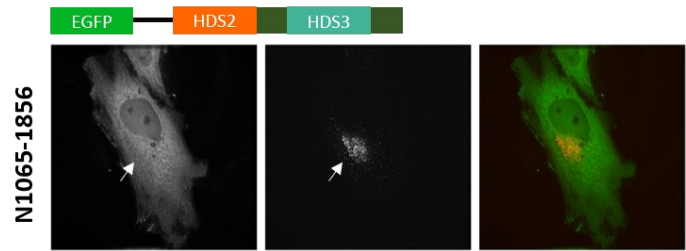
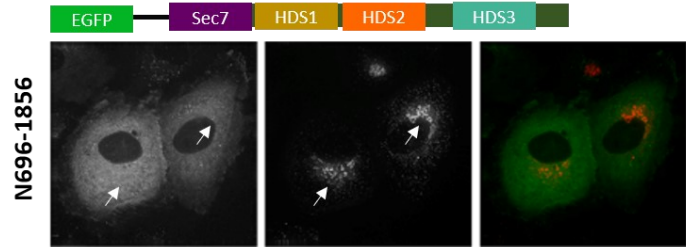
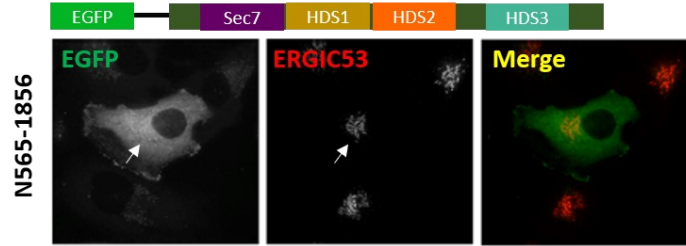


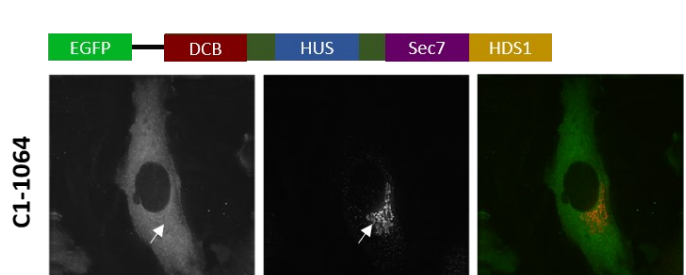
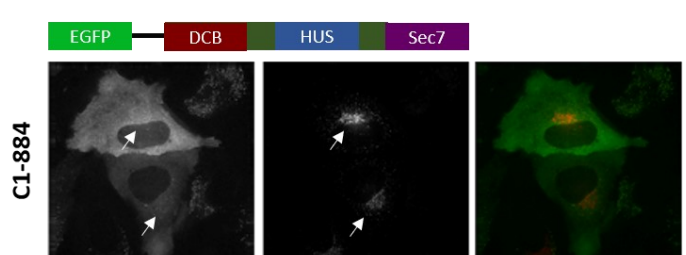
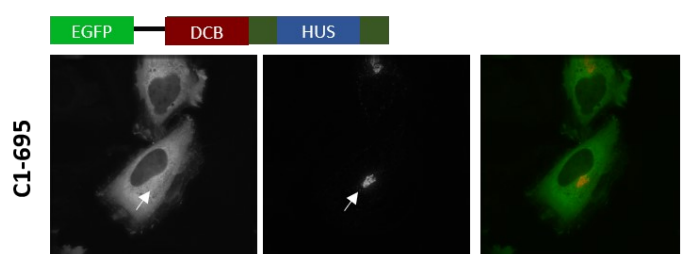
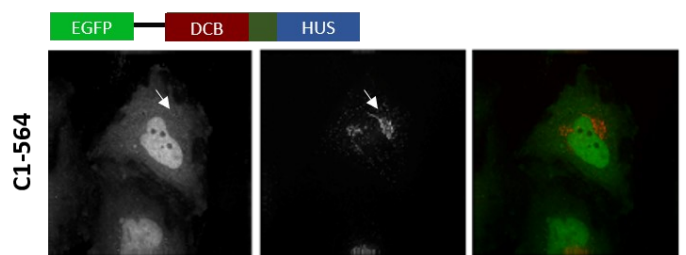
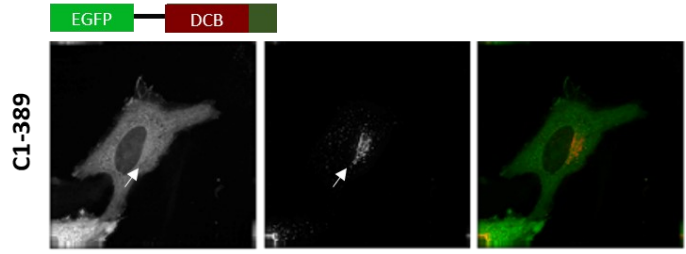
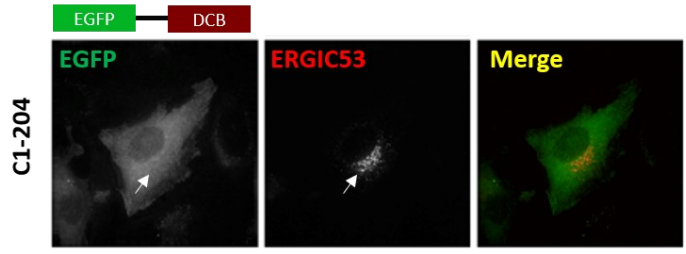
Figure 3.2 N205-1856, N390-1856, N885-1856, and C1-1275 localise to mCherry-ERGIC53-positive Golgi structures.

(Left) Images of live HeLa cells co-transfected with mCherry-ERGIC53, and plasmid encoding one of the following: GBF1, EGFP, N205-1856, N390-1856, N885-1856, or C1-1275. Schematic of the relevant construct is shown above each set of images. Live-cell images are shown as Z-projections. Image shown is representative of 35 cells examined across three independent biological replicates. Scale bar = 26 μm . Enlarged insets represent a 2.5x magnification. (Right) Li's intensity correlation plots of the corresponding representative cell shown on the left. Plots represent the comparison of EGFP and mCherry signal intensities against their respective $(\text{Intensity}_{C1} - \text{Mean}_{C1}) (\text{Intensity}_{C2} - \text{Mean}_{C2})$ values.

Full Length



Full Length



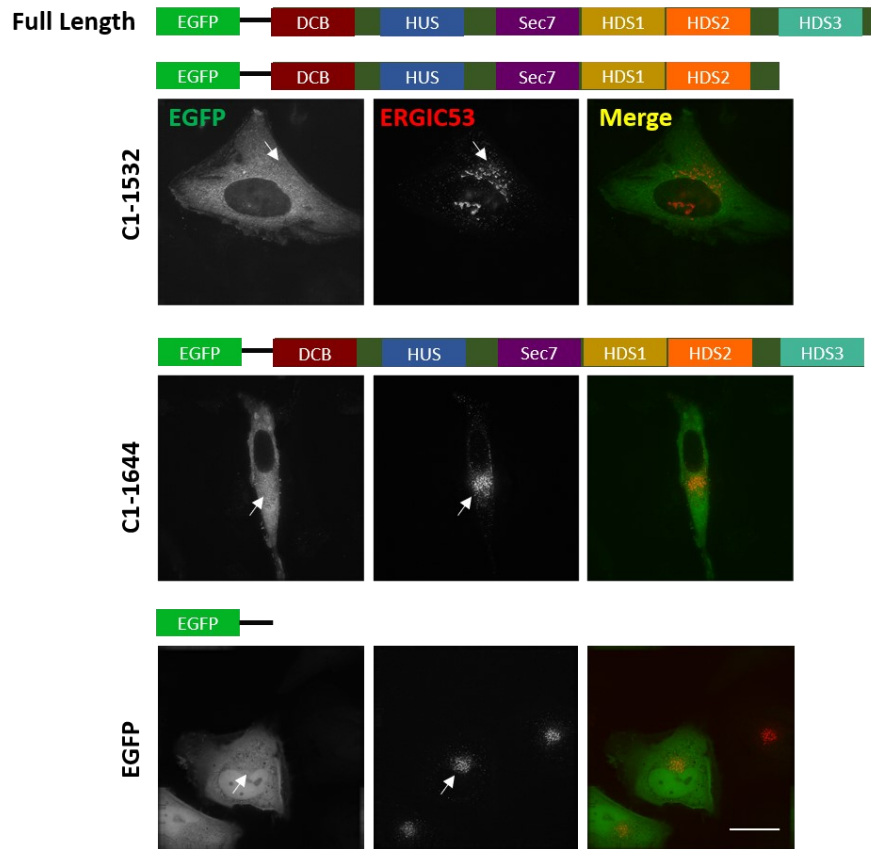


Figure 3.3 GBF1 truncations lacking HDS1 or HDS2 fail to co-localise with mCherry-ERGIC53.

Images of live HeLa cells co-transfected with N565-1856, N656-1856, N1065-1856, N1275-1856, N1533-1856, 1645-1856, C1-204, C1-389, C1-564, C1-695, C1-884, C1-1064, C1-1532, C1-1644, or EGFP alone and mCherry-ERGIC53. Live-cell images are representative of 35 cells examined for each construct over three independent biological replicates. Images are shown as Z-projections. Schematic of the relevant construct is shown above each set of images. None of the cells examined exhibited clear co-localisation with the mCherry-ERGIC53 marker. White arrows point to ERGIC-53 signal in the mCherry channel (middle images), but no corresponding accumulation of EGFP signal is observed in the EGFP channel. (left images). All images are shown as a projection of Z-slices. (n=3). Scale bar = 26 μ m.

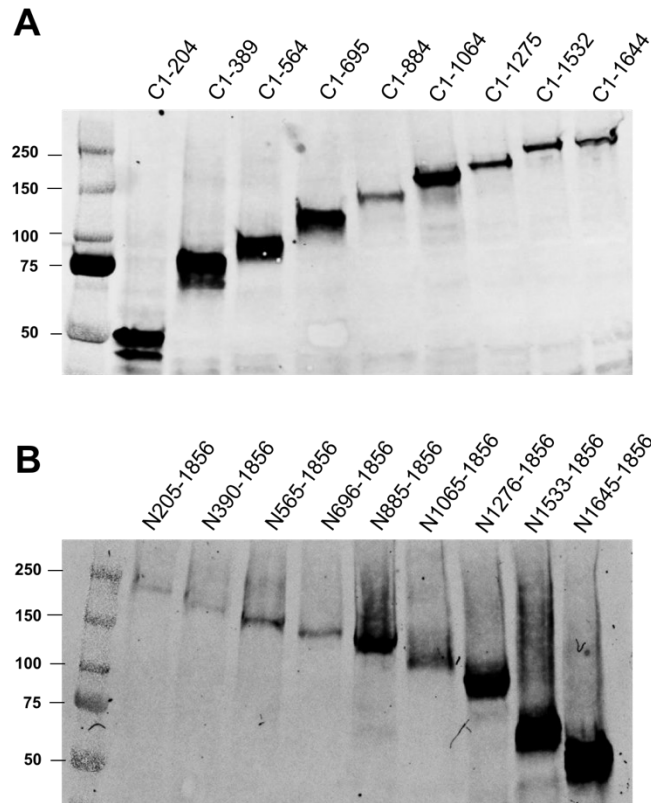


Figure 3.4 Western blotting confirms protein size for EGFP-tagged GBF1 truncations.

Both N and C-terminally truncated GBF1 constructs were expressed in HeLa cells and lysates collected after 18 hours for western blotting. Blots were probed with anti-EGFP antibodies to determine the size of the EGFP-tagged proteins. Numbers on the left side of the blots indicate molecular weight in kilodaltons. No obvious degradation products are observed for any of the truncations suggesting that the lack of localization observed for some constructs is likely not due to the separation from the truncation from the EGFP moiety. n = 1.

3.2.2 Interaction between HDS1, HDS2, and the membrane is sensitive to formaldehyde fixation

Additional confirmation in the form co-localisation with the mCherry-ERGIC53 marker and ICQ analysis was performed in part because the initial observation that HDS1 and HDS2 were essential in membrane binding, conflicted with previously published observations. Jackson and colleagues had shown that deletion of the DCB and HUS domains impaired GBF1 localisation to ERGIC and Golgi structures, initially suggesting that dimerization via the DCB and HUS may be essential for membrane targeting (Bouvet et al., 2013). However, our observations found that the DCB and HUS domains were dispensable (see N390-1856 in Figure 3.2). Upon further examination in live-cells, we discovered that formaldehyde fixation interfered with Golgi targeting of DCB- and HUS-deletion truncations (Figure 3.5). Previous observations by Bouvet et al. relied strictly on data collected from fixed cells. Across three independent replicates, fixation in 4% paraformaldehyde appeared to abrogate Golgi localisation for truncations N205-1856, N390-1856, and N885-1856 – which all lacked DCB, HUS, and/or sec7d. We speculate that observations previously reported for DCB- and HUS- deletion truncations likely resulted from a fixation artefact. Our findings suggest that the N-terminal half of GBF1 is dispensable for localisation and that membrane targeting requires strictly HDS1 and HDS2. The discrepancy observed in the imaging of the GBF1 truncations convinced us to rely solely, where possible, on live-cell imaging methods to avoid potential pitfalls resulting from fixation artefacts.

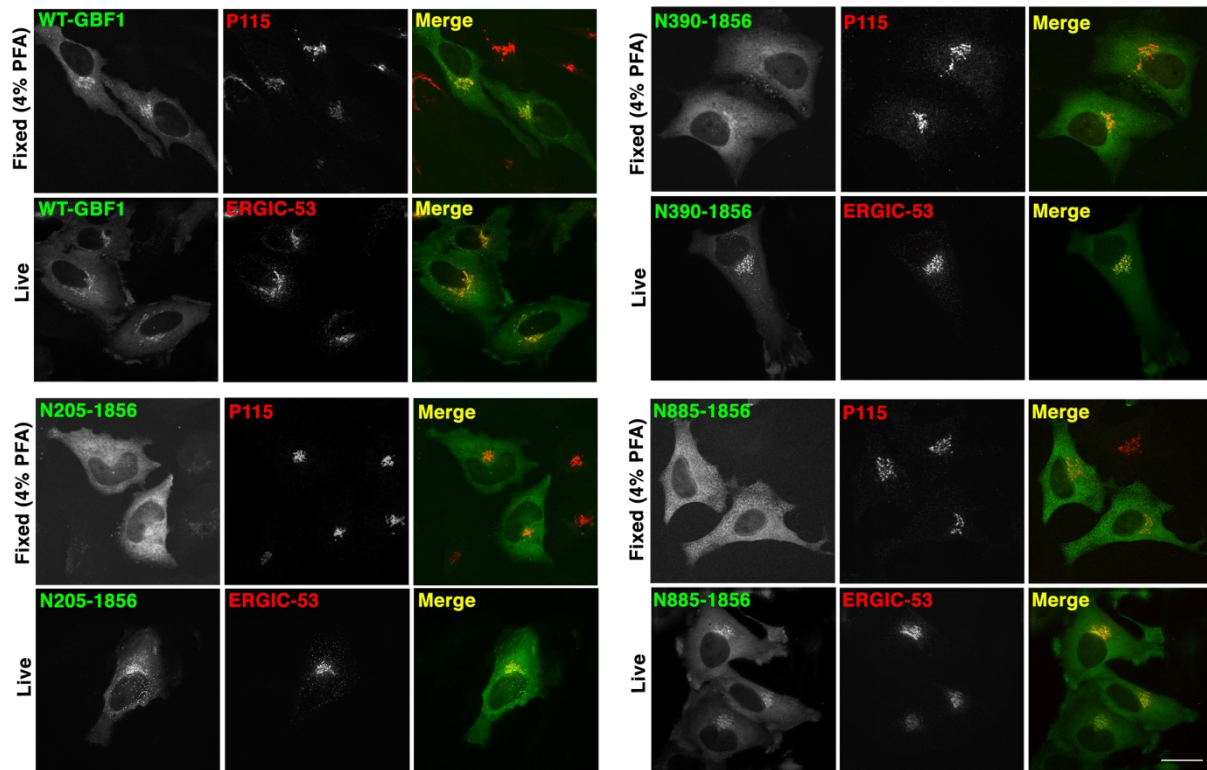


Figure 3.5 Localisation of GBF1 truncations appears sensitive to formaldehyde fixation. HeLa cells were transiently transfected with EGFP-tagged forms of full length GBF1, N205-1856, N390-1856, or N885-1856, and fixed in 4% paraformaldehyde and stained for the cis-Golgi marker p115. Alternatively, HeLa cells were co-transfected with the same EGFP-tagged GBF1 constructs and mCherry-ERGIC53. Cells were then subjected to wide-field fluorescence microscopy. While in live cells the N205-1856, N390-1856, and N885-1856 mutants exhibit clear colocalisation with the Golgi marker, no juxtannuclear localisation is observed in the fixed samples. Images are shown as a projection of all Z-slices. (n=3). Scale bar = 26 μ m.

3.2.3 HDS1 and HDS2 domains alone fail to localise to Golgi structures

Having identified HDS1 and HDS2 as likely being essential for membrane binding, we proceeded to determine whether these domains together were sufficient to target the protein to Golgi structures. Using a cloning strategy similar to that used for the GBF1 truncation library, we generated a EGFP-GBF1-885-1275 mutant containing only the HDS1 and HDS2 domains. When expressed in live-cells, the EGFP-tagged peptide failed to exhibit clear recruitment to a juxtannuclear structure and co-localisation with the mCherry-ERGIC53 marker (Figure 3.6). To confirm that the truncated protein could not be recruited to Golgi structures, we performed an additional experiment treating the live-cells with 10 $\mu\text{g}/\text{mL}$ BFA for 90 seconds. As mentioned, BFA is a potent inhibitor of GBF1 activity and can be used to stimulate GBF1 recruitment to Golgi membranes and ERGIC structures (Quilty et al., 2014; Zhao et al., 2006). However, while full length GBF1 was clearly recruited to both a juxtannuclear site and to cytosolic peripheral punctate or ERGIC structures upon BFA treatment, no obvious recruitment was observed with the 885-1275 mutant.

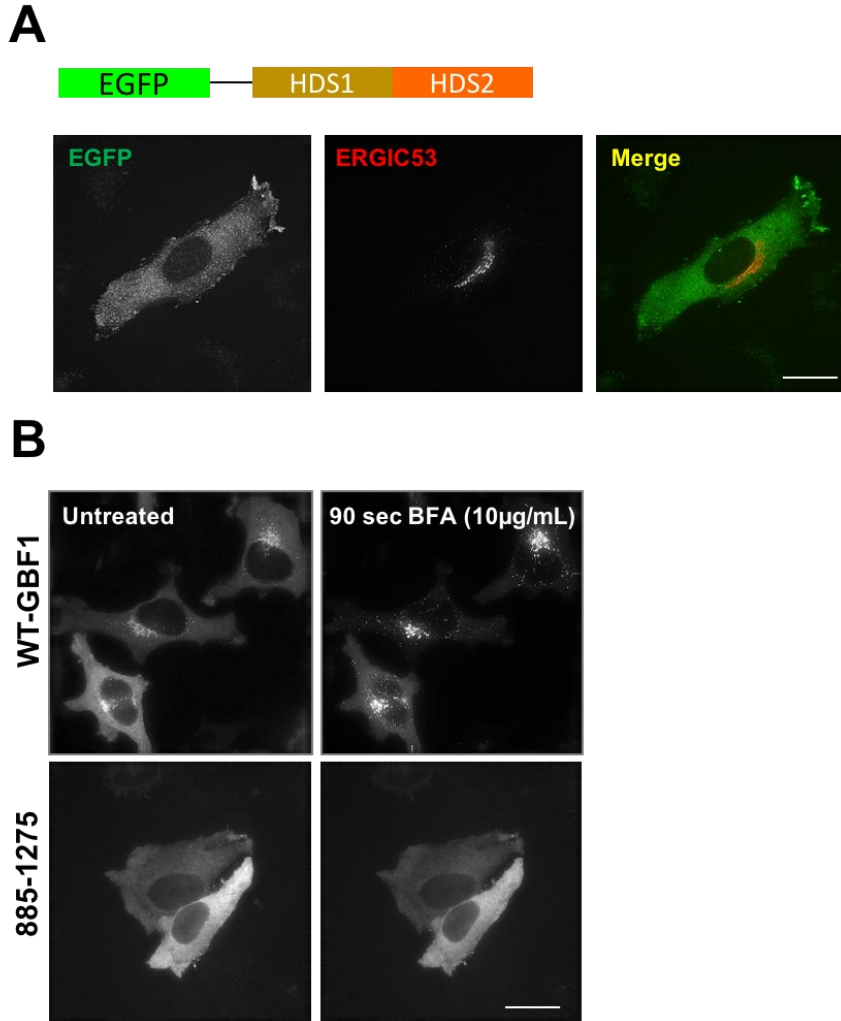


Figure 3.6 HDS1 and HDS2 domains alone fail to localise to Golgi structures.

A cartoon depiction illustrating the EGFP-tagged GBF1-885-1275 mutant is shown at the top. (A) Co-transfection of HeLa cells with mCherry-ERGIC53 and the EGFP-tagged 885-1275 GBF1 mutant. Under live-cell imaging, no clear co-localisation of the GBF1 mutant and the Golgi marker can be observed. Images are representative of 15 cells examined over three replicates and shown as projection of all Z-slices. (B) HeLa cells transfected with either the EGFP-tagged WT GBF1 or EGFP-tagged GBF1-885-1856 mutant were imaged in live-cells before and after a 90 second treatment with 10 $\mu\text{g}/\text{mL}$ BFA. While WT GBF1 was clearly recruited to juxtannuclear and peripheral punctate sites, no obvious changes in distribution was observed for the 885-1275 mutant. Images are representative of 15 cells examined over three replicates and shown as a projection of all Z-slices. Scale bar = 26 μm .

3.2.4 The catalytic Sec7d is not required for the active recruitment of GBF1 to the Golgi

To further characterize the recruitment of GBF1 to Golgi membranes, we chose to perform additional experiments to determine whether any of the Golgi-localised GBF1 truncations could be actively recruited to the Golgi upon treatment with BFA. The Golgi-localised truncation – N885-1856 – lacking *sec7d* was of particular interest, because BFA is a known uncompetitive inhibitor of the *sec7d* catalytic site, and can trap GBF1 on the membrane (Ting-Kuang et al., 2005; Zhao et al., 2006). Previous *in vitro* studies have suggested that the accumulation of GBF1 occurs through production of abortive GBF1-Arf-GDP complexes at the membrane. Other studies have since revealed that recruitment is also driven by an increase in Arf-GDP (Quilty et al., 2014). However, it remains unclear which domains regulatory Arf-GDP directly or indirectly acts upon to stimulate recruitment. Expression of the EGFP-tagged GBF1 truncations in live-cells before and after a 90 second treatment with 10 µg/mL BFA in DMSO revealed that all Golgi-localised truncations remained BFA sensitive (Figure 3.7). The fold increase at the Golgi after BFA treatment was quantified and displayed in panel B. Just as importantly, no increase in GBF1 membrane binding was observed in control cells treated with only DMSO. As before, we found that the catalytic *sec7d* is not essential in either the targeting of GBF1 to the Golgi, or for its active recruitment upon stimulation with BFA. Furthermore, the data illustrate that regulatory Arf-GDP likely acts either directly or indirectly on a domain other than *sec7d*. Instead, both localisation and recruitment of GBF1 to Golgi membranes likely occurs through HDS1 and HDS2.

However, interestingly, we found that none of the cells expressing the EGFP-N885-1856 truncation exhibited a clear recruitment to peripheral punctate or ERGIC structures upon BFA treatment. Cells expressing either the WT or the C1-1275 truncation – which contain DCB, HUS,

and sec7d – displayed recruitment to both a juxtannuclear site, and to peripheral punctate structures reminiscent of ERGIC.

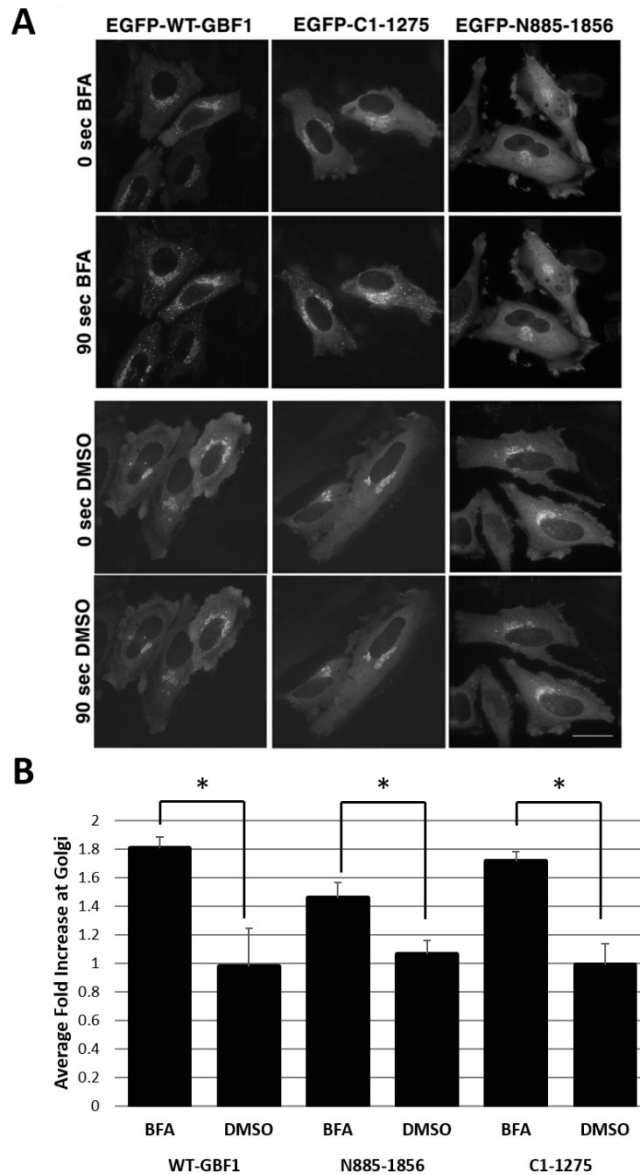


Figure 3.7 BFA stimulates Golgi recruitment of GBF1 truncations.

HeLa cells were transfected with plasmids encoding either EGFP-tagged WT GBF1, N885-1856 or C1-1275, and then imaged before and 90 seconds after the addition of BFA (10 $\mu\text{g}/\text{mL}$) using live-cell wide-field fluorescence microscopy. (A) Representative images from 15 cells across three independent replicates are displayed as a project of all Z-slices. Scale bar = 26 μm . (B) Fraction of GBF1 on juxtannuclear structures were quantified using images from panel A (15 cells over three independent replicates) as described in Chapter 2. Average fold increase in signal at existing GBF1 positive juxtannuclear Golgi sites are displayed \pm standard deviation. Statistical significance between BFA treated and DMSO treated cells was measured as described in Chapter 2 by a two-tailed unpaired *t*-test (WT-GBF1 $p = 0.0322$; N885-1856 $p = 0.0432$; C1-1275 $p = 0.0348$).

3.3 Discussion

3.3.1 DCB, HUS, Sec7ds are not needed for GBF1 localisation or recruitment to Golgi membranes

Previous data from our laboratory demonstrated that GBF1 recruitment to the Golgi requires, at least in part, a membranous protein component. To begin characterizing this putative protein-protein interaction, we began by generating a GBF1 truncation library to identify the minimal Golgi-binding domain(s) of GBF1. As described in the results, we found that the N-terminal half of GBF1, including the DCB and HUS domains (which were previously shown to facilitate GBF1 dimerization) and the catalytic sec7d, were all dispensable for localisation and recruitment (Figure 3.1 and 3.2). These observations were surprising as previous reports had indicated that the DCB and HUS domains were required for Golgi binding (Bouvet et al., 2013). However, these experiments were performed in fixed cells and likely did not capture the true localisation of the truncations. As we found, fixation with paraformaldehyde appears to interfere with the membrane interaction of the truncated GBF1 constructs (Figure 3.5). However, the cause of this sensitivity to formaldehyde is unclear. The observation may indicate that the nature of the membrane interaction between WT full length GBF1 and that of our truncated forms differ. While fixation is rapid, it is not instantaneous (Hoffman et al., 2015). Formaldehyde crosslinking is exothermic and can distort protein shape and cell structure. The loss of the N-terminal domains may weaken the already transient interaction between GBF1 and the membrane, leading to rapid dissociation upon treatment with paraformaldehyde. The stability of the interaction and the cycling dynamics of the GBF1 truncations on and off the membrane could be further examined using techniques such as FRAP.

The dispensability of the DCB and HUS domains also suggests that dimerization is non-essential for recruitment. No other domains apart from DCB and HUS has been implicated in

facilitating dimerization. This finding is supported by a recent report that mutations in the DCB domain abrogating GBF1 dimerization had no effect on localisation or function of GBF1 (Bhatt et al., 2016). Rather, dimerization appears to increase protein half-life, suggesting that dimerization through the DCB and HUS domains may regulate protein degradation.

3.3.2 HDS1 and HDS2 are likely essential in targeting GBF1 to Golgi membranes

Using live-cell imaging, we demonstrated that the loss of either HDS1 or HDS2 impaired the targeting and recruitment of GBF1 to Golgi membranes (Figure 3.1, 3.2, and 3.3). Previous reports had already established the role of HDS1 as a lipid binding domain and it was not surprising to find its deletion impaired Golgi localisation. Recent studies have further demonstrated that HDS1 functions as a phosphoinositide binding domain similar to the pleckstrin homology domain present in the smaller GEFs (Meissner et al., 2018). HDS1 appears to preferentially bind PI4P and PI4,5P₂. Mutations in amino acid residues 926 and 927 (LF to AA) of HDS1 disrupting a hydrophobic helix impaired GBF1 localisation to Golgi structures. This observation aligns well with another published study which found that pharmacological inhibitors of PI4P production reduced the quantity of observable GBF1 at the Golgi (Doiron-Dumaresq et al., 2010).

Our finding that HDS2 was also involved became recently supported by additional studies performed in both mammalian cell culture and zebrafish. In a zebrafish *N*-ethyl-*N*-nitrosourea mediated mutagenesis screen, researchers identified a mutation in HDS2 that lead to impaired Golgi localization and lethal vascular embryonic defects (Chen et al., 2017). Introduction of the L1246R mutation in mammalian cells also impaired GBF1 localisation to Golgi structures, impaired Golgi maintenance, and disrupted cell secretion and viability (Pocognoni et al., 2017).

However, when we tried to confirm that HDS1 and HDS2 alone were sufficient to target the protein to Golgi structures, we failed to observe the 885-1275 GBF1 truncation localising to a juxtannuclear site – even in the presence of BFA (Figure 3.6). One possibility could be that the truncation simply failed to fold into the proper conformation needed for membrane interaction. No crystal structure has yet been published for GBF1, and it is unclear whether each domain can fold into stable tertiary structures independently. In fact, many of the larger peptides in the truncation library containing HDS1 and HDS2 also failed to localise to Golgi structures. This includes N565-1856 and N696-1856 which contains all the domains present in the Golgi-localised N885-1856, as well as C1-1644 and C1-1532, which contains all the domains present in the Golgi-localised C1-1275. These truncations contained more than the minimum binding regions identified, and in theory should be capable of interacting with Golgi membranes. Their failure to do so may indicate some sort of altered tertiary structure: the additional peptide sequences either interfered with membrane interactions or interfered with folding. Another possibility could be the presence of negative regulation or inhibition. Additional domains may be required to relieve negative regulation present in the 885-1275 truncation containing only HDS1 and HDS2. Likewise, this may also explain why other truncations which contain the minimum binding region also failed to localise to the Golgi. Previous studies have attempted to identify GBF1 localisation domains by expressing domains independently (Bouvet et al., 2013). These authors found that neither HDS1 nor HDS2 alone localized to Golgi structures. Rather, HDS1 was shown to be targeted to lipid droplets, suggesting that it is sufficient to target GBF1 to these organelles. However, in terms of Golgi targeting, similar to our own work, the negative data observed in these studies cannot be readily interpreted.

Nonetheless, our findings confirm that DCB, HUS, *sec7d*, and HDS3 are all largely dispensable for localisation and recruitment, suggesting that HDS1 and HDS2 are essential. However, these domains may not be sufficient, as HDS1 and HDS2 alone fail to localize to Golgi structures. These negative data cannot rule out potential misfolding or other regulatory interactions between GBF1 domains.

3.3.3 *Sec7d* is not required for additional recruitment of GBF1 to Golgi structures

Using live-cell imaging we were also able to observe a clear recruitment of the N885-1856 truncation to juxtannuclear structures upon treatment with BFA (Figure 3.7). This was surprising as it lacked the catalytic *sec7d* that interacts with the drug. *In vitro* studies had argued that BFA causes an accumulation of membrane-bound GBF1 due to the formation of abortive GBF1-Arf-GDP complexes. Unable to complete the nucleotide exchange reaction, GBF1 remains trapped on the membrane (Ting-Kuang et al., 2005). However, previous work in our laboratory had shown that the recruitment of GBF1 to Golgi membranes can be promoted by the accumulation of regulatory Arf-GDP in the cell, a natural downstream effect of the inhibition of GBF1 by BFA (Quilty et al., 2014). Our observation that truncations lacking *sec7d* but containing both HDS1 and HDS2 could be recruited, supports the model that Arf-GDP can stimulate recruitment and suggests that HDS1 and HDS2 are involved. Whether the regulatory Arf-GDP acts on GBF1 itself or the putative membrane receptors to alter GBF1 recruitment is unclear. Identification of the putative receptor would allow for additional studies into how GBF1 affinity may be modulated by regulatory Arf-GDP.

Also of note is the lack of clear recruitment of N885-1856 to peripheral punctate or ERGIC structures where GBF1 also functions (Figure 3.7). In none of the cells examined did we observe a recruitment of N885-1856 to any obvious punctate structures. Substantial amount of

EGFP-tagged N885-1856 also remained in the cytosol. This observation is reflected in a lower quantified average fold increase at the Golgi upon BFA treatment, as compared to the WT GBF1 and C1-1275 truncations; both of which exhibited an increase of GBF1 at the Golgi and peripheral punctate sites, as well as a depletion of the cytosolic GBF1 pool (Figure 3.7). The residual cytosolic pool observed in the N885-1856 mutant could indicate that the protein may not be trapped at the Golgi in the same way due to the loss of *sec7d*. As mentioned previously, the inhibitory mechanism of BFA is thought to involve the stabilization of GBF1 at the membrane – potentially through the formation of a GBF1-Arf-GDP complex (Ting-Kuang et al., 2005; Zhao et al., 2006). However, without *sec7d*, the N885-1856 mutant, likely cannot be stably held at membrane sites, and may continue to cycle, as indicated by the presence of a cytosolic pool even upon treatment with BFA. FRAP experiments could be performed to test this hypothesis. This retained cytosolic pool may also mask recruitment to peripheral ERGIC structures. To determine whether the loss of the N-terminal domains may have interfered with ERGIC recruitment, additional experiments may prove useful. For instance, the quantity of EGFP-tagged N885-1856 could be measured through western blotting on enriched ERGIC membranes isolated from BFA treated cells using subcellular fractionation (Breuza et al., 2004).

3.3.4 GBF1 localisation to other membrane sites

While our work focused largely on the recruitment of GBF1 to Golgi structures due to the prominent role GBF1 plays in maintaining the organelle, the question of how GBF1 is recruited to other membrane sites remain a major unresolved topic in the field. As discussed previously, apart from Golgi and ERGIC structures, GBF1 also functions at numerous other cellular locations. At lipid droplets, GBF1 and its substrate, Arf1, is thought to regulate lipid metabolism through the COPI-dependent transport of surface proteins: including the triglyceride lipase

ATGL, and perilipin PLIN2 (Ellong et al., 2011; Kaczmarek et al., 2017). At the mitochondria, GBF1 regulates organelle positioning in a COPI-independent manner (Walch et al., 2018). At the cell periphery, GBF1 and Arf1 function in the clathrin-independent carriers/GPI-anchored protein enriched endosomal compartments (CLIC/GEEC) pathway – a form of clathrin and dynamin-independent endocytosis (Gupta et al., 2009). The numerous roles and localisation of GBF1 begs the question: how is the requirement for GBF1 at each of these sites differentially regulated? Previous data from our laboratory have shown that recruitment to Golgi membranes requires at least in part, a protein component, potentially suggesting that differentially localised membrane proteins may contribute to this regulation (Quilty et al., 2019). Our data here further suggest that at least for the Golgi, this interaction likely occurs through HDS1 and HDS2. Further work can be performed to confirm this upon identification of receptor components. Other reports have shown that interaction with lipid droplets is dependent on HDS1 (Bouvet et al., 2013). Using our truncation library, additional studies can be performed to identify whether similar domains are involved in the targeting of GBF1 to mitochondrial and plasma membrane sites. Understanding the interactions that regulate GBF1 localisation and recruitment to multiple cellular locations will be critical in developing a model for how GBF1 localisation and activity is regulated in a cell-wide context.

Chapter 4: Analysis of Golgi fractions obtained from proximity biotinylation with GBF1 chimera identifies unique proximal partners

A version of this chapter has been previously published (Chan, C.J., R. Le, K. Burns, K. Ahmed, E. Coyaud, E.M.N. Laurent, B. Raught, and P. Melançon. 2019. BioID performed on Golgi-enriched fractions identify C10orf76 as a GBF1 binding protein essential for Golgi maintenance and secretion. *Molecular & Cellular Proteomics*. 18:2285-2297). All copyright belongs to the respective authors.

Initial construction and characterization of the BirA*-FLAG and BirA*-FLAG-GBF1 cell lines, preparation of samples for mass spectrometry, and the shRNA screen was done with the help of undergraduate student Roberta Le. Mass spectrometry and SAINT analysis was performed by Dr. Etienne Coyaud and Estelle M.N. Laurent in Dr. Brian Raught's lab in the Department of Medical Biophysics at the University of Toronto, Toronto, ON, Canada. Several reagents were provided by Drs. Nicolas Touret and Ing Swie Goping. Dr. Paul Melançon helped in the planning of experiments, data analysis, and writing of the manuscript.

4.1 Background on BioID and rationale for using a Golgi enrichment procedure

4.1.1 Known GBF1 interactors and the putative GBF1 receptor

As discussed in Chapters 1 and 3, previous *in vitro* evidence argues for the existence of membrane-associated protein components that regulate GBF1 binding and recruitment to Golgi membranes (Quilty et al., 2019). In the previous chapter, we were able to further understand GBF1 membrane binding and recruitment by identifying two domains – HDS1 and HDS2 – that appear to be involved. However, due to the transient nature of GBF1's interaction with the membrane, the identification of putative GBF1 regulators has proven challenging. Yeast two-hybrid and immunoprecipitation assays performed in mammalian cell and yeast models have had some success in identifying GBF1 interactors. These include GMH1, GGAs, Rab1b, and the Rab1b effector, p115. However, none these identified interactors have been found to be essential in GBF1 localisation or recruitment.

GMH1 is a Golgi-localised protein with unknown function whose depletion has no observable impact on GBF1 localisation (Chantalat et al., 2003). The GGAs are TGN localised and their recruitment to TGN membranes appears to require GBF1 activity, not the other way around (Lefrançois and McCormick, 2007).

Rab1b and p115 are the only two interactors to have substantial evidence suggesting an involvement in GBF1 regulation. Rab1b binds directly to the N-terminal half of GBF1 (sequences upstream of Sec7, a region we had previously shown to be dispensable for membrane targeting and recruitment) and its constitutive activation appears to recruit additional GBF1 to peripheral ERGIC structures. Furthermore, interfering with the interaction between GBF1 and the Rab1 effector, p115, using competing peptides lead to Golgi disassembly (Sztul and García-Mata, 2003). However, neither protein appears essential for the targeting of GBF1 to Golgi

membranes, indicating that additional unidentified protein components are likely involved.

Despite the moderate success of co-immunoprecipitation approaches in the past, a more sensitive technique was needed to expand our understanding of GBF1 interactors and regulators.

4.1.2 Proximity-based biotinylation approaches to studying the GBF1 interactome

Recent developments in the study of protein-protein interactions has led to the popularization of two highly sensitive techniques – BioID and APEX (Chen and Perrimon, 2017; Roux et al., 2013; Trinkle-Mulcahy, 2019). Both methods rely on the tagging of a protein of interest to an enzyme that produces reactive biotin derivatives which label proteins in close proximity. Biotin labeled proximal proteins can then be pulled down, identified by mass spectrometry, and differentiated from background by subtracting candidates detected from control samples. BioID and APEX are advantageous over traditional affinity purification approaches for several reasons: 1) they capture transient and weak interactions that may be lost during purification, 2) they can identify both soluble and insoluble proteins, and 3) the strength of interaction between biotin and streptavidin allows for efficient protein extraction and stringent washing to remove background contaminants. Over a 100 publications have since utilized BioID and APEX techniques for the study of protein interactomes across multiple model systems (Trinkle-Mulcahy, 2019).

In BioID, the enzyme is a mutant biotin ligase, BirA* derived from *Escherichia coli*. WT BirA in bacteria facilitates the specific biotinylation of the biotin-dependent enzyme, acetyl-CoA carboxylase. The R118G mutation in the catalytic site of the ligase (BirA*) impairs its ability to retain activated biotin (Biotin + ATP → biotinyl-5'-AMP + PPi), which then dissociates from the mutant ligase and becomes free to react with primary amine residues on nearby lysines of neighbouring proteins – thus rendering the ligase promiscuous. BioID analysis of the well-

studied nuclear pore complex suggests a limited labeling radius of 10 nm for BirA* (Kim et al., 2014).

APEX, on the other hand, utilizes an engineered ascorbate peroxidase derived from plants. The enzyme catalyzes the oxidation of supplemented biotin-phenol into biotin-phenol radicals in the presence of hydrogen peroxide. The biotin-phenol radical can then react with electron rich amino acids in neighbouring proteins such as tyrosines, tryptophans, cysteines, and histidines. Unlike BirA*, the labeling distance of the reactive biotin molecules appears to be longer, at approximately 20 nm as measured in electron microscopy experiments (Martell et al., 2012).

BioID was chosen specifically for our study of the GBF1 interactome because of its gradual and continuous labeling of proximal partners *in vivo*. APEX requires the treatment of cells with biotin phenol for 30 minutes followed by hydrogen peroxide for 1-5 minutes to induce biotinylation. As illustrated in the previous chapter, GBF1 localisation appears to be highly sensitive to chemical stressors. To avoid conditions that may interfere with the labeling of GBF1 proximal partners on the membrane – such as treatment with high concentrations of hydrogen peroxide – we opted to use BioID instead.

To further enhance our chances of capturing membrane specific regulatory factors, we chose to adopt an additional Golgi enrichment step in the BioID procedure developed by Roux et al. (2013). Previous data have shown that enriched Golgi fractions were capable of recruiting GBF1, suggesting that the fractions themselves contained the minimum protein components required (Quilty et al., 2019). By isolating membranes prior to mass spectrometry, we can enrich for these components and avoid potential failed detection due to low protein abundance. A

diagram depicting proximity-based biotinylation and the adapted BioID workflow for use with GBF1 is shown in figure 4.1 and 4.2.

The following subsections will describe the characterization of two transgenic HeLa cell lines generated for the GBF1 BioID assay. We compare the difference in biotinylated targets between whole cell lysates and enriched Golgi fractions, and utilize a small-scale shRNA screen to identify putative GBF1 regulators of interest.

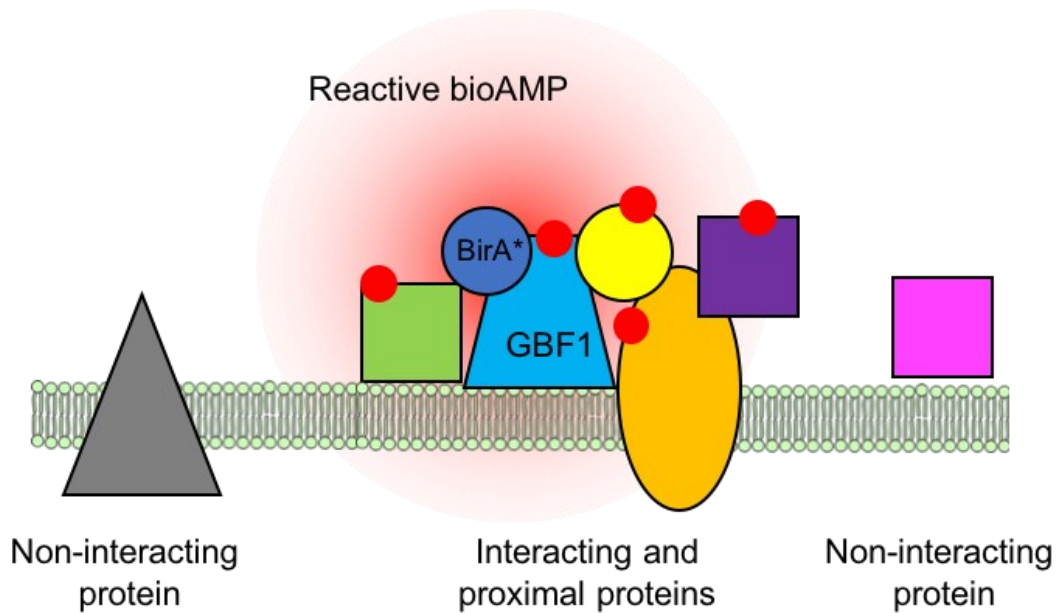


Figure 4.1 Depiction of the proximity-based biotinylation technique BioID with GBF1.

The Golgi-localised BirA*-FLAG-tagged GBF1 upon treatment with exogenous biotin will generate reactive biotinyl-5'-AMP (shown in red) that will dissociate from the BirA* ligase and diffuse towards proximal proteins. Biotinylated proteins may include integral and peripheral interactors that regulate GBF1 localisation and recruitment. Non-interacting or non-proximal proteins should not be labeled by reactive biotin.

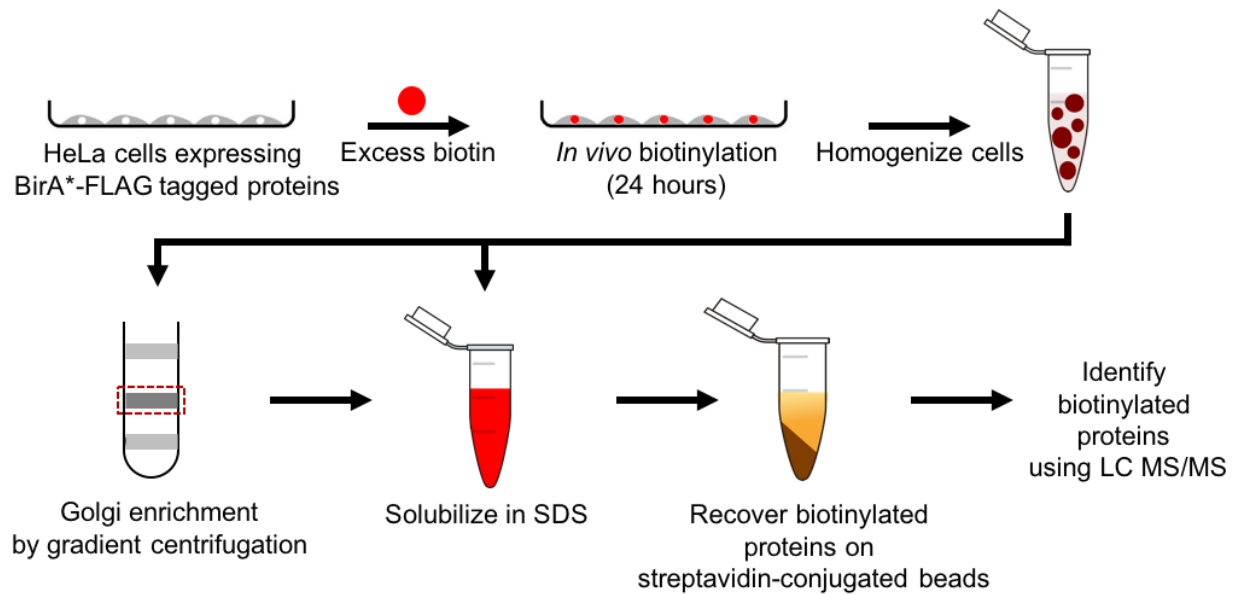


Figure 4.2 Application of the proximity-based biotinylation technique BioID for identifying GBF1 interactions on Golgi membranes.

HeLa cells stably expressing the BirA*-FLAG-GBF1 or BirA*-FLAG proteins are treated with excess biotin and cultured for 24 hours to allow for biotinylation *in vivo*. Cell homogenates are then either 1) solubilized in SDS directly, or 2) separated by gradient centrifugation and enriched Golgi membranes are collected for solubilization in SDS. In either case, biotinylated proteins are then captured using streptavidin-conjugated beads, and the proteins treated with trypsin, and identified using liquid chromatography coupled with tandem mass spectrometry (LC MS/MS).

4.2 Results of BioID Analysis

4.2.1 Characterization of the BirA*-FLAG and BirA*-FLAG-GBF1 HeLa cell lines

TREx system allows for the regulated expression of GBF1. By ensuring the transgenes are expressed at moderately low levels, we can curb potential toxicity and other nonspecific effects associated with overexpression (Kim and Roux, 2016). This is of particular importance as the labeling of proximal proteins takes place in living cells over a span of 24 hours. Nonspecific effects from extended overexpression may interfere with Golgi morphology or physiology, altering the identification of GBF1 interacting partners. After the cell lines were generated, preliminary experiments were performed to confirm their suitability for use in the BioID analysis.

First, western blotting using anti-FLAG antibodies was performed to confirm that addition of doxycycline, a more stable analogue of tetracycline, induced BirA*-FLAG-GBF1 expression at levels below that of endogenous GBF1 at 24 hours post-induction (Figure 4.3). At 0.1 $\mu\text{g/mL}$ doxycycline, we found that the exogenous BirA*-FLAG-GBF1 is expressed at approximately one-third of endogenous GBF1 – well below endogenous levels. Similar western blotting experiments established that BirA*-FLAG expressed at a level only moderately higher than BirA*-FLAG-GBF1.

To further confirm that under these conditions the BirA*-FLAG constructs were capable of biotinylating proteins *in vivo*, we repeated the western blotting experiment with the addition of 50 μM biotin (Figure 4.4). Samples were collected from either whole cells or as enriched Golgi fractions following density centrifugation. In our whole cell comparison, we found that both BirA*-FLAG-GBF1 and BirA*-FLAG HeLa cell lines biotinylated vastly different pools of

protein, with the BirA*-FLAG construct biotinylating much more protein overall. This is likely because BirA*-FLAG has a slightly higher expression as compared to BirA*-FLAG-GBF1 and because it is expected to be soluble and diffuse throughout the cell (Figure 4.3). BirA*-FLAG-GBF1 on the other hand should be Golgi-localised and biotinylated targets at either the Golgi membrane or the cytosol. Further examination of the enriched Golgi fractions revealed much more biotinylation for BirA*-FLAG-GBF1 on Golgi fractions as compared to whole cell lysates (Figure 4.4). Comparison with the Golgi-enriched BirA*-FLAG samples illustrates several key biotinylated protein bands that are present in the GBF1-tagged version only. Bands at 150, 100, and 75 kDa were the most obvious. Additional probing of the blot with anti-FLAG antibodies further revealed that BirA*-FLAG-GBF1 can be found in the Golgi-enriched fraction similar to Golgi marker GM130 while BirA*-FLAG was largely excluded. The mitochondrial marker VDAC1 was used to ensure that mitochondria, which contain several naturally biotinylated enzymes, were not enriched by the Golgi isolation procedure. Total protein load was not examined.

Following western blotting, we further examined the cells by fixed cell imaging to confirm the localisation of the BirA*-FLAG constructs and their biotinylated targets (Figure 4.5A). We found that BirA*-FLAG-GBF1 localised to giantin-positive Golgi structures and that most biotinylated proteins – as detected using streptavidin-Cy3 – similarly localised to the Golgi. In contrast, BirA*-FLAG and its biotinylated products were found dispersed through the cytosol and nucleus. Furthermore, treatment of cells for 24 hours with 50 μ M biotin did not alter the juxtannuclear distribution of the Golgi marker, giantin, in either cell line, indicating that the biotinylation of proteins at the Golgi did not severely impact Golgi maintenance.

Prior to the use of these cell lines in the subsequent BioID and mass spectrometry experiments, we lastly wanted to confirm that the BirA*-FLAG-GBF1 construct was subject to regulatory signals similar to that of endogenous GBF1. To do so, we examined whether the protein could be recruited to juxtannuclear Golgi structures upon treatment with BFA. As described previously, BFA inhibits GBF1 activity causing the accumulation of inactive Arf-GDP which triggers a feed-forward mechanism driving additional GBF1 recruitment to membranes (Quilty, 2016). Upon treatment with 10 $\mu\text{g}/\text{mL}$ BFA for 90 seconds, BirA*-FLAG-GBF1 largely cleared from the cytosol and accumulated at juxtannuclear structures as well as peripheral puncta. This suggests that the protein can be recruited to Golgi membranes like endogenous GBF1 and is likely subject to the same regulatory signals (Figure 4.5B).

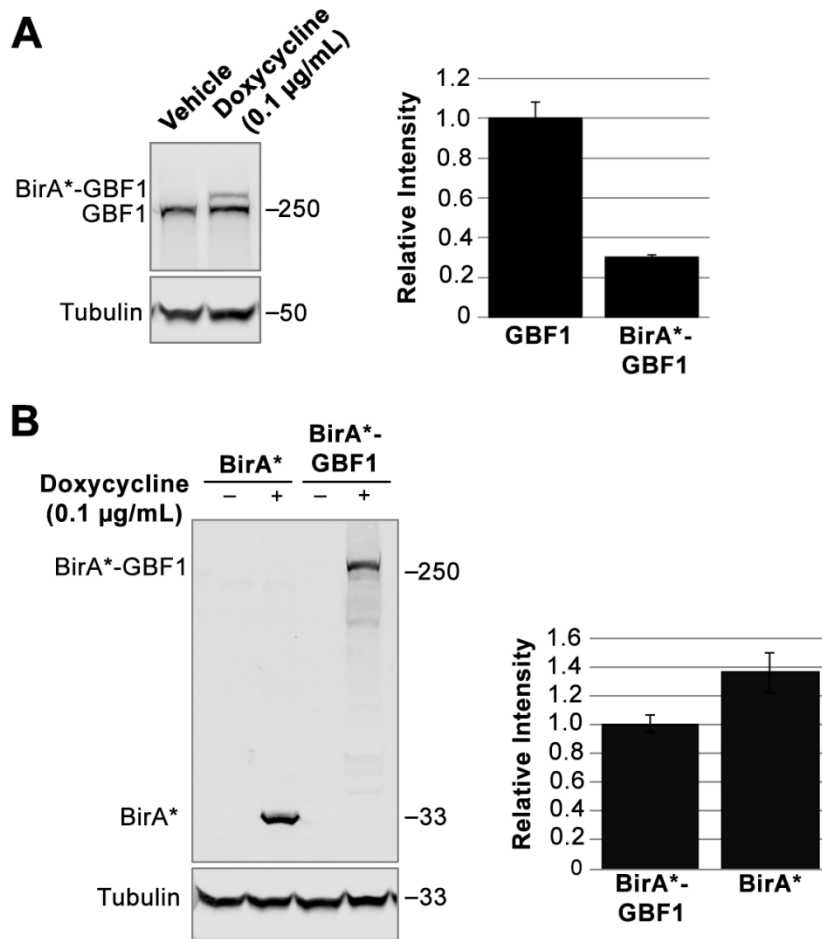


Figure 4.3 Both BirA*-FLAG and BirA*-FLAG-GBF1 are expressed at low levels upon induction with doxycycline.

HeLa cells stably expressing either BirA*-FLAG or BirA*-FLAG GBF1 were analyzed by western blotting using anti-FLAG antibodies or anti-GBF1 antibodies 24 hours post transduction with vehicle (water) or doxycycline (0.1 µg/mL). Numbers on the right side of the blots indicate molecular weight in kilodaltons. Samples were from three separate biological replicates and quantified. Values represent \pm standard deviation (error bars) (n=3). Representative blots are shown. (A) Western blot was probed with anti-GBF1 and anti-tubulin antibodies. Exogenous BirA*-FLAG-GBF1 is expressed at a level approximately one-third that of endogenous GBF1. (B) Western blot was probed with anti-FLAG and anti-tubulin antibodies. Exogenous BirA*-FLAG is expressed at a level approximately 40 percent higher than that of exogenous BirA*-FLAG-GBF1.

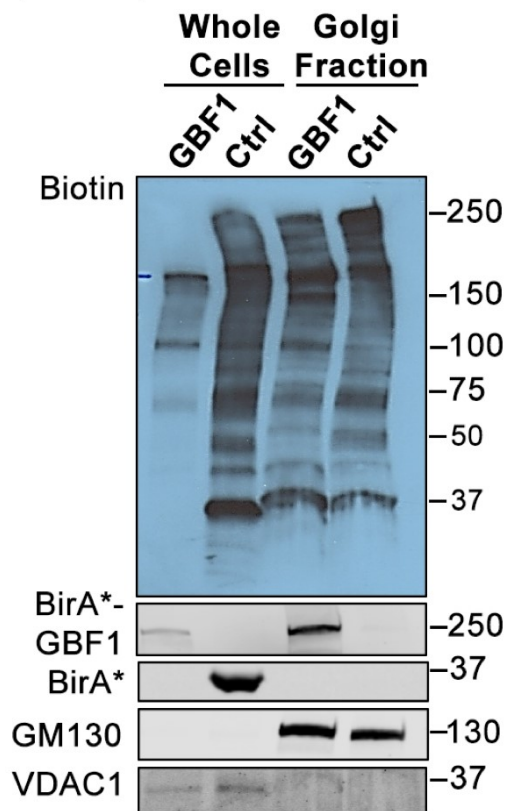


Figure 4.4 BirA*-FLAG-GBF1 biotinylates Golgi proteins vastly different than BirA*-FLAG.

HeLa cells stably expressing either BirA*-FLAG or BirA*-FLAG-GBF1 were analyzed 24 hours after induction with excess biotin (50 μ m). Western blotting performed using whole cells and sucrose-gradient separated Golgi fractions confirmed successful enrichment of GM130 positive Golgi membranes negative for mitochondrial marker VDAC1. BirA*-FLAG-GBF1 and BirA*-FLAG were probed for using anti-FLAG antibodies. GM130 and VDAC1 were probed for using anti-GM130 and anti-VDAC1 antibodies, respectively. Biotinylated proteins were probed for using fluorescently conjugated streptavidin without a secondary antibody. Numbers on the right side of the blots indicate molecular weight in kilodaltons. In both whole cell and Golgi fractions, BirA*-FLAG-GBF1 biotinylated proteins different than that of the control. Blot shown is representative of three independent replicates.

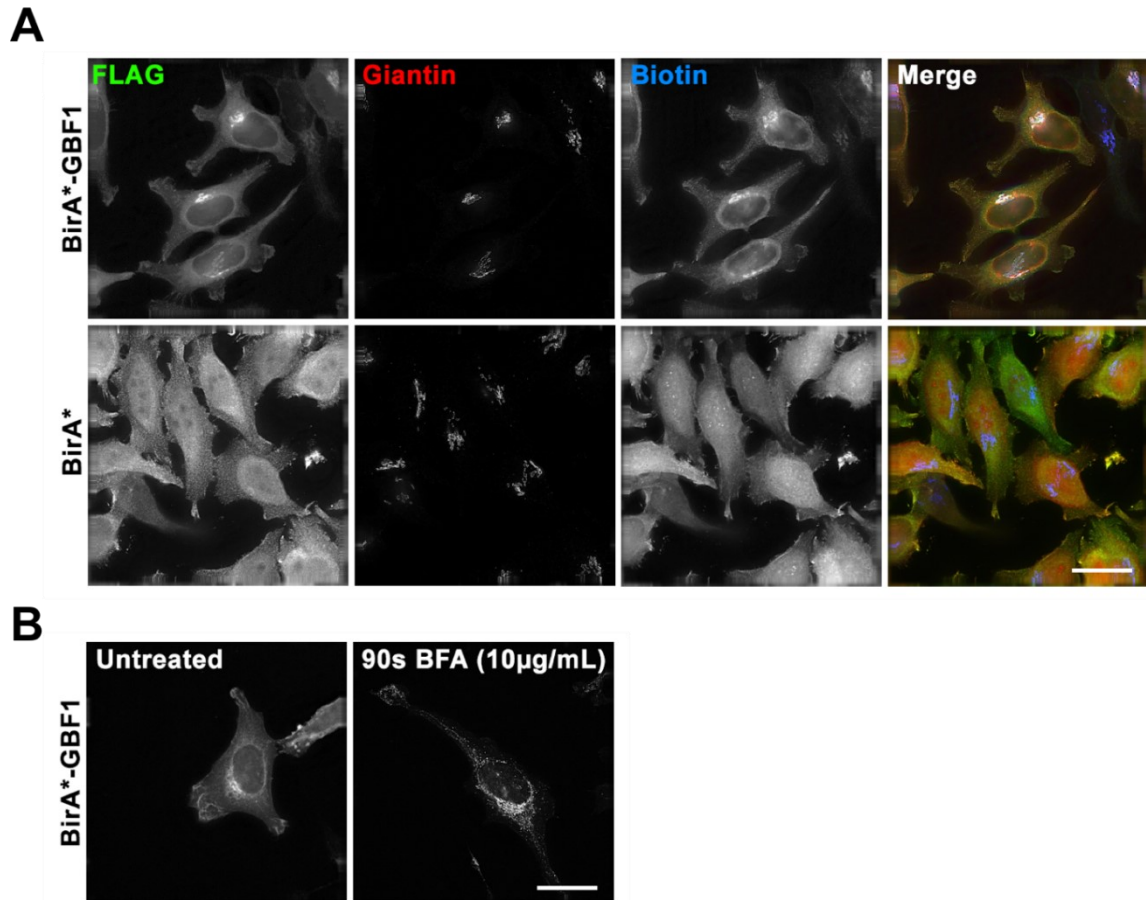


Figure 4.5 BirA*-FLAG-GBF1 can be recruited to and biotinylates proximal proteins at Golgi structures.

HeLa cells stably expressing either BirA*-FLAG-GBF1 or BirA*-FLAG were analyzed after 24-hour induction. (A) Upon treatment with excess biotin for 24 hours (50 μ M), BirA*-FLAG-GBF1 localised to and biotinylated proteins on giantin-positive Golgi membranes, unlike the nuclear and cytosolically diffuse BirA*-FLAG. (B) BirA*-FLAG-GBF1 remained sensitive to inhibitory drug BFA (10 μ g/mL) and can be recruited to juxtannuclear structures upon treatment. All images are representative of three replicates and are shown as projection of all z-slices. Scale bars = 26 μ m.

4.2.2 BioID analysis using Golgi-enriched fractions identify unique proximal partners

Having verified the cell lines for use in BioID experiments, whole cell lysates and Golgi-enriched fractions from biotin treated BirA*-FLAG-GBF1 and BirA*-FLAG expressing HeLa cells were collected. Biotinylated proteins were then isolated using streptavidin beads. After extensive washing, streptavidin-bound proteins were treated with trypsin and the eluted peptides identified using nanoflow liquid chromatography-electrospray ionization-tandem mass spectrometry (nLC-ESI-MS/MS). Two biological and two technical replicates were performed by our collaborators for each condition for a total of eight runs. Additional details can be found in Chapter 2. Data from the mass spectrometry analysis including total peptide counts and the associated false discovery rates for all protein identified can be found as part of appendices 9.1 and 9.2, on massive.ucsd.edu with the accession number MSV000083866, or as a supplementary table from Chan et al. 2019.

To begin identifying proximal proteins of interest, our collaborators performed SAINT analysis (Significance Analysis of Interactome) using the obtained peptide counts. SAINT is a computational tool that assigns confidence scores to protein-protein interaction data obtained through affinity-purification mass spectrometry and other AP-MS like experiments. Using this program, spectral counts for each prey protein identified in the GBF1 BioID experiment are converted into a SAINT value representing the probability of a true interaction. The analysis takes into consideration the spectral counts relative to the length of the protein (as larger proteins are more likely to be biotinylated and pulled down), the total number of spectra identified from the samples (i.e. fraction of spectra corresponding to a specific target), and the spectral distribution from the negative controls (in this case, the BirA*-FLAG samples). Proteins identified with two or more unique peptides and scoring above a false discovery rate of one

percent were considered to be high-confidence putative interactors (i.e. one percent of the candidates in the list are theoretically false positives). These thresholds were chosen based on previous proteomic studies comparing analysis methods (Choi et al., 2011). A false discovery rate of 1% was suggested to be a valuable baseline for identifying novel interactors. Surprisingly, we found that of the 212 proteins categorized as high-confidence in the whole cell lysates, only two (SLC30A6 and SLC30A5; also known as ZnT6 and ZnT5) were also identified as such in the Golgi-enriched fractions. Known GBF1 substrates including the class I and class II Arfs – Arf1, Arf4, and Arf5 – were identified but fell below the one percent false discovery rate cut off in both whole cell lysates and Golgi-enriched fractions (Wright et al., 2014). Of the GBF1 interactors previously identified using classical co-immunoprecipitation approaches (Rab1, p115, GGAs, and GMH1) only Rab1 and p115 were identified (Chantalat et al., 2003; Honda et al., 2005; Katayama et al., 2004; Monetta et al., 2007; Sztul and García-Mata, 2003). p115 was categorized as a high-confidence interactor from the whole cell lysates but not in enriched Golgi fractions, whereas Rab1 was identified in both but fell below the one percent false discovery rate cut off. Nonetheless, their presence in the proteomic data is consistent with other published work suggesting they are GBF1 interactors. Furthermore, Golgi-enriched fractions allowed for the identified seven unique high-confidence putative interactors, of which three failed to be identified at all from the whole cell lysates. A Venn diagram depicting the overlap in the high-confidence putative interactors identified between the whole cell lysates and Golgi-enriched fractions are shown in figure 4.6.

Initial western blotting for biotinylated targets in the Golgi fractions using fluorescently conjugated streptavidin highlighted several key biotinylated protein bands present in the GBF1-tagged version that appeared largely absent from the BirA*-FLAG expressing cells (Figure 4.4);

these include bands at 150, 100, and 75 kDa. From our list of high-confidence putative interactors, the 150 kDa band may correspond to the rhomboid like membrane protease, RHBDD2, which has a small and large splice isoform. The 100 kDa band may correspond to the *cis*-Golgi transmembrane protein, TMEM115. And the 75 kDa band may correspond to the uncharacterized C10orf76 and/or the huntingtin interacting protein ZDHHC17. A list of all the high-confidence putative interactors identified from the Golgi-enriched fractions and their associated spectral counts is provided in table 4.1.

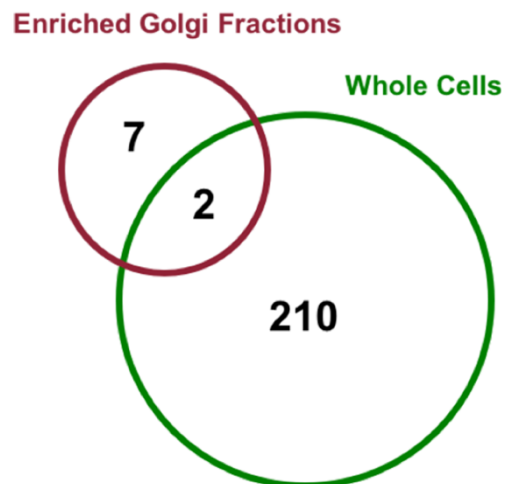


Figure 4.6 Venn diagram depicting the high-confidence candidates identified in the BioID experiment.

The diagram represents the 219 protein candidates scoring above a false discovery rate of one percent. The enriched Golgi fractions allowed for the identification of several unique preys that failed to meet the high-confidence cut off in the whole cell lysates and vice versa. The nine protein candidates identified from enriched Golgi fractions can be found in table 4.1. A list of all protein candidates can be found in appendices 9.1 and 9.2.

Table 4.1 Total spectral counts and SAINT scores for candidate GBF1 interactors identified in whole cell lysate (WCL) and Golgi-enriched fractions, as indicated.

Gene Symbol	Gene Name	WCL BirA*-FLAG Control	WCL BirA*-FLAG-GBF1	WCL SAINT	Golgi BirA*-FLAG-Control	Golgi BirA*-FLAG-GBF1	Golgi SAINT	Golgi False Discovery Rate
SLC30A6	Solute carrier family 30 member 6	0	158	1.00	12	327	1.00	0
SLC30A5	Solute carrier family 30 member 5	0	95	1.00	10	197	1.00	0
GOSR1	Golgi SNAP receptor complex member 1	0	10	0.92	10	135	1.00	0
TMEM115	Transmembrane protein 115	0	7	0.88	0	119	1.00	0
C10orf76	Chromosome 10 open reading frame 76	0	4	0.84	0	52	1.00	0
CANT1	Calcium activated nucleotidase 1	0	0	N/A	6	42	1.00	0
RHBDD2	Rhomboid domain containing 2	0	0	N/A	0	27	1.00	0
ZDHHC17	Zinc finger DHHC-type containing 17	0	0	N/A	0	20	1.00	0
TMEM87A	Transmembrane protein 87A	0	10	0.92	16	90	0.99	0.01

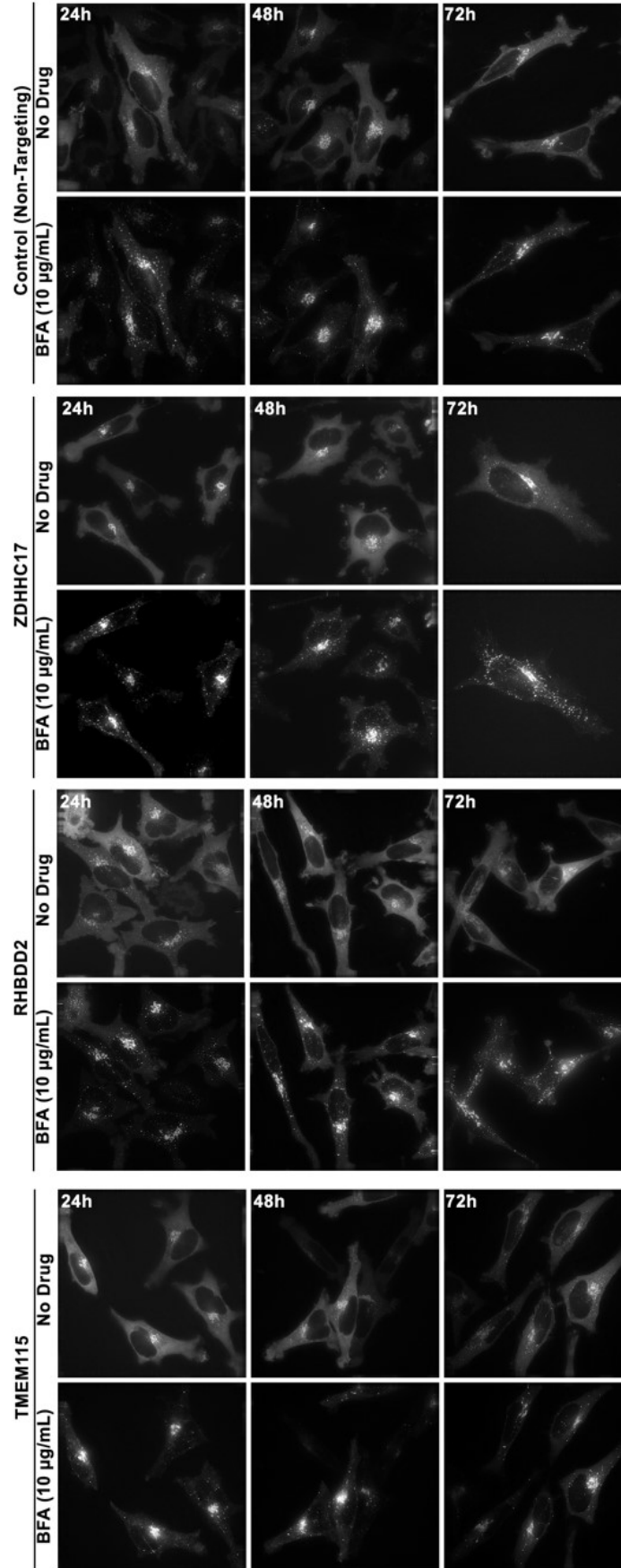
4.3 Results of the shRNA screen

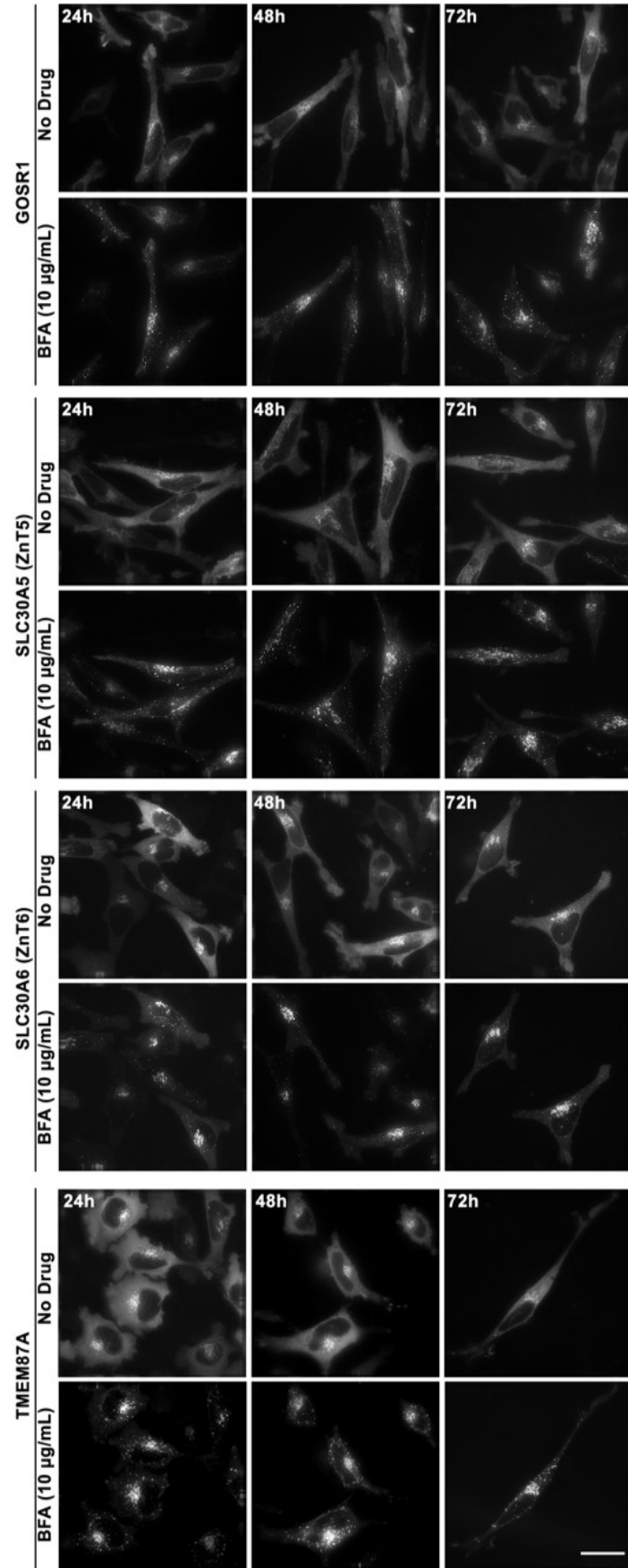
To begin identifying potential interactors involved in regulating GBF1 recruitment, we chose to start with a shRNA knockdown screen on the high-confidence candidates from the Golgi-enriched fraction. As mentioned, previous data from our laboratory had shown that enriched Golgi fractions were capable of recruiting GBF1 *in vitro*, indicating that the fractions themselves contained the protein components required for GBF1 recruitment (Quilty et al., 2019). BioID performed on the Golgi-enriched fractions also highlighted seven unique high-confidence hits, three of which were not detected at all in the whole cell lysates. This strongly suggests that our enrichment protocol can be utilized for the identification of certain GBF1 proximal membrane targets that may be missed when probing whole cell lysates alone. For this reason, we began first by examining the high-confidence candidates obtained from the Golgi-enriched fractions.

To achieve this, we performed our shRNA screen on EGFP-GBF1 expressing cells using an *in vivo* high-efficiency lentiviral vector delivery method developed by Sigma. As described in Chapter 2, lentiviral particles containing shRNA encoding plasmids were generated using the Sigma MISSION shRNA kits according to manufacturer protocols. The collected viral particles were then used to transduce HeLa cells at a multiplicity of infection of two. The effect on EGFP-GBF1 distribution and recruitment upon BFA treatment at 10 $\mu\text{g}/\text{mL}$ for 90 seconds was examined using live-cell imaging at 24, 48, and 72 hours post transduction. Transduced cells were selected for using 5 $\mu\text{g}/\text{mL}$ puromycin, which effectively killed untransduced HeLa cells after approximately 24 hours. For targets with obtainable commercial antibodies, their successful depletion via shRNA was confirmed by western blotting (Figure 4.8 and 4.9). Of the nine putative GBF1 interactors examined, only the treatment using shRNA targeting C10orf76 at 72

hours post-transduction yielded any observable alteration in EGFP-GBF1 distribution and recruitment upon BFA treatment (Figure 4.7; figure 4.9).

At 72 hours, we found the C10orf76 depletion caused a redistribution of EGFP-GBF1 in HeLa cells away from a juxtannuclear-like Golgi site towards peripheral punctate structures. This was not observed in the cells treated with the non-targeting shRNA or with shRNAs targeting the other eight candidates. Further, the addition of 10 $\mu\text{g}/\text{mL}$ BFA for 90 seconds promoted clear recruitment of additional EGFP-GBF1 to juxtannuclear sites in the non-targeting control, but not in the C10orf76-depleted cells. Depletion of C10orf76 was confirmed using western blotting, and the reduced ability of BFA to recruit additional EGFP-GBF1 to existing GBF1 positive membranes sites was quantified. In control cells, a 1.62 fold increase in EGFP signal at existing GBF1 positive sites were observed upon BFA treatment. However, in C10orf76-depleted cells, only a marginal 1.10 fold change was observed (two-tailed unpaired *t* test; ** $p = 0.0086$). These data suggest that C10orf76 may play essential roles in GBF1 recruitment as well as a function either in GBF1 distribution or the maintenance of GBF1 positive Golgi structures. The redistribution of GBF1 to dispersed punctate sites is similar to the redistribution of GBF1 upon treatment with the microtubule destabilizing agent, nocodazole, which fragments the Golgi (Szul et al., 2007; Zhao et al., 2006). Furthermore, even under conditions where the Golgi is fragmented upon nocodazole treatment, additional GBF1 can still be recruited to Golgi sites. As such, the lack of recruitment observed in C10orf76-depleted cells likely indicates an impairment in GBF1 recruitment. Additional experiments examining the role of C10orf76 will be discussed in Chapter 5. Images of the shRNA knockdown screen and their corresponding western blots are shown in figure 4.7 and 4.8. The effect of the C10orf76 targeting shRNA is shown separately in figure 4.9.





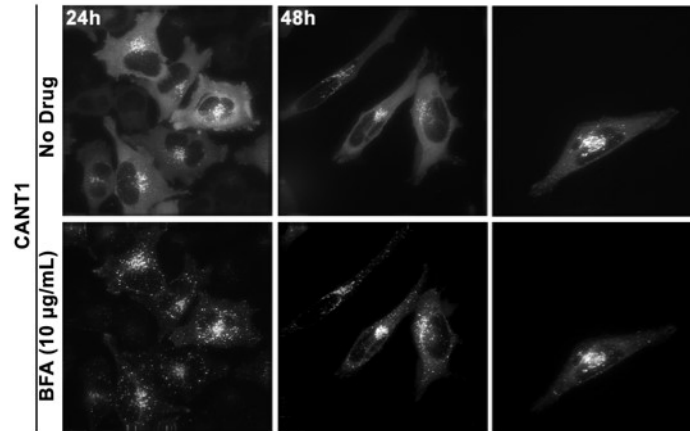


Figure 4.7 Knockdown of nearly all high-confidence GBF1 proximal proteins identified by BioID had little impact on GBF1 distribution at 72 hours.

Shown are live-cell imaging data for EGFP-GBF1 expressing HeLa cells after treatment with lentivirus particles containing plasmids encoding shRNAs against eight of the nine high-confidence GBF1 proximal proteins as identified by BioID from enriched Golgi fractions (ZDHHC17, RHBDD2, TMEM115, GOSR1, SLC30A5, SLC30A6, TMEM87A, and CANT1) or a non-targeting shRNA. All treated cells at all time points observed (24, 48, or 72 hours post transduction), exhibited a clear localisation of EGFP-GBF1 at juxtannuclear sites, and additional recruitment upon treatment with 10 µg/mL BFA for 90 seconds. All images are representative of 15 cells examined over three biological replicates and are shown as projections of all Z-slices. Scale bar = 26 µm.

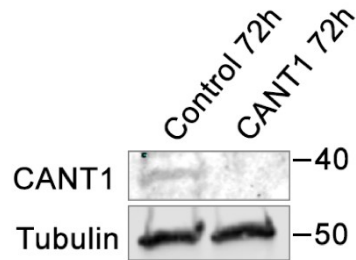
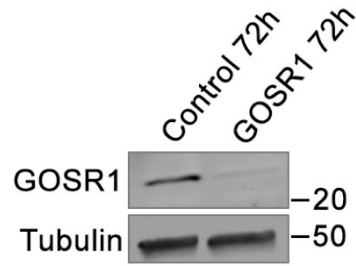


Figure 4.8 Confirmation of knockdown for high-confidence GBF1 proximal proteins identified by BioID.

Shown are western blots of samples from EGFP expressing HeLa cells after treatment with lentiviruses containing plasmids encoding shRNA against GOSR1 and CANT1 after 72 hours. Numbers on the right side of the blots indicate molecular weight in kilodaltons. Successful depletion of both proteins as compared to tubulin was observed using commercially available antibodies against GOSR1, CANT1, and tubulin. Blots are representative of two independent replicates.

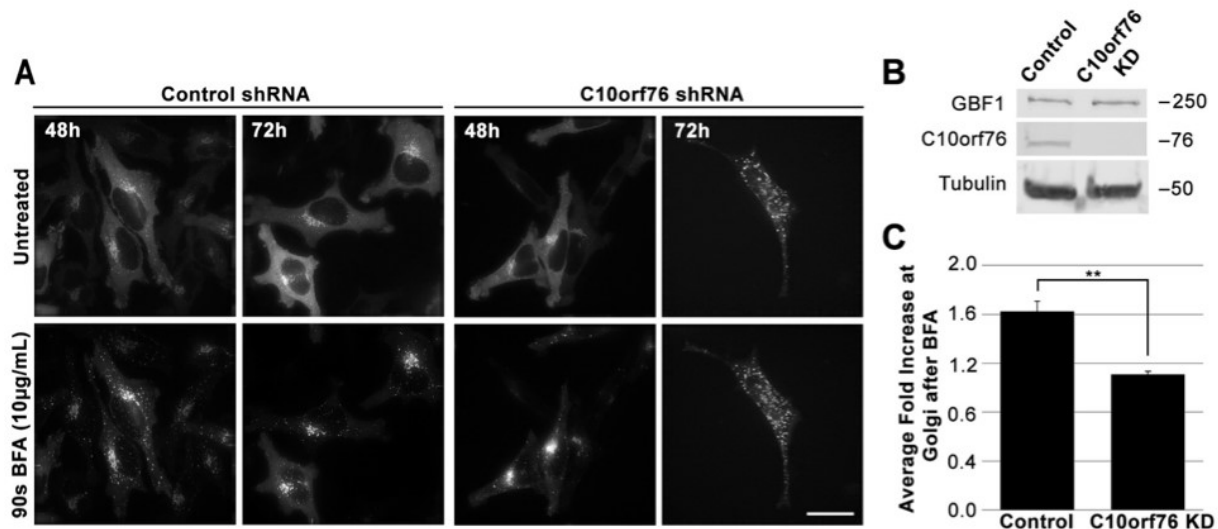


Figure 4.9 Knockdown of C10orf76 redistributed GBF1 and altered its recruitment.

EGFP-GBF1 expressing HeLa cells were transduced using lentiviral vectors containing plasmids encoding non-targeting or C10orf76 shRNAs and selected in the presence of puromycin. (A) At 72 hours, C10orf76-depleted cells showed a redistribution of EGFP-GBF1 to disperse punctate structures. Knockdown also caused GBF1 to enrich poorly at these sites upon treatment with BFA (10 µg/mL) for 90 seconds. All images are representative of 15 cells examined over three replicates and shown as projections of all Z-slices. Scale bar = 26 µm. (B) Confirmation of C10orf76 knockdown by western blotting using antibodies against GBF1, C10orf76, and tubulin. Numbers on the right side of the blots indicate molecular mass in kilodaltons. Images are representative of three replicates. (C) Quantitation of transduced cells at 72 hours. Bars indicate the average fold change of EGFP-GBF1 at existing EGFP-GBF1 positive sites after BFA treatment (10 µg/mL) for 90 seconds. Quantitation was performed as described in Chapter 2 (15 cells total examined over three replicates). A value of 1 translates as no impact of BFA and was chosen as the Y-intercept. Error bars represent mean values ± standard deviation. A statistically significant difference was observed between the C10orf76-depleted and control cells as measured by a two-tailed unpaired *t* test ($p = 0.0086$).

4.4 Discussion

4.4.1 Enrichment of Golgi organelles improved identification of certain proximal partners using BioID

Following the publication of the BioID method by Roux and colleagues in 2012, over 100 publications using BioID to study protein interactomes has since been published (Trinkle-Mulcahy, 2019). However, our work is the first published study demonstrating the applicability of the method on enriched Golgi fractions. This enrichment procedure allowed us to identify putative proximal proteins that were either not significantly detected in whole cell lysates (i.e. fell below our one percent false discovery rate threshold; C10orf76, GOSR1, TMEM115, TMEM87A) or were not detected at all (CANT1, RHBDD2, ZDHHC17; Table 4.1, Appendix 9.1 and 9.2). This is unexpected in that proximity partners identified from the enriched Golgi fractions are also present in the whole cell lysate, and should in theory, be similarly detected. The difference observed in these two analyses of local interactomes could potentially be due to differences in protein abundance. Although ideally mass spectrometry should facilitate the identification of all affinity purified proteins, the range in protein size, sequence, and quantity can often lead to the oversampling of abundant proteins, while peptides with low abundance are likely to be undersampled or undetected (Angel et al., 2012). In fact, C10orf76 could only be detected by WB of HeLa cell lysates after first concentrating proteins by acetone precipitation. This suggests that C10orf76 is likely a low abundance protein in HeLa cells. Therefore, organelle enrichment, where applicable, can allow for increased sensitivity for low abundance proteins and create a more robust BioID experiment.

Conversely, we also identified 157 high-confidence putative proximal proteins in whole cell lysates only and not in Golgi-enriched fractions (Figure 4.6, Appendix 9.1 and 9.2). By

similar logic, it is likely that these proximal proteins may interact with GBF1 at sites other than on Golgi membranes. As discussed, GBF1 has been shown to function at multiple cellular locations and likely has a unique interactome at each site. Additional examination of these high-confidence proximal proteins may yield novel insights into GBF1 function and regulation at other cellular locations. Our BioID data may prove useful for researchers in these other fields.

4.4.2 Comparison to previously published attempts at identifying GBF1 membrane interactors

Previously published research from our laboratory utilized a far-western approach to identify putative GBF1 membrane receptors (Quilty, 2016). Golgi membranes separated by gel electrophoresis was transferred onto nitrocellulose and probed with EGFP-GBF1 cell cytosols. This approach identified a 32 kDa protein of interest. Additional mass spectrometry revealed 76 proteins within this 32 kDa region. When compared to our BioID approach, none of the high-confidence candidates identified in our Golgi-enriched fractions (candidates within the one percent false discovery rate threshold) correspond to any of the 76 proteins previously identified. Expanding our false discovery rate threshold to 0.5 reveals three common candidates: STX5, GOLPH3, and TMED9. Depletion of STX5, or syntaxin 5, has been previously shown to have negligible effects on β -COP recruitment, suggesting that it likely does not play an essential role in GBF1 recruitment or function (Suga et al., 2005). GOLPH3 is a PI4P binding protein most abundantly found at the TGN where it interacts with myosin and connects the Golgi to the actin cytoskeleton (Dippold et al., 2009). Golgi remains compact in GOLPH3 depleted cells unlike cells depleted of GBF1 or COPI components, suggesting that GOLPH3 is likely uninvolved in COPI traffic. Lastly, TMED9 is a non-essential cargo receptor in COPI vesicles for the retrieval

of ER cargo (Gomez-Navarro and Miller, 2016). TMED9 functions downstream of GBF1 and Arf activation, indicating that it is also likely uninvolved in GBF1 recruitment.

4.4.3 Limitations of the BioID method and SAINT analysis

Utilizing BioID we were able to identify nine high-confidence GBF1 proximal proteins from Golgi-enriched fractions (Table 4.1, Figure 4.6). Within this list, none of them have been previously shown to be GBF1 interactors (we were able to confirm two new interactions to be discussed in Chapter 5 and 6). Within these nine, our shRNA screen identified one candidate, C10orf76, as having potential roles in regulating GBF1 recruitment and distribution. However, despite the success in identifying putative and novel GBF1 regulators of interest, our study has also been restricted by limitations in our approach.

Firstly, as mentioned, mass spectrometry itself is limited by multiple factors. Protein abundance and successful ionization of peptides can both influence whether a particular peptide can be successfully separated and detected (Lubec and Afjehi-Sadat, 2007). Even after successful detection, the subsequent identification of the protein is wholly dependent on our ability to discriminate with accuracy the peptide sequences determined by mass spectrometry. Only known mass peaks present in established databases can be assigned to the detected peptides, meaning mutations, miscleavages, undiscovered protein modifications, etc, can all influence whether a detected peptide can be identified as being part of a specific protein. Likewise, highly similar proteins may not be easily discriminated. For instance, of the known GBF1 substrates, Arf1, Arf3, Arf4, and Arf5, only Arf 1, Arf4, and Arf5 were detected in our analysis (all at false discovery rate of 0.6; appendix 9.1 and 9.2). This is likely because Arf1 and Arf3 share 96% identity and the identified peptides from both Arfs may not have been accurately discriminated (Kahn et al., 2006).

Secondly, the BioID method is also constrained by several physical limitations. For a proximal protein to be successfully biotinylated, it must be within the reactive biotin “cloud” created by the BirA* ligase, meaning its contact with reactive biotin cannot be blocked by the presence of other proteins. For instance in Roux and colleagues use of BioID to probe the nuclear pore complex, internal subunits neighboring the bait were not always biotinylated due to the spatial positioning of other subunits in between them (Kim et al., 2014). By similar logic, the position of the BirA* tag on the bait will likely also influence biotinylation of proximal targets. GBF1 being a large protein – 1856 amino acids and an observed molecular mass of over 250 kDa – with an unknown three-dimensional structure may mean that spatial positioning of the tag can have a pronounced influence on biotinylation. As such, C-terminally tagging of GBF1 may, in theory, lead to a similar but nonetheless uniquely different profile of the GBF1 interactome. We had initially constructed and sequenced a plasmid encoding a C-terminally tagged GBF1 for use in BioID, however, we were unable to determine why the construct would not express in HeLa cells and it was ultimately not used in the BioID analysis.

Thirdly, apart from the access to reactive biotin, successful biotinylation is also dependent on the availability of an exposed lysine to accept the reactive biotin molecule. Therefore, a lack of suitably positioned lysine side chains can lead to negative data.

Lastly, our assay is also limited by our ability to effectively differentiate using statistical methods the difference between background labeling and true GBF1 proximal proteins. Previously published GBF1 interactors including p115 and Rab1 were detected, but did not meet the one percent false discovery cut off (false discovery rate at 0.27 for Rab1 and 0.47 for p115 in Golgi-enriched samples; Appendix 9.1 and 9.2). P115 peptides were identified 33 times in the control and 99 times in the GBF1 sample; Rab1 peptides were identified 15 times in the control

and 49 times in the GBF1 sample. More abundant proteins are in general, more likely to be biotinylated regardless of interaction. The presence of known interactors in the list below our false discovery rate threshold suggests that there are likely other undiscovered novel interactors hidden below our cut off. A larger knockdown screen encompassing these additional candidates will require a more automated approach, possibly using automated imaging systems or an imaging flow cytometry method.

4.4.4 Limitations of the shRNA screen

In addition to the low number of candidates screened, our shRNA approach is also limited by other factors including potential functional redundancies and the availability of commercial antibodies to assess successful knockdown. Furthermore, proteins with long half-lives and transcripts resistant to RNA interference (for instance, those with high-turnover rates) may not have been successfully depleted within our 72-hour timespan. This is problematic because incomplete depletion of essential proteins may not yield easily observable phenotypes.

Complementary strategies may need to be implemented to strengthen the assay. For instance, we could utilize quantitative PCR as a measure of successful transcript depletion where antibodies are unavailable. The caveat here being that successful depletion at the mRNA level may not always lead to a comparable depletion at the protein level. However, based on the average rate at which HeLa cells divide, successful depletion of mRNA by 24 hours should lead to approximately one half or three-quarters reduction of protein level in cells by 72 hours, simply due to the partitioning of proteins into daughter cells. This reduction in protein levels should correspond to a reduction in GBF1 recruitment if the target is involved in the recruitment process. Additional experiments using reverse transcriptase mediated PCR can be performed to ascertain the ability of the selected shRNAs to target and deplete the mRNAs of interest. Aside

from shRNA, future experiments may also utilize RNA interference independent approaches such as CRISPR-Cas9 to knockout gene function. This method can eliminate confounding effects from low protein levels remaining after knockdown and RNA interference resistant transcripts. However, GBF1 function is essential for Golgi maintenance and cell survival. Therefore, the loss of essential GBF1 receptor components may lead to Golgi fragmentation and cell death which can complicate data interpretation.

Chapter 5: C10orf76 is a novel GBF1 interacting partner essential for Golgi maintenance

A version of this chapter has been previously published (Chan, C.J., R. Le, K. Burns, K. Ahmed, E. Coyaud, E.M.N. Laurent, B. Raught, and P. Melançon. 2019. BioID performed on Golgi-enriched fractions identify C10orf76 as a GBF1 binding protein essential for Golgi maintenance and secretion. *Molecular & Cellular Proteomics*. 18:2285-2297). All copyright belongs to the respective authors.

The electron microscopy was performed with Dr. Nasser Tahbaz. The GBF1 mutants used for the co-immunoprecipitation assays were generated with the help of undergraduate student Khadra Ahmed. The luciferase assay was performed with help from undergraduate student Kaylan Burns. Pulldowns were performed with advice from Dr. Richard Wozniak and with reagents provided by Dr. Thomas Simmen. The phylogeny of C10orf76 was examined using advice and guidelines suggested by Dr. Joel Dacks and Dr. Lael Barlow. Dr. Paul Melançon helped in the planning of experiments, data analysis, and writing of the manuscript.

5.1 Background on C10orf76

In our shRNA screen of GBF1 proximal candidates identified from Golgi-enriched fractions, we identified C10orf76 as potentially being involved in Golgi maintenance and the regulation of GBF1 recruitment. Depletion of C10orf76 using shRNA at 72 hours revealed a redistribution of EGFP-GBF1 to peripheral sites and poor recruitment upon treatment with BFA.

C10orf76 is a 76 kDa, 688 amino acids long protein (also referred to as ARMH3 or Armadillo-like helical domain-containing protein 3). The protein also contains a domain of unknown function (DUF1741) that is well conserved amongst C10orf76 orthologs but is not found in any other known protein.

At the time of study, little was known about the functional role of C10orf76. Data published as part of the International Mouse Phenotyping Consortium revealed that C10orf76 knockout in mice was lethal at the pre-weaning stage (Dickinson et al., 2016). In a large scale CRISPR-based screen for essential human genes, researchers also found that disruption of C10orf76 was lethal in near-haploid KBM7 cells (haploid except chromosome 8), but not in HAP1 cells (haploid except one region on chromosome 15; Blomen et al., 2015). It's unclear why the difference was observed. Nonetheless, Blomen et al., 2015 were able to demonstrate an interaction between C10orf76 and PI4KB (phosphatidylinositol 4-kinase beta) – which were both essential in a host factor screen with coxsackievirus A10 (i.e. required for coxsackievirus A10 viral replication.).

PI4KB, a type III PI4K, is involved in the production of PI4P at the early Golgi and TGN, and, like GBF1 is often hijacked by positive strand RNA viruses (Burke, 2018; Ferlin et al., 2018). Furthermore, GBF1 was recently shown to interact with PI4Ps, and as described previously, the

PI4KIII proteins are thought to play a role in GBF1 membrane binding (Doiron-Dumaresq et al., 2010; Meissner et al., 2018).

Following the identification of C10orf76 as a candidate of interest in the shRNA screen discussed in Chapter 4, the following subsections describe the characterization of this protein. This includes examining its interaction with GBF1, exploring its localization, distribution, and cycling dynamics, as well as examining its distribution across the eukaryotic tree.

5.2 Results

5.2.1 C10orf76 is essential for Golgi maintenance

As described in the last chapter, we found that depletion of C10orf76 caused a redistribution of EGFP-GBF1 in HeLa cells away from a juxtannuclear-like Golgi localisation toward peripheral puncta. Furthermore, treatment with BFA failed to recruit EGFP-GBF1 to existing GBF1 positive sites to the same extent as in control cells. Because the distribution of EGFP-GBF1 in these cells appear similar to that observed under conditions in which the Golgi is fragmented, we proceeded to examine the impact of C10orf76 depletion on the Golgi more closely – first using electron microscopy and then immunofluorescence. Transmission electron microscopy confirmed severe Golgi fragmentation (Figure 5.1A). No Golgi stacks could be observed in C10orf76-depleted cells (50 cells examined over two biological replicates) whereas Golgi stacks were observed in all cells treated with non-targeting shRNA. To further confirm our findings, we replicated the imaging experiment using immunofluorescence microscopy with the *cis*-Golgi and TGN markers, p115 and TGN46 (Figure 5.1B). These images further demonstrated that depletion of C10orf76 did indeed lead to the dispersal of Golgi stacks. GBF1 and p115 also remained largely redistributed to compartments proximal but distinct from TGN46, suggesting that the *cis*-Golgi localisation of GBF1 is not affected by C10orf76 depletion.

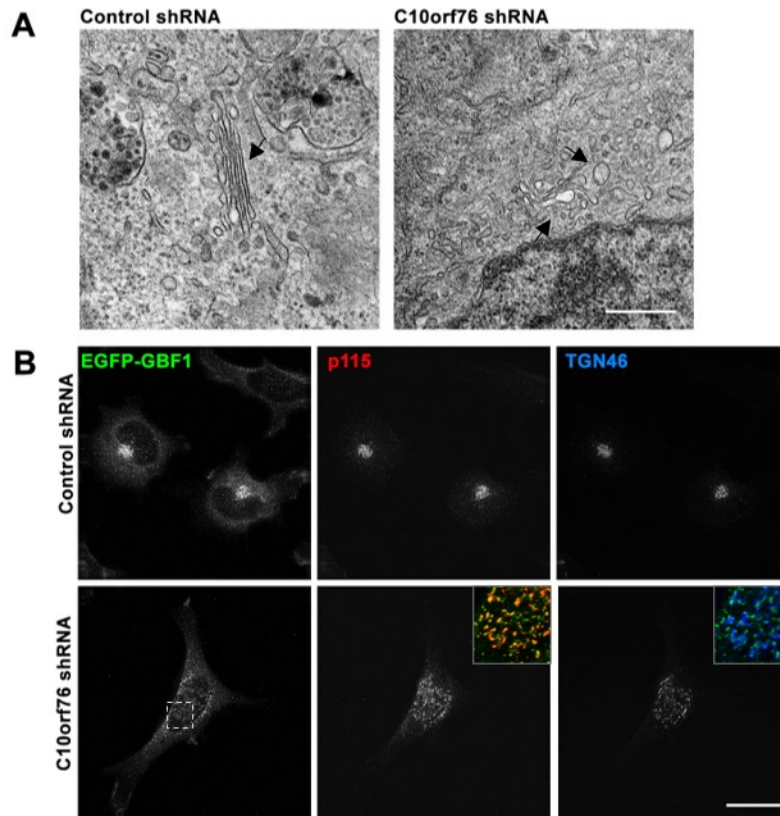


Figure 5.1 C10orf76 appears essential for Golgi maintenance.

EGFP-GBF1 expressing HeLa cells were transduced using lentiviral vectors with non-targeting or C10orf76 shRNAs, selected in the presence of puromycin, and grown for a total of 72 hours. (A) Transmission electron microscopy analysis found that although intact Golgi stacks were observed in all control cells examined, no C10orf76-depleted cells exhibited intact Golgi stacks. 50 cells were examined across two replicates. Black arrows point to an example of intact Golgi stacks in control shRNA treated or fragmented membrane compartments in C10orf76 shRNA treated cells. Scale bar = 2 μ m. (B) Immunofluorescence microscopy on fixed cells reveal a loss of intact Golgi upon C10orf76 depletion. EGFP-GBF1 as well as *cis*-Golgi and TGN markers, p115 and TGN46, are redistributed to disperse punctate structures. Panel B inset shows EGFP-GBF1 positive structures (green) largely distinct from those positive for TGN46 (blue). Images are representative of 15 cells examined across three replicates and are shown as projections of all z-slices. Inset represents a 3x magnification of the overlap with the EGFP signal in the selected area indicated by the dashed grey box. Scale bar = 26 μ m.

5.2.2 C10orf76 is required for maintaining cellular secretion

Having identified a role for C10orf76 in Golgi maintenance, we wanted to examine further whether secretory activity is similarly altered upon dispersal of the Golgi compartments. To measure global secretory activity, we chose to monitor the secretion of a nano luciferase. HeLa cells transduced with either non-targeting, C10orf76, or GBF1 shRNA encoding plasmids for 72 hours were additionally transfected with a plasmid encoding a secreted nano luciferase 18 hours prior to the secretion assay. After replacement with fresh media for collection of secretory products 72 hours post-transduction, the cells were then further exposed to either DMSO or 10 $\mu\text{g}/\text{mL}$ BFA for three hours. As previously observed, inhibition of GBF1 by either shRNA knockdown or treatment with BFA caused a severe reduction in luciferase secretion (Figure 5.2). Not surprisingly, we found that depletion of C10orf76 also led to a loss of secretory activity – likely due to disrupted Golgi. Together, our data indicate that C10orf76 is essential not only for Golgi maintenance but also for maintaining cellular secretion.

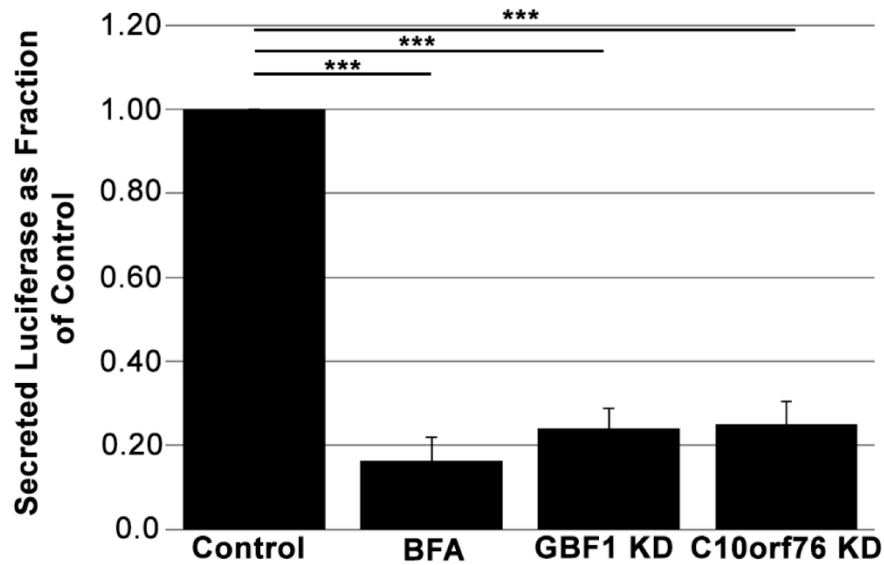


Figure 5.2 C10orf76 depletion impairs cellular secretion.

HeLa cells were transduced using lentiviral vectors with plasmids encoding non-targeting, c10orf76, or GBF1 shRNAs. All transductants were selected for using puromycin, and transfected with a plasmid encoding a secreted NanoLuc luciferase 18 hours prior to the assay at 72 hours post-transduction. During the assay, growth medium was analyzed for luciferase activity after a three hour incubation period with or without addition of BFA (1 $\mu\text{g}/\text{mL}$) as described in Chapter 2. Bars represent means \pm standard deviation (error bars) ($n = 3$). Depletion of c10orf76 causes a reduction in luciferase secretion similar to the inhibition of GBF1 activity by knockdown or treatment with BFA. Statistical significance was measured by a two-tailed unpaired *t*-test (control and BFA treatment $p = 0.0022$; control and GBF1 knockdown $p = 0.0019$; control and C10orf76 knockdown $p = 0.0027$).

5.2.3 C10orf76 interacts with the C-terminal half of GBF1

Our initial BioID analysis suggests that C10orf76 is likely a GBF1 proximal protein; however, to investigate potential GBF1 interaction we performed a traditional co-immunoprecipitation assay (Figure 5.3A). As mentioned, Blomen et al., 2014 had previously identified C10orf76 as an interactor of the Golgi enzyme, PI4KB, using a FLAG-tagged codon-optimized C10orf76 plasmid. Using the same codon-optimized C10orf76, we performed the co-immunoprecipitation alongside a mitochondrial localised Flag-tagged Rab32 as a control (Ortiz-Sandoval et al., 2014). Our results showed clear pulldown of GBF1 using FLAG-C10orf76 under conditions where FLAG-Rab32 pulled down its known interactor Drp1 but not GBF1 (Figure 5.3A). This suggests that C10orf76 is a novel GBF1 interactor.

To further examine the regions of GBF1 that C10orf76 interacts with, we performed additional co-immunoprecipitation experiments using our previously constructed EGFP-GBF1 truncations C1-884 and N885-1856; each truncation represents approximately one half of the GBF1 protein. C1-884 contains the N-terminal domains including the DCB and HUS domains previously shown to facilitate dimerization and the catalytic Sec7d. The Golgi-localised N885-1856 truncation contains the HDS1 and HDS2 domains essential for Golgi targeting and recruitment, as well as HDS3. In our assay, FLAG-tagged C10orf76 successfully pulled down the Golgi-localised N885-1856 but not the cytosolic C1-884 which lacks the membrane-association domains (Figure 5.3B). This suggests that C10orf76 likely interacts with GBF1 via its C-terminal half, the same fragment that was previously shown to be targeted to Golgi membranes (Figure 3.1 and 3.2)

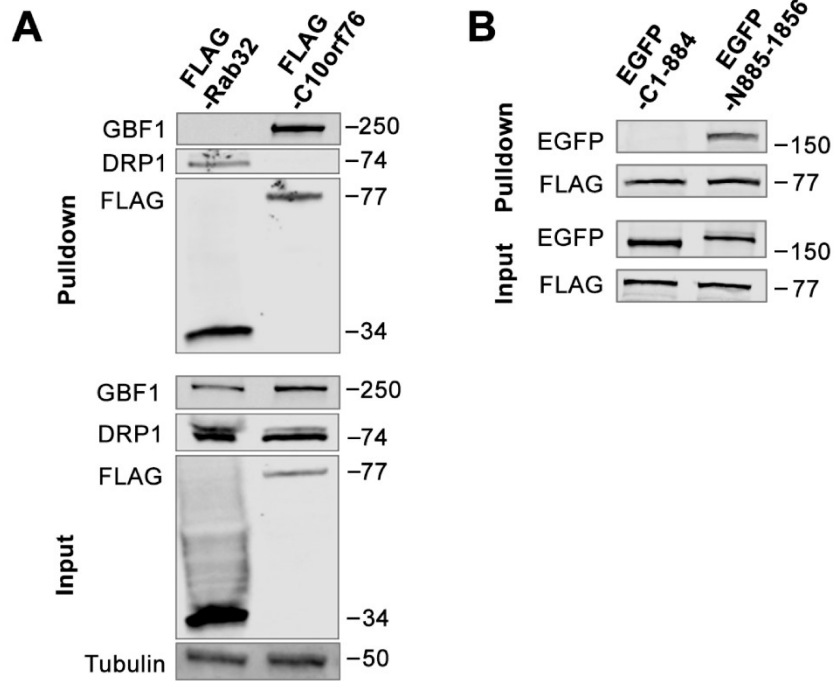


Figure 5.3 C10orf76 interacts with the C-terminal half of GBF1.

Pull-down was performed with either FLAG-C10orf76, FLAG-Rab32, EGFP C1-884, or EGFP-N885-1856. HeLa cells were transfected with plasmids encoding the appropriate constructs, grown for 18 hours, and co-immunoprecipitated as described in Chapter 2. Input represents collected lysates prior to pull-down using antibodies. Equivalent volumes were loaded. Numbers on the right side of the blots indicate molecular mass in kilodaltons. (A) Pull-down was performed with anti-FLAG antibodies. Western blotting shows distinct bands corresponding to the pulled-down endogenous GBF1 with FLAG-C10orf76 and DRP1 with FLAG-Rab32. (B) Pull-downs were performed with anti-EGFP-antibodies. Western blotting revealed distinct bands corresponding to the pulled-down EGFP-N885-1856 using FLAG-C10orf76. C1-885 was not pulled down by C10orf76. All images are representative of three replicates.

5.2.4 C10orf76 interaction is not sufficient to target GBF1 to the Golgi

Having identified that C10orf76 likely interacts with GBF1 via its C-terminal half, which contains the previously shown Golgi targeting domains, we wanted to further investigate whether this interaction may be involved in Golgi targeting of GBF1. Without knowing the select motifs and amino acids on GBF1 essential for C10orf76 interaction, we chose to instead work with known GBF1 mutants that fail to localise to the Golgi. As discussed in Chapter 3, mutating a key amino acid in HDS2 (L1246R mutation in the fifth alpha helix of HDS2) can impair Golgi localisation (Chen et al., 2017). We generated the L1246R mutation in the N885-1856 truncation, which facilitates site-directed mutagenesis because of its smaller size. Sanger sequencing confirmed successful mutation of the construct and live-cell imaging experiments confirmed that the mutation abrogated Golgi localisation as previously published (Figure 5.4). Using the mutant in our co-immunoprecipitation assay revealed that the L1246R change, while abrogating localisation, appeared to have no impact on C10orf76 interaction (Figure 5.5). The quantity of EGFP-tagged WT N885 or mutant N885 pulled down by FLAG-C10orf76 appears comparable, suggesting that the interaction with C10orf76 was not compromised by the mutation. This indicates that the interaction between C10orf76 and GBF1 is likely not sufficient for membrane targeting.

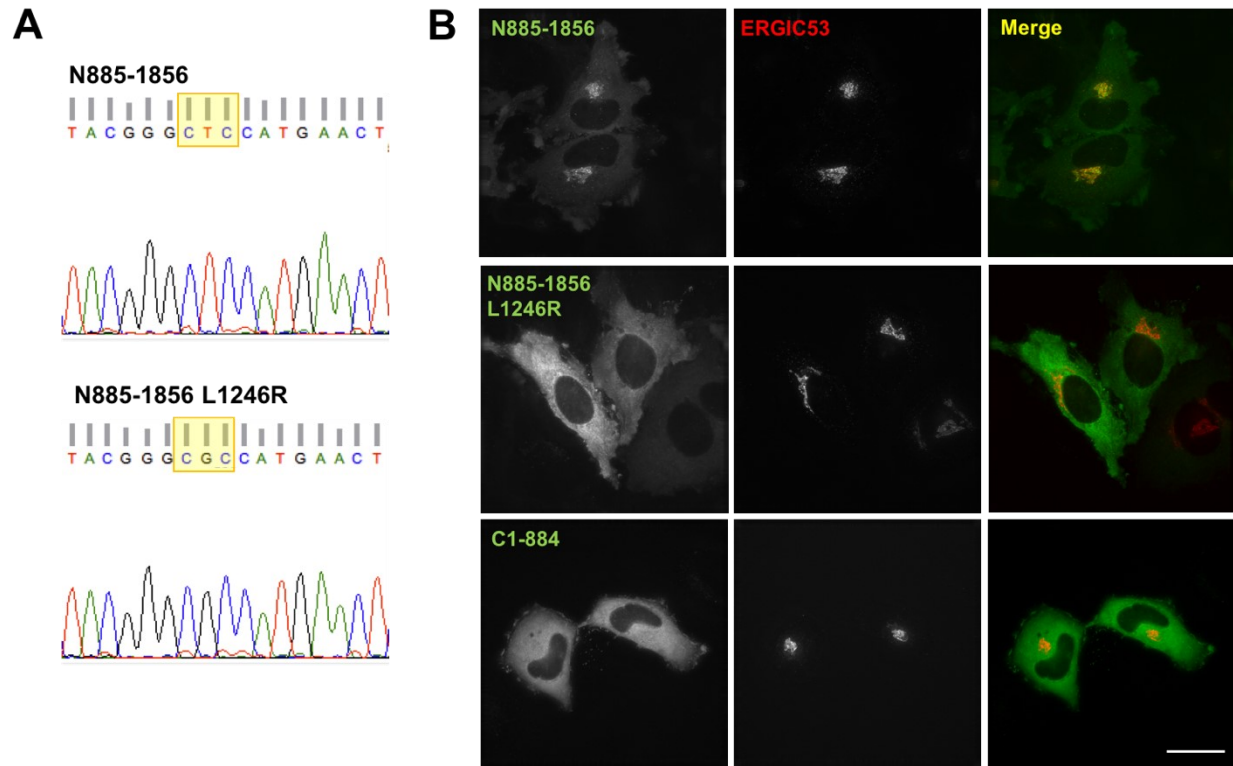


Figure 5.4 The L1246R mutation abrogates Golgi localisation in the N885-1856 truncation. (A) Sanger sequencing performed on the EGFP-tagged N885-1856 and N885-1856 L1246 mutant confirms successful introduction of a CTC to CGC change in nucleotide sequence (highlighted in yellow) corresponding to a leucine to arginine swap. (B) Live-cell imaging comparing the EGFP-tagged N885-1856, N885-1856 L1246R, and C1-884. The WT N885-1856 truncation colocalizes with ERGIC53 at juxtannuclear structures while the truncation lacking the appropriate targeting domains, C1-884, or containing the L1246 mutation both fail to colocalize with ERGIC53. All images are representative of 15 cells examined across three replicates. Scale bar = 26 μ m

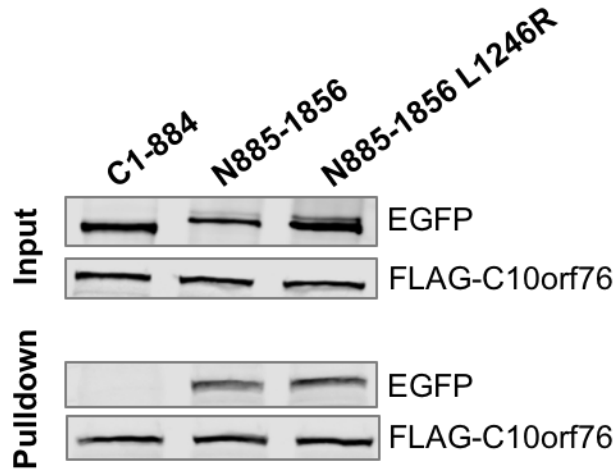


Figure 5.5 C10orf76 interaction appears not to be impaired by the L1246R mutation.

Pulldown was performed using anti-FLAG antibodies with cells transiently transfected with plasmid encoding FLAG-C10orf76 and either EGFP-C1-554, N885-1856, or the N885-1856 L1246R mutant. Proteins were detected by western blotting using anti-EGFP or anti-FLAG antibodies. Blot shows C10orf76 is pulling down both N885-1856 and the L1246R mutant, but not the C1-884 truncation. Input represents loading of lysates prior to pulldown with anti-FLAG antibodies. Images are representative of three replicates.

5.2.5 C10orf76 depletion does not impair GBF1 activity

Having identified C10orf76 as a novel interacting partner of GBF1, we next wanted to further examine whether the Golgi fragmentation associated with C10orf76 depletion may be caused by altered GBF1 function. One potential cause of fragmentation could be due to the loss of GBF1 activity, Arf activation, and COPI recruitment. To assess whether GBF1 activity is impaired, we looked to downstream Arf effectors for insight. GBF1 activated Arf1 on Golgi membranes are responsible for the recruitment of the COPI coatomer – including the β -COP subunit (García-Mata et al., 2003; Szul et al., 2007; Zhao et al., 2006). Extensive depletion of GBF1 or inhibition of GBF1 activity impairing Arf activation, blocks COPI recruitment to Golgi membranes (Manolea et al., 2008). Using immunofluorescence microscopy, we found that β -COP recruitment to GBF1 positive Golgi fragments were maintained in cells depleted of C10orf76 after 72 hours. Further treatment with GBF1 inhibitor, BFA (10 μ g/mL) for 2 minutes completely abrogated β -COP recruitment (Figure 5.6). These observations suggest that in cells depleted of C10orf76 at 72 hours post-transduction, sufficient GBF1 remains functional at fragmented Golgi sites in most cells to maintain Arf activation and COPI recruitment. Additional quantitation of GBF1 to existing GBF1 positive in these fixed samples reveal a comparable fold increase as observed by live-cell imaging performed in Figure 4.9.

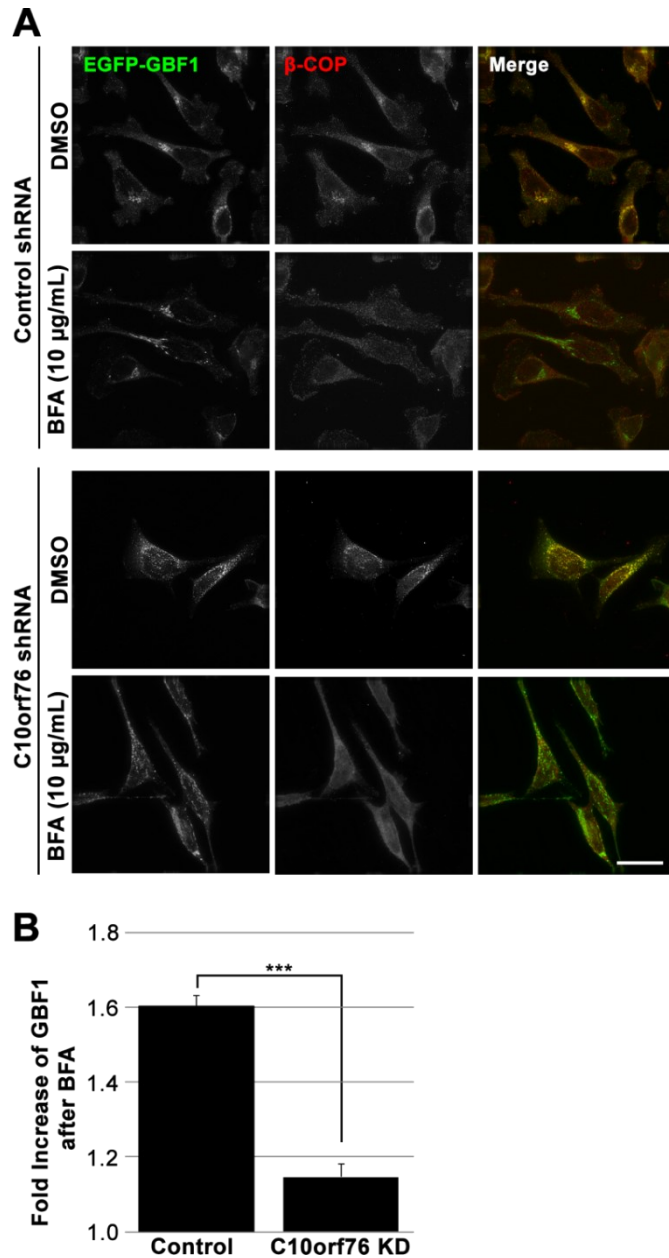


Figure 5.6 C10orf76 depletion does not prevent β -COP recruitment.

(A) HeLa cells were transduced using lentiviral vectors with plasmids encoding non-targeting or c10orf76 shRNAs for 72 hours. Fixed cell imaging reveals β -COP present on GBF1 positive Golgi fragments in c10orf76-depleted cells. Further treatment with BFA (10 μ g/mL) for 90 seconds as described in Chapter 2 abrogates β -COP recruitment to these sites suggesting GBF1 remains functional despite treatment with c10orf76 targeting shRNA. (B) Quantitation of the fold increase of GBF1 at after BFA treatment (10 μ g/mL) for 90 seconds in panel A. Quantitation was performed as described in described in Chapter 2 (six cells per replicate, n=3) (Mean values are 1.60 for control and 1.15 for c10orf76-depleted cells). Bars represent mean values \pm standard deviation (error bars). A statistically significant difference was observed between the c10orf76-depleted and control cells as measured by a two-tailed unpaired *t*-test ($p = 0.00015$).

5.2.6 C10orf76 is a Golgi-localised protein but is not sensitive to BFA

The interaction between C10orf76 and GBF1, as well as the previously shown Golgi resident enzyme PI4KB, suggests that C10orf76 may also be present on Golgi membranes (Blomen et al., 2015; Burke, 2018). Furthermore, our identification of C10orf76 from BioID performed on Golgi-enriched fractions further suggests a potential Golgi localisation. To confirm the localisation of C10orf76 without an antibody validated for use in immunofluorescence, we opted to examine the localisation using a fluorescently tagged version. In HeLa cells, the majority of mCherry-C10orf76 appeared cytosolic, with a portion colocalising with the previously characterized EGFP-GBF1 at juxtannuclear Golgi sites (Figure 5.7). This observation indicates a Golgi localisation for C10orf76.

The presence of a clear cytosolic pool of C10orf76 similar to GBF1, prompted us to examine whether the recruitment of C10orf76 to the membrane may be similarly regulated by Arf-GDP. To this end we examined the effects of the drug BFA on the recruitment of C10orf76 to membranes. In cells expressing both EGFP-GBF1 and mCherry-C10orf76, treatment with BFA (10 µg/mL) for up to four minutes clearly stimulated the recruitment of GBF1 to juxtannuclear sites, while C10orf76 distribution remained unchanged. No additional C10orf76 appeared to be required at the membrane for additional GBF1 recruitment.

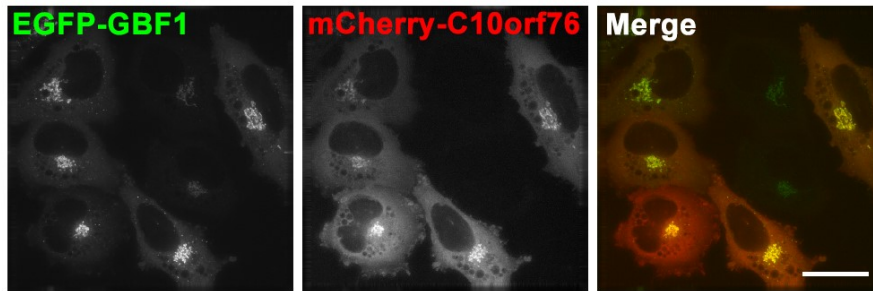
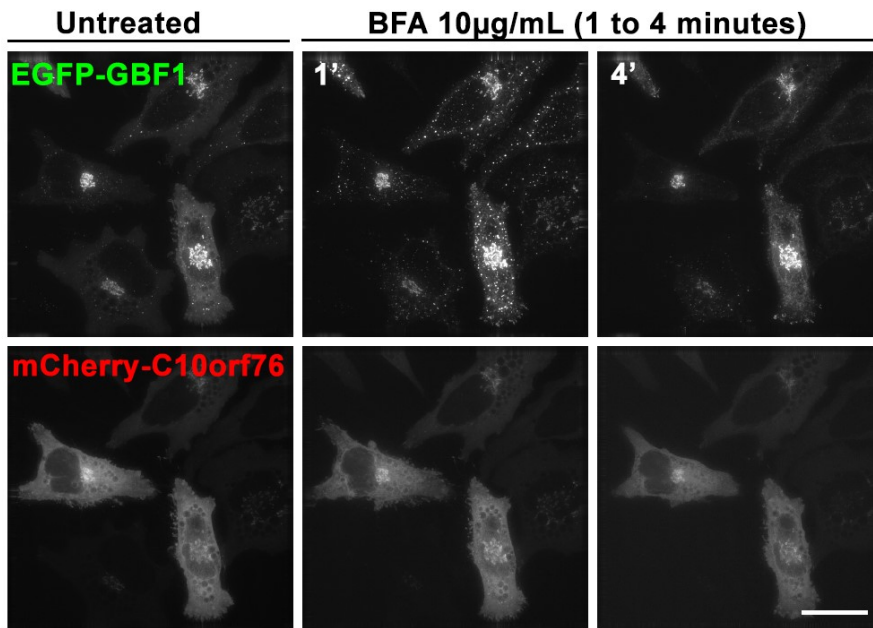
A**B**

Figure 5.7 C10orf76 localises to GBF1 positive Golgi structures but appears insensitive to BFA.

Live-cell imaging of EGFP-GBF1 expressing HeLa cells transfected with mCherry-C10orf76. (A) Both GBF1 and C10orf76 constructs occupy cytosolic pools and co-localise at juxtannuclear Golgi sites. (B) Live cells were treatment with BFA (10 μ g/mL) for up to four minutes and examined at one-minute intervals as described in Chapter 2. BFA treatment promotes recruitment of EGFP-GBF1 to juxtannuclear and peripheral punctate sites, and a clearing of GBF1 from the cytosol. mCherry-C10orf76 however, exhibits a similar distribution before and after BFA addition even after four minutes. Images are representative of twenty cells examined across three replicates and are shown as projections of all Z-slices. Scale bar = 26 μ m.

5.2.7 C10orf76 is a peripheral protein that cycles on and off Golgi membranes

To further investigate the interaction between C10orf76 and Golgi membranes, we utilized subcellular fractionation and FRAP. *In vitro* experiments showed that both GBF1 and C10orf76 can be detected on pelleted membrane fractions and washed off using a high pH carbonate solution (Figure 5.8). This confirms that C10orf76, like GBF1, is a peripheral membrane protein. Giantin, a known Golgi-localised integral membrane protein was resistant to the high pH wash and remained in the pellet, confirming that only peripheral membrane proteins were extracted.

In vivo FRAP experiments performed on cells expressing either EGFP-GBF1 or EGFP-C10orf76 revealed that both proteins cycled rapidly with their cytosolic pools at steady state. Surprisingly, C10orf76 appeared to cycle ($t_{1/2} = 6.6$ seconds) dramatically faster than GBF1 ($t_{1/2} = 21.2$ seconds; Figure 5.9). Furthermore, FRAP experiments performed in the presence of BFA (10 $\mu\text{g}/\text{mL}$) after 90 seconds revealed that while GBF1 cycling could be abrogated using the drug, BFA only slowed C10orf76 exchange ($t_{1/2} = 12.4$ seconds; two-tailed *t*-test $p < 0.0007$). Together with section 5.2.5, our data suggest that C10orf76 is a Golgi-localised peripheral membrane protein, but not regulated by Arf-GDP in the same manner as GBF1.

As described earlier, HeLa cells depleted of C10orf76 exhibited a clear redistribution of p115 and GBF1, fragmenting the Golgi. With the availability of our shRNA-resistant mCherry-C10orf76, we were now able to confirm the specificity of this observation. To do so, we repeated the knockdown experiments again in EGFP-GBF1 expressing HeLa cells, this time transfected with the codon-optimized shRNA-resistant mCherry-C10orf76. At 72 hours, cells expressing the mCherry-C10orf76 construct retained a juxtannuclear distribution of Golgi markers unlike those non-transfected with the construct (Figure 5.10). This suggests that the Golgi fragmentation observed in the C10orf76 shRNA transduced cells was specific and resulted from loss of

C10orf76 as opposed to result from an off-target effect. Further observations demonstrated that although C10orf76 depletion led to eventual cell death, cells overexpressing C10orf76 continued to survive at least until 80 hours post-transduction.

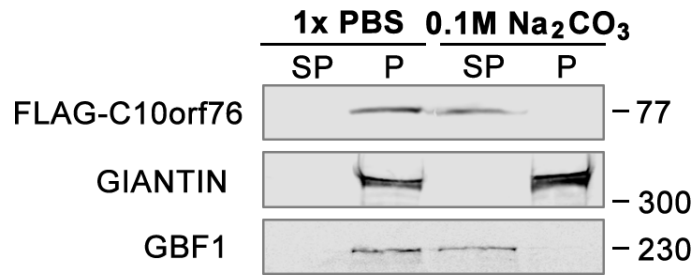


Figure 5.8 C10orf76 is a peripheral membrane protein.

Sucrose-gradient separated Golgi fractions were incubated either in 0.1 M Na₂CO₃ (pH 11.3) buffer or PBS with added protease inhibitors on ice for 30 minutes. Supernatants and membrane pellets were then collected and analyzed by western blotting and probed with anti-GBF1, anti-giantin, or anti-FLAG antibodies. Numbers on the right side of the blots indicate molecular mass in kilodaltons. Incubation with 0.1 M Na₂CO₃ (pH 11.3) successfully extracted peripheral membrane protein GBF1, and FLAG-C10orf76. Integral membrane protein, giantin, remains in the pellet suggesting that C10orf76 is indeed a peripherally protein. Images are representative of three replicates.

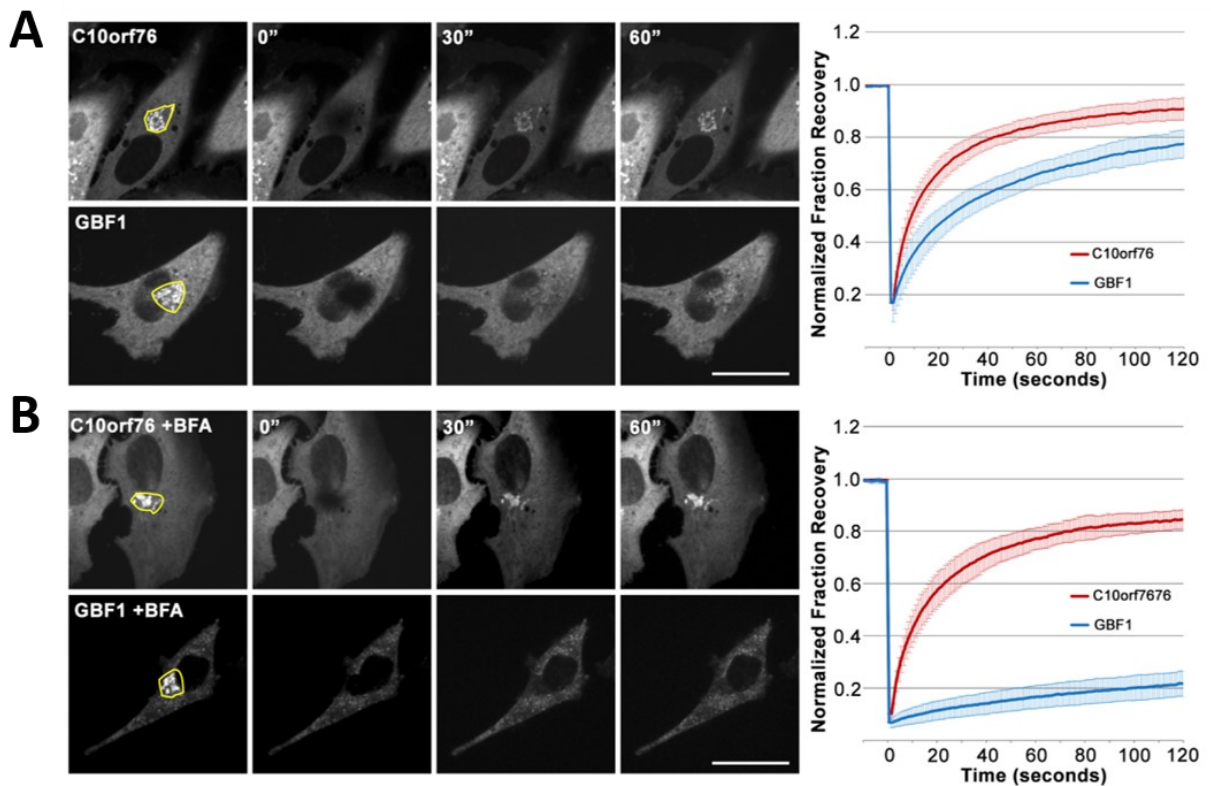


Figure 5.9 C10orf76 cycles on and off membranes rapidly.

FRAP analyses were performed on cells expressing either EGFP-GBF1 or EGFP-C10orf76 and with or without BFA (10 $\mu\text{g}/\text{mL}$). Cells were imaged before and after photobleaching of the Golgi region (outlined in yellow) by illumination with a high-intensity laser. After photobleaching, images were acquired at one second intervals for 120 seconds to monitor fluorescence recovery. 15 cells were examined across three biological replicates. Images at 0, 30, and 60 seconds are shown. The fraction of EGFP signal in the Golgi area was normalized to 1 at $t = 0$ and quantified as described in Chapter 2. Error bars represent $\pm 26 \mu\text{m}$. (A) EGFP-C10orf76 cycles more rapidly than GBF1 ($t_{1/2} = 6.6$ seconds vs 21.2 seconds). (B) BFA impairs EGFP-GBF1 cycling but only slows EGFP-C10orf76 (C10orf76 $t_{1/2} = 12.4$ seconds after BFA; two-tailed t -test $p < 0.0007$).

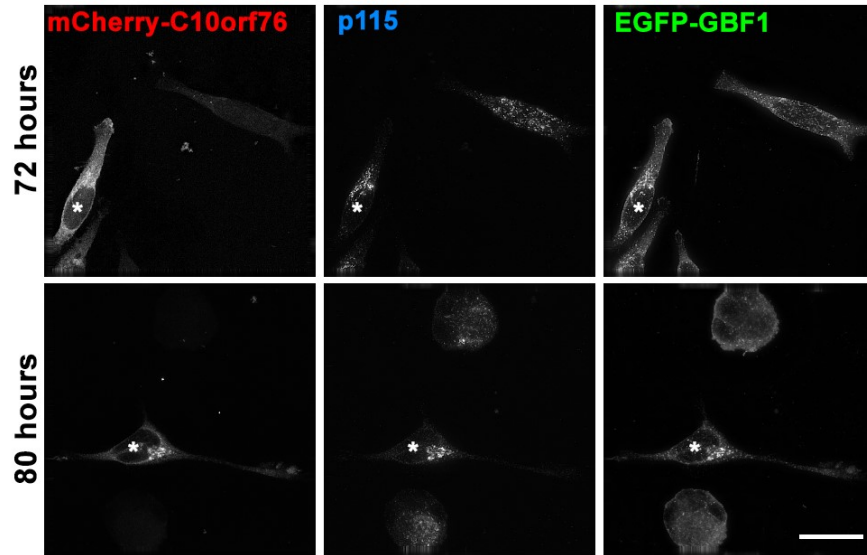


Figure 5.10 C10orf76 overexpression prevents Golgi fragmentation in knockdown cells.

EGFP-GBF1 expressing HeLa cells were transduced using lentiviral vectors with C10orf76 shRNA for 72 or 80 hours. Transfection with an shRNA resistant mCherry-C10orf76 rescues dispersal of p115 and EGFP-GBF1 observed at 72 hours, and cell death observed at 80 hours. Transfected cells are indicated by a white asterisk. Non-transfected cells exhibit a loss of juxtannuclear p115 staining and EGFP-GBF1 localisation. All images are representative of 15 cells examined across three replicates and are shown as projections of all Z-slices. Scale bar = 26 μm .

5.2.8 C10orf76 truncations fail to reveal a Golgi localising domain

As mentioned at the beginning of this chapter, the only known conserved region of C10orf76 is a domain of unknown function (DUF1741; amino acids 431-669). DUF1741 appears to present in all known C10orf76 orthologs, but is absent from other known proteins. To test whether DUF1741 was involved in targeting C10orf76 to the Golgi, we tested two EGFP-tagged C10orf76 truncation mutants: one containing the N-terminal half (amino acids 1 to 430) and the other, the C-terminal half with DUF1741 (amino acids 431-688). When expressed in HeLa cells, neither half exhibited any clear membrane localisation in live-cells (Figure 11). This may indicate that neither half of the protein is capable of membrane targeting on its own, or more likely, that the deletion mutants severely compromised protein structure and function.

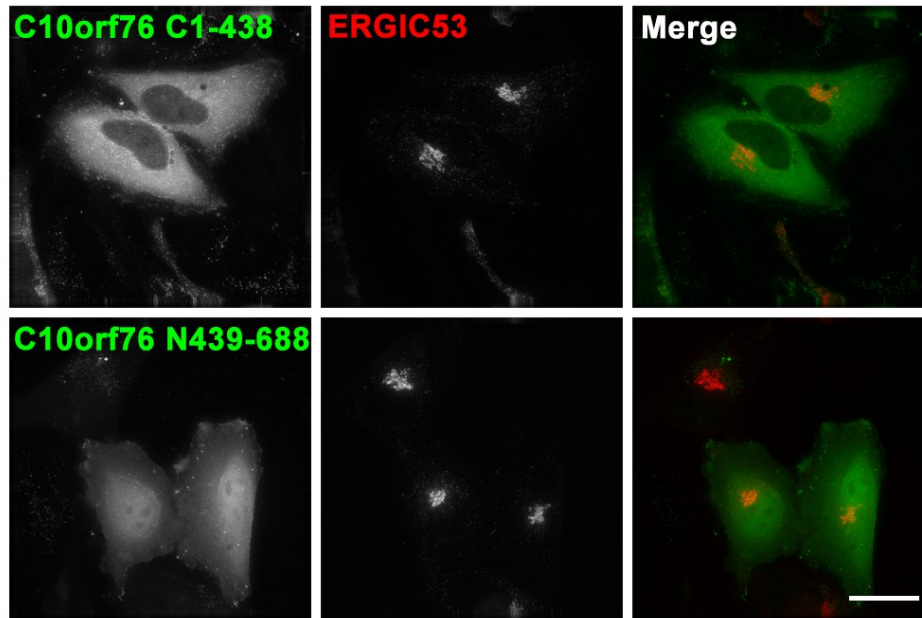


Figure 5.11 N- and C- terminal C10orf76 truncations fail to localise to ERGIC53-positive Golgi structures.

Live-cell imaging of EGFP-tagged c10orf76 truncation mutants co-transfected in HeLa cells with mCherry-ERGIC53. The C-terminal truncation with amino acids 1 to 438 (C1-438) appear cytosolic and is excluded from the nucleus likely due to size. The smaller, N-terminal truncation with amino acids 439 to 688, is present in both the cytosol and nucleus. Images are representative of 20 cells examined across three replicates and are shown as projections of all Z-slices. Scale bar = 26 μm .

5.2.9 C10orf76 is likely present in the last eukaryotic common ancestor, similar to GBF1

The GBF family of orthologs are found in all eukaryotic supergroups, and alongside BIGs and cyoohesins, are the only ArfGEF family members predicted to be present in the last eukaryotic common ancestor (LECA) (Pipaliya et al., 2019). We therefore assumed that the protein(s) involved in facilitating membrane targeting for GBF1 should also be present in the LECA and similarly inherited across eukaryotic lineages. To identify orthologs of C10orf76 across eukaryotes, we performed BLASTp searches using human C10orf76 protein sequence as a query. Using a reciprocal best hit strategy (where sequences were only characterized as true orthologs if they retrieve each other as the best hit in the opposite genome) and an E-value cutoff of 10^{-12} , related sequences were identified in a large variety of clades (Figure 5.12). However, no orthologs could be identified in the yeast *Saccharomyces cerevisiae*, plant *Arabidopsis thaliana*, or nematode *Caenorhabditis elegans*. Despite being missing in these common model systems, C10orf76 orthologues were readily identified in other plantae, fungi, and nematode species including the common liverwort *Marchantia polymorpha* (OAE23309.1, PTQ49274.1), fission yeast, *Schizosaccharomyces pombe* (NP_596366.1), and the nematode, *Trichinella spiralis* (KRY28766.1). To confirm that potentially divergent sequences from *S. cerevisiae*, *A. thaliana*, or *C. elegans*, were not missed, we performed additional searches using the identified protein sequences from their related plantae, fungi, and nematode species (*M. polymorpha*, *S. pombe*, *T. spiralis*), but no hits were identified. We also further performed tBLASTn searches into the nucleotide scaffolds of these organisms but were unable to identify any related sequences. This suggests that C10orf76 was likely inherited in the plantae, fungi, and nematode kingdoms but rather lost in certain plantae, fungi, and nematode species. Outside the achaeplastida and opisthokonta supergroups, we also identified C10orf76 orthologs in the protist *Naegleria gruberi*

(XP_002680913.1) from the excavate supergroup and the slime mold *Dictyostelium discoideum* (XP_643233.1) from the amoebozoan supergroup. The presence of C10orf76 in multiple eukaryotic lineages suggests that it was likely present in the last eukaryotic common ancestor similar to GBF1. All species examined, the top hits identified, and their corresponding accession numbers can be found in table 5.1.

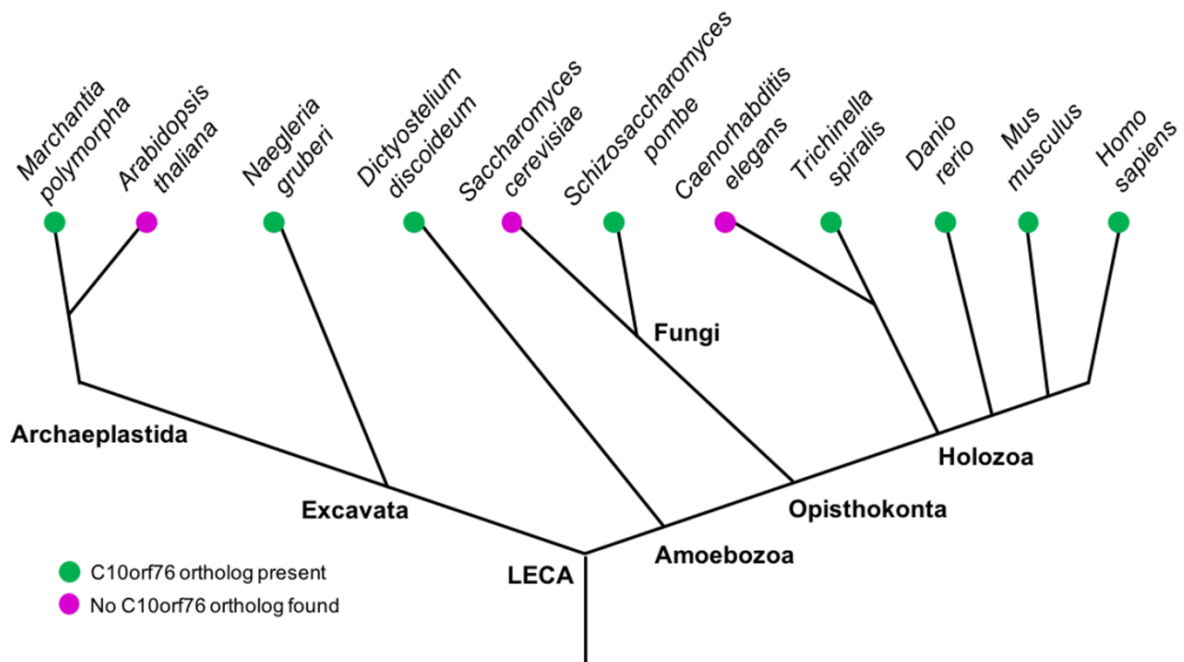


Figure 5.12 C10orf76 is likely an ancestral protein.

Presence and absence of C10orf76 orthologs in various eukaryotic species as identified using reciprocal best hit BLASTp searches with the human C10orf76 query. Green circles signify the presence of a C10orf76 ortholog while magenta circles signify the absence. An E-value cutoff of 10^{-12} was used for all searches. The C10orf76 orthologs identified and their corresponding accession number can be found in table 5.1.

Table 5.1 Accession numbers and associated E-values for BLASTp searches using human C10orf76 as a query.

Eukaryotic supergroup	Species	Accession	E-Value
Opisthokont	Homo sapiens (query)	NP_078817	
	Mus musculus	NP_938038.2	0.00E+00
	Danio rerio	NP_956913.2	0.00E+00
	Caenorhabditis elegans	NP_492912.1	8
	Trichinella spiralis	KRY28766.1	4.00E-155
	Drosophila melanogaster	NP_649841.1	0.00E+00
	Saccharomyces cerevisiae		NO HIT
	Schizosaccharomyces pombe	NP_596366.1	7.00E-14
	Aspergillus nidulans	XP_659579.1	3.00E-37
	Neurospora crassa	XP_963569.2	3.00E-44
Archaeplastida	Marchantia polymorpha	OAE23309.1	3.00E-32
	Physcomitrella patens	XP_024389176.1	3.00E-22
	Arabidopsis thaliana		NO HIT
Amoebozoa	Dictyostelium discoideum	XP_643233.1	9.00E-95
Excavata	Naegleria gruberi	XP_002680913.1	1.00E-62

5.3 Discussion

5.3.1 Links between C10orf76, PI4K, and GBF1

Our study identified several links between GBF1 and the poorly studied protein, C10orf76. With the depletion of C10orf76, we observed a clear fragmentation of the Golgi as well as a reduction in GBF1 recruitment to fragmented Golgi sites upon BFA treatment (Figure 4.9). Similar to previous experiments performed on near-haploid KBM7 cells, our data suggest that complete KD of C10orf76 in HeLa cells appear lethal, and as such, our observations on still living cells may have resulted from partial knockdown only. Previous research has shown that even under conditions where the Golgi is fragmented, such as upon treatment with nocodazole, GBF1 can still be recruited to fragmented Golgi membranes (Szul et al., 2005; Zhao et al., 2006). Our observation that C10orf76 depletion impaired the additional recruitment of GBF1 to fragmented Golgi sites suggest that C10orf76 is likely needed for recruitment of GBF1 to Golgi sites in mammalian cells. Furthermore, co-immunoprecipitation experiments found that GBF1 interacts with C10orf76 via its C-terminal half (Figure 5.3). However, additional experiments will be required to assay whether the interaction is direct. This can be examined using *in-vitro* co-immunoprecipitation experiments with recombinant GBF1. Likewise, we can ascertain whether the interaction takes place on Golgi membranes using imaging techniques such as fluorescence resonance energy transfer and by repeating the pulldown on Golgi-enriched fractions. As shown in Chapter 3, we previously established that GBF1 localisation to Golgi membranes is dependent on C-terminal domains. This may suggest that C10orf76 facilitates GBF1 interaction with the membrane via the GBF1 C-terminal domains. Since the publication of our work, an additional study reported additional links between C10orf76 and PI4KB – an

enzyme previously implicated in the regulation of GBF1 (Doiron-Dumaresq et al., 2010; McPhail et al., 2019).

In this recent study, researchers confirmed the previously reported interaction between PI4KB and C10orf76, and demonstrated that PI4KB functioned as a receptor for C10orf76 at Golgi membranes (McPhail et al., 2019). Redirecting PI4KB to mitochondrial membranes using the FRB domain of mTOR, similarly retargeted a portion of C10orf76 to mitochondria. Likewise, a C10orf76 mutation that disrupts PI4KB interaction prevents its Golgi localisation. Previous studies had already demonstrated that inhibition of PI4K activity reduced GBF1 levels at the Golgi (Doiron-Dumaresq et al., 2010). One potential model by which PI4K depletion might interfere with GBF1 localisation could be through reducing Golgi-localised C10orf76. McPhail et al., 2019 also found that depletion of C10orf76 reduced PI4P levels at the Golgi – likely through inhibition or disruption of PI4KB activity. As discussed, previous results have also shown that GBF1 is also a PI4P binding protein (Meissner et al., 2018). C10orf76 may thus regulate GBF1 binding through modulating PI4P levels via PI4KB activity.

Similar to our studies in HeLa cells, McPhail et al., 2019 found that reduction of C10orf76 in haploid human cells corresponded with reduced GBF1 at membrane sites. Together, published data strongly suggest that C10orf76 is a key modulator of GBF1 membrane binding, likely through a combination of physical interaction and modulation of PI4P levels through PI4KB.

5.3.2 Is C10orf76 a GBF1 co-receptor?

C10orf76 may be a regulator of GBF1 membrane binding, but is it a direct co-receptor for GBF1? Previous data have shown that high-temperature and trypsin treatment of enriched Golgi fractions impair GBF1 binding, suggesting the existence of a Golgi-localised receptor-like

protein for GBF1. If C10orf76 is a potential co-receptor for GBF1 at the membrane, one would expect that the recruitment of additional GBF1 to the Golgi might coincide with increased Golgi-localised C10orf76. Unfortunately, we did not observe C10orf76 localisation or recruitment alter upon BFA treatment (Figure 5.7). However, we also cannot exclude the possibility that levels of C10orf76 on membranes are already saturated in HeLa cells, and that other factors such as the recruitment of other co-receptor components or conformational changes to C10orf76 may regulate GBF1 binding. In fact, in both our study as well as in the work of McPhail et al., 2019, C10orf76 binding sites appear easily saturated. The Golgi localisation of fluorescently-tagged C10orf76 is only visible under low expression levels, with excess cytoplasmic C10orf76 masking Golgi-bound pools at higher levels of expression. Furthermore, our data also suggest that endogenous C10orf76 is likely naturally expressed at fairly low levels in the cell: C10orf76 was only detected in our BioID experiments in the Golgi-enriched fractions, and western blotting of C10orf76 required concentrating the protein first through acetone precipitation.

Nonetheless, despite a lack of change in localisation, C10orf76 cycling does appear to be sensitive to BFA treatment, suggesting that Arf-GDP may play a role in modifying C10orf76 dynamics and activity (Figure 5.9). Previous work has shown that Arf-GDP stimulates GBF1 recruitment to Golgi membranes in a feed-forward mechanism (Quilty, 2016). The reduced cycling of C10orf76 observed in BFA treated cells may act as a potential mechanism to facilitate additional GBF1 binding. This may occur by directly recruiting GBF1, by contributing to a receptor complex, or activating other protein components on the membrane. Additional experiments such as examining C10orf76 localisation and cycling in cells overexpressing Arf-GDP arrested or inactive GBF1 mutants may provide additional answers. Likewise, identifying

C10orf76 interacting partners through BioID or other similar methods may also yield novel insights.

While findings from both our laboratory and in McPhail et al., 2019 suggest that C10orf76 may act as a potential GBF1 co-receptor, several additional observations complicate this interpretation. Firstly, C10orf76 cycles much more rapidly than GBF1 (Figure 5.9). Indicating that it is not required at the membrane for the entire time GBF1 is present. For instance, it may only be required for the initial recruitment of GBF1, after which it is released from the membrane. Secondly, C10orf76 while likely ancestral, is also missing from several common model systems including *A. thaliana*, *S. cerevisiae*, and *C. elegans* (Figure 5.12). This may indicate that the function of C10orf76 may be replaced by some other protein in these organisms or that C10orf76 may not necessarily be essential for GBF1 recruitment. In fact, our work suggests that C10orf76 likely play additional roles in the cell apart from regulating GBF1. In cells depleted of C10orf76, we find that GBF1 remains active at fragmented Golgi sites as indicated by the recruitment of β -COP (Figure 5.6). C10orf76 could have functions in Golgi maintenance via other pathways. It is important to note that while GBF1 orthologs have been extensively studied in both yeast, worm, and plant systems, the mechanism regulating their recruitment remains similarly unresolved. The lack of readily identifiable C10orf76 sequences in these other model systems suggest that while C10orf76 may contribute to the regulation of GBF1 in mammalian cells, other more evolutionarily conserved components are likely involved. However, at this point, we also cannot exclude the possibility that the role of C10orf76 may be replaced by other proteins with low sequence similarity in these model systems. Little is known about the protein structure of C10orf76 apart from a conserved domain of unknown function, DUF1741, that is absent from other known human proteins.

To tease apart a GBF1 binding region in C10orf76, we generated two C10orf76 truncation mutants (one containing the DUF1741, and one without) and examined their localisation *in vivo*. Disappointingly, neither constructs localised to any clear membrane structure (Figure 5.11). McPhail et al., 2019 performed point mutations in the DUF1741 to determine if the region was involved in PI4KB binding, but none of the mutations tested appeared to have an effect. At this point, the function of the conserved DUF1741 remains unknown.

Chapter 6: ZnT6 is a novel GBF1 interacting partner and may regulate GBF1 dynamics at the Golgi

The work comprising this chapter has not yet been published. The construction of the ZnT6 knockdown cell line and the luciferase secretion assay was performed with help from undergraduate student Kaylan Burns.

6.1 Background on ZnT6

6.1.1 Zinc transporters at the Golgi

Zinc plays essential roles in the early secretory pathway by acting as a structural or catalytic component for enzymes, chaperones, and other protein functions (Huang and Tepasamorndech, 2013; Kambe, 2011; Kambe et al., 2017). Not surprisingly, disruption of zinc homeostasis can lead to ER stress and trigger the unfolded-protein response. The two main family of proteins involved in regulating zinc transport in the cell are the ZnTs and the ZIPs. The ZIP family is involved in the import of extracellular zinc and the export of zinc out of membrane-bound organelles – moving zinc into the cytosol. At the Golgi, ZIP13 is involved in the removal of zinc from the lumen. Unlike ZIPs, the ZnT family is involved in zinc import into membrane compartments.

At the Golgi, zinc import is regulated by two key complexes: ZnT7 homodimers, and ZnT5 and 6 heterodimers. However, unlike ZnTs found at other cellular locations, the Golgi-localised ZnT5, 6, and 7 have comparatively poor transport activities (Kambe, 2011). For instance, overexpression of ZnT5, 6, and 7 cannot confer resistance to high concentrations of zinc unlike vesicular ZnT2 or TGN-localised ZnT4. Furthermore, triple deletion of ZnT5, 6, and 7 do not significantly alter overall cellular concentrations of zinc and is dispensable for cell growth and survival in mammalian cells (Fukunaka et al., 2009). Mouse models missing either ZnT5 or ZnT7 survive until adulthood suggesting that neither proteins are essential for development (Huang and Tepasamorndech, 2013). However, the animals do exhibit poor growth and are leaner as compared to WT animals, and are also more susceptible to health problems such as cardiac arrhythmia and diabetes.

Nonetheless, deletion of ZnT5, 6, and 7 has been shown to reduce the activity of Golgi enzymes including the tissue nonspecific alkaline phosphatases (TNAP) (Suzuki et al., 2005). Re-expression of either ZnT5 and 6 or ZnT7 alone is sufficient to rescue TNAP activity, indicating that the two complexes are functionally redundant to a certain degree (Fukunaka et al., 2011). However, TNAP activity, unlike the function of other ZnT5, 6, and 7 activated enzymes (such as the metalloproteases 2 and 9, and autotaxin) cannot be rescued by zinc supplementation (Fukunaka et al., 2011; Kambe et al., 2017). Current work suggests that apart from zinc transport, ZnT5, 6, and 7 may also interact and facilitate the activation or stabilization of a subset of zinc enzymes, including TNAP.

6.1.2 ZnT5 and 6 are structurally unique compared to other ZnT proteins

Despite the perceived functional redundancy between the ZnT5 and 6 heterodimer and the ZnT7 homodimer, the ZnT5 and 6 complex is unique in several aspects. Firstly, all ZnTs function as homodimers except ZnT5 and 6 (Kambe, 2011). Furthermore, ZnT6 is particularly unusual in that it contains a serine-rich loop between transmembrane domains 4 and 5 even though most other ZnTs, including ZnT5, contain a histidine-rich loop (Suzuki et al., 2005). ZnT6 also lacks two of the four conserved hydrophilic residues (two histidine and two aspartic acids) in transmembrane 2 and 5 (Fukunaka et al., 2009). The histidine-rich loop and the hydrophilic residues are essential for the zinc transport activity of ZnTs (including ZnT5). In contrast, mutations in the serine-rich loop and transmembrane domain 2 and 5 of ZnT6 do not alter affect zinc transport, TNAP activation, localisation, or ZnT5 binding (Fukunaka et al., 2009). Furthermore, immunocytochemical analyses revealed that the ZnT5 subunit is essential in zinc transport, while ZnT6 is catalytically non-functional (Ohana et al., 2009). ZnT6 also contains a uniquely long, yet conserved, C-terminal cytosolic tail (203 amino acids) of unknown function

(Huang and Tepasamordech, 2013). Lastly, ZnT6 is the most divergent of the ZnT protein family, excluding ZnT9, which does not function as a true zinc transporter. ZnT9 is a zinc binding nuclear receptor and transcriptional co-activator of WNT- responsive genes (Chen et al., 2005b; Chen et al., 2007).

ZnT6 is the most abundantly identified proximal protein in the GBF1 BioID assay. The following subsections examines potential functional links between ZnT6 and GBF1. This includes examining its interaction with GBF1, as well as examining the impacts of ZnT6 depletion and overexpression on GBF1 distribution and cycling dynamics.

6.2 Results

6.2.1 ZnT6 is a novel GBF1 interactor

From our data in Chapter 5, we identified C10orf76 as a potential regulator of GBF1 membrane binding. However, our analysis also suggested that while C10orf76 may be involved, there were likely other more conserved protein components also present on the membrane facilitating GBF1 binding. To identify other potential regulators, we returned to the list of GBF1 proximal partners identified using BioID performed on Golgi-enriched fractions – as described in Chapter 5.

ZnT6 became of interest for several reasons: 1) the protein was the most abundantly identified prey in both Golgi fractions as well as whole cell lysates, indicating that GBF1 remains in close proximity to ZnT6 for extended periods of time. 2) ZnT6 is also not a canonical zinc transporter and past research has shown that it is incapable of binding and transporting zinc. ZnT6 also harbours several other physical attributes including a conserved serine-rich loop and a 203 amino acid long cytosolic C-terminal tail that indicates it may play functions outside of zinc transport, making it a potential candidate of interest.

To begin examining whether ZnT6 may be involved in GBF1 regulation, we started with co-immunoprecipitation assays to assess interaction. Kambe and colleagues had previously developed an EGFP-tagged form of ZnT6 and established a protocol for pulling down ZnT6 interacting partners using the detergent IPEGAL (Suzuki et al., 2005). Using the previously described construct and method, we repeated the co-immunoprecipitation experiments and investigated the presence of endogenous GBF1. Controls for the EGFP pulldown were performed using our previously constructed EGFP-C10orf76 and an EGFP-DRP1 from Dr. T. Simmen (Ortiz-Sandoval et al., 2014). As described and shown in Chapter 5, DRP1 is a mitochondrion localised protein and does not interact with GBF1 or C10orf76. Our results revealed clear pulldown of GBF1 using EGFP-ZnT6 as well as the positive control, EGFP-C10orf76, but not with EGFP-DRP1 (Figure 6.1). To confirm that pulldown of the integral membrane protein, did not erroneously precipitate membrane fragments that may contain GBF1, we further probed our blots for the Golgi integral membrane protein giantin. Our co-immunoprecipitation experiment demonstrated that under conditions that do not pulldown the Golgi protein giantin, we can observe interaction between C10orf76 and GBF1, as well as ZnT6 and GBF1. Furthermore, based on the fraction of samples loaded (input represents 10% of total protein used in pulldown), and assuming that all interacting complexes were recovered, our pulldown suggests that approximately 10% of GBF1 interact with the overexpressed C10orf76 and ZnT6 proteins.

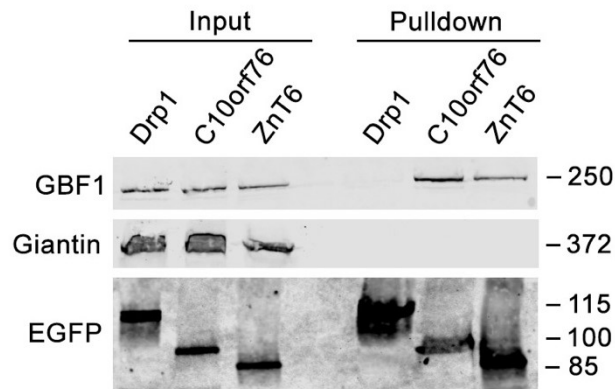


Figure 6.1 ZnT6 interacts with GBF1

Pulldown was performed with anti-EGFP antibodies with cells either expressing EGFP-ZnT6, EGFP-C10orf76, or EGFP-Drp1. HeLa cells were transfected with the appropriate constructs and co-immunoprecipitation was performed under conditions as previously published by Suzuki et al., 2005 and described in Chapter 2. Proteins were examined by western blotting using anti-GBF1, anti-Giantin, or anti-EGFP antibodies. Numbers on the right side of the blots indicate molecular weight in kilodaltons. Blots reveal distinct bands corresponding to the pulled-down endogenous GBF1 with EGFP-c10orf76 and EGFP-ZnT6, but not with EGFP-Drp1. All images are representative of three replicates.

6.2.2 ZnT6 depletion alters GBF1 dynamics on the membrane, but not distribution or recruitment

Following the pulldown experiment, we wanted to re-examine the effects of ZnT6 knock down on GBF1 distribution and recruitment. Previous studies on ZnT6 had shown that ZnT6 was non-essential in mammalian cells (Suzuki et al., 2005). We transduced HeLa cells stably expressing EGFP-GBF1 with lentiviral particles containing the ZnT6 targeting shRNA-encoding plasmids as described in previous experiments. We then selected for a population of ZnT6 targeting shRNA expressing cells with 5 $\mu\text{g}/\text{mL}$ puromycin over a two-week period. To confirm successful depletion of ZnT6 we obtained the antibody previously described by Kambe and colleagues (Suzuki et al., 2005).

Live-cell imaging of these stable ZnT6 knockdown cells led to the same initial conclusion from the earlier shRNA screen described in Chapter 5 (Figure 6.2A). EGFP-GBF1 distribution and recruitment upon BFA treatment appears comparable to control. We did observe slightly more juxtannuclear EGFP-GBF1 in ZnT6-depleted cells upon quantitation, but this was not significantly different (two-tailed t -test $p > 0.1418$). Additional quantitation performed further confirmed no difference in average fold increase of EGFP-GBF1 after BFA treatment for 90 seconds. However, unlike earlier experiments, we were able to confirm successful depletion of ZnT6 using an antibody (Figure 6.2B). Together, the data suggest that ZnT6 is not required for proper GBF1 localisation or recruitment.

These findings were initially disappointing, but the fact that ZnT6 interacted with GBF1 prompted us to examine the relationship further. To better assess whether ZnT6 depletion had any effect on GBF1 on Golgi membranes, we chose to perform additional FRAP experiments in ZnT6 knockdown cells. *In vivo* FRAP experiments revealed altered GBF1 dynamics at the

membrane (Figure 6.3). Upon photobleaching, EGFP-GBF1 appears to cycle slightly more rapidly in ZnT6-depleted cells ($t_{1/2} = 13.3$ s) as compared to control ($t_{1/2} = 23.0$ s) – however, not significantly so (two-tailed t -test $p > 0.0625$). Despite a comparable half-time, recovery rate in ZnT6-depleted cells began to plateau after approximately 60 seconds post-bleaching. In control cells, however, EGFP signal recovery at photobleached Golgi sites extended up to 170 seconds post-bleaching, reaching approximately 90% of original signal. This reduction in recovery in ZnT6-depleted cells suggests a potential ZnT6-dependent membrane-bound and immobile GBF1 fraction.

To document this in more detail, we chose to analyze the quantity of ZnT6 present in enriched Golgi membranes after subcellular fractionation. Despite not detecting significantly more EGFP-GBF1 at juxtannuclear sites by live-cell imaging, western blotting surprisingly revealed almost 2.5 fold more GBF1 in enriched Golgi fractions in ZnT6-depleted cells compared to control (Figure 6.4). One potential explanation could be that the non-cycling pool of GBF1 present in ZnT6-depleted cells may interact with membranes much more strongly compared the majority of GBF1 in WT cells. While a fraction of Golgi-localised GBF1 will likely disassociate from Golgi membranes during the Golgi enrichment procedure, the non-cycling pool of GBF1 in ZnT6-depleted cells may not, thus exaggerating the difference observed by western blotting. Additional work will be needed to further examine the nature of the membrane interaction of this non-cycling GBF1 pool. Nonetheless, our experiments on ZnT6 knockdown cells suggest that ZnT6 may be involved in fine-tuning the dynamics of GBF1 on membranes, potentially promoting the release of GBF1 off the membrane.

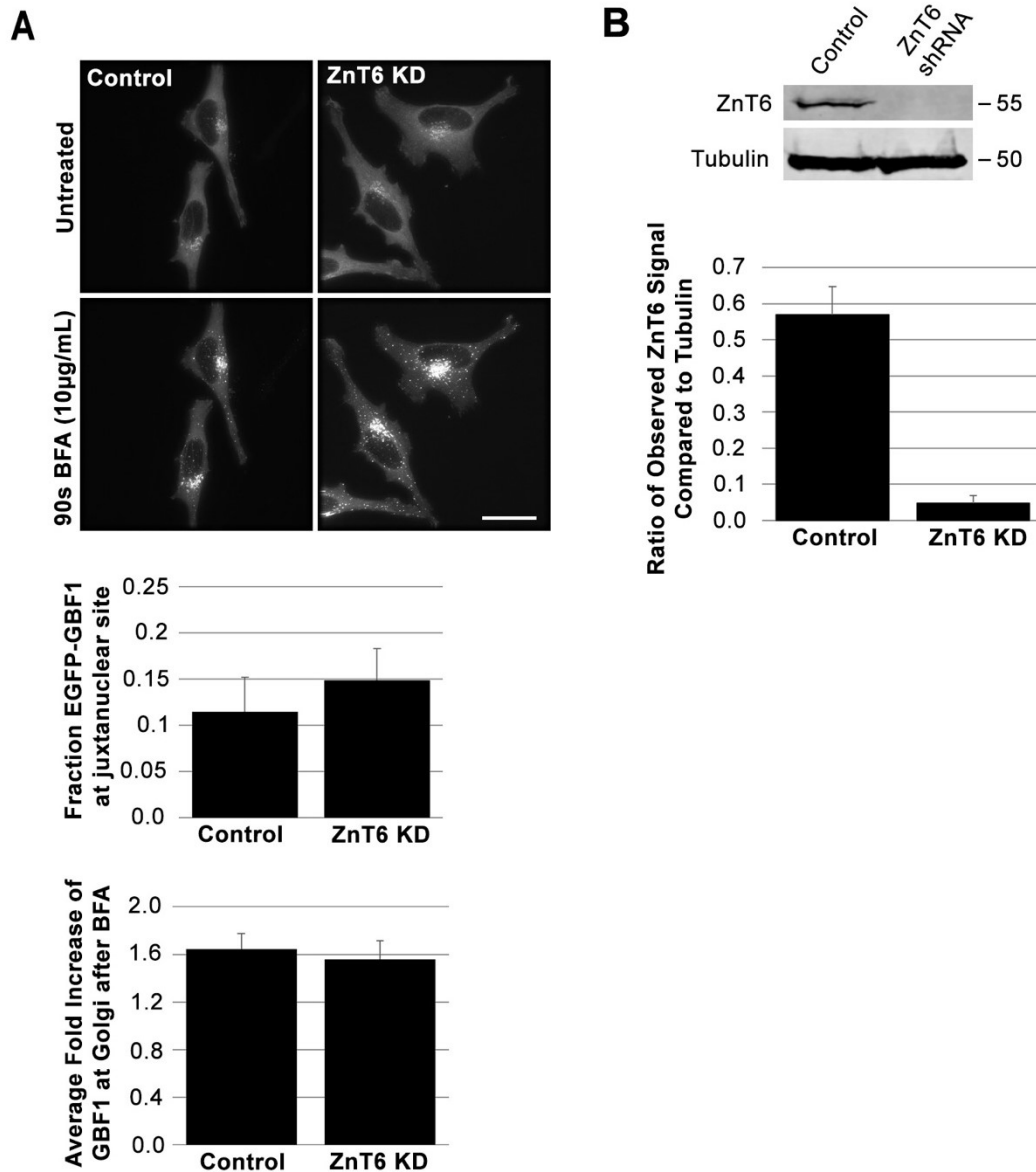


Figure 6.2 ZnT6 knockdown does not significantly alter GBF1 distribution or recruitment. Stable ZnT6 knockdown cells expressing EGFP-GBF1 were generated as described in Chapter 2 and analyzed by live-cell imaging and western blotting. (A) ZnT6-depleted cells show an EGFP-GBF1 distribution similar to control cells stably expressing a non-targeting shRNA. In live-cell imaging, ZnT6 knockdown cells exhibit slight but insignificant increase of EGFP-GBF1 at juxtannuclear sites upon quantitation ($p = 0.1544$) and no obvious difference in fold increase upon treatment with BFA for 90 seconds (10 µg/mL) ($p = 0.2107$). Quantitation was performed as described in Chapter 2. Live-cell images are shown as projections of all Z-slices. Scale bar = 26 µm. (B) Successful knockdown of ZnT6 as compared to tubulin was observed by western blotting using anti-ZnT6 and anti-tubulin antibodies. Numbers on the right side of the blots indicate molecular weight in kilodaltons. All images are representative of three replicates.

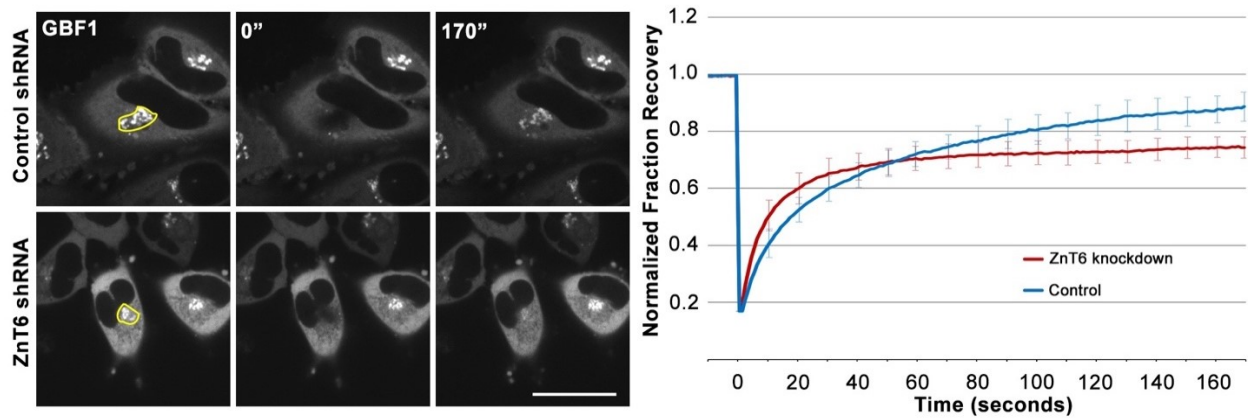


Figure 6.3 ZnT6 depletion alters GBF1 cycling on and off Golgi membranes.

FRAP analyses were performed on EGFP-GBF1 expressing ZnT6 knockdown cells. Cells were imaged before and after photobleaching of the Golgi region (outlined in yellow) by illumination with a high-intensity laser. Images were then acquired at single second intervals for 170 seconds to monitor fluorescence recovery. At least 15 movies were acquired from three separate replicates. Images at 0 and 170 seconds are shown. The fraction of EGFP signal in the Golgi area was normalized to 1 at $t = 0$ and quantitated as described in Chapter 2. While recovery continues in control cells as measured up to 170 seconds, recovery in ZnT6-depleted cells appear to halt after approximately 70 seconds. Error bars represent \pm standard deviation. Scale bars = 26 μm .

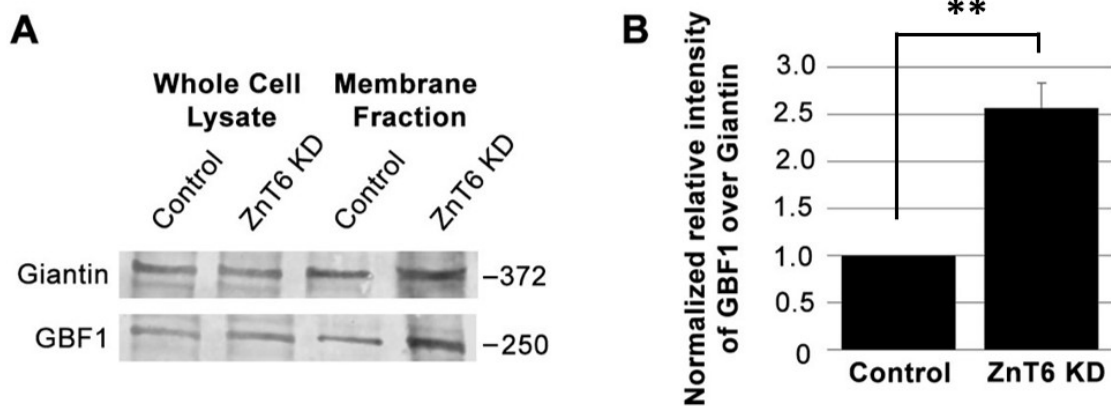


Figure 6.4 Golgi isolation reveals more membrane-bound GBF1 in ZnT6-depleted cells. Golgi membranes were enriched and isolated for using a sucrose-gradient density centrifugation as described in Chapter 2. Quantity of isolated endogenous GBF1 was compared to whole cell lysates by western blotting using anti-giantin and anti-GBF1 antibodies. (A) Western blot shows enrichment of Golgi marker giantin after separation of membrane fraction. Additional GBF1 was isolated from ZnT6-depleted cells as compared to control. No obvious difference in GBF1 expression is observed between control and ZnT6-depleted cells in whole cell lysates. Numbers on the right side of the blots indicate molecular weight in kilodaltons. Western blot shown is representative of three replicates. (B) Quantitation of western blots similar to those described for panel A. GBF1 signal relative to Golgi marker giantin was averaged over three replicates. Quantitation was performed as described in Chapter 2. Bars represent mean values \pm standard deviation (error bars). Statistical significance was measured by a two-tailed unpaired *t*-test ($p = 0.0022$).

6.2.3 ZnT6 overexpression reduces Golgi-localised GBF1 and alters GBF1 cycling on and off membranes

Having examined the effects of ZnT6 knockdown on GBF1 cycling, we next wanted to determine whether overexpression of ZnT6 led to similar or opposite effects. We transfected EGFP-GBF1 expressing HeLa cells with an mCherry-ZnT6 subcloned using the ZnT6 plasmid provided by Kambe and colleagues (Suzuki et al., 2005). Using live-cell imaging, we found that cells overexpressing ZnT6 had less juxtannuclear EGFP-GBF1 and exhibited reduced recruitment upon treatment with BFA (10 $\mu\text{g}/\text{mL}$) (Figure 6.5). The effect appears to be even more pronounced in cells transfected with twice as much mCherry-ZnT6 plasmid DNA: 500 ng to 1000 ng (Figure 6.6). Together, the data suggest that ZnT6 overexpression may alter the availability or quantity of GBF1 binding sites on the membrane. Likewise, the observations may also be due to altered cycling dynamics – i.e. GBF1 may remain on the membrane for much shorter durations of time.

To better determine whether cycling on and off membranes was altered by ZnT6 expression, we proceeded to perform additional FRAP experiments. Similar to the initial live-cell imaging experiments just described, we utilized EGFP-GBF1 expressing HeLa cells transfected with mCherry-ZnT6. While in the ZnT6-depleted cells we observed the emergence of a non-cycling GBF1 pool, this was not observed in the ZnT6 overexpressing cells (Figure 6.7). Instead, EGFP-GBF1 appears to cycle significantly faster ($t_{1/2} = 11.1$ s) as compared to control ($t_{1/2} = 22.3$ s) (two-tailed t -test $p = 0.0307$). However, as recovery continues, the fraction of signal recovered in both appear to even out at approximately 130 seconds post bleaching.

Together with the ZnT6 knockdown experiments, the data suggest that ZnT6 may have potential roles in regulating GBF1 dynamics on the membrane – either through altering the

availability or quantity of GBF1 binding sites, or perhaps modulating the overall rate of exchange.

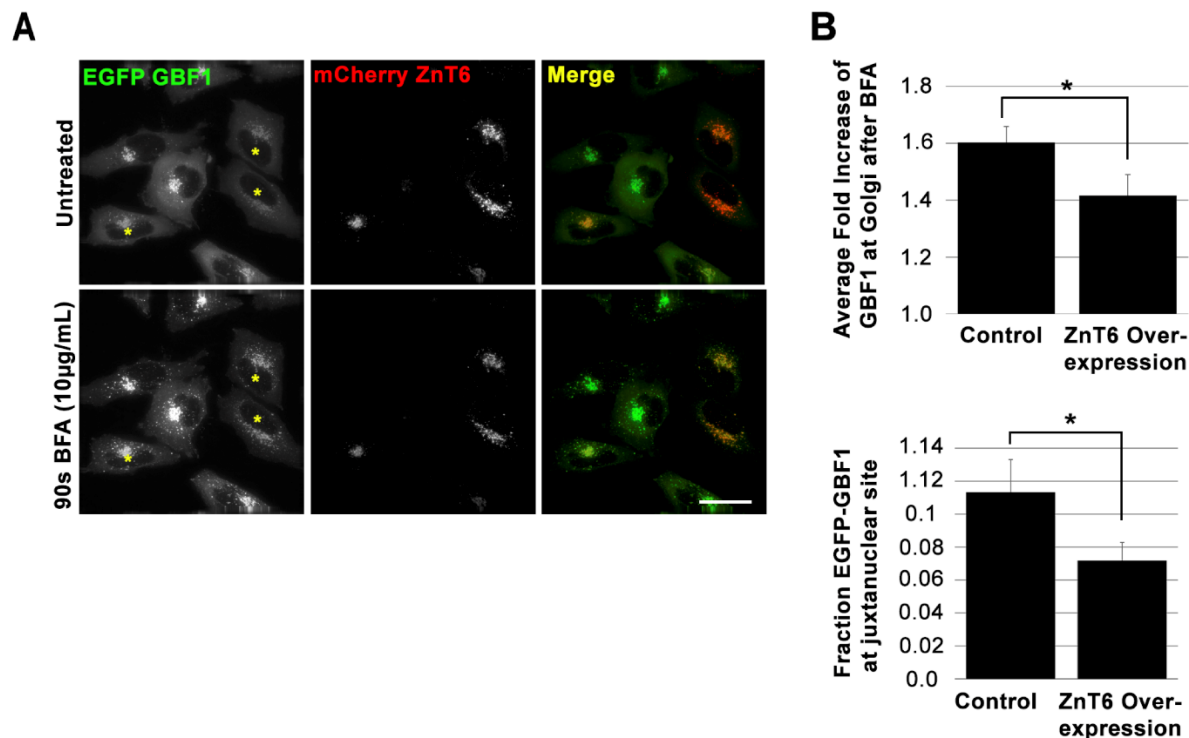


Figure 6.5 ZnT6 overexpression reduces quantity and recruitment of juxtannuclear GBF1. EGFP-GBF1 expressing HeLa cells were transfected with mCherry-ZnT6 and examined by live-cell imaging. (A) ZnT6 overexpressing cells (as indicated by a yellow asterisk) exhibit reduced juxtannuclear EGFP-GBF1 and reduced recruitment upon treatment with BFA (10 $\mu\text{g}/\text{mL}$) as compared to untransfected surrounding cells. Live images are shown as projections of all Z-slices. Scale bar = 26 μm . (B) Quantitation of average fold increase of GBF1 after BFA and quantitation of overall fraction of EGFP-GBF1 at juxtannuclear sites at steady state prior to drug treatment. Quantitation was performed as described in Chapter 2. Statistical significance was measured by a two-tailed unpaired *t*-test (fraction at juxtannuclear site $p = 0.0149$; average fold increase after BFA $p = 0.0260$).

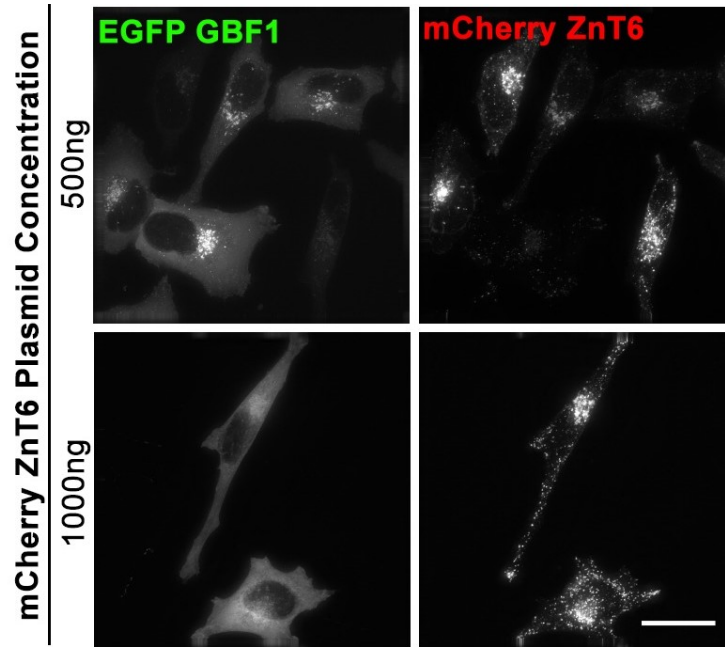


Figure 6.6 Fraction of juxtannuclear GBF1 appears to be sensitive to the amount of transfected ZnT6.

HeLa cells expressing EGFP-GBF1 were transfected with either 500 ng or 1000 ng mCherry-ZnT6 plasmid and examined 18 hours after transfection. Cells transfected with 1000 ng appears to have even less juxtannuclear EGFP signal as compared to those transfected with 500 ng of plasmid DNA. Live-cell images are shown as projections of all Z-slices and are representative of three independent replicates. Scale bar = 26 μ m.

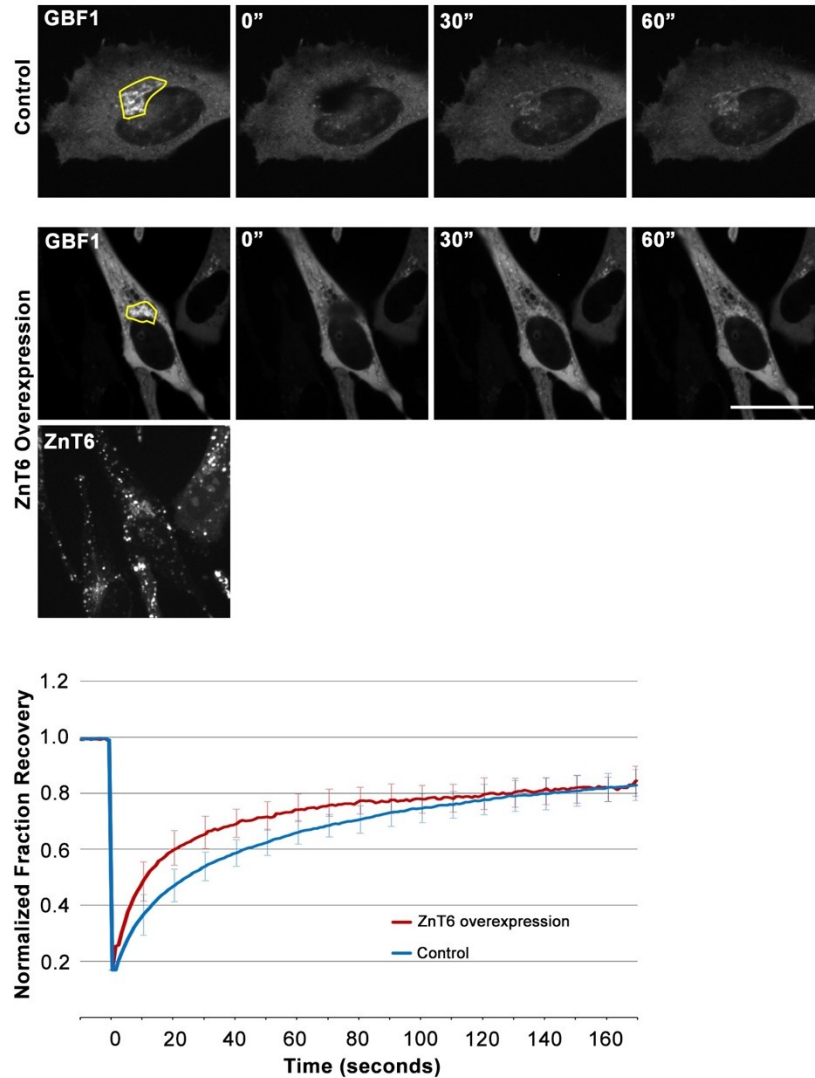


Figure 6.7 ZnT6 overexpression alters GBF1 cycling on and off Golgi membranes.

FRAP analyses were performed on EGFP-GBF1 expressing HeLa cells transfected with mCherry-ZnT6. Cells were imaged before and after photobleaching of the Golgi region (outlined in yellow) by illumination with a high-intensity laser. Post bleaching, images were acquired at single second intervals for 170 seconds to monitor fluorescence recovery. At least 15 movies were acquired from three separate replicates. Images at 0, 30, and 60 seconds are shown. The fraction of EGFP signal in the Golgi area was normalized to 1 at $t = 0$ and quantitated as described in Chapter 2. Recovery appears to be faster in cells overexpressing ZnT6 as compared to control ($t_{1/2} = 11.1$ s compared to $t_{1/2} = 22.3$ s; two-tailed t -test $p = 0.0307$). Error bars represent \pm standard deviation. Scale bars = 26 μm .

6.2.4 ZnT6 depletion does not significantly impact GBF1 activity or secretory activity

Having identified ZnT6 as potentially involved in regulating the dynamics of GBF1 association with membranes, we wanted to further examine whether depletion of ZnT6 altered the degree of GBF1 activity or the overall secretory activity of the cell. As previously described, ZnT6 is not an essential gene in mammalian cells and can be knocked out without dramatic impact on cell survival (Blomen et al., 2015; Suzuki et al., 2005). Previous studies further revealed that very little GBF1 is required for Golgi maintenance (Manolea et al., 2008; Quilty et al., 2014). However, cell survival does not necessarily preclude potential negative impacts on overall GBF1 activity or secretory activity. To measure these, we examined the fraction of Golgi-localised β -COP (a downstream effector of activated Arf1) and measured secreted luciferase in a secretion assay.

In ZnT6 knockdown cells fixed and stained for endogenous GBF1 and β -COP, no significant difference in the fraction of β -COP on GBF1 positive Golgi structures were observed (Figure 6.8). In both cases, additional treatment with BFA (10 μ g/mL) for two minutes completely abrogated β -COP recruitment. These observations suggest that overall Arf1 activation in ZnT6 cells is comparable to that of control.

The secretion of nano luciferase over a period of three hours was similarly unaltered. Indeed, we found that overall secretory activity of ZnT6 knockdown cells were comparable to control (Figure 6.9). As expected, treatment of cells with BFA (10 μ g/mL) to inhibit GBF1 activity led to a significant decline in overall cellular secretion. These observations suggest that ZnT6 depletion had negligible impact on overall GBF1 activity and cell secretory activity.

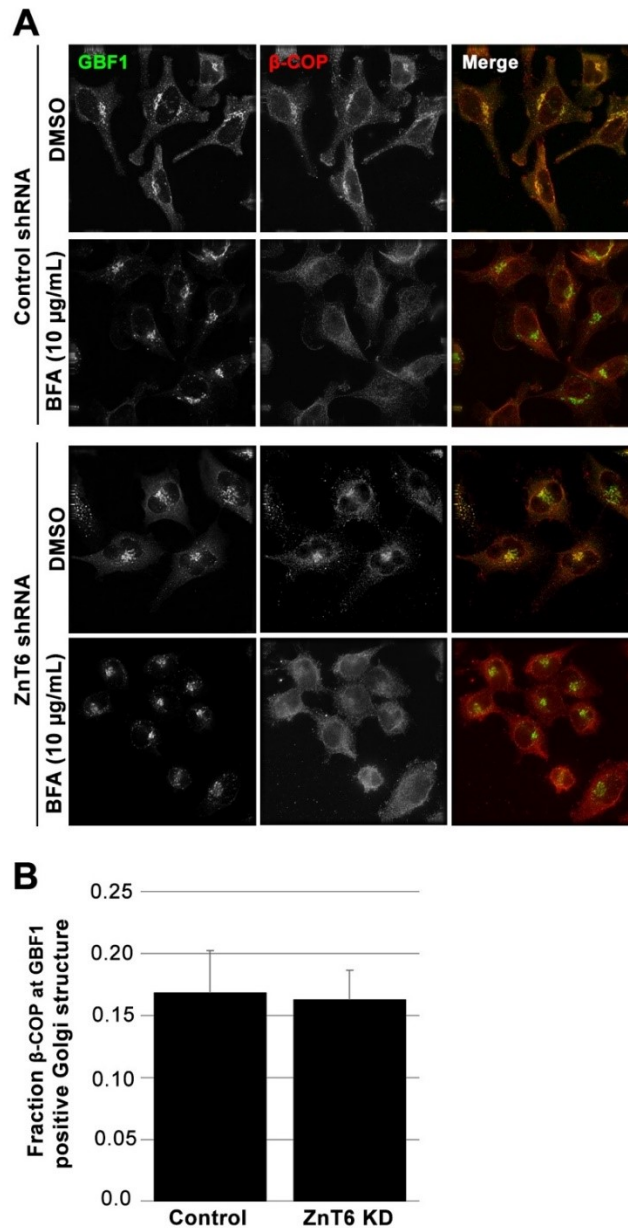


Figure 6.8 ZnT6 knockdown does not impair COP recruitment.

HeLa cells stably expressing a non-targeting or ZnT6 targeting shRNA were fixed and stained for endogenous β -COP and GBF1. (A) Imaging reveals that β -COP continues to be recruited to GBF1 positive Golgi membranes in ZnT6-depleted cells. Further treatment with BFA (10 μ g/mL) for two minutes abrogates recruitment to these sites, suggesting GBF1 remains comparably active despite ZnT6 depletion. (B) Quantitation of the images obtained from panel A. 18 cells were examined over three replicates and quantified as described in Chapter 2. Bars represent mean values \pm standard deviation (error bars). ZnT6 depletion was found to have no significant impact as estimated by a two-tailed unpaired *t*-test ($p = 0.4334$).

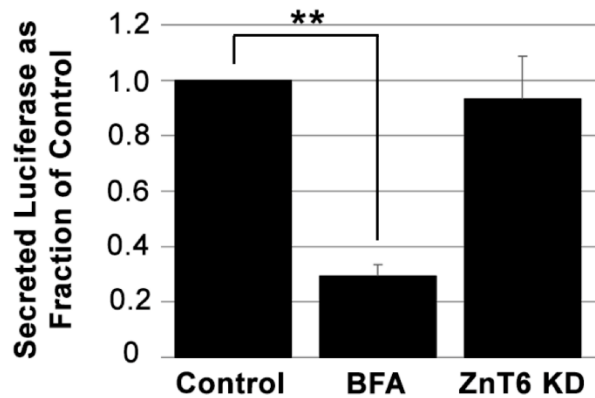


Figure 6.9 ZnT6 knockdown does not significantly alter secretory activity.

HeLa cells stably expressing a non-targeting or ZnT6 targeting shRNA were transfected with a plasmid encoding a secreted NanoLuc luciferase 18 hours prior to the assay. During the assay, growth medium was analyzed for luciferase activity after a 3 hour incubation period with or without addition of BFA (1 $\mu\text{g}/\text{mL}$) as described in Chapter 2. Bars represent means \pm standard deviation (error bars) ($n = 3$). Depletion of ZnT6 does not appear to alter luciferase secretion while inhibition of GBF1 activity with BFA does as compared to control. Statistical significance was measured by a two-tailed unpaired t -test (control and BFA $p = 0.0042$; control and ZnT6 knockdown $p = 0.3795$).

6.3 Discussion

6.3.1 ZnT6 is a novel GBF1 interactor and regulates GBF1 cycling on and off membranes

Our data suggest an interaction between GBF1 and ZnT6, and illustrates the impact of ZnT6 overexpression and depletion on GBF1 cycling. With the depletion of ZnT6, we observed an impact on GBF1 cycling. A fraction of Golgi-localised GBF1 appears to remain trapped on the membrane, no longer cycling between the usual membrane-bound and cytoplasmic states (Figure 6.3). In these same cells, we also observed a slight but non-statistically significant increase in the average rate of GBF1 signal recovery after photobleaching – potentially indicating that the still active, cycling pool of GBF1 may cycle moderately faster. However, this may simply be a secondary effect where the emergence of the non-cycling pool reduces the competition for free GBF1 surrounding the Golgi, meaning that there is more free GBF1 available nearby to exchange with the membrane-bound pool. In the ZnT6 overexpressed conditions, we observed a decrease in the fraction of Golgi-localised GBF1 (Figure 6.5 and 6.6). FRAP studies also revealed a moderate increase in the rate at which GBF1 cycles on and off membranes (Figure 6.7). Together, these data suggest that ZnT6 either directly or indirectly affects GBF1 cycling dynamics.

One potential mechanism to explain these observations could be that ZnT6 activity may be required to facilitate the release of GBF1 from membrane sites. Loss of ZnT6 would then lead to an accumulation of trapped GBF1 at the Golgi. Likewise, overexpression of ZnT6 may promote a more rapid release of GBF1 off the membrane, leading to the observed overall reduced Golgi-localised GBF1 and the moderate increase in GBF1 cycling. However, this model also raises several unresolved questions.

Firstly, is ZnT6 involved in nucleotide exchange? Previous studies have suggested that the release of GBF1 from the membrane is tied to the nucleotide exchange reaction. GBF1 mutants unable to catalyze the reaction fail to be released and remain on membranes significantly longer than WT (Szul et al., 2005). Likewise, WT GBF1 can also be held at the membrane in cells overexpressing GDP-arrested dominant negative Arf1, or using BFA, which is thought to arrest nucleotide exchange. This begs the question whether membrane-bound “non-cycling” GBF1 pool observed in ZnT6-depleted cells is similarly being held at the membrane because of an inability to effectively complete nucleotide exchange, or is it being held at the membrane due to some other mechanism? Determining this may require examining whether this “non-cycling” GBF1 pool in ZnT6-depleted cells remain catalytically active. Experiments examining the overall recruitment of β COP to Golgi sites and overall secretory activity suggest that the impaired GBF1 cycling observed in ZnT6-depleted cells do not significantly alter Arf activation, however, more sensitive *in vitro* measurements of nucleotide exchange may prove useful. Additional studies may also yield new insights into the mechanism of BFA in live-cells. As previously mentioned, BFA has been shown *in vitro* to arrest nucleotide exchange by stabilizing a GBF1-Arf-GDP abortive complex (Peyroche et al., 1999; Renault et al., 2003). However, this has never yet been confirmed *in vivo*. Instead, BFA induced recruitment of GBF1 coincides with a reduction in membrane-bound Arf (Chun et al., 2008). This suggests that the majority of membrane arrested GBF1 is likely not associated with Arfs. Bimolecular fluorescence assay using split YFP tagged GBF1 and Arf revealed that some Arf remains in close proximity to membrane-bound GBF1 (Ting-Kuang et al., 2005). Likewise, overexpression of GBF1 allows for increased retention of membrane localised Arfs. However, criticisms including the potential irreversibility of the reformed YFP and possible residual GBF1 activity from overexpression

have all raised doubts on the stability and formation of the GBF1-Arf complex. Currently, no proteins other than Arf and GBF1 itself have in been implicated in altering the rate at which GBF1 cycles on and off membranes. By further elucidating the mechanism by which ZnT6 is involved may yield novel insights into how GBF1 recruitment and release is regulated.

6.3.2 Does GBF1 regulation involve zinc?

A second major question in how ZnT6 regulates GBF1 cycling dynamics is whether the process is zinc-dependent. As discussed ZnT6 has been shown to be involved in the activation of zinc binding proteins in the Golgi lumen. While ZnT6 itself does not actively bind or transport zinc, the canonical zinc transporter ZnT5 cannot function without ZnT6 (Suzuki et al., 2005).

Currently no known GBF1 interacting partners have been shown to require zinc for function.

ArfGAPs do require zinc for their catalytic activity, and in turn, changes in Arf-GDP levels have been shown to modulate GBF1 recruitment (Kahn et al., 2008; Quilty et al., 2014); however, ZnT6 is involved in activating zinc proteins in the Golgi lumen, and ArfGAPs should not be a ZnT6 target. One way to determine whether zinc is involved would be to abrogate zinc import into the Golgi lumen. Methods that chelate zinc or cause global disruptions of zinc transport would severely interfere with other cellular processes which will complicate data interpretation.

As such, examining the impacts of ZnT5 and ZnT7 depletion on GBF1 dynamics may be the best option. ZnT6 facilitates zinc transport through ZnT5, and loss of either leads to comparable decline in the activity of the zinc-dependent enzyme, TNAP (Suzuki et al., 2005). ZnT7 homodimers have redundant zinc transport activities, but ZnT7 was not significantly detected in our BioID experiment. Determining whether ZnT5 and ZnT7 depletion has similar affects on GBF1 cycling may yield novel insights into whether zinc may play a role in regulating GBF1 dynamics. Additional experiments can also be performed to examine whether the effects of ZnT6

depletion on GBF1 can be rescued by zinc mobilization into the secretory pathway; this can be achieved through supplementing cells with excess zinc or overexpression of ER and TGN localised zinc transporters, or depletion of Golgi zinc exporters. Identification of motifs or mutations in ZnT6 that impair GBF1 interaction will also allow for additional experiments examining whether non-interacting ZnT6 can rescue the effects observed in ZnT6 knockdown cells.

Interestingly, despite a clear depletion of ZnT6 in our HeLa cells as confirmed by western blotting, only a small population of membrane-bound GBF1 appears to be affected. Majority of GBF1 appears to continually cycle, and no dramatic effects on either β COP recruitment of cellular secretion was observed (Figure 6.3 and 6.8). Furthermore, previously work has shown that complete impairment of zinc transport into the Golgi by knocking down ZnT5, 6, and 7 is not lethal in either cell culture or animal models (Huang and Tepasamordech, 2013). This indicates that whatever role ZnT6 plays in modulating GBF1 dynamics, it is not essential for cell survival. However, the impacts of ZnT6 depletion on the levels of Golgi membrane or Golgi morphology have not been examined. Our observations that ZnT6 overexpression altered the quantity of Golgi-localized GBF1 and that ZnT6 depletion impaired GBF1 cycling may be associated with other changes to either the quantity of Golgi membranes or Golgi morphology. Additional fluorescence and electron microscopy experiments using other Golgi markers can be done to examine changes to the Golgi more closely.

Chapter 7: General Discussion

7.1 Synopsis

Based on previous observations, we hypothesized that GBF1 interaction and recruitment to Golgi membranes require specific interactions between a number of protein components present on the *cis*-Golgi and critical domains found within GBF1. To identify essential domains in GBF1 required for Golgi targeting, we utilized an EGFP-tagged GBF1 truncation library. Live-cell imaging revealed that HDS1 and HDS2 were both essential in Golgi targeting and recruitment. As mentioned, HDS1 has been previously shown to be a lipid binding domain – interacting with PI4Ps. The role of HDS2 is not yet known, but may be involved in protein-protein interactions. Previous observations have shown that membrane binding of GBF1 is dependent on protein factors present on the Golgi membrane; HDS2 may be involved in interacting with these protein factors.

To identify potential Golgi-localised membrane proteins involved in GBF1 regulation, we proceeded to investigate the GBF1 interactome using a proximity biotinylation based (BioID) approach. The method relies on a modified BirA* tag that generates reactive biotin which irreversibly labels GBF1 proximal proteins. We generated and validated HeLa cell lines with regulatable expression of BirA*-FLAG tagged constructs for use in BioID. Mass spectrometry analysis performed on whole cell lysates and Golgi-enriched fractions identified a wide range of putative GBF1 interacting partners. Surprisingly, the Golgi-enriched fractions identified several unique hits not detected in the whole cell lysates, suggesting that the membrane enrichment procedure allowed for improved detection of Golgi-localised proteins. A small shRNA screen performed on candidates identified from the Golgi-enriched fractions highlighted C10orf76 as a potential regulator. C10orf76 depletion appears to impair GBF1 recruitment, Golgi maintenance, and secretory activity. However, C10orf76 appears to cycle on and off membrane much more

rapidly than GBF1. Likewise, the absence of C10orf76 in select model organisms with GBF family members, suggest there are likely other protein components involved in GBF1 recruitment.

Additional examination of the identified putative GBF1 interactors revealed the transmembrane protein ZnT6 as a potential regulator of GBF1 membrane dynamics. Depletion of ZnT6 interfered with proper GBF1 cycling on and off membranes, and overexpression altered the cytosol to Golgi-localised GBF1 ratio. However, whether these observed effects are due to GBF1 interactions with ZnT6 or the role of ZnT6 in facilitating the activation of zinc binding proteins is unclear.

Together, the work described in this thesis attributed a function to the previously undescribed HDS2 domain of GBF1, demonstrated the value of organelle isolation for BioID experiments, and briefly characterized two novel GBF1 interactors – C10orf76 and ZnT6. We were able to confirm both proteins as novel GBF1 interactors by co-immunoprecipitation. These data have not only extended our understanding of GBF1 recruitment to the *cis*-Golgi, but will also provide a platform for future mechanistic studies of GBF1 recruitment to the Golgi and other membrane sites.

7.2 Pairing organelle isolation with BioID

Our study is the first to report the successful pairing of Golgi enrichment with proximity biotinylation to identify Golgi specific proximal partners. Several GBF1 proximal proteins including CANT1, RHBDD2, ZDHHC17, and the novel interactor, C10orf76, were identified in Golgi-enriched fractions at a false discovery rate below 0.01 but were not detected at all from whole cell lysates. These candidates would have been missed completely had Golgi enrichment not been performed. This is likely due to limitations of mass spectrometry, where low-abundance

proteins such as C10orf76 may be easily undersampled or fail to be detected completely (Angel et al., 2012). Where possible, organelle enrichment can be advantageous for identifying unique protein interactors that may be missed from analyzing whole cell lysates alone.

7.3 GBF1 membrane binding and the HDS1 and HDS2 domains

In vivo live-cell imaging of EGFP-tagged GBF1 truncations revealed two essential domains in Golgi localisation – HDS1 and HDS2. Our work is the first demonstration that none of the N-terminal domains, including the highly conserved catalytic Sec7 are required for Golgi membrane binding. Further examination revealed that GBF1 mutants lacking sec7d can also be recruited to juxtannuclear sites upon treatment with BFA. Previous studies have suggested that GBF1 recruitment to the Golgi upon BFA addition involves the trapping of GBF1 at the membrane site. *In vitro* experiments have shown that BFA acts as a non-competitive inhibitor, binding a hydrophobic cavity that exists in the transitory Arf-GDP-Sec7 complex. This has been shown to create an abortive reaction intermediate *in vitro*: GBF1 remains bound to Arf-GDP as BFA insertion blocks the conformational change needed to electrostatically expel the bound nucleotide (Mossessova et al., 2003; Renault et al., 2003). Formation of this abortive intermediate has been used to explain the accumulation of GBF1 at the Golgi upon BFA treatment and the lack of GBF1 cycling (Ting-Kuang et al., 2005; Zhao et al., 2006). However, the existence of this abortive reaction intermediate *in vivo* remains debated. Imaging studies have shown that while GBF1 accumulates at Golgi membranes upon BFA treatment, Arf1 rapidly dissociates from the Golgi, suggesting that the majority of membrane-bound Arf is not trapped by GBF1 (Chun et al., 2008). Other reports have revealed that overexpressing GBF1 can allow for increased Arf1 retention at the membrane following BFA treatment (Ting-Kuang et al., 2005). Likewise, a bimolecular fluorescence complementation assay using GBF1 and Arf tagged

to split YFP also suggested that Arf remains in a complex with membrane-bound GBF1 upon BFA treatment. However, as discussed, criticisms including the irreversible nature of reformed YFP complexes and the effects of GBF1 overexpression on Arf activation have all raised doubts on whether these data reflect a true formation of an abortive complex. Quilty et al. (2014) has suggested that the additional recruitment of GBF1 upon BFA treatment may be better explained by the accumulation of inactive, regulatory Arf-GDP. As BFA inhibits Arf activation, Arf-GDP rapidly accumulates which triggers additional recruitment of GBF1 through an unknown mechanism. Overexpression of GDP-arrested Arfs or ArfGAP1 can similarly trigger additional recruitment. Our observations using the GBF1 truncation lacking the classic Sec7d (N885-1856) complements this model. Without sec7d, N885-1856 should not be a target of BFA, yet the addition of BFA similarly introduced a mild but reproducible recruitment of the mutant to the Golgi. In line with the observations from Quilty et al (2014), BFA treatment likely alters through some unexamined mechanism a change in the membrane binding potential of GBF1. This may occur through either altering GBF1's affinity for the membrane, or some membrane localised protein receptor's affinity for GBF1.

However, while this model may explain the observed increase in GBF1 at the membrane, it does not explain why GBF1 fails to continually cycle on and off membranes. FRAP studies have shown that in BFA treated cells, GBF1 becomes trapped on the membrane, and fails to cycle (Szul et al., 2007; Ting-Kuang et al., 2005; Zhao et al., 2006). We observed a similar effect in our own FRAP studies. Researchers have also observed that enzymatically dead GBF1(E794K) also fail to cycle, suggesting that GBF1 cycling may be tied to its nucleotide exchange activity. Comparing the cycling dynamics of GBF1 N885-1856 mutant with and without BFA treatment may yield additional novel insights. N885-1856 similarly lacks catalytic activity like previously

characterized enzymatically dead GBF1 mutants (E794K). But unlike these mutants, overexpression of N885-1856 does not lead to Golgi fragmentation (Saenz et al., 2012). In our experiments, overexpression of N885-1856 did not affect cell survival or Golgi integrity. This suggests that N885-1856 likely cycles comparably to WT and is not titrating away binding sites for catalytically functional WT GBF1.

Additional experiments can be done to confirm this hypothesis. This includes the examination of N885-1856 interaction with Golgi membranes through FRAP. As mentioned earlier, we also failed to observe N885-1856 recruitment to peripheral punctate or ERGIC structures upon treatment with BFA. To confirm whether GBF1 lacking N-terminal domains can still be targeted to ERGIC structures, ERGIC membranes from cells transfected with N885-1856 can be isolated and the presence of N885-1856 examined by western blotting. Future experiments may also investigate whether the domains present in N885-1856 which target the construct to Golgi membranes is sufficient to target it to other membrane sites where GBF1 functions, including the leading edge of migrating cells and at mitochondrial membranes.

7.4 ZnT6 and other zinc binding proteins in the BioID analysis

Depletion of ZnT6, a novel GBF1 interacting partner identified here, also appears to interfere with proper cycling of GBF1 on and off Golgi membranes. Depletion of ZnT6 introduces a pool of non-cycling membrane-bound GBF1. This is the first observation that GBF1 cycling can be disturbed through means other than an inhibitory drug or by altering the catalytic Sec7d. Similar to our observations with the N885-1856 mutant, our data suggest that regulating GBF1 cycling on the membrane likely involves components other than the GBF1 sec7d and Arf. As mentioned, the exact mechanism by which BFA impairs GBF1 cycling remains contentious. Identifying the

mechanism by which ZnT6 alters GBF1 cycling may yield new insights into how a similar effect is achieved with BFA.

While ZnT6 does not appear to directly bind or transport zinc, unlike other ZnT members, studies have shown that ZnT6 plays an important role in both stimulating the transport function of ZnT5, and in activating several luminal zinc binding proteins. This raises two mechanistic possibilities: 1) ZnT6 is directly involved in regulating GBF1 dynamics potentially through protein-protein interaction, or 2) ZnT6 is involved indirectly via the activation of some zinc binding component at the membrane (Figure 7.1). As described earlier, previous work has shown that deletion of all three Golgi-localised zinc transporters have little effect on luminal zinc levels and is not lethal in either cell culture or animal models (Fukunaka et al., 2009; Suzuki et al., 2005). The dispensability of ZnT6 and other Golgi-localised zinc transporters suggests that ZnT6 itself is not required to maintain GBF1 cycling. These observations may better align with the hypothesis that GBF1 dynamics is influenced by a zinc binding protein rather than ZnT6 directly. Although how luminal zinc levels might influence activity occurring at the cytosolic face is unclear; perhaps this occurs through unidentified transmembrane protein components.

Cross referencing known and suspected zinc binding proteins from the Gene Ontology Consortium with our BioID candidates yielded little insight. Apart from ZnT5 and 6, only nine zinc-binding proteins are present in the whole cell lysates analysis (False discovery rate above 0.20): this includes ArfGAP1 (the Golgi localized Arf GTPase activating protein), SQSTM1 (a ubiquitin binding protein involved in cargo selection for autophagy), PIKFYVE (a PI3P 5-kinase), BRAP (a regulator of BRCA1 translocation into the nucleus), Sec24A (a component of the COPII coat), TK1 (a thymidine kinase involved in nucleotide biosynthesis), ZDBF2 (an imprinted paternally expressed gene of unknown function), SNCA (or alpha-synuclein, a protein

with many neuroprotective functions), and TRIM26 (an E3 ligase involved in protein degradation) (Bendor et al., 2013; Chen et al., 2010; Kobayashi et al., 2009; Li et al., 1998; Martin-Sanchez and Komatsu, 2018; Williams and Parsons, 2018; Zolov et al., 2012). None of these are known *cis*-Golgi-localised proteins and appear to be involved in functions unrelated to GBF1. No ZnT proteins from other locations were identified, suggesting that if ZnT6 does play a direct role in regulating GBF1 dynamics, it is likely not conserved in other ZnTs. Similar cross referencing using candidates identified in the Golgi-enriched fractions (false discovery rate above 0.20) identified only Sec24A and ZDHHC17. Sec24A is a component of the COPII coat and is involved in protein sorting at ER exit sites; the protein is not known to have essential functions at the *cis*-Golgi. ZDHHC17 is a palmitoyltransferase highly expressed in neural tissues where it palmitoylates a number of synaptic proteins to regulate neuronal axon outgrowth and neurotransmitter release. No impact on GBF1 was observed in cells treated with plasmids encoding ZDHHC17 targeting shRNA. Likewise, ZDHHC17 has been shown to be non-essential for cell survival (Blomen et al., 2015; Shi et al., 2015).

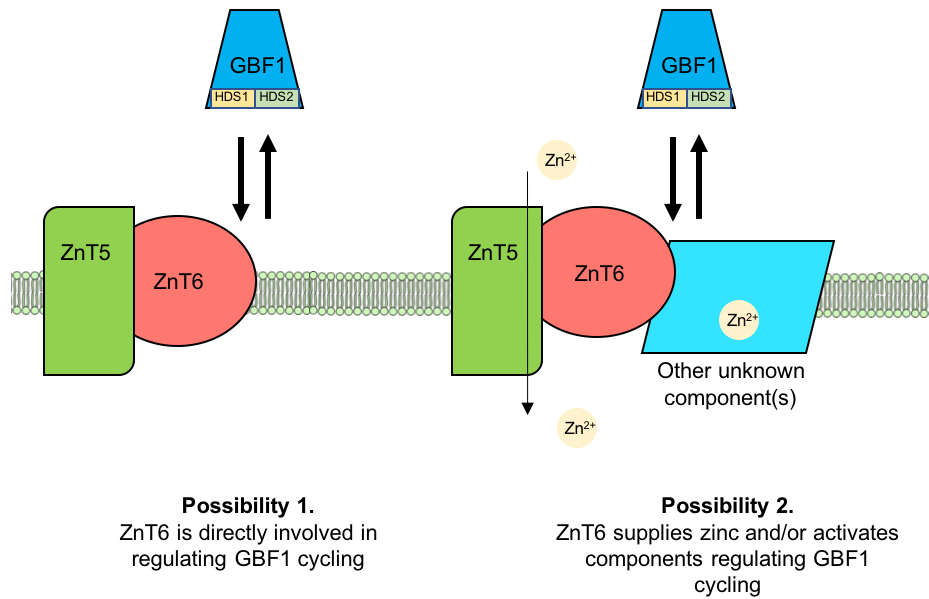


Figure 7.1 Models for ZnT6 regulation of GBF1 cycling.

ZnT6 may be involved in regulating GBF1 cycling on and off Golgi membranes either directly or indirectly. (Left) Co-immunoprecipitation demonstrated an interaction between GBF1 and ZnT6. This interaction with GBF1 may be involved in regulating its cycling dynamics. (Right) ZnT6 dimerizes with ZnT5 and is involved in stimulating zinc import into the Golgi lumen. ZnT6 may regulate GBF1 cycling indirectly by supplying zinc to integral membrane components that directly regulate GBF1.

7.5 Potential roles of C10orf76 in GBF1 regulation

As described previously, our study identified several links between GBF1 and the previously unstudied protein, C10orf76. In HeLa cells, we found that depletion of C10orf76 led to fragmentation of the Golgi and impaired recruitment of GBF1 to membrane sites. Additional work by McPhail et al., 2019 found a similar effect in human haploid cells (HAP1). C10orf76 knockout does not appear to be essential for Golgi maintenance in this cell type, but GBF1 recruitment to Golgi sites was similarly impaired. Furthermore, we demonstrated that GBF1 interaction with C10orf76 occurs through C-terminal domains which are essential for Golgi localization. However, the interaction could be direct or indirect. Together, the research indicates a key role for C10orf76 in facilitating the membrane binding of GBF1. However, it's important to note that C10orf76 appears to be missing in certain model organisms and is reportedly not essential in certain cell types such as HAP1. This indicates that while C10orf76 may play a role in GBF1 regulation, it is not the sole protein component involved. There likely exists other more conserved regulators.

McPhail et al., 2019 has shown that C10orf76 appears to be recruited to membranes by PI4KB. Furthermore, C10orf76 depletion reduces PI4P production *in vivo*. Previous work has also shown that the HDS1 domain of GBF1 is a PI4P binding domain (Meissner et al., 2018). Likewise, previous studies have suggested that Arf1 activation may also stimulate PI4KB activity, as constitutively active Arf1 leads to increased PI4KB and PI4P production at the Golgi (Godi et al., 1999). Together, these data may suggest a potential feed forward model by which C10orf76 regulates GBF1 membrane binding (Figure 7.2). GBF1 activation of Arf1 at the *cis*-Golgi facilitates the recruitment and activity PI4KB. PI4KB recruits C10orf76, which in turn stimulates PI4P production. Together, PI4P and C10orf76 may function as receptor-like

components for the recruitment of additional GBF1 to activate Arf1 which recruits additional PI4KB – thus maintaining a steady level of GBF1 at the membrane through a feed forward cycle. The exact mechanism by which active Arf1 recruits PI4KB is unclear, but is likely indirect as no interactions between Arf1 and PI4KB have been observed (Haynes et al., 2004). *In vitro* studies using recombinant C10orf76 and PI4KB initially suggested that C10orf76 interaction suppressed PI4KB activity (McPhail et al., 2019). However, observations *in vivo* suggest the opposite: C10orf76 knockout cells have reduced Golgi PI4P. This discrepancy may be due to the presence of additional factors such as GBF1. Understanding how C10orf76 participates in the production of increased binding sites for GBF1 upon stimulation with BFA and answering why C10orf76 appears essential in some cell types and organisms but not in others will require additional study.

Nonetheless the model described in figure 7.2 is attractive in that it may also explain GBF1's role in the replication of various positive-strand RNA viruses. As described, GBF1 appears to be essential to the successful replication for several positive-strand RNA viruses including polio and certain coxsackie viruses (Belov et al., 2010; Ferlin et al., 2018). Replication organelles – sites where positive-strand viral genome replication takes place in infected human cells – are highly enriched in PI4P (Dorobantu et al., 2015; Nagy et al., 2016). PI4K inhibitory drugs have been shown to block replication organelle assembly and viral replication (Melia et al., 2017). One potential explanation for GBF1's involvement could be through its ability to stimulate PI4P production upon recruitment by C10orf76. This hypothesis would also explain why BFA treatment interferes with poliovirus replication as well as C10orf76's initial discovery in a host factor screen for coxsackievirus A10 (Belov et al., 2010; Blomen et al., 2015).

Another GBF1 interactor, Rab1b, may also regulate GBF1 recruitment in a similar manner. As mentioned previously, Rab1b binds directly to the N-terminal half of GBF1 (sequences

upstream of Sec7) (Monetta et al., 2007). Constitutively active Rab1b also appears to recruit additional GBF1 to peripheral ERGIC structures. PI4KB has been suggested as a potential Rab1b effector, as dominant active Rab1 increase PI4P levels at the Golgi (Doiron-Dumaresq et al., 2010). However, no interaction between the two proteins have yet been reported. Rab1b mediated recruitment of PI4KB may help sustain adequate PI4P levels for GBF1 recruitment. This would link anterograde COPII traffic to retrograde COPI traffic between the ER and Golgi, allowing for balanced bi-directional movement. Links between COPII and COPI traffic via Rab1 had already been previously suggested when Rab1 knockdowns altered both COPII and COPI vesicle formation (García et al., 2011). Likewise, early genetics studies had revealed that overexpression of yeast Rab1, Ypt1, can rescue defects in yeast GBF1, Gea1 and Gea2 (Jones et al., 1999).

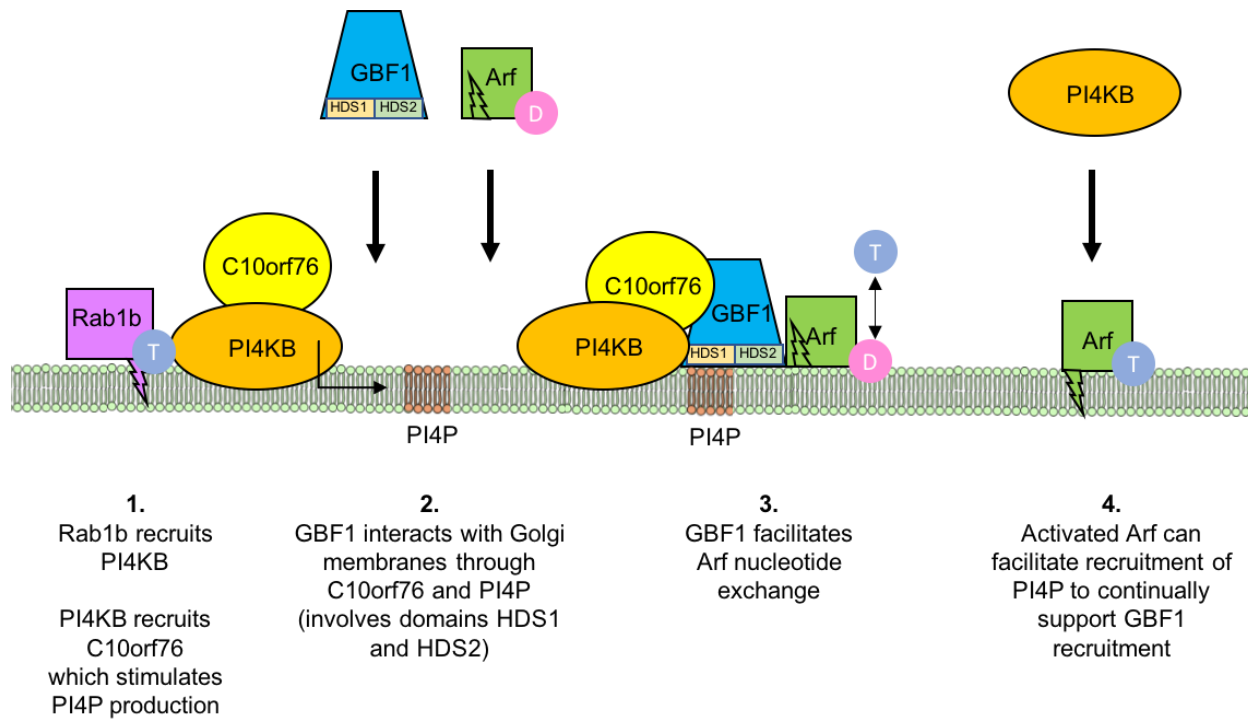


Figure 7.2 Potential model for C10orf76 mediated recruitment of GBF1.

C10orf76 may facilitate the recruitment of GBF1 to the *cis*-Golgi through both physical interaction and stimulation of PI4P production. 1) PI4KB has been previously suggested as a Rab1b effector and may facilitate recruitment of PI4KB to *cis*-Golgi membranes. PI4KB may then recruit C10orf76 to stimulate production of PI4Ps. 2) GBF1 interaction with PI4P and C10orf76 may then facilitate its recruitment to the *cis*-Golgi. This likely occurs through HDS1 and HDS2 which appear essential in Golgi targeting. HDS1 has also been previously shown to interact with PI4Ps. 3) At the membrane, GBF1 facilitates nucleotide exchange and the activation of Arfs. 4) Activated Arfs may recruit additional PI4KB to maintain continuous GBF1 recruitment.

7.6 Future experiments, BioID analysis, and other GBF1 regulators

While PI4P undoubtedly plays a role in GBF1 membrane binding, the act of recruitment appears to require facilitation by protein components – C10orf76 being one of them. Previous research has shown that no changes in *cis*-Golgi PI4P levels occur upon BFA treatment, suggesting that GBF1 recruitment is not caused by increased PI4P production (Quilty et al., 2014). Likewise PI4P can be found at multiple membrane sites outside the *cis*-Golgi, in fact PI4P is much more abundant at the TGN, endosomal, and plasma membrane as compared to the *cis*-Golgi (Jackson et al., 2016). These observations suggest that there must be other components at play in the *cis*-Golgi specific recruitment of GBF1.

While our research has expanded our knowledge of GBF1 regulation at the Golgi membrane, it remains clear that our current understanding remains incomplete. Firstly, additional studies need to be performed to better elucidate the role C10orf76 plays in GBF1 recruitment apart from PI4P production. Co-immunoprecipitation assays performed on C10orf76 and GBF1 in untreated and BFA treated cells will indicate whether C10orf76 affinity for GBF1 may change in response to regulatory signals. Likewise, mass spectrometry analysis of C10orf76 in untreated and BFA treated cells can reveal whether the protein may be differentially post-translationally modified. Furthermore, determining the C10orf76 interactome may also yield novel insights. Previous work has shown that membrane-associated Arf-GDP can stimulate GBF1 recruitment, yet the target of regulatory Arf-GDP remains unknown. Might C10orf76 interact with Arf-GDP, and if so, does it occur directly? If other protein components are at play, cross referencing the C10orf76 interactome with our list of BioID derived GBF1 proximal partners may allow for the identification of novel candidates of interest.

Additional experiments can also be performed to further evaluate the functional link between GBF1 and C10orf76. Firstly, we must determine whether the interaction between C10orf76 and GBF1 is direct. To do so we can perform co-immunoprecipitation experiments using recombinant GBF1 and C10orf76. Secondly, we must also determine whether the interaction is occurring on Golgi membranes. To do so we can take advantage of techniques such as fluorescence resonance energy transfer where both GBF1 and C10orf76 are tagged to either cyan fluorescent protein (CFP) or yellow fluorescent protein (YFP). If C10orf76 and GBF1 interact at the Golgi, fluorescence emission by excited of CFP will in turn excite nearby YFP which can be observed by imaging. Thirdly, to determine whether the activity of C10orf76 and PI4KB is sufficient to recruit GBF1 to membrane sites we can utilize the heterodimerization assay developed by McPhail et al., 2019. Using the FRB domain of mTOR attached to PI4KB, the researchers were able to retarget both PI4KB and C10orf76 to mitochondrial membranes. We can examine using a similar set up whether GBF1 distribution is altered by the retargeting of PI4KB and C10orf76 to the mitochondria.

Lastly, our phylogenetic analysis revealed that while ancestral, C10orf76 does not appear to be conserved in many model systems. This suggests the existence of other more conserved components involved in GBF1 regulation. Additional answers to major questions such as the mechanism by which ZnT6 affects GBF1 cycling and how C10orf76 modulates GBF1 recruitment in response to signals such as regulatory Arf-GDP or BFA may lie in these additional protein-protein interactions.

One way to identify additional protein regulators could be through revisiting the list of GBF1 proximal partners identified in our study. Our initial shRNA screen only examined nine candidates with a false discovery rate above 0.01. However, as discussed earlier, many

previously identified GBF1 interacting proteins such as p115 failed to meet the 0.01 false discovery rate cutoff, indicating that additional GBF1 interactors are likely present in the list. A large scale screen of these candidates using an automated microscopy of imaging flow cytometry approach might yield additional interacting partners of interest.

An alternative method could be by pairing the previously described APEX method of identifying proximal partners with BFA treatment. APEX was initially disregarded due to the requirement of additional chemicals including biotin phenol and hydrogen peroxide, which we feared may disrupt GBF1 membrane association. However, pairing the technique with BFA which traps GBF1 in a membrane-bound state may circumvent these issues and allow for the identification of regulatory components that trigger GBF1 recruitment and alter GBF1 cycling.

Similar to experiments proposed for the future studies of C10orf76, additional co-immunoprecipitation experiments can also be done to determine whether interaction between GBF1 and ZnT6 is direct. ZnT6 has two cytosolic loops, a C-terminal, and an N-terminal cytosolic tail. By repeating the pulldown experiments *in vitro* with tagged ZnT6 fragments and recombinant GBF1, we can try to determine which region of ZnT6 may be required for interaction and if the interaction is direct. To confirm whether the impact of ZnT6 depletion on GBF1 cycling is due to impaired zinc transport we can perform two different sets of experiments. The first involves examining whether GBF1 interacts with ZnT7 and whether the depletion of ZnT7 has an impact similar to Znt6 depletion on GBF1 cycling. If GBF1 cycling is not directly influenced by zinc, depletion of ZnT7 should have negligible impact. The second involves performing rescue experiments. If the defects in GBF1 cycling can be rescued by feeding cells excess zinc, overexpression of transport defective ZnT5 and ZnT6 in a ZnT5/6 knockout background, that would likely indicate a role for zinc in GBF1 regulation.

7.7 GBF1 recruitment at other membrane sites

GBF1 recruitment and membrane binding while incompletely understood at the Golgi, is even more poorly studied at other locations. As mentioned PI4Ps likely plays an essential role in membrane binding of GBF1, and the presence of PIPs at other locations including the plasma membrane likely facilitate GBF1 recruitment to those sites. But whether additional protein components are required have not yet been investigated.

In clathrin and dynamin independent CLIC/GEEC endocytosis, real-time super resolution imaging has demonstrated that GBF1 is rapidly recruited to endocytic pits approximately 60 seconds prior to the formation of GC vesicles (Sathe et al., 2018). GBF1 recruitment currently remains the earliest known initiators of the GC pathway. The concerted recruitment of GBF1, followed by Arf1 and other GC components suggest that GBF1 mediated GC endocytosis is a highly regulated cellular event, with the initial recruitment of GBF1 likely involving specific regulatory components. Uniquely, GC endocytosis only occurs on select cell types and has never been observed in HeLa cells (Mayor et al., 2014). While the components involved in GBF1 recruitment to endocytic sites may not have been identified in our HeLa BioID assay, the data may serve as a valuable baseline for identifying unique GBF1 partners at the plasma membrane when compared to cells that do exhibit GC (ex. AGS cells, a human gastric adenocarcinoma cell line).

At the mitochondria, GBF1 interacts with Miro1 and Miro2 – transmembrane adaptor proteins that link dynein and kinesin motors to the mitochondrial outer membrane (Ackema et al., 2014; Walch et al., 2018). Loss of GBF1 activity at these sites promote dynein mediated condensation of mitochondria towards the MTOC. Little is known about the exact mechanism by which GBF1 is recruited to these sites or the exact role activated Arf1 plays in modulating Miro,

activity. Our BioID analysis did not identify either Miro1 or Miro 2. Although, as our own analysis indicates, many interacting proteins may not be readily identified from whole cell lysates. Identification of GBF1 interactors at these unique membrane sites will likely require enriching for these proteins through organelle isolation or other methods prior to mass spectrometry.

The recruitment of GBF1 to the leading edge of cells for chemotaxis and migration similarly remains poorly understood. In cultured neutrophils (HL60), GBF1 appears to be specifically recruited to the leading edge upon stimulation of G-protein coupled receptors (Mazaki et al., 2012). This process appears to require membrane PI3P,s as loss of PI3 kinase activity impairs GBF1 recruitment. However, the presence of PI3P is itself insufficient, as no plasma membrane localised GBF1 is detected in unstimulated cells. The mechanism that recruits GBF1 to the leading edge upon stimulation is unclear, but likely also involves additional regulatory and signaling components. Inhibition of GBF1 activity or overexpression of GDP-arrested Arfs altered cell polarity leading to the formation of multiple leading edges and impaired migratory potential. GBF1 likely plays a role in these cells regulating leading edge formation. A subsequent publication has identified a similar requirement for GBF1 in cell adhesion and motility of the glioblastoma cell line (GBM) (Busby et al., 2017).

To determine whether the domains involved in targeting GBF1 to the Golgi are also involved in targeting GBF1 to these alternate membrane sites, we can utilize our previously generated GBF1 truncation library. For instance, we can look for the enrichment of EGFP-tagged N885-1856 at the leading edge of neutrophils upon stimulation of G-protein coupled receptors. Likewise, we can also assay for the presence of the EGFP-GBF1 truncations at mitochondrial

membranes using western blotting following the enrichment of the organelle by gradient centrifugation.

But no matter how GBF1 recruitment occurs at these alternate membrane sites, the mechanisms are likely different than those guiding Golgi recruitment. Neither BFA or other Arf-GDP altering treatments have been shown to increase GBF1 recruitment to sites other than the Golgi. Likewise, domains other than HDS1 and HDS2 may be involved. For instance, no function has yet been prescribed for HDS3, yet it's conservation amongst the GBF family indicates that it likely has some functional role (Mouratou et al., 2005; Pipaliya et al., 2019). Examining the recruitment of our characterized GBF1 truncation mutants to these alternate sites may provide valuable insight.

Apart from the potentially varied mechanisms by which GBF1 may be recruited to non-Golgi locations, it's important to note that the mechanism of GBF1 recruitment is already known to be unique compared to the other large-ArfGEFs: BIG1 and BIG2. The requirement for GBF1 at other membrane sites is likely reflected in these differences. In mammalian cells, BIG1 and BIG2 appear to be recruited to the TGN via GTP-bound Arf3, Arf4, and Arl1 (Christis and Munro, 2012; Lowery et al., 2013). This is in sharp contrast to the GDP-bound Arfs that stimulate GBF1 recruitment. The GTP-bound Arf mediated recruitment of BIG1 and BIG2 would suggest a feed-forward reaction where recruited BIG1 and BIG2 would activate additional Arfs fueling further recruitment. In fact, imaging studies have shown that majority of BIGs reside at the Golgi whereas only approximately 20% of GBF1 is Golgi-localised at homeostasis (Manolea et al., 2008; Quilty et al., 2014). The Arf-GDP mediated recruitment of GBF1 allows for a much more nuanced control of GBF1 distribution. GBF1 can be recruited to the Golgi-dependent on trafficking requirements while leaving a pool of cytoplasmic GBF1 for recruitment

to other sites when required. Further study into the components and mechanism involved in GBF1 recruitment and release from Golgi membranes will allow for a more complete understanding of the ways GBF1 activity and demand can be reconciled amongst multiple cellular locations.

7.8 Concluding remarks

The work described in this thesis contributes to our understanding of GBF1 recruitment to Golgi membranes. Firstly, we identified the minimum domains required for Golgi targeting and provided additional evidence that GBF1 recruitment can occur independently of *sec7d*, further pointing to the existence of membrane regulatory elements. Secondly, we identified two novel GBF1 interacting proteins: C10orf76 and ZnT6. Our data support other recently published evidence that C10orf76 is a peripheral membrane protein that facilitates the recruitment of GBF1. Additional phylogenetic analysis also revealed that C10orf76 was likely present in the LECA. Our identification of ZnT6 as a potential regulator of GBF1 dynamics at the Golgi is the first time a component other than GBF1 or Arf that appears to be involved in the release of GBF1 following recruitment. The exact mechanism remains unclear, but continued study will greatly add to our understanding of GBF1 membrane dynamics. Lastly, the GBF1 truncation library and the GBF1 BioID data generated through our work will serve as valuable tools for ongoing studies into GBF1 regulation and function. Since its initial discovery, GBF1 has been shown to play multiple essential cellular functions at the Golgi and beyond, including mitochondrial positioning, endocytosis, and cell migration. GBF1 has also been shown to be required in replication of various RNA viruses. A complete understanding of GBF1 recruitment to membrane sites will allow for a more nuanced picture of cellular physiology and potential methods by which to selectively alter GBF1 activity to treat human disease.

References

- Ackema, K.B., J. Hench, S. Böckler, S.C. Wang, U. Sauder, H. Mergentaler, B. Westermann, F. Bard, S. Frank, and A. Spang. 2014. The small GTPase Arf1 modulates mitochondrial morphology and function. *EMBO Journal*. 33:2659-2675.
- Aizawa, M., and M. Fukuda. 2015. Small GTPase Rab2B and Its Specific Binding Protein Golgi-associated Rab2B Interactor-like 4 (GARI-L4) Regulate Golgi Morphology. *Journal of Biological Chemistry*. 290:22250-22261.
- Allan, B.B., B.D. Moyer, and W.E. Balch. 2000. Rab1 recruitment of p115 into a cis-SNARE complex: programming budding COPII vesicles for fusion. *Science*. 289:444-448.
- Alvarez, C., H. Fujita, A. Hubbard, and E. Sztul. 1999. ER to Golgi transport: requirement for p115 at a pre-Golgi Vtc stage. *Journal of Cell Biology*. 147:1205-1222.
- Alvarez, C., R. García-Mata, E. Brandon, and E. Sztul. 2003. COPI recruitment is modulated by a Rab1b-dependent mechanism. *Molecular Biology of the Cell*. 14:2116-2127.
- Anders, N., M. Nielson, J. Keicher, Y.-D. Stierhof, M. Furutani, M. Tasaka, K. Skriver, and G. Jürgens. 2008. Membrane Association of the Arabidopsis ARF Exchange Factor GNOM Involves Interaction of Conserved Domains. *The Plant Cell*. 20:142-151.
- Angel, T.E., U.K. Aryal, S.M. Hengel, E.S. Baker, R.T. Kelly, E.W. Robinson, and R.D. Smith. 2012. Mass spectrometry based proteomics: existing capabilities and future directions. *Chemical Society Reviews*. 41:3912-3928.
- Appenzeller-Herzog, C., and H.-P. Hauri. 2006. The ER-Golgi intermediate compartment (ERGIC): in search of its identity and function. *Journal of Cell Science*. 119:2173-2183.
- Arakel, E.C., and B. Schwappach. 2018. Formation of COPI-coated vesicles at a glance. *Journal of Cell Science*. 131:jcs209890.
- Balla, T. 2013. Phosphoinositides: Tiny Lipids With Giant Impact on Cell Regulation. *Physiological Reviews*. 93:1019-1137.
- Beck, R., M. Rawet, F. Wieland, and D. Cassel. 2009. The COPI system: molecular mechanisms and function. *FEBS Letters*. 583:2701-2709.
- Beck, R., Z. Sun, F. Adolf, C. Rutz, J. Bassler, K. Wild, I. Sinning, E. Hurt, B. Brugger, J. Béthune, and F.T. Wieland. 2008. Membrane curvature induced by Arf1-GTP is essential for vesicle formation. *Proceedings of the National Academy of Science*. 105:11731-11736.
- Becker, B., and M. Melkonian. 1996. The secretory pathway of protists: spatial and functional organization and evolution. *Microbiology Reviews*. 60:697-721.
- Belov, G.A., G. Kovtunovych, C.L. Jackson, and E. Ehrenfeld. 2010. Poliovirus replication requires the N-terminus but not the catalytic sec7 domain of ArfGEF GBF1. *Cellular Microbiology*. 12:1463-1479.
- Ben-Tekaya, H., K. Miura, R. Pepperkok, and H.-P. Hauri. 2005. Live-imaging of bidirectional traffic from the ERGIC. *Journal of Cell Science*. 118:357-367.
- Bendor, J., T. Logan, and R.H. Edwards. 2013. The Function of alpha-Synuclein. *Neuron*. 79:1044-1066.
- Beznoussenko, G.V., S. Parashuraman, R. Rizzo, R. Polishchuk, O. Martella, D.D. Giandomenico, A. Fusella, A. Spaar, M. Salles, M.G. Capestrano, M. Pavelka, M.R. Vos, Y.G.M. Rikers, V. Helms, A.A. Mironov, and A. Luini. 2014. Transport

- of soluble proteins through the Golgi occurs by diffusion via continuities across the cisternae. *eLife*. 3:e02009.
- Bhatt, J.M., E.G. Viktorova, T. Busby, P. Wyrozumska, L.E. Newman, H. Lin, E. Lee, J. Wright, G.A. Belov, R.A. Kahn, and E. Sztul. 2016. Oligomerization of the Sec7 domain Arf guanine nucleotide exchange factor GBF1 is dispensable for Golgi localization and function but regulates degradation. *American Journal of Physiology Cell Physiology*. 310:456-469.
- Blomen, V.A., P. Májek, L.T. Jae, J.W. Bigenzahn, J. Nieuwenhuis, J. Staring, R. Sacco, F.R.V. Diemen, N. Olk, A. Stukalov, C. Marceau, H. Janssen, J.E. Carette, K.L. Bennett, J. Colinge, G. Superti-Furga, and T.R. Brummelkamp. 2015. Gene essentiality and synthetic lethality in haploid human cells. *Science*. 250:1092-1096.
- Boncompain, G., and F. Perez. 2013. The many routes of Golgi-dependent trafficking. *Histochemistry and Cell Biology*. 140:251-260.
- Bonfanti, L., A.A.J. Mironov, J.A. Martinez-Menárguez, O. Martella, A. Fusella, M. Baldassarre, R. Buccione, H.J. Geuze, A.A. Mironov, and A. Luini. 1998. Procollagen traverses the Golgi stack without leaving the lumen of cisternae: evidence for cisternal maturation. *Cell*. 95:993-1003.
- Bonifacino, J.S., and B.S. Glick. 2004. The mechanisms of vesicle budding and fusion. *Cell*. 116:153-166.
- Bouvet, S., M.P. Bgolinelli-Cohen, V. Contremoulins, and C.L. Jackson. 2013. Targeting of the Arf-GEF GBF1 to lipid droplets and Golgi membranes. *Journal of Cell Science*. 126:4794-4805.
- Braakman, I., and N.J. Bulleid. 2011. Protein Folding and Modification in the Mammalian Endoplasmic Reticulum. 80:71-99.
- Breuza, L., R. Halbeisen, P. Jenö, S. Otte, C. Barlowe, W. Hong, and H.-P. Hauri. 2004. Proteomics of endoplasmic reticulum-Golgi intermediate compartment (ERGIC) membranes from BrefeldinA-treated HepG2 cells indentifies ERGIC-32, a new cycling protein that interacts with human Erv46. *Journal of Biological Chemistry*. 279:47242-47253.
- Burke, J.B. 2018. Structural Basis for Regulation of Phosphoinositide Kinases and Their Involvement in Human Disease. *Molecular Cell*. 71:653-673.
- Busby, T., J.M. Meissner, M.L. Styers, J.M. Bhatt, A. Kaushik, A.B. Hjemeland, and E. Sztul. 2017. The Arf activator GBF1 localizes to plasma membrane sites involved in cell adhesion and motility. *Cellular Logistics*. 7:e1308900.
- Campa, F., and P.A. Randazzo. 2008. Arf GTPase-activating proteins and their potential role in cell migration and invasion. *Cell Adhesion and Migration*. 2:258-262.
- Casanova, J.E. 2007. Regulation of Arf activation: the Sec7 family of guanine nucleotide exchange factors. *Traffic*. 8:1476-1485.
- Chan, C.J., R. Le, K. Burns, K. Ahmed, E. Coyaud, E.M.N. Laurent, B. Raught, and P. Melançon. 2019. BioID Performed on Golgi-enriched Fractions Identify C10orf76 as a GBF1 Binding Protein Essential for Golgi Maintenance and Secretion. *Molecular & Cellular Proteomics*. 18:2285-2297.
- Chantalat, S., R. Courbeyrette, F. Senic-Matuglia, C.L. Jackson, B. Goud, and A. Peyroche. 2003. A novel Golgi membrane protein is a partner of the ARF exchange factors Gea1p and Gea2p. *Molecular Biology of the Cell*. 14.

- Chen, C.-L., and N. Perrimon. 2017. Proximity-dependent labeling methods for proteomic profiling in living cells. *Wiley Interdisciplinary Review Developmental Biology*. 6:10.1002/wdev.1272.
- Chen, J., X. Wu, L. Yao, L. Yan, L. Zhang, J. Qiu, X. Liu, S. Jia, and A. Meng. 2017. Impairment of cargo transportation caused by GBF1 mutation disrupts vascular integrity and causes hemorrhage in zebrafish embryos. *Journal of Biological Chemistry*. 292:2315-2327.
- Chen, Y., Y. Zhang, Y. Yin, G. Gao, S. Li, Y. Jiang, X. Gu, and J. Luo. 2005a. SPD—a web-based secreted protein database. *Nucleic Acids Research*. 33:D169–D173.
- Chen, Y.-H., J.H. Kim, and M.R. Stallcup. 2005b. GAC63, a GRIP1-dependent nuclear receptor coactivator. *Molecular and Cellular Biology*. 25:5965-5972.
- Chen, Y.-H., C.K. Yang, M. Xia, C.-Y. Ou, and M.R. Stallcup. 2007. Role of GAC63 in transcriptional activation mediated by beta-catenin. *Nucleic Acids Research*. 35:2084-2092.
- Chen, Y.-L., S. Eriksson, and Z.-F. Chang. 2010. Regulation and Functional Contribution of Thymidine Kinase 1 in Repair of DNA Damage. *Journal of Biological Chemistry*. 285:27327-27335.
- Choi, H., B. Larsen, Z.Y. Lin, A. Breitkreutz, D. Mellacheruvu, D. Fermin, Z.S. Qin, M. Tyers, A.C. Gingras, and A.I. Nesvizhskii. 2011. SAINT: probabilistic scoring of affinity purification-mass spectrometry data. *Nature Methods*. 8:70-73.
- Christis, C., and S. Munro. 2012. The small G protein Arf1 directs the trans-Golgi-specific targeting of the Arf1 exchange factors BIG1 and BIG2. *Journal of Cell Biology*. 196:327-335.
- Chun, J., Z. Shapovalova, S.Y. Dejgaard, J.F. Presley, and P. Melançon. 2008. Characterization of Class I and II ADP-Ribosylation Factors (Arfs) in Live-cells: GDP-bound Class II Arfs Associate with the ER-Golgi Intermediate Compartment Independently of GBF1. *Molecular Biology of the Cell*. 19:3488-3500.
- Claude, A., B.P. Zhao, C.E. Kuziemy, S. Dahan, S.J. Berger, J.P. Yan, A.D. Arnold, E.M. Sullivan, and P. Melançon. 1999. GBF1: A novel Golgi-associated BFA-resistant guanine nucleotide exchange factor that displays specificity for ADP-ribosylation factor 5. *Journal of Cell Biology*. 146:71-84.
- Claude, A., B.P. Zhao, and P. Melançon. 2003. Characterization of alternatively spliced and truncated forms of the Arf guanine nucleotide exchange factor GBF1 defines regions important for activity. *Biochemical and Biophysical Research Communications*. 303.
- Couzens, A.L., J.D. Knight, M.J. Kean, G. Teo, A. Weiss, W.H. Dunham, Z.Y. Lin, R.D. Bagshaw, F. Sicheri, T. Pawson, J.L. Wrana, H. Choi, and A.C. Gingras. 2013. Protein interaction network of the mammalian Hippo pathway reveals mechanisms of kinase-phosphatase interactions. *Science Signaling*. 6.
- Cox, R., R.J. Mason-Gamer, C.L. Jackson, and N. Segev. 2004. Phylogenetic Analysis of Sec7-Domain-containing Arf Nucleotide Exchangers. *Molecular Biology of the Cell*. 15:1487–1505.
- Craig, R., and R.C. Beavis. 2004. TANDEM: matching proteins with tandem mass spectra. *Bioinformatics*. 20:1466-1467.
- De Graaf, P., W.T. Zwart, R.A. van Dijken, M. Deneka, T.K. Schulz, N. Geijsen, P.J. Coffers, B.M. Gadella, A.J. Verkleij, P. van der Sluijs, and P.M. van Bergen en

- Henegouwen. 2004. Phosphatidylinositol 4-kinase beta is critical for functional association of rab11 with the Golgi complex. *Molecular Biology of the Cell*. 15.
- Dickinson, M.E., A.M. Flenniken, X. Ji, L. Teboul, M.D. Wong, J.K. White, T.F. Meehan, W.J. Weninger, H. Westerberg, H. Adissu, and e. al. 2016. High-throughput discovery of novel developmental phenotypes. *Nature*. 537:508-514.
- DiNitto, J.P., T.C. Cronin, and D.G. Lambright. 2003. Membrane recognition and targeting by lipid-binding domains. *Science Signaling*. 2003:re16.
- Dippold, H.C., M.M. Ng, S.E. Faber-Katz, S.-K. Lee, M.L. Kerr, M.C. Peterman, R. Sim, P.A. Wiharto, K.A. Galbraith, S. Madhavarapu, G.J. Fuchs, T. Meerloo, M.G. Farquhar, H. Zhou, and S.J. Field. 2009. GOLPH3 Bridges Phosphatidylinositol-4-Phosphate and Actomyosin to Stretch and Shape the Golgi to Promote Budding. *Cell*. 139:337–351.
- Doiron-Dumaresq, K., M. Savard, S. Akam, S. Costantino, and S. Lefrançois. 2010. The phosphatidylinositol 4-kinase PI4KIII alpha is required for the recruitment of GBF1 to Golgi membranes. *Journal of Cell Science*. 123.
- Donaldson, J.G., A. Honda, and R. Weigert. 2005. Multiple activities for Arf1 at the Golgi complex. *Biochimica et Biophysica Acta (BBA) - Molecular Cell Research*. 1744:364-373.
- Donaldson, J.G., and C.L. Jackson. 2011. Arf Family G Proteins and their regulators: roles in membrane transport, development and disease. *Nature Reviews Molecular Cell Biology*. 12:362–375.
- Dorobantu, C.M., L. Albuлесcu, C. Harak, Q. Feng, M. van Kampen, J.R.P.M. Strating, A.E. Gorbalenya, V. Lohmann, H.M. van der Scharr, and F.J.M.v. Kuppeveld. 2015. Modulation of the Host Lipid Landscape to Promote RNA Virus Replication: The Picornavirus Encephalomyocarditis Virus Converges on the Pathway Used by Hepatitis C Virus. *PLoS Pathogens*. 11:e1005185.
- East, M. P. and R. A. Kahn. 2011. Models for the Functions of ArfGAPs. *Semin Cell Dev Biol*. 22: 3-9.
- Ellong, E.N., K.G. Soni, Q.-T. Bui, R. Sougrat, M.-P. Golinelli-Cohen, and C.L. Jackson. 2011. Interaction between the triglyceride lipase ATGL and the Arf1 activator GBF1. *PLOS One*. 6:e21889.
- Eugster, A., G. Frigerio, M. Dale, and R. Duden. 2000. COP I domains required for coatmer integrity, and novel interactions with ARF and ARF-GAP. *EMBO Journal*. 19:3905–3917.
- Eura, Y., N. Ishihara, S. Yokota, and K. Mihara. 2003. Two mitofusin proteins, mammalian homologues of FZO, with distinct functions are both required for mitochondrial fusion. *Journal of Biochemistry*. 134.
- Fan, J.Y., J. Roth, and C. Zuber. 2003. Ultrastructural analysis of transitional endoplasmic reticulum and pre-Golgi intermediates: a highway for cars and trucks. *Histochemistry and Cell Biology*. 120:455-463.
- Ferlin, J., R. Farhat, S. Blelouzard, L. Cocquerel, A. Bertin, D. Hober, J. Dubuisson, and Y. Rouillé. 2018. Investigation of the role of GBF1 in the replication of positive-sense single-stranded RNA viruses. *Journal of General Virology*. 99:1086-1096.
- Frigerio, G., N. Grimsey, M. Dale, I. Majoul, and R. Duden. 2007. Two Human ARFGAPs Associated with COP-I-Coated Vesicles. *Traffic*. 8:1644-1655.

- Fukunaka, A., Y. Kurokawa, F. Teranishi, I. Sekler, K. Oda, L.M. Ackland, V. Faundez, M. Hiromura, S. Masuda, M. Nagao, S. Enomoto, and T. Kambe. 2011. Tissue Nonspecific Alkaline Phosphatase Is Activated via a Two-step Mechanism by Zinc Transport Complexes in the Early Secretory Pathway. *Journal of Biological Chemistry*. 286.
- Fukunaka, A., T. Suzuki, Y. Kurokawa, T. Yamazaki, N. Fujiwara, K. Ishihara, H. Migaki, K. Okumura, S. Masuda, Y. Yamaguchi-Iwai, M. Nagao, and T. Kambe. 2009. Demonstration and characterization of the heterodimerization of ZnT5, and ZnT6 in the early secretory pathway. *Journal of Biological Chemistry*. 284:30798-30806.
- García, I.A., H.A. Martinez, and C. Alvarez. 2011. Rab1b regulates COPI and COPII dynamics in mammalian cells. *Cellular Logistics*. 1:159–163.
- García-Mata, R., T. Szul, C. Alvarez, and E. Sztul. 2003. ADP-Ribosylation Factor/COPI-dependent Events at the Endoplasmic Reticulum-Golgi Interface Are Regulated by the Guanine Nucleotide Exchange Factor GBF1. *Molecular Biology of the Cell*. 14:2250-2261.
- Gilchrist, A., C.E. Au, J. Hiding, A.W. Bell, J. Fernandez-Rodriguez, S. Lesimple, H. Nagaya, L. Roy, S.J.C. Gosline, M. Hallett, J. Paiement, R.E. Kearney, T. Nilsson, and J.J.M. Bergeron. 2006. Quantitative Proteomics Analysis of the Secretory Pathway. *Cell*. 127:1265-1281.
- Glick, B.S., and A. Luini. 2011. Models for Golgi Traffic: A Critical Assessment. *Cold Spring Harbor Perspectives in Biology*. 3:a005215.
- Glick, B.S., and A. Nakano. 2009. Membrane Traffic Within the Golgi Apparatus. *Annual Review of Cell and Developmental Biology*. 25:113-132.
- Godi, A., A. Di Campli, A. Konstantakopoulos, G. Di Tullio, D.R. Alessi, G.S. Kular, T. Daniele, P. Marra, J.M. Lucocq, and A. De Matteis. 2004. FAPPs control Golgi-to-cell-surface membrane traffic by binding to ARF and PtdIns(4)P. *Nature Cell Biology*. 6.
- Godi, A., P. Pertile, R. Meyers, P. Marra, G. Di Tullio, C. Iurisci, A. Luini, D. Corda, and A. De Matteis. 1999. ARF mediates recruitment of PtdIns-4-OH kinase- β and stimulates synthesis of PtdIns(4,5)P₂ on the Golgi complex. *Nature Cell Biology*. 1:280–287.
- Goldberg, J. 1998. Structural basis for activation of ARF GTPase. *Cell*. 95:237-248.
- Gomez-Navarro, N., and E. Miller. 2016. Protein sorting at the ER–Golgi interface. *Journal of Cell Biology*. 215:769–778.
- Goud, B., S. Liu, and B. Storrie. 2018. Rab proteins as major determinants of the Golgi complex structure. *Small GTPases*. 9:66-75
- Grebe, M., J. Gadea, T. Steinmann, M. Kientz, J.-U. Rahfeld, K. Salchert, C. Koncz, and G. Jürgens. 2000. A conserved domain of the Arabidopsis GNOM protein mediates subunit interaction and cyclophilin 5 binding. *Plant Cell*. 12:343-356.
- Guo, Y., V. Punj, D. Sengupta, and A.D. Linstedt. 2008. Coat-tether interaction in Golgi organization. *Molecular Biology of the Cell*. 19:2830-2843.
- Gupta, G.D., S. M G, S. Kumari, R. Lakshminarayan, G. Dey, and S. Mayor. 2009. Analysis of endocytic pathways in Drosophila cells reveals a conserved role for GBF1 in internalization via GEECs. *PLOS One*. 4:e6768.

- Hammond, C., and A. Helenius. 1994. Quality control in the secretory pathway: retention of a misfolded viral membrane glycoprotein involves cycling between the ER, intermediate compartment, and Golgi apparatus. *Journal of Cell Biology*. 126:41-52.
- Hara-Kuge, S., O. Kuge, L. Orci, M. Amherdt, M. Ravazzola, F.T. Wieland, and J.E. Rothman. 1994. En bloc incorporation of coatamer subunits during the assembly of COP-coated vesicles. *Journal of Cell Biology*. 124:883–892.
- Haynes, L.P., G.M.H. Thomas, and R.D. Buroyone. 2004. Interaction of Neuronal Calcium Sensor-1 and ADP-ribosylation Factor 1 Allows Bidirectional Control of Phosphatidylinositol 4-Kinase β and trans-Golgi Network-Plasma Membrane Traffic. *Journal of Biological Chemistry*. 280:6047-6054.
- Hoffman, E.A., B. L. Frey, L. M. Smith, and D.T. Auble. 2015. Formaldehyde crosslinking: a tool for the study of chromatin complexes. *Journal of Biological Chemistry*. 290: 26404-26411.
- Honda, A., O.S. Al-Awar, J.C. Hay, and J.G. Donaldson. 2005. Targeting of Arf-1 to the early Golgi by membrin, an ER-Golgi SNARE. *Journal of Cell Biology*. 168.
- Huang, L., and S. Tepasamorndech. 2013. The SLC30 family of zinc transporters - a review of current understanding of their biological and pathophysiological roles. *Molecular aspects of medicine*. 34:548-560.
- Huber, I., E. Cukierman, M. Rotman, T. Aoe, V.W. Hsu, and D. Cassel. 1998. Requirement for both the amino-terminal catalytic domain and a noncatalytic domain for in vivo activity of ADP-ribosylation factor GTPase-activating protein. *Journal of Biochemistry*. 273:24786-24791.
- Jackson, C.L., L. Walch, and J.-M. Verbavatz. 2016. Lipids and Their Trafficking: An Integral Part of Cellular Organization. *Developmental Cell*. 39:139-153.
- Jones, S., G. Jedd, R.A. Kahn, A. Franzusoff, F. Bartolini, and N. Segev. 1999. Genetic Interactions in Yeast Between Ypt GTPases and Arf Guanine Nucleotide Exchangers. *Genetics*. 152:1543-1556.
- Kaczmarek, B., J.-M. Verbavatz, and C.L. Jackson. 2017. GBF1 and Arf1 function in vesicular trafficking, lipid homeostasis and organelle dynamics. *Biology of the cell*. 109:391-399.
- Kahn, R.A., E. Bruford, H. Inoue, J.M.J. Logsdon, Z. Nie, R.T. Premont, P.A. Randazzo, M. Satake, A.B. Theibert, M.L. Zapp, and D. Cassel. 2008. Consensus nomenclature for the human ArfGAP domain-containing proteins. *Journal of Cell Biology*. 182:1039–1044.
- Kahn, R.A., J. Cherfils, M. Elias, R.C. Lovering, S. Munro, and A. Schurmann. 2006. Nomenclature for the human Arf family of GTP-binding proteins: ARF, ARL, and SAR proteins. *Journal of Cell Biology*. 172:645-650.
- Kambe, T. 2011. An overview of a wide range of functions of ZnT and Zip zinc transporters in the secretory pathway. *Bioscience, Biotechnology, and Biochemistry*. 75:1036-1043.
- Kambe, T., M. Matsunaga, and T.-a. Takeda. 2017. Understanding the contribution of zinc transporters in the function of the early secretory pathway. *International Journal of Molecular Sciences*. 18:2179.
- Kartberg, F., L. Asp, S.Y. Dejgaard, M. Smedh, J. Fernandez-Rodriguez, T. Nilsson, and J.F. Presley. 2010. ARFGAP2 and ARFGAP3 Are Essential for COPI Coat

- Assembly on the Golgi Membrane of Living Cells. *Journal of Biological Chemistry*. 285:36709-36720.
- Katayama, T., K. Imaizumi, T. Yoneda, M. Taniguchi, A. Honda, T. Manabe, J. Hitomi, K. Oono, K. Baba, S. Miyata, S. Matsuzaki, K. Takatsuji, and M. Tohyama. 2004. Role of ARF4L in recycling between endosomes and the plasma membrane. *Cellular and Molecular Neurobiology*. 24:137-147.
- Kessner, D., M. Chambers, R. Burke, D. Agus, and P. Mallick. 2008. ProteoWizard: open source software for rapid proteomics tools development. *Bioinformatics*. 24:2534-2536.
- Kim, D.I., K.C. Birendra, W. Zhu, K. Motamedchaboki, V. Doye, and K.J. Roux. 2014. Probing nuclear pore complex architecture with proximity-dependent biotinylation. *Proceedings of the National Academy of Science*. 111:E2453-2461.
- Kim, D.I., and K.J. Roux. 2016. Filling the void: proximity-based labeling of proteins in living cells. *Trends in Cell Biology*. 26:804-817.
- Kobayashi, H., K. Yamada, S. Morita, H. Hiura, A. Fukuda, M. Kagami, T. Ogata, K. Hata, Y. Sotomaru, and T. Kono. 2009. Identification of the mouse paternally expressed imprinted gene *Zdbf2* on chromosome 1 and its imprinted human homolog *zdbf2* on chromosome 2. *Genomics*. 93:461-472.
- Kökoer, T., A. Fernandez, and F. Pinaud. 2018. Characterization of split fluorescent protein variants and quantitative analyses of their self-assembly process. *Scientific Reports*. 8:5344.
- Kumar, A., S. Hou, A.M. Airo, D. Limonta, V. Mancinelli, W. Branton, C. Power, and T.C. Hobman. 2016. Zika virus inhibits type-I interferon production and downstream signaling. *EMBO Reports*. 17:1766-1775.
- Lanke, K.H.W., H.M. van der Scharr, G.A. Belov, Q. Feng, D. Duijsings, C.L. Jackson, E. Ehrenfeld, and F.J.M.v. Kuppeveld. 2009. GBF1, a Guanine Nucleotide Exchange Factor for Arf, Is Crucial for Coxsackievirus B3 RNA Replication. *Journal of Virology*. 83:11940-11949.
- Lee, C., and J. Goldberg. 2010. Structure of Coatamer Cage Proteins and the Relationship among COPI, COPII, and Clathrin Vesicle Coats. *Cell*. 142:123-132.
- Lee, S.Y., J.S. Yang, W. Hong, R.T. Premont, and V.W. Hsu. 2005. ARFGAP1 plays a central role in coupling COPI cargo sorting with vesicle formation. *Journal of Cell Biology*. 168:281-290.
- Lefrançois, S., and P.J. McCormick. 2007. The Arf GEF GBF1 is required for GGA recruitment to Golgi membranes. *Traffic*. 8:1440-1451.
- Lev, S. 2010. Non-vesicular lipid transport by lipid-transfer proteins and beyond. *Nature Reviews Molecular Cell Biology*. 11:739-750.
- Li, Q., A. Lau, T.J. Morris, L. Guo, C.B. Fordyce, and E.F. Stanley. 2004. A syntaxin 1, Gao, and N-Type Calcium Channel Complex at a Presynaptic Nerve Terminal: Analysis by Quantitative Immunocolocalization. *Journal of Neuroscience*. 24:4070-4081.
- Li, S., C.-Y. Ku, A.A. Farmer, Y.-S. Cong, C.-F. Chen, and W.-H. Lee. 1998. Identification of a Novel Cytoplasmic Protein that Specifically Binds to Nuclear Localization Signal Motifs. *Journal of Biological Chemistry*. 273:6183-6189.
- Liu, G., J. Zhang, B. Larsen, C. Stark, A. Breitkreutz, Z.Y. Lin, B.J. Breitkreutz, Y. Ding, K. Colwill, A. Pasulescu, T. Pawson, J.L. Wrana, A.I. Nesvizhskii, B. Raught, M.

- Tyers, and A.C. Gingras. 2010. ProHits: integrated software for mass spectrometry-based interaction proteomics. *Nature Biotechnology*. 28:1015-1017.
- Losev, E., C.A. Reinke, J. Jellen, D.E. Strongin, B.J. Bevis, and B.S. Glick. 2006. *Nature*. 441:1002-1006.
- Lowery, J., T. Szul, M.L. Styers, Z. Holloway, V. Oorschot, J. Klumperman, and E. Sztul. 2013. The Sec7 guanine nucleotide exchange factor GBF1 regulates membrane recruitment of BIG1 and BIG2 guanine nucleotide exchange factors to the trans-Golgi network (TGN). *Journal of Biological Chemistry*. 288:11532-11545.
- Lubec, G., and L. Afjehi-Sadat. 2007. Limitations and Pitfalls in Protein Identification by Mass Spectrometry. *Chemical Reviews*. 107:3568-3584.
- Mani, S., and M. Thattai. 2016. Stacking the odds for Golgi cisternal maturation. *eLife*:5:e16231.
- Manolea, F., A. Claude, J. Chun, J. Rosas, and P. Melançon. 2008. Distinct functions for Arf guanine nucleotide exchange factors at the Golgi complex: GBF1 and BIGs are required for assembly and maintenance of the Golgi stack and trans-Golgi network, respectively. *Molecular Biology of the Cell*. 19:523-535.
- Mansour, S.J., J. Skaug, X.H. Zhao, J. Giordano, S.W. Scherer, and P. Melançon. 1999. p200 ARF-GEP1: a Golgi-localized guanine nucleotide exchange protein whose Sec7 domain is targeted by the drug brefeldin A. *Proceedings of the National Academy of Science*. 96.
- Marsh, B.J., N. Volkmann, R.J. McIntosh, and K.E. Howell. 2004. Direct continuities between cisternae at different levels of the Golgi complex in glucose-stimulated mouse islet beta cells. *Proceedings of the National Academy of Science*. 101:5565-5570.
- Martell, J.D., T.J. Deerink, Y. Sancak, T.L. Poulos, V.K. Mootha, G.E. Sosinsky, M.H. Ellisman, and A.Y. Ting. 2012. Engineered ascorbate peroxidase as a genetically encoded reporter for electron microscopy. *Nature Biotechnology*. 30:1143-1148.
- Martin-Sanchez, P., and M. Komatsu. 2018. p62/SQSTM1 - steering the cell through health and disease. *Journal of Cell Science*. 131:jcs222836.
- Matsuura-Tokita, K., M. Takeuchi, A. Ichihara, K. Mikuyira, and A. Nakano. 2006. Live-imaging of yeast Golgi cisternal maturation. *Nature*. 441:1007-1010.
- Mayinger, P. 2011. Signaling at the Golgi. *Cold Spring Harbor Perspectives in Biology*. 3:a005314.
- Mayor, S., R.G. Parton, and J.G. Donaldson. 2014. Clathrin-Independent Pathways of Endocytosis. *Cold Spring Harbor Perspectives in Biology*. 6:a016758.
- Mazaki, Y., Y. Nishimura, and H. Sabe. 2012. GBF1 bears a novel phosphatidylinositol-phosphate binding module, BP3K, to link PI3K γ activity with Arf1 activation involved in GPCR-mediated neutrophil chemotaxis and superoxide production. *Molecular Biology of the Cell*. 23:2457-2467.
- McPhail, J.A., H. Lyoo, J.G. Pemberton, R.M. Hoffman, W.v. Elst, J.R.P.M. Strating, M.L. Jenkins, J.T.B. Stariha, C.J. Powell, M.J. Moulanger, T. Balla, F.J.M.v. Kuppeveld, and J.E. Burke. 2019. Characterization of the C10orf76-PI4KB complex and its necessity for Golgi PI4P levels and enterovirus replication. *EMBO Reports*:e48441.
- Meissner, J.M., J.M. Bhatt, E. Lee, M.L. Styers, A.A. Ivanova, R.A. Kahn, and E. Sztul. 2018. The ARF guanine nucleotide exchange factor GBF1 is targeted to Golgi membranes through a PIP-binding domain. *Journal of Cell Science*. 131:jcs210245.

- Melançon, P., B.S. Glick, V. Malhotra, P.J. Weidman, T. Serafini, M.L. Gleason, L. Orci, and J. Roth. 1987. Involvement of GTP-binding “G” proteins in transport through the Golgi stack. *Cell*. 51:1053-1062.
- Melia, C.E., H.M. van der Scharr, H. Lyoo, R.W.A.L. Limpens, Q. Feng, M. Wahedi, G.J. Overheul, R.P. van Rij, E.J. Snijder, A.J. Koster, M. Bárcena, and F.J.M.v. Kuppeveld. 2017. Escaping Host Factor PI4KB Inhibition: Enterovirus Genomic RNA Replication in the Absence of Replication Organelles. *Cell Reports*. 21:587–599.
- Millarte, V., and H. Farhan. 2012. The Golgi in cell migration: regulation by signal transduction and its implications for cancer cell metastasis. *The scientific world journal*. 2012:498278.
- Miller, V.J., P. Sharma, T.A. Kudlyk, L. Frost, A.P. Rofe, I.J. Watson, R. Duden, M. Lowe, V. Lupashin, and D. Ungar. 2013. Molecular insights into vesicle tethering at the Golgi by the conserved oligomeric Golgi (COG) complex and the golgin TATA element modulatory factor (TMF). *Journal of Biological Chemistry*. 288:4229-4240.
- Mironov, A.A., A.A.J. Mironov, G.V. Beznoussenko, A. Truco, P. Lupetti, J.D. Smith, W.J.C. Geerts, A.J. Koster, K.N.J. Burger, M. Martone, E, T.J. Deerink, M.H. Ellisman, and A. Luini. 2003. ER-to-Golgi Carriers Arise through Direct En Bloc Protrusion and Multistage Maturation of Specialized ER Exit Domains. *Developmental Cell*. 5:583-594.
- Moelleken, J., J. Malsam, M.J. Betts, A. Movafeghi, I. Reckmann, I. Meissner, A. Hellwig, R.B. Russell, T. Sollner, B. Brugger, and F. Wieland. 2007. Differential localization of coatamer complex isoforms within the Golgi apparatus. *Proceedings of the National Academy of Science*. 104:4425–4430.
- Monetta, P., I. Slavin, N. Romero, and C. Alvarez. 2007. Rab1b interacts with GBF1 and modulates both ARF1 dynamics and COPI association. *Molecular Biology of the Cell*. 18:2400-2410.
- Moravec, R., K.K. Conger, R. D’Souza, A.B. Allison, and J.E. Casanova. 2012. BRAG2/GEP100/IQSec1 interacts with clathrin and regulates $\alpha 5\beta 1$ integrin endocytosis through activation of ADP ribosylation factor 5 (Arf5). *Journal of Biological Chemistry*. 287:31138-31147.
- Mossessova, E., R.A. Corpina, and J. Goldberg. 2003. Crystal structure of ARF1*Sec7 complexed with Brefeldin A and its implications for the guanine nucleotide exchange mechanism. *Molecular Cell*. 12:1403-1411.
- Mouratou, B., V. Biou, J. Joubert, D.J. Cohen, N. Shields, G. Geldner, P. Jurgens, P. Melançon, and J. Cherfils. 2005. The domain architecture of large guanine nucleotide exchange factors for the small GTP-binding protein Arf. *BioMed Central*. 6.
- Moyer, B.D., B.B. Allan, and W.E. Balch. 2001. Rab1 Interaction with a GM130 Effector Complex Regulates COPII Vesicle cis-Golgi Tethering. *Traffic*. 2:268-276.
- Nagy, P.D., J.R.P.M. Strating, and F.J.M.v. Kuppeveld. 2016. Building Viral Replication Organelles: Close Encounters of the Membrane Types. *PLoS Pathogens*. 12:e1005912.
- Nakamura, N., M. Lowe, T.P. Levine, C. Rabouille, and G. Warren. 1997. The vesicle docking protein p115 binds GM130, a cis-Golgi matrix protein, in a mitotically regulated manner. *Cell*. 89:445-455.

- Nawrotek, A., M. Zeghouf, and J. Cherfils. 2016. Allosteric regulation of Arf GTPases and their GEFs at the membrane interface. *Small GTPases*. 7:283–296.
- Nelson, D.S., C. Alvarez, Y.S. Gao, R. García-Mata, E. Fialkowski, and E. Sztul. 1998. The membrane transport factor TAP/p115 cycles between the Golgi and earlier secretory compartments and contains distinct domains required for its localization and function. *Journal of Cell Biology*. 143:319-331.
- Nesvizhskii, A.I., A. Keller, E. Kolker, and R. Aebersold. 2003. A statistical model for identifying proteins by tandem mass spectrometry. *Analytical Chemistry*. 75.
- Ohana, E., E. Hoch, C. Keasar, T. Kambe, O. Yifrach, M. Hershfinkel, and I. Sekler. 2009. Identification of the Zn²⁺ binding site and mode of operation of a mammalian zn²⁺ transporter. *Journal of Biological Chemistry*. 284:17677-17686.
- Ortiz-Sandoval, C.G., H. S, J.B. Dacks, and T. Simmen. 2014. Interaction with the effector dynamin-related protein 1 (Drp1) is an ancient function of Rab32 subfamily proteins. *Cellular Logistics*. 4.
- Padilla, P.I., M. Uhart, G. Pacheco-Rodriguez, B.A. Peculis, J. Moss, and M. Vaughan. 2008. Association of guanine nucleotide-exchange protein BIG1 in HepG2 cell nuclei with nucleolin, U3 snoRNA, and fibrillarin. *Proceedings of the National Academy of Science*. 105:3357-3361.
- Pedrioli, P.G.A. 2010. Trans-proteomic pipeline: a pipeline for proteomic analysis. In *Proteome Bioinformatics*. S.J. Hubbard and A.R. Jones, editors. Humana Press, New York.
- Peyroche, A., B. Antonny, S. Robineau, J. Acker, J. Cherfils, and C.L. Jackson. 1999. Brefeldin A acts to stabilize an abortive ARF-GDP-Sec7 domain protein complex: involvement of specific residues of the Sec7 domain. *Molecular Cell*. 3.
- Peyroche, A., S. Paris, and C.L. Jackson. 1996. Nucleotide exchange on ARF mediated by yeast Gea1 protein. *Nature*. 384:479–481.
- Pfeffer, S. 2003. Membrane Domains in the Secretory and Endocytic Pathways. *Cell*. 112:507-517.
- Pfeffer, S. 2010. How the Golgi works: A cisternal progenitor model. *Proceedings of the National Academy of Science*. 107:19614–19618.
- Pipaliya, S.V., A. Schlacht, C.M. Klinger, R.A. Kahn, and J.B. Dacks. 2019. Ancient complement and lineage-specific evolution of the Sec7 ARF GEF proteins in eukaryotes. *Molecular Biology of the Cell*. 30:1846–1863.
- Pocognoni, C.A., E.G. Viktorova, J. Wright, J.M. Meissner, G. Sager, E. Lee, G.A. Belov, and E. Sztul. 2017. Highly conserved motifs within the large Sec7 ARF guanine nucleotide exchange factor GBF1 target it to the Golgi and are critical for GBF1 activity. *American Journal of Physiology Cell Physiology*. 314:675-689.
- Popoff, V., F. Adolf, B. Brügger, and F. Wieland. 2011. COPI Budding within the Golgi Stack. *Cold Spring Harbor Perspectives in Biology*. 3:a005231.
- Presley, J.F., T.H. Ward, A.C. Pfeifer, E.D. Siggia, R.D. Phair, and J. Lippincott-Schwartz. 2002. Dissection of COPI and Arf1 dynamics in vivo and role in Golgi membrane transport. *Nature*. 417:187-193.
- Pylypenko, O., H. Hammich, I.-M. Yu, and A. Houdusse. 2017. Rab GTPases and their interacting protein partners: Structural insights into Rab functional diversity. *Small GTPases*. 9:22-48.

- Quilty, D., G. Fraser, N. Summerfeldt, D. Cassel, and P. Melançon. 2014. Arf activation at the Golgi is modulated by feed-forward stimulation of the exchange factor GBF1. *Journal of Cell Science*. 127:354-364.
- Quilty, D. 2016. A molecular mechanism for GBF1 recruitment to cis-Golgi membranes. In Department of Cell Biology. Vol. Doctor of Philosophy. University of Alberta, Edmonton, Alberta, Canada. 174.
- Quilty, D., C.J. Chan, Y. Katherine, A. Bain, G. Babolmorad, and P. Melançon. 2019. The Arf-GDP-regulated recruitment of GBF1 to Golgi membranes requires domains HDS1 and HDS2 and a Golgi-localized protein receptor. *Journal of Cell Science*. 132.
- Rabouille, C., and V. Kondylis. 2007. Golgi ribbon unlinking: an organelle-based G2/M checkpoint. *Cell Cycle* 6:2723-2729.
- Ramaen, O., A. Joubert, P. Simister, N. Belgareh-Touzé, M.C. Olivares-Sanchez, J.-C. Zeeh, S. Chantalat, M.-P. Golinelli-Cohen, C.L. Jackson, V. Biou, and J. Cherfils. 2007. Interactions between conserved domains within homodimers in the BIG1, BIG2, and GBF1 Arf guanine nucleotide exchange factors. *Journal of Biological Chemistry*. 282:28834-28842.
- Renault, L., B. Guibert, and J. Cherfils. 2003. Structural snapshots of the mechanism and inhibition of a guanine nucleotide exchange factor. *Nature*. 426:525-530.
- Roux, K.J., D.I. Kim, and B. Burke. 2013. BioID: a screen for protein-protein interactions. *Current Protocols in Protein Science*. 74:19-23.
- Saenz, J.B., W.J. Sun, J.W. Chang, J. Li, B. Bursulaya, N.S. Gray, and D.B. Haslam. 2012. Golgicide A reveals essential roles for GBF1 in Golgi assembly and function. *Nature Chemical Biology*. 5:157-165.
- Sasaki, K., and H. Yoshida. 2015. Organelle autoregulation-stress responses in the ER, Golgi, mitochondria and lysosome. *Journal of Biochemistry*. 157:185-195.
- Sathe, M., G. Muthkrihnan, J. Rae, A. Disanza, M. Thattai, G. Scita, R.G. Parton, and S. Mayor. 2018. Small GTPases and BAR domain proteins regulate branched actin polymerisation for clathrin and dynamin-independent endocytosis. *Nature Communications*. 9:1835.
- Schlacht, A., K. Mowbrey, M. Elias, R.A. Kahn, and J.B. Dacks. 2013. Ancient Complexity, Opisthokont Plasticity, and Discovery of the 11th Subfamily of Arf GAP Proteins. *Traffic*. 14:636-649.
- Schweizer, A., J.A. Fransen, T. Bächli, L. Ginsel, and H.-P. Hauri. 1988. Identification, by a monoclonal antibody, of a 53-kD protein associated with a tubulo-vesicular compartment at the cis-side of the Golgi apparatus. *Journal of Cell Biology*. 107:1643-1653.
- Segev, N., J. Mulholland, and D. Botstein. 1988. The yeast GTP-binding YPT1 protein and a mammalian counterpart are associated with the secretion machinery. *Cell*. 52:915-924.
- Shi, W., F. Wang, M. Gao, Y. Yang, Z. Du, C. Wang, Y. Yao, K. He, X. Chen, and A. Hao. 2015. ZDHHC17 promotes axon outgrowth by regulating TrkA-tubulin complex formation. *Molecular and Cellular Neuroscience*. 68:194-202.
- Shiba, Y., S. Kametaka, S. Waguri, J.F. Presley, and P.A. Randazzo. 2013. ArfGAP3 regulates the transport of cation-independent mannose 6-phosphate receptor in the post-Golgi compartment. *Current Biology*. 23:1945-1951.

- Shinotsuka, C., S. Waguri, M. Wakasugi, Y. Uchiyama, and K. Nakayama. 2002. Dominant-negative mutant of BIG2, an ARF-guanine nucleotide exchange factor, specifically affects membrane trafficking from the trans-Golgi network through inhibiting membrane association of AP-1 and GGA coat proteins. *Biochemical and Biophysical Research Communications*. 294.
- Shorter, J., M.B. Beard, J. Seemann, B. Dirac-Svejstrup, and G. Warren. 2002. Sequential tethering of Golgins and catalysis of SNAREpin assembly by the vesicle-tethering protein p115. *Journal of Cell Biology*. 157:45-62.
- Slavin, I., I.A. García, P. Monetta, H.A. Martinez, N. Romero, and C. Alvarez. 2011. Role of Rab1b in COPII dynamics and function. *European Journal of Cell Biology*. 90:301-311.
- Sonnichsen, B., M. Lowe, E. Levine, B. Jamsa, B. Dirac-Svejstrup, and G. Warren. 1998. A role for giantin in docking COPI vesicles to Golgi membranes. *Journal of Cell Biology*. 140:1013-1021.
- Spiro, M.J., and R.G. Spiro. 2001. Release of polymannose oligosaccharides from vesicular stomatitis virus G protein during endoplasmic reticulum-associated degradation. *Glycobiology*. 11:803-811.
- Stephens, D.J., and R. Pepperkok. 2001. Illuminating the secretory pathway: when do we need vesicles? *Journal of Cell Science*. 114:1053-1059
- Suga, K., H. Hattori, A. Saito, and K. Akagawa. 2005. RNA interference-mediated silencing of the syntaxin 5 gene induces Golgi fragmentation but capable of transporting vesicles. *FEBS Letters*. 579:4226-4234.
- Suzuki, T., K. Ishihara, H. Migaki, K. Ishihara, M. Nagao, Y. Yamaguchi-Iwai, and T. Kambe. 2005. Two Different Zinc Transport Complexes of Cation Diffusion Facilitator Proteins Localized in the Secretory Pathway Operate to Activate Alkaline Phosphatases in Vertebrate Cells. *Journal of Biological Chemistry*. 280:30956-30962.
- Sztul, E., P.-W. Chen, J.E. Casanova, J. Cherfils, J.B. Dacks, D.G. Lambright, F.-J.S. Lee, P.A. Randazzo, L.C. Santy, A. Schürmann, I. Wilhelmi, M.E. Yohe, and R.A. Kahn. 2019. ARF GTPases and their GEFs and GAPs: concepts and challenges. *Molecular Biology of the Cell*. 30:1249–1271.
- Sztul, E., and R. García-Mata. 2003. The membrane-tethering protein p115 interacts with GBF1, an ARF guanine-nucleotide-exchange factor. *EMBO Reports*. 4:320-325.
- Sztul, E., and V. Lupashin. 2009. Role of vesicle tethering factors in the ER-Golgi membrane traffic. *FEBS Letters*. 583:33770-33783.
- Szul, T., R. García-Mata, E. Brandon, S. Shestopal, C. Alvarez, and E. Sztul. 2005. Dissection of Membrane Dynamics of the ARF-Guanine Nucleotide Exchange Factor GBF1. *Traffic*. 6:374-385.
- Szul, T., R. Grabski, S. Lyons, Y. Morohashi, S. Svetlana, M. Lowe, and E. Sztul. 2007. Dissecting the role of the ARF guanine nucleotide exchange factor GBF1 in Golgi biogenesis and protein trafficking. *Journal of Cell Science*. 120:3929-3940.
- Szul, T., and E. Sztul. 2011. COPII and COPI Traffic at the ER-Golgi Interface. *Physiology*. 26:348-364.
- Teo, G., G. Liu, J. Zhang, A.I. Nesvizhskii, A.C. Gingras, and H. Choi. 2014. SAINTexpress: improvements and additional features in Significance Analysis of INTERactome software. *Journal of Proteomics*. 100.

- Tie, H.C., A. Ludwig, S. Sandin, and L. Lu. 2018. The spatial separation of processing and transport functions to the interior and periphery of the Golgi stack. *eLife*. 7:e41301.
- Ting-Kuang, N., A.C. Pfeifer, J. Lippincott-Schwartz, and C.L. Jackson. 2005. Dynamics of GBF1, a Brefeldin A-sensitive Arf1 exchange factor at the Golgi. *Molecular Biology of the Cell*. 16:1213-1222.
- Trinkle-Mulcahy, L. 2019. Recent advances in proximity based labeling methods for interactome mapping. *F1000 Research*. 8:10.12688/f1000research.16903.12681.
- Trucco, A., R. Polishchuk, O. Martella, A.D. Pentima, A. Fusella, D.D. Giandomenico, E.S. Pietro, G.V. Beznoussenko, E.V. Polishchuk, M. Baldassarre, R. Buccione, W.J.C. Geerts, A.J. Koster, K.N.J. Burger, A.A. Mironov, and A. Luini. 2004. Secretory traffic triggers the formation of tubular continuities across Golgi sub-compartments. *Nature Cell Biology*. 6:1071-1081.
- Velasco, A., L. Hendricks, K.W. Moremen, D.R. Tulsiani, O. Touster, and M.G. Farquhar. 1993. Cell type-dependent variations in the subcellular distribution of alpha-mannosidase I and II. *Journal of Cell Biology*. 122:39-51.
- Volpicelli-Daley, L.A., Y. Li, C.J. Zhang, and R.A. Kahn. 2005. Isoform-selective effects of the depletion of ADP-ribosylation factors 1-5 on membrane traffic. *Molecular Biology of the Cell*. 16:4495-4508.
- Walch, L., E. Pellier, W. Leng, G. Lakisic, A. Gautreau, V. Contremoulins, J.-M. Verbavatz, and C.L. Jackson. 2018. GBF1 and Arf1 interact with Miro and regulate mitochondrial positioning within cells. *Scientific Reports*. 8.
- Waters, M.G., T. Serafini, and J.E. Rothman. 1991. 'Coatomer': a cytosolic protein complex containing subunits of non-clathrin-coated Golgi transport vesicles. *Nature*. 349:248-251.
- Wei, J.H., and J. Seemann. 2010. Unraveling the Golgi ribbon. *Traffic*. 11:1391-1400.
- Wessels, E., D. Duijings, K.H.W. Lanke, W.L.G. Melchers, C.L. Jackson, and F.J.M.v. Kuppeveld. 2007. Molecular determinants of the interaction between coxsackievirus protein 3A and guanine nucleotide exchange factor GBF1. *Journal of Virology*. 81:5238-5245.
- Wilfling, F., A.R. Thiam, M.-J. Olarte, J. Wang, R. Beck, T.J. Gould, E.S. Allgeyer, F. Pincet, and J. Bewersdorf. 2014. Arf1/COPI machinery acts directly on lipid droplets and enables their connection to the ER for protein targeting. *eLife*. 3:e01607.
- Williams, S.C., and J. Parsons. 2018. NTH1 is a new target for ubiquitylation-dependent regulation by TRIM26 required for the cellular response to oxidative stress. *Molecular and Cellular Biology*. 38:e00616-00617.
- Wong, K.A., and J.P. O'Bryan. 2011. Bimolecular Fluorescence Complementation. *Journal of Visualized Experiments*. 50:2643.
- Wright, J., R.A. Kahn, and E. Sztul. 2014. Regulating the large Sec7 ARF guanine nucleotide exchange factors: the when, where and how of activation. *Cellular and Molecular Life Sciences*. 71:3419-3438.
- Xu, D., and J.C. Hay. 2004. Reconstitution of COPII vesicle fusion to generate a pre-Golgi intermediate compartment. *Journal of Cell Biology*. 167:997-1003.
- Yamamoto, H., S. Kakuta, T.M. Watanabe, A. Kitamura, T. Sekito, C. Kondo-Kakuta, R. Ichikawa, M. Kinjo, and Y. Ohsumi. 2012. Atg9 vesicles are an important

- membrane source during early steps of autophagosome formation. *Journal of Cell Biology*. 198:219-233.
- Yamasaki, A., S. Menon, S. Yu, J. Barrowman, T. Meerloo, V. Oorschot, J. Klumperman, A. Satoh, and S. Ferronovick. 2009. mTrs130 is a component of a mammalian TRAPP II complex, a Rab1 GEF that binds to COPI-coated vesicles. *Molecular Biology of the Cell*. 20:4205-4215.
- Yan, J.P., M.E. Colon, L.A. Beebe, and P. Melançon. 1994. Isolation and Characterization of Mutant CHO Cell Lines with Compartment-specific Resistance to Brefeldin A. *Journal of Cell Biology*. 126:65-75.
- Yang, J.-S., S.Y. Lee, M. Gao, S. Bourgoïn, P.A. Randazzo, R.T. Premont, and V.W. Hsu. 2002. ARFGAP1 promotes the formation of COPI vesicles, suggesting function as a component of the coat. *Journal of Cell Biology*. 159:69-78.
- Yano, H., I. Kobayashi, Y. Onodera, F. Luton, M. Franco, Y. Mazaki, S. Hashimoto, K. Iwai, Z. Ronai, and H. Sabe. 2008. Fbx8 makes Arf6 refractory to function via ubiquitination. *Molecular Biology of the Cell*. 19:822-832.
- Zhao, L., J.B. Helms, B. Brugger, C. Harter, B. Martoglio, R. Graf, J. Brunner, and F.T. Wieland. 1997. Direct and GTP-dependent interaction of ADP ribosylation factor 1 with coatamer subunit beta. *Proceedings of the National Academy of Science*. 94:4418-4423.
- Zhao, L., J.B. Helms, J. Brunner, and F.T. Wieland. 1999. GTP-dependent binding of ADP-ribosylation factor to coatamer in close proximity to the binding site for dilysine retrieval motifs and p2. *Journal of Biological Chemistry*. 274:14198-14203.
- Zhao, X., A. Claude, J. Chun, D.J. Shields, J.F. Presley, and P. Melançon. 2006. GBF1, a cis-Golgi and VTCs-localized ARF-GEF, is implicated in ER-to-Golgi protein traffic. *Journal of Cell Science*. 119.
- Zhao, X., T.K. Lasell, and P. Melançon. 2002. Localization of large ADP-ribosylation factor-guanine nucleotide exchange factors to different Golgi compartments: evidence for distinct functions in protein traffic. *Molecular Biology of the Cell*. 13:119-133.
- Zolov, S.N., D. Bridges, Y. Zhang, W.-W. Lee, E. Riehle, R. Verma, G.M. Lenk, K. Converso-Baran, T. Weide, R.L. Albin, A.R. Saltiel, M.H. Meisler, M.W. Russell, and L.S. Weisman. 2012. In vivo, PIKfyve generates PI(3,5)P₂, which serves as both a signaling lipid and the major precursor for PI5P. *Proceedings of the National Academy of Science*. 109:17472-17477.
- Zuber, C., J.Y. Fan, B. Guhl, A. Parodi, J.H. Fessler, C. Parker, and J. Roth. 2001. Immunolocalization of UDP-glucose:glycoprotein glucosyltransferase indicates involvement of pre-Golgi intermediates in protein quality control. *Proceedings of the National Academy of Science*. 98:10710-10715.

Appendix

9.1 Total peptide counts and associated Bayesian false discovery rates for proteins identified from whole cell lysates

Gene Symbol	Gene Name	WCL FlagBirA-Only Controls					WCL FlagBirA-GBF1					BFDR
		A1	A2	B1	B2	Total	A1	A2	B1	B2	Total	
GBF1	<i>golgi brefeldin A resistant guanine nucleotide exchange factor 1</i>	0	0	0	0	0	1412	1283	1299	1332	5326	na
birA	<i>E. coli biotin carboxylase</i>	133	115	116	116	480	1403	1376	1346	1636	5761	0
AHNAK	<i>AHNAK nucleoprotein</i>	118	110	35	30	293	876	773	730	676	3055	0
FASN	<i>fatty acid synthase</i>	98	90	55	54	297	494	451	574	614	2133	0
FLNB	<i>filamin B</i>	21	19	11	8	59	99	78	96	82	355	0
WARS	<i>tryptophanyl-tRNA synthetase</i>	14	6	10	9	39	29	28	28	39	124	0
KIF5B	<i>kinesin family member 5B</i>	10	11	8	8	37	39	31	34	32	136	0
CTTN	<i>cortactin</i>	9	8	5	2	24	61	67	60	48	236	0
RANBP2	<i>RAN binding protein 2</i>	9	9	6	7	31	55	49	42	46	192	0
MYH9	<i>myosin heavy chain 9</i>	8	7	2	2	19	44	31	28	31	134	0
MKL2	<i>myocardin related transcription factor B</i>	8	7	0	2	17	88	73	74	64	299	0
EIF4G1	<i>eukaryotic translation initiation factor 4 gamma 1</i>	7	9	9	5	30	41	29	38	39	147	0
TAGLN2	<i>transgelin 2</i>	7	5	2	2	16	42	31	29	29	131	0
RANGAP1	<i>Ran GTPase activating protein 1</i>	6	6	5	4	21	49	44	34	51	178	0
EIF5	<i>eukaryotic translation initiation factor 5</i>	6	7	0	2	15	26	31	32	22	111	0
COPG2	<i>coatamer protein complex subunit gamma 2</i>	6	3	2	0	11	16	17	21	20	74	0
ZBTB33	<i>zinc finger and BTB domain containing 33</i>	5	5	0	0	10	17	21	24	22	84	0
CAPZA1	<i>capping actin protein of muscle Z-line subunit alpha 1</i>	5	0	0	0	5	28	31	24	18	101	0
LARP1	<i>La ribonucleoprotein domain family member 1</i>	4	6	5	6	21	39	28	26	30	123	0
CORO1B	<i>coronin 1B</i>	4	5	0	0	9	90	79	79	114	362	0
DCTN1	<i>dynactin subunit 1</i>	4	0	5	5	14	12	14	13	23	62	0
GCN1L1	<i>GCN1 activator of EIF2AK4</i>	4	8	9	11	32	86	77	55	92	310	0
PAICS	<i>phosphoribosylaminoimidazole</i>	3	0	3	0	6	28	29	31	22	110	0

	<i>carboxylase and phosphoribosylaminoimidazolesuccinocarboxamide synthase tripartite motif family like 2</i>											
TRIML2		3	0	0	0	3	8	9	8	9	34	0
SEPT9	<i>septin9</i>	3	0	0	0	3	13	11	10	11	45	0
YWHAZ	<i>tyrosine 3-monooxygenase/tryptophan 5-monooxygenase activation protein zeta</i>	2	0	0	0	2	6	8	8	9	31	0
HDLBP	<i>high density lipoprotein binding protein</i>	2	3	5	2	12	35	32	27	30	124	0
CALD1	<i>caldesmon 1</i>	2	2	0	0	4	35	39	19	33	126	0
PSMA7	<i>proteasome subunit alpha 7</i>	2	0	4	3	9	9	10	7	12	38	0
CNN2	<i>calponin 2</i>	2	4	2	2	10	10	11	8	15	44	0
USP14	<i>ubiquitin specific peptidase 14</i>	2	0	2	2	6	7	8	9	7	31	0
ZC3HAV1	<i>zinc finger CCCH-type containing, antiviral 1</i>	2	0	2	0	4	11	6	5	8	30	0
EIF4G2	<i>eukaryotic translation initiation factor 4 gamma 2</i>	2	0	0	0	2	45	45	30	29	149	0
KPNA2	<i>karyopherin subunit alpha 2</i>	2	0	0	3	5	6	9	12	9	36	0
TLN1	<i>talin 1</i>	0	5	0	0	5	85	77	72	80	314	0
RPL7L1	<i>ribosomal protein L7 like 1</i>	0	2	0	3	5	11	10	16	12	49	0
BAG3	<i>BCL2 associated athanogene 3</i>	0	2	2	0	4	7	5	14	12	38	0
USO1	<i>USO1 vesicle transport factor</i>	0	2	0	0	2	32	33	22	41	128	0
STAT3	<i>signal transducer and activator of transcription 3</i>	0	0	3	0	3	38	28	37	44	147	0
LRBA	<i>LPS responsive beige-like anchor protein</i>	0	0	3	0	3	15	11	6	8	40	0
KIF11	<i>kinesin family member 11</i>	0	0	3	3	6	7	6	10	13	36	0
HSPH1	<i>heat shock protein family H (Hsp110) member 1</i>	0	0	2	0	2	4	6	3	10	23	0
YTHDC2	<i>YTH domain containing 2</i>	0	0	2	3	5	11	5	8	13	37	0
SEPT2	<i>septin2</i>	0	0	2	0	2	27	21	18	29	95	0
TWF1	<i>twinfilin actin binding protein 1</i>	0	0	0	3	3	5	4	10	9	28	0
NUDC	<i>nuclear distribution C, dynein complex regulator</i>	0	0	0	2	2	11	11	15	11	48	0
PSMD5	<i>proteasome 26S subunit, non-ATPase 5</i>	0	0	0	2	2	10	5	12	10	37	0

CLINT1	<i>clathrin interactor 1</i>	0	0	0	2	2	22	20	16	15	73	0
TPR	<i>translocated promoter region, nuclear basket protein</i>	0	0	0	0	0	69	51	72	68	260	0
ATG2B	<i>autophagy related 2B</i>	0	0	0	0	0	62	50	47	59	218	0
CKAP5	<i>cytoskeleton associated protein 5</i>	0	0	0	0	0	54	48	36	36	174	0
MRE11A	<i>MRE11 homolog, double strand break repair nuclease</i>	0	0	0	0	0	45	35	44	44	168	0
CD2AP	<i>CD2 associated protein</i>	0	0	0	0	0	44	51	50	58	203	0
USP15	<i>ubiquitin specific peptidase 15</i>	0	0	0	0	0	43	49	39	41	172	0
SLC30A6	<i>solute carrier family 30 member 6</i>	0	0	0	0	0	43	42	36	37	158	0
TUBA1C	<i>tubulin alpha 1c</i>	0	0	0	0	0	38	42	39	37	156	0
AHNAK2	<i>AHNAK nucleoprotein 2</i>	0	0	0	0	0	38	31	35	49	153	0
XRN1	<i>5'-3' exoribonuclease 1</i>	0	0	0	0	0	33	20	22	28	103	0
LIMCH1	<i>LIM and calponin homology domains 1</i>	0	0	0	0	0	31	28	23	24	106	0
SLK	<i>STE20 like kinase</i>	0	0	0	0	0	30	30	25	26	111	0
TJP1	<i>tight junction protein 1</i>	0	0	0	0	0	28	21	30	29	108	0
SRP68	<i>signal recognition particle 68</i>	0	0	0	0	0	26	24	21	28	99	0
PLA2G4A	<i>phospholipase A2 group IVA</i>	0	0	0	0	0	25	24	20	17	86	0
LIMA1	<i>LIM domain and actin binding 1</i>	0	0	0	0	0	25	24	21	36	106	0
CRKL	<i>CRK like proto-oncogene, adaptor protein</i>	0	0	0	0	0	23	21	12	17	73	0
CSDE1	<i>cold shock domain containing E1</i>	0	0	0	0	0	23	24	21	18	86	0
SLC30A5	<i>solute carrier family 30 member 5</i>	0	0	0	0	0	22	21	26	26	95	0
CORO1C	<i>coronin 1C</i>	0	0	0	0	0	22	21	19	25	87	0
PLIN3	<i>perilipin 3</i>	0	0	0	0	0	21	18	24	24	87	0
GAPVD1	<i>GTPase activating protein and VPS9 domains 1</i>	0	0	0	0	0	21	16	19	18	74	0
GIGYF2	<i>GRB10 interacting GYF protein 2</i>	0	0	0	0	0	21	17	17	19	74	0
CRK	<i>CRK proto-oncogene, adaptor protein</i>	0	0	0	0	0	21	18	16	17	72	0
FERMT2	<i>fermitin family member 2</i>	0	0	0	0	0	19	19	18	24	80	0
PUF60	<i>poly(U) binding splicing factor 60</i>	0	0	0	0	0	18	19	13	22	72	0
UNC45A	<i>unc-45 myosin chaperone A</i>	0	0	0	0	0	18	20	19	17	74	0

SNX1	<i>sorting nexin 1</i>	0	0	0	0	0	18	18	13	12	61	0
WDR11	<i>WD repeat domain 11</i>	0	0	0	0	0	18	23	19	21	81	0
RAPH1	<i>Ras association (RalGDS/AF-6) and pleckstrin homology domains 1</i>	0	0	0	0	0	18	22	16	18	74	0
TANC1	<i>tetratricopeptide repeat, ankyrin repeat and coiled-coil containing 1</i>	0	0	0	0	0	17	9	7	10	43	0
PDE1A	<i>phosphodiesterase 1A</i>	0	0	0	0	0	17	20	15	16	68	0
TXNL1	<i>thioredoxin like 1</i>	0	0	0	0	0	16	11	6	19	52	0
RPS27L	<i>ribosomal protein S27 like</i>	0	0	0	0	0	15	17	3	12	47	0
WIPI2	<i>WD repeat domain, phosphoinositide interacting 2</i>	0	0	0	0	0	15	11	10	18	54	0
TIPRL	<i>TOR signaling pathway regulator</i>	0	0	0	0	0	15	10	18	16	59	0
EIF4B	<i>eukaryotic translation initiation factor 4B</i>	0	0	0	0	0	15	19	16	28	78	0
ZYX	<i>zyxin</i>	0	0	0	0	0	14	9	8	7	38	0
DBT	<i>dihydroipoamide branched chain transacylase E2</i>	0	0	0	0	0	14	10	11	9	44	0
VCL	<i>vinculin</i>	0	0	0	0	0	13	13	12	15	53	0
FAM91A1	<i>family with sequence similarity 91 member A1</i>	0	0	0	0	0	13	15	8	9	45	0
DAB2	<i>DAB adaptor protein 2</i>	0	0	0	0	0	13	10	11	11	45	0
DBNL	<i>drebrin like</i>	0	0	0	0	0	13	10	10	12	45	0
C17orf81	<i>elongator acetyltransferase complex subunit 5</i>	0	0	0	0	0	13	11	11	6	41	0
GOLGA3	<i>golgin A3</i>	0	0	0	0	0	13	11	8	13	45	0
EPS15L1	<i>epidermal growth factor receptor pathway substrate 15 like 1</i>	0	0	0	0	0	12	10	11	14	47	0
KLC1	<i>kinesin light chain 1</i>	0	0	0	0	0	12	13	8	11	44	0
DLG5	<i>discs large MAGUK scaffold protein 5</i>	0	0	0	0	0	12	8	2	4	26	0
ERC1	<i>ELKS/RAB6-interacting/CAST family member 1</i>	0	0	0	0	0	12	10	8	6	36	0
PDLIM5	<i>PDZ and LIM domain 5</i>	0	0	0	0	0	12	11	8	7	38	0
GEMIN5	<i>gem nuclear organelle associated protein 5</i>	0	0	0	0	0	12	10	15	23	60	0
XIAP	<i>X-linked inhibitor of apoptosis</i>	0	0	0	0	0	11	12	5	13	41	0
SQSTM1	<i>sequestosome 1</i>	0	0	0	0	0	11	6	6	6	29	0

TTK	<i>TTK protein kinase</i>	0	0	0	0	0	11	16	12	13	52	0
NUP133	<i>nucleoporin 133</i>	0	0	0	0	0	11	10	5	9	35	0
GOLGA2	<i>golgin A2</i>	0	0	0	0	0	11	12	10	6	39	0
KIAA1524	<i>cell proliferation regulating inhibitor of protein phosphatase 2A</i>	0	0	0	0	0	11	10	3	4	28	0
KANK2	<i>KN motif and ankyrin repeat domains 2</i>	0	0	0	0	0	11	9	6	5	31	0
MYOF	<i>myoferlin</i>	0	0	0	0	0	11	8	6	6	31	0
EIF4E2	<i>eukaryotic translation initiation factor 4E family member 2</i>	0	0	0	0	0	10	8	4	6	28	0
KIAA1598	<i>shootin 1</i>	0	0	0	0	0	10	6	4	8	28	0
ACTN4	<i>actinin alpha 4</i>	0	0	0	0	0	10	6	10	16	42	0
EIF3A	<i>eukaryotic translation initiation factor 3 subunit A</i>	0	0	0	0	0	10	9	10	11	40	0
ARFGAP1	<i>ADP ribosylation factor GTPase activating protein 1</i>	0	0	0	0	0	10	14	12	12	48	0
PDAP1	<i>PDGFA associated protein 1</i>	0	0	0	0	0	9	7	10	14	40	0
DVL3	<i>dishevelled segment polarity protein 3</i>	0	0	0	0	0	9	13	11	16	49	0
VCPIP1	<i>valosin containing protein interacting protein 1</i>	0	0	0	0	0	9	8	6	7	30	0
ARHGEF16	<i>Rho guanine nucleotide exchange factor 16</i>	0	0	0	0	0	9	2	5	9	25	0
PLS3	<i>plastin 3</i>	0	0	0	0	0	9	6	4	2	21	0
STK38	<i>serine/threonine kinase 38</i>	0	0	0	0	0	9	9	7	8	33	0
DIAPH3	<i>diaphanous related formin 3</i>	0	0	0	0	0	9	6	11	13	39	0
IPO9	<i>importin 9</i>	0	0	0	0	0	9	10	6	7	32	0
SPG20	<i>spartin</i>	0	0	0	0	0	9	5	5	7	26	0
GTF3C5	<i>general transcription factor IIIC subunit 5</i>	0	0	0	0	0	8	4	10	9	31	0
ELP4	<i>elongator acetyltransferase complex subunit 4</i>	0	0	0	0	0	8	8	8	22	46	0
UBB	<i>ubiquitin B</i>	0	0	0	0	0	8	10	9	9	36	0
ASCC3	<i>activating signal cointegrator 1 complex subunit 3</i>	0	0	0	0	0	8	4	10	10	32	0
SEPT7	<i>septin7</i>	0	0	0	0	0	8	8	6	11	33	0
ANKRD17	<i>ankyrin repeat domain 17</i>	0	0	0	0	0	8	6	12	21	47	0

PSMD12	<i>proteasome 26S subunit, non-ATPase 12</i>	0	0	0	0	0	8	5	5	12	30	0
DFNA5	<i>gasdermin E</i>	0	0	0	0	0	8	4	7	9	28	0
RANBP3	<i>RAN binding protein 3</i>	0	0	0	0	0	8	9	5	6	28	0
YWHAE	<i>tyrosine 3-monooxygenase/tryptophan 5-monooxygenase activation protein epsilon</i>	0	0	0	0	0	7	10	9	10	36	0
CCDC25	<i>coiled-coil domain containing 25</i>	0	0	0	0	0	7	6	6	7	26	0
HAUS6	<i>HAUS augmin like complex subunit 6</i>	0	0	0	0	0	7	8	9	8	32	0
TBC1D15	<i>TBC1 domain family member 15</i>	0	0	0	0	0	7	10	6	4	27	0
MYPN	<i>myopalladin</i>	0	0	0	0	0	7	3	5	8	23	0
PDCD5	<i>programmed cell death 5</i>	0	0	0	0	0	7	6	4	5	22	0
MAP7D3	<i>MAP7 domain containing 3</i>	0	0	0	0	0	6	8	6	8	28	0
SH3GL1	<i>SH3 domain containing GRB2 like 1, endophilin A2</i>	0	0	0	0	0	6	6	5	3	20	0
RPL18A	<i>ribosomal protein L18a</i>	0	0	0	0	0	6	5	7	3	21	0
EFHD2	<i>EF-hand domain family member D2</i>	0	0	0	0	0	6	6	9	7	28	0
SEPT11	<i>septin11</i>	0	0	0	0	0	6	3	3	4	16	0
YWHAG	<i>tyrosine 3-monooxygenase/tryptophan 5-monooxygenase activation protein gamma</i>	0	0	0	0	0	6	3	4	3	16	0
KIF15	<i>kinesin family member 15</i>	0	0	0	0	0	6	9	4	6	25	0
DSG2	<i>desmoglein 2</i>	0	0	0	0	0	6	7	4	9	26	0
CAP1	<i>cyclase associated actin cytoskeleton regulatory protein 1</i>	0	0	0	0	0	6	4	6	11	27	0
DENND4C	<i>DENN domain containing 4C</i>	0	0	0	0	0	6	4	4	7	21	0
SEC23IP	<i>SEC23 interacting protein</i>	0	0	0	0	0	6	3	8	4	21	0
CACYBP	<i>calcyclin binding protein</i>	0	0	0	0	0	6	4	8	10	28	0
C11orf49	<i>chromosome 11 open reading frame 49</i>	0	0	0	0	0	6	9	7	7	29	0
C3orf75	<i>elongator acetyltransferase complex subunit 6</i>	0	0	0	0	0	6	11	11	10	38	0
NACA	<i>nascent polypeptide associated complex subunit alpha</i>	0	0	0	0	0	5	9	10	12	36	0

PRRC2C	<i>proline rich coiled-coil 2C</i>	0	0	0	0	0	5	3	5	7	20	0
CTNND1	<i>catenin delta 1</i>	0	0	0	0	0	5	7	2	6	20	0
TARS	<i>threonyl-tRNA synthetase</i>	0	0	0	0	0	5	4	5	3	17	0
ARHGAP35	<i>Rho GTPase activating protein 35</i>	0	0	0	0	0	5	5	3	10	23	0
DCTN2	<i>dynactin subunit 2</i>	0	0	0	0	0	5	5	9	10	29	0
TTC28	<i>tetratricopeptide repeat domain 28</i>	0	0	0	0	0	5	5	6	7	23	0
SHC1	<i>SHC adaptor protein 1</i>	0	0	0	0	0	5	4	5	8	22	0
AAK1	<i>AP2 associated kinase 1</i>	0	0	0	0	0	5	3	4	5	17	0
EZR	<i>ezrin</i>	0	0	0	0	0	5	6	8	7	26	0
DHX29	<i>DExH-box helicase 29</i>	0	0	0	0	0	5	5	3	5	18	0
DVL2	<i>dishevelled segment polarity protein 2</i>	0	0	0	0	0	5	15	7	4	31	0
NCKAP1	<i>NCK associated protein 1</i>	0	0	0	0	0	5	6	5	4	20	0
WDR45	<i>WD repeat domain 45</i>	0	0	0	0	0	5	5	3	3	16	0
SWAP70	<i>switching B cell complex subunit SWAP70</i>	0	0	0	0	0	5	7	9	7	28	0
HN1L	<i>Jupiter microtubule associated homolog 2</i>	0	0	0	0	0	4	2	4	3	13	0
SNX2	<i>sorting nexin 2</i>	0	0	0	0	0	4	2	3	7	16	0
UBAP2	<i>ubiquitin associated protein 2</i>	0	0	0	0	0	4	3	4	6	17	0
PIKFYVE	<i>phosphoinositide kinase, FYVE-type zinc finger containing</i>	0	0	0	0	0	4	5	4	5	18	0
JUP	<i>junction plakoglobin</i>	0	0	0	0	0	4	3	2	3	12	0
BRAP	<i>BRCA1 associated protein</i>	0	0	0	0	0	4	7	8	8	27	0
KIAA0368	<i>Ecm29 proteasome adaptor and scaffold</i>	0	0	0	0	0	4	2	3	4	13	0
PATL1	<i>PAT1 homolog 1, processing body mRNA decay factor</i>	0	0	0	0	0	4	3	3	4	14	0
DNMBP	<i>dynamamin binding protein</i>	0	0	0	0	0	4	4	5	3	16	0
SCYL2	<i>SCY1 like pseudokinase 2</i>	0	0	0	0	0	4	4	5	4	17	0
NUMBL	<i>NUMB like endocytic adaptor protein</i>	0	0	0	0	0	3	3	2	3	11	0
EPB41	<i>erythrocyte membrane protein band 4.1</i>	0	0	0	0	0	3	3	6	10	22	0
CHTOP	<i>chromatin target of PRMT1</i>	0	0	0	0	0	3	4	5	6	18	0

MB21D1	<i>cyclic GMP-AMP synthase</i>	0	0	0	0	0	3	3	2	3	11	0
GAK	<i>cyclin G associated kinase</i>	0	0	0	0	0	3	2	3	6	14	0
HN1	<i>Jupiter microtubule associated homolog 1</i>	0	0	0	0	0	3	5	8	10	26	0
ECD	<i>ecdysoneless cell cycle regulator</i>	0	0	0	0	0	3	3	4	4	14	0
PARVA	<i>parvin alpha</i>	0	0	0	0	0	3	4	4	4	15	0
GOLGA5	<i>golgin A5</i>	0	0	0	0	0	3	5	4	2	14	0
KLC2	<i>kinesin light chain 2</i>	0	0	0	0	0	3	5	3	6	17	0
FAM98A	<i>family with sequence similarity 98 member A</i>	0	0	0	0	0	3	3	2	2	10	0
EPB41L2	<i>erythrocyte membrane protein band 4.1 like 2</i>	0	0	0	0	0	3	3	4	9	19	0
PTPN11	<i>protein tyrosine phosphatase non-receptor type 11</i>	0	0	0	0	0	3	5	2	6	16	0
RPAP3	<i>RNA polymerase II associated protein 3</i>	0	0	0	0	0	3	4	7	4	18	0
TMCO7	<i>transport and golgi organization 6 homolog</i>	0	0	0	0	0	3	5	7	3	18	0
TPD52L2	<i>TPD52 like 2</i>	0	0	0	0	0	3	7	7	7	24	0
CDK6	<i>cyclin dependent kinase 6</i>	0	0	0	0	0	3	3	2	2	10	0
EIF3E	<i>eukaryotic translation initiation factor 3 subunit E</i>	0	0	0	0	0	2	5	4	3	14	0
ERBB2IP	<i>erb2 interacting protein</i>	0	0	0	0	0	2	3	2	4	11	0
SCFD1	<i>sec1 family domain containing 1</i>	0	0	0	0	0	2	2	3	6	13	0
PRMT1	<i>protein arginine methyltransferase 1</i>	0	0	0	0	0	2	3	4	3	12	0
PRMT7	<i>protein arginine methyltransferase 7</i>	0	0	0	0	0	2	3	4	2	11	0
ECHDC1	<i>ethylmalonyl-CoA decarboxylase 1</i>	0	0	0	0	0	2	4	5	10	21	0
IARS2	<i>isoleucyl-tRNA synthetase 2, mitochondrial</i>	0	0	0	0	0	2	3	2	3	10	0
CCT8	<i>chaperonin containing TCP1 subunit 8</i>	17	16	13	10	56	60	48	49	34	191	0.01
RPS11	<i>ribosomal protein S11</i>	8	7	8	5	28	22	21	22	17	82	0.01
IMPDH2	<i>inosine monophosphate dehydrogenase 2</i>	5	0	2	0	7	12	8	8	8	36	0.01
IPO7	<i>importin 7</i>	5	4	5	11	25	27	17	24	26	94	0.01
STRAP	<i>serine/threonine kinase receptor associated protein</i>	4	9	6	7	26	19	23	17	23	82	0.01

ACTA1	<i>actin alpha 1, skeletal muscle</i>	0	17	0	0	17	22	21	21	17	81	0.01
RPL35	<i>ribosomal protein L35</i>	0	3	0	2	5	8	5	7	5	25	0.01
GSPT1	<i>G1 to S phase transition 1</i>	0	3	0	0	3	7	2	4	8	21	0.01
PDLIM7	<i>PDZ and LIM domain 7</i>	0	0	4	0	4	6	5	10	12	33	0.01
ABCF3	<i>ATP binding cassette subfamily F member 3</i>	0	0	3	0	3	4	4	3	6	17	0.01
PRPF4	<i>pre-mRNA processing factor 4</i>	0	0	2	0	2	2	7	4	2	15	0.01
EIF3M	<i>eukaryotic translation initiation factor 3 subunit M</i>	0	0	0	5	5	7	5	7	12	31	0.01
PPME1	<i>protein phosphatase methylesterase 1</i>	0	0	0	5	5	8	7	8	8	31	0.01
NPM3	<i>nucleophosmin/nucleoplamin 3</i>	0	0	0	2	2	3	2	5	3	13	0.01
PRPF31	<i>pre-mRNA processing factor 31</i>	0	0	0	2	2	5	3	2	6	16	0.01
MAP4	<i>microtubule associated protein 4</i>	26	25	18	24	93	69	73	57	74	273	0.02
CXorf56	<i>chromosome X open reading frame 56</i>	0	0	0	0	0	8	7	5	0	20	0.02
STMN1	<i>stathmin 1</i>	0	0	0	0	0	8	5	0	5	18	0.02
MAPRE2	<i>microtubule associated protein RP/EB family member 2</i>	0	0	0	0	0	6	4	0	7	17	0.02
ARFIP2	<i>ADP ribosylation factor interacting protein 2</i>	0	0	0	0	0	5	0	4	6	15	0.02
DNAJC13	<i>DnaJ heat shock protein family (Hsp40) member C13</i>	0	0	0	0	0	5	5	0	6	16	0.02
SNRPF	<i>small nuclear ribonucleoprotein polypeptide F</i>	0	0	0	0	0	5	4	0	6	15	0.02
SH3PXD2	<i>SH3 and PX domains 2B</i>	0	0	0	0	0	4	0	6	5	15	0.02
B												
H2AFV	<i>H2A histone family member V</i>	0	0	0	0	0	0	7	6	5	18	0.02
SYAP1	<i>synapse associated protein 1</i>	0	0	0	0	0	0	7	5	10	22	0.02
BUB1B	<i>BUB1 mitotic checkpoint serine/threonine kinase B</i>	0	0	0	0	0	10	6	0	3	19	0.03
SEC24A	<i>SEC24 homolog A, COPII coat complex component</i>	0	0	0	0	0	6	0	4	4	14	0.03
PLEKHA5	<i>pleckstrin homology domain containing A5</i>	0	0	0	0	0	5	7	0	3	15	0.03
STAM	<i>signal transducing adaptor molecule</i>	0	0	0	0	0	5	0	4	5	14	0.03
VPS33B	<i>VPS33B late endosome and lysosome associated</i>	0	0	0	0	0	4	0	4	4	12	0.03

TK1	<i>thymidine kinase 1</i>	0	0	0	0	0	4	0	5	4	13	0.03
TRIP11	<i>thyroid hormone receptor interactor 11</i>	0	0	0	0	0	4	5	0	4	13	0.03
TP53BP2	<i>tumor protein p53 binding protein 2</i>	0	0	0	0	0	4	5	0	5	14	0.03
HINT1	<i>histidine triad nucleotide binding protein 1</i>	0	0	0	0	0	3	6	0	7	16	0.03
PDXDC1	<i>pyridoxal dependent decarboxylase domain containing 1</i>	0	0	0	0	0	0	7	3	8	18	0.03
SPAG9	<i>sperm associated antigen 9</i>	0	0	0	0	0	7	4	0	3	14	0.04
CEP170	<i>centrosomal protein 170</i>	0	0	0	0	0	5	4	3	0	12	0.04
PPP6R3	<i>protein phosphatase 6 regulatory subunit 3</i>	0	0	0	0	0	5	6	0	3	14	0.04
SKP2	<i>S-phase kinase associated protein 2</i>	0	0	0	0	0	5	0	3	6	14	0.04
LMAN1	<i>lectin, mannose binding 1</i>	0	0	0	0	0	4	0	3	6	13	0.04
SMARCA D1	<i>SWI/SNF-related, matrix-associated actin-dependent regulator of chromatin, subfamily a, containing DEAD/H box 1</i>	0	0	0	0	0	4	4	0	3	11	0.04
ANKS1A	<i>ankyrin repeat and sterile alpha motif domain containing 1A</i>	0	0	0	0	0	3	3	0	6	12	0.04
HSPA4	<i>heat shock protein family A (Hsp70) member 4</i>	0	0	0	0	0	3	0	4	9	16	0.04
AHCYL1	<i>adenosylhomocysteinase like 1</i>	0	0	0	0	0	3	0	3	5	11	0.04
PPP6C	<i>protein phosphatase 6 catalytic subunit</i>	0	0	0	0	0	0	4	4	3	11	0.04
DHX36	<i>DEAH-box helicase 36</i>	0	0	0	0	0	0	3	4	6	13	0.04
LUZP1	<i>leucine zipper protein 1</i>	0	0	0	0	0	6	0	5	2	13	0.05
IFIT5	<i>interferon induced protein with tetratricopeptide repeats 5</i>	0	0	0	0	0	6	9	2	0	17	0.05
PSMD11	<i>proteasome 26S subunit, non-ATPase 11</i>	0	0	0	0	0	4	3	3	0	10	0.05
GOLGB1	<i>golgin B1</i>	0	0	0	0	0	3	2	0	5	10	0.05
NFKB2	<i>nuclear factor kappa B subunit 2</i>	0	0	0	0	0	3	0	2	5	10	0.05
YWHAB	<i>tyrosine 3-monooxygenase/tryptophan 5-monooxygenase activation protein beta</i>	0	0	0	0	0	3	0	2	5	10	0.05
TRIP6	<i>thyroid hormone receptor interactor 6</i>	0	0	0	0	0	3	0	3	4	10	0.05

MAT2A	<i>methionine adenosyltransferase 2A</i>	0	0	0	0	0	3	0	2	4	9	0.05
DPYSL2	<i>dihydropyrimidinase like 2</i>	0	0	0	0	0	3	2	0	4	9	0.05
GOSR1	<i>golgi SNAP receptor complex member 1</i>	0	0	0	0	0	2	3	5	0	10	0.05
TMEM87A	<i>transmembrane protein 87A</i>	0	0	0	0	0	2	4	4	0	10	0.05
MYO1E	<i>myosin IE</i>	0	0	0	0	0	2	3	0	4	9	0.05
CIAPIN1	<i>cytokine induced apoptosis inhibitor 1</i>	0	0	0	0	0	2	4	4	0	10	0.05
TNKS1BP1	<i>tankyrase 1 binding protein 1</i>	0	0	0	0	0	0	3	2	4	9	0.05
KIAA1967	<i>cell cycle and apoptosis regulator 2</i>	0	0	0	0	0	0	2	4	3	9	0.05
DLGAP5	<i>DLG associated protein 5</i>	0	0	0	0	0	5	2	0	2	9	0.06
EHBP1	<i>EH domain binding protein 1</i>	0	0	0	0	0	4	2	0	2	8	0.06
SNRPN	<i>small nuclear ribonucleoprotein polypeptide N</i>	0	0	0	0	0	3	2	0	2	7	0.06
MGEA5	<i>O-GlcNAcase</i>	0	0	0	0	0	3	0	3	2	8	0.06
PTPN12	<i>protein tyrosine phosphatase non-receptor type 12</i>	0	0	0	0	0	2	0	3	2	7	0.06
PLK1	<i>polo like kinase 1</i>	0	0	0	0	0	2	0	3	3	8	0.06
KIF14	<i>kinesin family member 14</i>	0	0	0	0	0	2	0	2	5	9	0.06
COPS4	<i>COP9 signalosome subunit 4</i>	0	0	0	0	0	2	0	2	3	7	0.06
PSME3	<i>proteasome activator subunit 3</i>	0	0	0	0	0	0	2	2	4	8	0.06
CNOT1	<i>CCR4-NOT transcription complex subunit 1</i>	0	0	0	0	0	0	2	2	4	8	0.06
PFDN2	<i>prefoldin subunit 2</i>	0	0	0	0	0	0	2	4	2	8	0.06
STAT1	<i>signal transducer and activator of transcription 1</i>	8	9	12	9	38	28	18	29	27	102	0.07
SSB	<i>small RNA binding exonuclease protection factor La</i>	4	0	0	0	4	3	3	3	11	20	0.07
NSA2	<i>NSA2 ribosome biogenesis factor</i>	3	0	0	0	3	7	5	0	5	17	0.07
SPCS3	<i>signal peptidase complex subunit 3</i>	3	0	0	0	3	6	3	3	2	14	0.07
MTHFD1L	<i>methylenetetrahydrofolate dehydrogenase (NADP+ dependent) 1 like</i>	3	2	3	0	8	6	4	8	10	28	0.07
PAK2	<i>p21 (RAC1) activated kinase 2</i>	2	0	0	0	2	5	5	0	3	13	0.07
DNM1L	<i>dynammin 1 like</i>	0	0	3	3	6	5	4	5	10	24	0.07

CSNK1A1	<i>casein kinase 1 alpha 1</i>	0	0	2	2	4	7	9	0	4	20	0.07
DDX19B	<i>DEAD-box helicase 19B</i>	0	0	0	3	3	8	7	0	8	23	0.07
SYNJ2	<i>synaptojanin 2</i>	0	0	0	0	0	2	2	0	2	6	0.07
ATXN2L	<i>ataxin 2 like</i>	0	0	0	0	0	2	2	0	2	6	0.07
SNRPD1	<i>small nuclear ribonucleoprotein D1 polypeptide</i>	4	3	2	2	11	9	6	8	9	32	0.08
PSMC3	<i>proteasome 26S subunit, ATPase 3</i>	3	0	3	0	6	6	2	5	11	24	0.08
CAPZB	<i>capping actin protein of muscle Z-line subunit beta</i>	3	2	0	4	9	8	8	6	5	27	0.08
SMARCA4	<i>SWI/SNF related, matrix associated, actin dependent regulator of chromatin, subfamily a, member 4</i>	2	0	0	0	2	0	2	4	5	11	0.08
DDX27	<i>DEAD-box helicase 27</i>	0	2	4	2	8	6	4	8	7	25	0.08
SPTLC1	<i>serine palmitoyltransferase long chain base subunit 1</i>	0	2	3	0	5	6	4	5	3	18	0.08
TUBB2B	<i>tubulin beta 2B class IIb</i>	0	0	6	0	6	11	7	9	0	27	0.08
ADNP	<i>activity dependent neuroprotector homeobox</i>	0	0	3	0	3	2	3	4	2	11	0.08
ZC3H15	<i>zinc finger CCCH-type containing 15</i>	0	0	3	0	3	5	4	0	4	13	0.08
FAM120A	<i>family with sequence similarity 120A</i>	0	0	2	4	6	7	4	4	6	21	0.08
KPNA1	<i>karyopherin subunit alpha 1</i>	0	0	0	4	4	5	6	0	7	18	0.08
ATP5L	<i>ATP synthase membrane subunit g</i>	5	0	0	0	5	6	5	0	4	15	0.09
ACLY	<i>ATP citrate lyase</i>	4	6	3	0	13	9	9	9	13	40	0.09
RARS	<i>arginyl-tRNA synthetase</i>	4	6	10	6	26	19	15	16	27	77	0.09
EIF3CL	<i>eukaryotic translation initiation factor 3 subunit C like</i>	3	4	4	0	11	9	10	6	7	32	0.09
SRSF11	<i>serine and arginine rich splicing factor 11</i>	2	0	0	2	4	4	3	4	2	13	0.09
TOP2A	<i>DNA topoisomerase II alpha</i>	2	0	4	5	11	14	12	6	7	39	0.09
NSDHL	<i>NAD(P) dependent steroid dehydrogenase-like</i>	0	2	2	4	8	6	6	4	8	24	0.09
ACTR2	<i>actin related protein 2</i>	0	0	3	0	3	4	0	4	3	11	0.09
STOM	<i>stomatin</i>	4	0	5	6	15	13	12	10	8	43	0.1
ATP6V1A	<i>ATPase H⁺ transporting V1 subunit A</i>	4	3	2	0	9	3	4	9	10	26	0.1

HNRNPU L1	<i>heterogeneous nuclear ribonucleoprotein U like 1</i>	2	0	0	0	2	0	2	4	2	8	0.1
ACTR1A	<i>actin related protein 1A</i>	2	2	0	5	9	6	6	6	10	28	0.1
FRG1	<i>FSHD region gene 1</i>	0	0	0	0	0	6	7	0	0	13	0.1
HIST2H3 D	<i>histone cluster 2 H3 family member d</i>	0	0	0	0	0	6	4	0	0	10	0.1
HIST1H1 E	<i>histone cluster 1 H1 family member e</i>	0	0	0	0	0	0	0	25	14	39	0.1
NUDT5	<i>nudix hydrolase 5</i>	0	0	0	0	0	0	0	5	4	9	0.1
ZDBF2	<i>zinc finger DBF-type containing 2</i>	0	0	0	0	0	6	0	3	0	9	0.11
TNRC6B	<i>trinucleotide repeat containing adaptor 6B</i>	0	0	0	0	0	4	0	0	3	7	0.11
RASSF8	<i>Ras association domain family member 8</i>	0	0	0	0	0	4	3	0	0	7	0.11
C15orf38- AP3S2	<i>ARPIN-AP3S2 readthrough</i>	0	0	0	0	0	4	0	0	3	7	0.11
MON2	<i>MON2 homolog, regulator of endosome-to-Golgi trafficking</i>	0	0	0	0	0	4	0	0	3	7	0.11
FAM21C	<i>WASH complex subunit 2C</i>	0	0	0	0	0	3	0	0	5	8	0.11
ACBD3	<i>acyl-CoA binding domain containing 3</i>	0	0	0	0	0	3	4	0	0	7	0.11
TMEM115	<i>transmembrane protein 115</i>	0	0	0	0	0	0	4	3	0	7	0.11
SCD	<i>stearoyl-CoA desaturase</i>	0	0	0	0	0	0	3	0	4	7	0.11
RPS6KA1	<i>ribosomal protein S6 kinase A1</i>	0	0	0	0	0	0	3	0	5	8	0.11
CCDC43	<i>coiled-coil domain containing 43</i>	0	0	0	0	0	0	3	0	5	8	0.11
PDLIM1	<i>PDZ and LIM domain 1</i>	0	0	0	0	0	0	0	4	3	7	0.11
CBX1	<i>chromobox 1</i>	0	0	0	0	0	0	0	4	3	7	0.11
BET1	#N/A	0	0	0	0	0	0	0	3	4	7	0.11
VAPA	#N/A	0	0	0	0	0	0	0	3	4	7	0.11
ARHGAP 18	<i>Rho GTPase activating protein 18</i>	0	0	0	0	0	3	3	0	0	6	0.12
RANBP1	<i>RAN binding protein 1</i>	0	0	0	0	0	3	3	0	0	6	0.12
CDC16	<i>cell division cycle 16</i>	0	0	0	0	0	3	0	0	3	6	0.12
PRPSAP1	<i>phosphoribosyl pyrophosphate synthetase associated protein 1</i>	0	0	0	0	0	3	0	0	3	6	0.12

SUGT1	<i>SGT1 homolog, MIS12 kinetochore complex assembly cochaperone</i>	0	0	0	0	0	3	0	0	3	6	0.12
CEP44	<i>centrosomal protein 44</i>	0	0	0	0	0	3	3	0	0	6	0.12
ADD1	<i>adducin 1</i>	0	0	0	0	0	0	0	3	3	6	0.12
CAMSAP1	<i>calmodulin regulated spectrin associated protein 1</i>	0	0	0	0	0	5	0	2	0	7	0.13
EXOC4	<i>exocyst complex component 4</i>	0	0	0	0	0	4	0	2	0	6	0.13
PIH1D1	<i>PIH1 domain containing 1</i>	0	0	0	0	0	2	5	0	0	7	0.13
CASC5	<i>kinetochore scaffold 1</i>	0	0	0	0	0	2	4	0	0	6	0.13
HAUS5	<i>HAUS augmin like complex subunit 5</i>	0	0	0	0	0	2	4	0	0	6	0.13
PFDN5	<i>prefoldin subunit 5</i>	0	0	0	0	0	2	0	0	4	6	0.13
ANKHD1-EIF4EBP3	<i>ANKHD1-EIF4EBP3 readthrough</i>	0	0	0	0	0	2	4	0	0	6	0.13
AGFG1	<i>ArfGAP with FG repeats 1</i>	0	0	0	0	0	2	4	0	0	6	0.13
BMS1	<i>BMS1 ribosome biogenesis factor</i>	0	0	0	0	0	0	2	0	4	6	0.13
TDRD3	<i>tudor domain containing 3</i>	0	0	0	0	0	0	2	0	4	6	0.13
TNS3	<i>tensin 3</i>	0	0	0	0	0	0	0	2	4	6	0.13
KIF1B	<i>kinesin family member 1B</i>	0	0	0	0	0	0	0	2	4	6	0.13
EYA4	<i>EYA transcriptional coactivator and phosphatase 4</i>	0	0	0	0	0	0	0	2	7	9	0.13
IGBP1	<i>immunoglobulin binding protein 1</i>	0	0	0	0	0	0	0	2	4	6	0.13
LASP1	<i>LIM and SH3 protein 1</i>	0	0	0	0	0	0	0	2	4	6	0.13
CDC37	<i>cell division cycle 37</i>	0	0	0	0	0	3	0	0	2	5	0.15
CSTF2T	<i>cleavage stimulation factor subunit 2 tau variant</i>	0	0	0	0	0	3	2	0	0	5	0.15
MRPL16	<i>mitochondrial ribosomal protein L16</i>	0	0	0	0	0	3	0	2	0	5	0.15
TBC1D8	<i>TBC1 domain family member 8</i>	0	0	0	0	0	3	2	0	0	5	0.15
ATG3	<i>autophagy related 3</i>	0	0	0	0	0	3	2	0	0	5	0.15
ANKRD28	<i>ankyrin repeat domain 28</i>	0	0	0	0	0	3	2	0	0	5	0.15
RICTOR	<i>RPTOR independent companion of MTOR complex 2</i>	0	0	0	0	0	2	0	3	0	5	0.15
BET1L	<i>Bet1 golgi vesicular membrane trafficking protein like</i>	0	0	0	0	0	2	0	0	3	5	0.15
PALLD	<i>palladin, cytoskeletal associated protein</i>	0	0	0	0	0	2	0	0	3	5	0.15

BCR	<i>BCR activator of RhoGEF and GTPase</i>	0	0	0	0	0	0	3	2	0	5	0.15
KIF21A	<i>kinesin family member 21A</i>	0	0	0	0	0	0	3	0	2	5	0.15
DLAT	<i>dihydrolipoamide S-acetyltransferase</i>	0	0	0	0	0	0	3	2	0	5	0.15
ANXA1	<i>annexin A1</i>	0	0	0	0	0	0	3	2	0	5	0.15
STX5	<i>syntaxin 5</i>	0	0	0	0	0	0	3	0	2	5	0.15
KIF2C	<i>kinesin family member 2C</i>	0	0	0	0	0	0	2	3	0	5	0.15
SNCA	<i>synuclein alpha</i>	0	0	0	0	0	0	2	3	0	5	0.15
PGAM5	<i>PGAM family member 5, mitochondrial serine/threonine protein phosphatase</i>	0	0	0	0	0	0	0	3	2	5	0.15
EPS15	<i>epidermal growth factor receptor pathway substrate 15</i>	0	0	0	0	0	0	0	3	2	5	0.15
NUFIP2	<i>nuclear FMR1 interacting protein 2</i>	0	0	0	0	0	0	0	2	3	5	0.15
ERCC6L	<i>ERCC excision repair 6 like, spindle assembly checkpoint helicase</i>	0	0	0	0	0	0	0	2	3	5	0.15
GOPC	<i>golgi associated PDZ and coiled-coil motif containing</i>	0	0	0	0	0	0	0	2	3	5	0.15
FYTTD1	<i>forty-two-three domain containing 1</i>	0	0	0	0	0	0	0	2	3	5	0.15
EIF5A	<i>eukaryotic translation initiation factor 5A</i>	4	2	0	0	6	4	4	4	5	17	0.17
TSN	<i>translin</i>	0	0	0	0	0	2	0	2	0	4	0.17
C10orf76	<i>armadillo like helical domain containing 3</i>	0	0	0	0	0	2	0	0	2	4	0.17
CDC20	<i>cell division cycle 20</i>	0	0	0	0	0	2	2	0	0	4	0.17
ANKRD52	<i>ankyrin repeat domain 52</i>	0	0	0	0	0	2	0	0	2	4	0.17
NCK1	<i>NCK adaptor protein 1</i>	0	0	0	0	0	2	2	0	0	4	0.17
TRIM26	<i>tripartite motif containing 26</i>	0	0	0	0	0	2	2	0	0	4	0.17
CCDC124	<i>coiled-coil domain containing 124</i>	0	0	0	0	0	0	2	0	2	4	0.17
ERH	<i>ERH mRNA splicing and mitosis factor</i>	0	0	0	0	0	0	2	2	0	4	0.17
NAE1	<i>NEDD8 activating enzyme E1 subunit 1</i>	0	0	0	0	0	0	0	2	2	4	0.17
FIBP	<i>FGF1 intracellular binding protein</i>	0	0	0	0	0	0	0	2	2	4	0.17
RPL18	<i>ribosomal protein L18</i>	15	16	15	15	61	47	41	23	24	135	0.18

RAB1A	<i>RAB1A, member RAS oncogene family</i>	5	0	0	10	15	15	5	6	23	49	0.18
RPSA	<i>ribosomal protein SA</i>	0	4	2	0	6	5	5	3	4	17	0.18
RPS21	<i>ribosomal protein S21</i>	0	2	0	0	2	4	4	0	0	8	0.18
SCAMP3	<i>secretory carrier membrane protein 3</i>	0	0	0	4	4	2	0	4	4	10	0.18
ATL3	<i>atlastin GTPase 3</i>	0	0	0	2	2	0	0	3	8	11	0.18
DDX24	<i>DEAD-box helicase 24</i>	3	2	2	3	10	6	7	6	7	26	0.19
PTPN23	<i>protein tyrosine phosphatase non-receptor type 23</i>	2	0	0	0	2	0	3	0	5	8	0.19
FAM101B	<i>refilin B</i>	0	3	0	0	3	0	8	4	0	12	0.19
C20orf4	<i>AAR2 splicing factor</i>	0	3	0	0	3	4	0	0	8	12	0.19
DNAJB1	<i>DnaJ heat shock protein family (Hsp40) member B1</i>	0	2	0	0	2	4	0	0	3	7	0.19
FMR1	<i>fragile X mental retardation 1</i>	0	2	0	0	2	0	0	5	3	8	0.19
ADAR	<i>adenosine deaminase RNA specific</i>	0	2	3	3	8	6	3	5	6	20	0.19
AP2A1	<i>adaptor related protein complex 2 subunit alpha 1</i>	0	0	4	3	7	3	5	7	4	19	0.19
MAP2K2	<i>mitogen-activated protein kinase kinase 2</i>	0	0	4	0	4	0	0	4	10	14	0.19
TBK1	<i>TANK binding kinase 1</i>	0	0	3	2	5	4	0	2	11	17	0.19
RPS23	<i>ribosomal protein S23</i>	10	6	0	0	16	13	10	10	12	45	0.2
DNM2	<i>dynamain 2</i>	4	0	0	0	4	0	0	4	5	9	0.2
CDK2	<i>cyclin dependent kinase 2</i>	4	7	7	8	26	12	11	17	19	59	0.2
PSMC2	<i>proteasome 26S subunit, ATPase 2</i>	2	0	7	4	13	7	3	9	17	36	0.2
SKP1	<i>S-phase kinase associated protein 1</i>	2	0	2	2	6	3	3	5	4	15	0.2
TUBGCP3	<i>tubulin gamma complex associated protein 3</i>	0	2	2	0	4	0	0	3	5	8	0.2
SLC25A17	<i>solute carrier family 25 member 17</i>	0	2	0	0	2	3	0	0	3	6	0.2
VRK1	<i>VRK serine/threonine kinase 1</i>	0	0	2	0	2	0	0	3	3	6	0.2
NOC3L	<i>NOC3 like DNA replication regulator</i>	0	0	2	0	2	0	2	0	3	5	0.2
PIGU	<i>phosphatidylinositol glycan anchor biosynthesis class U</i>	0	0	0	3	3	4	3	0	0	7	0.2
GTPBP4	<i>GTP binding protein 4</i>	5	3	7	8	23	15	9	16	13	53	0.21
GTF2I	<i>general transcription factor Ili</i>	4	0	0	2	6	0	2	6	4	12	0.21

TNPO3	<i>transportin 3</i>	4	3	5	0	12	0	0	9	9	18	0.21
NOP56	<i>NOP56 ribonucleoprotein</i>	4	0	2	3	9	4	8	3	6	21	0.21
RCC1	<i>regulator of chromosome condensation 1</i>	3	0	0	0	3	4	2	0	0	6	0.21
BCAS2	<i>BCAS2 pre-mRNA processing factor</i>	3	0	0	0	3	0	0	2	4	6	0.21
SRPRB	<i>SRP receptor subunit beta</i>	2	0	4	0	6	4	3	2	5	14	0.21
EMD	<i>emerin</i>	0	2	0	3	5	4	2	3	3	12	0.21
PACS1	<i>phosphofurin acidic cluster sorting protein 1</i>	0	0	2	0	2	2	0	0	2	4	0.21
PSMD2	<i>proteasome 26S subunit, non-ATPase 2</i>	7	6	2	2	17	8	11	5	15	39	0.22
UBAP2L	<i>ubiquitin associated protein 2 like</i>	5	2	2	5	14	4	6	11	8	29	0.22
HNRNPA B	<i>heterogeneous nuclear ribonucleoprotein A/B</i>	4	0	0	5	9	6	6	5	5	22	0.22
FASTKD2	<i>FAST kinase domains 2</i>	2	5	2	0	9	3	2	5	9	19	0.22
LSM12	<i>LSM12 homolog</i>	2	0	2	0	4	3	4	0	0	7	0.22
PTDSS1	<i>phosphatidylserine synthase 1</i>	0	4	3	3	10	4	4	7	7	22	0.22
SF3B2	<i>splicing factor 3b subunit 2</i>	0	3	0	0	3	0	0	3	2	5	0.22
IDH3B	<i>isocitrate dehydrogenase (NAD(+)) 3 beta</i>	0	0	3	3	6	5	0	4	3	12	0.22
EEF1D	<i>eukaryotic translation elongation factor 1 delta</i>	4	7	6	6	23	0	0	0	27	27	0.23
UGDH	<i>UDP-glucose 6-dehydrogenase</i>	0	0	3	0	3	0	0	2	2	4	0.23
PPP1CA	<i>protein phosphatase 1 catalytic subunit alpha</i>	0	0	0	0	0	10	0	0	0	10	0.23
PFN1	<i>profilin 1</i>	0	0	0	0	0	6	0	0	0	6	0.23
RBMXL1	<i>RBMX like 1</i>	0	0	0	0	0	0	6	0	0	6	0.23
CTPS2	<i>CTP synthase 2</i>	0	0	0	0	0	0	0	12	0	12	0.23
DDX19A	<i>DEAD-box helicase 19A</i>	0	0	0	0	0	0	0	6	0	6	0.23
CHD3	<i>chromodomain helicase DNA binding protein 3</i>	0	0	0	0	0	0	0	6	0	6	0.23
ACTB	<i>actin beta</i>	0	0	0	0	0	0	0	0	79	79	0.23
TXNDC9	<i>thioredoxin domain containing 9</i>	0	0	0	0	0	0	0	0	8	8	0.23
FAM129B	<i>niban apoptosis regulator 2</i>	0	0	0	0	0	0	0	0	7	7	0.23
RRM2	<i>ribonucleotide reductase regulatory subunit M2</i>	0	0	0	0	0	0	0	0	6	6	0.23

TUBB2A	<i>tubulin beta 2A class IIa</i>	0	0	0	0	0	0	0	0	6	6	0.23
AP2B1	<i>adaptor related protein complex 2 subunit beta 1</i>	3	2	6	7	18	9	6	5	15	35	0.24
TIMM23B	<i>translocase of inner mitochondrial membrane 23 homolog B</i>	0	0	0	0	0	0	5	0	0	5	0.24
THOC2	<i>THO complex 2</i>	0	0	0	0	0	0	0	0	5	5	0.24
COMMD8	<i>COMM domain containing 8</i>	0	0	0	0	0	0	0	0	5	5	0.24
SEC31A	<i>SEC31 homolog A, COPII coat complex component</i>	0	0	0	0	0	4	0	0	0	4	0.25
ARPC4	<i>actin related protein 2/3 complex subunit 4</i>	0	0	0	0	0	4	0	0	0	4	0.25
HAUS3	<i>HAUS augmin like complex subunit 3</i>	0	0	0	0	0	4	0	0	0	4	0.25
RASGEF1 B	<i>RasGEF domain family member 1B</i>	0	0	0	0	0	4	0	0	0	4	0.25
CAST	<i>calpastatin</i>	0	0	0	0	0	4	0	0	0	4	0.25
PFDN6	<i>prefoldin subunit 6</i>	0	0	0	0	0	4	0	0	0	4	0.25
SMAP1	<i>small ArfGAP 1</i>	0	0	0	0	0	4	0	0	0	4	0.25
PPIB	<i>peptidylprolyl isomerase B</i>	0	0	0	0	0	4	0	0	0	4	0.25
RAI14	<i>retinoic acid induced 14</i>	0	0	0	0	0	0	4	0	0	4	0.25
SYNJ1	<i>synaptojanin 1</i>	0	0	0	0	0	0	4	0	0	4	0.25
TFB2M	<i>transcription factor B2, mitochondrial</i>	0	0	0	0	0	0	0	4	0	4	0.25
CSRP1	<i>cysteine and glycine rich protein 1</i>	0	0	0	0	0	0	0	4	0	4	0.25
SF1	<i>splicing factor 1</i>	0	0	0	0	0	0	0	4	0	4	0.25
ZC3H11A	<i>zinc finger CCCH-type containing 11A</i>	0	0	0	0	0	0	0	4	0	4	0.25
TMEM126 A	<i>transmembrane protein 126A</i>	0	0	0	0	0	0	0	4	0	4	0.25
ARFGAP2	<i>ADP ribosylation factor GTPase activating protein 2</i>	0	0	0	0	0	0	0	4	0	4	0.25
TPD52	<i>tumor protein D52</i>	0	0	0	0	0	0	0	0	4	4	0.25
DDX52	<i>DEXD-box helicase 52</i>	0	0	0	0	0	0	0	0	4	4	0.25
TTC27	<i>tetratricopeptide repeat domain 27</i>	0	0	0	0	0	0	0	0	4	4	0.25
MAPT	<i>microtubule associated protein tau</i>	0	0	0	0	0	0	0	0	4	4	0.25
RER1	<i>retention in endoplasmic reticulum sorting receptor 1</i>	0	0	0	0	0	0	0	0	4	4	0.25

KIAA1033	<i>WASH complex subunit 4</i>	0	0	0	0	0	0	0	0	4	4	0.25
SMARCD2	<i>SWI/SNF related, matrix associated, actin dependent regulator of chromatin, subfamily d, member 2</i>	0	0	0	0	0	0	0	0	4	4	0.25
KIAA0196	<i>WASH complex subunit 5</i>	0	0	0	0	0	0	0	0	4	4	0.25
NCAPD2	<i>non-SMC condensin I complex subunit D2</i>	0	0	0	0	0	0	0	0	4	4	0.25
NSF	<i>N-ethylmaleimide sensitive factor, vesicle fusing ATPase</i>	0	0	0	0	0	0	0	0	4	4	0.25
IKBKKG	<i>inhibitor of nuclear factor kappa B kinase regulatory subunit gamma</i>	0	0	0	0	0	0	0	0	4	4	0.25
IPO11	<i>importin 11</i>	0	0	0	0	0	0	0	0	4	4	0.25
RYR2	<i>ryanodine receptor 2</i>	0	0	0	0	0	0	0	0	4	4	0.25
C9orf86	<i>RAB, member RAS oncogene family like 6</i>	0	0	0	0	0	0	0	0	4	4	0.25
RAPGEF6	<i>Rap guanine nucleotide exchange factor 6</i>	0	0	0	0	0	0	0	0	4	4	0.25
RBM3	<i>RNA binding motif protein 3</i>	0	0	0	0	0	0	0	0	4	4	0.25
ITGA4	<i>integrin subunit alpha 4</i>	0	0	0	0	0	3	0	0	0	3	0.28
ALMS1	<i>ALMS1 centrosome and basal body associated protein</i>	0	0	0	0	0	3	0	0	0	3	0.28
SPAG5	<i>sperm associated antigen 5</i>	0	0	0	0	0	3	0	0	0	3	0.28
KIF22	<i>kinesin family member 22</i>	0	0	0	0	0	3	0	0	0	3	0.28
SLC35B2	<i>solute carrier family 35 member B2</i>	0	0	0	0	0	3	0	0	0	3	0.28
HEATR1	<i>HEAT repeat containing 1</i>	0	0	0	0	0	3	0	0	0	3	0.28
MED23	<i>mediator complex subunit 23</i>	0	0	0	0	0	3	0	0	0	3	0.28
COG7	<i>component of oligomeric golgi complex 7</i>	0	0	0	0	0	3	0	0	0	3	0.28
PAIP1	<i>poly(A) binding protein interacting protein 1</i>	0	0	0	0	0	3	0	0	0	3	0.28
SNAP29	<i>synaptosome associated protein 29</i>	0	0	0	0	0	0	3	0	0	3	0.28
SPTAN1	<i>spectrin alpha, non-erythrocytic 1</i>	0	0	0	0	0	0	3	0	0	3	0.28
KDM3A	<i>lysine demethylase 3A</i>	0	0	0	0	0	0	3	0	0	3	0.28
NDRG1	<i>N-myc downstream regulated 1</i>	0	0	0	0	0	0	3	0	0	3	0.28
PYCR1	<i>pyrroline-5-carboxylate reductase 3</i>	0	0	0	0	0	0	3	0	0	3	0.28
NEK9	<i>NIMA related kinase 9</i>	0	0	0	0	0	0	3	0	0	3	0.28

RELA	<i>RELA proto-oncogene, NF-kB subunit</i>	0	0	0	0	0	0	0	3	0	3	0.28
MRPS11	<i>mitochondrial ribosomal protein S11</i>	0	0	0	0	0	0	0	3	0	3	0.28
MAGEA1	<i>MAGE family member A1</i>	0	0	0	0	0	0	0	3	0	3	0.28
ZNF207	<i>zinc finger protein 207</i>	0	0	0	0	0	0	0	3	0	3	0.28
TUBGCP4	<i>tubulin gamma complex associated protein 4</i>	0	0	0	0	0	0	0	0	3	3	0.28
EIF2C2	<i>argonaute RISC catalytic component 2</i>	0	0	0	0	0	0	0	0	3	3	0.28
EIF3L	<i>eukaryotic translation initiation factor 3 subunit L</i>	0	0	0	0	0	0	0	0	3	3	0.28
PYCR2	<i>pyrroline-5-carboxylate reductase 2</i>	0	0	0	0	0	0	0	0	3	3	0.28
KIF23	<i>kinesin family member 23</i>	0	0	0	0	0	0	0	0	3	3	0.28
WWC1	<i>WW and C2 domain containing 1</i>	0	0	0	0	0	0	0	0	3	3	0.28
ATXN10	<i>ataxin 10</i>	0	0	0	0	0	0	0	0	3	3	0.28
XPO7	<i>exportin 7</i>	0	0	0	0	0	0	0	0	3	3	0.28
TMEM111	<i>ER membrane protein complex subunit 3</i>	0	0	0	0	0	0	0	0	3	3	0.28
LARS2	<i>leucyl-tRNA synthetase 2, mitochondrial</i>	0	0	0	0	0	0	0	0	3	3	0.28
PDHA1	<i>pyruvate dehydrogenase E1 alpha 1 subunit</i>	0	0	0	0	0	0	0	0	3	3	0.28
INF2	<i>inverted formin, FH2 and WH2 domain containing</i>	0	0	0	0	0	0	0	0	3	3	0.28
GTPBP1	<i>GTP binding protein 1</i>	0	0	0	0	0	0	0	0	3	3	0.28
EXOSC7	<i>exosome component 7</i>	0	0	0	0	0	0	0	0	3	3	0.28
GCC1	<i>GRIP and coiled-coil domain containing 1</i>	0	0	0	0	0	0	0	0	3	3	0.28
ZW10	<i>zw10 kinetochore protein</i>	0	0	0	0	0	0	0	0	3	3	0.28
KANK4	<i>KN motif and ankyrin repeat domains 4</i>	0	0	0	0	0	0	0	0	3	3	0.28
EIF3H	<i>eukaryotic translation initiation factor 3 subunit H</i>	0	0	0	0	0	0	0	0	3	3	0.28
RPA1	<i>replication protein A1</i>	0	0	0	0	0	0	0	0	3	3	0.28
BZW2	<i>basic leucine zipper and W2 domains 2</i>	0	0	0	0	0	0	0	0	3	3	0.28
CNOT3	<i>CCR4-NOT transcription complex subunit 3</i>	0	0	0	0	0	0	0	0	3	3	0.28

RIPK2	<i>receptor interacting serine/threonine kinase 2</i>	0	0	0	0	0	0	0	0	3	3	0.28
MFSD12	<i>major facilitator superfamily domain containing 12</i>	0	0	0	0	0	0	0	0	3	3	0.28
STIP1	<i>stress induced phosphoprotein 1</i>	0	0	0	0	0	0	0	0	3	3	0.28
XRCC5	<i>X-ray repair cross complementing 5</i>	9	12	8	5	34	12	10	13	25	60	0.32
SNRNP200	<i>small nuclear ribonucleoprotein U5 subunit 200</i>	6	12	3	3	24	15	12	9	22	58	0.32
PRKAA1	<i>protein kinase AMP-activated catalytic subunit alpha 1</i>	2	0	0	2	4	2	4	0	0	6	0.32
MEPCE	<i>methylphosphate capping enzyme</i>	0	0	0	0	0	2	0	0	0	2	0.32
SNRPD2	<i>small nuclear ribonucleoprotein D2 polypeptide</i>	0	0	0	0	0	2	0	0	0	2	0.32
HAUS8	<i>HAUS augmin like complex subunit 8</i>	0	0	0	0	0	2	0	0	0	2	0.32
VPS4B	<i>vacuolar protein sorting 4 homolog B</i>	0	0	0	0	0	2	0	0	0	2	0.32
CCDC6	<i>coiled-coil domain containing 6</i>	0	0	0	0	0	2	0	0	0	2	0.32
EXOC3	<i>exocyst complex component 3</i>	0	0	0	0	0	2	0	0	0	2	0.32
TFEC	<i>transcription factor EC</i>	0	0	0	0	0	2	0	0	0	2	0.32
DDX26B	<i>integrator complex subunit 6 like</i>	0	0	0	0	0	2	0	0	0	2	0.32
PSMD13	<i>proteasome 26S subunit, non-ATPase 13</i>	0	0	0	0	0	2	0	0	0	2	0.32
TBCB	<i>tubulin folding cofactor B</i>	0	0	0	0	0	2	0	0	0	2	0.32
USP7	<i>ubiquitin specific peptidase 7</i>	0	0	0	0	0	2	0	0	0	2	0.32
SPTBN5	<i>spectrin beta, non-erythrocytic 5</i>	0	0	0	0	0	2	0	0	0	2	0.32
MYCBP2	<i>MYC binding protein 2</i>	0	0	0	0	0	2	0	0	0	2	0.32
WNK1	<i>WNK lysine deficient protein kinase 1</i>	0	0	0	0	0	2	0	0	0	2	0.32
AURKB	<i>aurora kinase B</i>	0	0	0	0	0	2	0	0	0	2	0.32
USP8	<i>ubiquitin specific peptidase 8</i>	0	0	0	0	0	2	0	0	0	2	0.32
ATF7IP2	<i>activating transcription factor 7 interacting protein 2</i>	0	0	0	0	0	2	0	0	0	2	0.32
SAP18	<i>Sin3A associated protein 18</i>	0	0	0	0	0	2	0	0	0	2	0.32
ARHGEF18	<i>Rho/Rac guanine nucleotide exchange factor 18</i>	0	0	0	0	0	2	0	0	0	2	0.32
PELI2	<i>pellino E3 ubiquitin protein ligase</i>	0	0	0	0	0	2	0	0	0	2	0.32

<i>family member 2</i>												
TPM3	<i>tropomyosin 3</i>	0	0	0	0	0	2	0	0	0	2	0.32
INPPL1	<i>inositol polyphosphate phosphatase like 1</i>	0	0	0	0	0	2	0	0	0	2	0.32
LPP	<i>LIM domain containing preferred translocation partner in lipoma</i>	0	0	0	0	0	2	0	0	0	2	0.32
EIF2B2	<i>eukaryotic translation initiation factor 2B subunit beta</i>	0	0	0	0	0	2	0	0	0	2	0.32
STAU2	<i>staufen double-stranded RNA binding protein 2</i>	0	0	0	0	0	2	0	0	0	2	0.32
TJP2	<i>tight junction protein 2</i>	0	0	0	0	0	2	0	0	0	2	0.32
BAIAP2	<i>BAI1 associated protein 2</i>	0	0	0	0	0	2	0	0	0	2	0.32
CDKN2A	<i>cyclin dependent kinase inhibitor 2A</i>	0	0	0	0	0	2	0	0	0	2	0.32
GNL2	<i>G protein nucleolar 2</i>	0	0	0	0	0	2	0	0	0	2	0.32
NT5C2	<i>5'-nucleotidase, cytosolic II</i>	0	0	0	0	0	2	0	0	0	2	0.32
MYL6	<i>myosin light chain 6</i>	0	0	0	0	0	2	0	0	0	2	0.32
WDR77	<i>WD repeat domain 77</i>	0	0	0	0	0	2	0	0	0	2	0.32
OCRL	<i>OCRL inositol polyphosphate-5-phosphatase</i>	0	0	0	0	0	2	0	0	0	2	0.32
BICD2	<i>BICD cargo adaptor 2</i>	0	0	0	0	0	2	0	0	0	2	0.32
CPSF2	<i>cleavage and polyadenylation specific factor 2</i>	0	0	0	0	0	2	0	0	0	2	0.32
DNAJC21	<i>DnaJ heat shock protein family (Hsp40) member C21</i>	0	0	0	0	0	2	0	0	0	2	0.32
LRRC40	<i>leucine rich repeat containing 40</i>	0	0	0	0	0	2	0	0	0	2	0.32
PDE8A	<i>phosphodiesterase 8A</i>	0	0	0	0	0	0	2	0	0	2	0.32
CEP350	<i>centrosomal protein 350</i>	0	0	0	0	0	0	2	0	0	2	0.32
MSN	<i>moesin</i>	0	0	0	0	0	0	2	0	0	2	0.32
COMMD4	<i>COMM domain containing 4</i>	0	0	0	0	0	0	2	0	0	2	0.32
SMG9	<i>SMG9 nonsense mediated mRNA decay factor</i>	0	0	0	0	0	0	2	0	0	2	0.32
HSPA12B	<i>heat shock protein family A (Hsp70) member 12B</i>	0	0	0	0	0	0	2	0	0	2	0.32
KBTBD6	<i>kelch repeat and BTB domain containing 6</i>	0	0	0	0	0	0	2	0	0	2	0.32
PRDX5	<i>peroxiredoxin 5</i>	0	0	0	0	0	0	2	0	0	2	0.32

SCRIB	<i>scribble planar cell polarity protein</i>	0	0	0	0	0	0	2	0	0	2	0.32
ADD3	<i>adducin 3</i>	0	0	0	0	0	0	2	0	0	2	0.32
MPDZ	<i>multiple PDZ domain crumbs cell polarity complex component</i>	0	0	0	0	0	0	2	0	0	2	0.32
ESYT1	<i>extended synaptotagmin 1</i>	0	0	0	0	0	0	2	0	0	2	0.32
UBIAD1	<i>UbiA prenyltransferase domain containing 1</i>	0	0	0	0	0	0	2	0	0	2	0.32
PCDH11Y	<i>protocadherin 11 Y-linked</i>	0	0	0	0	0	0	2	0	0	2	0.32
BCLAF1	<i>BCL2 associated transcription factor 1</i>	0	0	0	0	0	0	2	0	0	2	0.32
TBCE	<i>tubulin folding cofactor E</i>	0	0	0	0	0	0	2	0	0	2	0.32
TAB1	<i>TGF-beta activated kinase 1 (MAP3K7) binding protein 1</i>	0	0	0	0	0	0	2	0	0	2	0.32
PAK3	<i>p21 (RAC1) activated kinase 3</i>	0	0	0	0	0	0	0	2	0	2	0.32
PM20D2	<i>peptidase M20 domain containing 2</i>	0	0	0	0	0	0	0	2	0	2	0.32
IKBKAP	<i>elongator complex protein 1</i>	0	0	0	0	0	0	0	2	0	2	0.32
EHD4	<i>EH domain containing 4</i>	0	0	0	0	0	0	0	2	0	2	0.32
OXSR1	<i>oxidative stress responsive kinase 1</i>	0	0	0	0	0	0	0	2	0	2	0.32
EHD1	<i>EH domain containing 1</i>	0	0	0	0	0	0	0	2	0	2	0.32
EPT1	<i>selenoprotein 1</i>	0	0	0	0	0	0	0	2	0	2	0.32
PNN	<i>pinin, desmosome associated protein</i>	0	0	0	0	0	0	0	2	0	2	0.32
UBE2N	<i>ubiquitin conjugating enzyme E2 N</i>	0	0	0	0	0	0	0	2	0	2	0.32
TNIP1	<i>TNFAIP3 interacting protein 1</i>	0	0	0	0	0	0	0	2	0	2	0.32
CPSF3	<i>cleavage and polyadenylation specific factor 3</i>	0	0	0	0	0	0	0	2	0	2	0.32
MOB3B	<i>MOB kinase activator 3B</i>	0	0	0	0	0	0	0	2	0	2	0.32
TRMT112	<i>tRNA methyltransferase subunit 11-2</i>	0	0	0	0	0	0	0	2	0	2	0.32
RAC1	<i>Rac family small GTPase 1</i>	0	0	0	0	0	0	0	2	0	2	0.32
NME1	<i>NME/NM23 nucleoside diphosphate kinase 1</i>	0	0	0	0	0	0	0	2	0	2	0.32
ALDH3A2	<i>aldehyde dehydrogenase 3 family member A2</i>	0	0	0	0	0	0	0	2	0	2	0.32
PAPSS2	<i>3'-phosphoadenosine 5'-phosphosulfate synthase 2</i>	0	0	0	0	0	0	0	2	0	2	0.32
PGAM1	<i>phosphoglycerate mutase 1</i>	0	0	0	0	0	0	0	0	2	2	0.32

SEC23B	<i>SEC23 homolog B, coat complex II component</i>	0	0	0	0	0	0	0	0	2	2	0.32
DIP2A	<i>disco interacting protein 2 homolog A</i>	0	0	0	0	0	0	0	0	2	2	0.32
RFC4	<i>replication factor C subunit 4</i>	0	0	0	0	0	0	0	0	2	2	0.32
MRPS22	<i>mitochondrial ribosomal protein S22</i>	0	0	0	0	0	0	0	0	2	2	0.32
TRAM1	<i>translocation associated membrane protein 1</i>	0	0	0	0	0	0	0	0	2	2	0.32
HEATR5A	<i>HEAT repeat containing 5A</i>	0	0	0	0	0	0	0	0	2	2	0.32
POLD1	<i>DNA polymerase delta 1, catalytic subunit</i>	0	0	0	0	0	0	0	0	2	2	0.32
IBTK	<i>inhibitor of Bruton tyrosine kinase</i>	0	0	0	0	0	0	0	0	2	2	0.32
SLC27A4	<i>solute carrier family 27 member 4</i>	0	0	0	0	0	0	0	0	2	2	0.32
RQCD1	<i>CCR4-NOT transcription complex subunit 9</i>	0	0	0	0	0	0	0	0	2	2	0.32
ARFIP1	<i>ADP ribosylation factor interacting protein 1</i>	0	0	0	0	0	0	0	0	2	2	0.32
STARD7	<i>StAR related lipid transfer domain containing 7</i>	0	0	0	0	0	0	0	0	2	2	0.32
CAMSAP2	<i>calmodulin regulated spectrin associated protein family member 2</i>	0	0	0	0	0	0	0	0	2	2	0.32
UBE3C	<i>ubiquitin protein ligase E3C</i>	0	0	0	0	0	0	0	0	2	2	0.32
DYNC1LI1	<i>dynein cytoplasmic 1 light intermediate chain 1</i>	0	0	0	0	0	0	0	0	2	2	0.32
CDC27	<i>cell division cycle 27</i>	0	0	0	0	0	0	0	0	2	2	0.32
PKN2	<i>protein kinase N2</i>	0	0	0	0	0	0	0	0	2	2	0.32
POLR2A	<i>RNA polymerase II subunit A</i>	0	0	0	0	0	0	0	0	2	2	0.32
SCYL3	<i>SCY1 like pseudokinase 3</i>	0	0	0	0	0	0	0	0	2	2	0.32
ARMC5	<i>armadillo repeat containing 5</i>	0	0	0	0	0	0	0	0	2	2	0.32
PXN	<i>paxillin</i>	0	0	0	0	0	0	0	0	2	2	0.32
SERPINE2	<i>serpin family E member 2</i>	0	0	0	0	0	0	0	0	2	2	0.32
SBNO1	<i>strawberry notch homolog 1</i>	0	0	0	0	0	0	0	0	2	2	0.32
PPP2R5C	<i>protein phosphatase 2 regulatory subunit B'gamma</i>	0	0	0	0	0	0	0	0	2	2	0.32
AARS	<i>alanyl-tRNA synthetase</i>	0	0	0	0	0	0	0	0	2	2	0.32

DARS2	<i>aspartyl-tRNA synthetase 2, mitochondrial</i>	0	0	0	0	0	0	0	0	2	2	0.32
USP24	<i>ubiquitin specific peptidase 24</i>	0	0	0	0	0	0	0	0	2	2	0.32
POLR2E	<i>RNA polymerase II subunit E</i>	0	0	0	0	0	0	0	0	2	2	0.32
C14orf133	<i>VPS33B interacting protein, apical-basolateral polarity regulator, spe-39 homolog</i>	0	0	0	0	0	0	0	0	2	2	0.32
LPCAT1	<i>lysophosphatidylcholine acyltransferase 1</i>	0	0	0	0	0	0	0	0	2	2	0.32
ILK	<i>integrin linked kinase</i>	0	0	0	0	0	0	0	0	2	2	0.32
PPIP5K2	<i>diphosphoinositol pentakisphosphate kinase 2</i>	0	0	0	0	0	0	0	0	2	2	0.32
ARHGAP17	<i>Rho GTPase activating protein 17</i>	0	0	0	0	0	0	0	0	2	2	0.32
DDB1	<i>damage specific DNA binding protein 1</i>	0	0	0	0	0	0	0	0	2	2	0.32
XAB2	<i>XPA binding protein 2</i>	0	0	0	0	0	0	0	0	2	2	0.32
ARHGEF2	<i>Rho/Rac guanine nucleotide exchange factor 2</i>	0	0	0	0	0	0	0	0	2	2	0.32
RRAGB	<i>Ras related GTP binding B</i>	0	0	0	0	0	0	0	0	2	2	0.32
YAP1	<i>Yes associated protein 1</i>	0	0	0	0	0	0	0	0	2	2	0.32
TACC3	<i>transforming acidic coiled-coil containing protein 3</i>	0	0	0	0	0	0	0	0	2	2	0.32
TOX4	<i>TOX high mobility group box family member 4</i>	0	0	0	0	0	0	0	0	2	2	0.32
MGST1	<i>microsomal glutathione S-transferase 1</i>	0	0	0	0	0	0	0	0	2	2	0.32
SIKE1	<i>suppressor of IKBKE 1</i>	0	0	0	0	0	0	0	0	2	2	0.32
SPCS2	<i>signal peptidase complex subunit 2</i>	0	0	0	0	0	0	0	0	2	2	0.32
NR3C1	<i>nuclear receptor subfamily 3 group C member 1</i>	0	0	0	0	0	0	0	0	2	2	0.32
CLPX	<i>caseinolytic mitochondrial matrix peptidase chaperone subunit</i>	0	0	0	0	0	0	0	0	2	2	0.32
NCAPG	<i>non-SMC condensin I complex subunit G</i>	6	5	9	4	24	12	9	12	18	51	0.4
DIAPH1	<i>diaphanous related formin 1</i>	5	5	2	4	16	10	5	7	11	33	0.4
UFL1	<i>UFM1 specific ligase 1</i>	0	0	2	0	2	0	0	5	0	5	0.4
EIF2B1	<i>eukaryotic translation initiation factor 2B subunit alpha</i>	0	0	0	2	2	0	0	0	5	5	0.4

RPL28	<i>ribosomal protein L28</i>	9	8	5	11	33	23	15	16	17	71	0.41
DNAJA2	<i>DnaJ heat shock protein family (Hsp40) member A2</i>	7	2	4	9	22	7	8	12	18	45	0.41
MAP2K1	<i>mitogen-activated protein kinase kinase 1</i>	4	0	0	2	6	5	3	0	2	10	0.41
EEF1B2	<i>eukaryotic translation elongation factor 1 beta 2</i>	4	6	4	0	14	0	7	9	10	26	0.41
PSMC5	<i>proteasome 26S subunit, ATPase 5</i>	4	0	2	4	10	4	4	5	8	21	0.41
GCLM	<i>glutamate-cysteine ligase modifier subunit</i>	3	0	2	0	5	0	0	6	0	6	0.41
CBX3	<i>chromobox 3</i>	3	0	0	2	5	0	4	0	3	7	0.41
MYBBP1	<i>MYB binding protein 1a</i>	0	3	7	5	15	6	3	3	15	27	0.41
A												
GSK3B	<i>glycogen synthase kinase 3 beta</i>	0	2	0	0	2	0	0	0	3	3	0.41
HNRPDL	<i>heterogeneous nuclear ribonucleoprotein D like</i>	0	2	0	0	2	0	0	0	3	3	0.41
KPNA6	<i>karyopherin subunit alpha 6</i>	0	0	4	0	4	0	0	7	0	7	0.41
UQCRCF1	<i>ubiquinol-cytochrome c reductase, Rieske iron-sulfur polypeptide 1</i>	0	0	3	0	3	0	0	0	4	4	0.41
C12orf23	<i>transmembrane protein 263</i>	0	0	3	3	6	0	0	3	5	8	0.41
CAPRIN1	<i>cell cycle associated protein 1</i>	0	0	3	3	6	3	2	4	3	12	0.41
CDC45	<i>cell division cycle 45</i>	0	0	2	0	2	0	0	3	0	3	0.41
AIMP2	<i>aminoacyl tRNA synthetase complex interacting multifunctional protein 2</i>	0	0	0	3	3	0	0	0	4	4	0.41
COX2	<i>mitochondrially encoded cytochrome c oxidase II</i>	0	0	0	2	2	0	0	0	3	3	0.41
NUP188	<i>nucleoporin 188</i>	0	0	0	2	2	0	0	0	3	3	0.41
MSH3	<i>mutS homolog 3</i>	0	0	0	2	2	0	0	0	3	3	0.41
NEB	<i>nebulin</i>	3	0	0	0	3	0	0	3	0	3	0.42
PSMD1	<i>proteasome 26S subunit, non-ATPase 1</i>	2	0	2	0	4	0	0	0	4	4	0.42
KPNA5	<i>karyopherin subunit alpha 5</i>	2	0	0	4	6	0	0	0	6	6	0.42
CYFIP2	<i>cytoplasmic FMR1 interacting protein 2</i>	2	0	0	0	2	0	0	0	2	2	0.42
HK2	<i>hexokinase 2</i>	2	0	0	0	2	0	0	0	2	2	0.42
EIF3I	<i>eukaryotic translation initiation factor 3 subunit I</i>	2	2	2	3	9	5	2	4	6	17	0.42

RAB18	<i>RAB18, member RAS oncogene family</i>	0	5	0	0	5	4	0	0	0	4	0.42
SF3A2	<i>splicing factor 3a subunit 2</i>	0	3	0	0	3	0	0	0	3	3	0.42
RPS6KA3	<i>ribosomal protein S6 kinase A3</i>	0	0	3	0	3	0	0	3	0	3	0.42
MLH1	<i>mutL homolog 1</i>	0	0	3	0	3	0	0	3	0	3	0.42
YTHDF2	<i>YTH N6-methyladenosine RNA binding protein 2</i>	0	0	2	0	2	2	0	0	0	2	0.42
EIF3D	<i>eukaryotic translation initiation factor 3 subunit D</i>	0	0	2	2	4	3	0	0	2	5	0.42
UBR4	<i>ubiquitin protein ligase E3 component n-recognin 4</i>	0	0	0	5	5	0	4	0	0	4	0.42
EXOSC4	<i>exosome component 4</i>	0	0	0	2	2	0	0	0	2	2	0.42
AFAP1	<i>actin filament associated protein 1</i>	0	0	0	2	2	0	0	0	2	2	0.42
RAP2C	<i>RAP2C, member of RAS oncogene family</i>	0	0	0	2	2	2	0	0	0	2	0.42
FBXL12	<i>F-box and leucine rich repeat protein 12</i>	0	0	0	2	2	0	0	0	2	2	0.42
PSMC4	<i>proteasome 26S subunit, ATPase 4</i>	0	0	0	2	2	0	2	0	0	2	0.42
FADS1	<i>fatty acid desaturase 1</i>	0	0	0	2	2	0	0	2	0	2	0.42
DIMT1	<i>DIMT1 rRNA methyltransferase and ribosome maturation factor</i>	4	4	6	4	18	4	3	12	6	25	0.43
FXR1	<i>FMR1 autosomal homolog 1</i>	4	5	0	6	15	10	5	7	9	31	0.43
PRPF8	<i>pre-mRNA processing factor 8</i>	4	5	8	4	21	8	6	7	14	35	0.43
SENP3	<i>SUMO specific peptidase 3</i>	3	0	4	0	7	0	5	2	0	7	0.43
RPS25	<i>ribosomal protein S25</i>	2	0	4	3	9	4	5	5	4	18	0.43
DSTN	<i>destrin, actin depolymerizing factor</i>	2	0	2	0	4	0	2	2	0	4	0.43
TBL2	<i>transducin beta like 2</i>	0	2	3	0	5	0	0	2	3	5	0.43
PCNA	<i>proliferating cell nuclear antigen</i>	0	0	5	5	10	3	3	4	7	17	0.43
NPEPPS	<i>aminopeptidase puromycin sensitive</i>	0	0	4	3	7	0	0	0	5	5	0.43
PRKAG1	<i>protein kinase AMP-activated non-catalytic subunit gamma 1</i>	0	0	4	3	7	2	0	2	5	9	0.43
CYFIP1	<i>cytoplasmic FMR1 interacting protein 1</i>	0	0	3	2	5	2	3	0	0	5	0.43
DDX23	<i>DEAD-box helicase 23</i>	0	0	2	2	4	0	0	0	3	3	0.43
HDAC2	<i>histone deacetylase 2</i>	8	5	3	0	16	7	5	7	11	30	0.44
CDC123	<i>cell division cycle 123</i>	7	3	3	2	15	4	5	9	9	27	0.44

RTN4	<i>reticulon 4</i>	5	4	0	2	11	4	5	7	5	21	0.44
CDIPT	<i>CDP-diacylglycerol--inositol 3-phosphatidyltransferase</i>	4	3	3	0	10	4	6	5	3	18	0.44
SLC16A3	<i>solute carrier family 16 member 3</i>	3	3	0	0	6	2	2	3	2	9	0.44
ALDH1B1	<i>aldehyde dehydrogenase 1 family member B1</i>	2	2	2	2	8	0	0	0	5	5	0.44
TWF2	<i>twinfilin actin binding protein 2</i>	2	0	4	0	6	0	0	0	4	4	0.44
RPL19	<i>ribosomal protein L19</i>	0	7	11	9	27	13	19	17	17	66	0.44
TTN	<i>titin</i>	0	4	0	0	4	0	2	0	0	2	0.44
AIMP1	<i>aminoacyl tRNA synthetase complex interacting multifunctional protein 1</i>	0	4	0	0	4	2	0	0	0	2	0.44
RFC2	<i>replication factor C subunit 2</i>	0	2	4	3	9	0	2	0	6	8	0.44
TRNT1	<i>tRNA nucleotidyl transferase 1</i>	0	0	4	0	4	0	0	2	0	2	0.44
FUBP3	<i>far upstream element binding protein 3</i>	0	0	4	2	6	0	0	0	4	4	0.44
ASNS	<i>asparagine synthetase (glutamine-hydrolyzing)</i>	0	0	4	3	7	0	0	3	4	7	0.44
SARIA	<i>secretion associated Ras related GTPase 1A</i>	0	0	3	3	6	0	0	0	4	4	0.44
SAFB2	<i>scaffold attachment factor B2</i>	4	2	2	0	8	2	2	0	5	9	0.45
FEN1	<i>flap structure-specific endonuclease 1</i>	4	3	2	3	12	6	4	5	7	22	0.45
NDUFS3	<i>NADH:ubiquinone oxidoreductase core subunit S3</i>	3	3	0	0	6	0	0	3	2	5	0.45
MAP7	<i>microtubule associated protein 7</i>	2	3	5	2	12	7	4	6	3	20	0.45
PLEKHA2	<i>pleckstrin homology domain containing A2</i>	2	0	2	3	7	0	0	0	4	4	0.45
QARS	<i>glutamyl-tRNA synthetase</i>	2	0	2	0	4	0	0	0	2	2	0.45
MRPS5	<i>mitochondrial ribosomal protein S5</i>	2	6	0	0	8	4	3	3	0	10	0.45
BUB3	<i>BUB3 mitotic checkpoint protein</i>	0	3	0	3	6	3	0	0	0	3	0.45
COPE	<i>coatamer protein complex subunit epsilon</i>	0	3	6	5	14	4	5	5	9	23	0.45
ATP6V1H	<i>ATPase H⁺ transporting V1 subunit H</i>	0	2	4	0	6	0	0	0	3	3	0.45
CENPM	<i>centromere protein M</i>	0	2	0	2	4	0	0	0	2	2	0.45
UBE2I	<i>ubiquitin conjugating enzyme E2 I</i>	0	2	0	2	4	0	0	2	0	2	0.45
AAAS	<i>aladin WD repeat nucleoporin</i>	0	2	2	3	7	0	0	4	0	4	0.45

FAR1	<i>fatty acyl-CoA reductase 1</i>	0	0	3	3	6	0	2	0	3	5	0.45
FARP1	<i>FERM, ARH/RhoGEF and pleckstrin domain protein 1</i>	0	0	2	2	4	0	2	0	0	2	0.45
RPL32	<i>ribosomal protein L32</i>	9	9	0	9	27	18	15	13	14	60	0.46
DRG1	<i>developmentally regulated GTP binding protein 1</i>	6	5	7	7	25	13	11	13	15	52	0.46
RPS20	<i>ribosomal protein S20</i>	4	4	5	6	19	11	8	7	8	34	0.46
C14orf166	<i>RNA transcription, translation and transport factor</i>	4	8	3	4	19	6	5	6	11	28	0.46
RBM15	<i>RNA binding motif protein 15</i>	3	0	2	3	8	0	0	0	4	4	0.46
SEC23A	<i>Sec23 homolog A, coat complex II component</i>	2	3	6	2	13	7	6	5	3	21	0.46
CPSF6	<i>cleavage and polyadenylation specific factor 6</i>	2	0	2	4	8	4	0	0	0	4	0.46
AFG3L2	<i>AFG3 like matrix AAA peptidase subunit 2</i>	0	2	2	2	6	0	0	0	3	3	0.46
HIST1H3F	<i>histone cluster 1 H3 family member f</i>	0	0	10	0	10	0	0	5	0	5	0.46
DHCR7	<i>7-dehydrocholesterol reductase</i>	0	0	4	6	10	3	3	0	5	11	0.46
PUS1	<i>pseudouridine synthase 1</i>	0	0	3	2	5	0	0	0	2	2	0.46
PLRG1	<i>pleiotropic regulator 1</i>	0	0	3	2	5	0	0	0	2	2	0.46
LMNB2	<i>lamin B2</i>	0	0	2	3	5	0	0	0	2	2	0.46
UBLCP1	<i>ubiquitin like domain containing CTD phosphatase 1</i>	0	0	2	3	5	0	0	0	2	2	0.46
ABCC3	<i>ATP binding cassette subfamily C member 3</i>	8	0	0	0	8	0	0	3	0	3	0.47
RAP1B	<i>RAP1B, member of RAS oncogene family</i>	6	0	3	0	9	3	0	4	0	7	0.47
EEF1A2	<i>eukaryotic translation elongation factor 1 alpha 2</i>	5	4	4	5	18	9	8	5	8	30	0.47
HCFC1	<i>host cell factor C1</i>	4	5	3	2	14	7	5	3	6	21	0.47
H1FX	<i>H1 histone family member X</i>	3	5	0	0	8	0	0	3	0	3	0.47
SNRNP70	<i>small nuclear ribonucleoprotein U1 subunit 70</i>	3	2	3	2	10	5	3	2	3	13	0.47
NUP85	<i>nucleoporin 85</i>	3	0	3	5	11	0	3	2	5	10	0.47
AKAP8L	<i>A-kinase anchoring protein 8 like</i>	3	0	7	3	13	5	5	5	4	19	0.47
NMT1	<i>N-myristoyltransferase 1</i>	3	3	3	5	14	7	3	0	7	17	0.47
SFXN3	<i>sideroflexin 3</i>	3	0	2	4	9	0	0	3	3	6	0.47

DNAJC10	<i>DnaJ heat shock protein family (Hsp40) member C10</i>	2	0	2	3	7	0	0	0	3	3	0.47
SLC25A1	<i>solute carrier family 25 member 1</i>	2	3	5	0	10	2	0	3	4	9	0.47
GFPT1	<i>glutamine--fructose-6-phosphate transaminase 1</i>	2	4	6	10	22	8	12	11	13	44	0.47
TMED10	<i>transmembrane p24 trafficking protein 10</i>	0	4	3	0	7	0	0	0	3	3	0.47
SMARCA1	<i>SWI/SNF related, matrix associated, actin dependent regulator of chromatin, subfamily a, member 1</i>	0	0	5	5	10	3	0	0	4	7	0.47
HBS1L	<i>HBS1 like translational GTPase</i>	7	5	8	5	25	11	8	12	13	44	0.48
BAG2	<i>BCL2 associated athanogene 2</i>	5	8	6	4	23	8	6	7	12	33	0.48
RHEB	<i>Ras homolog, mTORC1 binding</i>	5	3	5	7	20	8	9	10	5	32	0.48
AP2M1	<i>adaptor related protein complex 2 subunit mu 1</i>	4	3	5	6	18	5	6	9	6	26	0.48
DRG2	<i>developmentally regulated GTP binding protein 2</i>	3	3	4	7	17	0	4	8	7	19	0.48
SNRPA1	<i>small nuclear ribonucleoprotein polypeptide A'</i>	3	2	2	0	7	0	0	2	0	2	0.48
PDE3A	<i>phosphodiesterase 3A</i>	3	3	6	3	15	7	6	5	2	20	0.48
LUC7L2	<i>LUC7 like 2, pre-mRNA splicing factor</i>	2	0	4	4	10	0	4	0	0	4	0.48
SKIV2L2	<i>Mtr4 exosome RNA helicase</i>	2	2	0	3	7	0	0	0	2	2	0.48
DUT	<i>deoxyuridine triphosphatase</i>	0	6	2	2	10	3	3	0	0	6	0.48
DIS3	<i>DIS3 homolog, exosome endoribonuclease and 3'-5' exoribonuclease</i>	0	5	0	4	9	0	0	2	3	5	0.48
TMEM165	<i>transmembrane protein 165</i>	0	3	4	5	12	4	0	0	5	9	0.48
MSH2	<i>mutS homolog 2</i>	0	3	4	4	11	3	3	4	3	13	0.48
CNP	<i>2',3'-cyclic nucleotide 3' phosphodiesterase</i>	0	2	2	3	7	0	0	0	2	2	0.48
RPL10	<i>ribosomal protein L10</i>	9	9	7	7	32	14	15	17	14	60	0.49
GLUD1	<i>glutamate dehydrogenase 1</i>	7	6	0	0	13	0	0	3	5	8	0.49
SLC2A1	<i>solute carrier family 2 member 1</i>	6	0	4	0	10	0	0	3	2	5	0.49
C22orf28	<i>RNA 2',3'-cyclic phosphate and 5'-OH ligase</i>	6	4	7	7	24	6	7	10	12	35	0.49
PSMC6	<i>proteasome 26S subunit, ATPase 6</i>	5	4	2	3	14	0	2	4	6	12	0.49

RPL36	<i>ribosomal protein L36</i>	5	5	4	6	20	9	8	7	9	33	0.49
MYO1C	<i>myosin IC</i>	4	0	6	7	17	8	5	0	6	19	0.49
PRPS2	<i>phosphoribosyl pyrophosphate synthetase 2</i>	4	7	4	0	15	4	6	5	6	21	0.49
PSMC1	<i>proteasome 26S subunit, ATPase 1</i>	4	4	7	9	24	6	7	8	12	33	0.49
MRT04	<i>MRT4 homolog, ribosome maturation factor</i>	3	0	3	4	10	3	2	0	3	8	0.49
PRKACB	<i>protein kinase cAMP-activated catalytic subunit beta</i>	3	0	3	3	9	3	0	0	0	3	0.49
MAGED2	<i>MAGE family member D2</i>	2	4	5	2	13	5	2	4	4	15	0.49
ATP1A1	<i>ATPase Na⁺/K⁺ transporting subunit alpha 1</i>	2	3	2	2	9	2	3	0	0	5	0.49
ZNF622	<i>zinc finger protein 622</i>	2	4	3	0	9	0	3	0	0	3	0.49
TAF15	<i>TATA-box binding protein associated factor 15</i>	0	0	7	5	12	0	0	4	3	7	0.49
ABCF2	<i>ATP binding cassette subfamily F member 2</i>	11	10	21	15	57	34	32	31	24	121	0.5
LBR	<i>lamin B receptor</i>	8	0	5	7	20	7	8	7	9	31	0.5
RAB34	<i>RAB34, member RAS oncogene family</i>	7	0	5	3	15	6	4	3	0	13	0.5
G6PD	<i>glucose-6-phosphate dehydrogenase</i>	7	7	16	11	41	20	23	18	15	76	0.5
YBX1	<i>Y-box binding protein 1</i>	6	4	7	9	26	13	11	3	12	39	0.5
GRWD1	<i>glutamate rich WD repeat containing 1</i>	6	5	8	7	26	8	10	11	13	42	0.5
KDELR2	<i>KDEL endoplasmic reticulum protein retention receptor 2</i>	6	4	2	0	12	0	2	3	4	9	0.5
RPL27A	<i>ribosomal protein L27a</i>	6	7	8	6	27	12	13	13	10	48	0.5
ACTBL2	<i>actin beta like 2</i>	5	0	4	3	12	4	0	0	2	6	0.5
DSP	<i>desmoplakin</i>	4	9	16	10	39	5	3	9	23	40	0.5
C19orf21	<i>mitotic spindle positioning</i>	4	2	8	12	26	7	8	12	13	40	0.5
SF3B1	<i>splicing factor 3b subunit 1</i>	4	6	4	6	20	3	7	7	9	26	0.5
RPS5	<i>ribosomal protein S5</i>	2	3	2	3	10	0	3	0	0	3	0.5
NUP160	<i>nucleoporin 160</i>	0	4	4	4	12	0	0	0	4	4	0.5
BZW1	<i>basic leucine zipper and W2 domains 1</i>	0	2	5	7	14	4	4	4	0	12	0.5
AP3S1	<i>adaptor related protein complex 3 subunit sigma 1</i>	0	0	6	6	12	3	4	0	0	7	0.5

XPO1	<i>exportin 1</i>	14	16	19	16	65	12	10	20	37	79	0.51
PABPC4	<i>poly(A) binding protein cytoplasmic 4</i>	12	0	7	6	25	8	10	9	12	39	0.51
EIF2A	<i>eukaryotic translation initiation factor 2A</i>	9	7	9	12	37	14	13	6	19	52	0.51
MYO1B	<i>myosin 1B</i>	8	4	5	3	20	3	3	4	8	18	0.51
EIF2S1	<i>eukaryotic translation initiation factor 2 subunit alpha</i>	7	6	10	6	29	12	9	14	9	44	0.51
RAB32	<i>RAB32, member RAS oncogene family</i>	7	6	9	8	30	10	0	12	14	36	0.51
EIF3G	<i>eukaryotic translation initiation factor 3 subunit G</i>	5	4	0	5	14	4	0	0	3	7	0.51
DDX54	<i>DEAD-box helicase 54</i>	5	6	3	7	21	7	9	5	5	26	0.51
CDC5L	<i>cell division cycle 5 like</i>	5	2	2	4	13	3	0	0	4	7	0.51
EIF5B	<i>eukaryotic translation initiation factor 5B</i>	5	7	3	13	28	14	10	6	11	41	0.51
ARL8B	<i>ADP ribosylation factor like GTPase 8B</i>	5	6	4	5	20	8	3	4	5	20	0.51
HSD17B12	<i>hydroxysteroid 17-beta dehydrogenase 12</i>	5	6	6	9	26	3	8	12	6	29	0.51
TRIM25	<i>tripartite motif containing 25</i>	4	3	4	3	14	0	2	4	4	10	0.51
SLC16A1	<i>solute carrier family 16 member 1</i>	4	4	3	7	18	3	4	7	5	19	0.51
EFTUD2	<i>elongation factor Tu GTP binding domain containing 2</i>	4	4	4	4	16	4	3	5	5	17	0.51
HLTF	<i>helicase like transcription factor</i>	3	3	5	0	11	0	0	0	3	3	0.51
LDHB	<i>lactate dehydrogenase B</i>	3	4	3	4	14	2	2	3	4	11	0.51
KPNB1	<i>karyopherin subunit beta 1</i>	15	14	10	15	54	25	25	24	28	102	0.52
EIF3F	<i>eukaryotic translation initiation factor 3 subunit F</i>	11	10	8	10	39	19	14	16	13	62	0.52
NDUFA9	<i>NADH:ubiquinone oxidoreductase subunit A9</i>	9	8	4	6	27	8	6	11	7	32	0.52
EWSR1	<i>EWS RNA binding protein 1</i>	9	7	8	6	30	13	12	11	7	43	0.52
SLC25A6	<i>solute carrier family 25 member 6</i>	8	5	9	12	34	10	15	6	6	37	0.52
RBBP7	<i>RB binding protein 7, chromatin remodeling factor</i>	7	4	5	4	20	5	4	7	7	23	0.52
PARP1	<i>poly(ADP-ribose) polymerase 1</i>	7	10	6	5	28	10	10	11	9	40	0.52
USP10	<i>ubiquitin specific peptidase 10</i>	6	6	6	3	21	5	6	6	8	25	0.52
PICALM	<i>phosphatidylinositol binding clathrin assembly protein</i>	5	5	5	5	20	3	3	6	6	18	0.52

XRN2	<i>5'-3' exoribonuclease 2</i>	5	3	5	4	17	2	3	4	5	14	0.52
DDX6	<i>DEAD-box helicase 6</i>	5	9	7	6	27	6	3	8	12	29	0.52
PURA	<i>purine rich element binding protein A</i>	4	0	5	6	15	0	0	0	4	4	0.52
IGF2BP1	<i>insulin like growth factor 2 mRNA binding protein 1</i>	3	2	5	9	19	4	2	2	6	14	0.52
HSDL2	<i>hydroxysteroid dehydrogenase like 2</i>	3	5	6	6	20	6	5	4	6	21	0.52
NDUFS1	<i>NADH:ubiquinone oxidoreductase core subunit S1</i>	2	2	5	6	15	3	0	2	4	9	0.52
HADHB	<i>hydroxyacyl-CoA dehydrogenase trifunctional multienzyme complex subunit beta</i>	2	4	5	4	15	2	0	2	4	8	0.52
HIST1H2AA	<i>histone cluster 1 H2A family member a</i>	0	0	0	26	26	9	0	0	0	9	0.52
PABPC1	<i>poly(A) binding protein cytoplasmic 1</i>	20	10	11	8	49	18	24	18	16	76	0.53
RUVBL1	<i>RuvB like AAA ATPase 1</i>	20	18	19	17	74	39	39	27	36	141	0.53
CCT2	<i>chaperonin containing TCP1 subunit 2</i>	17	15	12	13	57	23	16	22	29	90	0.53
RPS3A	<i>ribosomal protein S3A</i>	12	9	15	14	50	18	15	25	17	75	0.53
RPL38	<i>ribosomal protein L38</i>	11	8	7	9	35	9	11	15	14	49	0.53
ETF1	<i>eukaryotic translation termination factor 1</i>	10	9	14	14	47	17	19	22	14	72	0.53
EIF3B	<i>eukaryotic translation initiation factor 3 subunit B</i>	9	3	8	10	30	11	12	5	11	39	0.53
FTSJ3	<i>FtsJ RNA 2'-O-methyltransferase 3</i>	9	6	7	9	31	10	8	4	13	35	0.53
RAB13	<i>RAB13, member RAS oncogene family</i>	7	3	6	7	23	3	5	7	0	15	0.53
TMEM33	<i>transmembrane protein 33</i>	7	6	8	5	26	7	5	9	8	29	0.53
NUP205	<i>nucleoporin 205</i>	7	6	12	3	28	7	3	5	11	26	0.53
TIMM23	<i>translocase of inner mitochondrial membrane 23</i>	6	9	7	5	27	6	0	10	10	26	0.53
PCID2	<i>PCI domain containing 2</i>	5	8	8	4	25	7	5	7	8	27	0.53
NXF1	<i>nuclear RNA export factor 1</i>	5	4	5	8	22	3	4	7	4	18	0.53
RPP30	<i>ribonuclease P/MRP subunit p30</i>	5	5	8	5	23	4	5	6	7	22	0.53
ACSL3	<i>acyl-CoA synthetase long chain family member 3</i>	5	0	9	8	22	3	3	6	0	12	0.53
MSH6	<i>mutS homolog 6</i>	4	6	8	12	30	2	5	6	11	24	0.53

CKAP4	<i>cytoskeleton associated protein 4</i>	4	8	6	5	23	6	7	6	3	22	0.53
RPS7	<i>ribosomal protein S7</i>	37	37	33	39	146	61	57	64	84	266	0.54
CHD4	<i>chromodomain helicase DNA binding protein 4</i>	14	12	12	9	47	16	10	16	20	62	0.54
RPS27	<i>ribosomal protein S27</i>	14	10	14	14	52	7	9	22	7	45	0.54
RPS13	<i>ribosomal protein S13</i>	11	6	10	4	31	11	7	10	8	36	0.54
NCAPH	<i>non-SMC condensin I complex subunit H</i>	11	6	10	8	35	10	9	9	14	42	0.54
CCT7	<i>chaperonin containing TCP1 subunit 7</i>	10	7	7	5	29	9	7	8	9	33	0.54
TUBB3	<i>tubulin beta 3 class III</i>	10	6	4	8	28	0	7	8	9	24	0.54
PPP2R1A	<i>protein phosphatase 2 scaffold subunit Aalpha</i>	10	6	9	3	28	7	8	5	8	28	0.54
PELO	<i>pelota mRNA surveillance and ribosome rescue factor</i>	8	8	7	6	29	6	8	7	6	27	0.54
NUP93	<i>nucleoporin 93</i>	8	8	21	13	50	12	12	12	23	59	0.54
MATR3	<i>matrin 3</i>	8	8	9	6	31	2	3	3	9	17	0.54
SUPT16H	<i>SPT16 homolog, facilitates chromatin remodeling subunit</i>	8	6	6	9	29	6	10	8	8	32	0.54
SRP14	<i>signal recognition particle 14</i>	8	8	8	8	32	9	9	7	4	29	0.54
VARS	<i>valyl-tRNA synthetase</i>	7	10	9	6	32	7	7	10	6	30	0.54
AP3B1	<i>adaptor related protein complex 3 subunit beta 1</i>	5	4	15	10	34	13	11	8	12	44	0.54
PTPLAD1	<i>3-hydroxyacyl-CoA dehydratase 3</i>	3	5	9	6	23	0	0	4	6	10	0.54
U2AF2	<i>U2 small nuclear RNA auxiliary factor 2</i>	3	6	9	5	23	0	0	0	6	6	0.54
RFC5	<i>replication factor C subunit 5</i>	3	4	9	7	23	5	4	6	3	18	0.54
TUBA4A	<i>tubulin alpha 4a</i>	20	22	9	5	56	15	13	23	22	73	0.55
CCT5	<i>chaperonin containing TCP1 subunit 5</i>	14	18	17	17	66	29	26	27	27	109	0.55
NOP58	<i>NOP58 ribonucleoprotein</i>	13	12	12	7	44	9	16	7	9	41	0.55
PFKP	<i>phosphofructokinase, platelet</i>	12	10	18	18	58	14	21	25	21	81	0.55
TECR	<i>trans-2,3-enoyl-CoA reductase</i>	12	12	9	11	44	13	16	15	13	57	0.55
BAZ1B	<i>bromodomain adjacent to zinc finger domain 1B</i>	11	4	9	9	33	3	2	5	10	20	0.55
RPL31	<i>ribosomal protein L31</i>	11	12	11	12	46	15	14	17	15	61	0.55
HNRNPR	<i>heterogeneous nuclear</i>	10	11	6	7	34	9	5	4	3	21	0.55

<i>ribonucleoprotein R</i>												
G3BP2	<i>G3BP stress granule assembly factor 2</i>	10	9	6	13	38	11	10	12	11	44	0.55
CUL4A	<i>cullin 4A</i>	9	8	13	9	39	12	8	13	12	45	0.55
ARL2	<i>ADP ribosylation factor like GTPase 2</i>	9	6	11	9	35	4	2	10	9	25	0.55
EEF1G	<i>eukaryotic translation elongation factor 1 gamma</i>	9	11	10	10	40	10	9	13	10	42	0.55
CHORDC1	<i>cysteine and histidine rich domain containing 1</i>	9	7	10	8	34	8	9	0	6	23	0.55
GART	<i>phosphoribosylglycinamide formyltransferase, phosphoribosylglycinamide synthetase, phosphoribosylaminoimidazole synthetase</i>	8	6	13	15	42	5	6	9	14	34	0.55
MCM6	<i>minichromosome maintenance complex component 6</i>	8	8	20	16	52	17	16	21	20	74	0.55
ABCE1	<i>ATP binding cassette subfamily E member 1</i>	8	11	11	9	39	6	7	8	13	34	0.55
MCM5	<i>minichromosome maintenance complex component 5</i>	7	8	12	11	38	11	9	13	10	43	0.55
RPL14	<i>ribosomal protein L14</i>	7	8	10	8	33	8	9	9	6	32	0.55
DDOST	<i>dolichyl-diphosphooligosaccharide-protein glycosyltransferase non-catalytic subunit</i>	7	5	13	9	34	6	3	8	10	27	0.55
RBM39	<i>RNA binding motif protein 39</i>	7	8	10	7	32	8	8	9	8	33	0.55
ESYT2	<i>extended synaptotagmin 2</i>	5	7	13	10	35	10	8	8	8	34	0.55
RUVBL2	<i>RuvB like AAA ATPase 2</i>	25	19	17	24	85	34	39	37	31	141	0.56
RPS15	<i>ribosomal protein S15</i>	20	15	0	13	48	10	8	15	8	41	0.56
HNRNPF	<i>heterogeneous nuclear ribonucleoprotein F</i>	14	0	18	17	49	13	10	11	15	49	0.56
MCM3	<i>minichromosome maintenance complex component 3</i>	13	8	10	13	44	10	13	11	9	43	0.56
RPL11	<i>ribosomal protein L11</i>	13	8	12	11	44	15	10	0	13	38	0.56
AP3M1	<i>adaptor related protein complex 3 subunit mu 1</i>	13	7	17	11	48	7	14	11	11	43	0.56
SMC4	<i>structural maintenance of chromosomes 4</i>	12	16	15	13	56	19	18	15	17	69	0.56
DNAJA1	<i>DnaJ heat shock protein family (Hsp40) member A1</i>	12	17	17	15	61	19	17	19	23	78	0.56

CAPZA2	<i>capping actin protein of muscle Z-line subunit alpha 2</i>	12	10	12	11	45	9	12	7	13	41	0.56
RAB21	<i>RAB21, member RAS oncogene family</i>	11	11	12	12	46	13	11	9	8	41	0.56
PFKM	<i>phosphofructokinase, muscle</i>	11	11	12	18	52	16	14	15	17	62	0.56
TMPO	<i>thymopoietin</i>	10	9	9	10	38	6	6	11	0	23	0.56
EIF2S2	<i>eukaryotic translation initiation factor 2 subunit beta</i>	10	11	8	16	45	13	14	11	8	46	0.56
DHFR	<i>dihydrofolate reductase</i>	9	8	14	12	43	10	10	12	11	43	0.56
RAB9A	<i>RAB9A, member RAS oncogene family</i>	9	10	15	11	45	6	8	7	12	33	0.56
RPL22	<i>ribosomal protein L22</i>	9	11	15	11	46	6	8	8	13	35	0.56
PPA1	<i>pyrophosphatase (inorganic) 1</i>	9	8	13	8	38	6	4	10	7	27	0.56
SLC1A5	<i>solute carrier family 1 member 5</i>	8	8	11	11	38	8	10	7	8	33	0.56
DDX18	<i>DEAD-box helicase 18</i>	7	10	10	10	37	10	10	7	8	35	0.56
ANXA2	<i>annexin A2</i>	36	33	29	25	123	54	53	59	48	214	0.57
RPS4X	<i>ribosomal protein S4 X-linked</i>	29	19	24	18	90	37	34	35	33	139	0.57
NAP1L1	<i>nucleosome assembly protein 1 like 1</i>	27	20	20	23	90	32	33	26	34	125	0.57
CCT4	<i>chaperonin containing TCP1 subunit 4</i>	27	22	34	33	116	34	31	48	40	153	0.57
SET	<i>SET nuclear proto-oncogene</i>	26	20	17	21	84	28	31	27	23	109	0.57
RPS6	<i>ribosomal protein S6</i>	22	22	21	22	87	25	30	36	26	117	0.57
PCBP1	<i>poly(rC) binding protein 1</i>	20	21	22	30	93	19	21	29	40	109	0.57
RPL5	<i>ribosomal protein L5</i>	19	21	19	15	74	28	20	26	26	100	0.57
RPL17	<i>ribosomal protein L17</i>	18	13	18	16	65	14	18	21	17	70	0.57
NAP1L4	<i>nucleosome assembly protein 1 like 4</i>	18	21	15	20	74	25	21	27	25	98	0.57
HNRNPC	<i>heterogeneous nuclear ribonucleoprotein C (C1/C2)</i>	18	17	11	16	62	21	15	19	16	71	0.57
ILF2	<i>interleukin enhancer binding factor 2</i>	18	17	12	16	63	16	13	10	12	51	0.57
EIF2S3	<i>eukaryotic translation initiation factor 2 subunit gamma</i>	18	21	22	19	80	31	31	25	27	114	0.57
XRCC6	<i>X-ray repair cross complementing 6</i>	17	16	16	13	62	14	8	13	18	53	0.57
SURF4	<i>surfeit 4</i>	15	18	25	15	73	12	15	21	25	73	0.57
HSD17B10	<i>hydroxysteroid 17-beta</i>	14	11	15	16	56	14	7	8	15	44	0.57

dehydrogenase 10

MARS	<i>methionyl-tRNA synthetase</i>	13	16	19	25	73	9	12	11	22	54	0.57
RPL10A	<i>ribosomal protein L10a</i>	12	14	10	13	49	6	11	13	14	44	0.57
SMC2	<i>structural maintenance of chromosomes 2</i>	12	14	25	27	78	25	23	27	26	101	0.57
RAB5C	<i>RAB5C, member RAS oncogene family</i>	12	14	12	15	53	11	12	9	14	46	0.57
NSUN2	<i>NOP2/Sun RNA methyltransferase 2</i>	10	12	14	14	50	12	7	11	15	45	0.57
GAPDH	<i>glyceraldehyde-3-phosphate dehydrogenase</i>	40	43	34	33	150	50	41	57	57	205	0.58
PCBP2	<i>poly(rC) binding protein 2</i>	35	31	33	25	124	30	29	37	41	137	0.58
CTPS	<i>CTP synthase 1</i>	34	37	44	40	155	52	42	55	56	205	0.58
CFL1	<i>cofilin 1</i>	32	26	29	27	114	33	38	39	33	143	0.58
CAND1	<i>cullin associated and neddylation dissociated 1</i>	32	27	30	27	116	25	22	39	36	122	0.58
CDK1	<i>cyclin dependent kinase 1</i>	32	25	29	34	120	47	30	33	45	155	0.58
RPS9	<i>ribosomal protein S9</i>	31	20	33	27	111	18	30	24	22	94	0.58
DDX39B	<i>DEAD-box helicase 39B</i>	30	22	29	31	112	30	26	30	21	107	0.58
HNRNPA1	<i>heterogeneous nuclear ribonucleoprotein A1</i>	30	31	29	27	117	22	25	31	17	95	0.58
COPB1	<i>coatomer protein complex subunit beta 1</i>	29	25	40	41	135	34	26	33	43	136	0.58
DDX5	<i>DEAD-box helicase 5</i>	27	23	35	29	114	31	22	27	29	109	0.58
RPN2	<i>ribophorin II</i>	27	26	21	21	95	25	27	25	30	107	0.58
HSPA5	<i>heat shock protein family A (Hsp70) member 5</i>	26	19	32	33	110	20	24	36	27	107	0.58
TUBB6	<i>tubulin beta 6 class V</i>	25	25	36	28	114	27	25	26	40	118	0.58
IQGAP1	<i>IQ motif containing GTPase activating protein 1</i>	25	26	27	36	114	24	21	20	32	97	0.58
TUBB4B	<i>tubulin beta 4B class IVb</i>	24	16	29	26	95	34	23	31	24	112	0.58
HNRNPK	<i>heterogeneous nuclear ribonucleoprotein K</i>	22	24	22	21	89	17	16	23	20	76	0.58
RPL23	<i>ribosomal protein L23</i>	22	18	35	38	113	32	39	39	40	150	0.58
MCM4	<i>minichromosome maintenance complex component 4</i>	21	21	30	27	99	23	18	30	34	105	0.58
PHB	<i>prohibitin</i>	20	19	25	22	86	22	17	16	17	72	0.58

NAMPT	<i>nicotinamide phosphoribosyltransferase</i>	20	25	31	27	103	23	21	27	36	107	0.58
GNL3	<i>G protein nucleolar 3</i>	15	18	21	23	77	19	21	17	22	79	0.58
FLNA	<i>filamin A</i>	454	444	247	225	1370	759	724	695	673	2851	0.59
EEF1A1	<i>eukaryotic translation elongation factor 1 alpha 1</i>	132	141	157	134	564	116	101	146	154	517	0.59
VIM	<i>vimentin</i>	129	137	126	130	522	219	214	213	225	871	0.59
PKM2	<i>pyruvate kinase M1/2</i>	114	115	97	97	423	123	107	117	125	472	0.59
RPS3	<i>ribosomal protein S3</i>	81	81	95	101	358	95	68	79	69	311	0.59
HIST1H2BB	<i>histone cluster 1 H2B family member b</i>	66	54	72	64	256	67	58	55	69	249	0.59
HIST1H2BD	<i>histone cluster 1 H2B family member d</i>	63	55	69	64	251	66	58	54	69	247	0.59
RPS2	<i>ribosomal protein S2</i>	63	56	55	59	233	55	61	55	62	233	0.59
RPL9	<i>ribosomal protein L9</i>	55	51	59	56	221	57	54	64	70	245	0.59
RPL3	<i>ribosomal protein L3</i>	54	50	55	64	223	58	56	56	69	239	0.59
RPS15A	<i>ribosomal protein S15a</i>	52	49	39	49	189	46	32	61	57	196	0.59
MCM7	<i>minichromosome maintenance complex component 7</i>	50	46	68	63	227	57	48	59	66	230	0.59
RPS8	<i>ribosomal protein S8</i>	49	46	44	42	181	54	61	58	52	225	0.59
RPL4	<i>ribosomal protein L4</i>	46	47	51	44	188	47	48	44	44	183	0.59
DDX39A	<i>DEAD-box helicase 39A</i>	45	32	44	44	165	40	34	49	32	155	0.59
CCT3	<i>chaperonin containing TCP1 subunit 3</i>	41	37	34	43	155	43	33	33	34	143	0.59
DDX3X	<i>DEAD-box helicase 3 X-linked</i>	41	41	37	34	153	47	45	44	46	182	0.59
NONO	<i>non-POU domain containing octamer binding</i>	38	31	46	52	167	61	59	52	60	232	0.59
GNB2L1	<i>receptor for activated C kinase 1</i>	37	37	43	42	159	32	38	41	35	146	0.59
CCT6A	<i>chaperonin containing TCP1 subunit 6A</i>	37	42	51	38	168	35	33	26	43	137	0.59
EPPK1	<i>epiplakin 1</i>	36	29	46	33	144	11	15	20	37	83	0.59
TRIP13	<i>thyroid hormone receptor interactor 13</i>	34	33	42	39	148	31	28	32	43	134	0.59
RPL15	<i>ribosomal protein L15</i>	30	29	33	33	125	34	35	25	25	119	0.59
EIF4A3	<i>eukaryotic translation initiation factor 4A3</i>	26	29	32	33	120	26	17	32	31	106	0.59

PC	<i>pyruvate carboxylase</i>	3243	3361	3762	3361	13727	1543	1500	1645	1679	6367	0.6
SAV_STR AV	<i>Streptavidin</i>	1125	1032	958	1022	4137	298	314	341	367	1320	0.6
PCCA	<i>propionyl-CoA carboxylase subunit alpha</i>	732	738	756	686	2912	236	225	295	244	1000	0.6
ACACB	<i>acetyl-CoA carboxylase beta</i>	713	697	749	685	2844	133	144	170	194	641	0.6
MCCC1	<i>methylcrotonoyl-CoA carboxylase 1</i>	431	419	348	328	1526	230	217	248	260	955	0.6
PCCB	<i>propionyl-CoA carboxylase subunit beta</i>	398	439	474	397	1708	177	169	192	228	766	0.6
MCCC2	<i>methylcrotonoyl-CoA carboxylase 2</i>	294	271	264	236	1065	101	94	117	106	418	0.6
CPS1	<i>carbamoyl-phosphate synthase 1</i>	273	245	309	307	1134	166	151	153	185	655	0.6
ASS1	<i>argininosuccinate synthase 1</i>	184	175	228	207	794	68	63	97	108	336	0.6
ENO1	<i>enolase 1</i>	144	148	161	167	620	112	97	97	102	408	0.6
HSP90AB 1	<i>heat shock protein 90 alpha family class B member 1</i>	134	122	152	138	546	94	83	98	83	358	0.6
PLEC	<i>plectin</i>	128	110	137	129	504	63	55	57	75	250	0.6
ATP5A1	<i>ATP synthase F1 subunit alpha</i>	124	109	136	137	506	85	82	92	77	336	0.6
PRKDC	<i>protein kinase, DNA-activated, catalytic subunit</i>	114	102	138	127	481	71	62	65	69	267	0.6
HSPA9	<i>heat shock protein family A (Hsp70) member 9</i>	114	108	108	112	442	84	84	81	85	334	0.6
HSPA8	<i>heat shock protein family A (Hsp70) member 8</i>	114	105	121	115	455	100	92	109	98	399	0.6
ACTG1	<i>actin gamma 1</i>	109	121	123	145	498	64	67	63	0	194	0.6
TCP1	<i>t-complex 1</i>	95	89	109	100	393	68	65	69	79	281	0.6
DYNC1H1	<i>dynein cytoplasmic 1 heavy chain 1</i>	94	82	100	109	385	49	37	42	65	193	0.6
DHX9	<i>DExH-box helicase 9</i>	89	86	88	89	352	34	33	34	33	134	0.6
EEF2	<i>eukaryotic translation elongation factor 2</i>	89	80	77	58	304	47	58	62	51	218	0.6
PTBP1	<i>polypyrimidine tract binding protein 1</i>	77	69	62	55	263	37	31	29	50	147	0.6
HSPA1B	<i>heat shock protein family A (Hsp70) member 1B</i>	76	77	81	83	317	46	47	49	45	187	0.6
HSP90AA 1	<i>heat shock protein 90 alpha family class A member 1</i>	75	71	86	93	325	56	49	65	54	224	0.6
NPM1	<i>nucleophosmin 1</i>	70	62	69	74	275	45	46	67	63	221	0.6
RAN	<i>RAN, member RAS oncogene family</i>	68	76	88	70	302	67	56	53	66	242	0.6

EIF4A1	<i>eukaryotic translation initiation factor 4A1</i>	67	65	99	89	320	69	53	69	60	251	0.6
AHSA1	<i>activator of HSP90 ATPase activity 1</i>	67	53	59	69	248	43	35	42	43	163	0.6
HSPD1	<i>heat shock protein family D (Hsp60) member 1</i>	65	63	49	60	237	27	21	16	31	95	0.6
ALDH18A1	<i>aldehyde dehydrogenase 18 family member A1</i>	65	61	74	70	270	42	35	39	42	158	0.6
SERPINH1	<i>serpin family H member 1</i>	64	59	74	67	264	33	28	46	48	155	0.6
TUFM	<i>Tu translation elongation factor, mitochondrial</i>	63	55	60	65	243	41	43	48	48	180	0.6
TUBB	<i>tubulin beta class I</i>	63	70	88	76	297	47	52	67	73	239	0.6
ACACA	<i>acetyl-CoA carboxylase alpha</i>	62	59	1889	41	2051	559	494	649	666	2368	0.6
HNRNPU	<i>heterogeneous nuclear ribonucleoprotein U</i>	61	64	53	59	237	42	38	52	46	178	0.6
TRAP1	<i>TNF receptor associated protein 1</i>	56	54	58	60	228	33	23	24	32	112	0.6
RPL6	<i>ribosomal protein L6</i>	55	45	61	46	207	50	42	41	39	172	0.6
HSPB1	<i>heat shock protein family B (small) member 1</i>	55	48	48	55	206	20	18	15	20	73	0.6
PRDX1	<i>peroxiredoxin 1</i>	53	49	46	43	191	43	25	31	31	130	0.6
ATP5B	<i>ATP synthase F1 subunit beta</i>	52	61	49	50	212	31	32	33	47	143	0.6
PHB2	<i>prohibitin 2</i>	51	54	60	53	218	35	39	36	31	141	0.6
HNRNPM	<i>heterogeneous nuclear ribonucleoprotein M</i>	50	49	46	53	198	30	29	38	35	132	0.6
SYNCRIP	<i>synaptotagmin binding cytoplasmic RNA interacting protein</i>	48	42	40	42	172	30	28	26	34	118	0.6
DDX21	<i>DEXD-box helicase 21</i>	48	56	49	42	195	39	30	34	36	139	0.6
LARS	<i>leucyl-tRNA synthetase</i>	46	31	48	54	179	25	27	30	26	108	0.6
NCL	<i>nucleolin</i>	45	44	36	37	162	11	9	9	12	41	0.6
IARS	<i>isoleucyl-tRNA synthetase</i>	45	37	48	58	188	18	25	26	31	100	0.6
PLOD1	<i>procollagen-lysine,2-oxoglutarate 5-dioxygenase 1</i>	44	42	39	38	163	8	7	7	9	31	0.6
SFPQ	<i>splicing factor proline and glutamine rich</i>	43	37	41	39	160	25	20	25	26	96	0.6
NUP214	<i>nucleoporin 214</i>	41	48	37	32	158	20	10	11	15	56	0.6
HNRNPH1	<i>heterogeneous nuclear ribonucleoprotein H1</i>	41	37	46	45	169	22	23	23	23	91	0.6

HNRNPA2 B1	<i>heterogeneous nuclear ribonucleoprotein A2/B1</i>	40	43	44	38	165	16	17	20	17	70	0.6
SND1	<i>staphylococcal nuclease and tudor domain containing 1</i>	40	38	40	42	160	20	20	17	27	84	0.6
G3BP1	<i>G3BP stress granule assembly factor 1</i>	39	27	30	31	127	23	25	25	30	103	0.6
HIST1H1 C	<i>histone cluster 1 H1 family member c</i>	39	38	48	42	167	20	24	0	0	44	0.6
EPRS	<i>glutamyl-prolyl-tRNA synthetase</i>	39	43	42	42	166	19	20	22	32	93	0.6
CLTC	<i>clathrin heavy chain</i>	38	34	41	40	153	14	13	15	16	58	0.6
PSMD3	<i>proteasome 26S subunit, non-ATPase 3</i>	35	32	41	34	142	27	22	27	25	101	0.6
RPS24	<i>ribosomal protein S24</i>	35	33	32	36	136	23	16	25	17	81	0.6
SLC3A2	<i>solute carrier family 3 member 2</i>	35	32	33	36	136	8	7	6	5	26	0.6
HIST1H4J	<i>histone cluster 1 H4 family member j</i>	35	38	43	37	153	34	27	27	29	117	0.6
VDAC2	<i>voltage dependent anion channel 2</i>	33	31	26	35	125	25	21	22	17	85	0.6
RPL7A	<i>ribosomal protein L7a</i>	33	32	36	35	136	30	32	34	34	130	0.6
RAB14	<i>RAB14, member RAS oncogene family</i>	32	25	35	35	127	20	20	18	24	82	0.6
NUMA1	<i>nuclear mitotic apparatus protein 1</i>	32	25	29	31	117	24	13	14	16	67	0.6
MTHFD1	<i>methylenetetrahydrofolate dehydrogenase, cyclohydrolase and formyltetrahydrofolate synthetase 1</i>	32	24	25	29	110	26	20	18	21	85	0.6
RPN1	<i>ribophorin 1</i>	31	20	24	18	93	17	16	15	22	70	0.6
RPL21	<i>ribosomal protein L21</i>	31	32	32	33	128	18	16	14	16	64	0.6
LMNA	<i>lamin A/C</i>	30	27	36	44	137	27	31	25	16	99	0.6
VDAC1	<i>voltage dependent anion channel 1</i>	30	25	34	29	118	13	11	17	16	57	0.6
FUS	<i>FUS RNA binding protein</i>	29	29	21	15	94	14	13	14	13	54	0.6
HSP90B1	<i>heat shock protein 90 beta family member 1</i>	29	23	37	29	118	12	9	8	9	38	0.6
ARF1	<i>ADP ribosylation factor 1</i>	29	21	25	22	97	20	16	18	16	70	0.6
ATP2A2	<i>ATPase sarcoplasmic/endoplasmic reticulum Ca²⁺ transporting 2</i>	29	23	32	35	119	19	17	19	29	84	0.6
NAT10	<i>N-acetyltransferase 10</i>	29	34	37	28	128	17	16	16	14	63	0.6
UQCRC2	<i>ubiquinol-cytochrome c reductase core protein 2</i>	29	31	38	41	139	27	23	27	28	105	0.6

LRPPRC	<i>leucine rich pentatricopeptide repeat containing</i>	28	25	14	7	74	3	0	0	4	7	0.6
SLC25A5	<i>solute carrier family 25 member 5</i>	28	39	37	31	135	32	24	22	18	96	0.6
RPS16	<i>ribosomal protein S16</i>	27	21	31	27	106	21	21	20	15	77	0.6
XPOT	<i>exportin for tRNA</i>	27	26	40	42	135	25	15	20	26	86	0.6
RPL7	<i>ribosomal protein L7</i>	27	25	34	35	121	24	22	26	21	93	0.6
DDX17	<i>DEAD-box helicase 17</i>	27	22	34	32	115	23	15	18	15	71	0.6
RAB2A	<i>RAB2A, member RAS oncogene family</i>	27	28	34	30	119	13	14	21	19	67	0.6
VDAC3	<i>voltage dependent anion channel 3</i>	26	24	25	31	106	13	14	17	16	60	0.6
RPL23A	<i>ribosomal protein L23a</i>	26	24	24	28	102	23	23	20	20	86	0.6
HNRNPL	<i>heterogeneous nuclear ribonucleoprotein L</i>	25	25	16	20	86	10	8	4	8	30	0.6
RBM14	<i>RNA binding motif protein 14</i>	25	26	24	33	108	11	12	10	8	41	0.6
RPS14	<i>ribosomal protein S14</i>	25	27	28	29	109	14	19	16	18	67	0.6
SLC25A13	<i>solute carrier family 25 member 13</i>	25	22	26	30	103	22	24	18	25	89	0.6
TOMM40	<i>translocase of outer mitochondrial membrane 40</i>	24	17	16	20	77	6	6	7	14	33	0.6
RAB7A	<i>RAB7A, member RAS oncogene family</i>	24	24	20	24	92	11	9	10	4	34	0.6
AP3D1	<i>adaptor related protein complex 3 subunit delta 1</i>	23	16	13	16	68	10	5	6	8	29	0.6
LDHA	<i>lactate dehydrogenase A</i>	23	13	12	8	56	13	9	13	9	44	0.6
DHX15	<i>DEAH-box helicase 15</i>	23	13	25	30	91	22	14	16	19	71	0.6
RPL13A	<i>ribosomal protein L13a</i>	22	16	21	21	80	12	13	13	8	46	0.6
SLC25A3	<i>solute carrier family 25 member 3</i>	21	23	26	20	90	8	10	9	12	39	0.6
COPG1	<i>coatamer protein complex subunit gamma 1</i>	21	22	27	28	98	14	10	16	24	64	0.6
ILF3	<i>interleukin enhancer binding factor 3</i>	21	20	14	22	77	13	11	15	11	50	0.6
ATAD3A	<i>ATPase family AAA domain containing 3A</i>	21	16	8	13	58	5	4	10	4	23	0.6
RAB6A	<i>RAB6A, member RAS oncogene family</i>	21	19	19	21	80	14	14	12	11	51	0.6
RPLP2	<i>ribosomal protein lateral stalk subunit P2</i>	21	17	14	19	71	12	7	13	9	41	0.6
SLC25A11	<i>solute carrier family 25 member 11</i>	21	21	20	18	80	6	7	7	7	27	0.6

TKT	<i>transketolase</i>	20	12	25	22	79	13	10	5	7	35	0.6
BRIX1	<i>biogenesis of ribosomes BRX1</i>	19	17	19	20	75	0	0	0	5	5	0.6
HIST1H1B	<i>histone cluster 1 H1 family member b</i>	19	17	23	17	76	11	14	13	10	48	0.6
RSL1D1	<i>ribosomal L1 domain containing 1</i>	19	22	17	16	74	10	10	7	7	34	0.6
PA2G4	<i>proliferation-associated 2G4</i>	19	20	17	25	81	4	3	9	8	24	0.6
C1QBP	<i>complement C1q binding protein</i>	19	17	25	23	84	21	14	15	15	65	0.6
PDCD6IP	<i>programmed cell death 6 interacting protein</i>	19	15	21	22	77	17	18	17	18	70	0.6
PRDX6	<i>peroxiredoxin 6</i>	19	22	18	17	76	8	5	0	8	21	0.6
CANX	<i>calnexin</i>	19	19	20	18	76	6	7	4	3	20	0.6
RPL13	<i>ribosomal protein L13</i>	18	13	16	15	62	15	11	15	14	55	0.6
RPL26	<i>ribosomal protein L26</i>	18	13	17	23	71	13	10	9	7	39	0.6
HNRNPH2	<i>heterogeneous nuclear ribonucleoprotein H2</i>	18	15	21	20	74	0	12	13	12	37	0.6
CAD	<i>carbamoyl-phosphate synthetase 2, aspartate transcarbamylase, and dihydroorotase</i>	18	19	31	31	99	4	3	5	6	18	0.6
TOMM22	<i>translocase of outer mitochondrial membrane 22</i>	18	17	20	21	76	12	12	17	16	57	0.6
ACOT9	<i>acyl-CoA thioesterase 9</i>	18	16	24	19	77	4	3	8	5	20	0.6
SSR4	<i>signal sequence receptor subunit 4</i>	18	20	22	25	85	8	8	13	14	43	0.6
GARS	<i>glycyl-tRNA synthetase</i>	18	16	15	13	62	0	0	2	4	6	0.6
RPL12	<i>ribosomal protein L12</i>	18	18	18	14	68	14	11	16	12	53	0.6
ATP5C1	<i>ATP synthase F1 subunit gamma</i>	17	19	25	21	82	15	14	16	12	57	0.6
RPL27	<i>ribosomal protein L27</i>	17	14	16	15	62	7	4	5	4	20	0.6
PRDX2	<i>peroxiredoxin 2</i>	17	20	13	13	63	12	6	11	12	41	0.6
HNRNPA0	<i>heterogeneous nuclear ribonucleoprotein A0</i>	17	18	21	21	77	17	17	11	17	62	0.6
DDX1	<i>DEAD-box helicase 1</i>	17	14	21	22	74	7	10	10	18	45	0.6
FBL	<i>fibrillarlin</i>	17	16	19	19	71	13	14	12	14	53	0.6
PRPF19	<i>pre-mRNA processing factor 19</i>	17	13	13	16	59	12	10	7	6	35	0.6
RPL24	<i>ribosomal protein L24</i>	16	16	18	15	65	14	12	8	7	41	0.6
RPS26	<i>ribosomal protein S26</i>	16	13	13	14	56	9	8	10	13	40	0.6

PHGDH	<i>phosphoglycerate dehydrogenase</i>	16	20	19	17	72	8	9	7	8	32	0.6
RAB1B	<i>RAB1B, member RAS oncogene family</i>	16	29	33	12	90	10	10	21	8	49	0.6
DPM1	<i>dolichyl-phosphate mannosyltransferase subunit 1, catalytic</i>	16	14	18	15	63	10	11	14	11	46	0.6
ALYREF	<i>Aly/REF export factor</i>	16	11	14	13	54	4	7	6	6	23	0.6
COPA	<i>coatamer protein complex subunit alpha</i>	16	15	13	20	64	13	7	10	13	43	0.6
GANAB	<i>glucosidase II alpha subunit</i>	16	10	16	12	54	6	4	3	12	25	0.6
RPLP0	<i>ribosomal protein lateral stalk subunit P0</i>	15	17	19	14	65	13	5	3	7	28	0.6
CLU	<i>clusterin</i>	15	16	20	17	68	3	5	0	0	8	0.6
DNAJA3	<i>DnaJ heat shock protein family (Hsp40) member A3</i>	15	12	19	11	57	11	11	13	13	48	0.6
SMC3	<i>structural maintenance of chromosomes 3</i>	15	15	27	25	82	11	11	15	18	55	0.6
SERBP1	<i>SERPINE1 mRNA binding protein 1</i>	14	15	13	13	55	6	11	11	12	40	0.6
HNRNPA3	<i>heterogeneous nuclear ribonucleoprotein A3</i>	14	9	10	11	44	5	6	3	4	18	0.6
ABCD3	<i>ATP binding cassette subfamily D member 3</i>	14	10	16	21	61	13	7	2	10	32	0.6
RPL8	<i>ribosomal protein L8</i>	14	18	13	20	65	15	11	14	12	52	0.6
FH	<i>fumarate hydratase</i>	14	8	9	7	38	0	0	0	3	3	0.6
H2AFY	<i>H2A histone family member Y</i>	14	11	9	9	43	9	4	9	8	30	0.6
LRRC59	<i>leucine rich repeat containing 59</i>	13	14	13	9	49	6	7	7	7	27	0.6
ABCF1	<i>ATP binding cassette subfamily F member 1</i>	13	11	13	15	52	11	6	6	6	29	0.6
PPP2R2A	<i>protein phosphatase 2 regulatory subunit Balpha</i>	13	13	10	7	43	5	4	2	8	19	0.6
YARS	<i>tyrosyl-tRNA synthetase</i>	12	6	15	16	49	5	0	7	5	17	0.6
RECQL	<i>RecQ like helicase</i>	12	4	7	8	31	6	0	0	7	13	0.6
SFXN1	<i>sideroflexin 1</i>	12	11	28	23	74	5	9	5	10	29	0.6
DDX47	<i>DEAD-box helicase 47</i>	12	16	9	12	49	12	8	10	7	37	0.6
SEC61A1	<i>SEC61 translocon alpha 1 subunit</i>	12	10	14	7	43	7	5	6	8	26	0.6
SMC1A	<i>structural maintenance of chromosomes 1A</i>	12	15	15	15	57	3	3	5	6	17	0.6
KARS	<i>lysyl-tRNA synthetase</i>	11	8	7	11	37	5	4	4	2	15	0.6

ELAVL1	<i>ELAV like RNA binding protein 1</i>	11	16	11	14	52	8	7	10	13	38	0.6
HNRNPD	<i>heterogeneous nuclear ribonucleoprotein D</i>	11	13	13	9	46	8	8	8	7	31	0.6
IPO5	<i>importin 5</i>	11	13	17	11	52	3	2	3	8	16	0.6
PPIA	<i>peptidylprolyl isomerase A</i>	11	5	5	4	25	0	3	5	2	10	0.6
ARF5	<i>ADP ribosylation factor 5</i>	11	7	7	3	28	3	3	2	2	10	0.6
NDUFA10	<i>NADH:ubiquinone oxidoreductase subunit A10</i>	11	12	10	12	45	4	0	0	6	10	0.6
ARF4	<i>ADP ribosylation factor 4</i>	10	8	16	14	48	2	4	11	3	20	0.6
SF3B3	<i>splicing factor 3b subunit 3</i>	10	8	13	13	44	4	0	6	10	20	0.6
ZNF326	<i>zinc finger protein 326</i>	10	9	12	16	47	10	6	4	5	25	0.6
PDCD6	<i>programmed cell death 6</i>	10	12	11	14	47	6	5	5	7	23	0.6
SMARCA5	<i>SWI/SNF related, matrix associated, actin dependent regulator of chromatin, subfamily a, member 5</i>	10	11	8	12	41	8	6	6	2	22	0.6
MKI67	<i>marker of proliferation Ki-67</i>	10	11	9	3	33	5	5	8	8	26	0.6
RBMX	<i>RNA binding motif protein X-linked</i>	10	9	10	8	37	6	0	0	0	6	0.6
CSRP2	<i>cysteine and glycine rich protein 2</i>	10	11	0	0	21	2	3	3	0	8	0.6
DNAJC11	<i>DnaJ heat shock protein family (Hsp40) member C11</i>	10	14	16	13	53	9	9	8	6	32	0.6
RAE1	<i>ribonucleic acid export 1</i>	10	12	8	4	34	4	4	0	5	13	0.6
RPS17	<i>ribosomal protein S17</i>	10	7	8	8	33	2	0	0	0	2	0.6
TARDBP	<i>TAR DNA binding protein</i>	9	10	8	5	32	0	3	0	3	6	0.6
RAB5A	<i>RAB5A, member RAS oncogene family</i>	9	10	9	9	37	8	9	8	7	32	0.6
ARL1	<i>ADP ribosylation factor like GTPase 1</i>	9	6	16	22	53	6	7	7	10	30	0.6
ERLIN2	<i>ER lipid raft associated 2</i>	9	7	8	12	36	2	2	0	7	11	0.6
RPL34	<i>ribosomal protein L34</i>	9	7	9	7	32	5	3	3	0	11	0.6
ARCN1	<i>archain 1</i>	9	9	15	13	46	6	6	6	8	26	0.6
PFKL	<i>phosphofructokinase, liver type</i>	9	5	10	7	31	6	0	4	6	16	0.6
LMNB1	<i>lamin B1</i>	9	11	12	17	49	7	8	6	11	32	0.6
CLPTM1L	<i>CLPTM1 like</i>	8	6	12	11	37	0	0	3	8	11	0.6
CSE1L	<i>chromosome segregation 1 like</i>	8	12	5	6	31	5	5	6	5	21	0.6

IMPA2	<i>inositol monophosphatase 2</i>	8	7	6	5	26	0	2	3	3	8	0.6
ECH1	<i>enoyl-CoA hydratase 1</i>	8	9	7	6	30	3	3	5	5	16	0.6
KHDRBS1	<i>KH RNA binding domain containing, signal transduction associated 1</i>	8	10	14	11	43	4	3	4	5	16	0.6
BLVRA	<i>biliverdin reductase A</i>	8	6	9	6	29	4	3	3	3	13	0.6
RCC2	<i>regulator of chromosome condensation 2</i>	8	7	4	5	24	2	0	2	0	4	0.6
LYAR	<i>Ly1 antibody reactive</i>	8	8	3	2	21	0	0	3	0	3	0.6
DARS	<i>aspartyl-tRNA synthetase</i>	7	8	12	10	37	0	5	5	3	13	0.6
SLC25A10	<i>solute carrier family 25 member 10</i>	7	7	10	13	37	6	6	8	7	27	0.6
RG9MTD1	<i>tRNA methyltransferase 10C, mitochondrial RNase P subunit 1</i>	7	2	6	5	20	2	3	4	5	14	0.6
SRSF7	<i>serine and arginine rich splicing factor 7</i>	7	8	5	4	24	5	6	0	6	17	0.6
RPS28	<i>ribosomal protein S28</i>	7	9	6	8	30	6	7	5	5	23	0.6
U2AF1	<i>U2 small nuclear RNA auxiliary factor 1</i>	7	5	7	6	25	0	2	4	6	12	0.6
NUP98	<i>nucleoporin 98</i>	7	6	2	3	18	0	2	4	3	9	0.6
KDELR1	<i>KDEL endoplasmic reticulum protein retention receptor 1</i>	7	9	0	0	16	0	4	0	0	4	0.6
TUBG1	<i>tubulin gamma 1</i>	7	11	18	15	51	9	6	4	8	27	0.6
TIMM50	<i>translocase of inner mitochondrial membrane 50</i>	7	11	8	13	39	5	7	0	0	12	0.6
RPL35A	<i>ribosomal protein L35a</i>	7	5	9	9	30	2	4	0	0	6	0.6
NNT	<i>nicotinamide nucleotide transhydrogenase</i>	6	7	5	0	18	0	0	0	4	4	0.6
SRP72	<i>signal recognition particle 72</i>	6	5	5	7	23	0	2	2	5	9	0.6
TFRC	<i>transferrin receptor</i>	6	7	6	9	28	4	5	0	0	9	0.6
HYOU1	<i>hypoxia up-regulated 1</i>	6	6	8	12	32	0	3	5	7	15	0.6
EMG1	<i>EMG1 NI-specific pseudouridine methyltransferase</i>	6	4	0	6	16	3	0	0	0	3	0.6
RPS12	<i>ribosomal protein S12</i>	6	0	6	5	17	0	3	2	2	7	0.6
MYL12B	<i>myosin light chain 12B</i>	6	6	5	7	24	2	0	5	3	10	0.6
PTGR1	<i>prostaglandin reductase 1</i>	6	9	4	5	24	3	0	0	0	3	0.6
YWHAQ	<i>tyrosine 3-monooxygenase/tryptophan 5-</i>	6	6	8	9	29	0	2	2	5	9	0.6

	<i>monooxygenase activation protein theta</i>											
SEC16A	<i>SEC16 homolog A, endoplasmic reticulum export factor</i>	6	3	7	4	20	0	3	0	4	7	0.6
PDIA6	<i>protein disulfide isomerase family A member 6</i>	6	8	7	11	32	0	4	6	8	18	0.6
PGRMC1	<i>progesterone receptor membrane component 1</i>	5	5	5	5	20	2	0	0	0	2	0.6
SHMT2	<i>serine hydroxymethyltransferase 2</i>	5	4	5	7	21	0	0	0	3	3	0.6
RPS18	<i>ribosomal protein S18</i>	5	3	7	4	19	3	3	4	4	14	0.6
CALU	<i>calumenin</i>	5	4	2	2	13	2	0	0	0	2	0.6
PSMD4	<i>proteasome 26S subunit, non-ATPase 4</i>	5	3	6	5	19	4	0	3	4	11	0.6
MCM2	<i>minichromosome maintenance complex component 2</i>	5	6	7	6	24	2	2	0	3	7	0.6
UPF1	<i>UPF1 RNA helicase and ATPase</i>	5	5	6	8	24	3	0	2	4	9	0.6
LONP1	<i>lon peptidase 1, mitochondrial</i>	5	7	5	0	17	0	0	0	2	2	0.6
SLC7A5	<i>solute carrier family 7 member 5</i>	5	7	4	7	23	4	3	4	2	13	0.6
MCU	<i>mitochondrial calcium uniporter</i>	5	5	6	5	21	2	0	0	2	4	0.6
HNRNPU L2	<i>heterogeneous nuclear ribonucleoprotein U like 2</i>	5	7	3	7	22	3	2	5	5	15	0.6
STT3A	<i>STT3 oligosaccharyltransferase complex catalytic subunit A</i>	5	5	10	4	24	5	2	0	2	9	0.6
SBDS	<i>SBDS ribosome maturation factor</i>	5	6	6	6	23	2	2	2	0	6	0.6
TRIM28	<i>tripartite motif containing 28</i>	4	5	6	5	20	0	3	4	4	11	0.6
PSMD14	<i>proteasome 26S subunit, non-ATPase 14</i>	4	2	3	6	15	0	3	0	0	3	0.6
SSRP1	<i>structure specific recognition protein 1</i>	4	6	5	4	19	3	4	0	0	7	0.6
DDX46	<i>DEAD-box helicase 46</i>	4	6	5	9	24	6	5	5	6	22	0.6
RRS1	<i>ribosome biogenesis regulator 1 homolog</i>	4	6	6	0	16	0	0	2	0	2	0.6
GMPS	<i>guanine monophosphate synthase</i>	4	2	7	3	16	0	0	0	4	4	0.6
RPS19	<i>ribosomal protein S19</i>	4	2	5	6	17	0	0	2	0	2	0.6
IDI1	<i>isopentenyl-diphosphate delta isomerase 1</i>	4	3	6	6	19	0	0	0	4	4	0.6
HIGD1A	<i>HIG1 hypoxia inducible domain family member 1A</i>	4	4	4	5	17	0	2	0	0	2	0.6

NUDT21	<i>nudix hydrolase 21</i>	4	4	4	0	12	3	0	3	2	8	0.6
DHX30	<i>DExH-box helicase 30</i>	4	4	7	5	20	4	5	4	4	17	0.6
PDHB	<i>pyruvate dehydrogenase E1 beta subunit</i>	4	4	5	7	20	3	3	5	5	16	0.6
UBXN1	<i>UBX domain protein 1</i>	4	3	8	6	21	0	2	3	5	10	0.6
PFN2	<i>profilin 2</i>	4	6	4	6	20	0	0	2	2	4	0.6
RHOG	<i>ras homolog family member G</i>	3	5	5	4	17	4	2	0	3	9	0.6
PARK7	<i>Parkinsonism associated deglycase</i>	3	0	3	3	9	0	2	2	0	4	0.6
ERLIN1	<i>ER lipid raft associated 1</i>	3	4	3	0	10	0	0	2	0	2	0.6
NCLN	<i>nicalin</i>	3	4	7	6	20	3	0	2	4	9	0.6
RAD50	<i>RAD50 double strand break repair protein</i>	2	2	4	6	14	3	2	2	0	7	0.6
NAA10	<i>N(alpha)-acetyltransferase 10, NatA catalytic subunit</i>	2	0	3	4	9	0	2	0	0	2	0.6
YTHDF1	<i>YTH N6-methyladenosine RNA binding protein 1</i>	2	3	6	6	17	0	0	2	3	5	0.6
RAD21	<i>RAD21 cohesin complex component</i>	2	5	0	5	12	0	0	2	0	2	0.6
FARSA	<i>phenylalanyl-tRNA synthetase subunit alpha</i>	0	4	5	5	14	0	0	0	2	2	0.6
IGF2BP3	<i>insulin like growth factor 2 mRNA binding protein 3</i>	0	4	7	4	15	0	0	0	3	3	0.6
TUBA1A	<i>tubulin alpha 1a</i>	49	51	13	9	122	0	0	0	0	0	#N/A
RPS27A	<i>ribosomal protein S27a</i>	27	23	21	19	90	0	0	0	0	0	#N/A
NUP62	<i>nucleoporin 62</i>	13	8	6	7	34	0	0	0	0	0	#N/A
SLC25A4	<i>solute carrier family 25 member 4</i>	11	11	14	8	44	0	0	0	0	0	#N/A
AK1	<i>adenylate kinase 1</i>	11	5	7	2	25	0	0	0	0	0	#N/A
RAB10	<i>RAB10, member RAS oncogene family</i>	9	5	6	8	28	0	0	0	0	0	#N/A
NUP88	<i>nucleoporin 88</i>	9	11	8	9	37	0	0	0	0	0	#N/A
EBNA1BP2	<i>EBNA1 binding protein 2</i>	9	7	7	4	27	0	0	0	0	0	#N/A
RAB8A	<i>RAB8A, member RAS oncogene family</i>	8	11	10	13	42	0	0	0	0	0	#N/A
PRKACA	<i>protein kinase cAMP-activated catalytic subunit alpha</i>	8	15	8	10	41	0	0	0	0	0	#N/A
TXN	<i>thioredoxin</i>	8	9	6	3	26	0	0	0	0	0	#N/A
AHCTF1	<i>AT-hook containing transcription</i>	7	3	4	6	20	0	0	0	0	0	#N/A

<i>factor 1</i>												
SRSF3	<i>serine and arginine rich splicing factor 3</i>	7	6	0	0	13	0	0	0	0	0	#N/A
SDHA	<i>succinate dehydrogenase complex flavoprotein subunit A</i>	7	5	5	3	20	0	0	0	0	0	#N/A
ATP5J2-PTCD1	<i>ATP5MF-PTCD1 readthrough</i>	7	7	8	7	29	0	0	0	0	0	#N/A
CRYZ	<i>crystallin zeta</i>	7	8	6	5	26	0	0	0	0	0	#N/A
ATAD3B	<i>ATPase family AAA domain containing 3B</i>	7	5	0	0	12	0	0	0	0	0	#N/A
MTDH	<i>metadherin</i>	6	4	3	4	17	0	0	0	0	0	#N/A
SAR1B	<i>secretion associated Ras related GTPase 1B</i>	6	5	6	6	23	0	0	0	0	0	#N/A
LOC101060252		0	6	0	0	6	0	0	0	0	0	#N/A
RBFOX2	<i>RNA binding fox-1 homolog 2</i>	6	5	8	9	28	0	0	0	0	0	#N/A
MOV10	<i>Mov10 RISC complex RNA helicase</i>	6	7	0	3	16	0	0	0	0	0	#N/A
API5	<i>apoptosis inhibitor 5</i>	6	0	2	0	8	0	0	0	0	0	#N/A
NMD3	<i>NMD3 ribosome export adaptor</i>	6	2	5	2	15	0	0	0	0	0	#N/A
RPL30	<i>ribosomal protein L30</i>	6	5	6	5	22	0	0	0	0	0	#N/A
ACOT7	<i>acyl-CoA thioesterase 7</i>	6	8	8	5	27	0	0	0	0	0	#N/A
RHOA	<i>ras homolog family member A</i>	6	7	5	4	22	0	0	0	0	0	#N/A
SRM	<i>spermidine synthase</i>	5	3	0	5	13	0	0	0	0	0	#N/A
SLC38A2	<i>solute carrier family 38 member 2</i>	5	5	3	0	13	0	0	0	0	0	#N/A
SRPK1	<i>SRSF protein kinase 1</i>	5	0	4	0	9	0	0	0	0	0	#N/A
RAB11B	<i>RAB11B, member RAS oncogene family</i>	5	6	7	7	25	0	0	0	0	0	#N/A
UBE2D3	<i>ubiquitin conjugating enzyme E2 D3</i>	5	5	4	0	14	0	0	0	0	0	#N/A
LGALS1	<i>galectin 1</i>	5	0	7	8	20	0	0	0	0	0	#N/A
ILVBL	<i>ilvB acetolactate synthase like</i>	5	5	5	7	22	0	0	0	0	0	#N/A
FAF2	<i>Fas associated factor family member 2</i>	5	0	3	0	8	0	0	0	0	0	#N/A
CSTB	<i>cystatin B</i>	5	0	4	3	12	0	0	0	0	0	#N/A
RPL36A	<i>ribosomal protein L36a</i>	5	5	6	4	20	0	0	0	0	0	#N/A
YIF1A	<i>Yip1 interacting factor homolog A,</i>	4	4	0	0	8	0	0	0	0	0	#N/A

<i>membrane trafficking protein</i>												
DAD1	<i>defender against cell death 1</i>	4	3	6	7	20	0	0	0	0	0	#N/A
RNPS1	<i>RNA binding protein with serine rich domain 1</i>	4	0	2	4	10	0	0	0	0	0	#N/A
MAD2L1	<i>mitotic arrest deficient 2 like 1</i>	4	4	8	5	21	0	0	0	0	0	#N/A
SPOCK3	<i>SPARC (osteonectin), cwcv and kazal like domains proteoglycan 3 PDS5 cohesin associated factor B</i>	4	0	0	0	4	0	0	0	0	0	#N/A
PDS5B	<i>PDS5 cohesin associated factor B</i>	4	0	2	0	6	0	0	0	0	0	#N/A
BSG	<i>basigin (Ok blood group)</i>	4	0	0	4	8	0	0	0	0	0	#N/A
USMG5	<i>ATP synthase membrane subunit DAPIT</i>	4	5	0	4	13	0	0	0	0	0	#N/A
IMMT	<i>inner membrane mitochondrial protein</i>	4	3	6	7	20	0	0	0	0	0	#N/A
TRA2B	<i>transformer 2 beta homolog</i>	4	0	0	0	4	0	0	0	0	0	#N/A
LRP1B	<i>LDL receptor related protein 1B</i>	4	0	0	2	6	0	0	0	0	0	#N/A
CLPB	<i>ClpB homolog, mitochondrial AAA ATPase chaperonin</i>	4	0	3	4	11	0	0	0	0	0	#N/A
TSMF	<i>Ts translation elongation factor, mitochondrial</i>	4	2	0	5	11	0	0	0	0	0	#N/A
LUC7L3	<i>LUC7 like 3 pre-mRNA splicing factor</i>	4	4	5	5	18	0	0	0	0	0	#N/A
IER3IP1	<i>immediate early response 3 interacting protein 1</i>	3	0	0	0	3	0	0	0	0	0	#N/A
DNAJB6	<i>DnaJ heat shock protein family (Hsp40) member B6</i>	3	3	2	3	11	0	0	0	0	0	#N/A
CYB5R3	<i>cytochrome b5 reductase 3</i>	3	4	2	2	11	0	0	0	0	0	#N/A
RDH11	<i>retinol dehydrogenase 11</i>	3	2	2	4	11	0	0	0	0	0	#N/A
PRPF6	<i>pre-mRNA processing factor 6</i>	3	0	0	0	3	0	0	0	0	0	#N/A
MYH14	<i>myosin heavy chain 14</i>	3	0	0	0	3	0	0	0	0	0	#N/A
SART1	<i>spliceosome associated factor 1, recruiter of U4/U6.U5 tri-snRNP</i>	3	0	0	0	3	0	0	0	0	0	#N/A
NUP155	<i>nucleoporin 155</i>	3	4	2	3	12	0	0	0	0	0	#N/A
KTN1	<i>kinectin 1</i>	3	0	2	4	9	0	0	0	0	0	#N/A
SEC22B	<i>SEC22 homolog B, vesicle trafficking protein (gene/pseudogene)</i>	3	0	3	3	9	0	0	0	0	0	#N/A
EMILIN3	<i>elastin microfibril interfacier 3</i>	3	0	0	0	3	0	0	0	0	0	#N/A
FUBP1	<i>far upstream element binding</i>	3	0	0	0	3	0	0	0	0	0	#N/A

<i>protein 1</i>												
MRI1	<i>methylthioribose-1-phosphate isomerase 1</i>	3	3	7	5	18	0	0	0	0	0	#N/A
TNPO1	<i>transportin 1</i>	3	3	0	0	6	0	0	0	0	0	#N/A
H2AFZ	<i>H2A histone family member Z</i>	3	4	4	4	15	0	0	0	0	0	#N/A
TOP1	<i>DNA topoisomerase I</i>	3	4	4	4	15	0	0	0	0	0	#N/A
MEST	<i>mesoderm specific transcript</i>	3	0	2	0	5	0	0	0	0	0	#N/A
EIF2AK2	<i>eukaryotic translation initiation factor 2 alpha kinase 2</i>	3	2	2	0	7	0	0	0	0	0	#N/A
APOBEC3 C	<i>apolipoprotein B mRNA editing enzyme catalytic subunit 3C</i>	3	2	3	6	14	0	0	0	0	0	#N/A
HADHA	<i>hydroxyacyl-CoA dehydrogenase trifunctional multienzyme complex subunit alpha</i>	3	5	0	0	8	0	0	0	0	0	#N/A
POLR2H	<i>RNA polymerase II subunit H</i>	3	5	4	5	17	0	0	0	0	0	#N/A
SLC35E1	<i>solute carrier family 35 member E1</i>	3	2	0	0	5	0	0	0	0	0	#N/A
ACAT1	<i>acetyl-CoA acetyltransferase 1</i>	2	0	4	2	8	0	0	0	0	0	#N/A
MAPKAP K2	<i>MAPK activated protein kinase 2</i>	2	0	0	0	2	0	0	0	0	0	#N/A
ARAF	<i>A-Raf proto-oncogene, serine/threonine kinase</i>	2	0	0	0	2	0	0	0	0	0	#N/A
ALDH1L2	<i>aldehyde dehydrogenase 1 family member L2</i>	2	2	5	5	14	0	0	0	0	0	#N/A
NDUFS2	<i>NADH:ubiquinone oxidoreductase core subunit S2</i>	2	0	0	0	2	0	0	0	0	0	#N/A
PKD2L2	<i>polycystin 2 like 2, transient receptor potential cation channel</i>	2	0	0	0	2	0	0	0	0	0	#N/A
MCF2	<i>MCF.2 cell line derived transforming sequence</i>	2	0	0	0	2	0	0	0	0	0	#N/A
PRKCSH	<i>protein kinase C substrate 80K-H</i>	2	0	0	0	2	0	0	0	0	0	#N/A
C8orf55	<i>thioesterase superfamily member 6</i>	2	0	2	0	4	0	0	0	0	0	#N/A
WDR3	<i>WD repeat domain 3</i>	2	2	2	0	6	0	0	0	0	0	#N/A
NUP153	<i>nucleoporin 153</i>	2	0	0	0	2	0	0	0	0	0	#N/A
SUCLA2	<i>succinate-CoA ligase ADP-forming beta subunit</i>	2	0	0	0	2	0	0	0	0	0	#N/A
RRP1B	<i>ribosomal RNA processing 1B</i>	2	0	0	0	2	0	0	0	0	0	#N/A
NKRF	<i>NFkB repressing factor</i>	2	0	2	2	6	0	0	0	0	0	#N/A

FAM208B	<i>transcription activation suppressor family member 2</i>	2	0	0	0	2	0	0	0	0	0	#N/A
ATP5O	<i>ATP synthase peripheral stalk subunit OSCP</i>	2	3	0	3	8	0	0	0	0	0	#N/A
FHL2	<i>four and a half LIM domains 2</i>	2	0	0	0	2	0	0	0	0	0	#N/A
KIAA0090	<i>ER membrane protein complex subunit 1</i>	2	0	0	2	4	0	0	0	0	0	#N/A
MOGS	<i>mannosyl-oligosaccharide glucosidase</i>	2	0	4	0	6	0	0	0	0	0	#N/A
TCOF1	<i>treacle ribosome biogenesis factor 1</i>	2	4	0	0	6	0	0	0	0	0	#N/A
BAG5	<i>BCL2 associated athanogene 5</i>	2	2	2	2	8	0	0	0	0	0	#N/A
ETFA	<i>electron transfer flavoprotein subunit alpha</i>	2	0	0	0	2	0	0	0	0	0	#N/A
RAB5B	<i>RAB5B, member RAS oncogene family</i>	2	2	4	2	10	0	0	0	0	0	#N/A
CCDC47	<i>coiled-coil domain containing 47</i>	2	0	0	0	2	0	0	0	0	0	#N/A
PARVB	<i>parvin beta</i>	2	0	3	2	7	0	0	0	0	0	#N/A
BOP1	<i>BOP1 ribosomal biogenesis factor</i>	2	5	0	0	7	0	0	0	0	0	#N/A
PIGT	<i>phosphatidylinositol glycan anchor biosynthesis class T</i>	2	0	0	0	2	0	0	0	0	0	#N/A
PGD	<i>phosphogluconate dehydrogenase</i>	2	2	0	3	7	0	0	0	0	0	#N/A
PIGK	<i>phosphatidylinositol glycan anchor biosynthesis class K</i>	2	0	0	3	5	0	0	0	0	0	#N/A
SEC24C	<i>SEC24 homolog C, COPII coat complex component</i>	2	3	2	3	10	0	0	0	0	0	#N/A
CCDC86	<i>coiled-coil domain containing 86</i>	2	2	2	0	6	0	0	0	0	0	#N/A
CAPN1	<i>calpain 1</i>	2	0	0	0	2	0	0	0	0	0	#N/A
GNAS	<i>GNAS complex locus</i>	2	0	2	0	4	0	0	0	0	0	#N/A
ARF6	<i>ADP ribosylation factor 6</i>	2	3	0	5	10	0	0	0	0	0	#N/A
NOP16	<i>NOP16 nucleolar protein</i>	2	4	0	0	6	0	0	0	0	0	#N/A
SMARCB1	<i>SWI/SNF related, matrix associated, actin dependent regulator of chromatin, subfamily b, member 1</i>	2	0	0	0	2	0	0	0	0	0	#N/A
TBRG4	<i>transforming growth factor beta regulator 4</i>	0	5	2	2	9	0	0	0	0	0	#N/A
COTL1	<i>coactosin like F-actin binding protein 1</i>	0	5	3	4	12	0	0	0	0	0	#N/A

PSIP1	<i>PC4 and SFRS1 interacting protein 1</i>	0	4	5	4	13	0	0	0	0	0	#N/A
PSPC1	<i>paraspeckle component 1</i>	0	4	0	2	6	0	0	0	0	0	#N/A
SMCHD1	<i>structural maintenance of chromosomes flexible hinge domain containing 1</i>	0	4	2	3	9	0	0	0	0	0	#N/A
XIRP1	<i>xin actin binding repeat containing 1</i>	0	4	0	0	4	0	0	0	0	0	#N/A
MTCH2	<i>mitochondrial carrier 2</i>	0	4	4	0	8	0	0	0	0	0	#N/A
MKI67IP	<i>nucleolar protein interacting with the FHA domain of MKI67</i>	0	4	0	0	4	0	0	0	0	0	#N/A
MGC50722	<i>coiled-coil domain containing 1872</i>	0	3	0	0	3	0	0	0	0	0	#N/A
ARL6IP5	<i>ADP ribosylation factor like GTPase 6 interacting protein 5</i>	0	3	0	0	3	0	0	0	0	0	#N/A
PTGES3	<i>prostaglandin E synthase 3</i>	0	3	0	0	3	0	0	0	0	0	#N/A
RRBP1	<i>ribosome binding protein 1</i>	0	3	6	2	11	0	0	0	0	0	#N/A
HSDL1	<i>hydroxysteroid dehydrogenase like 1</i>	0	3	5	4	12	0	0	0	0	0	#N/A
EBP	<i>EBP cholesterol delta-isomerase</i>	0	3	0	2	5	0	0	0	0	0	#N/A
FFAR1	<i>free fatty acid receptor 1</i>	0	3	0	0	3	0	0	0	0	0	#N/A
KRAS	<i>KRAS proto-oncogene, GTPase</i>	0	3	0	0	3	0	0	0	0	0	#N/A
NOLC1	<i>nucleolar and coiled-body phosphoprotein 1</i>	0	3	4	0	7	0	0	0	0	0	#N/A
GALNT2	<i>polypeptide N-acetylgalactosaminyltransferase 2</i>	0	3	3	5	11	0	0	0	0	0	#N/A
SF3B14	⁰	0	3	0	2	5	0	0	0	0	0	#N/A
TNRC6A	<i>trinucleotide repeat containing adaptor 6A</i>	0	3	3	0	6	0	0	0	0	0	#N/A
RPS10	<i>ribosomal protein S10</i>	0	3	2	5	10	0	0	0	0	0	#N/A
RAB3D	<i>RAB3D, member RAS oncogene family</i>	0	3	0	0	3	0	0	0	0	0	#N/A
DLD	<i>dihydrolipoamide dehydrogenase</i>	0	3	0	0	3	0	0	0	0	0	#N/A
PPM1G	<i>protein phosphatase, Mg²⁺/Mn²⁺ dependent 1G</i>	0	3	0	0	3	0	0	0	0	0	#N/A
EEF1E1	<i>eukaryotic translation elongation factor 1 epsilon 1</i>	0	2	2	0	4	0	0	0	0	0	#N/A
HNRPLL	<i>heterogeneous nuclear ribonucleoprotein L like</i>	0	2	4	0	6	0	0	0	0	0	#N/A

DNMT1	<i>DNA methyltransferase 1</i>	0	2	0	0	2	0	0	0	0	0	#N/A
SF3B4	<i>splicing factor 3b subunit 4</i>	0	2	0	2	4	0	0	0	0	0	#N/A
SORCS3	<i>sortilin related VPS10 domain containing receptor 3</i>	0	2	0	0	2	0	0	0	0	0	#N/A
SRSF1	<i>serine and arginine rich splicing factor 1</i>	0	2	0	2	4	0	0	0	0	0	#N/A
USP54	<i>ubiquitin specific peptidase 54</i>	0	2	0	0	2	0	0	0	0	0	#N/A
KHSRP	<i>KH-type splicing regulatory protein</i>	0	2	4	5	11	0	0	0	0	0	#N/A
MTA2	<i>metastasis associated 1 family member 2</i>	0	2	0	0	2	0	0	0	0	0	#N/A
C16orf80	<i>cilia and flagella associated protein 20</i>	0	2	0	0	2	0	0	0	0	0	#N/A
HDAC1	<i>histone deacetylase 1</i>	0	2	0	3	5	0	0	0	0	0	#N/A
DYNLT1	<i>dynein light chain Tctex-type 1</i>	0	2	0	0	2	0	0	0	0	0	#N/A
FOXRED1	<i>FAD dependent oxidoreductase domain containing 1</i>	0	2	0	0	2	0	0	0	0	0	#N/A
EIF4A2	<i>eukaryotic translation initiation factor 4A2</i>	0	2	0	0	2	0	0	0	0	0	#N/A
NAA11	<i>N(alpha)-acetyltransferase 11, NatA catalytic subunit</i>	0	2	0	0	2	0	0	0	0	0	#N/A
SRSF2	<i>serine and arginine rich splicing factor 2</i>	0	2	4	0	6	0	0	0	0	0	#N/A
LRRC47	<i>leucine rich repeat containing 47</i>	0	2	0	0	2	0	0	0	0	0	#N/A
CIC	<i>capicua transcriptional repressor</i>	0	2	0	0	2	0	0	0	0	0	#N/A
ABCB7	<i>ATP binding cassette subfamily B member 7</i>	0	2	2	3	7	0	0	0	0	0	#N/A
MRPS2	<i>mitochondrial ribosomal protein S2</i>	0	2	0	0	2	0	0	0	0	0	#N/A
TMC7	<i>transmembrane channel like 7</i>	0	0	7	0	7	0	0	0	0	0	#N/A
ATAD1	<i>ATPase family AAA domain containing 1</i>	0	0	5	0	5	0	0	0	0	0	#N/A
TIMMDC1	<i>translocase of inner mitochondrial membrane domain containing 1</i>	0	0	4	0	4	0	0	0	0	0	#N/A
TXNIP	<i>thioredoxin interacting protein</i>	0	0	4	2	6	0	0	0	0	0	#N/A
MTPAP	<i>mitochondrial poly(A) polymerase</i>	0	0	4	2	6	0	0	0	0	0	#N/A
HLA-A	<i>major histocompatibility complex, class I, A</i>	0	0	4	3	7	0	0	0	0	0	#N/A
NOP2	<i>NOP2 nucleolar protein</i>	0	0	4	0	4	0	0	0	0	0	#N/A
PYCR1	<i>pyrroline-5-carboxylate reductase 1</i>	0	0	4	0	4	0	0	0	0	0	#N/A

STT3B	<i>STT3 oligosaccharyltransferase complex catalytic subunit B</i>	0	0	4	2	6	0	0	0	0	0	#N/A
FBXO7	<i>F-box protein 7</i>	0	0	4	0	4	0	0	0	0	0	#N/A
ATPAF2	<i>ATP synthase mitochondrial F1 complex assembly factor 2</i>	0	0	4	4	8	0	0	0	0	0	#N/A
RANBP6	<i>RAN binding protein 6</i>	0	0	3	0	3	0	0	0	0	0	#N/A
TSR1	<i>TSR1 ribosome maturation factor</i>	0	0	3	4	7	0	0	0	0	0	#N/A
MDN1	<i>midasin AAA ATPase 1</i>	0	0	3	0	3	0	0	0	0	0	#N/A
C2orf47	<i>matrix AAA peptidase interacting protein 1</i>	0	0	3	0	3	0	0	0	0	0	#N/A
HK1	<i>hexokinase 1</i>	0	0	3	3	6	0	0	0	0	0	#N/A
HRAS	<i>HRas proto-oncogene, GTPase</i>	0	0	3	5	8	0	0	0	0	0	#N/A
NT5DC2	<i>5'-nucleotidase domain containing 2</i>	0	0	3	0	3	0	0	0	0	0	#N/A
P4HA1	<i>prolyl 4-hydroxylase subunit alpha 1</i>	0	0	3	3	6	0	0	0	0	0	#N/A
SEC63	<i>SEC63 homolog, protein translocation regulator</i>	0	0	3	2	5	0	0	0	0	0	#N/A
CLPP	<i>caseinolytic mitochondrial matrix peptidase proteolytic subunit</i>	0	0	3	3	6	0	0	0	0	0	#N/A
NDUFS7	<i>NADH:ubiquinone oxidoreductase core subunit S7</i>	0	0	3	4	7	0	0	0	0	0	#N/A
ATXN2	<i>ataxin 2</i>	0	0	3	0	3	0	0	0	0	0	#N/A
PLOD3	<i>procollagen-lysine,2-oxoglutarate 5-dioxygenase 3</i>	0	0	3	0	3	0	0	0	0	0	#N/A
NAT1	<i>N-acetyltransferase 1</i>	0	0	2	0	2	0	0	0	0	0	#N/A
NOMO2	<i>NODAL modulator 2</i>	0	0	2	0	2	0	0	0	0	0	#N/A
APRT	<i>adenine phosphoribosyltransferase</i>	0	0	2	0	2	0	0	0	0	0	#N/A
TRMT5	<i>tRNA methyltransferase 5</i>	0	0	2	0	2	0	0	0	0	0	#N/A
PCK2	<i>phosphoenolpyruvate carboxykinase 2, mitochondrial</i>	0	0	2	0	2	0	0	0	0	0	#N/A
MTFP1	<i>mitochondrial fission process 1</i>	0	0	2	0	2	0	0	0	0	0	#N/A
ERGIC2	<i>ERGIC and golgi 2</i>	0	0	2	2	4	0	0	0	0	0	#N/A
ISOC2	<i>isochorismatase domain containing 2</i>	0	0	2	0	2	0	0	0	0	0	#N/A
PRRC2B	<i>proline rich coiled-coil 2B</i>	0	0	2	0	2	0	0	0	0	0	#N/A
RFK	<i>riboflavin kinase</i>	0	0	2	0	2	0	0	0	0	0	#N/A

CACNA1D	<i>calcium voltage-gated channel subunit alpha1 D</i>	0	0	2	0	2	0	0	0	0	0	#N/A
PGLS	<i>6-phosphogluconolactonase</i>	0	0	2	0	2	0	0	0	0	0	#N/A
PRPSAP2	<i>phosphoribosyl pyrophosphate synthetase associated protein 2</i>	0	0	2	0	2	0	0	0	0	0	#N/A
AP1S1	<i>adaptor related protein complex 1 subunit sigma 1</i>	0	0	2	2	4	0	0	0	0	0	#N/A
NIPBL	<i>NIPBL cohesin loading factor</i>	0	0	2	2	4	0	0	0	0	0	#N/A
ARHGEF1	<i>Rho guanine nucleotide exchange factor 1</i>	0	0	2	2	4	0	0	0	0	0	#N/A
SRPR	<i>SRP receptor subunit alpha</i>	0	0	2	0	2	0	0	0	0	0	#N/A
PYGB	<i>glycogen phosphorylase B</i>	0	0	2	0	2	0	0	0	0	0	#N/A
MRPL22	<i>mitochondrial ribosomal protein L22</i>	0	0	2	0	2	0	0	0	0	0	#N/A
MLEC	<i>malectin</i>	0	0	2	0	2	0	0	0	0	0	#N/A
USP9X	<i>ubiquitin specific peptidase 9 X-linked</i>	0	0	2	2	4	0	0	0	0	0	#N/A
METAP2	<i>methionyl aminopeptidase 2</i>	0	0	2	2	4	0	0	0	0	0	#N/A
ARAP1	<i>ArfGAP with RhoGAP domain, ankyrin repeat and PH domain 1</i>	0	0	2	3	5	0	0	0	0	0	#N/A
PGM3	<i>phosphoglucomutase 3</i>	0	0	2	0	2	0	0	0	0	0	#N/A
ALPL	<i>alkaline phosphatase, biomineralization associated</i>	0	0	2	0	2	0	0	0	0	0	#N/A
C9orf64	<i>chromosome 9 open reading frame 64</i>	0	0	2	0	2	0	0	0	0	0	#N/A
ODZ3	<i>teneurin transmembrane protein 1</i>	0	0	0	5	5	0	0	0	0	0	#N/A
HSPA6	<i>heat shock protein family A (Hsp70) member 6</i>	0	0	0	5	5	0	0	0	0	0	#N/A
POLD3	<i>DNA polymerase delta 3, accessory subunit</i>	0	0	0	5	5	0	0	0	0	0	#N/A
KCNQ2	<i>potassium voltage-gated channel subfamily Q member 2</i>	0	0	0	4	4	0	0	0	0	0	#N/A
BCCIP	<i>BRCA2 and CDKN1A interacting protein</i>	0	0	0	4	4	0	0	0	0	0	#N/A
ACSL4	<i>acyl-CoA synthetase long chain family member 4</i>	0	0	0	4	4	0	0	0	0	0	#N/A
RAP1A	<i>RAP1A, member of RAS oncogene family</i>	0	0	0	4	4	0	0	0	0	0	#N/A
DDX50	<i>DEXD-box helicase 50</i>	0	0	0	3	3	0	0	0	0	0	#N/A
RPS6KA2	<i>ribosomal protein S6 kinase A2</i>	0	0	0	3	3	0	0	0	0	0	#N/A

DKC1	<i>dyskerin pseudouridine synthase 1</i>	0	0	0	3	3	0	0	0	0	0	#N/A
NAA40	<i>N(alpha)-acetyltransferase 40, NatD catalytic subunit</i>	0	0	0	3	3	0	0	0	0	0	#N/A
SLC12A7	<i>solute carrier family 12 member 7</i>	0	0	0	3	3	0	0	0	0	0	#N/A
HUWE1	<i>HECT, UBA and WWE domain containing E3 ubiquitin protein ligase 1</i>	0	0	0	3	3	0	0	0	0	0	#N/A
CHCHD1	<i>coiled-coil-helix-coiled-coil-helix domain containing 1</i>	0	0	0	2	2	0	0	0	0	0	#N/A
REPIN1	<i>replication initiator 1</i>	0	0	0	2	2	0	0	0	0	0	#N/A
KDM1A	<i>lysine demethylase 1A</i>	0	0	0	2	2	0	0	0	0	0	#N/A
SYNE1	<i>spectrin repeat containing nuclear envelope protein 1</i>	0	0	0	2	2	0	0	0	0	0	#N/A
CNN3	<i>calponin 3</i>	0	0	0	2	2	0	0	0	0	0	#N/A
DNAJB11	<i>DnaJ heat shock protein family (Hsp40) member B11</i>	0	0	0	2	2	0	0	0	0	0	#N/A
PSMA4	<i>proteasome subunit alpha 4</i>	0	0	0	2	2	0	0	0	0	0	#N/A
CCNT1	<i>cyclin T1</i>	0	0	0	2	2	0	0	0	0	0	#N/A
ELOVL1	<i>ELOVL fatty acid elongase 1</i>	0	0	0	2	2	0	0	0	0	0	#N/A
CPSF1	<i>cleavage and polyadenylation specific factor 1</i>	0	0	0	2	2	0	0	0	0	0	#N/A
SCCPDH	<i>saccharopine dehydrogenase (putative)</i>	0	0	0	2	2	0	0	0	0	0	#N/A
HM13	<i>histocompatibility minor 13</i>	0	0	0	2	2	0	0	0	0	0	#N/A
CBR1	<i>carbonyl reductase 1</i>	0	0	0	2	2	0	0	0	0	0	#N/A
SLC25A15	<i>solute carrier family 25 member 15</i>	0	0	0	2	2	0	0	0	0	0	#N/A
STOML2	<i>stomatin like 2</i>	0	0	0	2	2	0	0	0	0	0	#N/A
DIP2B	<i>disco interacting protein 2 homolog B</i>	0	0	0	2	2	0	0	0	0	0	#N/A
GEMIN4	<i>gem nuclear organelle associated protein 4</i>	0	0	0	2	2	0	0	0	0	0	#N/A
HLCS	<i>holocarboxylase synthetase</i>	0	0	0	2	2	0	0	0	0	0	#N/A
NUDT4	<i>nudix hydrolase 4</i>	0	0	0	2	2	0	0	0	0	0	#N/A
COPZ1	<i>coatamer protein complex subunit zeta 1</i>	0	0	0	2	2	0	0	0	0	0	#N/A
USP39	<i>ubiquitin specific peptidase 39</i>	0	0	0	2	2	0	0	0	0	0	#N/A
RRAS	<i>RAS related</i>	0	0	0	2	2	0	0	0	0	0	#N/A

SAFB	<i>scaffold attachment factor B</i>	0	0	0	2	2	0	0	0	0	0	#N/A
SIN3B	<i>SIN3 transcription regulator family member B</i>	0	0	0	0	0	0	0	0	0	0	#N/A
PAPOLA	<i>poly(A) polymerase alpha</i>	0	0	0	0	0	0	0	0	0	0	#N/A
PPP1R10	<i>protein phosphatase 1 regulatory subunit 10</i>	0	0	0	0	0	0	0	0	0	0	#N/A
DIDO1	<i>death inducer-obliterator 1</i>	0	0	0	0	0	0	0	0	0	0	#N/A
DDX42	<i>DEAD-box helicase 42</i>	0	0	0	0	0	0	0	0	0	0	#N/A
NASP	<i>nuclear autoantigenic sperm protein</i>	0	0	0	0	0	0	0	0	0	0	#N/A
KDM3B	<i>lysine demethylase 3B</i>	0	0	0	0	0	0	0	0	0	0	#N/A
RIF1	<i>replication timing regulatory factor 1</i>	0	0	0	0	0	0	0	0	0	0	#N/A
SART3	<i>spliceosome associated factor 3, U4/U6 recycling protein</i>	0	0	0	0	0	0	0	0	0	0	#N/A
WAPAL	<i>WAPL cohesin release factor</i>	0	0	0	0	0	0	0	0	0	0	#N/A
KIF4A	<i>kinesin family member 4A</i>	0	0	0	0	0	0	0	0	0	0	#N/A
ACIN1	<i>apoptotic chromatin condensation inducer 1</i>	0	0	0	0	0	0	0	0	0	0	#N/A
JMJD1C	<i>jumonji domain containing 1C</i>	0	0	0	0	0	0	0	0	0	0	#N/A
EXOSC10	<i>exosome component 10</i>	0	0	0	0	0	0	0	0	0	0	#N/A
SMEK1	<i>protein phosphatase 4 regulatory subunit 3A</i>	0	0	0	0	0	0	0	0	0	0	#N/A
SF3A1	<i>splicing factor 3a subunit 1</i>	0	0	0	0	0	0	0	0	0	0	#N/A
RBM27	<i>RNA binding motif protein 27</i>	0	0	0	0	0	0	0	0	0	0	#N/A
U2SURP	<i>U2 snRNP associated SURP domain containing</i>	0	0	0	0	0	0	0	0	0	0	#N/A
SUGP2	<i>SURP and G-patch domain containing 2</i>	0	0	0	0	0	0	0	0	0	0	#N/A
TPX2	<i>TPX2 microtubule nucleation factor</i>	0	0	0	0	0	0	0	0	0	0	#N/A
CHERP	<i>calcium homeostasis endoplasmic reticulum protein</i>	0	0	0	0	0	0	0	0	0	0	#N/A
THRAP3	<i>thyroid hormone receptor associated protein 3</i>	0	0	0	0	0	0	0	0	0	0	#N/A
TCERG1	<i>transcription elongation regulator 1</i>	0	0	0	0	0	0	0	0	0	0	#N/A
LRWD1	<i>leucine rich repeats and WD repeat domain containing 1</i>	0	0	0	0	0	0	0	0	0	0	#N/A
TH1L	<i>negative elongation factor complex member C/D</i>	0	0	0	0	0	0	0	0	0	0	#N/A

GTF2E2	<i>general transcription factor IIE subunit 2</i>	0	0	0	0	0	0	0	0	0	0	#N/A
SCML2	<i>Scm polycomb group protein like 2</i>	0	0	0	0	0	0	0	0	0	0	#N/A
RDBP	<i>negative elongation factor complex member E</i>	0	0	0	0	0	0	0	0	0	0	#N/A
SON	<i>SON DNA binding protein</i>	0	0	0	0	0	0	0	0	0	0	#N/A
YLPM1	<i>YLP motif containing 1</i>	0	0	0	0	0	0	0	0	0	0	#N/A
EDC4	<i>enhancer of mRNA decapping 4</i>	0	0	0	0	0	0	0	0	0	0	#N/A
WDR70	<i>WD repeat domain 70</i>	0	0	0	0	0	0	0	0	0	0	#N/A
DBN1	<i>drebrin 1</i>	0	0	0	0	0	0	0	0	0	0	#N/A
CHD8	<i>chromodomain helicase DNA binding protein 8</i>	0	0	0	0	0	0	0	0	0	0	#N/A
DDX10	<i>DEAD-box helicase 10</i>	0	0	0	0	0	0	0	0	0	0	#N/A
ORC2	<i>origin recognition complex subunit 2</i>	0	0	0	0	0	0	0	0	0	0	#N/A
RBM17	<i>RNA binding motif protein 17</i>	0	0	0	0	0	0	0	0	0	0	#N/A
WDR82	<i>WD repeat domain 82</i>	0	0	0	0	0	0	0	0	0	0	#N/A
WRNIP1	<i>WRN helicase interacting protein 1</i>	0	0	0	0	0	0	0	0	0	0	#N/A
SUGP1	<i>SURP and G-patch domain containing 1</i>	0	0	0	0	0	0	0	0	0	0	#N/A
ANAPC1	<i>anaphase promoting complex subunit 1</i>	0	0	0	0	0	0	0	0	0	0	#N/A
WDHD1	<i>WD repeat and HMG-box DNA binding protein 1</i>	0	0	0	0	0	0	0	0	0	0	#N/A
ZNF148	<i>zinc finger protein 148</i>	0	0	0	0	0	0	0	0	0	0	#N/A
GTF3C4	<i>general transcription factor IIIC subunit 4</i>	0	0	0	0	0	0	0	0	0	0	#N/A
EXOSC2	<i>exosome component 2</i>	0	0	0	0	0	0	0	0	0	0	#N/A
KEAP1	<i>kelch like ECH associated protein 1</i>	0	0	0	0	0	0	0	0	0	0	#N/A
SNW1	<i>SNW domain containing 1</i>	0	0	0	0	0	0	0	0	0	0	#N/A
ATRX	<i>ATRX chromatin remodeler</i>	0	0	0	0	0	0	0	0	0	0	#N/A
CHAMP1	<i>chromosome alignment maintaining phosphoprotein 1</i>	0	0	0	0	0	0	0	0	0	0	#N/A
CDCA2	<i>cell division cycle associated 2</i>	0	0	0	0	0	0	0	0	0	0	#N/A
POLH	<i>DNA polymerase eta</i>	0	0	0	0	0	0	0	0	0	0	#N/A
PHF3	<i>PHD finger protein 3</i>	0	0	0	0	0	0	0	0	0	0	#N/A

RPRD2	<i>regulation of nuclear pre-mRNA domain containing 2</i>	0	0	0	0	0	0	0	0	0	0	#N/A
RBM10	<i>RNA binding motif protein 10</i>	0	0	0	0	0	0	0	0	0	0	#N/A
ZNF638	<i>zinc finger protein 638</i>	0	0	0	0	0	0	0	0	0	0	#N/A
SUB1	<i>SUB1 regulator of transcription</i>	0	0	0	0	0	0	0	0	0	0	#N/A
NUP50	<i>nucleoporin 50</i>	0	0	0	0	0	0	0	0	0	0	#N/A
PES1	<i>pescadillo ribosomal biogenesis factor 1</i>	0	0	0	0	0	0	0	0	0	0	#N/A
PHAX	<i>phosphorylated adaptor for RNA export</i>	0	0	0	0	0	0	0	0	0	0	#N/A
SYNM	<i>synemin</i>	0	0	0	0	0	0	0	0	0	0	#N/A
PCM1	<i>pericentriolar material 1</i>	0	0	0	0	0	0	0	0	0	0	#N/A
BAZ1A	<i>bromodomain adjacent to zinc finger domain 1A</i>	0	0	0	0	0	0	0	0	0	0	#N/A
PHACTR4	<i>phosphatase and actin regulator 4</i>	0	0	0	0	0	0	0	0	0	0	#N/A
CDK11A	<i>cyclin dependent kinase 11A</i>	0	0	0	0	0	0	0	0	0	0	#N/A
CCDC99	<i>spindle apparatus coiled-coil protein 1</i>	0	0	0	0	0	0	0	0	0	0	#N/A
RBM26	<i>RNA binding motif protein 26</i>	0	0	0	0	0	0	0	0	0	0	#N/A
C19orf29	<i>cactin, spliceosome C complex subunit</i>	0	0	0	0	0	0	0	0	0	0	#N/A
GTF2F1	<i>general transcription factor IIF subunit 1</i>	0	0	0	0	0	0	0	0	0	0	#N/A
SYNPO	<i>synaptopodin</i>	0	0	0	0	0	0	0	0	0	0	#N/A
ZC3H14	<i>zinc finger CCCH-type containing 14</i>	0	0	0	0	0	0	0	0	0	0	#N/A
PGRMC2	<i>progesterone receptor membrane component 2</i>	0	0	0	0	0	0	0	0	0	0	#N/A
SNRPB2	<i>small nuclear ribonucleoprotein polypeptide B2</i>	0	0	0	0	0	0	0	0	0	0	#N/A
BPTF	<i>bromodomain PHD finger transcription factor</i>	0	0	0	0	0	0	0	0	0	0	#N/A
MBD3	<i>methyl-CpG binding domain protein 3</i>	0	0	0	0	0	0	0	0	0	0	#N/A
GTF2F2	<i>general transcription factor IIF subunit 2</i>	0	0	0	0	0	0	0	0	0	0	#N/A
PCNP	<i>PEST proteolytic signal containing nuclear protein</i>	0	0	0	0	0	0	0	0	0	0	#N/A
ANAPC5	<i>anaphase promoting complex subunit 5</i>	0	0	0	0	0	0	0	0	0	0	#N/A

HDGF	<i>heparin binding growth factor</i>	0	0	0	0	0	0	0	0	0	0	#N/A
PRPF40A	<i>pre-mRNA processing factor 40 homolog A</i>	0	0	0	0	0	0	0	0	0	0	#N/A
GATAD2A	<i>GATA zinc finger domain containing 2A</i>	0	0	0	0	0	0	0	0	0	0	#N/A
FIP1L1	<i>factor interacting with PAPOLA and CPSF1</i>	0	0	0	0	0	0	0	0	0	0	#N/A
WDR36	<i>WD repeat domain 36</i>	0	0	0	0	0	0	0	0	0	0	#N/A
HTATSF1	<i>HIV-1 Tat specific factor 1</i>	0	0	0	0	0	0	0	0	0	0	#N/A
MED1	<i>mediator complex subunit 1</i>	0	0	0	0	0	0	0	0	0	0	#N/A
SF3A3	<i>splicing factor 3a subunit 3</i>	0	0	0	0	0	0	0	0	0	0	#N/A
MTA1	<i>metastasis associated 1</i>	0	0	0	0	0	0	0	0	0	0	#N/A
TACC1	<i>transforming acidic coiled-coil containing protein 1</i>	0	0	0	0	0	0	0	0	0	0	#N/A
SMARCC1	<i>SWI/SNF related, matrix associated, actin dependent regulator of chromatin subfamily c member 1</i>	0	0	0	0	0	0	0	0	0	0	#N/A
OGT	<i>O-linked N-acetylglucosamine (GlcNAc) transferase</i>	0	0	0	0	0	0	0	0	0	0	#N/A
MEF2D	<i>myocyte enhancer factor 2D</i>	0	0	0	0	0	0	0	0	0	0	#N/A
NOL8	<i>nucleolar protein 8</i>	0	0	0	0	0	0	0	0	0	0	#N/A
TFIP11	<i>tuftelin interacting protein 11</i>	0	0	0	0	0	0	0	0	0	0	#N/A
SAP30BP	<i>SAP30 binding protein</i>	0	0	0	0	0	0	0	0	0	0	#N/A
BRD4	<i>bromodomain containing 4</i>	0	0	0	0	0	0	0	0	0	0	#N/A
LARP1B	<i>La ribonucleoprotein domain family member 1B</i>	0	0	0	0	0	0	0	0	0	0	#N/A
SEPT6	<i>septin6</i>	0	0	0	0	0	0	0	0	0	0	#N/A
POLA1	<i>DNA polymerase alpha 1, catalytic subunit</i>	0	0	0	0	0	0	0	0	0	0	#N/A
SPAG7	<i>sperm associated antigen 7</i>	0	0	0	0	0	0	0	0	0	0	#N/A
SF3B5	<i>splicing factor 3b subunit 5</i>	0	0	0	0	0	0	0	0	0	0	#N/A
NACC1	<i>nucleus accumbens associated 1</i>	0	0	0	0	0	0	0	0	0	0	#N/A
ESF1	<i>ESF1 nucleolar pre-rRNA processing protein homolog</i>	0	0	0	0	0	0	0	0	0	0	#N/A
UBE2O	<i>ubiquitin conjugating enzyme E2 O</i>	0	0	0	0	0	0	0	0	0	0	#N/A
URB1	<i>URB1 ribosome biogenesis</i>	0	0	0	0	0	0	0	0	0	0	#N/A

<i>homolog</i>												
TP53BP1	<i>tumor protein p53 binding protein 1</i>	0	0	0	0	0	0	0	0	0	0	#N/A
SIN3A	<i>SIN3 transcription regulator family member A</i>	0	0	0	0	0	0	0	0	0	0	#N/A
PPP4R2	<i>protein phosphatase 4 regulatory subunit 2</i>	0	0	0	0	0	0	0	0	0	0	#N/A
NBN	<i>nibrin</i>	0	0	0	0	0	0	0	0	0	0	#N/A
RBBP6	<i>RB binding protein 6, ubiquitin ligase</i>	0	0	0	0	0	0	0	0	0	0	#N/A
RNF20	<i>ring finger protein 20</i>	0	0	0	0	0	0	0	0	0	0	#N/A
PAF1	<i>PAF1 homolog, Paf1/RNA polymerase II complex component</i>	0	0	0	0	0	0	0	0	0	0	#N/A
CDC73	<i>cell division cycle 73</i>	0	0	0	0	0	0	0	0	0	0	#N/A
DHX8	<i>DEAH-box helicase 8</i>	0	0	0	0	0	0	0	0	0	0	#N/A
DNTTIP2	<i>deoxynucleotidyltransferase terminal interacting protein 2</i>	0	0	0	0	0	0	0	0	0	0	#N/A
HP1BP3	<i>heterochromatin protein 1 binding protein 3</i>	0	0	0	0	0	0	0	0	0	0	#N/A
C11orf58	<i>chromosome 11 open reading frame 58</i>	0	0	0	0	0	0	0	0	0	0	#N/A
BOD1L	<i>biorientation of chromosomes in cell division 1 like 1</i>	0	0	0	0	0	0	0	0	0	0	#N/A
CDKN2AIP	<i>CDKN2A interacting protein</i>	0	0	0	0	0	0	0	0	0	0	#N/A
FAM208A	<i>transcription activation suppressor</i>	0	0	0	0	0	0	0	0	0	0	#N/A
CSNK2A1	<i>casein kinase 2 alpha 1</i>	0	0	0	0	0	0	0	0	0	0	#N/A
LMO7	<i>LIM domain 7</i>	0	0	0	0	0	0	0	0	0	0	#N/A
GTF2A1	<i>general transcription factor IIA subunit 1</i>	0	0	0	0	0	0	0	0	0	0	#N/A
PABPN1	<i>poly(A) binding protein nuclear 1</i>	0	0	0	0	0	0	0	0	0	0	#N/A
CDC23	<i>cell division cycle 23</i>	0	0	0	0	0	0	0	0	0	0	#N/A
ZNF318	<i>zinc finger protein 318</i>	0	0	0	0	0	0	0	0	0	0	#N/A
MDC1	<i>mediator of DNA damage checkpoint 1</i>	0	0	0	0	0	0	0	0	0	0	#N/A
PRRC2A	<i>proline rich coiled-coil 2A</i>	0	0	0	0	0	0	0	0	0	0	#N/A
PNISR	<i>PNN interacting serine and arginine rich protein</i>	0	0	0	0	0	0	0	0	0	0	#N/A
SENP6	<i>SUMO specific peptidase 6</i>	0	0	0	0	0	0	0	0	0	0	#N/A

MASTL	<i>microtubule associated serine/threonine kinase like</i>	0	0	0	0	0	0	0	0	0	0	#N/A
EXOSC6	<i>exosome component 6</i>	0	0	0	0	0	0	0	0	0	0	#N/A
CPSF7	<i>cleavage and polyadenylation specific factor 7</i>	0	0	0	0	0	0	0	0	0	0	#N/A
GATAD2B	<i>GATA zinc finger domain containing 2B</i>	0	0	0	0	0	0	0	0	0	0	#N/A
ZBTB9	<i>zinc finger and BTB domain containing 9</i>	0	0	0	0	0	0	0	0	0	0	#N/A
BRIP1	<i>BRCA1 interacting protein C-terminal helicase 1</i>	0	0	0	0	0	0	0	0	0	0	#N/A
MUC13	<i>mucin 13, cell surface associated</i>	0	0	0	0	0	0	0	0	0	0	#N/A
EXOSC8	<i>exosome component 8</i>	0	0	0	0	0	0	0	0	0	0	#N/A
SRRM1	<i>serine and arginine repetitive matrix 1</i>	0	0	0	0	0	0	0	0	0	0	#N/A
CSNK2A2	<i>casein kinase 2 alpha 2</i>	0	0	0	0	0	0	0	0	0	0	#N/A
FAU	<i>FAU ubiquitin like and ribosomal protein S30 fusion</i>	0	0	0	0	0	0	0	0	0	0	#N/A
NCBP1	<i>nuclear cap binding protein subunit 1</i>	0	0	0	0	0	0	0	0	0	0	#N/A
PPP4C	<i>protein phosphatase 4 catalytic subunit</i>	0	0	0	0	0	0	0	0	0	0	#N/A
PEX14	<i>peroxisomal biogenesis factor 14</i>	0	0	0	0	0	0	0	0	0	0	#N/A
VCP	<i>valosin containing protein</i>	0	0	0	0	0	0	0	0	0	0	#N/A
C9orf78	<i>chromosome 9 open reading frame 78</i>	0	0	0	0	0	0	0	0	0	0	#N/A
NUP107	<i>nucleoporin 107</i>	0	0	0	0	0	0	0	0	0	0	#N/A
PDS5A	<i>PDS5 cohesin associated factor A</i>	0	0	0	0	0	0	0	0	0	0	#N/A
CDV3	<i>CDV3 homolog</i>	0	0	0	0	0	0	0	0	0	0	#N/A
SKA3	<i>spindle and kinetochore associated complex subunit 3</i>	0	0	0	0	0	0	0	0	0	0	#N/A
LARP4	<i>La ribonucleoprotein domain family member 4</i>	0	0	0	0	0	0	0	0	0	0	#N/A
LSG1	<i>large 60S subunit nuclear export GTPase 1</i>	0	0	0	0	0	0	0	0	0	0	#N/A
PPIL1	<i>peptidylprolyl isomerase like 1</i>	0	0	0	0	0	0	0	0	0	0	#N/A
PSME2	<i>proteasome activator subunit 2</i>	0	0	0	0	0	0	0	0	0	0	#N/A
BTF3	<i>basic transcription factor 3</i>	0	0	0	0	0	0	0	0	0	0	#N/A
TMSB10	<i>thymosin beta 10</i>	0	0	0	0	0	0	0	0	0	0	#N/A

HIVEP1	<i>human immunodeficiency virus type 1 enhancer binding protein 1</i>	0	0	0	0	0	0	0	0	0	0	#N/A
SRRM2	<i>serine/arginine repetitive matrix 2</i>	0	0	0	0	0	0	0	0	0	0	#N/A
TAF7	<i>TATA-box binding protein associated factor 7</i>	0	0	0	0	0	0	0	0	0	0	#N/A
RSBN1L	<i>round spermatid basic protein 1 like</i>	0	0	0	0	0	0	0	0	0	0	#N/A
TOP2B	<i>DNA topoisomerase II beta</i>	0	0	0	0	0	0	0	0	0	0	#N/A
C11orf30	<i>EMSY transcriptional repressor, BRCA2 interacting</i>	0	0	0	0	0	0	0	0	0	0	#N/A
NSFL1C	<i>NSFL1 cofactor</i>	0	0	0	0	0	0	0	0	0	0	#N/A
PPIL4	<i>peptidylprolyl isomerase like 4</i>	0	0	0	0	0	0	0	0	0	0	#N/A
LTV1	<i>LTV1 ribosome biogenesis factor</i>	0	0	0	0	0	0	0	0	0	0	#N/A
WDR12	<i>WD repeat domain 12</i>	0	0	0	0	0	0	0	0	0	0	#N/A
RNF40	<i>ring finger protein 40</i>	0	0	0	0	0	0	0	0	0	0	#N/A
AKAP1	<i>A-kinase anchoring protein 1</i>	0	0	0	0	0	0	0	0	0	0	#N/A
NFIC	<i>nuclear factor I C</i>	0	0	0	0	0	0	0	0	0	0	#N/A
CDCA8	<i>cell division cycle associated 8</i>	0	0	0	0	0	0	0	0	0	0	#N/A
GLYR1	<i>glyoxylate reductase 1 homolog</i>	0	0	0	0	0	0	0	0	0	0	#N/A
VBP1	<i>VHL binding protein 1</i>	0	0	0	0	0	0	0	0	0	0	#N/A
NARS	<i>asparaginyl-tRNA synthetase</i>	0	0	0	0	0	0	0	0	0	0	#N/A
PRKAR2A	<i>protein kinase cAMP-dependent type II regulatory subunit alpha</i>	0	0	0	0	0	0	0	0	0	0	#N/A
PUS7	<i>pseudouridine synthase 7</i>	0	0	0	0	0	0	0	0	0	0	#N/A
AFF4	<i>AF4/FMR2 family member 4</i>	0	0	0	0	0	0	0	0	0	0	#N/A
RPRD1B	<i>regulation of nuclear pre-mRNA domain containing 1B</i>	0	0	0	0	0	0	0	0	0	0	#N/A
ATP6V1B2	<i>ATPase H⁺ transporting V1 subunit B2</i>	0	0	0	0	0	0	0	0	0	0	#N/A
PALM2-AKAP2	<i>PALM2-AKAP2 fusion</i>	0	0	0	0	0	0	0	0	0	0	#N/A
TPM1	<i>tropomyosin 1</i>	0	0	0	0	0	0	0	0	0	0	#N/A
TXLNG	<i>taxilin gamma</i>	0	0	0	0	0	0	0	0	0	0	#N/A
ZHX3	<i>zinc fingers and homeoboxes 3</i>	0	0	0	0	0	0	0	0	0	0	#N/A
WDR44	<i>WD repeat domain 44</i>	0	0	0	0	0	0	0	0	0	0	#N/A

CDK9	<i>cyclin dependent kinase 9</i>	0	0	0	0	0	0	0	0	0	0	#N/A
VAMP3	<i>vesicle associated membrane protein 3</i>	0	0	0	0	0	0	0	0	0	0	#N/A
FXR2	<i>FMR1 autosomal homolog 2</i>	0	0	0	0	0	0	0	0	0	0	#N/A
QSER1	<i>glutamine and serine rich 1</i>	0	0	0	0	0	0	0	0	0	0	#N/A
CWC15	<i>CWC15 spliceosome associated protein homolog</i>	0	0	0	0	0	0	0	0	0	0	#N/A
KDM2A	<i>lysine demethylase 2A</i>	0	0	0	0	0	0	0	0	0	0	#N/A
DCP1A	<i>decapping mRNA 1A</i>	0	0	0	0	0	0	0	0	0	0	#N/A
ANP32B	<i>acidic nuclear phosphoprotein 32 family member B</i>	0	0	0	0	0	0	0	0	0	0	#N/A
FAM21A	<i>WASH complex subunit 2A</i>	0	0	0	0	0	0	0	0	0	0	#N/A
ASF1B	<i>anti-silencing function 1B histone chaperone</i>	0	0	0	0	0	0	0	0	0	0	#N/A
CCDC168	<i>coiled-coil domain containing 168</i>	0	0	0	0	0	0	0	0	0	0	#N/A
PRIM2	<i>DNA primase subunit 2</i>	0	0	0	0	0	0	0	0	0	0	#N/A
ANLN	<i>anillin actin binding protein</i>	0	0	0	0	0	0	0	0	0	0	#N/A
KPNA4	<i>karyopherin subunit alpha 4</i>	0	0	0	0	0	0	0	0	0	0	#N/A
BRMS1L	<i>BRMS1 like transcriptional repressor</i>	0	0	0	0	0	0	0	0	0	0	#N/A
MAPRE1	<i>microtubule associated protein RP/EB family member 1</i>	0	0	0	0	0	0	0	0	0	0	#N/A
GTF2E1	<i>general transcription factor IIE subunit 1</i>	0	0	0	0	0	0	0	0	0	0	#N/A
COPS3	<i>COP9 signalosome subunit 3</i>	0	0	0	0	0	0	0	0	0	0	#N/A
PRPF3	<i>pre-mRNA processing factor 3</i>	0	0	0	0	0	0	0	0	0	0	#N/A
SALL4	<i>spalt like transcription factor 4</i>	0	0	0	0	0	0	0	0	0	0	#N/A
EIF3K	<i>eukaryotic translation initiation factor 3 subunit K</i>	0	0	0	0	0	0	0	0	0	0	#N/A
GNB4	<i>G protein subunit beta 4</i>	0	0	0	0	0	0	0	0	0	0	#N/A
PHC3	<i>polyhomeotic homolog 3</i>	0	0	0	0	0	0	0	0	0	0	#N/A
RBM33	<i>RNA binding motif protein 33</i>	0	0	0	0	0	0	0	0	0	0	#N/A
GPKOW	<i>G-patch domain and KOW motifs</i>	0	0	0	0	0	0	0	0	0	0	#N/A
EIF4E	<i>eukaryotic translation initiation factor 4E</i>	0	0	0	0	0	0	0	0	0	0	#N/A
SETD2	<i>SET domain containing 2, histone lysine methyltransferase</i>	0	0	0	0	0	0	0	0	0	0	#N/A

TRMT6	<i>tRNA methyltransferase 6</i>	0	0	0	0	0	0	0	0	0	0	#N/A
NSD1	<i>nuclear receptor binding SET domain protein 1</i>	0	0	0	0	0	0	0	0	0	0	#N/A
PRMT5	<i>protein arginine methyltransferase 5</i>	0	0	0	0	0	0	0	0	0	0	#N/A
SEPT10	<i>septin10</i>	0	0	0	0	0	0	0	0	0	0	#N/A
NCOR1	<i>nuclear receptor corepressor 1</i>	0	0	0	0	0	0	0	0	0	0	#N/A
FTSJD2	<i>cap methyltransferase 1</i>	0	0	0	0	0	0	0	0	0	0	#N/A
ZNF280C	<i>zinc finger protein 280C</i>	0	0	0	0	0	0	0	0	0	0	#N/A
PRPF38A	<i>pre-mRNA processing factor 38A</i>	0	0	0	0	0	0	0	0	0	0	#N/A
DHX16	<i>DEAH-box helicase 16</i>	0	0	0	0	0	0	0	0	0	0	#N/A
ATAD5	<i>ATPase family AAA domain containing 5</i>	0	0	0	0	0	0	0	0	0	0	#N/A
UBAP1	<i>ubiquitin associated protein 1</i>	0	0	0	0	0	0	0	0	0	0	#N/A
EPB41L1	<i>erythrocyte membrane protein band 4.1 like 1</i>	0	0	0	0	0	0	0	0	0	0	#N/A
DVL1	<i>dishevelled segment polarity protein 1</i>	0	0	0	0	0	0	0	0	0	0	#N/A
EP400	<i>E1A binding protein p400</i>	0	0	0	0	0	0	0	0	0	0	#N/A
RPA3	<i>replication protein A3</i>	0	0	0	0	0	0	0	0	0	0	#N/A
MFAP1	<i>microfibril associated protein 1</i>	0	0	0	0	0	0	0	0	0	0	#N/A
CFDP1	<i>craniofacial development protein 1</i>	0	0	0	0	0	0	0	0	0	0	#N/A
ZNF281	<i>zinc finger protein 281</i>	0	0	0	0	0	0	0	0	0	0	#N/A
USP47	<i>ubiquitin specific peptidase 47</i>	0	0	0	0	0	0	0	0	0	0	#N/A
KIAA0664	<i>clustered mitochondria homolog</i>	0	0	0	0	0	0	0	0	0	0	#N/A
LYPLA2	<i>lysophospholipase 2</i>	0	0	0	0	0	0	0	0	0	0	#N/A
SRSF10	<i>serine and arginine rich splicing factor 10</i>	0	0	0	0	0	0	0	0	0	0	#N/A
ZFR	<i>zinc finger RNA binding protein</i>	0	0	0	0	0	0	0	0	0	0	#N/A
TOR1AIP1	<i>torsin 1A interacting protein 1</i>	0	0	0	0	0	0	0	0	0	0	#N/A
FAM50A	<i>family with sequence similarity 50 member A</i>	0	0	0	0	0	0	0	0	0	0	#N/A
CUL4B	<i>cullin 4B</i>	0	0	0	0	0	0	0	0	0	0	#N/A
WDR83	<i>WD repeat domain 83</i>	0	0	0	0	0	0	0	0	0	0	#N/A

PEX5	<i>peroxisomal biogenesis factor 5</i>	0	0	0	0	0	0	0	0	0	0	#N/A
COIL	<i>coilin</i>	0	0	0	0	0	0	0	0	0	0	#N/A
CC2D1A	<i>coiled-coil and C2 domain containing 1A</i>	0	0	0	0	0	0	0	0	0	0	#N/A
RPP38	<i>ribonuclease P/MRP subunit p38</i>	0	0	0	0	0	0	0	0	0	0	#N/A
DIS3L	<i>DIS3 like exosome 3'-5' exoribonuclease</i>	0	0	0	0	0	0	0	0	0	0	#N/A
PPF1BP1	<i>PPF1A binding protein 1</i>	0	0	0	0	0	0	0	0	0	0	#N/A
ZCCHC8	<i>zinc finger CCHC-type containing 8</i>	0	0	0	0	0	0	0	0	0	0	#N/A
STAG2	<i>stromal antigen 2</i>	0	0	0	0	0	0	0	0	0	0	#N/A
CIRBP	<i>cold inducible RNA binding protein</i>	0	0	0	0	0	0	0	0	0	0	#N/A
CBX5	<i>chromobox 5</i>	0	0	0	0	0	0	0	0	0	0	#N/A
UTP3	<i>UTP3 small subunit processome component</i>	0	0	0	0	0	0	0	0	0	0	#N/A
ADAMTS L4	<i>ADAMTS like 4</i>	0	0	0	0	0	0	0	0	0	0	#N/A
RAB11FIP1	<i>RAB11 family interacting protein 1</i>	0	0	0	0	0	0	0	0	0	0	#N/A
NPLOC4	<i>NPL4 homolog, ubiquitin recognition factor</i>	0	0	0	0	0	0	0	0	0	0	#N/A
SREK1	<i>splicing regulatory glutamic acid and lysine rich protein 1</i>	0	0	0	0	0	0	0	0	0	0	#N/A
MNAT1	<i>MNAT1 component of CDK activating kinase</i>	0	0	0	0	0	0	0	0	0	0	#N/A
INCENP	<i>inner centromere protein</i>	0	0	0	0	0	0	0	0	0	0	#N/A
STBD1	<i>starch binding domain 1</i>	0	0	0	0	0	0	0	0	0	0	#N/A
SNRNP40	<i>small nuclear ribonucleoprotein U5 subunit 40</i>	0	0	0	0	0	0	0	0	0	0	#N/A
APC	<i>APC regulator of WNT signaling pathway</i>	0	0	0	0	0	0	0	0	0	0	#N/A
AHCYL2	<i>adenosylhomocysteinase like 2</i>	0	0	0	0	0	0	0	0	0	0	#N/A
RAB3GAP2	<i>RAB3 GTPase activating non-catalytic protein subunit 2</i>	0	0	0	0	0	0	0	0	0	0	#N/A
TAF9B	<i>TATA-box binding protein associated factor 9b</i>	0	0	0	0	0	0	0	0	0	0	#N/A
TCEB3	<i>elongin A</i>	0	0	0	0	0	0	0	0	0	0	#N/A
PPP1R12A	<i>protein phosphatase 1 regulatory subunit 12A</i>	0	0	0	0	0	0	0	0	0	0	#N/A

ARPC2	<i>actin related protein 2/3 complex subunit 2</i>	0	0	0	0	0	0	0	0	0	0	#N/A
UBA1	<i>ubiquitin like modifier activating enzyme 1</i>	0	0	0	0	0	0	0	0	0	0	#N/A
LENG8	<i>leukocyte receptor cluster member 8</i>	0	0	0	0	0	0	0	0	0	0	#N/A
NFKB1	<i>nuclear factor kappa B subunit 1</i>	0	0	0	0	0	0	0	0	0	0	#N/A
SLU7	<i>SLU7 homolog, splicing factor</i>	0	0	0	0	0	0	0	0	0	0	#N/A
C15orf63	<i>huntingtin interacting protein K</i>	0	0	0	0	0	0	0	0	0	0	#N/A
BCAR1	<i>BCAR1 scaffold protein, Cas family member</i>	0	0	0	0	0	0	0	0	0	0	#N/A
CCDC50	<i>coiled-coil domain containing 50</i>	0	0	0	0	0	0	0	0	0	0	#N/A
EGFR	<i>epidermal growth factor receptor</i>	0	0	0	0	0	0	0	0	0	0	#N/A
PFAS	<i>phosphoribosylformylglycinamide synthase</i>	0	0	0	0	0	0	0	0	0	0	#N/A
COPS8	<i>COP9 signalosome subunit 8</i>	0	0	0	0	0	0	0	0	0	0	#N/A
ZRANB2	<i>zinc finger RANBP2-type containing 2</i>	0	0	0	0	0	0	0	0	0	0	#N/A
TYMS	<i>thymidylate synthetase</i>	0	0	0	0	0	0	0	0	0	0	#N/A
RBM25	<i>RNA binding motif protein 25</i>	0	0	0	0	0	0	0	0	0	0	#N/A
BAZ2A	<i>bromodomain adjacent to zinc finger domain 2A</i>	0	0	0	0	0	0	0	0	0	0	#N/A
SRGAP2	<i>SLIT-ROBO Rho GTPase activating protein 2</i>	0	0	0	0	0	0	0	0	0	0	#N/A
PHF2	<i>PHD finger protein 2</i>	0	0	0	0	0	0	0	0	0	0	#N/A
EIF4G3	<i>eukaryotic translation initiation factor 4 gamma 3</i>	0	0	0	0	0	0	0	0	0	0	#N/A
HARS	<i>histidyl-tRNA synthetase</i>	0	0	0	0	0	0	0	0	0	0	#N/A
MORF4L1	<i>mortality factor 4 like 1</i>	0	0	0	0	0	0	0	0	0	0	#N/A
CCNL2	<i>cyclin L2</i>	0	0	0	0	0	0	0	0	0	0	#N/A
GTF3C1	<i>general transcription factor IIIC subunit 1</i>	0	0	0	0	0	0	0	0	0	0	#N/A
LARP7	<i>La ribonucleoprotein domain family member 7</i>	0	0	0	0	0	0	0	0	0	0	#N/A
DNAJC9	<i>DnaJ heat shock protein family (Hsp40) member C9</i>	0	0	0	0	0	0	0	0	0	0	#N/A
WBP11	<i>WW domain binding protein 11</i>	0	0	0	0	0	0	0	0	0	0	#N/A
RUFY1	<i>RUN and FYVE domain containing 1</i>	0	0	0	0	0	0	0	0	0	0	#N/A

FLYWCH2	<i>FLYWCH family member 2</i>	0	0	0	0	0	0	0	0	0	0	#N/A
PPIL3	<i>peptidylprolyl isomerase like 3</i>	0	0	0	0	0	0	0	0	0	0	#N/A
SARNP	<i>SAP domain containing ribonucleoprotein</i>	0	0	0	0	0	0	0	0	0	0	#N/A
GPATCH1	<i>G-patch domain containing 1</i>	0	0	0	0	0	0	0	0	0	0	#N/A
STAT5B	<i>signal transducer and activator of transcription 5B</i>	0	0	0	0	0	0	0	0	0	0	#N/A
CRTC1	<i>CREB regulated transcription coactivator 1</i>	0	0	0	0	0	0	0	0	0	0	#N/A
RRP12	<i>ribosomal RNA processing 12 homolog</i>	0	0	0	0	0	0	0	0	0	0	#N/A
RACGAP1	<i>Rac GTPase activating protein 1</i>	0	0	0	0	0	0	0	0	0	0	#N/A
COPS7A	<i>COP9 signalosome subunit 7A</i>	0	0	0	0	0	0	0	0	0	0	#N/A
SNRPA	<i>small nuclear ribonucleoprotein polypeptide A</i>	0	0	0	0	0	0	0	0	0	0	#N/A
GPX4	<i>glutathione peroxidase 4</i>	0	0	0	0	0	0	0	0	0	0	#N/A
FARSB	<i>phenylalanyl-tRNA synthetase subunit beta</i>	0	0	0	0	0	0	0	0	0	0	#N/A
TRIM33	<i>tripartite motif containing 33</i>	0	0	0	0	0	0	0	0	0	0	#N/A
RTF1	<i>RTF1 homolog, Paf1/RNA polymerase II complex component</i>	0	0	0	0	0	0	0	0	0	0	#N/A
PMS1	<i>PMS1 homolog 1, mismatch repair system component</i>	0	0	0	0	0	0	0	0	0	0	#N/A
BAZ2B	<i>bromodomain adjacent to zinc finger domain 2B</i>	0	0	0	0	0	0	0	0	0	0	#N/A
PRPS1	<i>phosphoribosyl pyrophosphate synthetase 1</i>	0	0	0	0	0	0	0	0	0	0	#N/A
LIG3	<i>DNA ligase 3</i>	0	0	0	0	0	0	0	0	0	0	#N/A
EIF3C	<i>eukaryotic translation initiation factor 3 subunit C</i>	0	0	0	0	0	0	0	0	0	0	#N/A
BANF1	<i>barrier to autointegration factor 1</i>	0	0	0	0	0	0	0	0	0	0	#N/A
TOP3B	<i>DNA topoisomerase III beta</i>	0	0	0	0	0	0	0	0	0	0	#N/A
SPTBN1	<i>spectrin beta, non-erythrocytic 1</i>	0	0	0	0	0	0	0	0	0	0	#N/A
RC3H2	<i>ring finger and CCCH-type domains 2</i>	0	0	0	0	0	0	0	0	0	0	#N/A
MLL	<i>lysine methyltransferase 2A</i>	0	0	0	0	0	0	0	0	0	0	#N/A
SRP54	<i>signal recognition particle 54</i>	0	0	0	0	0	0	0	0	0	0	#N/A

INADL	<i>PATJ crumbs cell polarity complex component</i>	0	0	0	0	0	0	0	0	0	0	#N/A
GLTSCR2	<i>NOP53 ribosome biogenesis factor</i>	0	0	0	0	0	0	0	0	0	0	#N/A
HEXIM1	<i>HEXIM P-TEFb complex subunit 1</i>	0	0	0	0	0	0	0	0	0	0	#N/A
PPP1CC	<i>protein phosphatase 1 catalytic subunit gamma</i>	0	0	0	0	0	0	0	0	0	0	#N/A
ZMYM1	<i>zinc finger MYM-type containing 1</i>	0	0	0	0	0	0	0	0	0	0	#N/A
MTAP	<i>methylthioadenosine phosphorylase</i>	0	0	0	0	0	0	0	0	0	0	#N/A
CHD7	<i>chromodomain helicase DNA binding protein 7</i>	0	0	0	0	0	0	0	0	0	0	#N/A
ZC3H4	<i>zinc finger CCH-type containing 4</i>	0	0	0	0	0	0	0	0	0	0	#N/A
CLIC1	<i>chloride intracellular channel 1</i>	0	0	0	0	0	0	0	0	0	0	#N/A
CCNK	<i>cyclin K</i>	0	0	0	0	0	0	0	0	0	0	#N/A
RBBP4	<i>RB binding protein 4, chromatin remodeling factor</i>	0	0	0	0	0	0	0	0	0	0	#N/A
POP1	<i>POP1 homolog, ribonuclease P/MRP subunit</i>	0	0	0	0	0	0	0	0	0	0	#N/A
RIOK1	<i>RIO kinase 1</i>	0	0	0	0	0	0	0	0	0	0	#N/A
NCOR2	<i>nuclear receptor corepressor 2</i>	0	0	0	0	0	0	0	0	0	0	#N/A
YEATS2	<i>YEATS domain containing 2</i>	0	0	0	0	0	0	0	0	0	0	#N/A
RANBP9	<i>RAN binding protein 9</i>	0	0	0	0	0	0	0	0	0	0	#N/A
ANAPC4	<i>anaphase promoting complex subunit 4</i>	0	0	0	0	0	0	0	0	0	0	#N/A
LIN54	<i>lin-54 DREAM MuvB core complex component</i>	0	0	0	0	0	0	0	0	0	0	#N/A
WAC	<i>WW domain containing adaptor with coiled-coil</i>	0	0	0	0	0	0	0	0	0	0	#N/A
HMGA1	<i>high mobility group AT-hook 1</i>	0	0	0	0	0	0	0	0	0	0	#N/A
DAZAP1	<i>DAZ associated protein 1</i>	0	0	0	0	0	0	0	0	0	0	#N/A
UBFD1	<i>ubiquitin family domain containing 1</i>	0	0	0	0	0	0	0	0	0	0	#N/A
WDR75	<i>WD repeat domain 75</i>	0	0	0	0	0	0	0	0	0	0	#N/A
CHMP5	<i>charged multivesicular body protein 5</i>	0	0	0	0	0	0	0	0	0	0	#N/A
GAR1	<i>GAR1 ribonucleoprotein</i>	0	0	0	0	0	0	0	0	0	0	#N/A
TRIP12	<i>thyroid hormone receptor interactor 12</i>	0	0	0	0	0	0	0	0	0	0	#N/A

PRKCI	<i>protein kinase C iota</i>	0	0	0	0	0	0	0	0	0	0	#N/A
WIZ	<i>WIZ zinc finger</i>	0	0	0	0	0	0	0	0	0	0	#N/A
NOL6	<i>nucleolar protein 6</i>	0	0	0	0	0	0	0	0	0	0	#N/A
DEPDC1B	<i>DEP domain containing 1B</i>	0	0	0	0	0	0	0	0	0	0	#N/A
PCMT1	<i>protein-L-isoaspartate (D-aspartate) O-methyltransferase</i>	0	0	0	0	0	0	0	0	0	0	#N/A
POGZ	<i>pogo transposable element derived with ZNF domain</i>	0	0	0	0	0	0	0	0	0	0	#N/A
MPHOSP H10	<i>M-phase phosphoprotein 10</i>	0	0	0	0	0	0	0	0	0	0	#N/A
PPP1R2	<i>protein phosphatase 1 regulatory inhibitor subunit 2</i>	0	0	0	0	0	0	0	0	0	0	#N/A
TMOD3	<i>tropomodulin 3</i>	0	0	0	0	0	0	0	0	0	0	#N/A
CTR9	<i>CTR9 homolog, Paf1/RNA polymerase II complex component</i>	0	0	0	0	0	0	0	0	0	0	#N/A
CNOT7	<i>CCR4-NOT transcription complex subunit 7</i>	0	0	0	0	0	0	0	0	0	0	#N/A
ANP32E	<i>acidic nuclear phosphoprotein 32 family member E</i>	0	0	0	0	0	0	0	0	0	0	#N/A
REPS1	<i>RALBP1 associated Eps domain containing 1</i>	0	0	0	0	0	0	0	0	0	0	#N/A
CSNK1D	<i>casein kinase 1 delta</i>	0	0	0	0	0	0	0	0	0	0	#N/A
ARHGAP 21	<i>Rho GTPase activating protein 21</i>	0	0	0	0	0	0	0	0	0	0	#N/A
MICAL3	<i>microtubule associated monooxygenase, calponin and LIM domain containing 3</i>	0	0	0	0	0	0	0	0	0	0	#N/A
GCFC1	<i>PAX3 and PAX7 binding protein 1</i>	0	0	0	0	0	0	0	0	0	0	#N/A
TPM2	<i>tropomyosin 2</i>	0	0	0	0	0	0	0	0	0	0	#N/A
ZNF644	<i>zinc finger protein 644</i>	0	0	0	0	0	0	0	0	0	0	#N/A
SRFBP1	<i>serum response factor binding protein 1</i>	0	0	0	0	0	0	0	0	0	0	#N/A
NCOA7	<i>nuclear receptor coactivator 7</i>	0	0	0	0	0	0	0	0	0	0	#N/A
FAM135A	<i>family with sequence similarity 135 member A</i>	0	0	0	0	0	0	0	0	0	0	#N/A
NCOA6	<i>nuclear receptor coactivator 6</i>	0	0	0	0	0	0	0	0	0	0	#N/A
RPA2	<i>replication protein A2</i>	0	0	0	0	0	0	0	0	0	0	#N/A
KPNA3	<i>karyopherin subunit alpha 3</i>	0	0	0	0	0	0	0	0	0	0	#N/A

EIF3J	<i>eukaryotic translation initiation factor 3 subunit J</i>	0	0	0	0	0	0	0	0	0	0	#N/A
ELAC2	<i>elaC ribonuclease Z 2</i>	0	0	0	0	0	0	0	0	0	0	#N/A
ZNF131	<i>zinc finger protein 131</i>	0	0	0	0	0	0	0	0	0	0	#N/A
ACTL6A	<i>actin like 6A</i>	0	0	0	0	0	0	0	0	0	0	#N/A
IK	<i>IK cytokine</i>	0	0	0	0	0	0	0	0	0	0	#N/A
RFX1	<i>regulatory factor X1</i>	0	0	0	0	0	0	0	0	0	0	#N/A
INTS3	<i>integrator complex subunit 3</i>	0	0	0	0	0	0	0	0	0	0	#N/A
CHMP7	<i>charged multivesicular body protein 7</i>	0	0	0	0	0	0	0	0	0	0	#N/A
NRBF2	<i>nuclear receptor binding factor 2</i>	0	0	0	0	0	0	0	0	0	0	#N/A
C19orf43	<i>telomerase RNA component interacting RNase</i>	0	0	0	0	0	0	0	0	0	0	#N/A
MTMR6	<i>myotubularin related protein 6</i>	0	0	0	0	0	0	0	0	0	0	#N/A
THOC3	<i>THO complex 3</i>	0	0	0	0	0	0	0	0	0	0	#N/A
WDR62	<i>WD repeat domain 62</i>	0	0	0	0	0	0	0	0	0	0	#N/A
FNBP4	<i>formin binding protein 4</i>	0	0	0	0	0	0	0	0	0	0	#N/A
LSM14A	<i>LSM14A mRNA processing body assembly factor</i>	0	0	0	0	0	0	0	0	0	0	#N/A
BBX	<i>BBX high mobility group box domain containing</i>	0	0	0	0	0	0	0	0	0	0	#N/A
XPR1	<i>xenotropic and polytropic retrovirus receptor 1</i>	0	0	0	0	0	0	0	0	0	0	#N/A
DDX41	<i>DEAD-box helicase 41</i>	0	0	0	0	0	0	0	0	0	0	#N/A
TAF6	<i>TATA-box binding protein associated factor 6</i>	0	0	0	0	0	0	0	0	0	0	#N/A
ROBO1	<i>roundabout guidance receptor 1</i>	0	0	0	0	0	0	0	0	0	0	#N/A
BTAF1	<i>B-TFIID TATA-box binding protein associated factor 1</i>	0	0	0	0	0	0	0	0	0	0	#N/A
POLDIP3	<i>DNA polymerase delta interacting protein 3</i>	0	0	0	0	0	0	0	0	0	0	#N/A
COPS5	<i>COP9 signalosome subunit 5</i>	0	0	0	0	0	0	0	0	0	0	#N/A
NOSIP	<i>nitric oxide synthase interacting protein</i>	0	0	0	0	0	0	0	0	0	0	#N/A
DCP1B	<i>decapping mRNA 1B</i>	0	0	0	0	0	0	0	0	0	0	#N/A
PMS2	<i>PMS1 homolog 2, mismatch repair system component</i>	0	0	0	0	0	0	0	0	0	0	#N/A

EXOSC5	<i>exosome component 5</i>	0	0	0	0	0	0	0	0	0	0	#N/A
UBA2	<i>ubiquitin like modifier activating enzyme 2</i>	0	0	0	0	0	0	0	0	0	0	#N/A
TSG101	<i>tumor susceptibility 101</i>	0	0	0	0	0	0	0	0	0	0	#N/A
ARID2	<i>AT-rich interaction domain 2</i>	0	0	0	0	0	0	0	0	0	0	#N/A
IRAK1	<i>interleukin 1 receptor associated kinase 1</i>	0	0	0	0	0	0	0	0	0	0	#N/A
EFTUD1	<i>elongation factor like GTPase 1</i>	0	0	0	0	0	0	0	0	0	0	#N/A
YTHDF3	<i>YTH N6-methyladenosine RNA binding protein 3</i>	0	0	0	0	0	0	0	0	0	0	#N/A
CLASP1	<i>cytoplasmic linker associated protein 1</i>	0	0	0	0	0	0	0	0	0	0	#N/A
CRTC3	<i>CREB regulated transcription coactivator 3</i>	0	0	0	0	0	0	0	0	0	0	#N/A
CDK12	<i>cyclin dependent kinase 12</i>	0	0	0	0	0	0	0	0	0	0	#N/A
PAPOLG	<i>poly(A) polymerase gamma</i>	0	0	0	0	0	0	0	0	0	0	#N/A
PRUNE	<i>prune exopolyphosphatase 1</i>	0	0	0	0	0	0	0	0	0	0	#N/A
POLR2B	<i>RNA polymerase II subunit B</i>	0	0	0	0	0	0	0	0	0	0	#N/A
LARP4B	<i>La ribonucleoprotein domain family member 4B</i>	0	0	0	0	0	0	0	0	0	0	#N/A
DHX38	<i>DEAH-box helicase 38</i>	0	0	0	0	0	0	0	0	0	0	#N/A
SUDS3	<i>SDS3 homolog, SIN3A corepressor complex component</i>	0	0	0	0	0	0	0	0	0	0	#N/A
C16orf88	<i>lysine rich nucleolar protein 1</i>	0	0	0	0	0	0	0	0	0	0	#N/A
TFCP2	<i>transcription factor CP2</i>	0	0	0	0	0	0	0	0	0	0	#N/A
CALM2	<i>calmodulin 2</i>	0	0	0	0	0	0	0	0	0	0	#N/A
CSNK2B	<i>casein kinase 2 beta</i>	0	0	0	0	0	0	0	0	0	0	#N/A
ELP3	<i>elongator acetyltransferase complex subunit 3</i>	0	0	0	0	0	0	0	0	0	0	#N/A
IDH1	<i>isocitrate dehydrogenase (NADP(+)) 1, cytosolic</i>	0	0	0	0	0	0	0	0	0	0	#N/A
GPHN	<i>gephyrin</i>	0	0	0	0	0	0	0	0	0	0	#N/A
DCAF7	<i>DDB1 and CUL4 associated factor 7</i>	0	0	0	0	0	0	0	0	0	0	#N/A
WHSC1	<i>nuclear receptor binding SET domain protein 2</i>	0	0	0	0	0	0	0	0	0	0	#N/A
UBTF	<i>upstream binding transcription factor</i>	0	0	0	0	0	0	0	0	0	0	#N/A

ZFYVE16	<i>zinc finger FYVE-type containing 16</i>	0	0	0	0	0	0	0	0	0	0	#N/A
MYO9B	<i>myosin IXB</i>	0	0	0	0	0	0	0	0	0	0	#N/A
TOPBP1	<i>DNA topoisomerase II binding protein 1</i>	0	0	0	0	0	0	0	0	0	0	#N/A
SMARCE1	<i>SWI/SNF related, matrix associated, actin dependent regulator of chromatin, subfamily e, member 1</i>	0	0	0	0	0	0	0	0	0	0	#N/A
AKAP13	<i>A-kinase anchoring protein 13</i>	0	0	0	0	0	0	0	0	0	0	#N/A
SFSWAP	<i>splicing factor SWAP</i>	0	0	0	0	0	0	0	0	0	0	#N/A
TES	<i>testin LIM domain protein</i>	0	0	0	0	0	0	0	0	0	0	#N/A
SYNRG	<i>synergin gamma</i>	0	0	0	0	0	0	0	0	0	0	#N/A
DDX20	<i>DEAD-box helicase 20</i>	0	0	0	0	0	0	0	0	0	0	#N/A
SPECC1	<i>sperm antigen with calponin homology and coiled-coil domains 1</i>	0	0	0	0	0	0	0	0	0	0	#N/A
PTRF	<i>caveolae associated protein 1</i>	0	0	0	0	0	0	0	0	0	0	#N/A
BUB1	<i>BUB1 mitotic checkpoint serine/threonine kinase</i>	0	0	0	0	0	0	0	0	0	0	#N/A
KIDINS220	<i>kinase D interacting substrate 220</i>	0	0	0	0	0	0	0	0	0	0	#N/A
CWC27	<i>CWC27 spliceosome associated cyclophilin</i>	0	0	0	0	0	0	0	0	0	0	#N/A
CCNL1	<i>cyclin L1</i>	0	0	0	0	0	0	0	0	0	0	#N/A
PIP4K2C	<i>phosphatidylinositol-5-phosphate 4-kinase type 2 gamma</i>	0	0	0	0	0	0	0	0	0	0	#N/A
CHD1	<i>chromodomain helicase DNA binding protein 1</i>	0	0	0	0	0	0	0	0	0	0	#N/A
NR2C1	<i>nuclear receptor subfamily 2 group C member 1</i>	0	0	0	0	0	0	0	0	0	0	#N/A
KIAA0182	<i>Gse1 coiled-coil protein</i>	0	0	0	0	0	0	0	0	0	0	#N/A
STAMBP	<i>STAM binding protein</i>	0	0	0	0	0	0	0	0	0	0	#N/A
PDCL	<i>phosducin like</i>	0	0	0	0	0	0	0	0	0	0	#N/A
ATP6V1E1	<i>ATPase H⁺ transporting V1 subunit E1</i>	0	0	0	0	0	0	0	0	0	0	#N/A
MYSM1	<i>Myb like, SWIRM and MPN domains 1</i>	0	0	0	0	0	0	0	0	0	0	#N/A

PARD3	<i>par-3 family cell polarity regulator</i>	0	0	0	0	0	0	0	0	0	0	#N/A
COBL	<i>cordon-bleu WH2 repeat protein</i>	0	0	0	0	0	0	0	0	0	0	#N/A
CD3EAP	<i>CD3e molecule associated protein</i>	0	0	0	0	0	0	0	0	0	0	#N/A
WHSC2	<i>negative elongation factor complex member A</i>	0	0	0	0	0	0	0	0	0	0	#N/A
SRSF12	<i>serine and arginine rich splicing factor 12</i>	0	0	0	0	0	0	0	0	0	0	#N/A
RAVER1	<i>ribonucleoprotein, PTB binding 1</i>	0	0	0	0	0	0	0	0	0	0	#N/A
SLAIN2	<i>SLAIN motif family member 2</i>	0	0	0	0	0	0	0	0	0	0	#N/A
FAM193A	<i>family with sequence similarity 193 member A</i>	0	0	0	0	0	0	0	0	0	0	#N/A
MYO6	<i>myosin VI</i>	0	0	0	0	0	0	0	0	0	0	#N/A
SUPT6H	<i>SPT6 homolog, histone chaperone and transcription elongation factor</i>	0	0	0	0	0	0	0	0	0	0	#N/A
RAB3GAP1	<i>RAB3 GTPase activating protein catalytic subunit 1</i>	0	0	0	0	0	0	0	0	0	0	#N/A
FKBP3	<i>FKBP prolyl isomerase 3</i>	0	0	0	0	0	0	0	0	0	0	#N/A
CCDC72	<i>translation machinery associated 7 homolog</i>	0	0	0	0	0	0	0	0	0	0	#N/A
COMMD9	<i>COMM domain containing 9</i>	0	0	0	0	0	0	0	0	0	0	#N/A
BAP1	<i>BRCA1 associated protein 1</i>	0	0	0	0	0	0	0	0	0	0	#N/A
COPB2	<i>coatamer protein complex subunit beta 2</i>	0	0	0	0	0	0	0	0	0	0	#N/A
VAPB	<i>VAMP associated protein B and C</i>	0	0	0	0	0	0	0	0	0	0	#N/A
CCS	<i>copper chaperone for superoxide dismutase</i>	0	0	0	0	0	0	0	0	0	0	#N/A
RCL1	<i>RNA terminal phosphate cyclase like 1</i>	0	0	0	0	0	0	0	0	0	0	#N/A
LSM6	<i>LSM6 homolog, U6 small nuclear RNA and mRNA degradation associated</i>	0	0	0	0	0	0	0	0	0	0	#N/A
BCAS3	<i>BCAS3 microtubule associated cell migration factor</i>	0	0	0	0	0	0	0	0	0	0	#N/A
MCM3AP	<i>minichromosome maintenance complex component 3 associated protein</i>	0	0	0	0	0	0	0	0	0	0	#N/A
POLA2	<i>DNA polymerase alpha 2, accessory subunit</i>	0	0	0	0	0	0	0	0	0	0	#N/A
ASCC1	<i>activating signal cointegrator 1 complex subunit 1</i>	0	0	0	0	0	0	0	0	0	0	#N/A

KIF13A	<i>kinesin family member 13A</i>	0	0	0	0	0	0	0	0	0	0	#N/A
DHPS	<i>deoxyhypusine synthase</i>	0	0	0	0	0	0	0	0	0	0	#N/A
SIPA1L1	<i>signal induced proliferation associated 1 like 1</i>	0	0	0	0	0	0	0	0	0	0	#N/A
KIAA0586	<i>KIAA0586</i>	0	0	0	0	0	0	0	0	0	0	#N/A
VANGL1	<i>VANGL planar cell polarity protein 1</i>	0	0	0	0	0	0	0	0	0	0	#N/A
PGK1	<i>phosphoglycerate kinase 1</i>	0	0	0	0	0	0	0	0	0	0	#N/A
DLST	<i>dihydrolipoamide S-succinyltransferase</i>	0	0	0	0	0	0	0	0	0	0	#N/A
RNH1	<i>ribonuclease/angiogenin inhibitor 1</i>	0	0	0	0	0	0	0	0	0	0	#N/A
GLO1	<i>glyoxalase 1</i>	0	0	0	0	0	0	0	0	0	0	#N/A
CPNE8	<i>copine 8</i>	0	0	0	0	0	0	0	0	0	0	#N/A
UQCRC1	<i>ubiquinol-cytochrome c reductase core protein 1</i>	0	0	0	0	0	0	0	0	0	0	#N/A
PRDX3	<i>peroxiredoxin 3</i>	0	0	0	0	0	0	0	0	0	0	#N/A
VPS35	<i>VPS35 retromer complex component</i>	0	0	0	0	0	0	0	0	0	0	#N/A
GNAI2	<i>G protein subunit alpha i2</i>	0	0	0	0	0	0	0	0	0	0	#N/A
ANXA6	<i>annexin A6</i>	0	0	0	0	0	0	0	0	0	0	#N/A
PLD3	<i>phospholipase D family member 3</i>	0	0	0	0	0	0	0	0	0	0	#N/A
NAPA	<i>NSF attachment protein alpha</i>	0	0	0	0	0	0	0	0	0	0	#N/A
AHCY	<i>adenosylhomocysteinase</i>	0	0	0	0	0	0	0	0	0	0	#N/A
PDIA3	<i>protein disulfide isomerase family A member 3</i>	0	0	0	0	0	0	0	0	0	0	#N/A
P4HB	<i>prolyl 4-hydroxylase subunit beta</i>	0	0	0	0	0	0	0	0	0	0	#N/A
ANXA11	<i>annexin A11</i>	0	0	0	0	0	0	0	0	0	0	#N/A
AGPS	<i>alkylglycerone phosphate synthase</i>	0	0	0	0	0	0	0	0	0	0	#N/A
HSD17B4	<i>hydroxysteroid 17-beta dehydrogenase 4</i>	0	0	0	0	0	0	0	0	0	0	#N/A
GNAI3	<i>G protein subunit alpha i3</i>	0	0	0	0	0	0	0	0	0	0	#N/A
ATP1B3	<i>ATPase Na⁺/K⁺ transporting subunit beta 3</i>	0	0	0	0	0	0	0	0	0	0	#N/A
SLC30A1	<i>solute carrier family 30 member 1</i>	0	0	0	0	0	0	0	0	0	0	#N/A
ATP2C1	<i>ATPase secretory pathway Ca²⁺ transporting 1</i>	0	0	0	0	0	0	0	0	0	0	#N/A

FKBP8	<i>FKBP prolyl isomerase 8</i>	0	0	0	0	0	0	0	0	0	0	#N/A
ATP11A	<i>ATPase phospholipid transporting 11A</i>	0	0	0	0	0	0	0	0	0	0	#N/A
TRIM27	<i>tripartite motif containing 27</i>	0	0	0	0	0	0	0	0	0	0	#N/A
RAB35	<i>RAB35, member RAS oncogene family</i>	0	0	0	0	0	0	0	0	0	0	#N/A
AP1M1	<i>adaptor related protein complex 1 subunit mu 1</i>	0	0	0	0	0	0	0	0	0	0	#N/A
SNAP23	<i>synaptosome associated protein 23</i>	0	0	0	0	0	0	0	0	0	0	#N/A
PTPN1	<i>protein tyrosine phosphatase non-receptor type 1</i>	0	0	0	0	0	0	0	0	0	0	#N/A
AP1G1	<i>adaptor related protein complex 1 subunit gamma 1</i>	0	0	0	0	0	0	0	0	0	0	#N/A
ACTN1	<i>actinin alpha 1</i>	0	0	0	0	0	0	0	0	0	0	#N/A
LAMTOR 1	<i>late endosomal/lysosomal adaptor, MAPK and MTOR activator 1</i>	0	0	0	0	0	0	0	0	0	0	#N/A
ROCK2	<i>Rho associated coiled-coil containing protein kinase 2</i>	0	0	0	0	0	0	0	0	0	0	#N/A
AP1B1	<i>adaptor related protein complex 1 subunit beta 1</i>	0	0	0	0	0	0	0	0	0	0	#N/A
CUL3	<i>cullin 3</i>	0	0	0	0	0	0	0	0	0	0	#N/A
CISD2	<i>CDGSH iron sulfur domain 2</i>	0	0	0	0	0	0	0	0	0	0	#N/A
SEC61B	<i>SEC61 translocon beta subunit</i>	0	0	0	0	0	0	0	0	0	0	#N/A
NBAS	<i>neuroblastoma amplified sequence</i>	0	0	0	0	0	0	0	0	0	0	#N/A
CD97	<i>adhesion G protein-coupled receptor E5</i>	0	0	0	0	0	0	0	0	0	0	#N/A
VPS28	<i>VPS28 subunit of ESCRT-1</i>	0	0	0	0	0	0	0	0	0	0	#N/A
GNB1	<i>G protein subunit beta 1</i>	0	0	0	0	0	0	0	0	0	0	#N/A
SBF1	<i>SET binding factor 1</i>	0	0	0	0	0	0	0	0	0	0	#N/A
SLC39A14	<i>solute carrier family 39 member 14</i>	0	0	0	0	0	0	0	0	0	0	#N/A
KIAA0528	<i>C2 calcium dependent domain containing 5</i>	0	0	0	0	0	0	0	0	0	0	#N/A
FLOT2	<i>flotillin 2</i>	0	0	0	0	0	0	0	0	0	0	#N/A
TMF1	<i>TATA element modulatory factor 1</i>	0	0	0	0	0	0	0	0	0	0	#N/A
MAN1B1	<i>mannosidase alpha class 1B member 1</i>	0	0	0	0	0	0	0	0	0	0	#N/A
S100A10	<i>S100 calcium binding protein A10</i>	0	0	0	0	0	0	0	0	0	0	#N/A

GOLGA4	<i>golgin A4</i>	0	0	0	0	0	0	0	0	0	0	#N/A
HIST1H2AE	<i>histone cluster 1 H2A family member e</i>	0	0	0	0	0	0	0	0	0	0	#N/A
GCC2	<i>GRIP and coiled-coil domain containing 2</i>	0	0	0	0	0	0	0	0	0	0	#N/A
GOSR2	<i>golgi SNAP receptor complex member 2</i>	0	0	0	0	0	0	0	0	0	0	#N/A
TM9SF3	<i>transmembrane 9 superfamily member 3</i>	0	0	0	0	0	0	0	0	0	0	#N/A
SGMS1	<i>sphingomyelin synthase 1</i>	0	0	0	0	0	0	0	0	0	0	#N/A
SLC35A2	<i>solute carrier family 35 member A2</i>	0	0	0	0	0	0	0	0	0	0	#N/A
CANT1	<i>calcium activated nucleotidase 1</i>	0	0	0	0	0	0	0	0	0	0	#N/A
SEC24B	<i>SEC24 homolog B, COPII coat complex component</i>	0	0	0	0	0	0	0	0	0	0	#N/A
HLA-B	<i>major histocompatibility complex, class I, B</i>	0	0	0	0	0	0	0	0	0	0	#N/A
ATP6V1G1	<i>ATPase H+ transporting V1 subunit G1</i>	0	0	0	0	0	0	0	0	0	0	#N/A
RHBDD2	<i>rhomboid domain containing 2</i>	0	0	0	0	0	0	0	0	0	0	#N/A
PACSIN3	<i>protein kinase C and casein kinase substrate in neurons 3</i>	0	0	0	0	0	0	0	0	0	0	#N/A
NRAS	<i>NRAS proto-oncogene, GTPase</i>	0	0	0	0	0	0	0	0	0	0	#N/A
ZFPL1	<i>zinc finger protein like 1</i>	0	0	0	0	0	0	0	0	0	0	#N/A
GORASP2	<i>golgi reassembly stacking protein 2</i>	0	0	0	0	0	0	0	0	0	0	#N/A
MAN2A1	<i>mannosidase alpha class 2A member 1</i>	0	0	0	0	0	0	0	0	0	0	#N/A
PRAF2	<i>PRA1 domain family member 2</i>	0	0	0	0	0	0	0	0	0	0	#N/A
STX10	<i>syntaxin 10</i>	0	0	0	0	0	0	0	0	0	0	#N/A
B3GALT6	<i>beta-1,3-galactosyltransferase 6</i>	0	0	0	0	0	0	0	0	0	0	#N/A
PKP4	<i>plakophilin 4</i>	0	0	0	0	0	0	0	0	0	0	#N/A
IGF2R	<i>insulin like growth factor 2 receptor</i>	0	0	0	0	0	0	0	0	0	0	#N/A
GLT8D1	<i>glycosyltransferase 8 domain containing 1</i>	0	0	0	0	0	0	0	0	0	0	#N/A
GORAB	<i>golgin, RAB6 interacting</i>	0	0	0	0	0	0	0	0	0	0	#N/A
VPS13B	<i>vacuolar protein sorting 13 homolog B</i>	0	0	0	0	0	0	0	0	0	0	#N/A
TMEM30	<i>transmembrane protein 30A</i>	0	0	0	0	0	0	0	0	0	0	#N/A

A												
ABI2	<i>abl interactor 2</i>	0	0	0	0	0	0	0	0	0	0	#N/A
TPM4	<i>tropomyosin 4</i>	0	0	0	0	0	0	0	0	0	0	#N/A
ZDHHC13	<i>zinc finger DHHC-type containing 13</i>	0	0	0	0	0	0	0	0	0	0	#N/A
GRIN2B	<i>glutamate ionotropic receptor NMDA type subunit 2B</i>	0	0	0	0	0	0	0	0	0	0	#N/A
RRAS2	<i>RAS related 2</i>	0	0	0	0	0	0	0	0	0	0	#N/A
ZDHHC17	<i>zinc finger DHHC-type containing 17</i>	0	0	0	0	0	0	0	0	0	0	#N/A
MUC16	<i>mucin 16, cell surface associated</i>	0	0	0	0	0	0	0	0	0	0	#N/A
CAV1	<i>caveolin 1</i>	0	0	0	0	0	0	0	0	0	0	#N/A
HS2ST1	<i>heparan sulfate 2-O-sulfotransferase 1</i>	0	0	0	0	0	0	0	0	0	0	#N/A
GLG1	<i>golgi glycoprotein 1</i>	0	0	0	0	0	0	0	0	0	0	#N/A
KCNN4	<i>potassium calcium-activated channel subfamily N member 4</i>	0	0	0	0	0	0	0	0	0	0	#N/A
PKP3	<i>plakophilin 3</i>	0	0	0	0	0	0	0	0	0	0	#N/A
FRAS1	<i>Fraser extracellular matrix complex subunit 1</i>	0	0	0	0	0	0	0	0	0	0	#N/A
SLC38A1	<i>solute carrier family 38 member 1</i>	0	0	0	0	0	0	0	0	0	0	#N/A
OSBPL11	<i>oxysterol binding protein like 11</i>	0	0	0	0	0	0	0	0	0	0	#N/A
AKAP9	<i>A-kinase anchoring protein 9</i>	0	0	0	0	0	0	0	0	0	0	#N/A
TM9SF2	<i>transmembrane 9 superfamily member 2</i>	0	0	0	0	0	0	0	0	0	0	#N/A
FLOT1	<i>flotillin 1</i>	0	0	0	0	0	0	0	0	0	0	#N/A
RALA	<i>RAS like proto-oncogene A</i>	0	0	0	0	0	0	0	0	0	0	#N/A
SLC30A7	<i>solute carrier family 30 member 7</i>	0	0	0	0	0	0	0	0	0	0	#N/A
DAB2IP	<i>DAB2 interacting protein</i>	0	0	0	0	0	0	0	0	0	0	#N/A
CCDC82	<i>coiled-coil domain containing 82</i>	0	0	0	0	0	0	0	0	0	0	#N/A
OSBPL9	<i>oxysterol binding protein like 9</i>	0	0	0	0	0	0	0	0	0	0	#N/A
KIF5C	<i>kinesin family member 5C</i>	0	0	0	0	0	0	0	0	0	0	#N/A
BSDC1	<i>BSD domain containing 1</i>	0	0	0	0	0	0	0	0	0	0	#N/A
SH3BP4	<i>SH3 domain binding protein 4</i>	0	0	0	0	0	0	0	0	0	0	#N/A
DSG1	<i>desmoglein 1</i>	0	0	0	0	0	0	0	0	0	0	#N/A

PLCB4	<i>phospholipase C beta 4</i>	0	0	0	0	0	0	0	0	0	0	#N/A
MAP4K4	<i>mitogen-activated protein kinase kinase kinase 4</i>	0	0	0	0	0	0	0	0	0	0	#N/A
RAB11FIP5	<i>RAB11 family interacting protein 5</i>	0	0	0	0	0	0	0	0	0	0	#N/A
FYN	<i>FYN proto-oncogene, Src family tyrosine kinase</i>	0	0	0	0	0	0	0	0	0	0	#N/A
MPRIP	<i>myosin phosphatase Rho interacting protein</i>	0	0	0	0	0	0	0	0	0	0	#N/A
WDR91	<i>WD repeat domain 91</i>	0	0	0	0	0	0	0	0	0	0	#N/A
ATP6V0D1	<i>ATPase H+ transporting V0 subunit d1</i>	0	0	0	0	0	0	0	0	0	0	#N/A
CDKAL1	<i>CDK5 regulatory subunit associated protein 1 like 1</i>	0	0	0	0	0	0	0	0	0	0	#N/A
KIF26B	<i>kinesin family member 26B</i>	0	0	0	0	0	0	0	0	0	0	#N/A
ATP6V0A2	<i>ATPase H+ transporting V0 subunit a2</i>	0	0	0	0	0	0	0	0	0	0	#N/A
EFR3A	<i>EFR3 homolog A</i>	0	0	0	0	0	0	0	0	0	0	#N/A
WDR81	<i>WD repeat domain 81</i>	0	0	0	0	0	0	0	0	0	0	#N/A
LNPEP	<i>leucyl and cystinyl aminopeptidase</i>	0	0	0	0	0	0	0	0	0	0	#N/A
FLG2	<i>filaggrin family member 2</i>	0	0	0	0	0	0	0	0	0	0	#N/A
ATP6V0A1	<i>ATPase H+ transporting V0 subunit a1</i>	0	0	0	0	0	0	0	0	0	0	#N/A
VAMP7	<i>vesicle associated membrane protein 7</i>	0	0	0	0	0	0	0	0	0	0	#N/A
LAMTOR3	<i>late endosomal/lysosomal adaptor, MAPK and MTOR activator 3</i>	0	0	0	0	0	0	0	0	0	0	#N/A
CASK	<i>calcium/calmodulin dependent serine protein kinase</i>	0	0	0	0	0	0	0	0	0	0	#N/A
B4GALT1	<i>beta-1,4-galactosyltransferase 1</i>	0	0	0	0	0	0	0	0	0	0	#N/A
SDCBP	<i>syndecan binding protein</i>	0	0	0	0	0	0	0	0	0	0	#N/A
TRIOBP	<i>TRIO and F-actin binding protein</i>	0	0	0	0	0	0	0	0	0	0	#N/A
TM9SF4	<i>transmembrane 9 superfamily member 4</i>	0	0	0	0	0	0	0	0	0	0	#N/A
SGPL1	<i>sphingosine-1-phosphate lyase 1</i>	0	0	0	0	0	0	0	0	0	0	#N/A
CPD	<i>carboxypeptidase D</i>	0	0	0	0	0	0	0	0	0	0	#N/A
MGAT1	<i>mannosyl (alpha-1,3-)-glycoprotein</i>	0	0	0	0	0	0	0	0	0	0	#N/A

<i>beta-1,2-N-acetylglucosaminyltransferase</i>												
S100A11	<i>S100 calcium binding protein A11</i>	0	0	0	0	0	0	0	0	0	0	#N/A
QSOX2	<i>quiescin sulfhydryl oxidase 2</i>	0	0	0	0	0	0	0	0	0	0	#N/A
NBR1	<i>NBR1 autophagy cargo receptor</i>	0	0	0	0	0	0	0	0	0	0	#N/A
TRPM7	<i>transient receptor potential cation channel subfamily M member 7</i>	0	0	0	0	0	0	0	0	0	0	#N/A
SLMAP	<i>sarcolemma associated protein</i>	0	0	0	0	0	0	0	0	0	0	#N/A
DSC1	<i>desmocollin 1</i>	0	0	0	0	0	0	0	0	0	0	#N/A
EMID2	<i>collagen type XXVI alpha 1 chain</i>	0	0	0	0	0	0	0	0	0	0	#N/A
VT11B	<i>vesicle transport through interaction with t-SNAREs 1B</i>	0	0	0	0	0	0	0	0	0	0	#N/A
RPS10-NUDT3	<i>RPS10-NUDT3 readthrough</i>	0	0	0	0	0	0	0	0	0	0	#N/A
PI4K2B	<i>phosphatidylinositol 4-kinase type 2 beta</i>	0	0	0	0	0	0	0	0	0	0	#N/A
KCTD14	<i>potassium channel tetramerization domain containing 14</i>	0	0	0	0	0	0	0	0	0	0	#N/A
PEF1	<i>penta-EF-hand domain containing 1</i>	0	0	0	0	0	0	0	0	0	0	#N/A
STX7	<i>syntaxin 7</i>	0	0	0	0	0	0	0	0	0	0	#N/A
ERP29	<i>endoplasmic reticulum protein 29</i>	0	0	0	0	0	0	0	0	0	0	#N/A
ZDHHC5	<i>zinc finger DHHC-type containing 5</i>	0	0	0	0	0	0	0	0	0	0	#N/A
BAIAP2L1	<i>BAI1 associated protein 2 like 1</i>	0	0	0	0	0	0	0	0	0	0	#N/A
VPS45	<i>vacuolar protein sorting 45 homolog</i>	0	0	0	0	0	0	0	0	0	0	#N/A
DSC3	<i>desmocollin 3</i>	0	0	0	0	0	0	0	0	0	0	#N/A
CDK5RAP3	<i>CDK5 regulatory subunit associated protein 3</i>	0	0	0	0	0	0	0	0	0	0	#N/A
CHMP2A	<i>charged multivesicular body protein 2A</i>	0	0	0	0	0	0	0	0	0	0	#N/A
AFTPH	<i>aftiphilin</i>	0	0	0	0	0	0	0	0	0	0	#N/A
MTMR1	<i>myotubularin related protein 1</i>	0	0	0	0	0	0	0	0	0	0	#N/A
STRN4	<i>striatin 4</i>	0	0	0	0	0	0	0	0	0	0	#N/A
VRK2	<i>VRK serine/threonine kinase 2</i>	0	0	0	0	0	0	0	0	0	0	#N/A
ATP13A3	<i>ATPase 13A3</i>	0	0	0	0	0	0	0	0	0	0	#N/A

ADCY9	<i>adenylate cyclase 9</i>	0	0	0	0	0	0	0	0	0	0	#N/A
GLT8D2	<i>glycosyltransferase 8 domain containing 2</i>	0	0	0	0	0	0	0	0	0	0	#N/A
ANKLE2	<i>ankyrin repeat and LEM domain containing 2</i>	0	0	0	0	0	0	0	0	0	0	#N/A
SNAPIN	<i>SNAP associated protein</i>	0	0	0	0	0	0	0	0	0	0	#N/A
TAX1BP1	<i>Tax1 binding protein 1</i>	0	0	0	0	0	0	0	0	0	0	#N/A
UTRN	<i>utrophin</i>	0	0	0	0	0	0	0	0	0	0	#N/A
GPRIN1	<i>G protein regulated inducer of neurite outgrowth 1</i>	0	0	0	0	0	0	0	0	0	0	#N/A
ABI1	<i>abl interactor 1</i>	0	0	0	0	0	0	0	0	0	0	#N/A
STEAP3	<i>STEAP3 metalloredutase</i>	0	0	0	0	0	0	0	0	0	0	#N/A
MAGT1	<i>magnesium transporter 1</i>	0	0	0	0	0	0	0	0	0	0	#N/A
PEG10	<i>paternally expressed 10</i>	0	0	0	0	0	0	0	0	0	0	#N/A
MPP7	<i>membrane palmitoylated protein 7</i>	0	0	0	0	0	0	0	0	0	0	#N/A
RAB7L1	<i>RAB29, member RAS oncogene family</i>	0	0	0	0	0	0	0	0	0	0	#N/A
POR	<i>cytochrome p450 oxidoreductase</i>	0	0	0	0	0	0	0	0	0	0	#N/A
ROR2	<i>receptor tyrosine kinase like orphan receptor 2</i>	0	0	0	0	0	0	0	0	0	0	#N/A
STX8	<i>syntaxin 8</i>	0	0	0	0	0	0	0	0	0	0	#N/A
RAP2B	<i>RAP2B, member of RAS oncogene family</i>	0	0	0	0	0	0	0	0	0	0	#N/A
CALR	<i>calreticulin</i>	0	0	0	0	0	0	0	0	0	0	#N/A
ATP6V1D	<i>ATPase H⁺ transporting V1 subunit D</i>	0	0	0	0	0	0	0	0	0	0	#N/A
SRGAP1	<i>SLIT-ROBO Rho GTPase activating protein 1</i>	0	0	0	0	0	0	0	0	0	0	#N/A
ACOX3	<i>acyl-CoA oxidase 3, pristanoyl</i>	0	0	0	0	0	0	0	0	0	0	#N/A
KIF16B	<i>kinesin family member 16B</i>	0	0	0	0	0	0	0	0	0	0	#N/A
WASF2	<i>WASP family member 2</i>	0	0	0	0	0	0	0	0	0	0	#N/A
KPRP	<i>keratinocyte proline rich protein</i>	0	0	0	0	0	0	0	0	0	0	#N/A
CHST14	<i>carbohydrate sulfotransferase 14</i>	0	0	0	0	0	0	0	0	0	0	#N/A
TMEM237	<i>transmembrane protein 237</i>	0	0	0	0	0	0	0	0	0	0	#N/A
ITCH	<i>itchy E3 ubiquitin protein ligase</i>	0	0	0	0	0	0	0	0	0	0	#N/A
STX6	<i>syntaxin 6</i>	0	0	0	0	0	0	0	0	0	0	#N/A

MACF1	<i>microtubule actin crosslinking factor 1</i>	0	0	0	0	0	0	0	0	0	0	#N/A
TMED9	<i>transmembrane p24 trafficking protein 9</i>	0	0	0	0	0	0	0	0	0	0	#N/A
DST	<i>dystonin</i>	0	0	0	0	0	0	0	0	0	0	#N/A
STARD9	<i>StAR related lipid transfer domain containing 9</i>	0	0	0	0	0	0	0	0	0	0	#N/A
STON2	<i>stonin 2</i>	0	0	0	0	0	0	0	0	0	0	#N/A
MOSPD2	<i>motile sperm domain containing 2</i>	0	0	0	0	0	0	0	0	0	0	#N/A
AP3M2	<i>adaptor related protein complex 3 subunit mu 2</i>	0	0	0	0	0	0	0	0	0	0	#N/A
PALM2	<i>paralemmin 2</i>	0	0	0	0	0	0	0	0	0	0	#N/A
PRDX4	<i>peroxiredoxin 4</i>	0	0	0	0	0	0	0	0	0	0	#N/A
PIP5K1A	<i>phosphatidylinositol-4-phosphate 5-kinase type 1 alpha</i>	0	0	0	0	0	0	0	0	0	0	#N/A
GOLPH3	<i>golgi phosphoprotein 3</i>	0	0	0	0	0	0	0	0	0	0	#N/A
TXNDC5	<i>thioredoxin domain containing 5</i>	0	0	0	0	0	0	0	0	0	0	#N/A
LPL	<i>lipoprotein lipase</i>	0	0	0	0	0	0	0	0	0	0	#N/A
COL12A1	<i>collagen type XII alpha 1 chain</i>	0	0	0	0	0	0	0	0	0	0	#N/A
NUCB1	<i>nucleobindin 1</i>	0	0	0	0	0	0	0	0	0	0	#N/A
LMAN2	<i>lectin, mannose binding 2</i>	0	0	0	0	0	0	0	0	0	0	#N/A
ECE1	<i>endothelin converting enzyme 1</i>	0	0	0	0	0	0	0	0	0	0	#N/A
KDEL3	<i>KDEL endoplasmic reticulum protein retention receptor 3</i>	0	0	0	0	0	0	0	0	0	0	#N/A
ABCB6	<i>ATP binding cassette subfamily B member 6 (Langereis blood group)</i>	0	0	0	0	0	0	0	0	0	0	#N/A
SYPL1	<i>synaptophysin like 1</i>	0	0	0	0	0	0	0	0	0	0	#N/A
IMPAD1	<i>inositol monophosphatase domain containing 1</i>	0	0	0	0	0	0	0	0	0	0	#N/A
SACM1L	<i>SAC1 like phosphatidylinositide phosphatase</i>	0	0	0	0	0	0	0	0	0	0	#N/A
FAM3C	<i>family with sequence similarity 3 member C</i>	0	0	0	0	0	0	0	0	0	0	#N/A
M6PR	<i>mannose-6-phosphate receptor, cation dependent</i>	0	0	0	0	0	0	0	0	0	0	#N/A
ERP44	<i>endoplasmic reticulum protein 44</i>	0	0	0	0	0	0	0	0	0	0	#N/A
ITGAV	<i>integrin subunit alpha V</i>	0	0	0	0	0	0	0	0	0	0	#N/A

TXNDC12	<i>thioredoxin domain containing 12</i>	0	0	0	0	0	0	0	0	0	0	#N/A
SCARB2	<i>scavenger receptor class B member 2</i>	0	0	0	0	0	0	0	0	0	0	#N/A
ITGB1	<i>integrin subunit beta 1</i>	0	0	0	0	0	0	0	0	0	0	#N/A
NDFIP1	<i>Nedd4 family interacting protein 1</i>	0	0	0	0	0	0	0	0	0	0	#N/A
STX16	<i>syntaxin 16</i>	0	0	0	0	0	0	0	0	0	0	#N/A
CD47	<i>CD47 molecule</i>	0	0	0	0	0	0	0	0	0	0	#N/A
TM9SF1	<i>transmembrane 9 superfamily member 1</i>	0	0	0	0	0	0	0	0	0	0	#N/A
SCARB1	<i>scavenger receptor class B member 1</i>	0	0	0	0	0	0	0	0	0	0	#N/A
ZMPSTE24	<i>zinc metalloproteinase STE24</i>	0	0	0	0	0	0	0	0	0	0	#N/A
MFSD5	<i>major facilitator superfamily domain containing 5</i>	0	0	0	0	0	0	0	0	0	0	#N/A
CTSD	<i>cathepsin D</i>	0	0	0	0	0	0	0	0	0	0	#N/A
C5orf15	<i>chromosome 5 open reading frame 15</i>	0	0	0	0	0	0	0	0	0	0	#N/A
GOLIM4	<i>golgi integral membrane protein 4</i>	0	0	0	0	0	0	0	0	0	0	#N/A
ARFRP1	<i>ADP ribosylation factor related protein 1</i>	0	0	0	0	0	0	0	0	0	0	#N/A
RABL3	<i>RAB, member of RAS oncogene family like 3</i>	0	0	0	0	0	0	0	0	0	0	#N/A
MRC2	<i>mannose receptor C type 2</i>	0	0	0	0	0	0	0	0	0	0	#N/A
CUX1	<i>cut like homeobox 1</i>	0	0	0	0	0	0	0	0	0	0	#N/A
HEXB	<i>hexosaminidase subunit beta</i>	0	0	0	0	0	0	0	0	0	0	#N/A
RCN1	<i>reticulocalbin 1</i>	0	0	0	0	0	0	0	0	0	0	#N/A
TMED2	<i>transmembrane p24 trafficking protein 2</i>	0	0	0	0	0	0	0	0	0	0	#N/A
SLC7A1	<i>solute carrier family 7 member 1</i>	0	0	0	0	0	0	0	0	0	0	#N/A
SPNS1	<i>sphingolipid transporter 1 (putative)</i>	0	0	0	0	0	0	0	0	0	0	#N/A
CERS2	<i>ceramide synthase 2</i>	0	0	0	0	0	0	0	0	0	0	#N/A
MGAT2	<i>mannosyl (alpha-1,6-)-glycoprotein beta-1,2-N-acetylglucosaminyltransferase</i>	0	0	0	0	0	0	0	0	0	0	#N/A
KIAA2013	<i>KIAA2013</i>	0	0	0	0	0	0	0	0	0	0	#N/A

BST2	<i>bone marrow stromal cell antigen 2</i>	0	0	0	0	0	0	0	0	0	0	#N/A
UXS1	<i>UDP-glucuronate decarboxylase 1</i>	0	0	0	0	0	0	0	0	0	0	#N/A
NAPG	<i>NSF attachment protein gamma</i>	0	0	0	0	0	0	0	0	0	0	#N/A
SLC2A14	<i>solute carrier family 2 member 14</i>	0	0	0	0	0	0	0	0	0	0	#N/A
GALNT1	<i>polypeptide N-acetylgalactosaminyltransferase 1</i>	0	0	0	0	0	0	0	0	0	0	#N/A
PLXNB2	<i>plexin B2</i>	0	0	0	0	0	0	0	0	0	0	#N/A
LAMTOR2	<i>late endosomal/lysosomal adaptor, MAPK and MTOR activator 2</i>	0	0	0	0	0	0	0	0	0	0	#N/A
SYNGR2	<i>synaptogyrin 2</i>	0	0	0	0	0	0	0	0	0	0	#N/A
ATP6V1C1	<i>ATPase H+ transporting V1 subunit C1</i>	0	0	0	0	0	0	0	0	0	0	#N/A
POLE	<i>DNA polymerase epsilon, catalytic subunit</i>	0	0	0	0	0	0	0	0	0	0	#N/A
CLCN7	<i>chloride voltage-gated channel 7</i>	0	0	0	0	0	0	0	0	0	0	#N/A
GOLGA1	<i>golgin A1</i>	0	0	0	0	0	0	0	0	0	0	#N/A
SCAMP4	<i>secretory carrier membrane protein 4</i>	0	0	0	0	0	0	0	0	0	0	#N/A
LAMP1	<i>lysosomal associated membrane protein 1</i>	0	0	0	0	0	0	0	0	0	0	#N/A
NCSTN	<i>nicastrin</i>	0	0	0	0	0	0	0	0	0	0	#N/A
RAB31	<i>RAB31, member RAS oncogene family</i>	0	0	0	0	0	0	0	0	0	0	#N/A
THBS3	<i>thrombospondin 3</i>	0	0	0	0	0	0	0	0	0	0	#N/A
GALNT7	<i>polypeptide N-acetylgalactosaminyltransferase 7</i>	0	0	0	0	0	0	0	0	0	0	#N/A
RHOB	<i>ras homolog family member B</i>	0	0	0	0	0	0	0	0	0	0	#N/A
GNA11	<i>G protein subunit alpha 11</i>	0	0	0	0	0	0	0	0	0	0	#N/A
ATP1B1	<i>ATPase Na+/K+ transporting subunit beta 1</i>	0	0	0	0	0	0	0	0	0	0	#N/A
SLC35C1	<i>solute carrier family 35 member C1</i>	0	0	0	0	0	0	0	0	0	0	#N/A
SLC12A4	<i>solute carrier family 12 member 4</i>	0	0	0	0	0	0	0	0	0	0	#N/A
BASP1	<i>brain abundant membrane attached signal protein 1</i>	0	0	0	0	0	0	0	0	0	0	#N/A
FTL	<i>ferritin light chain</i>	0	0	0	0	0	0	0	0	0	0	#N/A
RTN3	<i>reticulon 3</i>	0	0	0	0	0	0	0	0	0	0	#N/A

LDLR	<i>low density lipoprotein receptor</i>	0	0	0	0	0	0	0	0	0	0	#N/A
BCAP31	<i>B cell receptor associated protein 31</i>	0	0	0	0	0	0	0	0	0	0	#N/A
ERGIC1	<i>endoplasmic reticulum-golgi intermediate compartment 1</i>	0	0	0	0	0	0	0	0	0	0	#N/A

9.2 Total peptide counts and associated Bayesian false discovery rates for proteins identified from enriched Golgi fractions

Gene Symbol	Gene Name	Golgi FlagBirA-Only Controls					Golgi FlagBirA-GBF1					BFDR
		A1	A2	B1	B2	Total	A1	A2	B1	B2	Total	
GBF1	<i>golgi brefeldin A resistant guanine nucleotide exchange factor 1</i>	0	0	12	9	21	649	619	613	581	2462	na
SLC30A6	<i>solute carrier family 30 member 6</i>	0	0	7	5	12	78	80	89	80	327	0
SLC30A5	<i>solute carrier family 30 member 5</i>	0	0	6	4	10	44	52	58	43	197	0
GOSR1	<i>golgi SNAP receptor complex member 1</i>	0	0	4	6	10	31	37	43	24	135	0
TMEM115	<i>transmembrane protein 115</i>	0	0	0	0	0	35	30	28	26	119	0
C10orf76	<i>armadillo like helical domain containing 3</i>	0	0	0	0	0	15	10	15	12	52	0
CANT1	<i>calcium activated nucleotidase 1</i>	0	0	3	3	6	10	7	13	12	42	0
RHBDD2	<i>rhomboid domain containing 2</i>	0	0	0	0	0	6	8	6	7	27	0
ZDHHC17	<i>zinc finger DHHC-type containing 17</i>	0	0	0	0	0	3	5	7	5	20	0
TMEM87	<i>transmembrane protein 87A</i>	0	0	7	9	16	21	20	24	25	90	0.01
A												
SGMS1	<i>sphingomyelin synthase 1</i>	0	0	4	5	9	11	12	11	10	44	0.02
MAN1B1	<i>mannosidase alpha class 1B member 1</i>	0	0	23	13	36	39	45	40	36	160	0.04
STX5	<i>syntaxin 5</i>	0	0	10	9	19	16	27	24	26	93	0.05
STX10	<i>syntaxin 10</i>	0	0	0	0	0	4	0	9	13	26	0.07
ROCK2	<i>Rho associated coiled-coil containing protein kinase 2</i>	0	0	0	0	0	8	5	4	0	17	0.08
BET1L	<i>Bet1 golgi vesicular membrane trafficking protein like</i>	0	0	0	0	0	0	3	5	6	14	0.09
SLC30A7	<i>solute carrier family 30 member 7</i>	0	0	0	0	0	0	3	5	3	11	0.1
RRAS2	<i>RAS related 2</i>	0	0	0	0	0	3	3	0	3	9	0.11
GLG1	<i>golgi glycoprotein 1</i>	0	0	0	0	0	2	0	10	9	21	0.12
GORASP2	<i>golgi reassembly stacking protein 2</i>	0	0	0	5	5	5	8	9	7	29	0.13
BET1	#N/A	0	0	4	0	4	5	8	9	4	26	0.14

RAB35	<i>RAB35, member RAS oncogene family</i>	0	0	0	0	0	2	0	7	3	12	0.14
DNAJB6	<i>DnaJ heat shock protein family (Hsp40) member B6</i>	0	0	0	0	0	0	3	3	2	8	0.15
ACBD3	<i>acyl-CoA binding domain containing 3</i>	0	0	0	0	0	7	0	2	2	11	0.16
RAB34	<i>RAB34, member RAS oncogene family</i>	0	0	0	6	6	14	12	0	14	40	0.16
AAAS	<i>aladin WD repeat nucleoporin</i>	0	0	5	0	5	5	6	8	6	25	0.17
LMAN1	<i>lectin, mannose binding 1</i>	0	2	9	6	17	10	15	39	29	93	0.18
TM9SF3	<i>transmembrane 9 superfamily member 3</i>	0	0	7	5	12	12	5	19	20	56	0.18
ATP2C1	<i>ATPase secretory pathway Ca²⁺ transporting 1</i>	0	0	13	14	27	23	30	31	23	107	0.19
RER1	<i>retention in endoplasmic reticulum sorting receptor 1</i>	0	0	4	0	4	7	0	7	5	19	0.2
SEC24B	<i>SEC24 homolog B, COPII coat complex component</i>	0	0	7	3	10	10	9	10	9	38	0.2
TM9SF2	<i>transmembrane 9 superfamily member 2</i>	0	0	4	0	4	2	0	17	14	33	0.21
NUCB1	<i>nucleobindin 1</i>	0	0	0	0	0	0	0	16	18	34	0.23
LMAN2	<i>lectin, mannose binding 2</i>	0	0	0	0	0	0	0	15	21	36	0.24
P4HB	<i>proyl 4-hydroxylase subunit beta</i>	0	0	0	0	0	0	0	10	10	20	0.25
ECE1	<i>endothelin converting enzyme 1</i>	0	0	0	0	0	0	0	13	14	27	0.25
ABCB6	<i>ATP binding cassette subfamily B member 6 (Langereis blood group)</i>	0	0	0	0	0	0	0	10	9	19	0.26
RAB1A	<i>RAB1A, member RAS oncogene family</i>	0	0	0	0	0	0	0	7	12	19	0.27
IMPAD1	<i>inositol monophosphatase domain containing 1</i>	0	0	0	0	0	0	0	8	9	17	0.27
ARF5	<i>ADP ribosylation factor 5</i>	0	0	0	0	0	9	7	0	0	16	0.28
FAM3C	<i>family with sequence similarity 3 member C</i>	0	0	0	0	0	0	0	7	7	14	0.28
ERP44	<i>endoplasmic reticulum protein 44</i>	0	0	0	0	0	0	0	6	8	14	0.29
ITGAV	<i>integrin subunit alpha V</i>	0	0	0	0	0	0	0	6	6	12	0.29
TXNDC5	<i>thioredoxin domain containing 5</i>	0	0	0	0	0	0	0	11	5	16	0.3
SACM1L	<i>SAC1 like phosphatidylinositide phosphatase</i>	0	0	0	0	0	0	0	7	5	12	0.3
M6PR	<i>mannose-6-phosphate receptor, cation dependent</i>	0	0	0	0	0	0	0	7	5	12	0.3

POR	<i>cytochrome p450 oxidoreductase</i>	0	0	2	0	2	0	0	14	13	27	0.31
CYB5R3	<i>cytochrome b5 reductase 3</i>	0	0	0	0	0	0	0	5	5	10	0.32
NRAS	<i>NRAS proto-oncogene, GTPase</i>	0	0	0	0	0	5	0	5	0	10	0.32
GOLIM4	<i>golgi integral membrane protein 4</i>	0	0	0	0	0	0	0	4	7	11	0.32
ATP1B3	<i>ATPase Na⁺/K⁺ transporting subunit beta 3</i>	0	0	0	0	0	0	0	5	4	9	0.33
HLA-B	<i>major histocompatibility complex, class I, B</i>	0	0	0	0	0	6	0	4	0	10	0.33
GORAB	<i>golgin, RAB6 interacting</i>	0	0	0	0	0	4	5	0	0	9	0.33
RALA	<i>RAS like proto-oncogene A</i>	0	0	0	0	0	0	5	0	4	9	0.33
LPL	<i>lipoprotein lipase</i>	0	0	0	0	0	0	0	6	4	10	0.33
NDFIP1	<i>Nedd4 family interacting protein 1</i>	0	0	0	0	0	0	0	4	5	9	0.33
ZMPSTE24	<i>zinc metalloproteinase STE24</i>	0	0	0	0	0	0	0	4	5	9	0.33
C5orf15	<i>chromosome 5 open reading frame 15</i>	0	0	0	0	0	0	0	4	5	9	0.33
RAB5A	<i>RAB5A, member RAS oncogene family</i>	0	0	0	0	0	0	0	4	4	8	0.35
COL12A1	<i>collagen type XII alpha 1 chain</i>	0	0	0	0	0	0	0	4	4	8	0.35
RAP2C	<i>RAP2C, member of RAS oncogene family</i>	0	0	0	0	0	4	3	0	0	7	0.36
YWHAQ	<i>tyrosine 3-monooxygenase/tryptophan 5-monooxygenase activation protein theta</i>	0	0	0	0	0	11	0	0	3	14	0.36
PRAF2	<i>PRA1 domain family member 2</i>	0	0	0	0	0	4	0	3	0	7	0.36
TXNDC12	<i>thioredoxin domain containing 12</i>	0	0	0	0	0	0	0	5	3	8	0.36
ITGB1	<i>integrin subunit beta 1</i>	0	0	0	0	0	0	0	4	3	7	0.36
CTSD	<i>cathepsin D</i>	0	0	0	0	0	0	0	4	3	7	0.36
MRC2	<i>mannose receptor C type 2</i>	0	0	0	0	0	0	0	3	4	7	0.36
BST2	<i>bone marrow stromal cell antigen 2</i>	0	0	0	0	0	0	0	3	4	7	0.36
CUX1	<i>cut like homeobox 1</i>	0	0	0	0	0	0	0	3	3	6	0.37
SPNS1	<i>sphingolipid transporter 1 (putative)</i>	0	0	0	0	0	0	0	3	3	6	0.37
CERS2	<i>ceramide synthase 2</i>	0	0	0	0	0	0	0	3	3	6	0.37
B4GALT1	<i>beta-1,4-galactosyltransferase 1</i>	0	0	5	6	11	0	0	22	21	43	0.38

QSOX2	<i>quiescin sulfhydryl oxidase 2</i>	0	0	4	5	9	0	0	18	18	36	0.38
CALR	<i>calreticulin</i>	0	0	0	3	3	0	0	10	13	23	0.38
CANX	<i>calnexin</i>	0	3	9	11	23	0	0	35	31	66	0.39
CLPTMIL	<i>CLPTM1 like</i>	0	0	0	0	0	0	0	4	2	6	0.39
MYL12B	<i>myosin light chain 12B</i>	0	0	0	0	0	0	0	5	2	7	0.39
GALNT2	<i>polypeptide N-acetylgalactosaminyltransferase 2</i>	0	0	19	21	40	8	8	70	66	152	0.39
PDIA3	<i>protein disulfide isomerase family A member 3</i>	0	0	6	5	11	0	0	19	23	42	0.39
ZFPL1	<i>zinc finger protein like 1</i>	0	0	2	3	5	5	7	3	4	19	0.39
SCARB2	<i>scavenger receptor class B member 2</i>	0	0	0	0	0	0	0	4	2	6	0.39
STX16	<i>syntaxin 16</i>	0	0	0	0	0	0	0	4	2	6	0.39
RAB6A	<i>RAB6A, member RAS oncogene family</i>	4	0	31	0	35	27	29	36	40	132	0.4
TFRC	<i>transferrin receptor</i>	3	3	47	34	87	62	60	124	107	353	0.4
CHST14	<i>carbohydrate sulfotransferase 14</i>	0	0	0	2	2	0	0	7	6	13	0.4
ARFRP1	<i>ADP ribosylation factor related protein 1</i>	0	0	0	0	0	0	0	3	2	5	0.4
TMED2	<i>transmembrane p24 trafficking protein 2</i>	0	0	0	0	0	0	0	3	2	5	0.4
KIAA2013	<i>KIAA2013</i>	0	0	0	0	0	0	0	3	2	5	0.4
LAMP1	<i>lysosomal associated membrane protein 1</i>	0	0	0	0	0	0	0	2	3	5	0.4
PPIB	<i>peptidylprolyl isomerase B</i>	2	0	4	6	12	0	0	15	15	30	0.41
PTPLAD1	<i>3-hydroxyacyl-CoA dehydratase 3</i>	0	0	4	0	4	0	0	11	13	24	0.41
CALU	<i>calumenin</i>	0	0	0	0	0	0	0	2	2	4	0.41
NUP155	<i>nucleoporin 155</i>	0	0	0	0	0	0	2	2	0	4	0.41
HSD17B4	<i>hydroxysteroid 17-beta dehydrogenase 4</i>	0	0	2	0	2	0	0	5	8	13	0.41
TM9SF4	<i>transmembrane 9 superfamily member 4</i>	0	0	5	6	11	0	0	18	20	38	0.41
TMED9	<i>transmembrane p24 trafficking protein 9</i>	0	0	0	2	2	0	0	6	6	12	0.41
SYNGR2	<i>synaptogyrin 2</i>	0	0	0	0	0	0	0	2	2	4	0.41
GOLGB1	<i>golgin B1</i>	0	0	263	5	268	282	314	9	293	898	0.42
TMED10	<i>transmembrane p24 trafficking</i>	0	0	4	6	10	0	0	18	14	32	0.42

<i>protein 10</i>												
HSP90B1	<i>heat shock protein 90 beta family member 1</i>	0	4	17	16	37	2	0	41	40	83	0.42
PDIA6	<i>protein disulfide isomerase family A member 6</i>	0	0	3	0	3	0	0	8	6	14	0.42
PGRMC1	<i>progesterone receptor membrane component 1</i>	0	0	0	3	3	0	2	7	4	13	0.42
MAN2A1	<i>mannosidase alpha class 2A member 1</i>	0	0	13	11	24	5	0	34	31	70	0.42
DHCR7	<i>7-dehydrocholesterol reductase</i>	0	0	4	0	4	3	0	6	5	14	0.43
RAB21	<i>RAB21, member RAS oncogene family</i>	0	0	5	4	9	4	6	11	9	30	0.43
GANAB	<i>glucosidase II alpha subunit</i>	0	0	11	10	21	0	4	35	23	62	0.43
RAB11B	<i>RAB11B, member RAS oncogene family</i>	0	0	10	9	19	3	11	23	22	59	0.43
PRDX3	<i>peroxiredoxin 3</i>	0	0	0	3	3	0	0	5	8	13	0.43
MGAT1	<i>mannosyl (alpha-1,3-)-glycoprotein beta-1,2-N-acetylglucosaminyltransferase</i>	0	0	4	0	4	0	0	9	8	17	0.43
ERP29	<i>endoplasmic reticulum protein 29</i>	0	0	3	0	3	0	0	6	7	13	0.43
STX6	<i>syntaxin 6</i>	0	0	0	2	2	0	0	6	4	10	0.43
RAC1	<i>Rac family small GTPase 1</i>	0	0	4	0	4	0	3	5	5	13	0.44
CNP	<i>2',3'-cyclic nucleotide 3' phosphodiesterase</i>	0	0	0	4	4	2	0	7	4	13	0.44
LMNB1	<i>lamin B1</i>	3	2	2	2	9	0	0	7	10	17	0.44
SLC35A2	<i>solute carrier family 35 member A2</i>	0	0	6	6	12	11	8	8	11	38	0.44
ZDHHC13	<i>zinc finger DHHC-type containing 13</i>	0	0	3	2	5	3	2	7	4	16	0.44
ATP6V0A1	<i>ATPase H⁺ transporting V0 subunit a1</i>	0	0	6	2	8	0	0	11	12	23	0.44
CPD	<i>carboxypeptidase D</i>	0	0	4	0	4	0	0	8	7	15	0.44
MFSD12	<i>major facilitator superfamily domain containing 12</i>	0	0	5	4	9	0	0	10	9	19	0.45
SEC23A	<i>Sec23 homolog A, coat complex II component</i>	0	6	14	14	34	31	30	24	26	111	0.45
KDELR2	<i>KDEL endoplasmic reticulum protein retention receptor 2</i>	0	0	8	3	11	8	0	18	7	33	0.45
RAB10	<i>RAB10, member RAS oncogene family</i>	0	0	0	8	8	0	0	8	8	16	0.45

RAB8A	<i>RAB8A, member RAS oncogene family</i>	0	5	5	0	10	2	4	11	10	27	0.45
STX7	<i>syntaxin 7</i>	0	0	3	0	3	0	0	7	3	10	0.45
SCD	<i>stearoyl-CoA desaturase</i>	0	0	0	3	3	0	0	3	4	7	0.46
DDOST	<i>dolichyl-diphosphooligosaccharide-protein glycosyltransferase non-catalytic subunit</i>	0	0	6	5	11	0	0	21	8	29	0.46
PFN2	<i>profilin 2</i>	0	0	3	0	3	0	0	4	3	7	0.46
BSG	<i>basigin (Ok blood group)</i>	0	0	6	3	9	0	0	9	8	17	0.46
ATP6V0D1	<i>ATPase H⁺ transporting V0 subunit d1</i>	0	0	7	4	11	0	0	10	11	21	0.46
VAMP7	<i>vesicle associated membrane protein 7</i>	0	0	6	4	10	0	0	10	9	19	0.46
USO1	<i>USO1 vesicle transport factor</i>	6	3	15	9	33	23	22	30	24	99	0.47
VPS35	<i>VPS35 retromer complex component</i>	0	0	3	4	7	0	0	6	7	13	0.47
TMEM30A	<i>transmembrane protein 30A</i>	0	0	3	2	5	3	0	4	5	12	0.47
VPS45	<i>vacuolar protein sorting 45 homolog</i>	0	0	3	2	5	0	0	6	4	10	0.47
SLC16A1	<i>solute carrier family 16 member 1</i>	0	2	4	3	9	2	0	7	7	16	0.48
CSRP2	<i>cysteine and glycine rich protein 2</i>	0	0	2	0	2	3	2	0	0	5	0.48
KDELR1	<i>KDEL endoplasmic reticulum protein retention receptor 1</i>	0	0	0	0	0	0	0	11	0	11	0.48
CD97	<i>adhesion G protein-coupled receptor E5</i>	0	0	4	0	4	0	0	3	5	8	0.48
KDELR3	<i>KDEL endoplasmic reticulum protein retention receptor 3</i>	0	0	0	0	0	0	0	10	0	10	0.48
CYFIP2	<i>cytoplasmic FMR1 interacting protein 2</i>	0	0	0	0	0	5	0	0	0	5	0.49
PRKCSH	<i>protein kinase C substrate 80K-H</i>	0	0	0	0	0	0	0	5	0	5	0.49
C8orf55	<i>thioesterase superfamily member 6</i>	0	0	0	0	0	0	0	5	0	5	0.49
RPS10	<i>ribosomal protein S10</i>	0	0	0	0	0	5	0	0	0	5	0.49
PRDX4	<i>peroxiredoxin 4</i>	0	0	0	0	0	0	0	6	0	6	0.49
SYPL1	<i>synaptophysin like 1</i>	0	0	0	0	0	0	0	8	0	8	0.49
GALNT7	<i>polypeptide N-acetylgalactosaminyltransferase 7</i>	0	0	0	0	0	0	0	0	5	5	0.49
RHOB	<i>ras homolog family member B</i>	0	0	0	0	0	0	0	0	5	5	0.49

RAB5B	<i>RAB5B, member RAS oncogene family</i>	0	0	0	0	0	0	0	4	0	4	0.5
GOLPH3	<i>golgi phosphoprotein 3</i>	0	0	0	0	0	0	0	0	4	4	0.5
CD47	<i>CD47 molecule</i>	0	0	0	0	0	0	0	4	0	4	0.5
TM9SF1	<i>transmembrane 9 superfamily member 1</i>	0	0	0	0	0	0	0	4	0	4	0.5
SCARB1	<i>scavenger receptor class B member 1</i>	0	0	0	0	0	0	0	4	0	4	0.5
MFSD5	<i>major facilitator superfamily domain containing 5</i>	0	0	0	0	0	0	0	4	0	4	0.5
GNA11	<i>G protein subunit alpha 11</i>	0	0	0	0	0	0	0	0	4	4	0.5
ATP1B1	<i>ATPase Na⁺/K⁺ transporting subunit beta 1</i>	0	0	0	0	0	0	0	0	4	4	0.5
GOPC	<i>golgi associated PDZ and coiled-coil motif containing</i>	0	0	0	0	0	0	0	3	0	3	0.51
ACTBL2	<i>actin beta like 2</i>	0	0	0	0	0	3	0	0	0	3	0.51
SEC63	<i>SEC63 homolog, protein translocation regulator</i>	0	0	0	0	0	0	0	3	0	3	0.51
ARAP1	<i>ArfGAP with RhoGAP domain, ankyrin repeat and PH domain 1</i>	0	0	0	0	0	0	0	0	3	3	0.51
ELOVL1	<i>ELOVL fatty acid elongase 1</i>	0	0	0	0	0	0	0	0	3	3	0.51
AHCY	<i>adenosylhomocysteinase</i>	0	0	0	0	0	0	0	3	0	3	0.51
SEC61B	<i>SEC61 translocon beta subunit</i>	0	0	0	0	0	0	0	0	3	3	0.51
GRIN2B	<i>glutamate ionotropic receptor NMDA type subunit 2B</i>	0	0	0	0	0	3	0	0	0	3	0.51
MUC16	<i>mucin 16, cell surface associated</i>	0	0	0	0	0	3	0	0	0	3	0.51
RABL3	<i>RAB, member of RAS oncogene family like 3</i>	0	0	0	0	0	0	0	3	0	3	0.51
HEXB	<i>hexosaminidase subunit beta</i>	0	0	0	0	0	0	0	3	0	3	0.51
RCN1	<i>reticulocalbin 1</i>	0	0	0	0	0	0	0	3	0	3	0.51
SLC7A1	<i>solute carrier family 7 member 1</i>	0	0	0	0	0	0	0	3	0	3	0.51
MGAT2	<i>mannosyl (alpha-1,6-)-glycoprotein beta-1,2-N-acetylglucosaminyltransferase</i>	0	0	0	0	0	0	0	3	0	3	0.51
SLC35C1	<i>solute carrier family 35 member C1</i>	0	0	0	0	0	0	0	0	3	3	0.51
SLC12A4	<i>solute carrier family 12 member 4</i>	0	0	0	0	0	0	0	0	3	3	0.51
YWHAZ	<i>tyrosine 3-monooxygenase/tryptophan 5-monooxygenase activation protein</i>	0	3	0	0	3	0	0	3	3	6	0.54

zeta												
ATL3	<i>atlastin GTPase 3</i>	0	0	0	0	0	0	0	2	0	2	0.54
RPS19	<i>ribosomal protein S19</i>	0	0	0	0	0	2	0	0	0	2	0.54
RPL30	<i>ribosomal protein L30</i>	0	0	0	0	0	2	0	0	0	2	0.54
SLC35E1	<i>solute carrier family 35 member E1</i>	0	0	11	10	21	14	13	20	16	63	0.54
PIGT	<i>phosphatidylinositol glycan anchor biosynthesis class T</i>	0	0	0	0	0	0	0	0	2	2	0.54
XIRP1	<i>xin actin binding repeat containing 1</i>	0	0	0	0	0	0	0	0	2	2	0.54
KRAS	<i>KRAS proto-oncogene, GTPase</i>	0	0	0	0	0	0	2	0	0	2	0.54
DNAJB11	<i>DnaJ heat shock protein family (Hsp40) member B11</i>	0	0	0	0	0	0	0	0	2	2	0.54
SCCPDH	<i>saccharopine dehydrogenase (putative)</i>	0	0	0	0	0	0	0	2	0	2	0.54
AP1M1	<i>adaptor related protein complex 1 subunit mu 1</i>	0	0	0	0	0	0	0	2	0	2	0.54
AP1G1	<i>adaptor related protein complex 1 subunit gamma 1</i>	0	0	3	0	3	0	0	8	0	8	0.54
KCNN4	<i>potassium calcium-activated channel subfamily N member 4</i>	0	0	0	0	0	2	0	0	0	2	0.54
FRAS1	<i>Fraser extracellular matrix complex subunit 1</i>	0	0	0	0	0	2	0	0	0	2	0.54
AKAP9	<i>A-kinase anchoring protein 9</i>	0	0	0	0	0	2	0	0	0	2	0.54
DAB2IP	<i>DAB2 interacting protein</i>	0	0	0	0	0	0	2	0	0	2	0.54
CCDC82	<i>coiled-coil domain containing 82</i>	0	0	0	0	0	0	2	0	0	2	0.54
KIF5C	<i>kinesin family member 5C</i>	0	0	0	0	0	0	2	0	0	2	0.54
BSDC1	<i>BSD domain containing 1</i>	0	0	0	0	0	0	2	0	0	2	0.54
PIP5K1A	<i>phosphatidylinositol-4-phosphate 5-kinase type 1 alpha</i>	0	0	0	0	0	0	0	0	2	2	0.54
UXS1	<i>UDP-glucuronate decarboxylase 1</i>	0	0	0	0	0	0	0	2	0	2	0.54
NAPG	<i>NSF attachment protein gamma</i>	0	0	0	0	0	0	0	2	0	2	0.54
SLC2A14	<i>solute carrier family 2 member 14</i>	0	0	0	0	0	0	0	2	0	2	0.54
GALNT1	<i>polypeptide N-acetylgalactosaminyltransferase 1</i>	0	0	0	0	0	0	0	2	0	2	0.54
PLXNB2	<i>plexin B2</i>	0	0	0	0	0	0	0	2	0	2	0.54
LAMTOR2	<i>late endosomal/lysosomal adaptor, MAPK and MTOR activator 2</i>	0	0	0	0	0	0	0	2	0	2	0.54

ATP6V1C1	<i>ATPase H⁺ transporting VI subunit C1</i>	0	0	0	0	0	0	0	2	0	2	0.54
POLE	<i>DNA polymerase epsilon, catalytic subunit</i>	0	0	0	0	0	0	0	2	0	2	0.54
CLCN7	<i>chloride voltage-gated channel 7</i>	0	0	0	0	0	0	0	2	0	2	0.54
GOLGA1	<i>golgin A1</i>	0	0	0	0	0	0	0	2	0	2	0.54
SCAMP4	<i>secretory carrier membrane protein 4</i>	0	0	0	0	0	0	0	2	0	2	0.54
NCSTN	<i>nicastrin</i>	0	0	0	0	0	0	0	2	0	2	0.54
RAB31	<i>RAB31, member RAS oncogene family</i>	0	0	0	0	0	0	0	2	0	2	0.54
THBS3	<i>thrombospondin 3</i>	0	0	0	0	0	0	0	2	0	2	0.54
BASP1	<i>brain abundant membrane attached signal protein 1</i>	0	0	0	0	0	0	0	0	2	2	0.54
FTL	<i>ferritin light chain</i>	0	0	0	0	0	0	0	0	2	2	0.54
RTN3	<i>reticulon 3</i>	0	0	0	0	0	0	0	0	2	2	0.54
LDLR	<i>low density lipoprotein receptor</i>	0	0	0	0	0	0	0	0	2	2	0.54
BCAP31	<i>B cell receptor associated protein 31</i>	0	0	0	0	0	0	0	0	2	2	0.54
ERGIC1	<i>endoplasmic reticulum-golgi intermediate compartment 1</i>	0	0	0	0	0	0	0	0	2	2	0.54
SCFD1	<i>sec1 family domain containing 1</i>	0	0	9	12	21	8	8	21	16	53	0.58
SPTLC1	<i>serine palmitoyltransferase long chain base subunit 1</i>	0	2	0	0	2	0	0	5	0	5	0.58
HSD17B12	<i>hydroxysteroid 17-beta dehydrogenase 12</i>	0	0	6	4	10	0	0	10	6	16	0.58
SSR4	<i>signal sequence receptor subunit 4</i>	0	2	0	0	2	0	0	2	2	4	0.58
SEC22B	<i>SEC22 homolog B, vesicle trafficking protein (gene/pseudogene)</i>	0	2	17	11	30	22	26	25	23	96	0.58
NAPA	<i>NSF attachment protein alpha</i>	0	0	15	13	28	3	5	23	26	57	0.58
STX8	<i>syntaxin 8</i>	0	0	0	4	4	0	0	4	3	7	0.58
FARP1	<i>FERM, ARH/RhoGEF and pleckstrin domain protein 1</i>	0	0	0	5	5	0	0	4	3	7	0.59
SLC2A1	<i>solute carrier family 2 member 1</i>	0	0	9	7	16	0	4	13	12	29	0.59
HRAS	<i>HRas proto-oncogene, GTPase</i>	0	0	5	3	8	0	0	0	8	8	0.59
TPM2	<i>tropomyosin 2</i>	0	4	0	0	4	0	6	0	0	6	0.59

ABI2	<i>abl interactor 2</i>	0	0	0	2	2	3	0	0	0	3	0.59
SLC38A1	<i>solute carrier family 38 member 1</i>	0	0	3	4	7	2	4	5	4	15	0.59
PEF1	<i>penta-EF-hand domain containing 1</i>	0	0	3	0	3	0	0	3	0	3	0.59
CDK5RAP3	<i>CDK5 regulatory subunit associated protein 3</i>	0	0	3	0	3	0	0	0	3	3	0.59
MTMR1	<i>myotubularin related protein 1</i>	0	0	3	0	3	0	0	3	0	3	0.59
RAP2B	<i>RAP2B, member of RAS oncogene family</i>	0	0	0	4	4	0	0	2	3	5	0.59
ATP6V1D	<i>ATPase H⁺ transporting V1 subunit D</i>	0	0	0	3	3	0	0	0	4	4	0.59
ACOX3	<i>acyl-CoA oxidase 3, pristanoyl</i>	0	0	0	3	3	0	0	3	0	3	0.59
EMD	<i>emerin</i>	4	0	0	3	7	5	0	4	3	12	0.6
KIAA0586	<i>KIAA0586</i>	0	2	0	0	2	0	0	2	0	2	0.6
GNAI3	<i>G protein subunit alpha i3</i>	0	0	7	9	16	8	12	9	11	40	0.6
VPS28	<i>VPS28 subunit of ESCRT-I</i>	0	0	0	2	2	0	0	2	0	2	0.6
GNB1	<i>G protein subunit beta 1</i>	0	0	0	6	6	0	0	0	5	5	0.6
SEC24A	<i>SEC24 homolog A, COPII coat complex component</i>	0	4	0	0	4	2	0	0	2	4	0.61
UBIAD1	<i>UbiA prenyltransferase domain containing 1</i>	0	0	7	7	14	10	9	8	6	33	0.61
HSPA5	<i>heat shock protein family A (Hsp70) member 5</i>	15	20	21	26	82	9	9	53	49	120	0.61
HLA-A	<i>major histocompatibility complex, class I, A</i>	0	0	10	9	19	8	8	15	12	43	0.61
UQCRC1	<i>ubiquinol-cytochrome c reductase core protein 1</i>	0	0	4	5	9	0	0	7	0	7	0.61
PLD3	<i>phospholipase D family member 3</i>	0	0	9	9	18	0	0	12	14	26	0.61
LNPEP	<i>leucyl and cystinyl aminopeptidase</i>	0	0	6	9	15	0	0	12	8	20	0.61
VTI1B	<i>vesicle transport through interaction with t-SNAREs 1B</i>	0	0	4	0	4	0	0	3	0	3	0.61
VDAC1	<i>voltage dependent anion channel 1</i>	4	5	0	0	9	0	0	6	5	11	0.62
STT3B	<i>STT3 oligosaccharyltransferase complex catalytic subunit B</i>	0	0	3	0	3	0	0	2	0	2	0.62
ERGIC2	<i>ERGIC and golgi 2</i>	0	0	9	9	18	2	7	14	9	32	0.62
ANXA11	<i>annexin A11</i>	0	0	3	0	3	0	0	2	0	2	0.62
FKBP8	<i>FKBP prolyl isomerase 8</i>	0	0	8	5	13	0	0	9	8	17	0.62

AP1B1	<i>adaptor related protein complex 1 subunit beta 1</i>	0	0	13	0	13	0	0	9	7	16	0.62
CUL3	<i>cullin 3</i>	0	0	3	0	3	0	0	0	2	2	0.62
GOSR2	<i>golgi SNAP receptor complex member 2</i>	0	0	14	12	26	19	18	19	17	73	0.62
GLT8D1	<i>glycosyltransferase 8 domain containing 1</i>	0	0	10	10	20	4	2	11	16	33	0.62
WASF2	<i>WASP family member 2</i>	0	0	0	3	3	0	0	0	2	2	0.62
VAPA	#N/A	0	0	18	10	28	0	6	23	16	45	0.63
SCAMP3	<i>secretory carrier membrane protein 3</i>	0	0	9	10	19	9	7	12	14	42	0.63
RAB18	<i>RAB18, member RAS oncogene family</i>	0	0	15	15	30	19	21	0	24	64	0.63
SEC24C	<i>SEC24 homolog C, COPII coat complex component</i>	0	0	11	10	21	15	14	13	10	52	0.63
ATP6V1E1	<i>ATPase H⁺ transporting V1 subunit E1</i>	0	2	4	0	6	0	0	4	2	6	0.63
TPM4	<i>tropomyosin 4</i>	0	0	5	5	10	3	0	7	4	14	0.63
NSF	<i>N-ethylmaleimide sensitive factor, vesicle fusing ATPase</i>	0	0	25	17	42	14	14	34	31	93	0.64
MSN	<i>moesin</i>	0	2	4	7	13	0	0	9	5	14	0.64
TBL2	<i>transducin beta like 2</i>	0	0	3	6	9	0	0	6	3	9	0.64
TMEM165	<i>transmembrane protein 165</i>	0	0	23	20	43	9	18	36	23	86	0.64
AP3M1	<i>adaptor related protein complex 3 subunit mu 1</i>	3	3	0	0	6	0	0	4	2	6	0.64
ARF4	<i>ADP ribosylation factor 4</i>	4	5	2	0	11	6	5	6	6	23	0.64
RUFY1	<i>RUN and FYVE domain containing 1</i>	2	0	2	2	6	0	3	3	3	9	0.64
SLC39A14	<i>solute carrier family 39 member 14</i>	0	0	4	5	9	0	3	6	4	13	0.64
GLT8D2	<i>glycosyltransferase 8 domain containing 2</i>	0	0	2	2	4	0	0	2	2	4	0.64
TUBA1C	<i>tubulin alpha 1c</i>	32	0	0	0	32	0	17	23	0	40	0.65
SPCS3	<i>signal peptidase complex subunit 3</i>	0	0	6	0	6	3	0	0	0	3	0.65
SLC35B2	<i>solute carrier family 35 member B2</i>	0	0	12	13	25	12	11	16	17	56	0.65
TPM3	<i>tropomyosin 3</i>	0	0	5	4	9	4	2	5	2	13	0.65
COPG1	<i>coatamer protein complex subunit gamma 1</i>	5	7	0	0	12	0	0	7	0	7	0.65
DPM1	<i>dolichyl-phosphate</i>	0	4	9	8	21	3	2	14	13	32	0.65

	<i>mannosyltransferase subunit 1, catalytic</i>											
PNISR	<i>PNN interacting serine and arginine rich protein</i>	5	0	0	0	5	0	2	0	0	2	0.65
VAPB	<i>VAMP associated protein B and C</i>	0	2	6	2	10	0	0	0	6	6	0.65
GOLGA5	<i>golgin A5</i>	0	0	20	21	41	30	29	21	23	103	0.66
ATP6V1H	<i>ATPase H+ transporting V1 subunit H</i>	0	0	6	4	10	0	0	4	5	9	0.66
SLC25A6	<i>solute carrier family 25 member 6</i>	7	9	4	0	20	0	0	13	4	17	0.66
SEC61A1	<i>SEC61 translocon alpha 1 subunit</i>	2	3	2	0	7	0	0	3	3	6	0.66
RPL34	<i>ribosomal protein L34</i>	3	0	2	3	8	3	3	3	3	12	0.66
RPS18	<i>ribosomal protein S18</i>	0	0	10	7	17	4	5	9	10	28	0.66
SLC38A2	<i>solute carrier family 38 member 2</i>	0	0	8	8	16	3	5	9	8	25	0.66
VPS13B	<i>vacuolar protein sorting 13 homolog B</i>	0	0	3	7	10	4	4	4	0	12	0.66
FYN	<i>FYN proto-oncogene, Src family tyrosine kinase</i>	0	0	9	10	19	0	0	8	12	20	0.66
NSDHL	<i>NAD(P) dependent steroid dehydrogenase-like</i>	3	0	8	7	18	4	4	11	7	26	0.67
SRPRB	<i>SRP receptor subunit beta</i>	2	0	7	7	16	0	0	9	6	15	0.67
ARL8B	<i>ADP ribosylation factor like GTPase 8B</i>	0	3	15	13	31	7	5	20	20	52	0.67
RAB9A	<i>RAB9A, member RAS oncogene family</i>	4	0	5	7	16	4	4	9	5	22	0.67
RHOA	<i>ras homolog family member A</i>	0	2	6	5	13	2	3	7	6	18	0.67
RDH11	<i>retinol dehydrogenase 11</i>	0	0	5	6	11	0	0	5	5	10	0.67
SRPR	<i>SRP receptor subunit alpha</i>	0	0	7	9	16	0	0	8	8	16	0.67
ATP6V1G1	<i>ATPase H+ transporting V1 subunit G1</i>	0	0	10	7	17	6	5	9	8	28	0.67
ATP6V0A2	<i>ATPase H+ transporting V0 subunit a2</i>	0	0	7	7	14	0	0	7	6	13	0.67
TACC3	<i>transforming acidic coiled-coil containing protein 3</i>	2	4	0	0	6	0	0	2	0	2	0.68
ATP1A1	<i>ATPase Na+/K+ transporting subunit alpha 1</i>	2	0	26	26	54	8	13	38	40	99	0.68
SURF4	<i>surfeit 4</i>	7	6	12	15	40	12	5	25	21	63	0.68
RAB14	<i>RAB14, member RAS oncogene family</i>	13	13	20	21	67	24	22	40	36	122	0.68

GNAS	<i>GNAS complex locus</i>	2	0	8	9	19	4	0	9	10	23	0.68
VCP	<i>valosin containing protein</i>	5	7	0	0	12	0	0	4	5	9	0.68
COBL	<i>cordon-bleu WH2 repeat protein</i>	0	2	6	3	11	0	2	5	3	10	0.68
ANXA6	<i>annexin A6</i>	0	0	22	26	48	7	13	34	32	86	0.68
PACSIN3	<i>protein kinase C and casein kinase substrate in neurons 3</i>	0	0	10	4	14	6	5	0	4	15	0.68
LAMTOR3	<i>late endosomal/lysosomal adaptor, MAPK and MTOR activator 3</i>	0	0	6	5	11	0	0	5	0	5	0.68
YWHAE	<i>tyrosine 3-monooxygenase/tryptophan 5-monooxygenase activation protein epsilon</i>	8	0	0	3	11	0	3	0	3	6	0.69
DIAPH1	<i>diaphanous related formin 1</i>	4	8	0	2	14	5	6	3	0	14	0.69
RAB32	<i>RAB32, member RAS oncogene family</i>	0	6	10	8	24	8	8	12	12	40	0.69
PHGDH	<i>phosphoglycerate dehydrogenase</i>	2	0	8	6	16	0	7	5	6	18	0.69
ATP11A	<i>ATPase phospholipid transporting 11A</i>	0	0	9	9	18	0	0	7	9	16	0.69
PTPN1	<i>protein tyrosine phosphatase non-receptor type 1</i>	0	0	9	6	15	0	2	6	6	14	0.69
S100A10	<i>S100 calcium binding protein A10</i>	0	0	33	28	61	35	33	45	44	157	0.69
HIST1H2AE	<i>histone cluster 1 H2A family member e</i>	0	0	18	18	36	22	0	13	12	47	0.69
MAP4K4	<i>mitogen-activated protein kinase kinase kinase 4</i>	0	0	11	3	14	0	0	5	4	9	0.69
WDR81	<i>WD repeat domain 81</i>	0	0	6	7	13	0	0	0	5	5	0.69
TPD52L2	<i>TPD52 like 2</i>	5	9	0	0	14	0	0	4	5	9	0.7
UFL1	<i>UFM1 specific ligase 1</i>	0	3	4	6	13	0	0	0	5	5	0.7
TECR	<i>trans-2,3-enoyl-CoA reductase</i>	0	8	9	10	27	9	7	11	14	41	0.7
VDAC3	<i>voltage dependent anion channel 3</i>	9	7	0	0	16	0	0	6	5	11	0.7
ARL1	<i>ADP ribosylation factor like GTPase 1</i>	3	3	8	4	18	5	6	8	3	22	0.7
RAP1A	<i>RAP1A, member of RAS oncogene family</i>	0	0	22	20	42	17	17	26	20	80	0.7
LAMTOR1	<i>late endosomal/lysosomal adaptor, MAPK and MTOR activator 1</i>	0	0	14	11	25	3	0	12	10	25	0.7
FLOT2	<i>flotillin 2</i>	0	0	11	13	24	0	0	12	3	15	0.7

PKP4	<i>plakophilin 4</i>	0	0	7	7	14	4	2	5	4	15	0.7
IGF2R	<i>insulin like growth factor 2 receptor</i>	0	0	22	16	38	4	9	22	23	58	0.7
UBB	<i>ubiquitin B</i>	0	0	20	21	41	13	15	20	22	70	0.71
STOM	<i>stomatin</i>	5	6	13	18	42	10	14	24	22	70	0.71
RPSA	<i>ribosomal protein SA</i>	3	3	8	7	21	0	0	9	5	14	0.71
SLC16A3	<i>solute carrier family 16 member 3</i>	2	2	11	12	27	12	8	11	11	42	0.71
RAB13	<i>RAB13, member RAS oncogene family</i>	4	3	4	4	15	5	3	4	4	16	0.71
COPA	<i>coatamer protein complex subunit alpha</i>	5	11	8	6	30	6	3	14	9	32	0.71
ATP6V1B2	<i>ATPase H+ transporting V1 subunit B2</i>	4	3	15	13	35	0	2	18	6	26	0.71
GNAI2	<i>G protein subunit alpha i2</i>	0	0	8	8	16	0	0	4	5	9	0.71
CISD2	<i>CDGSH iron sulfur domain 2</i>	0	0	7	11	18	0	3	6	6	15	0.71
B3GALT6	<i>beta-1,3-galactosyltransferase 6</i>	0	0	13	10	23	4	4	10	9	27	0.71
HS2ST1	<i>heparan sulfate 2-O-sulfotransferase 1</i>	0	0	15	12	27	3	7	12	9	31	0.71
PTDSS1	<i>phosphatidylserine synthase 1</i>	0	5	9	9	23	3	0	8	6	17	0.72
ACSL3	<i>acyl-CoA synthetase long chain family member 3</i>	0	0	29	26	55	8	7	33	31	79	0.72
RPS13	<i>ribosomal protein S13</i>	2	2	11	9	24	0	0	9	9	18	0.72
RPL22	<i>ribosomal protein L22</i>	5	5	3	5	18	3	5	3	5	16	0.72
ATP2A2	<i>ATPase sarcoplasmic/endoplasmic reticulum Ca2+ transporting 2</i>	7	12	20	20	59	0	3	34	32	69	0.72
RBM14	<i>RNA binding motif protein 14</i>	4	4	3	5	16	5	3	0	0	8	0.72
CLU	<i>clusterin</i>	0	0	28	28	56	23	25	31	33	112	0.72
ROBO1	<i>roundabout guidance receptor 1</i>	0	3	12	9	24	8	8	3	2	21	0.72
SPECC1	<i>sperm antigen with calponin homology and coiled-coil domains 1</i>	0	2	12	11	25	8	8	10	9	35	0.72
SNAP23	<i>synaptosome associated protein 23</i>	0	0	11	13	24	0	0	8	6	14	0.72
FLOT1	<i>flotillin 1</i>	0	0	18	14	32	0	6	13	13	32	0.72
OSBPL9	<i>oxysterol binding protein like 9</i>	0	0	7	12	19	0	2	6	5	13	0.72
PPP1CA	<i>protein phosphatase 1 catalytic subunit alpha</i>	3	2	10	10	25	4	0	7	7	18	0.73
SPTAN1	<i>spectrin alpha, non-erythrocytic 1</i>	4	6	4	6	20	0	0	6	4	10	0.73

MYL6	<i>myosin light chain 6</i>	5	4	10	8	27	7	4	6	8	25	0.73
FXR1	<i>FMR1 autosomal homolog 1</i>	7	4	9	4	24	0	0	8	0	8	0.73
RPL14	<i>ribosomal protein L14</i>	6	5	6	6	23	0	0	6	0	6	0.73
RAB5C	<i>RAB5C, member RAS oncogene family</i>	8	8	14	11	41	18	12	17	11	58	0.73
CLTC	<i>clathrin heavy chain</i>	4	5	22	21	52	12	14	26	23	75	0.73
RPS16	<i>ribosomal protein S16</i>	9	5	9	12	35	12	11	11	15	49	0.73
RAB2A	<i>RAB2A, member RAS oncogene family</i>	9	13	27	33	82	18	24	47	47	136	0.73
RPS28	<i>ribosomal protein S28</i>	6	6	6	5	23	3	3	6	5	17	0.73
VAMP3	<i>vesicle associated membrane protein 3</i>	4	4	9	9	26	6	6	5	8	25	0.73
PTRF	<i>caveolae associated protein 1</i>	0	2	10	11	23	0	0	7	6	13	0.73
RAB11FIP5	<i>RAB11 family interacting protein 5</i>	0	0	10	13	23	0	0	6	3	9	0.73
ACTA1	<i>actin alpha 1, skeletal muscle</i>	13	0	17	12	42	0	13	13	0	26	0.74
CYFIP1	<i>cytoplasmic FMR1 interacting protein 1</i>	2	8	15	8	33	0	5	9	6	20	0.74
MYO1C	<i>myosin IC</i>	0	3	31	24	58	22	23	24	28	97	0.74
RPL27A	<i>ribosomal protein L27a</i>	9	7	4	6	26	0	0	2	7	9	0.74
TMEM33	<i>transmembrane protein 33</i>	5	6	13	13	37	5	5	10	10	30	0.74
RPN2	<i>ribophorin II</i>	10	13	25	22	70	7	8	36	25	76	0.74
IQGAP1	<i>IQ motif containing GTPase activating protein 1</i>	5	4	25	28	62	17	18	28	18	81	0.74
HSPD1	<i>heat shock protein family D (Hsp60) member 1</i>	18	16	9	5	48	0	0	19	13	32	0.74
RPN1	<i>ribophorin I</i>	6	9	23	23	61	7	2	28	23	60	0.74
RPL27	<i>ribosomal protein L27</i>	9	8	7	7	31	4	6	7	8	25	0.74
PPIA	<i>peptidylprolyl isomerase A</i>	4	5	17	12	38	8	6	8	12	34	0.74
TUBA1A	<i>tubulin alpha 1a</i>	0	0	29	28	57	27	0	0	19	46	0.74
BANF1	<i>barrier to autointegration factor 1</i>	0	11	12	11	34	0	0	11	6	17	0.74
SBF1	<i>SET binding factor 1</i>	0	0	19	17	36	8	7	12	6	33	0.74
GOLGA2	<i>golgin A2</i>	0	2	83	84	169	82	103	108	88	381	0.75
TRIP11	<i>thyroid hormone receptor interactor 11</i>	0	0	84	73	157	72	76	75	75	298	0.75

ATP6V1A	<i>ATPase H⁺ transporting VI subunit A</i>	13	13	26	29	81	14	14	27	26	81	0.75
RPS25	<i>ribosomal protein S25</i>	9	9	17	17	52	14	12	16	14	56	0.75
CKAP4	<i>cytoskeleton associated protein 4</i>	6	12	33	26	77	4	10	24	18	56	0.75
SLC1A5	<i>solute carrier family 1 member 5</i>	9	13	12	13	47	5	8	13	14	40	0.75
SERPINH1	<i>serpin family H member 1</i>	13	25	16	12	66	5	11	27	21	64	0.75
HSPB1	<i>heat shock protein family B (small) member 1</i>	19	23	16	12	70	17	15	20	17	69	0.75
ARF1	<i>ADP ribosylation factor 1</i>	19	17	8	5	49	13	12	11	12	48	0.75
SLC25A5	<i>solute carrier family 25 member 5</i>	16	26	22	25	89	15	18	20	28	81	0.75
RAB7A	<i>RAB7A, member RAS oncogene family</i>	8	9	46	38	101	32	24	51	47	154	0.75
PRDX2	<i>peroxiredoxin 2</i>	14	12	16	12	54	0	11	14	13	38	0.75
SEC16A	<i>SEC16 homolog A, endoplasmic reticulum export factor</i>	2	4	39	33	78	18	14	19	21	72	0.75
MUC13	<i>mucin 13, cell surface associated</i>	5	5	17	13	40	4	5	11	7	27	0.75
RAB11FIP1	<i>RAB11 family interacting protein 1</i>	3	4	52	37	96	10	15	35	26	86	0.75
EGFR	<i>epidermal growth factor receptor</i>	2	0	25	27	54	11	8	18	19	56	0.75
CLINT1	<i>clathrin interactor 1</i>	22	22	55	45	144	38	34	40	37	149	0.76
AHNAK2	<i>AHNAK nucleoprotein 2</i>	24	27	337	303	691	136	151	204	171	662	0.76
GOLGA3	<i>golgin A3</i>	4	5	83	70	162	48	63	49	46	206	0.76
MYOF	<i>myoferlin</i>	5	4	144	134	287	97	84	174	166	521	0.76
DNAJC13	<i>DnaJ heat shock protein family (Hsp40) member C13</i>	0	10	436	399	845	127	134	250	219	730	0.76
C19orf21	<i>mitotic spindle positioning</i>	11	21	37	33	102	16	16	27	15	74	0.76
ANXA2	<i>annexin A2</i>	54	65	242	227	588	142	162	247	231	782	0.76
RPS2	<i>ribosomal protein S2</i>	27	30	22	27	106	11	13	28	20	72	0.76
ACTG1	<i>actin gamma 1</i>	53	86	61	62	262	80	79	90	87	336	0.76
ACACA	<i>acetyl-CoA carboxylase alpha</i>	348	338	387	320	1393	306	324	354	363	1347	0.76
SLC3A2	<i>solute carrier family 3 member 2</i>	31	35	76	71	213	28	38	80	71	217	0.76
RAB1B	<i>RAB1B, member RAS oncogene family</i>	18	16	38	41	113	20	17	34	33	104	0.76
LRRC59	<i>leucine rich repeat containing 59</i>	9	10	46	43	108	25	25	40	36	126	0.76

TMF1	<i>TATA element modulatory factor 1</i>	0	0	75	68	143	41	51	48	48	188	0.76
GOLGA4	<i>golgin A4</i>	0	0	63	58	121	31	44	42	21	138	0.76
GCC2	<i>GRIP and coiled-coil domain containing 2</i>	0	0	54	43	97	22	28	28	26	104	0.76
birA	<i>E. coli biotin carboxylase</i>	1416	1639	106	88	3249	383	389	376	372	1520	0.77
AHNAK	<i>AHNAK nucleoprotein</i>	1026	1096	2905	2577	7604	1800	1730	1801	1713	7044	0.77
FASN	<i>fatty acid synthase</i>	520	513	177	154	1364	59	63	82	71	275	0.77
FLNB	<i>filamin B</i>	144	151	81	61	437	18	10	29	13	70	0.77
KIF5B	<i>kinesin family member 5B</i>	44	51	8	4	107	2	0	0	2	4	0.77
CTTN	<i>cortactin</i>	88	67	14	9	178	6	12	8	7	33	0.77
MYH9	<i>myosin heavy chain 9</i>	65	88	119	104	376	32	30	58	47	167	0.77
MKL2	<i>myocardin related transcription factor B</i>	72	87	11	10	180	0	0	3	3	6	0.77
TAGLN2	<i>transgelin 2</i>	41	43	6	10	100	0	0	0	5	5	0.77
COPG2	<i>coatamer protein complex subunit gamma 2</i>	64	74	30	29	197	6	4	0	6	16	0.77
CAPZA1	<i>capping actin protein of muscle Z-line subunit alpha 1</i>	41	35	26	24	126	12	15	19	21	67	0.77
LARP1	<i>La ribonucleoprotein domain family member 1</i>	73	78	9	4	164	0	0	2	2	4	0.77
CORO1B	<i>coronin 1B</i>	78	101	17	15	211	11	13	12	9	45	0.77
PAICS	<i>phosphoribosylaminoimidazole carboxylase and phosphoribosylaminoimidazolesuccinocarboxamide synthase</i>	39	43	4	3	89	3	6	0	4	13	0.77
SEPT9	<i>septin9</i>	20	21	5	5	51	2	0	0	0	2	0.77
CALD1	<i>caldesmon 1</i>	44	53	10	15	122	9	7	7	15	38	0.77
ZC3HAV1	<i>zinc finger CCCH-type containing, antiviral 1</i>	18	19	12	16	65	4	3	4	0	11	0.77
TLN1	<i>talin 1</i>	99	124	30	32	285	0	4	10	4	18	0.77
SEPT2	<i>septin2</i>	26	36	11	9	82	0	3	2	3	8	0.77
CKAP5	<i>cytoskeleton associated protein 5</i>	79	95	42	40	256	3	3	9	7	22	0.77
CD2AP	<i>CD2 associated protein</i>	54	69	29	32	184	16	19	14	5	54	0.77
LIMA1	<i>LIM domain and actin binding 1</i>	47	67	37	34	185	8	12	19	16	55	0.77
CORO1C	<i>coronin 1C</i>	26	24	9	8	67	0	0	8	4	12	0.77
FERMT2	<i>fermitin family member 2</i>	36	40	11	12	99	0	0	9	7	16	0.77

WDR11	<i>WD repeat domain 11</i>	25	20	25	24	94	5	3	6	10	24	0.77
FAM91A1	<i>family with sequence similarity 91 member A1</i>	10	17	17	14	58	0	3	6	0	9	0.77
DAB2	<i>DAB adaptor protein 2</i>	8	10	4	7	29	3	3	2	2	10	0.77
EPS15L1	<i>epidermal growth factor receptor pathway substrate 15 like 1</i>	39	42	16	14	111	0	0	5	0	5	0.77
DLG5	<i>discs large MAGUK scaffold protein 5</i>	27	37	30	27	121	0	0	7	4	11	0.77
SQSTM1	<i>sequestosome 1</i>	42	50	91	80	263	9	11	22	24	66	0.77
ACTN4	<i>actinin alpha 4</i>	38	45	35	15	133	5	9	20	14	48	0.77
ARFGAP1	<i>ADP ribosylation factor GTPase activating protein 1</i>	10	8	4	6	28	0	4	4	3	11	0.77
SEPT7	<i>septin7</i>	9	8	12	6	35	3	0	0	0	3	0.77
YWHAG	<i>tyrosine 3-monooxygenase/tryptophan 5-monooxygenase activation protein gamma</i>	5	6	0	0	11	0	0	0	2	2	0.77
DSG2	<i>desmoglein 2</i>	20	25	53	56	154	11	13	16	12	52	0.77
CTNND1	<i>catenin delta 1</i>	5	18	24	18	65	13	14	13	8	48	0.77
EZR	<i>ezrin</i>	12	14	18	9	53	0	4	5	3	12	0.77
NCKAP1	<i>NCK associated protein 1</i>	4	4	11	10	29	0	0	2	3	5	0.77
JUP	<i>junction plakoglobin</i>	28	31	83	84	226	21	30	34	20	105	0.77
EPB41L2	<i>erythrocyte membrane protein band 4.1 like 2</i>	31	44	40	36	151	5	7	5	6	23	0.77
ERBB2IP	<i>erb2 interacting protein</i>	23	25	66	64	178	14	12	17	15	58	0.77
CCT8	<i>chaperonin containing TCP1 subunit 8</i>	80	84	24	24	212	3	3	6	5	17	0.77
RPS11	<i>ribosomal protein S11</i>	9	9	2	2	22	0	0	2	4	6	0.77
MAP4	<i>microtubule associated protein 4</i>	170	171	14	10	365	0	3	0	2	5	0.77
SYAP1	<i>synapse associated protein 1</i>	6	10	13	9	38	8	7	6	5	26	0.77
LUZP1	<i>leucine zipper protein 1</i>	20	20	17	14	71	0	4	4	4	12	0.77
CAPZB	<i>capping actin protein of muscle Z-line subunit beta</i>	22	18	18	12	70	7	7	6	8	28	0.77
ACLY	<i>ATP citrate lyase</i>	13	17	4	0	34	3	0	2	0	5	0.77
EPS15	<i>epidermal growth factor receptor pathway substrate 15</i>	7	8	16	12	43	0	0	4	0	4	0.77
RPL18	<i>ribosomal protein L18</i>	18	19	8	9	54	0	0	3	6	9	0.77

AP2A1	<i>adaptor related protein complex 2 subunit alpha 1</i>	2	4	24	19	49	0	0	7	7	14	0.77
EEF1D	<i>eukaryotic translation elongation factor 1 delta</i>	45	8	15	0	68	0	2	5	6	13	0.77
AP2B1	<i>adaptor related protein complex 2 subunit beta 1</i>	9	19	26	31	85	0	4	13	9	26	0.77
RAI14	<i>retinoic acid induced 14</i>	29	29	53	46	157	0	0	0	3	3	0.77
KIAA0196	<i>WASH complex subunit 5</i>	0	4	4	3	11	0	0	2	0	2	0.77
SNAP29	<i>synaptosome associated protein 29</i>	5	2	2	0	9	0	0	2	0	2	0.77
INF2	<i>inverted formin, FH2 and WH2 domain containing</i>	3	7	24	24	58	0	2	7	5	14	0.77
SCRIB	<i>scribble planar cell polarity protein</i>	12	34	52	46	144	16	14	13	15	58	0.77
ESYT1	<i>extended synaptotagmin 1</i>	16	20	41	38	115	0	0	14	14	28	0.77
EEF1B2	<i>eukaryotic translation elongation factor 1 beta 2</i>	21	20	8	4	53	4	5	0	6	15	0.77
CAPRIN1	<i>cell cycle associated protein 1</i>	9	7	5	4	25	2	0	3	0	5	0.77
RTN4	<i>reticulon 4</i>	14	14	11	11	50	0	0	10	8	18	0.77
RPL19	<i>ribosomal protein L19</i>	12	10	0	0	22	2	0	0	0	2	0.77
C14orf166	<i>RNA transcription, translation and transport factor</i>	12	16	3	3	34	0	0	2	0	2	0.77
HIST1H3F	<i>histone cluster 1 H3 family member f</i>	6	6	0	0	12	0	0	2	0	2	0.77
BAG2	<i>BCL2 associated athanogene 2</i>	11	12	18	10	51	7	8	7	3	25	0.77
AP2M1	<i>adaptor related protein complex 2 subunit mu 1</i>	5	8	21	22	56	0	0	8	8	16	0.77
LBR	<i>lamin B receptor</i>	12	14	9	8	43	2	0	6	7	15	0.77
PABPC4	<i>poly(A) binding protein cytoplasmic 4</i>	23	14	0	4	41	0	0	0	5	5	0.77
MYO1B	<i>myosin IB</i>	14	27	56	53	150	14	14	19	21	68	0.77
PABPC1	<i>poly(A) binding protein cytoplasmic 1</i>	36	35	22	14	107	7	8	15	13	43	0.77
CCT2	<i>chaperonin containing TCP1 subunit 2</i>	18	30	6	3	57	0	0	2	0	2	0.77
RPS3A	<i>ribosomal protein S3A</i>	19	18	14	20	71	13	9	16	14	52	0.77
RPS7	<i>ribosomal protein S7</i>	32	48	24	21	125	3	6	21	20	50	0.77
RPS27	<i>ribosomal protein S27</i>	13	9	0	0	22	0	0	3	0	3	0.77
TUBA4A	<i>tubulin alpha 4a</i>	12	171	30	23	236	13	4	2	13	32	0.77

CCT5	<i>chaperonin containing TCP1 subunit 5</i>	17	23	4	3	47	0	0	5	3	8	0.77
RPL31	<i>ribosomal protein L31</i>	12	7	9	9	37	0	4	9	9	22	0.77
ESYT2	<i>extended synaptotagmin 2</i>	0	6	0	5	11	0	0	2	2	4	0.77
RPL11	<i>ribosomal protein L11</i>	8	11	6	6	31	0	0	6	2	8	0.77
DNAJA1	<i>DnaJ heat shock protein family (Hsp40) member A1</i>	8	9	2	2	21	0	0	2	2	4	0.77
CAPZA2	<i>capping actin protein of muscle Z-line subunit alpha 2</i>	14	19	9	10	52	0	0	11	7	18	0.77
TMPO	<i>thymopoietin</i>	27	31	19	17	94	2	0	18	18	38	0.77
RPS4X	<i>ribosomal protein S4 X-linked</i>	31	21	26	23	101	0	5	25	23	53	0.77
CCT4	<i>chaperonin containing TCP1 subunit 4</i>	26	25	5	8	64	0	3	9	5	17	0.77
RPS6	<i>ribosomal protein S6</i>	24	16	5	0	45	2	0	7	0	9	0.77
RPL17	<i>ribosomal protein L17</i>	13	13	4	5	35	0	0	4	5	9	0.77
ILF2	<i>interleukin enhancer binding factor 2</i>	16	32	6	4	58	0	0	3	0	3	0.77
EIF2S3	<i>eukaryotic translation initiation factor 2 subunit gamma</i>	23	23	4	5	55	0	2	3	0	5	0.77
RPL10A	<i>ribosomal protein L10a</i>	6	13	12	12	43	0	0	9	4	13	0.77
SMC2	<i>structural maintenance of chromosomes 2</i>	16	26	0	0	42	0	2	0	0	2	0.77
GAPDH	<i>glyceraldehyde-3-phosphate dehydrogenase</i>	64	75	24	21	184	4	10	19	14	47	0.77
CFL1	<i>cofilin 1</i>	24	27	19	22	92	7	10	20	18	55	0.77
RPS9	<i>ribosomal protein S9</i>	13	21	3	6	43	0	0	5	3	8	0.77
COPB1	<i>coatamer protein complex subunit beta 1</i>	27	30	12	5	74	4	9	14	5	32	0.77
DDX5	<i>DEAD-box helicase 5</i>	25	27	9	8	69	6	4	6	7	23	0.77
TUBB4B	<i>tubulin beta 4B class IVb</i>	18	15	19	17	69	0	6	10	5	21	0.77
HNRNPK	<i>heterogeneous nuclear ribonucleoprotein K</i>	43	42	12	12	109	0	2	0	3	5	0.77
FLNA	<i>filamin A</i>	1278	1293	650	596	3817	342	325	376	354	1397	0.77
EEF1A1	<i>eukaryotic translation elongation factor 1 alpha 1</i>	79	86	28	32	225	20	26	31	25	102	0.77
VIM	<i>vimentin</i>	134	124	43	41	342	17	14	20	19	70	0.77
PKM2	<i>pyruvate kinase M1/2</i>	100	106	55	49	310	15	15	25	19	74	0.77

RPS3	<i>ribosomal protein S3</i>	67	49	21	17	154	14	12	21	25	72	0.77
HIST1H2BB	<i>histone cluster 1 H2B family member b</i>	87	110	19	0	216	22	24	0	0	46	0.77
HIST1H2BD	<i>histone cluster 1 H2B family member d</i>	88	111	0	13	212	0	0	11	14	25	0.77
RPL9	<i>ribosomal protein L9</i>	20	17	5	0	42	0	0	3	0	3	0.77
RPL3	<i>ribosomal protein L3</i>	25	25	10	10	70	2	2	5	7	16	0.77
RPS15A	<i>ribosomal protein S15a</i>	16	22	4	3	45	4	3	4	5	16	0.77
RPS8	<i>ribosomal protein S8</i>	37	36	20	21	114	7	9	15	14	45	0.77
RPL4	<i>ribosomal protein L4</i>	41	47	30	28	146	5	4	23	15	47	0.77
CCT3	<i>chaperonin containing TCP1 subunit 3</i>	28	28	3	3	62	4	0	4	3	11	0.77
DDX3X	<i>DEAD-box helicase 3 X-linked</i>	39	46	8	5	98	5	7	3	4	19	0.77
NONO	<i>non-POU domain containing octamer binding</i>	67	76	9	7	159	2	4	2	3	11	0.77
GNB2L1	<i>receptor for activated C kinase 1</i>	36	35	29	21	121	16	21	16	18	71	0.77
CCT6A	<i>chaperonin containing TCP1 subunit 6A</i>	21	25	4	0	50	3	0	0	0	3	0.77
RPL15	<i>ribosomal protein L15</i>	24	26	12	10	72	6	4	7	9	26	0.77
PC	<i>pyruvate carboxylase</i>	1019	954	296	297	2566	162	166	311	302	941	0.77
SAV_STRAV	<i>Streptavidin</i>	533	349	1800	1805	4487	2300	2084	1823	1988	8195	0.77
PCCA	<i>propionyl-CoA carboxylase subunit alpha</i>	152	142	58	58	410	25	17	51	46	139	0.77
MCCC1	<i>methylcrotonoyl-CoA carboxylase 1</i>	136	135	40	28	339	9	6	41	27	83	0.77
PCCB	<i>propionyl-CoA carboxylase subunit beta</i>	127	120	50	48	345	17	19	56	48	140	0.77
MCCC2	<i>methylcrotonoyl-CoA carboxylase 2</i>	91	84	4	2	181	0	0	3	4	7	0.77
CPS1	<i>carbamoyl-phosphate synthase 1</i>	111	123	48	42	324	14	12	59	54	139	0.77
ENO1	<i>enolase 1</i>	45	50	29	21	145	0	0	9	4	13	0.77
HSP90AB1	<i>heat shock protein 90 alpha family class B member 1</i>	82	75	23	19	199	5	6	21	23	55	0.77
PLEC	<i>plectin</i>	32	47	6	4	89	0	0	5	2	7	0.77
ATP5A1	<i>ATP synthase F1 subunit alpha</i>	57	58	30	25	170	15	20	30	26	91	0.77
HSPA9	<i>heat shock protein family A (Hsp70) member 9</i>	58	67	7	11	143	0	0	11	14	25	0.77

HSPA8	<i>heat shock protein family A (Hsp70) member 8</i>	119	112	76	82	389	51	61	64	68	244	0.77
TCP1	<i>t-complex 1</i>	57	60	5	6	128	3	3	7	6	19	0.77
DYNC1H1	<i>dynein cytoplasmic 1 heavy chain 1</i>	29	39	0	0	68	3	4	2	0	9	0.77
EEF2	<i>eukaryotic translation elongation factor 2</i>	68	63	23	20	174	11	7	11	8	37	0.77
PTBP1	<i>polypyrimidine tract binding protein 1</i>	39	50	8	8	105	0	0	2	0	2	0.77
HSPA1B	<i>heat shock protein family A (Hsp70) member 1B</i>	57	62	24	29	172	16	17	23	21	77	0.77
HSP90AA1	<i>heat shock protein 90 alpha family class A member 1</i>	48	39	18	13	118	0	0	22	21	43	0.77
NPM1	<i>nucleophosmin 1</i>	119	112	29	25	285	5	0	14	10	29	0.77
EIF4A1	<i>eukaryotic translation initiation factor 4A1</i>	51	42	13	12	118	4	0	7	6	17	0.77
TUFM	<i>Tu translation elongation factor, mitochondrial</i>	21	26	3	0	50	0	0	5	3	8	0.77
TUBB	<i>tubulin beta class 1</i>	39	39	46	39	163	13	23	30	26	92	0.77
HNRNPU	<i>heterogeneous nuclear ribonucleoprotein U</i>	57	47	11	5	120	0	0	3	6	9	0.77
RPL6	<i>ribosomal protein L6</i>	36	35	40	44	155	9	9	31	26	75	0.77
PRDX1	<i>peroxiredoxin 1</i>	35	40	27	23	125	21	22	29	28	100	0.77
ATP5B	<i>ATP synthase F1 subunit beta</i>	17	20	0	4	41	0	0	8	8	16	0.77
PHB2	<i>prohibitin 2</i>	28	26	9	5	68	2	0	16	14	32	0.77
HNRNPM	<i>heterogeneous nuclear ribonucleoprotein M</i>	34	25	23	27	109	21	14	23	21	79	0.77
SYNCRIP	<i>synaptotagmin binding cytoplasmic RNA interacting protein</i>	35	40	20	16	111	0	0	17	10	27	0.77
DDX21	<i>DEXD-box helicase 21</i>	56	41	10	9	116	0	0	2	4	6	0.77
NCL	<i>nucleolin</i>	38	40	15	13	106	6	5	5	2	18	0.77
SFPQ	<i>splicing factor proline and glutamine rich</i>	31	38	12	16	97	4	0	6	4	14	0.77
SND1	<i>staphylococcal nuclease and tudor domain containing 1</i>	32	38	18	20	108	3	3	7	7	20	0.77
G3BP1	<i>G3BP stress granule assembly factor 1</i>	49	47	16	13	125	3	5	8	5	21	0.77
HIST1H1C	<i>histone cluster 1 H1 family member c</i>	22	19	6	7	54	6	8	5	4	23	0.77
EPRS	<i>glutamyl-prolyl-tRNA synthetase</i>	40	44	9	7	100	0	0	2	0	2	0.77

HIST1H4J	<i>histone cluster 1 H4 family member j</i>	57	53	14	11	135	9	8	11	7	35	0.77
VDAC2	<i>voltage dependent anion channel 2</i>	18	15	6	6	45	0	2	8	7	17	0.77
RPL7A	<i>ribosomal protein L7a</i>	27	28	17	15	87	3	4	6	8	21	0.77
MTHFD1	<i>methylenetetrahydrofolate dehydrogenase, cyclohydrolase and formyltetrahydrofolate synthetase 1</i>	9	11	5	7	32	3	7	8	4	22	0.77
RPL21	<i>ribosomal protein L21</i>	7	5	3	0	15	0	0	3	0	3	0.77
LMNA	<i>lamin A/C</i>	11	17	6	6	40	0	4	3	6	13	0.77
UQCRC2	<i>ubiquinol-cytochrome c reductase core protein 2</i>	8	12	0	0	20	0	0	2	3	5	0.77
RPL7	<i>ribosomal protein L7</i>	20	10	12	8	50	2	3	6	5	16	0.77
RPL23A	<i>ribosomal protein L23a</i>	19	18	4	4	45	0	0	0	5	5	0.77
RPS14	<i>ribosomal protein S14</i>	11	11	4	4	30	0	0	4	4	8	0.77
AP3D1	<i>adaptor related protein complex 3 subunit delta 1</i>	19	20	26	23	88	0	2	6	6	14	0.77
LDHA	<i>lactate dehydrogenase A</i>	9	8	2	0	19	0	0	3	0	3	0.77
RPL13A	<i>ribosomal protein L13a</i>	18	8	5	5	36	0	0	5	5	10	0.77
ILF3	<i>interleukin enhancer binding factor 3</i>	22	19	3	4	48	0	0	0	2	2	0.77
RPLP2	<i>ribosomal protein lateral stalk subunit P2</i>	13	15	8	11	47	3	3	7	7	20	0.77
PDCD6IP	<i>programmed cell death 6 interacting protein</i>	5	11	8	4	28	0	4	5	5	14	0.77
RPL13	<i>ribosomal protein L13</i>	10	12	7	6	35	4	0	6	8	18	0.77
RPL26	<i>ribosomal protein L26</i>	8	7	5	6	26	0	0	5	6	11	0.77
CAD	<i>carbamoyl-phosphate synthetase 2, aspartate transcarbamylase, and dihydroorotase</i>	0	0	11	8	19	3	3	0	0	6	0.77
RPL12	<i>ribosomal protein L12</i>	7	11	0	7	25	0	0	4	2	6	0.77
ATP5C1	<i>ATP synthase F1 subunit gamma</i>	10	8	5	4	27	0	0	5	3	8	0.77
HNRNPA0	<i>heterogeneous nuclear ribonucleoprotein A0</i>	13	17	0	3	33	0	0	0	2	2	0.77
FBL	<i>fibrillarin</i>	23	30	0	2	55	0	0	2	0	2	0.77
RPL24	<i>ribosomal protein L24</i>	12	7	7	10	36	0	4	5	9	18	0.77
RPS26	<i>ribosomal protein S26</i>	8	5	6	4	23	0	0	0	5	5	0.77
RPLP0	<i>ribosomal protein lateral stalk</i>	12	12	6	10	40	4	2	9	8	23	0.77

subunit P0												
SERBP1	<i>SERPINE1 mRNA binding protein 1</i>	25	34	9	12	80	0	0	9	8	17	0.77
ABCD3	<i>ATP binding cassette subfamily D member 3</i>	0	5	20	15	40	2	0	5	3	10	0.77
RPL8	<i>ribosomal protein L8</i>	10	11	2	2	25	0	0	2	3	5	0.77
PPP2R2A	<i>protein phosphatase 2 regulatory subunit Balpha</i>	7	8	4	2	21	0	0	4	4	8	0.77
RPL35A	<i>ribosomal protein L35a</i>	5	5	2	3	15	2	2	0	0	4	0.77
SRP72	<i>signal recognition particle 72</i>	9	9	17	17	52	0	0	4	7	11	0.77
SLC7A5	<i>solute carrier family 7 member 5</i>	8	5	13	11	37	5	6	6	9	26	0.77
MTDH	<i>metadherin</i>	12	13	33	33	91	0	0	13	9	22	0.77
KTN1	<i>kinectin 1</i>	0	11	37	25	73	0	0	12	11	23	0.77
RRBP1	<i>ribosome binding protein 1</i>	0	4	13	11	28	0	0	4	0	4	0.77
DIP2B	<i>disco interacting protein 2 homolog B</i>	0	0	9	6	15	0	0	3	0	3	0.77
DBN1	<i>drebrin 1</i>	17	14	18	17	66	3	3	15	15	36	0.77
TACC1	<i>transforming acidic coiled-coil containing protein 1</i>	8	15	31	23	77	0	4	5	6	15	0.77
SEPT6	<i>septin6</i>	7	0	5	4	16	0	0	2	0	2	0.77
LSG1	<i>large 60S subunit nuclear export GTPase 1</i>	5	3	11	7	26	0	0	4	4	8	0.77
SPTBN1	<i>spectrin beta, non-erythrocytic 1</i>	0	10	7	8	25	0	0	6	4	10	0.77
XPR1	<i>xenotropic and polytropic retrovirus receptor 1</i>	0	3	14	15	32	0	0	2	0	2	0.77
KIDINS220	<i>kinase D interacting substrate 220</i>	0	2	69	69	140	11	6	9	9	35	0.77
VANGL1	<i>VANGL planar cell polarity protein 1</i>	0	2	8	5	15	0	0	3	3	6	0.77
CPNE8	<i>copine 8</i>	0	0	18	13	31	4	5	7	7	23	0.77
CAV1	<i>caveolin 1</i>	0	0	6	7	13	3	2	0	0	5	0.77
PKP3	<i>plakophilin 3</i>	0	0	8	3	11	2	0	0	0	2	0.77
OSBPL11	<i>oxysterol binding protein like 11</i>	0	0	11	12	23	2	0	5	5	12	0.77
SH3BP4	<i>SH3 domain binding protein 4</i>	0	0	3	6	9	0	2	0	0	2	0.77
PLCB4	<i>phospholipase C beta 4</i>	0	0	20	16	36	0	0	7	7	14	0.77
WDR91	<i>WD repeat domain 91</i>	0	0	7	3	10	0	0	2	2	4	0.77

EFR3A	<i>EFR3 homolog A</i>	0	0	6	4	10	0	0	2	0	2	0.77
WARS	<i>tryptophanyl-tRNA synthetase</i>	47	57	0	0	104	0	0	0	0	0	#N/A
RANBP2	<i>RAN binding protein 2</i>	172	157	5	0	334	0	0	0	0	0	#N/A
EIF4G1	<i>eukaryotic translation initiation factor 4 gamma 1</i>	63	82	0	0	145	0	0	0	0	0	#N/A
RANGAP1	<i>Ran GTPase activating protein 1</i>	73	86	0	2	161	0	0	0	0	0	#N/A
EIF5	<i>eukaryotic translation initiation factor 5</i>	48	39	0	3	90	0	0	0	0	0	#N/A
ZBTB33	<i>zinc finger and BTB domain containing 33</i>	66	67	0	0	133	0	0	0	0	0	#N/A
DCTN1	<i>dynactin subunit 1</i>	22	40	0	0	62	0	0	0	0	0	#N/A
GCN1L1	<i>GCN1 activator of EIF2AK4</i>	114	140	0	0	254	0	0	0	0	0	#N/A
TRIML2	<i>tripartite motif family like 2</i>	17	14	0	0	31	0	0	0	0	0	#N/A
HDLBP	<i>high density lipoprotein binding protein</i>	31	46	0	0	77	0	0	0	0	0	#N/A
PSMA7	<i>proteasome subunit alpha 7</i>	5	10	0	0	15	0	0	0	0	0	#N/A
CNN2	<i>calponin 2</i>	10	18	0	0	28	0	0	0	0	0	#N/A
USP14	<i>ubiquitin specific peptidase 14</i>	8	16	0	0	24	0	0	0	0	0	#N/A
EIF4G2	<i>eukaryotic translation initiation factor 4 gamma 2</i>	41	52	0	0	93	0	0	0	0	0	#N/A
KPNA2	<i>karyopherin subunit alpha 2</i>	0	11	0	0	11	0	0	0	0	0	#N/A
RPL7L1	<i>ribosomal protein L7 like 1</i>	3	2	0	0	5	0	0	0	0	0	#N/A
BAG3	<i>BCL2 associated athanogene 3</i>	13	15	0	0	28	0	0	0	0	0	#N/A
STAT3	<i>signal transducer and activator of transcription 3</i>	47	54	0	0	101	0	0	0	0	0	#N/A
LRBA	<i>LPS responsive beige-like anchor protein</i>	7	11	0	0	18	0	0	0	0	0	#N/A
KIF11	<i>kinesin family member 11</i>	10	10	0	0	20	0	0	0	0	0	#N/A
HSPH1	<i>heat shock protein family H (Hsp110) member 1</i>	14	25	2	2	43	0	0	0	0	0	#N/A
YTHDC2	<i>YTH domain containing 2</i>	15	26	0	0	41	0	0	0	0	0	#N/A
TWF1	<i>twinfilin actin binding protein 1</i>	8	12	0	0	20	0	0	0	0	0	#N/A
NUDC	<i>nuclear distribution C, dynein complex regulator</i>	20	22	0	0	42	0	0	0	0	0	#N/A
PSMD5	<i>proteasome 26S subunit, non-ATPase 5</i>	8	11	0	0	19	0	0	0	0	0	#N/A
TPR	<i>translocated promoter region,</i>	197	201	0	3	401	0	0	0	0	0	#N/A

<i>nuclear basket protein</i>												
ATG2B	<i>autophagy related 2B</i>	66	71	0	0	137	0	0	0	0	0	#N/A
MRE11A	<i>MRE11 homolog, double strand break repair nuclease</i>	45	49	0	0	94	0	0	0	0	0	#N/A
USP15	<i>ubiquitin specific peptidase 15</i>	65	65	0	0	130	0	0	0	0	0	#N/A
XRN1	<i>5'-3' exoribonuclease 1</i>	29	43	0	0	72	0	0	0	0	0	#N/A
LIMCH1	<i>LIM and calponin homology domains 1</i>	104	93	9	8	214	0	0	0	0	0	#N/A
SLK	<i>STE20 like kinase</i>	39	52	0	0	91	0	0	0	0	0	#N/A
TJP1	<i>tight junction protein 1</i>	48	53	5	5	111	0	0	0	0	0	#N/A
SRP68	<i>signal recognition particle 68</i>	45	53	15	10	123	0	0	0	0	0	#N/A
PLA2G4A	<i>phospholipase A2 group IVA</i>	29	35	3	6	73	0	0	0	0	0	#N/A
CRKL	<i>CRK like proto-oncogene, adaptor protein</i>	14	17	0	0	31	0	0	0	0	0	#N/A
CSDE1	<i>cold shock domain containing E1</i>	37	44	0	0	81	0	0	0	0	0	#N/A
PLIN3	<i>perilipin 3</i>	25	39	0	0	64	0	0	0	0	0	#N/A
GAPVD1	<i>GTPase activating protein and VPS9 domains 1</i>	41	35	0	0	76	0	0	0	0	0	#N/A
GIGYF2	<i>GRB10 interacting GYF protein 2</i>	38	35	7	3	83	0	0	0	0	0	#N/A
CRK	<i>CRK proto-oncogene, adaptor protein</i>	24	28	0	0	52	0	0	0	0	0	#N/A
PUF60	<i>poly(U) binding splicing factor 60</i>	48	60	0	0	108	0	0	0	0	0	#N/A
UNC45A	<i>unc-45 myosin chaperone A</i>	26	25	0	0	51	0	0	0	0	0	#N/A
SNX1	<i>sorting nexin 1</i>	23	28	2	2	55	0	0	0	0	0	#N/A
RAPH1	<i>Ras association (RalGDS/AF-6) and pleckstrin homology domains 1</i>	23	25	0	0	48	0	0	0	0	0	#N/A
TANC1	<i>tetratricopeptide repeat, ankyrin repeat and coiled-coil containing 1</i>	6	8	0	0	14	0	0	0	0	0	#N/A
PDE1A	<i>phosphodiesterase 1A</i>	7	12	0	0	19	0	0	0	0	0	#N/A
TXNL1	<i>thioredoxin like 1</i>	2	2	0	0	4	0	0	0	0	0	#N/A
RPS27L	<i>ribosomal protein S27 like</i>	0	0	0	0	0	0	0	0	0	0	#N/A
WIP12	<i>WD repeat domain, phosphoinositide interacting 2</i>	13	11	0	0	24	0	0	0	0	0	#N/A
TIPRL	<i>TOR signaling pathway regulator</i>	29	24	0	0	53	0	0	0	0	0	#N/A
EIF4B	<i>eukaryotic translation initiation factor 4B</i>	42	47	0	0	89	0	0	0	0	0	#N/A

ZYX	<i>zyxin</i>	11	0	0	0	11	0	0	0	0	0	#N/A
DBT	<i>dihydrolipoamide branched chain transacylase E2</i>	5	5	0	0	10	0	0	0	0	0	#N/A
VCL	<i>vinculin</i>	3	6	0	0	9	0	0	0	0	0	#N/A
DBNL	<i>drebrin like</i>	13	13	0	0	26	0	0	0	0	0	#N/A
C17orf81	<i>elongator acetyltransferase complex subunit 5</i>	12	13	0	0	25	0	0	0	0	0	#N/A
KLC1	<i>kinesin light chain 1</i>	18	9	0	3	30	0	0	0	0	0	#N/A
ERC1	<i>ELKS/RAB6-interacting/CAST family member 1</i>	13	10	2	0	25	0	0	0	0	0	#N/A
PDLIM5	<i>PDZ and LIM domain 5</i>	12	14	0	0	26	0	0	0	0	0	#N/A
GEMIN5	<i>gem nuclear organelle associated protein 5</i>	98	87	0	0	185	0	0	0	0	0	#N/A
XIAP	<i>X-linked inhibitor of apoptosis</i>	9	18	0	0	27	0	0	0	0	0	#N/A
TTK	<i>TTK protein kinase</i>	17	19	0	0	36	0	0	0	0	0	#N/A
NUP133	<i>nucleoporin 133</i>	20	27	0	0	47	0	0	0	0	0	#N/A
KIAA1524	<i>cell proliferation regulating inhibitor of protein phosphatase 2A</i>	4	4	0	0	8	0	0	0	0	0	#N/A
KANK2	<i>KN motif and ankyrin repeat domains 2</i>	17	17	5	5	44	0	0	0	0	0	#N/A
EIF4E2	<i>eukaryotic translation initiation factor 4E family member 2</i>	10	11	0	0	21	0	0	0	0	0	#N/A
KIAA1598	<i>shootin 1</i>	24	34	0	0	58	0	0	0	0	0	#N/A
EIF3A	<i>eukaryotic translation initiation factor 3 subunit A</i>	25	31	0	0	56	0	0	0	0	0	#N/A
PDAP1	<i>PDGFA associated protein 1</i>	18	15	0	0	33	0	0	0	0	0	#N/A
DVL3	<i>dishevelled segment polarity protein 3</i>	9	13	3	0	25	0	0	0	0	0	#N/A
VCPIP1	<i>valosin containing protein interacting protein 1</i>	10	16	0	0	26	0	0	0	0	0	#N/A
ARHGEF16	<i>Rho guanine nucleotide exchange factor 16</i>	11	9	0	0	20	0	0	0	0	0	#N/A
PLS3	<i>plastin 3</i>	7	8	3	0	18	0	0	0	0	0	#N/A
STK38	<i>serine/threonine kinase 38</i>	12	17	0	0	29	0	0	0	0	0	#N/A
DIAPH3	<i>diaphanous related formin 3</i>	17	17	0	0	34	0	0	0	0	0	#N/A
IPO9	<i>importin 9</i>	6	9	0	0	15	0	0	0	0	0	#N/A
SPG20	<i>spartin</i>	8	9	0	0	17	0	0	0	0	0	#N/A

GTF3C5	<i>general transcription factor IIIC subunit 5</i>	18	25	0	0	43	0	0	0	0	0	#N/A
ELP4	<i>elongator acetyltransferase complex subunit 4</i>	12	16	0	0	28	0	0	0	0	0	#N/A
ASCC3	<i>activating signal cointegrator 1 complex subunit 3</i>	14	16	0	0	30	0	0	0	0	0	#N/A
ANKRD17	<i>ankyrin repeat domain 17</i>	38	28	0	0	66	0	0	0	0	0	#N/A
PSMD12	<i>proteasome 26S subunit, non-ATPase 12</i>	6	6	0	0	12	0	0	0	0	0	#N/A
DFNA5	<i>gasdermin E</i>	0	2	0	0	2	0	0	0	0	0	#N/A
RANBP3	<i>RAN binding protein 3</i>	19	20	0	0	39	0	0	0	0	0	#N/A
CCDC25	<i>coiled-coil domain containing 25</i>	4	3	0	0	7	0	0	0	0	0	#N/A
HAUS6	<i>HAUS augmin like complex subunit 6</i>	16	23	0	0	39	0	0	0	0	0	#N/A
TBC1D15	<i>TBC1 domain family member 15</i>	18	13	0	0	31	0	0	0	0	0	#N/A
MYPN	<i>myopalladin</i>	4	5	0	0	9	0	0	0	0	0	#N/A
PDCD5	<i>programmed cell death 5</i>	6	9	0	0	15	0	0	0	0	0	#N/A
MAP7D3	<i>MAP7 domain containing 3</i>	18	13	4	4	39	0	0	0	0	0	#N/A
SH3GL1	<i>SH3 domain containing GRB2 like 1, endophilin A2</i>	7	6	0	0	13	0	0	0	0	0	#N/A
RPL18A	<i>ribosomal protein L18a</i>	2	0	0	0	2	0	0	0	0	0	#N/A
EFHD2	<i>EF-hand domain family member D2</i>	12	5	0	0	17	0	0	0	0	0	#N/A
SEPT11	<i>septin11</i>	10	8	0	0	18	0	0	0	0	0	#N/A
KIF15	<i>kinesin family member 15</i>	3	8	0	0	11	0	0	0	0	0	#N/A
CAP1	<i>cyclase associated actin cytoskeleton regulatory protein 1</i>	5	9	0	0	14	0	0	0	0	0	#N/A
DENND4C	<i>DENN domain containing 4C</i>	8	14	0	0	22	0	0	0	0	0	#N/A
SEC23IP	<i>SEC23 interacting protein</i>	4	3	0	0	7	0	0	0	0	0	#N/A
CACYBP	<i>calcyclin binding protein</i>	3	5	0	0	8	0	0	0	0	0	#N/A
C11orf49	<i>chromosome 11 open reading frame 49</i>	9	12	0	0	21	0	0	0	0	0	#N/A
C3orf75	<i>elongator acetyltransferase complex subunit 6</i>	11	11	0	0	22	0	0	0	0	0	#N/A
NACA	<i>nascent polypeptide associated complex subunit alpha</i>	15	10	0	0	25	0	0	0	0	0	#N/A
PRRC2C	<i>proline rich coiled-coil 2C</i>	14	18	0	0	32	0	0	0	0	0	#N/A
TARS	<i>threonyl-tRNA synthetase</i>	11	9	0	0	20	0	0	0	0	0	#N/A

ARHGAP35	<i>Rho GTPase activating protein 35</i>	10	19	0	0	29	0	0	0	0	0	#N/A
DCTN2	<i>dynactin subunit 2</i>	10	24	0	0	34	0	0	0	0	0	#N/A
TTC28	<i>tetratricopeptide repeat domain 28</i>	5	14	2	0	21	0	0	0	0	0	#N/A
SHC1	<i>SHC adaptor protein 1</i>	2	4	0	0	6	0	0	0	0	0	#N/A
AAK1	<i>AP2 associated kinase 1</i>	5	8	0	0	13	0	0	0	0	0	#N/A
DHX29	<i>DEXH-box helicase 29</i>	20	22	0	0	42	0	0	0	0	0	#N/A
DVL2	<i>dishevelled segment polarity protein 2</i>	6	12	0	0	18	0	0	0	0	0	#N/A
WDR45	<i>WD repeat domain 45</i>	6	4	0	0	10	0	0	0	0	0	#N/A
SWAP70	<i>switching B cell complex subunit SWAP70</i>	18	16	0	0	34	0	0	0	0	0	#N/A
HN1L	<i>Jupiter microtubule associated homolog 2</i>	9	3	0	0	12	0	0	0	0	0	#N/A
SNX2	<i>sorting nexin 2</i>	10	4	0	0	14	0	0	0	0	0	#N/A
UBAP2	<i>ubiquitin associated protein 2</i>	26	42	0	0	68	0	0	0	0	0	#N/A
PIKFYVE	<i>phosphoinositide kinase, FYVE-type zinc finger containing</i>	0	0	0	0	0	0	0	0	0	0	#N/A
BRAP	<i>BRCA1 associated protein</i>	10	10	0	0	20	0	0	0	0	0	#N/A
KIAA0368	<i>Ecm29 proteasome adaptor and scaffold</i>	0	2	0	0	2	0	0	0	0	0	#N/A
PATL1	<i>PAT1 homolog 1, processing body mRNA decay factor</i>	0	6	0	0	6	0	0	0	0	0	#N/A
DNMBP	<i>dynamamin binding protein</i>	5	8	0	0	13	0	0	0	0	0	#N/A
SCYL2	<i>SCY1 like pseudokinase 2</i>	4	4	0	0	8	0	0	0	0	0	#N/A
NUMBL	<i>NUMB like endocytic adaptor protein</i>	2	3	9	8	22	0	0	0	0	0	#N/A
EPB41	<i>erythrocyte membrane protein band 4.1</i>	21	26	10	4	61	0	0	0	0	0	#N/A
CHTOP	<i>chromatin target of PRMT1</i>	4	0	0	0	4	0	0	0	0	0	#N/A
MB21D1	<i>cyclic GMP-AMP synthase</i>	2	0	0	0	2	0	0	0	0	0	#N/A
GAK	<i>cyclin G associated kinase</i>	4	10	0	0	14	0	0	0	0	0	#N/A
HN1	<i>Jupiter microtubule associated homolog 1</i>	9	14	0	0	23	0	0	0	0	0	#N/A
ECD	<i>ecdysoneless cell cycle regulator</i>	11	7	0	0	18	0	0	0	0	0	#N/A
PARVA	<i>parvin alpha</i>	2	6	0	0	8	0	0	0	0	0	#N/A
KLC2	<i>kinesin light chain 2</i>	4	0	0	0	4	0	0	0	0	0	#N/A

FAM98A	<i>family with sequence similarity 98 member A</i>	0	0	2	0	2	0	0	0	0	0	#N/A
PTPN11	<i>protein tyrosine phosphatase non-receptor type 11</i>	8	13	0	0	21	0	0	0	0	0	#N/A
RPAP3	<i>RNA polymerase II associated protein 3</i>	29	27	0	0	56	0	0	0	0	0	#N/A
TMCO7	<i>transport and golgi organization 6 homolog</i>	14	20	0	0	34	0	0	0	0	0	#N/A
CDK6	<i>cyclin dependent kinase 6</i>	3	2	0	0	5	0	0	0	0	0	#N/A
EIF3E	<i>eukaryotic translation initiation factor 3 subunit E</i>	7	6	0	0	13	0	0	0	0	0	#N/A
PRMT1	<i>protein arginine methyltransferase 1</i>	10	11	0	0	21	0	0	0	0	0	#N/A
PRMT7	<i>protein arginine methyltransferase 7</i>	6	6	0	0	12	0	0	0	0	0	#N/A
ECHDC1	<i>ethylmalonyl-CoA decarboxylase 1</i>	8	6	0	0	14	0	0	0	0	0	#N/A
IARS2	<i>isoleucyl-tRNA synthetase 2, mitochondrial</i>	0	0	0	0	0	0	0	0	0	0	#N/A
IMPDH2	<i>inosine monophosphate dehydrogenase 2</i>	4	7	0	0	11	0	0	0	0	0	#N/A
IPO7	<i>importin 7</i>	41	50	0	0	91	0	0	0	0	0	#N/A
STRAP	<i>serine/threonine kinase receptor associated protein</i>	28	34	0	0	62	0	0	0	0	0	#N/A
RPL35	<i>ribosomal protein L35</i>	8	6	0	0	14	0	0	0	0	0	#N/A
GSPT1	<i>G1 to S phase transition 1</i>	3	5	0	0	8	0	0	0	0	0	#N/A
PDLIM7	<i>PDZ and LIM domain 7</i>	6	5	0	0	11	0	0	0	0	0	#N/A
ABCF3	<i>ATP binding cassette subfamily F member 3</i>	4	7	0	0	11	0	0	0	0	0	#N/A
PRPF4	<i>pre-mRNA processing factor 4</i>	7	16	0	0	23	0	0	0	0	0	#N/A
EIF3M	<i>eukaryotic translation initiation factor 3 subunit M</i>	4	13	0	0	17	0	0	0	0	0	#N/A
PPME1	<i>protein phosphatase methylesterase 1</i>	14	14	0	0	28	0	0	0	0	0	#N/A
NPM3	<i>nucleophosmin/nucleoplasmin 3</i>	6	8	0	0	14	0	0	0	0	0	#N/A
PRPF31	<i>pre-mRNA processing factor 31</i>	6	5	0	0	11	0	0	0	0	0	#N/A
CXorf56	<i>chromosome X open reading frame 56</i>	14	13	0	0	27	0	0	0	0	0	#N/A
STMN1	<i>stathmin 1</i>	9	10	0	0	19	0	0	0	0	0	#N/A
MAPRE2	<i>microtubule associated protein RP/EB family member 2</i>	5	7	0	0	12	0	0	0	0	0	#N/A

ARFIP2	<i>ADP ribosylation factor interacting protein 2</i>	0	0	0	0	0	0	0	0	0	0	#N/A
SNRPF	<i>small nuclear ribonucleoprotein polypeptide F</i>	0	6	0	0	6	0	0	0	0	0	#N/A
SH3PXD2	<i>SH3 and PX domains 2B</i>	3	0	0	0	3	0	0	0	0	0	#N/A
B												
H2AFV	<i>H2A histone family member V</i>	0	0	0	0	0	0	0	0	0	0	#N/A
BUB1B	<i>BUB1 mitotic checkpoint serine/threonine kinase B</i>	14	14	0	0	28	0	0	0	0	0	#N/A
PLEKHA5	<i>pleckstrin homology domain containing A5</i>	6	7	0	0	13	0	0	0	0	0	#N/A
STAM	<i>signal transducing adaptor molecule</i>	0	9	0	0	9	0	0	0	0	0	#N/A
VPS33B	<i>VPS33B late endosome and lysosome associated</i>	0	4	0	0	4	0	0	0	0	0	#N/A
TK1	<i>thymidine kinase 1</i>	0	0	0	0	0	0	0	0	0	0	#N/A
TP53BP2	<i>tumor protein p53 binding protein 2</i>	7	8	0	0	15	0	0	0	0	0	#N/A
HINT1	<i>histidine triad nucleotide binding protein 1</i>	0	6	0	0	6	0	0	0	0	0	#N/A
PDXDC1	<i>pyridoxal dependent decarboxylase domain containing 1</i>	0	4	0	0	4	0	0	0	0	0	#N/A
SPAG9	<i>sperm associated antigen 9</i>	7	11	0	0	18	0	0	0	0	0	#N/A
CEP170	<i>centrosomal protein 170</i>	20	26	3	0	49	0	0	0	0	0	#N/A
PPP6R3	<i>protein phosphatase 6 regulatory subunit 3</i>	10	12	0	0	22	0	0	0	0	0	#N/A
SKP2	<i>S-phase kinase associated protein 2</i>	0	9	0	0	9	0	0	0	0	0	#N/A
SMARCA D1	<i>SWI/SNF-related, matrix-associated actin-dependent regulator of chromatin, subfamily a, containing DEAD/H box 1</i>	5	2	0	0	7	0	0	0	0	0	#N/A
ANKS1A	<i>ankyrin repeat and sterile alpha motif domain containing 1A</i>	9	9	0	0	18	0	0	0	0	0	#N/A
HSPA4	<i>heat shock protein family A (Hsp70) member 4</i>	8	15	0	0	23	0	0	0	0	0	#N/A
AHCYL1	<i>adenosylhomocysteinase like 1</i>	0	0	0	0	0	0	0	0	0	0	#N/A
PPP6C	<i>protein phosphatase 6 catalytic subunit</i>	7	8	0	0	15	0	0	0	0	0	#N/A
DHX36	<i>DEAH-box helicase 36</i>	0	7	0	0	7	0	0	0	0	0	#N/A
IFIT5	<i>interferon induced protein with tetratricopeptide repeats 5</i>	8	11	0	0	19	0	0	0	0	0	#N/A

PSMD11	<i>proteasome 26S subunit, non-ATPase 11</i>	4	7	0	0	11	0	0	0	0	0	#N/A
NFKB2	<i>nuclear factor kappa B subunit 2</i>	6	6	0	0	12	0	0	0	0	0	#N/A
YWHAB	<i>tyrosine 3-monooxygenase/tryptophan 5-monooxygenase activation protein beta</i>	0	3	0	0	3	0	0	0	0	0	#N/A
TRIP6	<i>thyroid hormone receptor interactor 6</i>	0	0	0	0	0	0	0	0	0	0	#N/A
MAT2A	<i>methionine adenosyltransferase 2A</i>	0	2	0	0	2	0	0	0	0	0	#N/A
DPYSL2	<i>dihydropyrimidinase like 2</i>	5	10	0	0	15	0	0	0	0	0	#N/A
MYO1E	<i>myosin IE</i>	2	5	0	0	7	0	0	0	0	0	#N/A
CIAPIN1	<i>cytokine induced apoptosis inhibitor 1</i>	5	9	0	0	14	0	0	0	0	0	#N/A
TNKS1BP1	<i>tankyrase 1 binding protein 1</i>	10	13	0	0	23	0	0	0	0	0	#N/A
KIAA1967	<i>cell cycle and apoptosis regulator 2</i>	16	20	0	0	36	0	0	0	0	0	#N/A
DLGAP5	<i>DLG associated protein 5</i>	8	18	0	0	26	0	0	0	0	0	#N/A
EHBP1	<i>EH domain binding protein 1</i>	5	3	0	0	8	0	0	0	0	0	#N/A
SNRPN	<i>small nuclear ribonucleoprotein polypeptide N</i>	5	0	0	0	5	0	0	0	0	0	#N/A
MGEA5	<i>O-GlcNAcase</i>	3	8	0	0	11	0	0	0	0	0	#N/A
PTPN12	<i>protein tyrosine phosphatase non-receptor type 12</i>	6	8	0	0	14	0	0	0	0	0	#N/A
PLK1	<i>polo like kinase 1</i>	0	0	0	2	2	0	0	0	0	0	#N/A
KIF14	<i>kinesin family member 14</i>	0	10	2	2	14	0	0	0	0	0	#N/A
COPS4	<i>COP9 signalosome subunit 4</i>	4	5	0	0	9	0	0	0	0	0	#N/A
PSME3	<i>proteasome activator subunit 3</i>	32	33	0	0	65	0	0	0	0	0	#N/A
CNOT1	<i>CCR4-NOT transcription complex subunit 1</i>	3	3	0	0	6	0	0	0	0	0	#N/A
PFDN2	<i>prefoldin subunit 2</i>	4	0	0	0	4	0	0	0	0	0	#N/A
STAT1	<i>signal transducer and activator of transcription 1</i>	34	49	0	0	83	0	0	0	0	0	#N/A
SSB	<i>small RNA binding exonuclease protection factor La</i>	12	12	0	0	24	0	0	0	0	0	#N/A
NSA2	<i>NSA2 ribosome biogenesis factor</i>	0	0	0	0	0	0	0	0	0	0	#N/A
MTHFD1	<i>methylenetetrahydrofolate dehydrogenase (NADP+</i>	0	0	0	0	0	0	0	0	0	0	#N/A

L	<i>dependent) 1 like</i>											
PAK2	<i>p21 (RAC1) activated kinase 2</i>	0	8	0	0	8	0	0	0	0	0	#N/A
DNM1L	<i>dynamain 1 like</i>	12	24	0	0	36	0	0	0	0	0	#N/A
CSNK1A1	<i>casein kinase 1 alpha 1</i>	8	8	0	0	16	0	0	0	0	0	#N/A
DDX19B	<i>DEAD-box helicase 19B</i>	0	5	0	0	5	0	0	0	0	0	#N/A
SYNJ2	<i>synaptojanin 2</i>	2	4	0	0	6	0	0	0	0	0	#N/A
ATXN2L	<i>ataxin 2 like</i>	22	26	4	0	52	0	0	0	0	0	#N/A
SNRPD1	<i>small nuclear ribonucleoprotein D1 polypeptide</i>	7	8	0	0	15	0	0	0	0	0	#N/A
PSMC3	<i>proteasome 26S subunit, ATPase 3</i>	9	14	0	0	23	0	0	0	0	0	#N/A
SMARCA4	<i>SWI/SNF related, matrix associated, actin dependent regulator of chromatin, subfamily a, member 4</i>	9	17	0	0	26	0	0	0	0	0	#N/A
DDX27	<i>DEAD-box helicase 27</i>	7	7	0	0	14	0	0	0	0	0	#N/A
TUBB2B	<i>tubulin beta 2B class IIb</i>	6	6	0	5	17	0	0	0	0	0	#N/A
ADNP	<i>activity dependent neuroprotector homeobox</i>	24	18	0	0	42	0	0	0	0	0	#N/A
ZC3H15	<i>zinc finger CCCH-type containing 15</i>	10	14	0	0	24	0	0	0	0	0	#N/A
FAM120A	<i>family with sequence similarity 120A</i>	6	5	0	0	11	0	0	0	0	0	#N/A
KPNA1	<i>karyopherin subunit alpha 1</i>	4	6	0	0	10	0	0	0	0	0	#N/A
ATP5L	<i>ATP synthase membrane subunit g</i>	0	0	0	0	0	0	0	0	0	0	#N/A
RARS	<i>arginyl-tRNA synthetase</i>	34	38	2	4	78	0	0	0	0	0	#N/A
EIF3CL	<i>eukaryotic translation initiation factor 3 subunit C like</i>	14	0	0	0	14	0	0	0	0	0	#N/A
SRSF11	<i>serine and arginine rich splicing factor 11</i>	14	19	0	0	33	0	0	0	0	0	#N/A
TOP2A	<i>DNA topoisomerase II alpha</i>	69	73	0	0	142	0	0	0	0	0	#N/A
ACTR2	<i>actin related protein 2</i>	3	0	0	0	3	0	0	0	0	0	#N/A
HNRNPU L1	<i>heterogeneous nuclear ribonucleoprotein U like 1</i>	3	3	0	0	6	0	0	0	0	0	#N/A
ACTR1A	<i>actin related protein 1A</i>	3	4	0	0	7	0	0	0	0	0	#N/A
FRG1	<i>FSHD region gene 1</i>	0	6	0	0	6	0	0	0	0	0	#N/A
HIST2H3	<i>histone cluster 2 H3 family member d</i>	0	0	0	0	0	0	0	0	0	0	#N/A

D												
HIST1H1E	<i>histone cluster 1 H1 family member e</i>	0	0	0	0	0	0	0	0	0	0	#N/A
NUDT5	<i>nudix hydrolase 5</i>	0	5	0	0	5	0	0	0	0	0	#N/A
ZDBF2	<i>zinc finger DBF-type containing 2</i>	6	7	2	0	15	0	0	0	0	0	#N/A
TNRC6B	<i>trinucleotide repeat containing adaptor 6B</i>	3	4	0	0	7	0	0	0	0	0	#N/A
RASSF8	<i>Ras association domain family member 8</i>	0	0	0	0	0	0	0	0	0	0	#N/A
C15orf38-AP3S2	<i>ARPIN-AP3S2 readthrough</i>	4	0	0	0	4	0	0	0	0	0	#N/A
MON2	<i>MON2 homolog, regulator of endosome-to-Golgi trafficking</i>	0	2	0	0	2	0	0	0	0	0	#N/A
FAM21C	<i>WASH complex subunit 2C</i>	0	11	0	3	14	0	0	0	0	0	#N/A
RPS6KA1	<i>ribosomal protein S6 kinase A1</i>	0	0	0	0	0	0	0	0	0	0	#N/A
CCDC43	<i>coiled-coil domain containing 43</i>	5	6	0	0	11	0	0	0	0	0	#N/A
PDLIM1	<i>PDZ and LIM domain 1</i>	6	11	0	0	17	0	0	0	0	0	#N/A
CBX1	<i>chromobox 1</i>	0	0	0	0	0	0	0	0	0	0	#N/A
ARHGAP18	<i>Rho GTPase activating protein 18</i>	0	2	0	0	2	0	0	0	0	0	#N/A
RANBP1	<i>RAN binding protein 1</i>	0	4	0	0	4	0	0	0	0	0	#N/A
CDC16	<i>cell division cycle 16</i>	0	3	0	0	3	0	0	0	0	0	#N/A
PRPSAP1	<i>phosphoribosyl pyrophosphate synthetase associated protein 1</i>	0	0	0	0	0	0	0	0	0	0	#N/A
SUGT1	<i>SGT1 homolog, MIS12 kinetochore complex assembly cochaperone</i>	5	4	0	0	9	0	0	0	0	0	#N/A
CEP44	<i>centrosomal protein 44</i>	0	2	0	0	2	0	0	0	0	0	#N/A
ADD1	<i>adducin 1</i>	8	12	0	0	20	0	0	0	0	0	#N/A
CAMSAP1	<i>calmodulin regulated spectrin associated protein 1</i>	10	21	0	0	31	0	0	0	0	0	#N/A
EXOC4	<i>exocyst complex component 4</i>	0	0	0	0	0	0	0	0	0	0	#N/A
PIH1D1	<i>PIH1 domain containing 1</i>	10	16	0	0	26	0	0	0	0	0	#N/A
CASC5	<i>kinetochore scaffold 1</i>	14	33	0	0	47	0	0	0	0	0	#N/A
HAUS5	<i>HAUS augmin like complex subunit 5</i>	7	4	0	0	11	0	0	0	0	0	#N/A
PFDN5	<i>prefoldin subunit 5</i>	2	6	0	0	8	0	0	0	0	0	#N/A

ANKHD1-EIF4EBP3	<i>ANKHD1-EIF4EBP3 readthrough</i>	8	5	0	0	13	0	0	0	0	0	#N/A
AGFG1	<i>ArfGAP with FG repeats 1</i>	0	3	0	0	3	0	0	0	0	0	#N/A
BMS1	<i>BMS1 ribosome biogenesis factor</i>	5	11	0	0	16	0	0	0	0	0	#N/A
TDRD3	<i>tudor domain containing 3</i>	5	7	0	0	12	0	0	0	0	0	#N/A
TNS3	<i>tensin 3</i>	2	15	0	0	17	0	0	0	0	0	#N/A
KIF1B	<i>kinesin family member 1B</i>	0	0	0	0	0	0	0	0	0	0	#N/A
EYA4	<i>EYA transcriptional coactivator and phosphatase 4</i>	0	3	0	0	3	0	0	0	0	0	#N/A
IGBP1	<i>immunoglobulin binding protein 1</i>	9	8	0	0	17	0	0	0	0	0	#N/A
LASP1	<i>LIM and SH3 protein 1</i>	5	5	0	0	10	0	0	0	0	0	#N/A
CDC37	<i>cell division cycle 37</i>	3	2	0	0	5	0	0	0	0	0	#N/A
CSTF2T	<i>cleavage stimulation factor subunit 2 tau variant</i>	5	5	0	0	10	0	0	0	0	0	#N/A
MRPL16	<i>mitochondrial ribosomal protein L16</i>	0	0	0	0	0	0	0	0	0	0	#N/A
TBC1D8	<i>TBC1 domain family member 8</i>	0	3	0	0	3	0	0	0	0	0	#N/A
ATG3	<i>autophagy related 3</i>	5	6	0	0	11	0	0	0	0	0	#N/A
ANKRD28	<i>ankyrin repeat domain 28</i>	7	10	0	0	17	0	0	0	0	0	#N/A
RICTOR	<i>RPTOR independent companion of MTOR complex 2</i>	0	2	0	0	2	0	0	0	0	0	#N/A
PALLD	<i>palladin, cytoskeletal associated protein</i>	3	4	0	0	7	0	0	0	0	0	#N/A
BCR	<i>BCR activator of RhoGEF and GTPase</i>	3	0	2	3	8	0	0	0	0	0	#N/A
KIF21A	<i>kinesin family member 21A</i>	3	2	0	0	5	0	0	0	0	0	#N/A
DLAT	<i>dihydrolipoamide S-acetyltransferase</i>	0	0	0	0	0	0	0	0	0	0	#N/A
ANXA1	<i>annexin A1</i>	8	5	0	0	13	0	0	0	0	0	#N/A
KIF2C	<i>kinesin family member 2C</i>	4	2	0	0	6	0	0	0	0	0	#N/A
SNCA	<i>synuclein alpha</i>	0	5	0	0	5	0	0	0	0	0	#N/A
PGAM5	<i>PGAM family member 5, mitochondrial serine/threonine protein phosphatase</i>	4	6	0	0	10	0	0	0	0	0	#N/A
NUFIP2	<i>nuclear FMR1 interacting protein 2</i>	35	37	5	4	81	0	0	0	0	0	#N/A
ERCC6L	<i>ERCC excision repair 6 like, spindle assembly checkpoint</i>	2	2	0	0	4	0	0	0	0	0	#N/A

<i>helicase</i>												
FYTTD1	<i>forty-two-three domain containing 1</i>	0	0	0	0	0	0	0	0	0	0	#N/A
EIF5A	<i>eukaryotic translation initiation factor 5A</i>	12	14	0	0	26	0	0	0	0	0	#N/A
TSN	<i>translin</i>	2	5	0	0	7	0	0	0	0	0	#N/A
CDC20	<i>cell division cycle 20</i>	0	0	0	0	0	0	0	0	0	0	#N/A
ANKRD52	<i>ankyrin repeat domain 52</i>	0	5	0	0	5	0	0	0	0	0	#N/A
NCK1	<i>NCK adaptor protein 1</i>	2	2	0	0	4	0	0	0	0	0	#N/A
TRIM26	<i>tripartite motif containing 26</i>	0	0	0	0	0	0	0	0	0	0	#N/A
CCDC124	<i>coiled-coil domain containing 124</i>	2	2	0	0	4	0	0	0	0	0	#N/A
ERH	<i>ERH mRNA splicing and mitosis factor</i>	4	2	0	0	6	0	0	0	0	0	#N/A
NAE1	<i>NEDD8 activating enzyme E1 subunit 1</i>	0	3	0	0	3	0	0	0	0	0	#N/A
FIBP	<i>FGF1 intracellular binding protein</i>	0	0	5	0	5	0	0	0	0	0	#N/A
RPS21	<i>ribosomal protein S21</i>	3	0	3	0	6	0	0	0	0	0	#N/A
DDX24	<i>DEAD-box helicase 24</i>	0	0	0	0	0	0	0	0	0	0	#N/A
PTPN23	<i>protein tyrosine phosphatase non-receptor type 23</i>	3	7	0	0	10	0	0	0	0	0	#N/A
FAM101B	<i>refilin B</i>	13	17	7	7	44	0	0	0	0	0	#N/A
C20orf4	<i>AAR2 splicing factor</i>	0	6	0	0	6	0	0	0	0	0	#N/A
DNAJB1	<i>DnaJ heat shock protein family (Hsp40) member B1</i>	7	11	0	0	18	0	0	0	0	0	#N/A
FMR1	<i>fragile X mental retardation 1</i>	5	0	0	0	5	0	0	0	0	0	#N/A
ADAR	<i>adenosine deaminase RNA specific</i>	10	15	0	0	25	0	0	0	0	0	#N/A
MAP2K2	<i>mitogen-activated protein kinase kinase 2</i>	0	0	0	0	0	0	0	0	0	0	#N/A
TBK1	<i>TANK binding kinase 1</i>	2	9	0	0	11	0	0	0	0	0	#N/A
RPS23	<i>ribosomal protein S23</i>	6	5	0	0	11	0	0	0	0	0	#N/A
DNM2	<i>dynamain 2</i>	0	0	0	0	0	0	0	0	0	0	#N/A
CDK2	<i>cyclin dependent kinase 2</i>	9	18	0	0	27	0	0	0	0	0	#N/A
PSMC2	<i>proteasome 26S subunit, ATPase 2</i>	19	21	0	0	40	0	0	0	0	0	#N/A
SKP1	<i>S-phase kinase associated protein 1</i>	5	9	0	0	14	0	0	0	0	0	#N/A
TUBGCP3	<i>tubulin gamma complex associated protein 3</i>	0	3	0	0	3	0	0	0	0	0	#N/A

SLC25A17	<i>solute carrier family 25 member 17</i>	0	0	0	0	0	0	0	0	0	0	#N/A
VRK1	<i>VRK serine/threonine kinase 1</i>	0	0	0	0	0	0	0	0	0	0	#N/A
NOC3L	<i>NOC3 like DNA replication regulator</i>	0	0	0	0	0	0	0	0	0	0	#N/A
PIGU	<i>phosphatidylinositol glycan anchor biosynthesis class U</i>	0	0	0	0	0	0	0	0	0	0	#N/A
GTPBP4	<i>GTP binding protein 4</i>	6	10	0	0	16	0	0	0	0	0	#N/A
GTF2I	<i>general transcription factor Iii</i>	26	25	0	2	53	0	0	0	0	0	#N/A
TNPO3	<i>transportin 3</i>	3	2	0	0	5	0	0	0	0	0	#N/A
NOP56	<i>NOP56 ribonucleoprotein</i>	14	12	0	0	26	0	0	0	0	0	#N/A
RCC1	<i>regulator of chromosome condensation 1</i>	6	3	0	0	9	0	0	0	0	0	#N/A
BCAS2	<i>BCAS2 pre-mRNA processing factor</i>	10	14	0	0	24	0	0	0	0	0	#N/A
PACS1	<i>phosphofurin acidic cluster sorting protein 1</i>	0	0	0	0	0	0	0	0	0	0	#N/A
PSMD2	<i>proteasome 26S subunit, non-ATPase 2</i>	20	23	0	0	43	0	0	0	0	0	#N/A
UBAP2L	<i>ubiquitin associated protein 2 like</i>	37	49	0	4	90	0	0	0	0	0	#N/A
HNRNPAB	<i>heterogeneous nuclear ribonucleoprotein A/B</i>	10	11	0	0	21	0	0	0	0	0	#N/A
FASTKD2	<i>FAST kinase domains 2</i>	0	0	0	0	0	0	0	0	0	0	#N/A
LSM12	<i>LSM12 homolog</i>	7	4	0	0	11	0	0	0	0	0	#N/A
SF3B2	<i>splicing factor 3b subunit 2</i>	37	45	0	0	82	0	0	0	0	0	#N/A
IDH3B	<i>isocitrate dehydrogenase (NAD(+)) 3 beta</i>	0	0	0	0	0	0	0	0	0	0	#N/A
UGDH	<i>UDP-glucose 6-dehydrogenase</i>	0	0	0	0	0	0	0	0	0	0	#N/A
PFN1	<i>profilin 1</i>	6	6	0	0	12	0	0	0	0	0	#N/A
RBMXL1	<i>RBMX like 1</i>	8	5	0	0	13	0	0	0	0	0	#N/A
CTPS2	<i>CTP synthase 2</i>	0	0	0	0	0	0	0	0	0	0	#N/A
DDX19A	<i>DEAD-box helicase 19A</i>	0	0	0	0	0	0	0	0	0	0	#N/A
CHD3	<i>chromodomain helicase DNA binding protein 3</i>	16	13	0	0	29	0	0	0	0	0	#N/A
ACTB	<i>actin beta</i>	0	0	0	0	0	0	0	0	0	0	#N/A
TXNDC9	<i>thioredoxin domain containing 9</i>	0	0	0	0	0	0	0	0	0	0	#N/A
FAM129B	<i>niban apoptosis regulator 2</i>	20	20	0	0	40	0	0	0	0	0	#N/A

RRM2	<i>ribonucleotide reductase regulatory subunit M2</i>	0	0	0	0	0	0	0	0	0	0	#N/A
TUBB2A	<i>tubulin beta 2A class IIa</i>	0	0	0	0	0	0	0	0	0	0	#N/A
TIMM23B	<i>translocase of inner mitochondrial membrane 23 homolog B</i>	0	3	0	0	3	0	0	0	0	0	#N/A
THOC2	<i>THO complex 2</i>	23	18	0	0	41	0	0	0	0	0	#N/A
COMMD8	<i>COMM domain containing 8</i>	4	3	0	0	7	0	0	0	0	0	#N/A
SEC31A	<i>SEC31 homolog A, COPII coat complex component</i>	0	0	0	0	0	0	0	0	0	0	#N/A
ARPC4	<i>actin related protein 2/3 complex subunit 4</i>	0	4	0	0	4	0	0	0	0	0	#N/A
HAUS3	<i>HAUS augmin like complex subunit 3</i>	0	0	0	0	0	0	0	0	0	0	#N/A
RASGEF1B	<i>RasGEF domain family member 1B</i>	0	0	0	0	0	0	0	0	0	0	#N/A
CAST	<i>calpastatin</i>	9	8	0	0	17	0	0	0	0	0	#N/A
PFDN6	<i>prefoldin subunit 6</i>	0	4	0	0	4	0	0	0	0	0	#N/A
SMAP1	<i>small ArfGAP 1</i>	8	5	0	0	13	0	0	0	0	0	#N/A
SYNJ1	<i>synaptojanin 1</i>	0	2	0	0	2	0	0	0	0	0	#N/A
TFB2M	<i>transcription factor B2, mitochondrial</i>	0	0	0	0	0	0	0	0	0	0	#N/A
CSRP1	<i>cysteine and glycine rich protein 1</i>	4	4	0	0	8	0	0	0	0	0	#N/A
SF1	<i>splicing factor 1</i>	15	24	0	0	39	0	0	0	0	0	#N/A
ZC3H11A	<i>zinc finger CCCH-type containing 11A</i>	14	16	0	0	30	0	0	0	0	0	#N/A
TMEM126A	<i>transmembrane protein 126A</i>	0	0	0	0	0	0	0	0	0	0	#N/A
ARFGAP2	<i>ADP ribosylation factor GTPase activating protein 2</i>	2	3	0	0	5	0	0	0	0	0	#N/A
TPD52	<i>tumor protein D52</i>	4	9	0	0	13	0	0	0	0	0	#N/A
DDX52	<i>DEXD-box helicase 52</i>	0	0	0	0	0	0	0	0	0	0	#N/A
TTC27	<i>tetratricopeptide repeat domain 27</i>	0	0	0	0	0	0	0	0	0	0	#N/A
MAPT	<i>microtubule associated protein tau</i>	0	5	0	0	5	0	0	0	0	0	#N/A
KIAA1033	<i>WASH complex subunit 4</i>	4	5	2	4	15	0	0	0	0	0	#N/A
SMARCD2	<i>SWI/SNF related, matrix associated, actin dependent regulator of chromatin, subfamily</i>	0	0	0	0	0	0	0	0	0	0	#N/A

d, member 2

NCAPD2	<i>non-SMC condensin I complex subunit D2</i>	0	0	0	0	0	0	0	0	0	0	#N/A
IKBKKG	<i>inhibitor of nuclear factor kappa B kinase regulatory subunit gamma</i>	0	0	0	0	0	0	0	0	0	0	#N/A
IPO11	<i>importin 11</i>	0	0	0	0	0	0	0	0	0	0	#N/A
RYR2	<i>ryanodine receptor 2</i>	0	0	0	0	0	0	0	0	0	0	#N/A
C9orf86	<i>RAB, member RAS oncogene family like 6</i>	0	7	0	0	7	0	0	0	0	0	#N/A
RAPGEF6	<i>Rap guanine nucleotide exchange factor 6</i>	5	6	0	0	11	0	0	0	0	0	#N/A
RBM3	<i>RNA binding motif protein 3</i>	7	6	0	0	13	0	0	0	0	0	#N/A
ITGA4	<i>integrin subunit alpha 4</i>	0	0	0	0	0	0	0	0	0	0	#N/A
ALMS1	<i>ALMS1 centrosome and basal body associated protein</i>	0	2	0	0	2	0	0	0	0	0	#N/A
SPAG5	<i>sperm associated antigen 5</i>	0	7	0	0	7	0	0	0	0	0	#N/A
KIF22	<i>kinesin family member 22</i>	0	0	0	0	0	0	0	0	0	0	#N/A
HEATR1	<i>HEAT repeat containing 1</i>	5	10	0	0	15	0	0	0	0	0	#N/A
MED23	<i>mediator complex subunit 23</i>	0	0	0	0	0	0	0	0	0	0	#N/A
COG7	<i>component of oligomeric golgi complex 7</i>	0	0	0	0	0	0	0	0	0	0	#N/A
PAIP1	<i>poly(A) binding protein interacting protein 1</i>	0	3	0	0	3	0	0	0	0	0	#N/A
KDM3A	<i>lysine demethylase 3A</i>	0	6	0	0	6	0	0	0	0	0	#N/A
NDRG1	<i>N-myc downstream regulated 1</i>	6	4	0	0	10	0	0	0	0	0	#N/A
PYCRL	<i>pyrroline-5-carboxylate reductase 3</i>	0	0	0	3	3	0	0	0	0	0	#N/A
NEK9	<i>NIMA related kinase 9</i>	9	5	0	0	14	0	0	0	0	0	#N/A
RELA	<i>RELA proto-oncogene, NF-kB subunit</i>	3	3	0	0	6	0	0	0	0	0	#N/A
MRPS11	<i>mitochondrial ribosomal protein S11</i>	0	0	0	0	0	0	0	0	0	0	#N/A
MAGEA1	<i>MAGE family member A1</i>	4	3	0	0	7	0	0	0	0	0	#N/A
ZNF207	<i>zinc finger protein 207</i>	3	5	0	0	8	0	0	0	0	0	#N/A
TUBGCP4	<i>tubulin gamma complex associated protein 4</i>	0	0	0	0	0	0	0	0	0	0	#N/A
EIF2C2	<i>argonaute RISC catalytic component 2</i>	7	8	0	0	15	0	0	0	0	0	#N/A

EIF3L	<i>eukaryotic translation initiation factor 3 subunit L</i>	4	5	0	0	9	0	0	0	0	0	#N/A
PYCR2	<i>pyrroline-5-carboxylate reductase 2</i>	0	0	0	0	0	0	0	0	0	0	#N/A
KIF23	<i>kinesin family member 23</i>	8	9	0	0	17	0	0	0	0	0	#N/A
WWC1	<i>WW and C2 domain containing 1</i>	0	2	0	0	2	0	0	0	0	0	#N/A
ATXN10	<i>ataxin 10</i>	0	0	0	0	0	0	0	0	0	0	#N/A
XPO7	<i>exportin 7</i>	0	0	0	0	0	0	0	0	0	0	#N/A
TMEM111	<i>ER membrane protein complex subunit 3</i>	0	0	0	0	0	0	0	0	0	0	#N/A
LARS2	<i>leucyl-tRNA synthetase 2, mitochondrial</i>	0	0	0	0	0	0	0	0	0	0	#N/A
PDHA1	<i>pyruvate dehydrogenase E1 alpha 1 subunit</i>	0	0	0	0	0	0	0	0	0	0	#N/A
GTPBP1	<i>GTP binding protein 1</i>	0	0	0	0	0	0	0	0	0	0	#N/A
EXOSC7	<i>exosome component 7</i>	6	5	0	0	11	0	0	0	0	0	#N/A
GCC1	<i>GRIP and coiled-coil domain containing 1</i>	0	0	0	0	0	0	0	0	0	0	#N/A
ZW10	<i>zw10 kinetochore protein</i>	2	0	0	0	2	0	0	0	0	0	#N/A
KANK4	<i>KN motif and ankyrin repeat domains 4</i>	0	0	0	0	0	0	0	0	0	0	#N/A
EIF3H	<i>eukaryotic translation initiation factor 3 subunit H</i>	2	3	0	0	5	0	0	0	0	0	#N/A
RPA1	<i>replication protein A1</i>	13	16	0	0	29	0	0	0	0	0	#N/A
BZW2	<i>basic leucine zipper and W2 domains 2</i>	0	0	0	0	0	0	0	0	0	0	#N/A
CNOT3	<i>CCR4-NOT transcription complex subunit 3</i>	0	0	0	0	0	0	0	0	0	0	#N/A
RIPK2	<i>receptor interacting serine/threonine kinase 2</i>	3	9	0	0	12	0	0	0	0	0	#N/A
STIP1	<i>stress induced phosphoprotein 1</i>	3	4	0	0	7	0	0	0	0	0	#N/A
XRCC5	<i>X-ray repair cross complementing 5</i>	17	18	0	0	35	0	0	0	0	0	#N/A
SNRNP200	<i>small nuclear ribonucleoprotein U5 subunit 200</i>	76	97	0	0	173	0	0	0	0	0	#N/A
PRKAA1	<i>protein kinase AMP-activated catalytic subunit alpha 1</i>	3	0	0	0	3	0	0	0	0	0	#N/A
MEPCE	<i>methylphosphate capping enzyme</i>	0	4	0	0	4	0	0	0	0	0	#N/A
SNRPD2	<i>small nuclear ribonucleoprotein D2 polypeptide</i>	8	8	0	0	16	0	0	0	0	0	#N/A

HAUS8	<i>HAUS augmin like complex subunit 8</i>	4	5	0	0	9	0	0	0	0	0	#N/A
VPS4B	<i>vacuolar protein sorting 4 homolog B</i>	0	0	0	0	0	0	0	0	0	0	#N/A
CCDC6	<i>coiled-coil domain containing 6</i>	4	2	0	0	6	0	0	0	0	0	#N/A
EXOC3	<i>exocyst complex component 3</i>	0	0	0	0	0	0	0	0	0	0	#N/A
TFEC	<i>transcription factor EC</i>	0	0	0	0	0	0	0	0	0	0	#N/A
DDX26B	<i>integrator complex subunit 6 like</i>	0	0	0	0	0	0	0	0	0	0	#N/A
PSMD13	<i>proteasome 26S subunit, non-ATPase 13</i>	0	0	0	0	0	0	0	0	0	0	#N/A
TBCB	<i>tubulin folding cofactor B</i>	0	0	0	0	0	0	0	0	0	0	#N/A
USP7	<i>ubiquitin specific peptidase 7</i>	13	7	0	0	20	0	0	0	0	0	#N/A
SPTBN5	<i>spectrin beta, non-erythrocytic 5</i>	0	0	0	0	0	0	0	0	0	0	#N/A
MYCBP2	<i>MYC binding protein 2</i>	0	0	0	0	0	0	0	0	0	0	#N/A
WNK1	<i>WNK lysine deficient protein kinase 1</i>	2	2	2	0	6	0	0	0	0	0	#N/A
AURKB	<i>aurora kinase B</i>	0	0	0	0	0	0	0	0	0	0	#N/A
USP8	<i>ubiquitin specific peptidase 8</i>	4	7	0	0	11	0	0	0	0	0	#N/A
ATF7IP2	<i>activating transcription factor 7 interacting protein 2</i>	0	0	0	0	0	0	0	0	0	0	#N/A
SAP18	<i>Sin3A associated protein 18</i>	8	7	0	0	15	0	0	0	0	0	#N/A
ARHGEF18	<i>Rho/Rac guanine nucleotide exchange factor 18</i>	0	0	0	0	0	0	0	0	0	0	#N/A
PELI2	<i>pellino E3 ubiquitin protein ligase family member 2</i>	0	0	0	0	0	0	0	0	0	0	#N/A
INPPL1	<i>inositol polyphosphate phosphatase like 1</i>	0	2	0	0	2	0	0	0	0	0	#N/A
LPP	<i>LIM domain containing preferred translocation partner in lipoma</i>	0	0	0	0	0	0	0	0	0	0	#N/A
EIF2B2	<i>eukaryotic translation initiation factor 2B subunit beta</i>	0	0	0	0	0	0	0	0	0	0	#N/A
STAU2	<i>staufen double-stranded RNA binding protein 2</i>	0	0	0	0	0	0	0	0	0	0	#N/A
TJP2	<i>tight junction protein 2</i>	2	2	0	0	4	0	0	0	0	0	#N/A
BAIAP2	<i>BAI1 associated protein 2</i>	0	0	2	0	2	0	0	0	0	0	#N/A
CDKN2A	<i>cyclin dependent kinase inhibitor 2A</i>	0	0	0	0	0	0	0	0	0	0	#N/A
GNL2	<i>G protein nucleolar 2</i>	17	17	0	0	34	0	0	0	0	0	#N/A

NT5C2	<i>5'-nucleotidase, cytosolic II</i>	0	0	0	0	0	0	0	0	0	0	#N/A
WDR77	<i>WD repeat domain 77</i>	3	4	0	0	7	0	0	0	0	0	#N/A
OCRL	<i>OCRL inositol polyphosphate-5-phosphatase</i>	2	0	0	0	2	0	0	0	0	0	#N/A
BICD2	<i>BICD cargo adaptor 2</i>	0	2	0	0	2	0	0	0	0	0	#N/A
CPSF2	<i>cleavage and polyadenylation specific factor 2</i>	6	8	0	0	14	0	0	0	0	0	#N/A
DNAJC21	<i>DnaJ heat shock protein family (Hsp40) member C21</i>	0	0	0	0	0	0	0	0	0	0	#N/A
LRRC40	<i>leucine rich repeat containing 40</i>	0	0	0	0	0	0	0	0	0	0	#N/A
PDE8A	<i>phosphodiesterase 8A</i>	0	0	0	0	0	0	0	0	0	0	#N/A
CEP350	<i>centrosomal protein 350</i>	0	0	0	0	0	0	0	0	0	0	#N/A
COMMD4	<i>COMM domain containing 4</i>	2	3	0	0	5	0	0	0	0	0	#N/A
SMG9	<i>SMG9 nonsense mediated mRNA decay factor</i>	0	5	0	0	5	0	0	0	0	0	#N/A
HSPA12B	<i>heat shock protein family A (Hsp70) member 12B</i>	0	0	0	0	0	0	0	0	0	0	#N/A
KBTBD6	<i>kelch repeat and BTB domain containing 6</i>	0	0	0	0	0	0	0	0	0	0	#N/A
PRDX5	<i>peroxiredoxin 5</i>	0	0	0	0	0	0	0	0	0	0	#N/A
ADD3	<i>adducin 3</i>	0	4	0	0	4	0	0	0	0	0	#N/A
MPDZ	<i>multiple PDZ domain crumbs cell polarity complex component</i>	0	0	0	0	0	0	0	0	0	0	#N/A
PCDH11Y	<i>protocadherin 11 Y-linked</i>	0	0	0	0	0	0	0	0	0	0	#N/A
BCLAF1	<i>BCL2 associated transcription factor 1</i>	9	8	0	0	17	0	0	0	0	0	#N/A
TBCE	<i>tubulin folding cofactor E</i>	0	0	0	0	0	0	0	0	0	0	#N/A
TAB1	<i>TGF-beta activated kinase 1 (MAP3K7) binding protein 1</i>	2	3	0	0	5	0	0	0	0	0	#N/A
PAK3	<i>p21 (RAC1) activated kinase 3</i>	0	0	0	0	0	0	0	0	0	0	#N/A
PM20D2	<i>peptidase M20 domain containing 2</i>	0	0	0	0	0	0	0	0	0	0	#N/A
IKBKAP	<i>elongator complex protein 1</i>	0	4	0	0	4	0	0	0	0	0	#N/A
EHD4	<i>EH domain containing 4</i>	0	0	0	0	0	0	0	0	0	0	#N/A
OXSRI	<i>oxidative stress responsive kinase 1</i>	0	0	0	0	0	0	0	0	0	0	#N/A
EHD1	<i>EH domain containing 1</i>	0	0	0	0	0	0	0	0	0	0	#N/A
EPT1	<i>selenoprotein 1</i>	0	0	0	0	0	0	0	0	0	0	#N/A

PNN	<i>pinin, desmosome associated protein</i>	30	23	0	0	53	0	0	0	0	0	#N/A
UBE2N	<i>ubiquitin conjugating enzyme E2 N</i>	0	0	0	0	0	0	0	0	0	0	#N/A
TNIP1	<i>TNFAIP3 interacting protein 1</i>	0	0	0	0	0	0	0	0	0	0	#N/A
CPSF3	<i>cleavage and polyadenylation specific factor 3</i>	0	3	0	0	3	0	0	0	0	0	#N/A
MOB3B	<i>MOB kinase activator 3B</i>	3	0	0	0	3	0	0	0	0	0	#N/A
TRMT112	<i>tRNA methyltransferase subunit 11-2</i>	0	0	0	0	0	0	0	0	0	0	#N/A
NME1	<i>NME/NM23 nucleoside diphosphate kinase 1</i>	0	4	0	0	4	0	0	0	0	0	#N/A
ALDH3A2	<i>aldehyde dehydrogenase 3 family member A2</i>	9	4	9	5	27	0	0	0	0	0	#N/A
PAPSS2	<i>3'-phosphoadenosine 5'-phosphosulfate synthase 2</i>	0	0	0	0	0	0	0	0	0	0	#N/A
PGAM1	<i>phosphoglycerate mutase 1</i>	2	4	0	0	6	0	0	0	0	0	#N/A
SEC23B	<i>SEC23 homolog B, coat complex II component</i>	0	0	0	0	0	0	0	0	0	0	#N/A
DIP2A	<i>disco interacting protein 2 homolog A</i>	0	0	0	0	0	0	0	0	0	0	#N/A
RFC4	<i>replication factor C subunit 4</i>	7	13	0	0	20	0	0	0	0	0	#N/A
MRPS22	<i>mitochondrial ribosomal protein S22</i>	0	0	0	0	0	0	0	0	0	0	#N/A
TRAM1	<i>translocation associated membrane protein 1</i>	0	0	0	0	0	0	0	0	0	0	#N/A
HEATR5A	<i>HEAT repeat containing 5A</i>	0	4	0	0	4	0	0	0	0	0	#N/A
POLD1	<i>DNA polymerase delta 1, catalytic subunit</i>	3	2	0	0	5	0	0	0	0	0	#N/A
IBTK	<i>inhibitor of Bruton tyrosine kinase</i>	0	0	0	0	0	0	0	0	0	0	#N/A
SLC27A4	<i>solute carrier family 27 member 4</i>	0	0	0	0	0	0	0	0	0	0	#N/A
RQCD1	<i>CCR4-NOT transcription complex subunit 9</i>	0	0	0	0	0	0	0	0	0	0	#N/A
ARFIP1	<i>ADP ribosylation factor interacting protein 1</i>	0	0	0	0	0	0	0	0	0	0	#N/A
STARD7	<i>StAR related lipid transfer domain containing 7</i>	0	0	0	0	0	0	0	0	0	0	#N/A
CAMSAP2	<i>calmodulin regulated spectrin associated protein family member 2</i>	5	0	0	0	5	0	0	0	0	0	#N/A
UBE3C	<i>ubiquitin protein ligase E3C</i>	0	0	0	0	0	0	0	0	0	0	#N/A
DYNC1LI	<i>dynein cytoplasmic 1 light intermediate chain 1</i>	0	0	0	0	0	0	0	0	0	0	#N/A

1												
CDC27	<i>cell division cycle 27</i>	9	13	0	0	22	0	0	0	0	0	#N/A
PKN2	<i>protein kinase N2</i>	0	0	0	0	0	0	0	0	0	0	#N/A
POLR2A	<i>RNA polymerase II subunit A</i>	0	4	0	0	4	0	0	0	0	0	#N/A
SCYL3	<i>SCY1 like pseudokinase 3</i>	0	0	7	0	7	0	0	0	0	0	#N/A
ARMC5	<i>armadillo repeat containing 5</i>	0	0	0	0	0	0	0	0	0	0	#N/A
PXN	<i>paxillin</i>	0	3	0	0	3	0	0	0	0	0	#N/A
SERPINE	<i>serpin family E member 2</i>	0	0	0	0	0	0	0	0	0	0	#N/A
2												
SBNO1	<i>strawberry notch homolog 1</i>	13	13	0	0	26	0	0	0	0	0	#N/A
PPP2R5C	<i>protein phosphatase 2 regulatory subunit B'gamma</i>	0	0	0	0	0	0	0	0	0	0	#N/A
AARS	<i>alanyl-tRNA synthetase</i>	0	7	0	0	7	0	0	0	0	0	#N/A
DARS2	<i>aspartyl-tRNA synthetase 2, mitochondrial</i>	0	0	0	0	0	0	0	0	0	0	#N/A
USP24	<i>ubiquitin specific peptidase 24</i>	0	3	0	0	3	0	0	0	0	0	#N/A
POLR2E	<i>RNA polymerase II subunit E</i>	0	0	0	0	0	0	0	0	0	0	#N/A
C14orf133	<i>VPS33B interacting protein, apical-basolateral polarity regulator, spe-39 homolog</i>	0	0	0	0	0	0	0	0	0	0	#N/A
LPCAT1	<i>lysophosphatidylcholine acyltransferase 1</i>	0	0	0	0	0	0	0	0	0	0	#N/A
ILK	<i>integrin linked kinase</i>	0	0	0	0	0	0	0	0	0	0	#N/A
PPIP5K2	<i>diphosphoinositol pentakisphosphate kinase 2</i>	0	0	0	0	0	0	0	0	0	0	#N/A
ARHGAP	<i>Rho GTPase activating protein 17</i>	0	0	0	0	0	0	0	0	0	0	#N/A
17												
DDB1	<i>damage specific DNA binding protein 1</i>	0	0	0	0	0	0	0	0	0	0	#N/A
XAB2	<i>XPA binding protein 2</i>	18	31	0	0	49	0	0	0	0	0	#N/A
ARHGEF2	<i>Rho/Rac guanine nucleotide exchange factor 2</i>	0	0	0	0	0	0	0	0	0	0	#N/A
RRAGB	<i>Ras related GTP binding B</i>	0	0	0	0	0	0	0	0	0	0	#N/A
YAP1	<i>Yes associated protein 1</i>	5	8	0	0	13	0	0	0	0	0	#N/A
TOX4	<i>TOX high mobility group box family member 4</i>	30	42	0	0	72	0	0	0	0	0	#N/A
MGST1	<i>microsomal glutathione S-</i>	0	0	0	0	0	0	0	0	0	0	#N/A

<i>transferase 1</i>												
SIKE1	<i>suppressor of IKBKE 1</i>	0	0	0	0	0	0	0	0	0	0	#N/A
SPCS2	<i>signal peptidase complex subunit 2</i>	0	0	0	0	0	0	0	0	0	0	#N/A
NR3C1	<i>nuclear receptor subfamily 3 group C member 1</i>	5	8	0	0	13	0	0	0	0	0	#N/A
CLPX	<i>caseinolytic mitochondrial matrix peptidase chaperone subunit</i>	0	0	0	0	0	0	0	0	0	0	#N/A
NCAPG	<i>non-SMC condensin I complex subunit G</i>	22	26	0	0	48	0	0	0	0	0	#N/A
EIF2B1	<i>eukaryotic translation initiation factor 2B subunit alpha</i>	0	0	0	0	0	0	0	0	0	0	#N/A
RPL28	<i>ribosomal protein L28</i>	8	8	0	0	16	0	0	0	0	0	#N/A
DNAJA2	<i>DnaJ heat shock protein family (Hsp40) member A2</i>	0	0	0	0	0	0	0	0	0	0	#N/A
MAP2K1	<i>mitogen-activated protein kinase kinase 1</i>	0	0	0	0	0	0	0	0	0	0	#N/A
PSMC5	<i>proteasome 26S subunit, ATPase 5</i>	7	10	0	0	17	0	0	0	0	0	#N/A
GCLM	<i>glutamate-cysteine ligase modifier subunit</i>	0	0	0	0	0	0	0	0	0	0	#N/A
CBX3	<i>chromobox 3</i>	9	8	0	0	17	0	0	0	0	0	#N/A
MYBBP1A	<i>MYB binding protein 1a</i>	9	12	0	0	21	0	0	0	0	0	#N/A
GSK3B	<i>glycogen synthase kinase 3 beta</i>	0	0	0	0	0	0	0	0	0	0	#N/A
HNRPDL	<i>heterogeneous nuclear ribonucleoprotein D like</i>	6	8	0	0	14	0	0	0	0	0	#N/A
KPNA6	<i>karyopherin subunit alpha 6</i>	0	0	0	0	0	0	0	0	0	0	#N/A
UQCRCF1	<i>ubiquinol-cytochrome c reductase, Rieske iron-sulfur polypeptide 1</i>	0	0	0	0	0	0	0	0	0	0	#N/A
C12orf23	<i>transmembrane protein 263</i>	0	0	0	0	0	0	0	0	0	0	#N/A
CDC45	<i>cell division cycle 45</i>	0	0	0	0	0	0	0	0	0	0	#N/A
AIMP2	<i>aminoacyl tRNA synthetase complex interacting multifunctional protein 2</i>	0	0	0	0	0	0	0	0	0	0	#N/A
COX2	<i>mitochondrially encoded cytochrome c oxidase II</i>	0	0	0	0	0	0	0	0	0	0	#N/A
NUP188	<i>nucleoporin 188</i>	0	0	0	0	0	0	0	0	0	0	#N/A
MSH3	<i>mutS homolog 3</i>	0	0	0	0	0	0	0	0	0	0	#N/A
NEB	<i>nebulin</i>	0	0	0	0	0	0	0	0	0	0	#N/A

PSMD1	<i>proteasome 26S subunit, non-ATPase 1</i>	2	9	0	0	11	0	0	0	0	0	#N/A
KPNA5	<i>karyopherin subunit alpha 5</i>	0	0	0	0	0	0	0	0	0	0	#N/A
HK2	<i>hexokinase 2</i>	0	0	0	0	0	0	0	0	0	0	#N/A
EIF3I	<i>eukaryotic translation initiation factor 3 subunit I</i>	8	11	0	0	19	0	0	0	0	0	#N/A
SF3A2	<i>splicing factor 3a subunit 2</i>	0	3	0	0	3	0	0	0	0	0	#N/A
RPS6KA3	<i>ribosomal protein S6 kinase A3</i>	0	0	0	0	0	0	0	0	0	0	#N/A
MLH1	<i>mutL homolog 1</i>	5	7	0	0	12	0	0	0	0	0	#N/A
YTHDF2	<i>YTH N6-methyladenosine RNA binding protein 2</i>	0	2	0	0	2	0	0	0	0	0	#N/A
EIF3D	<i>eukaryotic translation initiation factor 3 subunit D</i>	2	6	0	0	8	0	0	0	0	0	#N/A
UBR4	<i>ubiquitin protein ligase E3 component n-recognin 4</i>	0	0	0	0	0	0	0	0	0	0	#N/A
EXOSC4	<i>exosome component 4</i>	8	7	0	0	15	0	0	0	0	0	#N/A
AFAP1	<i>actin filament associated protein 1</i>	0	0	0	0	0	0	0	0	0	0	#N/A
FBXL12	<i>F-box and leucine rich repeat protein 12</i>	0	0	0	0	0	0	0	0	0	0	#N/A
PSMC4	<i>proteasome 26S subunit, ATPase 4</i>	2	4	0	0	6	0	0	0	0	0	#N/A
FADS1	<i>fatty acid desaturase 1</i>	0	0	0	0	0	0	0	0	0	0	#N/A
DIMT1	<i>DIMT1 rRNA methyltransferase and ribosome maturation factor</i>	0	0	0	0	0	0	0	0	0	0	#N/A
PRPF8	<i>pre-mRNA processing factor 8</i>	64	67	0	0	131	0	0	0	0	0	#N/A
SENP3	<i>SUMO specific peptidase 3</i>	0	0	0	0	0	0	0	0	0	0	#N/A
DSTN	<i>destrin, actin depolymerizing factor</i>	0	0	0	0	0	0	0	0	0	0	#N/A
PCNA	<i>proliferating cell nuclear antigen</i>	0	0	0	0	0	0	0	0	0	0	#N/A
NPEPPS	<i>aminopeptidase puromycin sensitive</i>	0	0	0	0	0	0	0	0	0	0	#N/A
PRKAG1	<i>protein kinase AMP-activated non-catalytic subunit gamma 1</i>	0	4	0	0	4	0	0	0	0	0	#N/A
DDX23	<i>DEAD-box helicase 23</i>	13	14	0	0	27	0	0	0	0	0	#N/A
HDAC2	<i>histone deacetylase 2</i>	39	28	0	0	67	0	0	0	0	0	#N/A
CDC123	<i>cell division cycle 123</i>	3	5	0	0	8	0	0	0	0	0	#N/A
CDIPT	<i>CDP-diacylglycerol--inositol 3-phosphatidyltransferase</i>	0	0	0	0	0	0	0	0	0	0	#N/A
ALDH1B1	<i>aldehyde dehydrogenase 1 family</i>	0	0	0	0	0	0	0	0	0	0	#N/A

<i>member B1</i>												
TWF2	<i>twinfilin actin binding protein 2</i>	0	3	0	0	3	0	0	0	0	0	#N/A
TTN	<i>titin</i>	0	0	0	3	3	0	0	0	0	0	#N/A
AIMP1	<i>aminoacyl tRNA synthetase complex interacting multifunctional protein 1</i>	5	6	0	0	11	0	0	0	0	0	#N/A
RFC2	<i>replication factor C subunit 2</i>	0	3	0	0	3	0	0	0	0	0	#N/A
TRNT1	<i>tRNA nucleotidyl transferase 1</i>	0	0	0	0	0	0	0	0	0	0	#N/A
FUBP3	<i>far upstream element binding protein 3</i>	0	0	0	0	0	0	0	0	0	0	#N/A
ASNS	<i>asparagine synthetase (glutamine-hydrolyzing)</i>	0	5	0	0	5	0	0	0	0	0	#N/A
SAR1A	<i>secretion associated Ras related GTPase 1A</i>	0	0	0	0	0	0	0	0	0	0	#N/A
SAFB2	<i>scaffold attachment factor B2</i>	10	19	0	0	29	0	0	0	0	0	#N/A
FEN1	<i>flap structure-specific endonuclease 1</i>	18	21	0	0	39	0	0	0	0	0	#N/A
NDUFS3	<i>NADH:ubiquinone oxidoreductase core subunit S3</i>	0	0	0	0	0	0	0	0	0	0	#N/A
MAP7	<i>microtubule associated protein 7</i>	10	6	0	0	16	0	0	0	0	0	#N/A
PLEKHA2	<i>pleckstrin homology domain containing A2</i>	0	0	0	0	0	0	0	0	0	0	#N/A
QARS	<i>glutamyl-tRNA synthetase</i>	0	8	0	0	8	0	0	0	0	0	#N/A
MRPS5	<i>mitochondrial ribosomal protein S5</i>	0	0	0	0	0	0	0	0	0	0	#N/A
BUB3	<i>BUB3 mitotic checkpoint protein</i>	3	5	0	0	8	0	0	0	0	0	#N/A
COPE	<i>coatamer protein complex subunit epsilon</i>	0	0	0	0	0	0	0	0	0	0	#N/A
CENPM	<i>centromere protein M</i>	0	0	0	0	0	0	0	0	0	0	#N/A
UBE2I	<i>ubiquitin conjugating enzyme E2 I</i>	0	0	0	0	0	0	0	0	0	0	#N/A
FAR1	<i>fatty acyl-CoA reductase 1</i>	0	0	0	0	0	0	0	0	0	0	#N/A
RPL32	<i>ribosomal protein L32</i>	4	5	0	0	9	0	0	0	0	0	#N/A
DRG1	<i>developmentally regulated GTP binding protein 1</i>	22	21	8	2	53	0	0	0	0	0	#N/A
RPS20	<i>ribosomal protein S20</i>	0	4	3	2	9	0	0	0	0	0	#N/A
RBM15	<i>RNA binding motif protein 15</i>	0	0	0	0	0	0	0	0	0	0	#N/A
CPSF6	<i>cleavage and polyadenylation specific factor 6</i>	14	16	0	0	30	0	0	0	0	0	#N/A

AFG3L2	<i>AFG3 like matrix AAA peptidase subunit 2</i>	0	0	0	0	0	0	0	0	0	0	#N/A
PUS1	<i>pseudouridine synthase 1</i>	0	0	0	0	0	0	0	0	0	0	#N/A
PLRG1	<i>pleiotropic regulator 1</i>	0	0	0	0	0	0	0	0	0	0	#N/A
LMNB2	<i>lamin B2</i>	0	0	0	0	0	0	0	0	0	0	#N/A
UBLCP1	<i>ubiquitin like domain containing CTD phosphatase 1</i>	0	0	0	0	0	0	0	0	0	0	#N/A
ABCC3	<i>ATP binding cassette subfamily C member 3</i>	0	6	0	0	6	0	0	0	0	0	#N/A
RAP1B	<i>RAP1B, member of RAS oncogene family</i>	0	0	0	0	0	0	0	0	0	0	#N/A
EEF1A2	<i>eukaryotic translation elongation factor 1 alpha 2</i>	19	63	0	0	82	0	0	0	0	0	#N/A
HCFC1	<i>host cell factor C1</i>	50	64	0	0	114	0	0	0	0	0	#N/A
H1FX	<i>H1 histone family member X</i>	2	3	0	0	5	0	0	0	0	0	#N/A
SNRNP70	<i>small nuclear ribonucleoprotein U1 subunit 70</i>	9	5	0	0	14	0	0	0	0	0	#N/A
NUP85	<i>nucleoporin 85</i>	0	5	0	0	5	0	0	0	0	0	#N/A
AKAP8L	<i>A-kinase anchoring protein 8 like</i>	0	9	0	0	9	0	0	0	0	0	#N/A
NMT1	<i>N-myristoyltransferase 1</i>	10	10	0	0	20	0	0	0	0	0	#N/A
SFXN3	<i>sideroflexin 3</i>	0	0	0	0	0	0	0	0	0	0	#N/A
DNAJC10	<i>DnaJ heat shock protein family (Hsp40) member C10</i>	0	0	0	0	0	0	0	0	0	0	#N/A
SLC25A1	<i>solute carrier family 25 member 1</i>	0	0	0	0	0	0	0	0	0	0	#N/A
GFPT1	<i>glutamine--fructose-6-phosphate transaminase 1</i>	5	6	0	0	11	0	0	0	0	0	#N/A
SMARCA1	<i>SWI/SNF related, matrix associated, actin dependent regulator of chromatin, subfamily a, member 1</i>	25	25	0	0	50	0	0	0	0	0	#N/A
HBS1L	<i>HBS1 like translational GTPase</i>	11	16	0	0	27	0	0	0	0	0	#N/A
RHEB	<i>Ras homolog, mTORC1 binding</i>	7	5	0	0	12	0	0	0	0	0	#N/A
DRG2	<i>developmentally regulated GTP binding protein 2</i>	4	8	0	0	12	0	0	0	0	0	#N/A
SNRPA1	<i>small nuclear ribonucleoprotein polypeptide A'</i>	17	19	0	0	36	0	0	0	0	0	#N/A
PDE3A	<i>phosphodiesterase 3A</i>	6	11	0	0	17	0	0	0	0	0	#N/A
LUC7L2	<i>LUC7 like 2, pre-mRNA splicing factor</i>	3	3	0	0	6	0	0	0	0	0	#N/A

SKIV2L2	<i>Mtr4 exosome RNA helicase</i>	10	9	0	0	19	0	0	0	0	0	#N/A
DUT	<i>deoxyuridine triphosphatase</i>	6	8	0	0	14	0	0	0	0	0	#N/A
DIS3	<i>DIS3 homolog, exosome endoribonuclease and 3'-5' exoribonuclease</i>	4	0	0	0	4	0	0	0	0	0	#N/A
MSH2	<i>mutS homolog 2</i>	9	7	0	0	16	0	0	0	0	0	#N/A
RPL10	<i>ribosomal protein L10</i>	7	7	0	0	14	0	0	0	0	0	#N/A
GLUD1	<i>glutamate dehydrogenase 1</i>	2	2	0	0	4	0	0	0	0	0	#N/A
C22orf28	<i>RNA 2',3'-cyclic phosphate and 5'-OH ligase</i>	11	19	5	0	35	0	0	0	0	0	#N/A
PSMC6	<i>proteasome 26S subunit, ATPase 6</i>	6	13	0	0	19	0	0	0	0	0	#N/A
RPL36	<i>ribosomal protein L36</i>	6	3	0	0	9	0	0	0	0	0	#N/A
PRPS2	<i>phosphoribosyl pyrophosphate synthetase 2</i>	0	0	0	0	0	0	0	0	0	0	#N/A
PSMC1	<i>proteasome 26S subunit, ATPase 1</i>	12	13	0	0	25	0	0	0	0	0	#N/A
MRTO4	<i>MRT4 homolog, ribosome maturation factor</i>	0	0	0	0	0	0	0	0	0	0	#N/A
PRKACB	<i>protein kinase cAMP-activated catalytic subunit beta</i>	0	0	0	0	0	0	0	0	0	0	#N/A
MAGED2	<i>MAGE family member D2</i>	0	7	0	0	7	0	0	0	0	0	#N/A
ZNF622	<i>zinc finger protein 622</i>	0	0	0	0	0	0	0	0	0	0	#N/A
TAF15	<i>TATA-box binding protein associated factor 15</i>	0	8	0	0	8	0	0	0	0	0	#N/A
ABCF2	<i>ATP binding cassette subfamily F member 2</i>	24	29	0	0	53	0	0	0	0	0	#N/A
G6PD	<i>glucose-6-phosphate dehydrogenase</i>	15	18	0	0	33	0	0	0	0	0	#N/A
YBX1	<i>Y-box binding protein 1</i>	13	11	0	0	24	0	0	0	0	0	#N/A
GRWD1	<i>glutamate rich WD repeat containing 1</i>	6	7	0	0	13	0	0	0	0	0	#N/A
DSP	<i>desmoplakin</i>	3	4	23	12	42	0	0	0	0	0	#N/A
SF3B1	<i>splicing factor 3b subunit 1</i>	79	86	0	0	165	0	0	0	0	0	#N/A
RPS5	<i>ribosomal protein S5</i>	0	0	0	0	0	0	0	0	0	0	#N/A
NUP160	<i>nucleoporin 160</i>	0	0	0	0	0	0	0	0	0	0	#N/A
BZW1	<i>basic leucine zipper and W2 domains 1</i>	4	5	0	0	9	0	0	0	0	0	#N/A
AP3S1	<i>adaptor related protein complex 3 subunit sigma 1</i>	0	0	0	0	0	0	0	0	0	0	#N/A

XPO1	<i>exportin 1</i>	4	10	0	0	14	0	0	0	0	0	#N/A
EIF2A	<i>eukaryotic translation initiation factor 2A</i>	24	24	0	0	48	0	0	0	0	0	#N/A
EIF2S1	<i>eukaryotic translation initiation factor 2 subunit alpha</i>	7	5	0	0	12	0	0	0	0	0	#N/A
EIF3G	<i>eukaryotic translation initiation factor 3 subunit G</i>	5	4	0	0	9	0	0	0	0	0	#N/A
DDX54	<i>DEAD-box helicase 54</i>	0	8	0	0	8	0	0	0	0	0	#N/A
CDC5L	<i>cell division cycle 5 like</i>	30	32	0	0	62	0	0	0	0	0	#N/A
EIF5B	<i>eukaryotic translation initiation factor 5B</i>	30	32	0	0	62	0	0	0	0	0	#N/A
TRIM25	<i>tripartite motif containing 25</i>	5	6	0	0	11	0	0	0	0	0	#N/A
EFTUD2	<i>elongation factor Tu GTP binding domain containing 2</i>	38	39	0	0	77	0	0	0	0	0	#N/A
HLTF	<i>helicase like transcription factor</i>	3	0	0	0	3	0	0	0	0	0	#N/A
LDHB	<i>lactate dehydrogenase B</i>	3	4	0	0	7	0	0	0	0	0	#N/A
KPNB1	<i>karyopherin subunit beta 1</i>	44	55	0	0	99	0	0	0	0	0	#N/A
EIF3F	<i>eukaryotic translation initiation factor 3 subunit F</i>	13	10	2	2	27	0	0	0	0	0	#N/A
NDUFA9	<i>NADH:ubiquinone oxidoreductase subunit A9</i>	3	3	0	0	6	0	0	0	0	0	#N/A
EWSR1	<i>EWS RNA binding protein 1</i>	14	18	0	0	32	0	0	0	0	0	#N/A
RBBP7	<i>RB binding protein 7, chromatin remodeling factor</i>	16	16	0	0	32	0	0	0	0	0	#N/A
PARP1	<i>poly(ADP-ribose) polymerase 1</i>	32	30	6	4	72	0	0	0	0	0	#N/A
USP10	<i>ubiquitin specific peptidase 10</i>	16	15	0	0	31	0	0	0	0	0	#N/A
PICALM	<i>phosphatidylinositol binding clathrin assembly protein</i>	4	4	0	0	8	0	0	0	0	0	#N/A
XRN2	<i>5'-3' exoribonuclease 2</i>	7	10	0	0	17	0	0	0	0	0	#N/A
DDX6	<i>DEAD-box helicase 6</i>	8	9	0	0	17	0	0	0	0	0	#N/A
PURA	<i>purine rich element binding protein A</i>	0	0	0	0	0	0	0	0	0	0	#N/A
IGF2BP1	<i>insulin like growth factor 2 mRNA binding protein 1</i>	0	3	0	0	3	0	0	0	0	0	#N/A
HSDL2	<i>hydroxysteroid dehydrogenase like 2</i>	0	4	0	0	4	0	0	0	0	0	#N/A
NDUFS1	<i>NADH:ubiquinone oxidoreductase core subunit S1</i>	0	0	0	0	0	0	0	0	0	0	#N/A
HADHB	<i>hydroxyacyl-CoA dehydrogenase</i>	0	0	0	0	0	0	0	0	0	0	#N/A

<i>trifunctional multienzyme complex</i>												
<i>subunit beta</i>												
HIST1H2AA	<i>histone cluster 1 H2A family member a</i>	0	0	0	0	0	0	0	0	0	0	#N/A
RUVBL1	<i>RuvB like AAA ATPase 1</i>	90	90	8	9	197	0	0	0	0	0	#N/A
RPL38	<i>ribosomal protein L38</i>	0	5	4	5	14	0	0	0	0	0	#N/A
ETF1	<i>eukaryotic translation termination factor 1</i>	14	14	0	0	28	0	0	0	0	0	#N/A
EIF3B	<i>eukaryotic translation initiation factor 3 subunit B</i>	21	17	0	0	38	0	0	0	0	0	#N/A
FTSJ3	<i>FtsJ RNA 2'-O-methyltransferase 3</i>	22	31	0	0	53	0	0	0	0	0	#N/A
NUP205	<i>nucleoporin 205</i>	0	0	0	0	0	0	0	0	0	0	#N/A
TIMM23	<i>translocase of inner mitochondrial membrane 23</i>	0	0	0	0	0	0	0	0	0	0	#N/A
PCID2	<i>PCI domain containing 2</i>	0	0	0	0	0	0	0	0	0	0	#N/A
NXF1	<i>nuclear RNA export factor 1</i>	0	0	0	0	0	0	0	0	0	0	#N/A
RPP30	<i>ribonuclease P/MRP subunit p30</i>	14	16	0	0	30	0	0	0	0	0	#N/A
MSH6	<i>mutS homolog 6</i>	13	25	0	0	38	0	0	0	0	0	#N/A
CHD4	<i>chromodomain helicase DNA binding protein 4</i>	95	99	0	0	194	0	0	0	0	0	#N/A
NCAPH	<i>non-SMC condensin I complex subunit H</i>	15	16	0	0	31	0	0	0	0	0	#N/A
CCT7	<i>chaperonin containing TCP1 subunit 7</i>	8	14	2	0	24	0	0	0	0	0	#N/A
TUBB3	<i>tubulin beta 3 class III</i>	0	0	0	0	0	0	0	0	0	0	#N/A
PPP2R1A	<i>protein phosphatase 2 scaffold subunit Aalpha</i>	0	5	4	0	9	0	0	0	0	0	#N/A
PELO	<i>pelota mRNA surveillance and ribosome rescue factor</i>	0	0	0	0	0	0	0	0	0	0	#N/A
NUP93	<i>nucleoporin 93</i>	0	6	0	0	6	0	0	0	0	0	#N/A
MATR3	<i>matrin 3</i>	12	19	0	0	31	0	0	0	0	0	#N/A
SUPT16H	<i>SPT16 homolog, facilitates chromatin remodeling subunit</i>	20	17	0	0	37	0	0	0	0	0	#N/A
SRP14	<i>signal recognition particle 14</i>	5	6	0	0	11	0	0	0	0	0	#N/A
VARS	<i>valyl-tRNA synthetase</i>	9	12	0	0	21	0	0	0	0	0	#N/A
AP3B1	<i>adaptor related protein complex 3 subunit beta 1</i>	12	10	4	10	36	0	0	0	0	0	#N/A
U2AF2	<i>U2 small nuclear RNA auxiliary</i>	5	9	0	0	14	0	0	0	0	0	#N/A

<i>factor 2</i>												
RFC5	<i>replication factor C subunit 5</i>	0	0	0	0	0	0	0	0	0	0	#N/A
NOP58	<i>NOP58 ribonucleoprotein</i>	20	25	0	0	45	0	0	0	0	0	#N/A
PFKP	<i>phosphofructokinase, platelet</i>	8	7	4	0	19	0	0	0	0	0	#N/A
BAZ1B	<i>bromodomain adjacent to zinc finger domain 1B</i>	120	142	0	0	262	0	0	0	0	0	#N/A
HNRNPR	<i>heterogeneous nuclear ribonucleoprotein R</i>	16	23	0	0	39	0	0	0	0	0	#N/A
G3BP2	<i>G3BP stress granule assembly factor 2</i>	13	11	0	5	29	0	0	0	0	0	#N/A
CUL4A	<i>cullin 4A</i>	5	7	0	0	12	0	0	0	0	0	#N/A
ARL2	<i>ADP ribosylation factor like GTPase 2</i>	5	6	0	0	11	0	0	0	0	0	#N/A
EEF1G	<i>eukaryotic translation elongation factor 1 gamma</i>	23	21	0	6	50	0	0	0	0	0	#N/A
CHORDC1	<i>cysteine and histidine rich domain containing 1</i>	4	5	0	0	9	0	0	0	0	0	#N/A
GART	<i>phosphoribosylglycinamide formyltransferase, phosphoribosylglycinamide synthetase, phosphoribosylaminoimidazole synthetase</i>	3	8	0	2	13	0	0	0	0	0	#N/A
MCM6	<i>minichromosome maintenance complex component 6</i>	7	6	0	0	13	0	0	0	0	0	#N/A
ABCE1	<i>ATP binding cassette subfamily E member 1</i>	3	0	0	0	3	0	0	0	0	0	#N/A
MCM5	<i>minichromosome maintenance complex component 5</i>	4	6	0	0	10	0	0	0	0	0	#N/A
RBM39	<i>RNA binding motif protein 39</i>	13	14	0	0	27	0	0	0	0	0	#N/A
RUVBL2	<i>RuvB like AAA ATPase 2</i>	67	72	3	0	142	0	0	0	0	0	#N/A
RPS15	<i>ribosomal protein S15</i>	11	14	0	0	25	0	0	0	0	0	#N/A
HNRNPF	<i>heterogeneous nuclear ribonucleoprotein F</i>	8	12	0	0	20	0	0	0	0	0	#N/A
MCM3	<i>minichromosome maintenance complex component 3</i>	7	11	0	0	18	0	0	0	0	0	#N/A
SMC4	<i>structural maintenance of chromosomes 4</i>	14	19	0	0	33	0	0	0	0	0	#N/A
PFKM	<i>phosphofructokinase, muscle</i>	6	13	0	0	19	0	0	0	0	0	#N/A
EIF2S2	<i>eukaryotic translation initiation</i>	11	8	0	0	19	0	0	0	0	0	#N/A

<i>factor 2 subunit beta</i>												
DHFR	<i>dihydrofolate reductase</i>	2	0	0	0	2	0	0	0	0	0	#N/A
PPA1	<i>pyrophosphatase (inorganic) 1</i>	7	4	7	0	18	0	0	0	0	0	#N/A
DDX18	<i>DEAD-box helicase 18</i>	8	13	0	0	21	0	0	0	0	0	#N/A
NAP1L1	<i>nucleosome assembly protein 1 like 1</i>	34	34	0	0	68	0	0	0	0	0	#N/A
SET	<i>SET nuclear proto-oncogene</i>	34	26	0	0	60	0	0	0	0	0	#N/A
PCBP1	<i>poly(rC) binding protein 1</i>	22	30	0	0	52	0	0	0	0	0	#N/A
RPL5	<i>ribosomal protein L5</i>	20	19	0	0	39	0	0	0	0	0	#N/A
NAP1L4	<i>nucleosome assembly protein 1 like 4</i>	27	29	0	0	56	0	0	0	0	0	#N/A
HNRNPC	<i>heterogeneous nuclear ribonucleoprotein C (C1/C2)</i>	30	27	0	0	57	0	0	0	0	0	#N/A
XRCC6	<i>X-ray repair cross complementing 6</i>	23	21	0	0	44	0	0	0	0	0	#N/A
HSD17B10	<i>hydroxysteroid 17-beta dehydrogenase 10</i>	0	5	0	0	5	0	0	0	0	0	#N/A
MARS	<i>methionyl-tRNA synthetase</i>	6	14	3	5	28	0	0	0	0	0	#N/A
NSUN2	<i>NOP2/Sun RNA methyltransferase 2</i>	9	12	0	0	21	0	0	0	0	0	#N/A
PCBP2	<i>poly(rC) binding protein 2</i>	25	25	5	5	60	0	0	0	0	0	#N/A
CTPS	<i>CTP synthase 1</i>	59	60	0	0	119	0	0	0	0	0	#N/A
CAND1	<i>cullin associated and neddylation dissociated 1</i>	19	17	0	0	36	0	0	0	0	0	#N/A
CDK1	<i>cyclin dependent kinase 1</i>	12	17	0	0	29	0	0	0	0	0	#N/A
DDX39B	<i>DEAD-box helicase 39B</i>	0	0	0	0	0	0	0	0	0	0	#N/A
HNRNPA1	<i>heterogeneous nuclear ribonucleoprotein A1</i>	36	36	0	0	72	0	0	0	0	0	#N/A
TUBB6	<i>tubulin beta 6 class V</i>	11	19	0	0	30	0	0	0	0	0	#N/A
RPL23	<i>ribosomal protein L23</i>	0	0	0	0	0	0	0	0	0	0	#N/A
MCM4	<i>minichromosome maintenance complex component 4</i>	19	28	0	0	47	0	0	0	0	0	#N/A
PHB	<i>prohibitin</i>	7	11	0	0	18	0	0	0	0	0	#N/A
NAMPT	<i>nicotinamide phosphoribosyltransferase</i>	3	9	0	0	12	0	0	0	0	0	#N/A
GNL3	<i>G protein nucleolar 3</i>	20	21	0	0	41	0	0	0	0	0	#N/A
MCM7	<i>minichromosome maintenance complex component 7</i>	18	30	0	0	48	0	0	0	0	0	#N/A

DDX39A	<i>DExD-box helicase 39A</i>	30	32	0	0	62	0	0	0	0	0	#N/A
EPPK1	<i>epiplakin 1</i>	6	12	0	0	18	0	0	0	0	0	#N/A
TRIP13	<i>thyroid hormone receptor interactor 13</i>	12	13	0	0	25	0	0	0	0	0	#N/A
EIF4A3	<i>eukaryotic translation initiation factor 4A3</i>	14	16	0	0	30	0	0	0	0	0	#N/A
ACACB	<i>acetyl-CoA carboxylase beta</i>	51	57	0	0	108	0	0	0	0	0	#N/A
ASS1	<i>argininosuccinate synthase 1</i>	40	40	0	0	80	0	0	0	0	0	#N/A
PRKDC	<i>protein kinase, DNA-activated, catalytic subunit</i>	29	40	0	0	69	0	0	0	0	0	#N/A
DHX9	<i>DExH-box helicase 9</i>	46	62	7	6	121	0	0	0	0	0	#N/A
RAN	<i>RAN, member RAS oncogene family</i>	34	37	2	0	73	0	0	0	0	0	#N/A
AHSA1	<i>activator of HSP90 ATPase activity 1</i>	38	47	0	0	85	0	0	0	0	0	#N/A
ALDH18A1	<i>aldehyde dehydrogenase 18 family member A1</i>	13	22	0	0	35	0	0	0	0	0	#N/A
TRAP1	<i>TNF receptor associated protein 1</i>	13	14	0	0	27	0	0	0	0	0	#N/A
LARS	<i>leucyl-tRNA synthetase</i>	22	21	0	0	43	0	0	0	0	0	#N/A
IARS	<i>isoleucyl-tRNA synthetase</i>	13	39	9	0	61	0	0	0	0	0	#N/A
PLOD1	<i>procollagen-lysine,2-oxoglutarate 5-dioxygenase 1</i>	2	3	0	0	5	0	0	0	0	0	#N/A
NUP214	<i>nucleoporin 214</i>	39	39	0	0	78	0	0	0	0	0	#N/A
HNRNPH1	<i>heterogeneous nuclear ribonucleoprotein H1</i>	22	24	0	0	46	0	0	0	0	0	#N/A
HNRNPA2B1	<i>heterogeneous nuclear ribonucleoprotein A2/B1</i>	32	33	0	0	65	0	0	0	0	0	#N/A
PSMD3	<i>proteasome 26S subunit, non-ATPase 3</i>	14	13	0	0	27	0	0	0	0	0	#N/A
RPS24	<i>ribosomal protein S24</i>	16	9	12	11	48	0	0	0	0	0	#N/A
NUMA1	<i>nuclear mitotic apparatus protein 1</i>	111	125	0	0	236	0	0	0	0	0	#N/A
FUS	<i>FUS RNA binding protein</i>	11	15	0	0	26	0	0	0	0	0	#N/A
NAT10	<i>N-acetyltransferase 10</i>	55	55	0	0	110	0	0	0	0	0	#N/A
LRPPRC	<i>leucine rich pentatricopeptide repeat containing</i>	0	0	0	0	0	0	0	0	0	0	#N/A
XPOT	<i>exportin for tRNA</i>	12	23	0	0	35	0	0	0	0	0	#N/A
DDX17	<i>DEAD-box helicase 17</i>	17	14	0	0	31	0	0	0	0	0	#N/A

HNRNPL	<i>heterogeneous nuclear ribonucleoprotein L</i>	23	24	9	5	61	0	0	0	0	0	#N/A
SLC25A13	<i>solute carrier family 25 member 13</i>	7	8	0	0	15	0	0	0	0	0	#N/A
TOMM40	<i>translocase of outer mitochondrial membrane 40</i>	0	6	0	0	6	0	0	0	0	0	#N/A
DHX15	<i>DEAH-box helicase 15</i>	49	44	0	0	93	0	0	0	0	0	#N/A
SLC25A3	<i>solute carrier family 25 member 3</i>	2	4	0	0	6	0	0	0	0	0	#N/A
ATAD3A	<i>ATPase family AAA domain containing 3A</i>	2	0	0	0	2	0	0	0	0	0	#N/A
SLC25A11	<i>solute carrier family 25 member 11</i>	4	2	0	0	6	0	0	0	0	0	#N/A
TKT	<i>transketolase</i>	4	0	0	0	4	0	0	0	0	0	#N/A
BRX1	<i>biogenesis of ribosomes BRX1</i>	0	0	0	0	0	0	0	0	0	0	#N/A
HIST1H1B	<i>histone cluster 1 H1 family member b</i>	11	11	0	0	22	0	0	0	0	0	#N/A
RSL1D1	<i>ribosomal L1 domain containing 1</i>	12	16	0	0	28	0	0	0	0	0	#N/A
PA2G4	<i>proliferation-associated 2G4</i>	22	17	0	0	39	0	0	0	0	0	#N/A
C1QBP	<i>complement C1q binding protein</i>	32	28	0	0	60	0	0	0	0	0	#N/A
PRDX6	<i>peroxiredoxin 6</i>	13	16	0	0	29	0	0	0	0	0	#N/A
HNRNPH2	<i>heterogeneous nuclear ribonucleoprotein H2</i>	0	11	0	0	11	0	0	0	0	0	#N/A
TOMM22	<i>translocase of outer mitochondrial membrane 22</i>	2	3	0	0	5	0	0	0	0	0	#N/A
ACOT9	<i>acyl-CoA thioesterase 9</i>	0	0	0	0	0	0	0	0	0	0	#N/A
GARS	<i>glycyl-tRNA synthetase</i>	0	0	0	0	0	0	0	0	0	0	#N/A
DDX1	<i>DEAD-box helicase 1</i>	11	13	0	0	24	0	0	0	0	0	#N/A
PRPF19	<i>pre-mRNA processing factor 19</i>	30	27	0	0	57	0	0	0	0	0	#N/A
ALYREF	<i>Aly/REF export factor</i>	10	9	0	0	19	0	0	0	0	0	#N/A
DNAJA3	<i>DnaJ heat shock protein family (Hsp40) member A3</i>	4	6	0	0	10	0	0	0	0	0	#N/A
SMC3	<i>structural maintenance of chromosomes 3</i>	12	17	0	0	29	0	0	0	0	0	#N/A
HNRNPA3	<i>heterogeneous nuclear ribonucleoprotein A3</i>	5	7	0	2	14	0	0	0	0	0	#N/A
FH	<i>fumarate hydratase</i>	0	0	0	0	0	0	0	0	0	0	#N/A
H2AFY	<i>H2A histone family member Y</i>	17	13	0	0	30	0	0	0	0	0	#N/A
ABCF1	<i>ATP binding cassette subfamily F</i>	17	17	0	0	34	0	0	0	0	0	#N/A

<i>member 1</i>												
YARS	<i>tyrosyl-tRNA synthetase</i>	0	0	0	0	0	0	0	0	0	0	#N/A
RECQL	<i>RecQ like helicase</i>	3	4	0	0	7	0	0	0	0	0	#N/A
SFXN1	<i>sideroflexin 1</i>	0	4	0	0	4	0	0	0	0	0	#N/A
DDX47	<i>DEAD-box helicase 47</i>	3	4	0	0	7	0	0	0	0	0	#N/A
SMC1A	<i>structural maintenance of chromosomes 1A</i>	5	4	0	0	9	0	0	0	0	0	#N/A
KARS	<i>lysyl-tRNA synthetase</i>	4	9	2	0	15	0	0	0	0	0	#N/A
ELAVL1	<i>ELAV like RNA binding protein 1</i>	6	6	0	0	12	0	0	0	0	0	#N/A
HNRNPD	<i>heterogeneous nuclear ribonucleoprotein D</i>	13	16	0	0	29	0	0	0	0	0	#N/A
IPO5	<i>importin 5</i>	0	2	0	0	2	0	0	0	0	0	#N/A
NDUFA10	<i>NADH:ubiquinone oxidoreductase subunit A10</i>	0	0	0	0	0	0	0	0	0	0	#N/A
SF3B3	<i>splicing factor 3b subunit 3</i>	54	62	0	0	116	0	0	0	0	0	#N/A
ZNF326	<i>zinc finger protein 326</i>	2	2	0	0	4	0	0	0	0	0	#N/A
PDCD6	<i>programmed cell death 6</i>	0	0	3	3	6	0	0	0	0	0	#N/A
SMARCA5	<i>SWI/SNF related, matrix associated, actin dependent regulator of chromatin, subfamily a, member 5</i>	71	67	0	0	138	0	0	0	0	0	#N/A
MKI67	<i>marker of proliferation Ki-67</i>	100	105	0	0	205	0	0	0	0	0	#N/A
RBMX	<i>RNA binding motif protein X-linked</i>	0	0	0	0	0	0	0	0	0	0	#N/A
DNAJC11	<i>DnaJ heat shock protein family (Hsp40) member C11</i>	0	2	0	0	2	0	0	0	0	0	#N/A
RAE1	<i>ribonucleic acid export 1</i>	4	5	0	0	9	0	0	0	0	0	#N/A
RPS17	<i>ribosomal protein S17</i>	0	0	0	0	0	0	0	0	0	0	#N/A
TARDBP	<i>TAR DNA binding protein</i>	3	4	0	0	7	0	0	0	0	0	#N/A
ERLIN2	<i>ER lipid raft associated 2</i>	0	0	0	0	0	0	0	0	0	0	#N/A
ARCN1	<i>archain 1</i>	7	7	2	0	16	0	0	0	0	0	#N/A
PFKL	<i>phosphofructokinase, liver type</i>	0	3	0	0	3	0	0	0	0	0	#N/A
CSE1L	<i>chromosome segregation 1 like</i>	0	5	0	0	5	0	0	0	0	0	#N/A
IMPA2	<i>inositol monophosphatase 2</i>	0	0	0	0	0	0	0	0	0	0	#N/A
ECH1	<i>enoyl-CoA hydratase 1</i>	0	0	0	0	0	0	0	0	0	0	#N/A

KHDRBS1	<i>KH RNA binding domain containing, signal transduction associated 1</i>	13	10	0	0	23	0	0	0	0	0	#N/A
BLVRA	<i>biliverdin reductase A</i>	0	0	0	0	0	0	0	0	0	0	#N/A
RCC2	<i>regulator of chromosome condensation 2</i>	2	0	0	0	2	0	0	0	0	0	#N/A
LYAR	<i>Ly1 antibody reactive</i>	5	5	0	0	10	0	0	0	0	0	#N/A
DARS	<i>aspartyl-tRNA synthetase</i>	3	4	2	0	9	0	0	0	0	0	#N/A
SLC25A10	<i>solute carrier family 25 member 10</i>	0	0	0	0	0	0	0	0	0	0	#N/A
RG9MTD1	<i>tRNA methyltransferase 10C, mitochondrial RNase P subunit</i>	0	0	0	0	0	0	0	0	0	0	#N/A
SRSF7	<i>serine and arginine rich splicing factor 7</i>	7	9	0	0	16	0	0	0	0	0	#N/A
U2AF1	<i>U2 small nuclear RNA auxiliary factor 1</i>	3	4	0	0	7	0	0	0	0	0	#N/A
NUP98	<i>nucleoporin 98</i>	15	19	0	0	34	0	0	0	0	0	#N/A
TUBG1	<i>tubulin gamma 1</i>	0	0	0	0	0	0	0	0	0	0	#N/A
TIMM50	<i>translocase of inner mitochondrial membrane 50</i>	0	3	0	0	3	0	0	0	0	0	#N/A
NNT	<i>nicotinamide nucleotide transhydrogenase</i>	0	0	0	0	0	0	0	0	0	0	#N/A
HYOU1	<i>hypoxia up-regulated 1</i>	0	0	0	0	0	0	0	0	0	0	#N/A
EMG1	<i>EMG1 N1-specific pseudouridine methyltransferase</i>	4	3	0	0	7	0	0	0	0	0	#N/A
RPS12	<i>ribosomal protein S12</i>	2	0	2	0	4	0	0	0	0	0	#N/A
PTGR1	<i>prostaglandin reductase 1</i>	0	0	0	0	0	0	0	0	0	0	#N/A
SHMT2	<i>serine hydroxymethyltransferase 2</i>	0	0	0	0	0	0	0	0	0	0	#N/A
PSMD4	<i>proteasome 26S subunit, non-ATPase 4</i>	4	3	0	0	7	0	0	0	0	0	#N/A
MCM2	<i>minichromosome maintenance complex component 2</i>	0	0	0	0	0	0	0	0	0	0	#N/A
UPF1	<i>UPF1 RNA helicase and ATPase</i>	3	6	0	0	9	0	0	0	0	0	#N/A
LONP1	<i>lon peptidase 1, mitochondrial</i>	0	0	0	0	0	0	0	0	0	0	#N/A
MCU	<i>mitochondrial calcium uniporter</i>	0	0	0	0	0	0	0	0	0	0	#N/A
HNRNPU L2	<i>heterogeneous nuclear ribonucleoprotein U like 2</i>	3	4	0	0	7	0	0	0	0	0	#N/A
STT3A	<i>STT3 oligosaccharyltransferase complex catalytic subunit A</i>	0	0	0	0	0	0	0	0	0	0	#N/A

SBDS	<i>SBDS ribosome maturation factor</i>	0	0	0	0	0	0	0	0	0	0	#N/A
TRIM28	<i>tripartite motif containing 28</i>	55	48	4	4	111	0	0	0	0	0	#N/A
PSMD14	<i>proteasome 26S subunit, non-ATPase 14</i>	0	0	0	0	0	0	0	0	0	0	#N/A
SSRP1	<i>structure specific recognition protein 1</i>	6	11	0	0	17	0	0	0	0	0	#N/A
DDX46	<i>DEAD-box helicase 46</i>	88	85	0	0	173	0	0	0	0	0	#N/A
RRS1	<i>ribosome biogenesis regulator 1 homolog</i>	5	9	0	0	14	0	0	0	0	0	#N/A
GMPS	<i>guanine monophosphate synthase</i>	3	2	0	0	5	0	0	0	0	0	#N/A
IDI1	<i>isopentenyl-diphosphate delta isomerase 1</i>	0	0	0	0	0	0	0	0	0	0	#N/A
HIGD1A	<i>HIG1 hypoxia inducible domain family member 1A</i>	0	0	0	0	0	0	0	0	0	0	#N/A
NUDT21	<i>nudix hydrolase 21</i>	17	21	0	0	38	0	0	0	0	0	#N/A
DHX30	<i>DExH-box helicase 30</i>	0	0	0	0	0	0	0	0	0	0	#N/A
PDHB	<i>pyruvate dehydrogenase E1 beta subunit</i>	0	0	0	0	0	0	0	0	0	0	#N/A
UBXN1	<i>UBX domain protein 1</i>	0	0	0	0	0	0	0	0	0	0	#N/A
RHOG	<i>ras homolog family member G</i>	0	0	0	0	0	0	0	0	0	0	#N/A
PARK7	<i>Parkinsonism associated deglycase</i>	0	0	0	0	0	0	0	0	0	0	#N/A
ERLIN1	<i>ER lipid raft associated 1</i>	0	0	0	0	0	0	0	0	0	0	#N/A
NCLN	<i>nicalin</i>	0	0	0	0	0	0	0	0	0	0	#N/A
RAD50	<i>RAD50 double strand break repair protein</i>	0	3	0	0	3	0	0	0	0	0	#N/A
NAA10	<i>N(alpha)-acetyltransferase 10, NatA catalytic subunit</i>	0	0	0	0	0	0	0	0	0	0	#N/A
YTHDF1	<i>YTH N6-methyladenosine RNA binding protein 1</i>	3	0	0	0	3	0	0	0	0	0	#N/A
RAD21	<i>RAD21 cohesin complex component</i>	6	7	0	0	13	0	0	0	0	0	#N/A
FARSA	<i>phenylalanyl-tRNA synthetase subunit alpha</i>	4	11	0	2	17	0	0	0	0	0	#N/A
IGF2BP3	<i>insulin like growth factor 2 mRNA binding protein 3</i>	2	3	0	0	5	0	0	0	0	0	#N/A
RPS27A	<i>ribosomal protein S27a</i>	13	11	0	0	24	0	0	0	0	0	#N/A
NUP62	<i>nucleoporin 62</i>	3	4	0	0	7	0	0	0	0	0	#N/A
SLC25A4	<i>solute carrier family 25 member 4</i>	0	2	0	0	2	0	0	0	0	0	#N/A

AK1	<i>adenylate kinase 1</i>	0	0	0	0	0	0	0	0	0	0	#N/A
NUP88	<i>nucleoporin 88</i>	0	4	0	0	4	0	0	0	0	0	#N/A
EBNA1BP2	<i>EBNA1 binding protein 2</i>	2	5	0	0	7	0	0	0	0	0	#N/A
PRKACA	<i>protein kinase cAMP-activated catalytic subunit alpha</i>	0	0	0	0	0	0	0	0	0	0	#N/A
TXN	<i>thioredoxin</i>	0	5	0	0	5	0	0	0	0	0	#N/A
AHCTF1	<i>AT-hook containing transcription factor 1</i>	47	61	0	0	108	0	0	0	0	0	#N/A
SRSF3	<i>serine and arginine rich splicing factor 3</i>	0	0	0	0	0	0	0	0	0	0	#N/A
SDHA	<i>succinate dehydrogenase complex flavoprotein subunit A</i>	0	0	0	0	0	0	0	0	0	0	#N/A
ATP5J2-PTCD1	<i>ATP5MF-PTCD1 readthrough</i>	0	0	0	0	0	0	0	0	0	0	#N/A
CRYZ	<i>crystallin zeta</i>	0	0	0	0	0	0	0	0	0	0	#N/A
ATAD3B	<i>ATPase family AAA domain containing 3B</i>	0	0	0	0	0	0	0	0	0	0	#N/A
SAR1B	<i>secretion associated Ras related GTPase 1B</i>	0	0	0	0	0	0	0	0	0	0	#N/A
LOC101060252		0	0	0	0	0	0	0	0	0	0	#N/A
RBFOX2	<i>RNA binding fox-1 homolog 2</i>	0	0	0	0	0	0	0	0	0	0	#N/A
MOV10	<i>Mov10 RISC complex RNA helicase</i>	0	0	0	0	0	0	0	0	0	0	#N/A
API5	<i>apoptosis inhibitor 5</i>	4	7	0	0	11	0	0	0	0	0	#N/A
NMD3	<i>NMD3 ribosome export adaptor</i>	0	0	0	0	0	0	0	0	0	0	#N/A
ACOT7	<i>acyl-CoA thioesterase 7</i>	0	0	0	0	0	0	0	0	0	0	#N/A
SRM	<i>spermidine synthase</i>	0	0	0	0	0	0	0	0	0	0	#N/A
SRPK1	<i>SRSF protein kinase 1</i>	4	4	0	0	8	0	0	0	0	0	#N/A
UBE2D3	<i>ubiquitin conjugating enzyme E2 D3</i>	0	0	0	0	0	0	0	0	0	0	#N/A
LGALS1	<i>galectin 1</i>	3	6	8	5	22	0	0	0	0	0	#N/A
ILVBL	<i>ilvB acetolactate synthase like</i>	0	0	0	0	0	0	0	0	0	0	#N/A
FAF2	<i>Fas associated factor family member 2</i>	0	0	0	0	0	0	0	0	0	0	#N/A
CSTB	<i>cystatin B</i>	0	0	0	0	0	0	0	0	0	0	#N/A
RPL36A	<i>ribosomal protein L36a</i>	0	0	0	0	0	0	0	0	0	0	#N/A

YIF1A	<i>Yip1 interacting factor homolog A, membrane trafficking protein</i>	0	0	0	0	0	0	0	0	0	0	#N/A
DAD1	<i>defender against cell death 1</i>	0	0	0	0	0	0	0	0	0	0	#N/A
RNPS1	<i>RNA binding protein with serine rich domain 1</i>	18	15	0	0	33	0	0	0	0	0	#N/A
MAD2L1	<i>mitotic arrest deficient 2 like 1</i>	0	0	0	0	0	0	0	0	0	0	#N/A
SPOCK3	<i>SPARC (osteonectin), cwcw and kazal like domains proteoglycan 3</i>	0	0	0	0	0	0	0	0	0	0	#N/A
PDS5B	<i>PDS5 cohesin associated factor B</i>	0	0	0	0	0	0	0	0	0	0	#N/A
USMG5	<i>ATP synthase membrane subunit DAPIT</i>	0	0	0	0	0	0	0	0	0	0	#N/A
IMMT	<i>inner membrane mitochondrial protein</i>	0	0	0	0	0	0	0	0	0	0	#N/A
TRA2B	<i>transformer 2 beta homolog</i>	8	8	0	0	16	0	0	0	0	0	#N/A
LRP1B	<i>LDL receptor related protein 1B</i>	2	0	0	0	2	0	0	0	0	0	#N/A
CLPB	<i>ClpB homolog, mitochondrial AAA ATPase chaperonin</i>	0	0	0	0	0	0	0	0	0	0	#N/A
TSMF	<i>Ts translation elongation factor, mitochondrial</i>	0	0	0	0	0	0	0	0	0	0	#N/A
LUC7L3	<i>LUC7 like 3 pre-mRNA splicing factor</i>	3	7	0	0	10	0	0	0	0	0	#N/A
IER3IP1	<i>immediate early response 3 interacting protein 1</i>	0	0	0	0	0	0	0	0	0	0	#N/A
PRPF6	<i>pre-mRNA processing factor 6</i>	3	0	0	0	3	0	0	0	0	0	#N/A
MYH14	<i>myosin heavy chain 14</i>	0	0	0	0	0	0	0	0	0	0	#N/A
SART1	<i>spliceosome associated factor 1, recruiter of U4/U6.U5 tri-snRNP</i>	29	37	0	0	66	0	0	0	0	0	#N/A
EMILIN3	<i>elastin microfibril interfacier 3</i>	0	0	0	0	0	0	0	0	0	0	#N/A
FUBP1	<i>far upstream element binding protein 1</i>	11	6	0	0	17	0	0	0	0	0	#N/A
MRI1	<i>methylthioribose-1-phosphate isomerase 1</i>	0	0	0	0	0	0	0	0	0	0	#N/A
TNPO1	<i>transportin 1</i>	0	3	0	0	3	0	0	0	0	0	#N/A
H2AFZ	<i>H2A histone family member Z</i>	6	3	0	0	9	0	0	0	0	0	#N/A
TOP1	<i>DNA topoisomerase I</i>	0	0	0	0	0	0	0	0	0	0	#N/A
MEST	<i>mesoderm specific transcript</i>	0	0	0	0	0	0	0	0	0	0	#N/A
EIF2AK2	<i>eukaryotic translation initiation factor 2 alpha kinase 2</i>	0	0	0	0	0	0	0	0	0	0	#N/A
APOBEC3	<i>apolipoprotein B mRNA editing</i>	0	0	0	0	0	0	0	0	0	0	#N/A

C	<i>enzyme catalytic subunit 3C</i>											
HADHA	<i>hydroxyacyl-CoA dehydrogenase trifunctional multienzyme complex subunit alpha</i>	0	0	0	0	0	0	0	0	0	0	#N/A
POLR2H	<i>RNA polymerase II subunit H</i>	0	0	0	0	0	0	0	0	0	0	#N/A
ACAT1	<i>acetyl-CoA acetyltransferase 1</i>	0	0	0	0	0	0	0	0	0	0	#N/A
MAPKAPK2	<i>MAPK activated protein kinase 2</i>	0	0	0	0	0	0	0	0	0	0	#N/A
ARAF	<i>A-Raf proto-oncogene, serine/threonine kinase</i>	0	0	0	0	0	0	0	0	0	0	#N/A
ALDH1L2	<i>aldehyde dehydrogenase 1 family member L2</i>	0	0	0	0	0	0	0	0	0	0	#N/A
NDUFS2	<i>NADH:ubiquinone oxidoreductase core subunit S2</i>	0	0	0	0	0	0	0	0	0	0	#N/A
PKD2L2	<i>polycystin 2 like 2, transient receptor potential cation channel</i>	0	0	0	0	0	0	0	0	0	0	#N/A
MCF2	<i>MCF.2 cell line derived transforming sequence</i>	0	0	0	0	0	0	0	0	0	0	#N/A
WDR3	<i>WD repeat domain 3</i>	0	0	0	0	0	0	0	0	0	0	#N/A
NUP153	<i>nucleoporin 153</i>	37	35	0	0	72	0	0	0	0	0	#N/A
SUCLA2	<i>succinate-CoA ligase ADP-forming beta subunit</i>	0	0	0	0	0	0	0	0	0	0	#N/A
RRP1B	<i>ribosomal RNA processing 1B</i>	0	0	0	0	0	0	0	0	0	0	#N/A
NKRF	<i>NFKB repressing factor</i>	0	0	0	0	0	0	0	0	0	0	#N/A
FAM208B	<i>transcription activation suppressor family member 2</i>	0	0	0	0	0	0	0	0	0	0	#N/A
ATP5O	<i>ATP synthase peripheral stalk subunit OSCP</i>	0	0	0	0	0	0	0	0	0	0	#N/A
FHL2	<i>four and a half LIM domains 2</i>	0	0	0	0	0	0	0	0	0	0	#N/A
KIAA0090	<i>ER membrane protein complex subunit 1</i>	0	0	0	0	0	0	0	0	0	0	#N/A
MOGS	<i>mannosyl-oligosaccharide glucosidase</i>	0	0	0	0	0	0	0	0	0	0	#N/A
TCOF1	<i>treacle ribosome biogenesis factor 1</i>	28	34	0	3	65	0	0	0	0	0	#N/A
BAG5	<i>BCL2 associated athanogene 5</i>	0	0	0	0	0	0	0	0	0	0	#N/A
ETFA	<i>electron transfer flavoprotein subunit alpha</i>	0	0	0	0	0	0	0	0	0	0	#N/A
CCDC47	<i>coiled-coil domain containing 47</i>	0	0	0	0	0	0	0	0	0	0	#N/A

PARVB	<i>parvin beta</i>	0	0	0	0	0	0	0	0	0	0	#N/A
BOP1	<i>BOP1 ribosomal biogenesis factor</i>	8	13	0	0	21	0	0	0	0	0	#N/A
PGD	<i>phosphogluconate dehydrogenase</i>	0	0	0	0	0	0	0	0	0	0	#N/A
PIGK	<i>phosphatidylinositol glycan anchor biosynthesis class K</i>	2	0	0	0	2	0	0	0	0	0	#N/A
CCDC86	<i>coiled-coil domain containing 86</i>	0	0	0	0	0	0	0	0	0	0	#N/A
CAPN1	<i>calpain 1</i>	0	0	0	0	0	0	0	0	0	0	#N/A
ARF6	<i>ADP ribosylation factor 6</i>	0	0	0	0	0	0	0	0	0	0	#N/A
NOP16	<i>NOP16 nucleolar protein</i>	0	5	0	0	5	0	0	0	0	0	#N/A
SMARCB1	<i>SWI/SNF related, matrix associated, actin dependent regulator of chromatin, subfamily b, member 1</i>	0	2	0	0	2	0	0	0	0	0	#N/A
TBRG4	<i>transforming growth factor beta regulator 4</i>	0	0	0	0	0	0	0	0	0	0	#N/A
COTL1	<i>coactosin like F-actin binding protein 1</i>	0	0	0	0	0	0	0	0	0	0	#N/A
PSIP1	<i>PC4 and SFRS1 interacting protein 1</i>	6	6	0	0	12	0	0	0	0	0	#N/A
PSPC1	<i>paraspeckle component 1</i>	4	8	0	0	12	0	0	0	0	0	#N/A
SMCHD1	<i>structural maintenance of chromosomes flexible hinge domain containing 1</i>	3	3	0	0	6	0	0	0	0	0	#N/A
MTCH2	<i>mitochondrial carrier 2</i>	0	0	0	0	0	0	0	0	0	0	#N/A
MKI67IP	<i>nucleolar protein interacting with the FHA domain of MKI67</i>	0	7	0	0	7	0	0	0	0	0	#N/A
MGC50722	<i>coiled-coil domain containing 1872</i>	0	0	0	0	0	0	0	0	0	0	#N/A
ARL6IP5	<i>ADP ribosylation factor like GTPase 6 interacting protein 5</i>	0	0	0	0	0	0	0	0	0	0	#N/A
PTGES3	<i>prostaglandin E synthase 3</i>	0	0	0	0	0	0	0	0	0	0	#N/A
HSDL1	<i>hydroxysteroid dehydrogenase like 1</i>	0	0	0	0	0	0	0	0	0	0	#N/A
EBP	<i>EBP cholesterol delta-isomerase</i>	0	0	0	0	0	0	0	0	0	0	#N/A
FFAR1	<i>free fatty acid receptor 1</i>	0	0	0	0	0	0	0	0	0	0	#N/A
NOLC1	<i>nucleolar and coiled-body phosphoprotein 1</i>	4	7	0	0	11	0	0	0	0	0	#N/A
SF3B14		0	10	11	0	21	0	0	0	0	0	#N/A

TNRC6A	<i>trinucleotide repeat containing adaptor 6A</i>	0	0	0	0	0	0	0	0	0	0	#N/A
RAB3D	<i>RAB3D, member RAS oncogene family</i>	0	0	0	0	0	0	0	0	0	0	#N/A
DLD	<i>dihydrolipoamide dehydrogenase</i>	0	0	0	0	0	0	0	0	0	0	#N/A
PPM1G	<i>protein phosphatase, Mg2+/Mn2+ dependent 1G</i>	2	5	0	0	7	0	0	0	0	0	#N/A
EEF1E1	<i>eukaryotic translation elongation factor 1 epsilon 1</i>	0	3	2	0	5	0	0	0	0	0	#N/A
HNRPLL	<i>heterogeneous nuclear ribonucleoprotein L like</i>	0	0	0	0	0	0	0	0	0	0	#N/A
DNMT1	<i>DNA methyltransferase 1</i>	9	8	0	0	17	0	0	0	0	0	#N/A
SF3B4	<i>splicing factor 3b subunit 4</i>	12	17	0	0	29	0	0	0	0	0	#N/A
SORCS3	<i>sortilin related VPS10 domain containing receptor 3</i>	0	0	0	0	0	0	0	0	0	0	#N/A
SRSF1	<i>serine and arginine rich splicing factor 1</i>	5	3	0	0	8	0	0	0	0	0	#N/A
USP54	<i>ubiquitin specific peptidase 54</i>	0	0	0	0	0	0	0	0	0	0	#N/A
KHSRP	<i>KH-type splicing regulatory protein</i>	7	6	0	0	13	0	0	0	0	0	#N/A
MTA2	<i>metastasis associated 1 family member 2</i>	16	13	0	0	29	0	0	0	0	0	#N/A
C16orf80	<i>cilia and flagella associated protein 20</i>	2	2	0	0	4	0	0	0	0	0	#N/A
HDAC1	<i>histone deacetylase 1</i>	9	26	0	0	35	0	0	0	0	0	#N/A
DYNLT1	<i>dynein light chain Tctex-type 1</i>	0	0	0	0	0	0	0	0	0	0	#N/A
FOXRED1	<i>FAD dependent oxidoreductase domain containing 1</i>	0	0	0	0	0	0	0	0	0	0	#N/A
EIF4A2	<i>eukaryotic translation initiation factor 4A2</i>	0	0	0	0	0	0	0	0	0	0	#N/A
NAA11	<i>N(alpha)-acetyltransferase 11, NatA catalytic subunit</i>	0	0	0	0	0	0	0	0	0	0	#N/A
SRSF2	<i>serine and arginine rich splicing factor 2</i>	0	0	0	0	0	0	0	0	0	0	#N/A
LRRC47	<i>leucine rich repeat containing 47</i>	0	0	0	0	0	0	0	0	0	0	#N/A
CIC	<i>capicua transcriptional repressor</i>	0	0	0	0	0	0	0	0	0	0	#N/A
ABCB7	<i>ATP binding cassette subfamily B member 7</i>	0	0	0	0	0	0	0	0	0	0	#N/A
MRPS2	<i>mitochondrial ribosomal protein S2</i>	0	0	0	0	0	0	0	0	0	0	#N/A
TMC7	<i>transmembrane channel like 7</i>	0	0	0	0	0	0	0	0	0	0	#N/A

ATAD1	<i>ATPase family AAA domain containing 1</i>	0	0	0	0	0	0	0	0	0	0	#N/A
TIMMDC1	<i>translocase of inner mitochondrial membrane domain containing 1</i>	0	0	0	0	0	0	0	0	0	0	#N/A
TXNIP	<i>thioredoxin interacting protein</i>	0	0	0	0	0	0	0	0	0	0	#N/A
MTPAP	<i>mitochondrial poly(A) polymerase</i>	0	0	0	0	0	0	0	0	0	0	#N/A
NOP2	<i>NOP2 nucleolar protein</i>	0	6	0	0	6	0	0	0	0	0	#N/A
PYCR1	<i>pyrroline-5-carboxylate reductase 1</i>	0	0	0	0	0	0	0	0	0	0	#N/A
FBXO7	<i>F-box protein 7</i>	0	0	0	0	0	0	0	0	0	0	#N/A
ATPAF2	<i>ATP synthase mitochondrial F1 complex assembly factor 2</i>	0	0	0	0	0	0	0	0	0	0	#N/A
RANBP6	<i>RAN binding protein 6</i>	0	0	0	0	0	0	0	0	0	0	#N/A
TSR1	<i>TSR1 ribosome maturation factor</i>	16	14	0	0	30	0	0	0	0	0	#N/A
MDN1	<i>midasin AAA ATPase 1</i>	0	0	0	0	0	0	0	0	0	0	#N/A
C2orf47	<i>matrix AAA peptidase interacting protein 1</i>	0	0	0	0	0	0	0	0	0	0	#N/A
HK1	<i>hexokinase 1</i>	0	0	0	0	0	0	0	0	0	0	#N/A
NT5DC2	<i>5'-nucleotidase domain containing 2</i>	0	0	0	0	0	0	0	0	0	0	#N/A
P4HA1	<i>prolyl 4-hydroxylase subunit alpha 1</i>	0	0	0	0	0	0	0	0	0	0	#N/A
CLPP	<i>caseinolytic mitochondrial matrix peptidase proteolytic subunit</i>	0	0	0	0	0	0	0	0	0	0	#N/A
NDUFS7	<i>NADH:ubiquinone oxidoreductase core subunit S7</i>	0	0	0	0	0	0	0	0	0	0	#N/A
ATXN2	<i>ataxin 2</i>	2	5	0	0	7	0	0	0	0	0	#N/A
PLOD3	<i>procollagen-lysine,2-oxoglutarate 5-dioxygenase 3</i>	0	0	0	0	0	0	0	0	0	0	#N/A
NAT1	<i>N-acetyltransferase 1</i>	0	0	0	0	0	0	0	0	0	0	#N/A
NOMO2	<i>NODAL modulator 2</i>	0	0	0	0	0	0	0	0	0	0	#N/A
APRT	<i>adenine phosphoribosyltransferase</i>	0	0	0	0	0	0	0	0	0	0	#N/A
TRMT5	<i>tRNA methyltransferase 5</i>	0	0	0	0	0	0	0	0	0	0	#N/A
PCK2	<i>phosphoenolpyruvate carboxykinase 2, mitochondrial</i>	0	0	0	0	0	0	0	0	0	0	#N/A
MTFP1	<i>mitochondrial fission process 1</i>	0	0	0	0	0	0	0	0	0	0	#N/A
ISOC2	<i>isochorismatase domain containing 2</i>	0	0	0	0	0	0	0	0	0	0	#N/A

PRRC2B	<i>proline rich coiled-coil 2B</i>	2	4	0	0	6	0	0	0	0	0	#N/A
RFK	<i>riboflavin kinase</i>	0	0	0	0	0	0	0	0	0	0	#N/A
CACNA1D	<i>calcium voltage-gated channel subunit alpha1 D</i>	0	0	0	0	0	0	0	0	0	0	#N/A
PGLS	<i>6-phosphogluconolactonase</i>	0	0	0	0	0	0	0	0	0	0	#N/A
PRPSAP2	<i>phosphoribosyl pyrophosphate synthetase associated protein 2</i>	0	0	0	0	0	0	0	0	0	0	#N/A
AP1S1	<i>adaptor related protein complex 1 subunit sigma 1</i>	0	0	0	0	0	0	0	0	0	0	#N/A
NIPBL	<i>NIPBL cohesin loading factor</i>	4	2	0	0	6	0	0	0	0	0	#N/A
ARHGEF1	<i>Rho guanine nucleotide exchange factor 1</i>	0	0	0	0	0	0	0	0	0	0	#N/A
PYGB	<i>glycogen phosphorylase B</i>	0	0	0	0	0	0	0	0	0	0	#N/A
MRPL22	<i>mitochondrial ribosomal protein L22</i>	0	0	0	0	0	0	0	0	0	0	#N/A
MLEC	<i>malectin</i>	0	0	0	0	0	0	0	0	0	0	#N/A
USP9X	<i>ubiquitin specific peptidase 9 X-linked</i>	0	0	0	0	0	0	0	0	0	0	#N/A
METAP2	<i>methionyl aminopeptidase 2</i>	0	0	0	0	0	0	0	0	0	0	#N/A
PGM3	<i>phosphoglucomutase 3</i>	0	0	0	0	0	0	0	0	0	0	#N/A
ALPL	<i>alkaline phosphatase, biomineralization associated</i>	0	0	0	0	0	0	0	0	0	0	#N/A
C9orf64	<i>chromosome 9 open reading frame 64</i>	0	0	0	0	0	0	0	0	0	0	#N/A
ODZ3	<i>teneurin transmembrane protein 1</i>	0	0	0	0	0	0	0	0	0	0	#N/A
HSPA6	<i>heat shock protein family A (Hsp70) member 6</i>	0	0	0	0	0	0	0	0	0	0	#N/A
POLD3	<i>DNA polymerase delta 3, accessory subunit</i>	3	0	0	0	3	0	0	0	0	0	#N/A
KCNQ2	<i>potassium voltage-gated channel subfamily Q member 2</i>	0	0	0	0	0	0	0	0	0	0	#N/A
BCCIP	<i>BRCA2 and CDKN1A interacting protein</i>	0	0	0	0	0	0	0	0	0	0	#N/A
ACSL4	<i>acyl-CoA synthetase long chain family member 4</i>	0	0	0	0	0	0	0	0	0	0	#N/A
DDX50	<i>DEXD-box helicase 50</i>	0	0	0	0	0	0	0	0	0	0	#N/A
RPS6KA2	<i>ribosomal protein S6 kinase A2</i>	0	3	0	0	3	0	0	0	0	0	#N/A
DKC1	<i>dyskerin pseudouridine synthase 1</i>	0	6	0	0	6	0	0	0	0	0	#N/A

NAA40	<i>N(alpha)-acetyltransferase 40, NatD catalytic subunit</i>	0	0	0	0	0	0	0	0	0	0	#N/A
SLC12A7	<i>solute carrier family 12 member 7</i>	0	0	0	0	0	0	0	0	0	0	#N/A
HUWE1	<i>HECT, UBA and WWE domain containing E3 ubiquitin protein ligase 1</i>	0	0	0	0	0	0	0	0	0	0	#N/A
CHCHD1	<i>coiled-coil-helix-coiled-coil-helix domain containing 1</i>	0	0	0	0	0	0	0	0	0	0	#N/A
REPIN1	<i>replication initiator 1</i>	0	0	0	0	0	0	0	0	0	0	#N/A
KDM1A	<i>lysine demethylase 1A</i>	2	2	0	0	4	0	0	0	0	0	#N/A
SYNE1	<i>spectrin repeat containing nuclear envelope protein 1</i>	0	0	0	0	0	0	0	0	0	0	#N/A
CNN3	<i>calponin 3</i>	0	0	0	0	0	0	0	0	0	0	#N/A
PSMA4	<i>proteasome subunit alpha 4</i>	0	0	0	0	0	0	0	0	0	0	#N/A
CCNT1	<i>cyclin T1</i>	12	12	0	0	24	0	0	0	0	0	#N/A
CPSF1	<i>cleavage and polyadenylation specific factor 1</i>	2	0	0	0	2	0	0	0	0	0	#N/A
HM13	<i>histocompatibility minor 13</i>	0	0	0	0	0	0	0	0	0	0	#N/A
CBR1	<i>carbonyl reductase 1</i>	0	0	0	0	0	0	0	0	0	0	#N/A
SLC25A15	<i>solute carrier family 25 member 15</i>	0	0	0	0	0	0	0	0	0	0	#N/A
STOML2	<i>stomatin like 2</i>	0	0	0	0	0	0	0	0	0	0	#N/A
GEMIN4	<i>gem nuclear organelle associated protein 4</i>	0	3	0	0	3	0	0	0	0	0	#N/A
HLCS	<i>holocarboxylase synthetase</i>	0	0	0	0	0	0	0	0	0	0	#N/A
NUDT4	<i>nudix hydrolase 4</i>	0	0	0	0	0	0	0	0	0	0	#N/A
COPZ1	<i>coatamer protein complex subunit zeta 1</i>	0	0	0	0	0	0	0	0	0	0	#N/A
USP39	<i>ubiquitin specific peptidase 39</i>	7	9	0	0	16	0	0	0	0	0	#N/A
RRAS	<i>RAS related</i>	0	0	0	0	0	0	0	0	0	0	#N/A
SAFB	<i>scaffold attachment factor B</i>	3	7	0	0	10	0	0	0	0	0	#N/A
SIN3B	<i>SIN3 transcription regulator family member B</i>	60	70	0	0	130	0	0	0	0	0	#N/A
PAPOLA	<i>poly(A) polymerase alpha</i>	48	54	0	0	102	0	0	0	0	0	#N/A
PPP1R10	<i>protein phosphatase 1 regulatory subunit 10</i>	42	45	0	0	87	0	0	0	0	0	#N/A
DIDO1	<i>death inducer-obliterator 1</i>	39	48	0	0	87	0	0	0	0	0	#N/A
DDX42	<i>DEAD-box helicase 42</i>	38	39	0	0	77	0	0	0	0	0	#N/A

NASP	<i>nuclear autoantigenic sperm protein</i>	37	19	0	0	56	0	0	0	0	0	#N/A
KDM3B	<i>lysine demethylase 3B</i>	34	41	0	0	75	0	0	0	0	0	#N/A
RIF1	<i>replication timing regulatory factor 1</i>	33	54	0	0	87	0	0	0	0	0	#N/A
SART3	<i>spliceosome associated factor 3, U4/U6 recycling protein</i>	32	24	0	0	56	0	0	0	0	0	#N/A
WAPAL	<i>WAPL cohesin release factor</i>	30	35	0	0	65	0	0	0	0	0	#N/A
KIF4A	<i>kinesin family member 4A</i>	30	38	0	0	68	0	0	0	0	0	#N/A
ACIN1	<i>apoptotic chromatin condensation inducer 1</i>	29	33	0	0	62	0	0	0	0	0	#N/A
JMJD1C	<i>jumonji domain containing 1C</i>	28	36	0	0	64	0	0	0	0	0	#N/A
EXOSC10	<i>exosome component 10</i>	27	34	0	0	61	0	0	0	0	0	#N/A
SMEK1	<i>protein phosphatase 4 regulatory subunit 3A</i>	27	32	0	0	59	0	0	0	0	0	#N/A
SF3A1	<i>splicing factor 3a subunit 1</i>	25	18	0	0	43	0	0	0	0	0	#N/A
RBM27	<i>RNA binding motif protein 27</i>	23	29	0	0	52	0	0	0	0	0	#N/A
U2SURP	<i>U2 snRNP associated SURP domain containing</i>	22	31	0	0	53	0	0	0	0	0	#N/A
SUGP2	<i>SURP and G-patch domain containing 2</i>	22	19	0	0	41	0	0	0	0	0	#N/A
TPX2	<i>TPX2 microtubule nucleation factor</i>	21	22	0	0	43	0	0	0	0	0	#N/A
CHERP	<i>calcium homeostasis endoplasmic reticulum protein</i>	20	26	0	0	46	0	0	0	0	0	#N/A
THRAP3	<i>thyroid hormone receptor associated protein 3</i>	20	23	0	0	43	0	0	0	0	0	#N/A
TCERG1	<i>transcription elongation regulator 1</i>	20	20	0	0	40	0	0	0	0	0	#N/A
LRWD1	<i>leucine rich repeats and WD repeat domain containing 1</i>	19	27	0	0	46	0	0	0	0	0	#N/A
TH1L	<i>negative elongation factor complex member C/D</i>	19	22	0	0	41	0	0	0	0	0	#N/A
GTF2E2	<i>general transcription factor IIE subunit 2</i>	19	17	0	0	36	0	0	0	0	0	#N/A
SCML2	<i>Scm polycomb group protein like 2</i>	19	20	0	0	39	0	0	0	0	0	#N/A
RDBP	<i>negative elongation factor complex member E</i>	18	26	0	0	44	0	0	0	0	0	#N/A
SON	<i>SON DNA binding protein</i>	18	16	0	0	34	0	0	0	0	0	#N/A
YLPM1	<i>YLP motif containing 1</i>	17	20	0	0	37	0	0	0	0	0	#N/A
EDC4	<i>enhancer of mRNA decapping 4</i>	17	24	0	0	41	0	0	0	0	0	#N/A

WDR70	<i>WD repeat domain 70</i>	17	14	0	0	31	0	0	0	0	0	#N/A
CHD8	<i>chromodomain helicase DNA binding protein 8</i>	17	29	0	0	46	0	0	0	0	0	#N/A
DDX10	<i>DEAD-box helicase 10</i>	16	12	0	0	28	0	0	0	0	0	#N/A
ORC2	<i>origin recognition complex subunit 2</i>	15	28	0	0	43	0	0	0	0	0	#N/A
RBM17	<i>RNA binding motif protein 17</i>	14	13	0	0	27	0	0	0	0	0	#N/A
WDR82	<i>WD repeat domain 82</i>	14	15	0	0	29	0	0	0	0	0	#N/A
WRNIP1	<i>WRN helicase interacting protein 1</i>	14	13	0	0	27	0	0	0	0	0	#N/A
SUGP1	<i>SURP and G-patch domain containing 1</i>	14	16	0	0	30	0	0	0	0	0	#N/A
ANAPC1	<i>anaphase promoting complex subunit 1</i>	14	12	0	0	26	0	0	0	0	0	#N/A
WDHD1	<i>WD repeat and HMG-box DNA binding protein 1</i>	14	13	0	0	27	0	0	0	0	0	#N/A
ZNF148	<i>zinc finger protein 148</i>	13	13	0	0	26	0	0	0	0	0	#N/A
GTF3C4	<i>general transcription factor IIIC subunit 4</i>	13	10	0	0	23	0	0	0	0	0	#N/A
EXOSC2	<i>exosome component 2</i>	13	19	0	0	32	0	0	0	0	0	#N/A
KEAP1	<i>kelch like ECH associated protein 1</i>	13	17	13	10	53	0	0	0	0	0	#N/A
SNW1	<i>SNW domain containing 1</i>	13	21	0	0	34	0	0	0	0	0	#N/A
ATRX	<i>ATRX chromatin remodeler</i>	12	19	0	0	31	0	0	0	0	0	#N/A
CHAMP1	<i>chromosome alignment maintaining phosphoprotein 1</i>	12	12	0	0	24	0	0	0	0	0	#N/A
CDCA2	<i>cell division cycle associated 2</i>	12	14	0	0	26	0	0	0	0	0	#N/A
POLH	<i>DNA polymerase eta</i>	12	13	0	0	25	0	0	0	0	0	#N/A
PHF3	<i>PHD finger protein 3</i>	12	25	0	0	37	0	0	0	0	0	#N/A
RPRD2	<i>regulation of nuclear pre-mRNA domain containing 2</i>	11	19	0	0	30	0	0	0	0	0	#N/A
RBM10	<i>RNA binding motif protein 10</i>	11	8	0	0	19	0	0	0	0	0	#N/A
ZNF638	<i>zinc finger protein 638</i>	11	11	0	0	22	0	0	0	0	0	#N/A
SUB1	<i>SUB1 regulator of transcription</i>	11	9	0	0	20	0	0	0	0	0	#N/A
NUP50	<i>nucleoporin 50</i>	11	14	0	0	25	0	0	0	0	0	#N/A
PES1	<i>pescadillo ribosomal biogenesis factor 1</i>	11	16	0	0	27	0	0	0	0	0	#N/A
PHAX	<i>phosphorylated adaptor for RNA export</i>	11	11	0	0	22	0	0	0	0	0	#N/A

SYNM	<i>synemin</i>	11	12	0	0	23	0	0	0	0	0	#N/A
PCM1	<i>pericentriolar material 1</i>	11	13	15	10	49	0	0	0	0	0	#N/A
BAZ1A	<i>bromodomain adjacent to zinc finger domain 1A</i>	11	21	0	0	32	0	0	0	0	0	#N/A
PHACTR4	<i>phosphatase and actin regulator 4</i>	10	12	2	0	24	0	0	0	0	0	#N/A
CDK11A	<i>cyclin dependent kinase 11A</i>	10	16	0	0	26	0	0	0	0	0	#N/A
CCDC99	<i>spindle apparatus coiled-coil protein 1</i>	10	14	0	0	24	0	0	0	0	0	#N/A
RBM26	<i>RNA binding motif protein 26</i>	10	8	0	0	18	0	0	0	0	0	#N/A
C19orf29	<i>cactin, spliceosome C complex subunit</i>	9	14	0	0	23	0	0	0	0	0	#N/A
GTF2F1	<i>general transcription factor IIF subunit 1</i>	9	8	0	0	17	0	0	0	0	0	#N/A
SYNPO	<i>synaptopodin</i>	9	12	0	0	21	0	0	0	0	0	#N/A
ZC3H14	<i>zinc finger CCCH-type containing 14</i>	9	9	0	2	20	0	0	0	0	0	#N/A
PGRMC2	<i>progesterone receptor membrane component 2</i>	9	9	12	14	44	0	0	0	0	0	#N/A
SNRPB2	<i>small nuclear ribonucleoprotein polypeptide B2</i>	9	6	0	0	15	0	0	0	0	0	#N/A
BPTF	<i>bromodomain PHD finger transcription factor</i>	9	9	0	0	18	0	0	0	0	0	#N/A
MBD3	<i>methyl-CpG binding domain protein 3</i>	9	11	0	0	20	0	0	0	0	0	#N/A
GTF2F2	<i>general transcription factor IIF subunit 2</i>	9	8	0	0	17	0	0	0	0	0	#N/A
PCNP	<i>PEST proteolytic signal containing nuclear protein</i>	9	8	0	0	17	0	0	0	0	0	#N/A
ANAPC5	<i>anaphase promoting complex subunit 5</i>	9	20	0	0	29	0	0	0	0	0	#N/A
HDGF	<i>heparin binding growth factor</i>	9	8	0	0	17	0	0	0	0	0	#N/A
PRPF40A	<i>pre-mRNA processing factor 40 homolog A</i>	8	10	0	0	18	0	0	0	0	0	#N/A
GATAD2A	<i>GATA zinc finger domain containing 2A</i>	8	9	0	0	17	0	0	0	0	0	#N/A
FIP1L1	<i>factor interacting with PAPOLA and CPSF1</i>	8	17	0	0	25	0	0	0	0	0	#N/A
WDR36	<i>WD repeat domain 36</i>	8	13	0	0	21	0	0	0	0	0	#N/A
HTATSF1	<i>HIV-1 Tat specific factor 1</i>	8	6	0	0	14	0	0	0	0	0	#N/A
MED1	<i>mediator complex subunit 1</i>	8	9	0	0	17	0	0	0	0	0	#N/A

SF3A3	<i>splicing factor 3a subunit 3</i>	8	9	0	0	17	0	0	0	0	0	#N/A
MTA1	<i>metastasis associated 1</i>	8	14	0	0	22	0	0	0	0	0	#N/A
SMARCC1	<i>SWI/SNF related, matrix associated, actin dependent regulator of chromatin subfamily c member 1</i>	8	7	0	0	15	0	0	0	0	0	#N/A
OGT	<i>O-linked N-acetylglucosamine (GlcNAc) transferase</i>	8	14	0	0	22	0	0	0	0	0	#N/A
MEF2D	<i>myocyte enhancer factor 2D</i>	8	9	0	0	17	0	0	0	0	0	#N/A
NOL8	<i>nucleolar protein 8</i>	7	11	0	0	18	0	0	0	0	0	#N/A
TFIP11	<i>tuftelin interacting protein 11</i>	7	5	0	0	12	0	0	0	0	0	#N/A
SAP30BP	<i>SAP30 binding protein</i>	7	0	0	0	7	0	0	0	0	0	#N/A
BRD4	<i>bromodomain containing 4</i>	7	10	0	0	17	0	0	0	0	0	#N/A
LARP1B	<i>La ribonucleoprotein domain family member 1B</i>	7	5	0	0	12	0	0	0	0	0	#N/A
POLA1	<i>DNA polymerase alpha 1, catalytic subunit</i>	6	13	0	0	19	0	0	0	0	0	#N/A
SPAG7	<i>sperm associated antigen 7</i>	6	6	0	0	12	0	0	0	0	0	#N/A
SF3B5	<i>splicing factor 3b subunit 5</i>	6	0	0	0	6	0	0	0	0	0	#N/A
NACC1	<i>nucleus accumbens associated 1</i>	6	7	0	0	13	0	0	0	0	0	#N/A
ESF1	<i>ESF1 nucleolar pre-rRNA processing protein homolog</i>	6	8	0	0	14	0	0	0	0	0	#N/A
UBE2O	<i>ubiquitin conjugating enzyme E2 O</i>	6	9	0	0	15	0	0	0	0	0	#N/A
URB1	<i>URB1 ribosome biogenesis homolog</i>	6	9	0	0	15	0	0	0	0	0	#N/A
TP53BP1	<i>tumor protein p53 binding protein 1</i>	6	10	0	0	16	0	0	0	0	0	#N/A
SIN3A	<i>SIN3 transcription regulator family member A</i>	6	11	0	0	17	0	0	0	0	0	#N/A
PPP4R2	<i>protein phosphatase 4 regulatory subunit 2</i>	6	7	0	0	13	0	0	0	0	0	#N/A
NBN	<i>nibrin</i>	6	4	0	0	10	0	0	0	0	0	#N/A
RBBP6	<i>RB binding protein 6, ubiquitin ligase</i>	6	6	0	0	12	0	0	0	0	0	#N/A
RNF20	<i>ring finger protein 20</i>	6	9	0	0	15	0	0	0	0	0	#N/A
PAF1	<i>PAF1 homolog, Paf1/RNA polymerase II complex component</i>	6	8	0	0	14	0	0	0	0	0	#N/A
CDC73	<i>cell division cycle 73</i>	6	11	0	0	17	0	0	0	0	0	#N/A

DHX8	<i>DEAH-box helicase 8</i>	6	7	0	0	13	0	0	0	0	0	#N/A
DNTTIP2	<i>deoxynucleotidyltransferase terminal interacting protein 2</i>	6	12	0	0	18	0	0	0	0	0	#N/A
HP1BP3	<i>heterochromatin protein 1 binding protein 3</i>	6	5	0	0	11	0	0	0	0	0	#N/A
C11orf58	<i>chromosome 11 open reading frame 58</i>	6	4	0	0	10	0	0	0	0	0	#N/A
BOD1L	<i>biorientation of chromosomes in cell division 1 like 1</i>	6	11	0	0	17	0	0	0	0	0	#N/A
CDKN2A1P	<i>CDKN2A interacting protein</i>	6	8	0	0	14	0	0	0	0	0	#N/A
FAM208A	<i>transcription activation suppressor</i>	6	5	0	0	11	0	0	0	0	0	#N/A
CSNK2A1	<i>casein kinase 2 alpha 1</i>	6	14	0	0	20	0	0	0	0	0	#N/A
LMO7	<i>LIM domain 7</i>	6	7	0	2	15	0	0	0	0	0	#N/A
GTF2A1	<i>general transcription factor IIA subunit 1</i>	6	6	0	0	12	0	0	0	0	0	#N/A
PABPN1	<i>poly(A) binding protein nuclear 1</i>	6	4	0	0	10	0	0	0	0	0	#N/A
CDC23	<i>cell division cycle 23</i>	5	8	0	0	13	0	0	0	0	0	#N/A
ZNF318	<i>zinc finger protein 318</i>	5	8	0	0	13	0	0	0	0	0	#N/A
MDC1	<i>mediator of DNA damage checkpoint 1</i>	5	12	0	0	17	0	0	0	0	0	#N/A
PRRC2A	<i>proline rich coiled-coil 2A</i>	5	4	0	0	9	0	0	0	0	0	#N/A
SENP6	<i>SUMO specific peptidase 6</i>	5	12	0	0	17	0	0	0	0	0	#N/A
MASTL	<i>microtubule associated serine/threonine kinase like</i>	5	6	0	0	11	0	0	0	0	0	#N/A
EXOSC6	<i>exosome component 6</i>	5	0	0	0	5	0	0	0	0	0	#N/A
CPSF7	<i>cleavage and polyadenylation specific factor 7</i>	5	7	0	0	12	0	0	0	0	0	#N/A
GATAD2B	<i>GATA zinc finger domain containing 2B</i>	5	6	0	0	11	0	0	0	0	0	#N/A
ZBTB9	<i>zinc finger and BTB domain containing 9</i>	5	6	0	0	11	0	0	0	0	0	#N/A
BRIP1	<i>BRCA1 interacting protein C-terminal helicase 1</i>	5	12	0	0	17	0	0	0	0	0	#N/A
EXOSC8	<i>exosome component 8</i>	5	4	0	0	9	0	0	0	0	0	#N/A
SRRM1	<i>serine and arginine repetitive matrix 1</i>	5	4	0	0	9	0	0	0	0	0	#N/A
CSNK2A2	<i>casein kinase 2 alpha 2</i>	5	7	0	0	12	0	0	0	0	0	#N/A

FAU	<i>FAU ubiquitin like and ribosomal protein S30 fusion</i>	5	6	0	0	11	0	0	0	0	0	#N/A
NCBP1	<i>nuclear cap binding protein subunit 1</i>	5	3	0	0	8	0	0	0	0	0	#N/A
PPP4C	<i>protein phosphatase 4 catalytic subunit</i>	5	6	0	0	11	0	0	0	0	0	#N/A
PEX14	<i>peroxisomal biogenesis factor 14</i>	5	5	4	4	18	0	0	0	0	0	#N/A
C9orf78	<i>chromosome 9 open reading frame 78</i>	5	3	0	0	8	0	0	0	0	0	#N/A
NUP107	<i>nucleoporin 107</i>	5	10	0	0	15	0	0	0	0	0	#N/A
PDS5A	<i>PDS5 cohesin associated factor A</i>	5	8	0	0	13	0	0	0	0	0	#N/A
CDV3	<i>CDV3 homolog</i>	5	6	0	0	11	0	0	0	0	0	#N/A
SKA3	<i>spindle and kinetochore associated complex subunit 3</i>	5	4	0	0	9	0	0	0	0	0	#N/A
LARP4	<i>La ribonucleoprotein domain family member 4</i>	5	7	0	0	12	0	0	0	0	0	#N/A
PPIL1	<i>peptidylprolyl isomerase like 1</i>	5	5	0	0	10	0	0	0	0	0	#N/A
PSME2	<i>proteasome activator subunit 2</i>	5	4	0	0	9	0	0	0	0	0	#N/A
BTF3	<i>basic transcription factor 3</i>	5	10	0	0	15	0	0	0	0	0	#N/A
TMSB10	<i>thymosin beta 10</i>	5	0	0	0	5	0	0	0	0	0	#N/A
HIVEP1	<i>human immunodeficiency virus type 1 enhancer binding protein 1</i>	4	6	0	0	10	0	0	0	0	0	#N/A
SRRM2	<i>serine/arginine repetitive matrix 2</i>	4	2	0	0	6	0	0	0	0	0	#N/A
TAF7	<i>TATA-box binding protein associated factor 7</i>	4	5	0	0	9	0	0	0	0	0	#N/A
RSBN1L	<i>round spermatid basic protein 1 like</i>	4	0	0	0	4	0	0	0	0	0	#N/A
TOP2B	<i>DNA topoisomerase II beta</i>	4	10	0	0	14	0	0	0	0	0	#N/A
C11orf30	<i>EMSY transcriptional repressor, BRCA2 interacting</i>	4	9	0	0	13	0	0	0	0	0	#N/A
NSFL1C	<i>NSFL1 cofactor</i>	4	7	0	0	11	0	0	0	0	0	#N/A
PPIL4	<i>peptidylprolyl isomerase like 4</i>	4	0	0	0	4	0	0	0	0	0	#N/A
LTV1	<i>LTV1 ribosome biogenesis factor</i>	4	4	0	0	8	0	0	0	0	0	#N/A
WDR12	<i>WD repeat domain 12</i>	4	4	0	0	8	0	0	0	0	0	#N/A
RNF40	<i>ring finger protein 40</i>	4	5	0	0	9	0	0	0	0	0	#N/A
AKAP1	<i>A-kinase anchoring protein 1</i>	4	2	0	0	6	0	0	0	0	0	#N/A
NFIC	<i>nuclear factor I C</i>	4	0	0	0	4	0	0	0	0	0	#N/A

CDCA8	<i>cell division cycle associated 8</i>	4	4	0	0	8	0	0	0	0	0	#N/A
GLYR1	<i>glyoxylate reductase 1 homolog</i>	4	9	0	0	13	0	0	0	0	0	#N/A
VBP1	<i>VHL binding protein 1</i>	4	4	0	0	8	0	0	0	0	0	#N/A
NARS	<i>asparaginyl-tRNA synthetase</i>	4	3	0	0	7	0	0	0	0	0	#N/A
PRKAR2A	<i>protein kinase cAMP-dependent type II regulatory subunit alpha</i>	4	5	0	0	9	0	0	0	0	0	#N/A
PUS7	<i>pseudouridine synthase 7</i>	4	9	0	0	13	0	0	0	0	0	#N/A
AFF4	<i>AF4/FMR2 family member 4</i>	4	2	0	0	6	0	0	0	0	0	#N/A
RPRD1B	<i>regulation of nuclear pre-mRNA domain containing 1B</i>	4	5	0	0	9	0	0	0	0	0	#N/A
PALM2-AKAP2	<i>PALM2-AKAP2 fusion</i>	4	12	0	0	16	0	0	0	0	0	#N/A
TPM1	<i>tropomyosin 1</i>	4	3	0	0	7	0	0	0	0	0	#N/A
TXLNG	<i>taxilin gamma</i>	4	0	0	0	4	0	0	0	0	0	#N/A
ZHX3	<i>zinc fingers and homeoboxes 3</i>	4	6	0	0	10	0	0	0	0	0	#N/A
WDR44	<i>WD repeat domain 44</i>	4	4	0	0	8	0	0	0	0	0	#N/A
CDK9	<i>cyclin dependent kinase 9</i>	4	5	0	0	9	0	0	0	0	0	#N/A
FXR2	<i>FMR1 autosomal homolog 2</i>	4	8	0	0	12	0	0	0	0	0	#N/A
QSER1	<i>glutamine and serine rich 1</i>	4	8	0	0	12	0	0	0	0	0	#N/A
CWC15	<i>CWC15 spliceosome associated protein homolog</i>	4	8	0	0	12	0	0	0	0	0	#N/A
KDM2A	<i>lysine demethylase 2A</i>	4	3	0	0	7	0	0	0	0	0	#N/A
DCP1A	<i>decapping mRNA 1A</i>	4	6	0	0	10	0	0	0	0	0	#N/A
ANP32B	<i>acidic nuclear phosphoprotein 32 family member B</i>	4	7	0	0	11	0	0	0	0	0	#N/A
FAM21A	<i>WASH complex subunit 2A</i>	4	0	4	0	8	0	0	0	0	0	#N/A
ASF1B	<i>anti-silencing function 1B histone chaperone</i>	4	3	0	0	7	0	0	0	0	0	#N/A
CCDC168	<i>coiled-coil domain containing 168</i>	4	2	0	0	6	0	0	0	0	0	#N/A
PRIM2	<i>DNA primase subunit 2</i>	4	4	0	0	8	0	0	0	0	0	#N/A
ANLN	<i>anillin actin binding protein</i>	4	6	0	0	10	0	0	0	0	0	#N/A
KPNA4	<i>karyopherin subunit alpha 4</i>	4	0	0	0	4	0	0	0	0	0	#N/A
BRMS1L	<i>BRMS1 like transcriptional repressor</i>	4	5	0	0	9	0	0	0	0	0	#N/A
MAPRE1	<i>microtubule associated protein</i>	4	4	0	0	8	0	0	0	0	0	#N/A

RP/EB family member 1

GTF2E1	<i>general transcription factor IIE subunit 1</i>	4	8	0	0	12	0	0	0	0	0	#N/A
COPS3	<i>COP9 signalosome subunit 3</i>	4	0	0	0	4	0	0	0	0	0	#N/A
PRPF3	<i>pre-mRNA processing factor 3</i>	4	3	0	0	7	0	0	0	0	0	#N/A
SALL4	<i>spalt like transcription factor 4</i>	3	8	0	0	11	0	0	0	0	0	#N/A
EIF3K	<i>eukaryotic translation initiation factor 3 subunit K</i>	3	3	0	0	6	0	0	0	0	0	#N/A
GNB4	<i>G protein subunit beta 4</i>	3	0	0	0	3	0	0	0	0	0	#N/A
PHC3	<i>polyhomeotic homolog 3</i>	3	0	0	0	3	0	0	0	0	0	#N/A
RBM33	<i>RNA binding motif protein 33</i>	3	5	0	0	8	0	0	0	0	0	#N/A
GPKOW	<i>G-patch domain and KOW motifs</i>	3	6	0	0	9	0	0	0	0	0	#N/A
EIF4E	<i>eukaryotic translation initiation factor 4E</i>	3	2	0	0	5	0	0	0	0	0	#N/A
SETD2	<i>SET domain containing 2, histone lysine methyltransferase</i>	3	2	0	0	5	0	0	0	0	0	#N/A
TRMT6	<i>tRNA methyltransferase 6</i>	3	3	0	0	6	0	0	0	0	0	#N/A
NSD1	<i>nuclear receptor binding SET domain protein 1</i>	3	0	0	0	3	0	0	0	0	0	#N/A
PRMT5	<i>protein arginine methyltransferase 5</i>	3	5	0	0	8	0	0	0	0	0	#N/A
SEPT10	<i>septin10</i>	3	3	0	0	6	0	0	0	0	0	#N/A
NCOR1	<i>nuclear receptor corepressor 1</i>	3	5	0	0	8	0	0	0	0	0	#N/A
FTSJD2	<i>cap methyltransferase 1</i>	3	3	0	0	6	0	0	0	0	0	#N/A
ZNF280C	<i>zinc finger protein 280C</i>	3	0	0	0	3	0	0	0	0	0	#N/A
PRPF38A	<i>pre-mRNA processing factor 38A</i>	3	2	0	0	5	0	0	0	0	0	#N/A
DHX16	<i>DEAH-box helicase 16</i>	3	3	0	0	6	0	0	0	0	0	#N/A
ATAD5	<i>ATPase family AAA domain containing 5</i>	3	5	0	0	8	0	0	0	0	0	#N/A
UBAP1	<i>ubiquitin associated protein 1</i>	3	5	0	0	8	0	0	0	0	0	#N/A
EPB41L1	<i>erythrocyte membrane protein band 4.1 like 1</i>	3	2	0	0	5	0	0	0	0	0	#N/A
DVL1	<i>dishevelled segment polarity protein 1</i>	3	4	0	0	7	0	0	0	0	0	#N/A
EP400	<i>E1A binding protein p400</i>	3	8	0	0	11	0	0	0	0	0	#N/A
RPA3	<i>replication protein A3</i>	3	0	0	0	3	0	0	0	0	0	#N/A

MFAP1	<i>microfibril associated protein 1</i>	3	2	0	0	5	0	0	0	0	0	#N/A
CFDP1	<i>craniofacial development protein 1</i>	3	6	0	0	9	0	0	0	0	0	#N/A
ZNF281	<i>zinc finger protein 281</i>	3	6	0	0	9	0	0	0	0	0	#N/A
USP47	<i>ubiquitin specific peptidase 47</i>	3	2	0	0	5	0	0	0	0	0	#N/A
KIAA0664	<i>clustered mitochondria homolog</i>	3	2	0	0	5	0	0	0	0	0	#N/A
LYPLA2	<i>lysophospholipase 2</i>	3	7	0	0	10	0	0	0	0	0	#N/A
SRSF10	<i>serine and arginine rich splicing factor 10</i>	3	0	0	0	3	0	0	0	0	0	#N/A
ZFR	<i>zinc finger RNA binding protein</i>	3	11	0	0	14	0	0	0	0	0	#N/A
TOR1AIP1	<i>torsin 1A interacting protein 1</i>	3	3	0	0	6	0	0	0	0	0	#N/A
FAM50A	<i>family with sequence similarity 50 member A</i>	3	0	0	0	3	0	0	0	0	0	#N/A
CUL4B	<i>cullin 4B</i>	3	2	0	0	5	0	0	0	0	0	#N/A
WDR83	<i>WD repeat domain 83</i>	3	0	0	0	3	0	0	0	0	0	#N/A
PEX5	<i>peroxisomal biogenesis factor 5</i>	3	5	0	0	8	0	0	0	0	0	#N/A
COIL	<i>coilin</i>	3	4	0	0	7	0	0	0	0	0	#N/A
CC2D1A	<i>coiled-coil and C2 domain containing 1A</i>	3	3	0	0	6	0	0	0	0	0	#N/A
RPP38	<i>ribonuclease P/MRP subunit p38</i>	3	5	0	0	8	0	0	0	0	0	#N/A
DIS3L	<i>DIS3 like exosome 3'-5' exoribonuclease</i>	3	0	0	0	3	0	0	0	0	0	#N/A
PPF1BP1	<i>PPF1A binding protein 1</i>	3	4	0	0	7	0	0	0	0	0	#N/A
ZCCHC8	<i>zinc finger CCHC-type containing 8</i>	3	7	0	0	10	0	0	0	0	0	#N/A
STAG2	<i>stromal antigen 2</i>	3	7	0	0	10	0	0	0	0	0	#N/A
CIRBP	<i>cold inducible RNA binding protein</i>	3	0	0	0	3	0	0	0	0	0	#N/A
CBX5	<i>chromobox 5</i>	3	3	0	0	6	0	0	0	0	0	#N/A
UTP3	<i>UTP3 small subunit processome component</i>	3	2	0	0	5	0	0	0	0	0	#N/A
ADAMTS L4	<i>ADAMTS like 4</i>	3	0	0	0	3	0	0	0	0	0	#N/A
NPLOC4	<i>NPL4 homolog, ubiquitin recognition factor</i>	3	0	0	0	3	0	0	0	0	0	#N/A
SREK1	<i>splicing regulatory glutamic acid and lysine rich protein 1</i>	3	0	0	0	3	0	0	0	0	0	#N/A
MNAT1	<i>MNAT1 component of CDK</i>	3	5	0	0	8	0	0	0	0	0	#N/A

<i>activating kinase</i>												
INCENP	<i>inner centromere protein</i>	3	6	0	0	9	0	0	0	0	0	#N/A
STBD1	<i>starch binding domain 1</i>	3	3	8	7	21	0	0	0	0	0	#N/A
SNRNP40	<i>small nuclear ribonucleoprotein U5 subunit 40</i>	2	4	0	0	6	0	0	0	0	0	#N/A
APC	<i>APC regulator of WNT signaling pathway</i>	2	4	5	3	14	0	0	0	0	0	#N/A
AHCYL2	<i>adenosylhomocysteinase like 2</i>	2	0	0	0	2	0	0	0	0	0	#N/A
RAB3GAP2	<i>RAB3 GTPase activating non-catalytic protein subunit 2</i>	2	4	0	0	6	0	0	0	0	0	#N/A
TAF9B	<i>TATA-box binding protein associated factor 9b</i>	2	2	0	0	4	0	0	0	0	0	#N/A
TCEB3	<i>elongin A</i>	2	2	0	0	4	0	0	0	0	0	#N/A
PPP1R12A	<i>protein phosphatase 1 regulatory subunit 12A</i>	2	5	0	2	9	0	0	0	0	0	#N/A
ARPC2	<i>actin related protein 2/3 complex subunit 2</i>	2	0	0	0	2	0	0	0	0	0	#N/A
UBA1	<i>ubiquitin like modifier activating enzyme 1</i>	2	7	0	0	9	0	0	0	0	0	#N/A
LENG8	<i>leukocyte receptor cluster member 8</i>	2	5	0	0	7	0	0	0	0	0	#N/A
NFKB1	<i>nuclear factor kappa B subunit 1</i>	2	0	0	0	2	0	0	0	0	0	#N/A
SLU7	<i>SLU7 homolog, splicing factor</i>	2	9	0	0	11	0	0	0	0	0	#N/A
C15orf63	<i>huntingtin interacting protein K</i>	2	2	0	0	4	0	0	0	0	0	#N/A
BCAR1	<i>BCAR1 scaffold protein, Cas family member</i>	2	0	0	0	2	0	0	0	0	0	#N/A
CCDC50	<i>coiled-coil domain containing 50</i>	2	0	0	0	2	0	0	0	0	0	#N/A
PFAS	<i>phosphoribosylformylglycinamide synthase</i>	2	3	0	0	5	0	0	0	0	0	#N/A
COPS8	<i>COP9 signalosome subunit 8</i>	2	0	0	0	2	0	0	0	0	0	#N/A
ZRANB2	<i>zinc finger RANBP2-type containing 2</i>	2	0	0	0	2	0	0	0	0	0	#N/A
TYMS	<i>thymidylate synthetase</i>	2	0	0	0	2	0	0	0	0	0	#N/A
RBM25	<i>RNA binding motif protein 25</i>	2	4	0	0	6	0	0	0	0	0	#N/A
BAZ2A	<i>bromodomain adjacent to zinc finger domain 2A</i>	2	6	0	0	8	0	0	0	0	0	#N/A
SRGAP2	<i>SLIT-ROBO Rho GTPase activating protein 2</i>	2	0	0	0	2	0	0	0	0	0	#N/A

PHF2	<i>PHD finger protein 2</i>	2	2	0	0	4	0	0	0	0	0	#N/A
EIF4G3	<i>eukaryotic translation initiation factor 4 gamma 3</i>	2	0	0	0	2	0	0	0	0	0	#N/A
HARS	<i>histidyl-tRNA synthetase</i>	2	11	3	0	16	0	0	0	0	0	#N/A
MORF4L1	<i>mortality factor 4 like 1</i>	2	0	0	0	2	0	0	0	0	0	#N/A
CCNL2	<i>cyclin L2</i>	2	6	0	0	8	0	0	0	0	0	#N/A
GTF3C1	<i>general transcription factor III C subunit 1</i>	2	6	0	0	8	0	0	0	0	0	#N/A
LARP7	<i>La ribonucleoprotein domain family member 7</i>	2	5	0	0	7	0	0	0	0	0	#N/A
DNAJC9	<i>DnaJ heat shock protein family (Hsp40) member C9</i>	2	0	0	0	2	0	0	0	0	0	#N/A
WBP11	<i>WW domain binding protein 11</i>	2	0	0	0	2	0	0	0	0	0	#N/A
FLYWCH 2	<i>FLYWCH family member 2</i>	2	0	0	0	2	0	0	0	0	0	#N/A
PPIL3	<i>peptidylprolyl isomerase like 3</i>	2	0	0	0	2	0	0	0	0	0	#N/A
SARNP	<i>SAP domain containing ribonucleoprotein</i>	2	0	0	0	2	0	0	0	0	0	#N/A
GPATCH1	<i>G-patch domain containing 1</i>	2	6	0	0	8	0	0	0	0	0	#N/A
STAT5B	<i>signal transducer and activator of transcription 5B</i>	2	0	0	0	2	0	0	0	0	0	#N/A
CRTC1	<i>CREB regulated transcription coactivator 1</i>	2	5	0	0	7	0	0	0	0	0	#N/A
RRP12	<i>ribosomal RNA processing 12 homolog</i>	2	0	0	0	2	0	0	0	0	0	#N/A
RACGAP1	<i>Rac GTPase activating protein 1</i>	2	7	0	0	9	0	0	0	0	0	#N/A
COPS7A	<i>COP9 signalosome subunit 7A</i>	2	2	0	0	4	0	0	0	0	0	#N/A
SNRPA	<i>small nuclear ribonucleoprotein polypeptide A</i>	2	3	0	0	5	0	0	0	0	0	#N/A
GPX4	<i>glutathione peroxidase 4</i>	2	0	0	0	2	0	0	0	0	0	#N/A
FARSB	<i>phenylalanyl-tRNA synthetase subunit beta</i>	2	4	0	0	6	0	0	0	0	0	#N/A
TRIM33	<i>tripartite motif containing 33</i>	2	0	0	0	2	0	0	0	0	0	#N/A
RTF1	<i>RTF1 homolog, Paf1/RNA polymerase II complex component</i>	2	4	0	0	6	0	0	0	0	0	#N/A
PMS1	<i>PMS1 homolog 1, mismatch repair system component</i>	2	5	0	0	7	0	0	0	0	0	#N/A
BAZ2B	<i>bromodomain adjacent to zinc finger domain 2B</i>	2	0	0	0	2	0	0	0	0	0	#N/A

PRPS1	<i>phosphoribosyl pyrophosphate synthetase 1</i>	2	4	0	0	6	0	0	0	0	0	#N/A
LIG3	<i>DNA ligase 3</i>	2	0	0	0	2	0	0	0	0	0	#N/A
EIF3C	<i>eukaryotic translation initiation factor 3 subunit C</i>	0	20	0	0	20	0	0	0	0	0	#N/A
TOP3B	<i>DNA topoisomerase III beta</i>	0	11	0	0	11	0	0	0	0	0	#N/A
RC3H2	<i>ring finger and CCCH-type domains 2</i>	0	9	0	0	9	0	0	0	0	0	#N/A
MLL	<i>lysine methyltransferase 2A</i>	0	8	0	0	8	0	0	0	0	0	#N/A
SRP54	<i>signal recognition particle 54</i>	0	8	0	0	8	0	0	0	0	0	#N/A
INADL	<i>PATJ crumbs cell polarity complex component</i>	0	7	0	0	7	0	0	0	0	0	#N/A
GLTSCR2	<i>NOP53 ribosome biogenesis factor</i>	0	7	0	0	7	0	0	0	0	0	#N/A
HEXIM1	<i>HEXIM P-TEFb complex subunit 1</i>	0	7	0	0	7	0	0	0	0	0	#N/A
PPP1CC	<i>protein phosphatase 1 catalytic subunit gamma</i>	0	7	0	0	7	0	0	0	0	0	#N/A
ZMYM1	<i>zinc finger MYM-type containing 1</i>	0	6	0	0	6	0	0	0	0	0	#N/A
MTAP	<i>methylthioadenosine phosphorylase</i>	0	6	0	0	6	0	0	0	0	0	#N/A
CHD7	<i>chromodomain helicase DNA binding protein 7</i>	0	6	0	0	6	0	0	0	0	0	#N/A
ZC3H4	<i>zinc finger CCCH-type containing 4</i>	0	5	0	0	5	0	0	0	0	0	#N/A
CLIC1	<i>chloride intracellular channel 1</i>	0	5	0	0	5	0	0	0	0	0	#N/A
CCNK	<i>cyclin K</i>	0	5	0	0	5	0	0	0	0	0	#N/A
RBBP4	<i>RB binding protein 4, chromatin remodeling factor</i>	0	5	0	0	5	0	0	0	0	0	#N/A
POP1	<i>POP1 homolog, ribonuclease P/MRP subunit</i>	0	5	0	0	5	0	0	0	0	0	#N/A
RIOK1	<i>RIO kinase 1</i>	0	5	0	0	5	0	0	0	0	0	#N/A
NCOR2	<i>nuclear receptor corepressor 2</i>	0	5	0	0	5	0	0	0	0	0	#N/A
YEATS2	<i>YEATS domain containing 2</i>	0	5	0	0	5	0	0	0	0	0	#N/A
RANBP9	<i>RAN binding protein 9</i>	0	5	0	0	5	0	0	0	0	0	#N/A
ANAPC4	<i>anaphase promoting complex subunit 4</i>	0	5	0	0	5	0	0	0	0	0	#N/A
LIN54	<i>lin-54 DREAM MuvB core complex component</i>	0	5	0	0	5	0	0	0	0	0	#N/A
WAC	<i>WW domain containing adaptor with coiled-coil</i>	0	5	0	0	5	0	0	0	0	0	#N/A

HMGA1	<i>high mobility group AT-hook 1</i>	0	5	0	0	5	0	0	0	0	0	#N/A
DAZAP1	<i>DAZ associated protein 1</i>	0	5	0	0	5	0	0	0	0	0	#N/A
UBFD1	<i>ubiquitin family domain containing 1</i>	0	5	0	0	5	0	0	0	0	0	#N/A
WDR75	<i>WD repeat domain 75</i>	0	5	0	0	5	0	0	0	0	0	#N/A
CHMP5	<i>charged multivesicular body protein 5</i>	0	5	0	0	5	0	0	0	0	0	#N/A
GAR1	<i>GAR1 ribonucleoprotein</i>	0	5	0	0	5	0	0	0	0	0	#N/A
TRIP12	<i>thyroid hormone receptor interactor 12</i>	0	4	0	0	4	0	0	0	0	0	#N/A
PRKCI	<i>protein kinase C iota</i>	0	4	0	0	4	0	0	0	0	0	#N/A
WIZ	<i>WIZ zinc finger</i>	0	4	0	0	4	0	0	0	0	0	#N/A
NOL6	<i>nucleolar protein 6</i>	0	4	0	0	4	0	0	0	0	0	#N/A
DEPDC1B	<i>DEP domain containing 1B</i>	0	4	0	0	4	0	0	0	0	0	#N/A
PCMT1	<i>protein-L-isoaspartate (D-aspartate) O-methyltransferase</i>	0	4	0	0	4	0	0	0	0	0	#N/A
POGZ	<i>pogo transposable element derived with ZNF domain</i>	0	4	0	0	4	0	0	0	0	0	#N/A
MPHOSP H10	<i>M-phase phosphoprotein 10</i>	0	4	0	0	4	0	0	0	0	0	#N/A
PPP1R2	<i>protein phosphatase 1 regulatory inhibitor subunit 2</i>	0	4	0	0	4	0	0	0	0	0	#N/A
TMOD3	<i>tropomodulin 3</i>	0	4	0	0	4	0	0	0	0	0	#N/A
CTR9	<i>CTR9 homolog, Paf1/RNA polymerase II complex component</i>	0	4	0	0	4	0	0	0	0	0	#N/A
CNOT7	<i>CCR4-NOT transcription complex subunit 7</i>	0	4	0	0	4	0	0	0	0	0	#N/A
ANP32E	<i>acidic nuclear phosphoprotein 32 family member E</i>	0	4	0	0	4	0	0	0	0	0	#N/A
REPS1	<i>RALBP1 associated Eps domain containing 1</i>	0	4	0	0	4	0	0	0	0	0	#N/A
CSNK1D	<i>casein kinase 1 delta</i>	0	4	0	0	4	0	0	0	0	0	#N/A
ARHGAP 21	<i>Rho GTPase activating protein 21</i>	0	4	0	0	4	0	0	0	0	0	#N/A
MICAL3	<i>microtubule associated monooxygenase, calponin and LIM domain containing 3</i>	0	4	0	0	4	0	0	0	0	0	#N/A
GCFC1	<i>PAX3 and PAX7 binding protein 1</i>	0	4	0	0	4	0	0	0	0	0	#N/A

ZNF644	<i>zinc finger protein 644</i>	0	4	0	0	4	0	0	0	0	0	#N/A
SRFBP1	<i>serum response factor binding protein 1</i>	0	4	0	0	4	0	0	0	0	0	#N/A
NCOA7	<i>nuclear receptor coactivator 7</i>	0	4	0	0	4	0	0	0	0	0	#N/A
FAM135A	<i>family with sequence similarity 135 member A</i>	0	4	0	0	4	0	0	0	0	0	#N/A
NCOA6	<i>nuclear receptor coactivator 6</i>	0	4	0	0	4	0	0	0	0	0	#N/A
RPA2	<i>replication protein A2</i>	0	4	0	0	4	0	0	0	0	0	#N/A
KPNA3	<i>karyopherin subunit alpha 3</i>	0	4	0	0	4	0	0	0	0	0	#N/A
EIF3J	<i>eukaryotic translation initiation factor 3 subunit J</i>	0	4	0	0	4	0	0	0	0	0	#N/A
ELAC2	<i>elaC ribonuclease Z 2</i>	0	4	0	0	4	0	0	0	0	0	#N/A
ZNF131	<i>zinc finger protein 131</i>	0	4	0	0	4	0	0	0	0	0	#N/A
ACTL6A	<i>actin like 6A</i>	0	4	0	0	4	0	0	0	0	0	#N/A
IK	<i>IK cytokine</i>	0	4	0	0	4	0	0	0	0	0	#N/A
RFX1	<i>regulatory factor X1</i>	0	4	0	0	4	0	0	0	0	0	#N/A
INTS3	<i>integrator complex subunit 3</i>	0	4	0	0	4	0	0	0	0	0	#N/A
CHMP7	<i>charged multivesicular body protein 7</i>	0	4	0	0	4	0	0	0	0	0	#N/A
NRBF2	<i>nuclear receptor binding factor 2</i>	0	4	0	0	4	0	0	0	0	0	#N/A
C19orf43	<i>telomerase RNA component interacting RNase</i>	0	3	0	0	3	0	0	0	0	0	#N/A
MTMR6	<i>myotubularin related protein 6</i>	0	3	0	0	3	0	0	0	0	0	#N/A
THOC3	<i>THO complex 3</i>	0	3	0	0	3	0	0	0	0	0	#N/A
WDR62	<i>WD repeat domain 62</i>	0	3	0	0	3	0	0	0	0	0	#N/A
FNBP4	<i>formin binding protein 4</i>	0	3	0	0	3	0	0	0	0	0	#N/A
LSM14A	<i>LSM14A mRNA processing body assembly factor</i>	0	3	0	0	3	0	0	0	0	0	#N/A
BBX	<i>BBX high mobility group box domain containing</i>	0	3	0	0	3	0	0	0	0	0	#N/A
DDX41	<i>DEAD-box helicase 41</i>	0	3	0	0	3	0	0	0	0	0	#N/A
TAF6	<i>TATA-box binding protein associated factor 6</i>	0	3	0	0	3	0	0	0	0	0	#N/A
BTAF1	<i>B-TFIID TATA-box binding protein associated factor 1</i>	0	3	0	0	3	0	0	0	0	0	#N/A
POLDIP3	<i>DNA polymerase delta interacting protein 3</i>	0	3	0	0	3	0	0	0	0	0	#N/A

COPS5	<i>COP9 signalosome subunit 5</i>	0	3	0	0	3	0	0	0	0	0	#N/A
NOSIP	<i>nitric oxide synthase interacting protein</i>	0	3	0	0	3	0	0	0	0	0	#N/A
DCP1B	<i>decapping mRNA 1B</i>	0	3	0	0	3	0	0	0	0	0	#N/A
PMS2	<i>PMS1 homolog 2, mismatch repair system component</i>	0	3	0	0	3	0	0	0	0	0	#N/A
EXOSC5	<i>exosome component 5</i>	0	3	0	0	3	0	0	0	0	0	#N/A
UBA2	<i>ubiquitin like modifier activating enzyme 2</i>	0	3	0	0	3	0	0	0	0	0	#N/A
TSG101	<i>tumor susceptibility 101</i>	0	3	2	0	5	0	0	0	0	0	#N/A
ARID2	<i>AT-rich interaction domain 2</i>	0	3	0	0	3	0	0	0	0	0	#N/A
IRAK1	<i>interleukin 1 receptor associated kinase 1</i>	0	3	0	0	3	0	0	0	0	0	#N/A
EFTUD1	<i>elongation factor like GTPase 1</i>	0	3	0	0	3	0	0	0	0	0	#N/A
YTHDF3	<i>YTH N6-methyladenosine RNA binding protein 3</i>	0	3	0	0	3	0	0	0	0	0	#N/A
CLASP1	<i>cytoplasmic linker associated protein 1</i>	0	3	0	0	3	0	0	0	0	0	#N/A
CRTC3	<i>CREB regulated transcription coactivator 3</i>	0	3	0	0	3	0	0	0	0	0	#N/A
CDK12	<i>cyclin dependent kinase 12</i>	0	3	0	0	3	0	0	0	0	0	#N/A
PAPOLG	<i>poly(A) polymerase gamma</i>	0	3	0	0	3	0	0	0	0	0	#N/A
PRUNE	<i>prune exopolyphosphatase 1</i>	0	3	0	0	3	0	0	0	0	0	#N/A
POLR2B	<i>RNA polymerase II subunit B</i>	0	3	0	0	3	0	0	0	0	0	#N/A
LARP4B	<i>La ribonucleoprotein domain family member 4B</i>	0	3	0	0	3	0	0	0	0	0	#N/A
DHX38	<i>DEAH-box helicase 38</i>	0	3	0	0	3	0	0	0	0	0	#N/A
SUDS3	<i>SDS3 homolog, SIN3A corepressor complex component</i>	0	3	0	0	3	0	0	0	0	0	#N/A
C16orf88	<i>lysine rich nucleolar protein 1</i>	0	3	0	0	3	0	0	0	0	0	#N/A
TFCP2	<i>transcription factor CP2</i>	0	3	0	0	3	0	0	0	0	0	#N/A
CALM2	<i>calmodulin 2</i>	0	3	0	0	3	0	0	0	0	0	#N/A
CSNK2B	<i>casein kinase 2 beta</i>	0	3	0	0	3	0	0	0	0	0	#N/A
ELP3	<i>elongator acetyltransferase complex subunit 3</i>	0	3	0	0	3	0	0	0	0	0	#N/A
IDH1	<i>isocitrate dehydrogenase (NADP(+)) 1, cytosolic</i>	0	3	0	0	3	0	0	0	0	0	#N/A

GPHN	<i>gephyrin</i>	0	2	0	0	2	0	0	0	0	0	#N/A
DCAF7	<i>DDB1 and CUL4 associated factor 7</i>	0	2	0	0	2	0	0	0	0	0	#N/A
WHSC1	<i>nuclear receptor binding SET domain protein 2</i>	0	2	0	0	2	0	0	0	0	0	#N/A
UBTF	<i>upstream binding transcription factor</i>	0	2	0	0	2	0	0	0	0	0	#N/A
ZFYVE16	<i>zinc finger FYVE-type containing 16</i>	0	2	0	0	2	0	0	0	0	0	#N/A
MYO9B	<i>myosin IXB</i>	0	2	0	0	2	0	0	0	0	0	#N/A
TOPBP1	<i>DNA topoisomerase II binding protein 1</i>	0	2	0	0	2	0	0	0	0	0	#N/A
SMARCE1	<i>SWI/SNF related, matrix associated, actin dependent regulator of chromatin, subfamily e, member 1</i>	0	2	0	0	2	0	0	0	0	0	#N/A
AKAP13	<i>A-kinase anchoring protein 13</i>	0	2	3	3	8	0	0	0	0	0	#N/A
SFSWAP	<i>splicing factor SWAP</i>	0	2	0	0	2	0	0	0	0	0	#N/A
TES	<i>testin LIM domain protein</i>	0	2	0	0	2	0	0	0	0	0	#N/A
SYNRG	<i>synergin gamma</i>	0	2	0	0	2	0	0	0	0	0	#N/A
DDX20	<i>DEAD-box helicase 20</i>	0	2	0	0	2	0	0	0	0	0	#N/A
BUB1	<i>BUB1 mitotic checkpoint serine/threonine kinase</i>	0	2	0	0	2	0	0	0	0	0	#N/A
CWC27	<i>CWC27 spliceosome associated cyclophilin</i>	0	2	0	0	2	0	0	0	0	0	#N/A
CCNL1	<i>cyclin L1</i>	0	2	0	0	2	0	0	0	0	0	#N/A
PIP4K2C	<i>phosphatidylinositol-5-phosphate 4-kinase type 2 gamma</i>	0	2	0	0	2	0	0	0	0	0	#N/A
CHD1	<i>chromodomain helicase DNA binding protein 1</i>	0	2	0	0	2	0	0	0	0	0	#N/A
NR2C1	<i>nuclear receptor subfamily 2 group C member 1</i>	0	2	0	0	2	0	0	0	0	0	#N/A
KIAA0182	<i>Gse1 coiled-coil protein</i>	0	2	0	0	2	0	0	0	0	0	#N/A
STAMBP	<i>STAM binding protein</i>	0	2	0	0	2	0	0	0	0	0	#N/A
PDCL	<i>phosducin like</i>	0	2	0	0	2	0	0	0	0	0	#N/A
MYSM1	<i>Myb like, SWIRM and MPN domains 1</i>	0	2	0	0	2	0	0	0	0	0	#N/A
PARD3	<i>par-3 family cell polarity regulator</i>	0	2	0	0	2	0	0	0	0	0	#N/A
CD3EAP	<i>CD3e molecule associated protein</i>	0	2	0	0	2	0	0	0	0	0	#N/A

WHSC2	<i>negative elongation factor complex member A</i>	0	2	0	0	2	0	0	0	0	0	#N/A
SRSF12	<i>serine and arginine rich splicing factor 12</i>	0	2	0	0	2	0	0	0	0	0	#N/A
RAVER1	<i>ribonucleoprotein, PTB binding 1</i>	0	2	0	0	2	0	0	0	0	0	#N/A
SLAIN2	<i>SLAIN motif family member 2</i>	0	2	0	0	2	0	0	0	0	0	#N/A
FAM193A	<i>family with sequence similarity 193 member A</i>	0	2	0	0	2	0	0	0	0	0	#N/A
MYO6	<i>myosin VI</i>	0	2	0	0	2	0	0	0	0	0	#N/A
SUPT6H	<i>SPT6 homolog, histone chaperone and transcription elongation factor</i>	0	2	0	0	2	0	0	0	0	0	#N/A
RAB3GAP1	<i>RAB3 GTPase activating protein catalytic subunit 1</i>	0	2	3	0	5	0	0	0	0	0	#N/A
FKBP3	<i>FKBP prolyl isomerase 3</i>	0	2	0	0	2	0	0	0	0	0	#N/A
CCDC72	<i>translation machinery associated 7 homolog</i>	0	2	0	0	2	0	0	0	0	0	#N/A
COMMD9	<i>COMM domain containing 9</i>	0	2	0	0	2	0	0	0	0	0	#N/A
BAP1	<i>BRCA1 associated protein 1</i>	0	2	0	0	2	0	0	0	0	0	#N/A
COPB2	<i>coatamer protein complex subunit beta 2</i>	0	2	0	0	2	0	0	0	0	0	#N/A
CCS	<i>copper chaperone for superoxide dismutase</i>	0	2	0	0	2	0	0	0	0	0	#N/A
RCL1	<i>RNA terminal phosphate cyclase like 1</i>	0	2	0	0	2	0	0	0	0	0	#N/A
LSM6	<i>LSM6 homolog, U6 small nuclear RNA and mRNA degradation associated</i>	0	2	0	0	2	0	0	0	0	0	#N/A
BCAS3	<i>BCAS3 microtubule associated cell migration factor</i>	0	2	0	0	2	0	0	0	0	0	#N/A
MCM3AP	<i>minichromosome maintenance complex component 3 associated protein</i>	0	2	0	0	2	0	0	0	0	0	#N/A
POLA2	<i>DNA polymerase alpha 2, accessory subunit</i>	0	2	0	0	2	0	0	0	0	0	#N/A
ASCC1	<i>activating signal cointegrator 1 complex subunit 1</i>	0	2	0	0	2	0	0	0	0	0	#N/A
KIF13A	<i>kinesin family member 13A</i>	0	2	0	0	2	0	0	0	0	0	#N/A
DHPS	<i>deoxyhypusine synthase</i>	0	2	0	0	2	0	0	0	0	0	#N/A
SIPA1L1	<i>signal induced proliferation associated 1 like 1</i>	0	2	0	0	2	0	0	0	0	0	#N/A

PGK1	<i>phosphoglycerate kinase 1</i>	0	0	27	19	46	0	0	0	0	0	#N/A
DLST	<i>dihydrolipoamide S-succinyltransferase</i>	0	0	8	8	16	0	0	0	0	0	#N/A
RNH1	<i>ribonuclease/angiogenin inhibitor 1</i>	0	0	8	5	13	0	0	0	0	0	#N/A
GLO1	<i>glyoxalase 1</i>	0	0	8	5	13	0	0	0	0	0	#N/A
AGPS	<i>alkylglycerone phosphate synthase</i>	0	0	0	2	2	0	0	0	0	0	#N/A
SLC30A1	<i>solute carrier family 30 member 1</i>	0	0	4	4	8	0	0	0	0	0	#N/A
TRIM27	<i>tripartite motif containing 27</i>	0	0	4	5	9	0	0	0	0	0	#N/A
ACTN1	<i>actinin alpha 1</i>	0	0	0	7	7	0	0	0	0	0	#N/A
NBAS	<i>neuroblastoma amplified sequence</i>	0	0	2	3	5	0	0	0	0	0	#N/A
KIAA0528	<i>C2 calcium dependent domain containing 5</i>	0	0	5	3	8	0	0	0	0	0	#N/A
DSG1	<i>desmoglein 1</i>	0	0	28	21	49	0	0	0	0	0	#N/A
MPRIP	<i>myosin phosphatase Rho interacting protein</i>	0	0	7	6	13	0	0	0	0	0	#N/A
CDKAL1	<i>CDK5 regulatory subunit associated protein 1 like 1</i>	0	0	7	3	10	0	0	0	0	0	#N/A
KIF26B	<i>kinesin family member 26B</i>	0	0	7	5	12	0	0	0	0	0	#N/A
FLG2	<i>filaggrin family member 2</i>	0	0	6	6	12	0	0	0	0	0	#N/A
CASK	<i>calcium/calmodulin dependent serine protein kinase</i>	0	0	6	0	6	0	0	0	0	0	#N/A
SDCBP	<i>syndecan binding protein</i>	0	0	5	9	14	0	0	0	0	0	#N/A
TRIOBP	<i>TRIO and F-actin binding protein</i>	0	0	5	3	8	0	0	0	0	0	#N/A
SGPL1	<i>sphingosine-1-phosphate lyase 1</i>	0	0	5	0	5	0	0	0	0	0	#N/A
S100A11	<i>S100 calcium binding protein A11</i>	0	0	4	4	8	0	0	0	0	0	#N/A
NBR1	<i>NBR1 autophagy cargo receptor</i>	0	0	4	2	6	0	0	0	0	0	#N/A
TRPM7	<i>transient receptor potential cation channel subfamily M member 7</i>	0	0	4	3	7	0	0	0	0	0	#N/A
SLMAP	<i>sarcolemma associated protein</i>	0	0	4	6	10	0	0	0	0	0	#N/A
DSC1	<i>desmocollin 1</i>	0	0	4	6	10	0	0	0	0	0	#N/A
EMID2	<i>collagen type XXVI alpha 1 chain</i>	0	0	4	0	4	0	0	0	0	0	#N/A
RPS10-NUDT3	<i>RPS10-NUDT3 readthrough</i>	0	0	4	0	4	0	0	0	0	0	#N/A
PI4K2B	<i>phosphatidylinositol 4-kinase type 2 beta</i>	0	0	3	2	5	0	0	0	0	0	#N/A

KCTD14	<i>potassium channel tetramerization domain containing 14</i>	0	0	3	0	3	0	0	0	0	0	#N/A
ZDHHC5	<i>zinc finger DHHC-type containing 5</i>	0	0	3	3	6	0	0	0	0	0	#N/A
BAIAP2L1	<i>BAI1 associated protein 2 like 1</i>	0	0	3	0	3	0	0	0	0	0	#N/A
DSC3	<i>desmocollin 3</i>	0	0	3	0	3	0	0	0	0	0	#N/A
CHMP2A	<i>charged multivesicular body protein 2A</i>	0	0	3	0	3	0	0	0	0	0	#N/A
AFTPH	<i>aftiphilin</i>	0	0	3	3	6	0	0	0	0	0	#N/A
STRN4	<i>striatin 4</i>	0	0	2	2	4	0	0	0	0	0	#N/A
VRK2	<i>VRK serine/threonine kinase 2</i>	0	0	2	2	4	0	0	0	0	0	#N/A
ATP13A3	<i>ATPase 13A3</i>	0	0	2	0	2	0	0	0	0	0	#N/A
ADCY9	<i>adenylate cyclase 9</i>	0	0	2	0	2	0	0	0	0	0	#N/A
ANKLE2	<i>ankyrin repeat and LEM domain containing 2</i>	0	0	2	0	2	0	0	0	0	0	#N/A
SNAPIN	<i>SNAP associated protein</i>	0	0	2	0	2	0	0	0	0	0	#N/A
TAX1BP1	<i>Tax1 binding protein 1</i>	0	0	2	2	4	0	0	0	0	0	#N/A
UTRN	<i>utrophin</i>	0	0	2	0	2	0	0	0	0	0	#N/A
GPRIN1	<i>G protein regulated inducer of neurite outgrowth 1</i>	0	0	2	2	4	0	0	0	0	0	#N/A
ABI1	<i>abl interactor 1</i>	0	0	2	0	2	0	0	0	0	0	#N/A
STEAP3	<i>STEAP3 metalloredutase</i>	0	0	2	2	4	0	0	0	0	0	#N/A
MAGT1	<i>magnesium transporter 1</i>	0	0	2	2	4	0	0	0	0	0	#N/A
PEG10	<i>paternally expressed 10</i>	0	0	2	0	2	0	0	0	0	0	#N/A
MPP7	<i>membrane palmitoylated protein 7</i>	0	0	2	3	5	0	0	0	0	0	#N/A
RAB7L1	<i>RAB29, member RAS oncogene family</i>	0	0	2	2	4	0	0	0	0	0	#N/A
ROR2	<i>receptor tyrosine kinase like orphan receptor 2</i>	0	0	0	4	4	0	0	0	0	0	#N/A
SRGAP1	<i>SLIT-ROBO Rho GTPase activating protein 1</i>	0	0	0	3	3	0	0	0	0	0	#N/A
KIF16B	<i>kinesin family member 16B</i>	0	0	0	3	3	0	0	0	0	0	#N/A
KPRP	<i>keratinocyte proline rich protein</i>	0	0	0	2	2	0	0	0	0	0	#N/A
TMEM237	<i>transmembrane protein 237</i>	0	0	0	2	2	0	0	0	0	0	#N/A
ITCH	<i>itchy E3 ubiquitin protein ligase</i>	0	0	0	2	2	0	0	0	0	0	#N/A
MACF1	<i>microtubule actin crosslinking</i>	0	0	0	2	2	0	0	0	0	0	#N/A

<i>factor 1</i>												
DST	<i>dystonin</i>	0	0	0	2	2	0	0	0	0	0	#N/A
STARD9	<i>StAR related lipid transfer domain containing 9</i>	0	0	0	2	2	0	0	0	0	0	#N/A
STON2	<i>stonin 2</i>	0	0	0	2	2	0	0	0	0	0	#N/A
MOSPD2	<i>motile sperm domain containing 2</i>	0	0	0	2	2	0	0	0	0	0	#N/A
AP3M2	<i>adaptor related protein complex 3 subunit mu 2</i>	0	0	0	2	2	0	0	0	0	0	#N/A
PALM2	<i>paralemmin 2</i>	0	0	0	2	2	0	0	0	0	0	#N/A